HYPERBOLIC PROBLEMS

Theory, Numerical Methods and Applications

Second International Conference

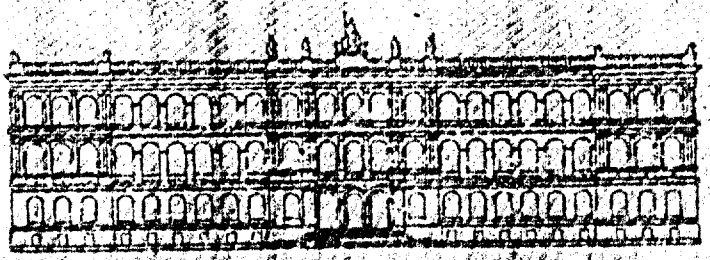

RWTH Aachen
March, 14—18 1988

BOOK OF ABSTRACTS

NONLINEAR HYPERBOLIC WAVES

John K. Hunter
Colorado State University
Ft Collins, CO 80524, U.S.A.

Joseph B. Keller
Stanford University
Stanford, CA 94305, U.S.A.

We develop a formal asymptotic theory for hyperbolic conservation laws with large amplitude, rapidly varying initial data [1]. For small times, the solution is described by a system of conservation laws in a single space variable. Shocks form, and the solution rapidly decays. For larger times, the solution propagates along rays according to weakly nonlinear geometrical optics. Initial data for the weakly nonlinear solution is obtained by matching with the long time behavior of the solution to the conservation laws in one space variable.

Let $u(x,t;\epsilon)$ be a solution of the strictly hyperbolic, genuinely nonlinear system of conservation laws,

$$\begin{aligned} &\partial_t u + \sum_{i=1}^{n} \partial_{x_i} f_i(u) = 0, \quad f_i : \mathbb{R}^m \to \mathbb{R}^m, \\ &u(x,0;\epsilon) = u_0[x,\epsilon^{-1}\Psi(x)], \end{aligned} \tag{1}$$

where $u_0(x,\eta)$ has compact support in η. We shall describe the asymptotic behavior of u as $\epsilon \to 0$. For short times, of the order ϵ,

$$u(x,t;\epsilon) \sim v[x,\epsilon^{-1}\Psi(x),\epsilon^{-1}t] \quad \text{as } \epsilon \to 0,$$

where $v(x,\eta,\tau)$ satisfies

$$\begin{aligned} &\partial_\tau v + \partial_\eta g(x,v) = 0, \qquad g(x,v) := \sum_{i=1}^{n} \partial_{x_i}\Psi(x)\, f_i(v), \\ &v(x,\eta,0) = u_0(x,\eta). \end{aligned} \tag{2}$$

Equation (2) is a system of conservation laws in one space dimension, in which x

occurs as a parameter.

For times of the order one, $u(x,t;\epsilon)$ is asymptotic to a weakly nonlinear geometrical optics solution [2], which has the form

$$(3) \qquad u(x,t;\epsilon) \sim \delta(\epsilon) \sum_{i=1}^{m} a_j[x,t,\delta^{-1}\phi_j(x,t)]R_j(x,t) \quad \text{as } \epsilon \to 0.$$

In (3), the wave amplitudes a_j, the phase functions ϕ_j and the eigenvectors R_j satisfy the equations derived in [1]. In particular, the wave amplitudes solve inviscid Burgers' equations of the form,

$$[\partial_t + C_j(x,t)\cdot\nabla]a_j + \tfrac{1}{2}M_j(x,t)\ \partial_\theta[a_j^2] + Q_j(x,t)a_j = 0.$$

These equations must be supplemented by initial values of the a_j and ϕ_j, and by specification of the amplitude parameter δ, which are obtained by matching (3) as $t \to 0+$, with the solution of (2) as $\tau \to +\infty$.

The solution of (2) approaches a superposition of N–waves as $\tau \to +\infty$ [3]. Matching implies that

$$\delta = \epsilon^{1/2},$$

$$\phi_j(x,0) = \Psi(x), \quad \partial_t\phi_j(x,0) = -\lambda_j(x),$$

where $\lambda_j(x)$ is the j^{th} eigenvalue of $D_v g(x,v)$. Also, as $t \to 0+$,

$$a_j(x,t,\theta) \sim M_j(x,0)^{-1}t^{-1}\theta, \text{ if } -[-2p_j(x)t]^{1/2} < \theta < [2q_j(x)t]^{1/2},$$

$$a_j(x,t,\theta) \sim 0, \qquad \text{otherwise.}$$

Here, M_j is a nonlinear self interaction coefficient (which is nonzero for genuinely nonlinear waves), and p_j and q_j are the N–wave invariants of the j^{th} N–wave in the large time asymptotic solution of (2).

A similar theory is possible when $u_0(x,\eta)$ is periodic in η, but it is only complete for a scalar equation and 2×2 systems. This is for two reasons: the large time behavior of periodic solutions to general systems of conservation laws in one space variable is not known; and there are difficulties in the weakly nonlinear

theory for resonantly interacting periodic waves.

References

[1] J. K. Hunter and J. B. Keller, "Nonlinear hyperbolic waves", to appear in *Proc. Roy. Soc. A.*

[2] J. K. Hunter and J. B. Keller, "Weakly nonlinear, high–frequency waves", *Comm. Pure Appl. Math.* 36 (1983), 547–569.

[3] T. P. Liu, "Decay to N–waves of solutions of general systems of nonlinear hyperbolic conservation laws", *Comm. Pure. Appl. Math.* 30 (1977), 585–610.

Numerical Solution of Flow Equations
An Aircraft Designer's View

Josef Mertens, Klaus Becker

Department of Theoretical Aerodynamics
MBB-UT, TE 212, Hünefelderstr. 1-5, D-2800 Bremen 1

Today the most accurate and cost effective industrial codes used for aircraft design are based on full potential equations coupled with boundary layer equations. But these are not capable to solve complicated three-dimensional problems of vortical flows and shocks. On the other hand Euler and Navier-Stokes codes are too expensive and not sufficiently accurate for design purposes, especially towards drag and interference prediction. The reasons for these deficiencies are investigated and a way to overcome them by future developments is demonstrated.

ON THE POSSIBILITY AND THE STRUCTURE OF OSCILLATING SOLUTIONS TO SOME NONLINEAR SYSTEMS OF CONSERVATION LAWS.

Michel RASCLE, Département de Mathématiques, Université de Nice, Parc Valrose
06034 NICE CEDEX, FRANCE

Abstract:

We study the convergence of a sequence of approximate solutions to some nonlinear 2 x 2 strictly hyperbolic systems of conservation laws, typically the (vanishing) viscosity method, in which the Cauchy problem:

$$(1)\quad \partial_t u + \partial_x f(u) = 0$$
$$u(x,0) = u_0(x)$$

(where $f: \mathbb{R}^2 \to \mathbb{R}^2$ is a smooth function) is approximated by:

$$(1_\varepsilon)\quad \partial_t u^\varepsilon + \partial_x f(u^\varepsilon) = \varepsilon\, \partial_x (D \partial_x u^\varepsilon)$$
$$u^\varepsilon(x,0) = u_0(x)$$

where D is a diffusion matrix. We only assume that this sequence (u^ε) satisfies a uniform L^∞ estimate:

$$(2)\quad \|u^\varepsilon\| \le c$$

and the easy energy estimate :

$$(3)\quad \varepsilon^{1/2} \|\partial_x u^\varepsilon\| \le c$$

Under these assumptions, we study the relations between the weak-star limits g^* in L^∞ of $g(u^\varepsilon)$, for any continuous function g. In other words, at any point (x,t) we study the so-called Young measure $\nu_{x,t}: g \to g^*(x,t)$. We recall that $(\nu_{x,t})$ is a

family of probability measures which operate in the phase plane, and that the strong convergence (no oscillation) corresponds to the case where these probability measures are delta-functions.

By using very simple ideas of compensated compactness, in the spirit of previous results of L. TARTAR, R.J. DIPERNA, D. SERRE, we have previously studied the structure of this family of Young measures. Roughly speaking, "we can pass to the limit on the product of the Riemann Invariants of the system". This is expressed by the formula:

$$(4) \qquad \nu_{x,t} = p(v,z)\mu_1 \times \mu_2$$

in which $p(v,z)$ is a precisely given function and was first conjectured by D. SERRE, while μ_1 and μ_2 respectively operate on functions of v and z. We had also shown that this is the key point to prove the convergence of the viscosity method. Namely, either for the "elasticity system or for the isentropic gas dynamics equations, (4) enables to show (very simply) a sequence of non positive functions whose weak limit is non negative: therefore the limit is zero and the convergence is strong. Moreover, the Young measure is a delta-function, except if the system is linearly degenerate.

Here, we show that this information (4) is also crucial to study the linearly degenerate case, so that, roughly speaking, the picture is the following:

-either the system is linearly degenerate, and then oscillations can just propagate (if they already exist in the initial data), but cannot be created

-or the system is not linearly degenerate(e.g. is genuinely nonlinear), and then possible oscillations in the initial data are immediately "killed" by the entropy conditions.

Large Time Step Glimm's Scheme for Hyperbolic Conservation Laws

Wang Jinghua

Institute of Systems Science
Academia Sinica
Beijing
China

We are concerned with systems of conservation laws of the form

$$u_t + f(u)_x = 0 \quad , \quad -\infty < x < \infty \quad , \quad t \geq 0 \tag{1}$$

with initial condition

$$u(x,0) = u_0(x) \quad . \tag{2}$$

Here $u(x,t) = (u^1(x,t), \ldots, u^m(x,t))$ and $f(u(x,t)) = (f^1(u(x,t)), \ldots, f^m(u(x,t)))$ is a smooth mapping from a region Ω of R^m to R^m. We assume that the system (1) is strictly hyperbolic, i.e. the matrix $\frac{\partial f}{\partial u}$ has real and distinct eigenvalues.

Solution to I.V.P. (1), (2) may develop discontinuities even when the initial data are smooth. Therefore we seek weak solutions to I.V.P. (1), (2), i.e., solutions $u(x,t)$ which satisfy

$$\int_0^\infty \int_{-\infty}^\infty (u\Phi_t + f(u)\Phi_x)\, dx\, dt + \int_{-\infty}^\infty u_0(x)\Phi(x,0)\, dx = 0$$

for all C^1 test functions $\Phi(x,t)$, vanishing for $|x| + t$ large.

Glimm's scheme, introduced in his celebrated paper [1], is an effective method for calculating discontinous solutions of systems of conservation laws. The main advantages of the scheme for numerical calculation is the sharp resolution of discontinuities and absence of over- and undershoots. A drawback of the scheme is to solve many Riemann problems. This is a time consuming procedure. Motivated by Le Veque's work [3], we introduce two types of large time step generalization of Glimm's scheme, [4], by linear superposition of conserved quantities and corresponding Riemann invariants respectively. Here we give a description of first one as follows.

We discretize $R \times (0,\infty)$ by spatial mesh length δ and time mesh length τ and allowing the Courant number c to be arbitrary (fixed) constant, i.e.,

$$\frac{\tau}{\delta}|\lambda| = c \leq N$$

where $|\lambda|$ is the maximum wave speed. Then for a random sequence $\{\alpha_i\}$ in $[0,1)$, assuming that $u(x,t,\delta)$, approximate solution to I.V.P. (1), (2) has been determined for $t < t_n = n\tau$, then we define $u(x,t_n,\delta) = u_{k,n} = u(x_k + \alpha_n\delta t_n - \delta)$ for $x \in I_k = [x_k, x_{k+1})$, where $x_k = k\delta$. Let $u_{k,n}(x,t)$ be solution of Riemann problem

$$\begin{cases} (1) \\ u(x,t_n) = \begin{cases} u_{k-1,n} & , \quad x < x_k \\ u_{k,n} & , \quad x > x_k \end{cases} . \end{cases}$$

We set $u(x,t,\delta)$ in the stripe $S_n = \{(x,t), \quad t_n \le t < t_{n+1}\}$ as

$$u(x,t,\delta) = u(x,t_n,\delta) + \sum_i (u_i(x,t) - u_i(x,t_n)) \quad , \quad (x,t) \in S_n \tag{3}$$

The above procedure may proceed for all $t > 0$ provided we have suitable bound on $u(x,t,\delta)$. To initiate the scheme, at $n = 0$, we set

$$u(x,0,\delta) = u_0(x) \quad .$$

These are at most $2N$ non-zero terms in the sum of right hand side of (3). In particular this large time generalization of Glimm's scheme, abbreviated as L.T.S. Glimm's scheme, reduces to Glimm's scheme when $c \le 1/2$.

We prove [4], the consistency of the L.T.S. Glimm's scheme, i.e., assume that each choice of the random sequence $\{\alpha_i\}$ yield a family $\{u(x,t,\delta), \quad 0 < \delta < \delta_0\}$ of approximate solution which are defined for $t > 0$ and T.V. $u(\cdot,t,\delta)$ are uniformly bounded in δ and t. Then there exists a sequence $\delta_l \to 0$ such that

$$u(x,t,\delta_l) \longrightarrow u(x,t) \quad , \quad \delta_l \to 0$$

and $u(x,t,\delta)$ is the weak solution to I.V.P. (1), (2).

We also prove in [4] that the L.T.S. Glimm's scheme is total variation diminishing for scalar conservation laws. Therefore by consistency of the scheme it follows that the weak solution to I.V.P. (1), (2) can be obtained as limit of sequence of the approximate solution $u(x,t,\delta)$ for almost all choices of random sequence $\{\alpha_i\}$ as the mesh is refined.

In [4], for general systems, if we assume the system is genuinely nonlinear and T.V. $u_0(\cdot)$ is sufficiently small, then T.V. $u(\cdot,t,\delta)$ is bounded uniformly in δ and $t > 0$. Thus the weak solution to I.V.P (1), (2) also can be obtained by L.T.S. Glimm's scheme. This means that the main theorem in Glimm's work [1] remains true for L.T.S. Glimm's scheme.

Harten and Lax [2] modify Glimm's scheme by replacing the exact solution of Riemann problem with an appropriate finite difference approximation and by building approximate solutions on a moving grid. Their modification is computationally more efficient and easier to extend to more general situations. In [5], we extend the random choice finite difference scheme by Harten and Lax to a large time step version and we prove the consistency of the scheme and the scheme is total variation diminishing for scalar conservation laws. We also make study on entropy condition for it.

References

1. *J. Glimm, Solutions in the large for nonlinear hyperbolic systems of equations, Comm., Pure Appl. Math., 18 (1965), 695–715*
2. *A. Harten and P.D. Lax, A random choice finite difference scheme for hyperbolic conservation laws, SIAM J. Numer. Anal. 18 (1981), 289–315*
3. *R.I. Le Veque, Convergence of a large time step generalization of Godunov's method for conservation laws. Comm. Pure Appl. Math., 37 (1984), 463–477*
4. *Wang Jinghua, Large time step generalizations of Glimm's scheme for systems of conservation laws.*
   Research report of Nankai Institute of Mathematics, Tianjin, China N8 (1986).
   To appear in Chinese Annals of Mathematics.
5. *Wang Jinghua, Large time step generalization of random choice finite difference scheme for hyperbolic conservation laws*
   To appear in Acta Mathematica Scientia

MBB UT

Second International Conference on Hyperbolic Problems

Numerical Solution of Flow Equations
An Aircraft Designer's View

Josef Mertens, Klaus Becker

Department of Theoretical Aerodynamics
MBB-UT, TE 212, Hünefeldstr. 1-5, D-2800 Bremen 1

Second International Conference on Hyperbolic Problems

Main Topic: 2. Numerical Methods

Contribution Title: Numerical Solution of Flow Equations
An Aircraft Designer's View

Authors: Josef Mertens, Klaus Becker *

Summary

Today the most accurate and cost effective industrial codes used for aircraft design are based on full potential equations coupled with boundary layer equations. But these are not capable to solve complicated three-dimensional problems of vortical flows and shocks. On the other hand Euler and Navier-Stokes codes are too expensive and not sufficiently accurate for design purposes, especially towards drag and interference prediction. The reasons for these deficiencies are investigated and a way to overcome them by future developments is demonstrated.

Nomenclature

a	speed of sound	p	pressure
a_o	stagnation speed of sound	R	special gas constant
dA	element of surface ∂V	s	specific entropy
div_n.	div in plane normal to $\underset{\sim}{n}$	t	time
D_M.	wave operator at Mach cone	T	temperature
D_p.	wave operator at path line	$\underset{\sim}{v}^*$	space-time velocity, stat. = $\underset{\sim}{v}$
$\frac{D.}{Dt}$	substantial derivative	$\underset{\sim}{v}$	space velocity
		v_n	normal comp. of velocity
∂V	surface of V	v_t	tangential comp. of velocity
e	specific inner energy	V	control volume
$\underset{\sim}{F}$	flux	γ	ratio of specific heats
h_o	specific stagnation enthalpy	λ	Riemann invariant
$\underset{\sim}{n}^*$	space-time like normal vector	ρ	density
$\underset{\sim}{n}$	space like part of $\underset{\sim}{n}^*$		

Deficiencies of Modern Numerical Methods

In the field of aerodynamic design of modern aircraft, especially transonic transport aircraft, numerical methods became one of the most important design tools. The mayority of the codes used nowadays heavily relies on the experience with the elliptic subsonic potential equation. To enable the solution of transonic problems with supersonic pockets the necessary numerical conditions for hyperbolic flows were introduced. And yet today the most accurate codes for drag prediction are full potential codes coupled with a boundary layer method. Especially at the points indicated in Fig. 1 the viscous effects strongly influence the solution: shock/boundary layer interaction, rear loaded profiles, transonic wakes. An H-type grid enables an accurate coupling of the inviscid and viscous solution including the wake and an easy capture of normal shocks [3].

* Department of Theoretical Aerodynamics
MBB-UT, TE 212, Hünefeldstr. 1-5, D-2800 Bremen 1

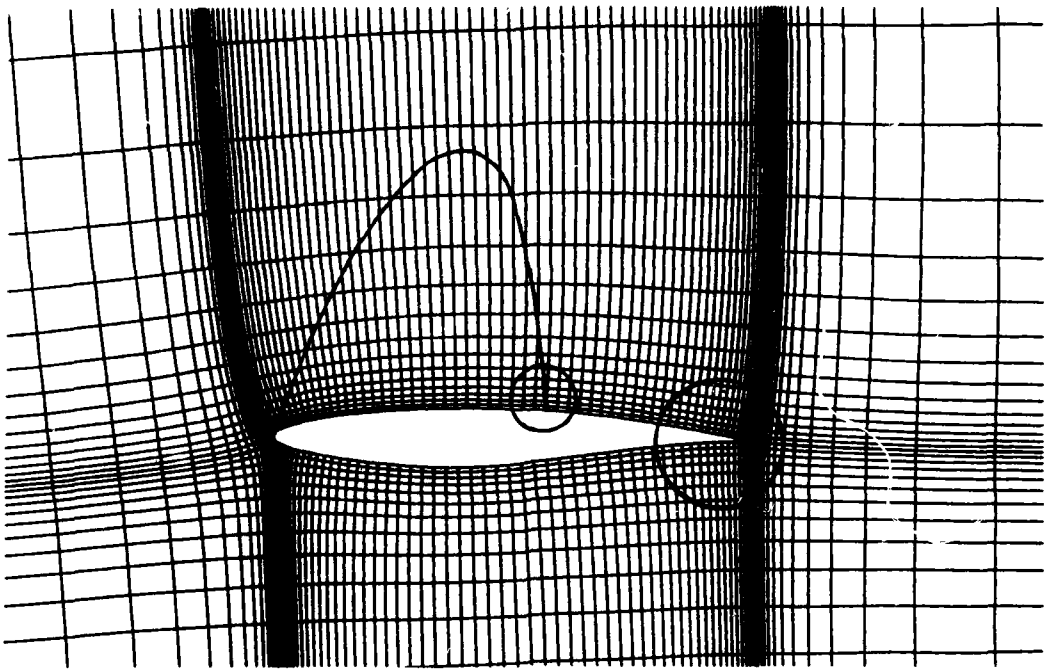

Fig. 1: Transonic airfoil calculation

These codes are restricted to two-dimensional or at least nearly two-dimensional flow problems because they cannot capture the typical three-dimensional effects shown in Fig. 2: unknown three-dimensional shocks, free vortices, wake interferencies, nacelle and jet interferencies, rotational flow fields.

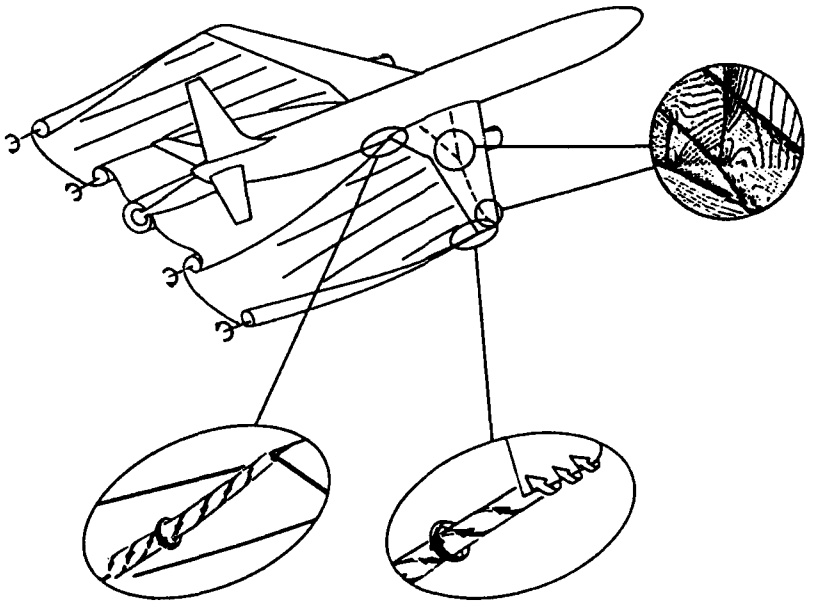

Fig. 2: Severe 3D-problems for transport aircraft

For aircraft of small aspect ratio (Fig. 3) the old methods are completely insufficient: the flow field is dominated by vortex systems; at higher Mach numbers the strong entropy gradients do not allow a potential approximation.

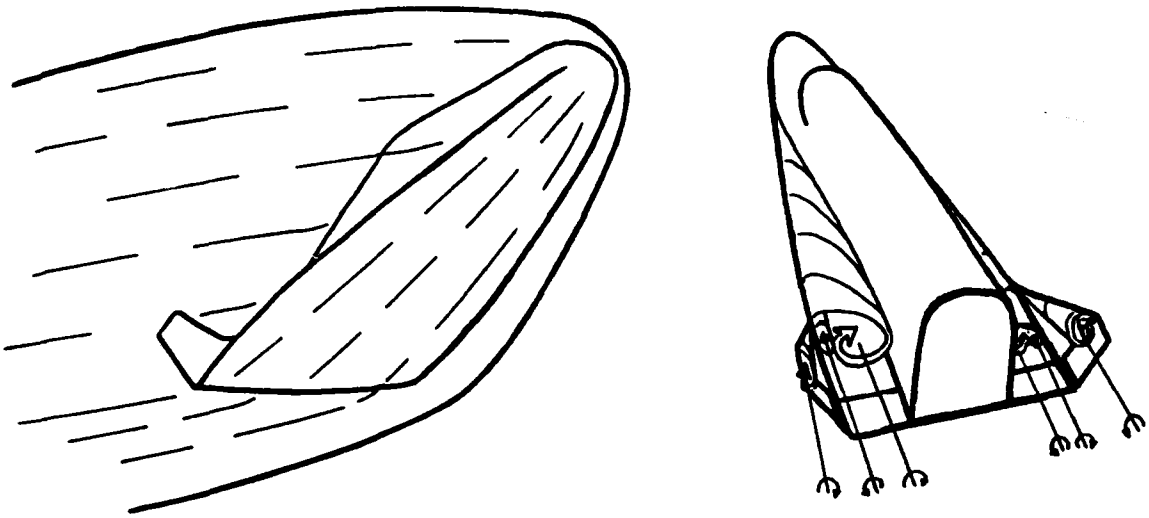

Fig. 3: Severe 3D-problems for reentry vehicle

On the other hand there exist a lot of Euler and Navier-Stokes (NS) codes which should be able to solve these problems. The following figures show some typical 3D-results of two modern Euler codes representing the state of the art. Fig. 4 shows total pressure losses on a midwing airfoil.

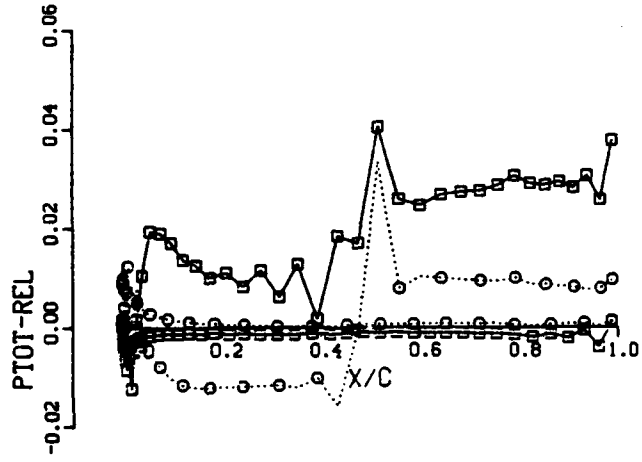

Fig. 4: Total pressure loss on midwing airfoil
(Solutions of two different 3D Euler codes)

Due to smearing and wiggles shock location and strength cannot be determined accurately. At the leading edge spurious pressure raises resp. entropy losses and other numerical errors occur; the trailing edge solution shows similar errors.
Inviscid wave and induced drag has to be determined by integration in the direction perpendicular to the free stream.

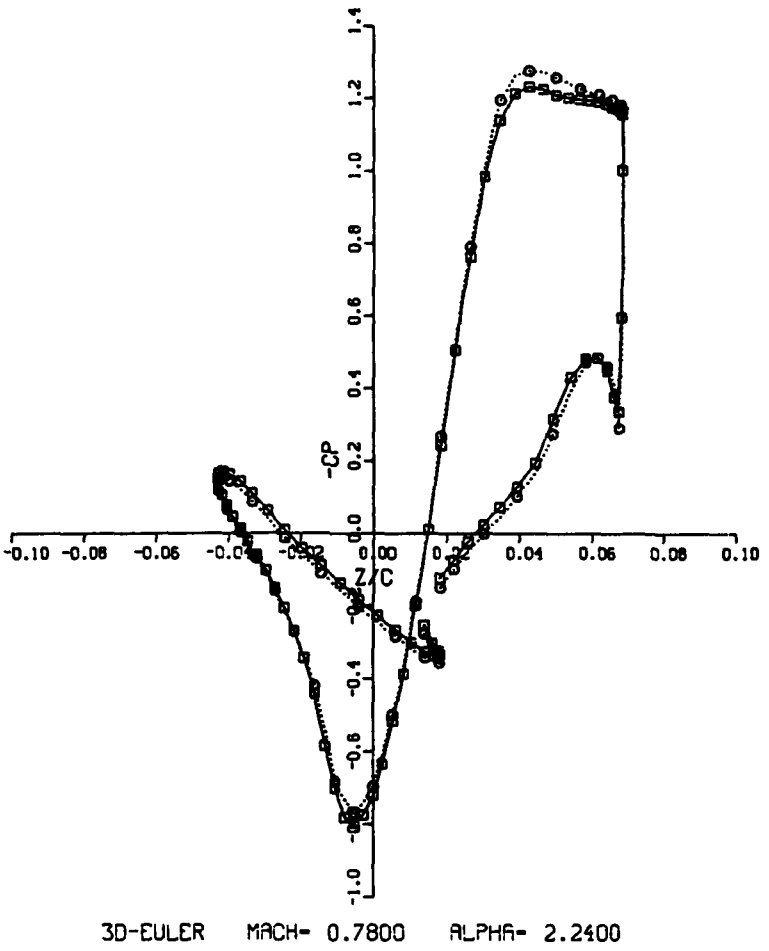

Fig. 5: Inviscid drag by pressure integration
(Solutions of two different 3D Euler codes)

Inviscid drag is given as the small difference of the large areas enclosed by the pressure curves; errors mainly result from the wrong pressure computation at leading and trailing edges.
Another possibility of inviscid drag calculation is to calculate wave drag by entropy rise at the shock and induced drag in the Treffz plane. This method requires accurate shock determination and vorticity transport (Fig. 6, 7); both are not sufficiently guaranteed by current codes.

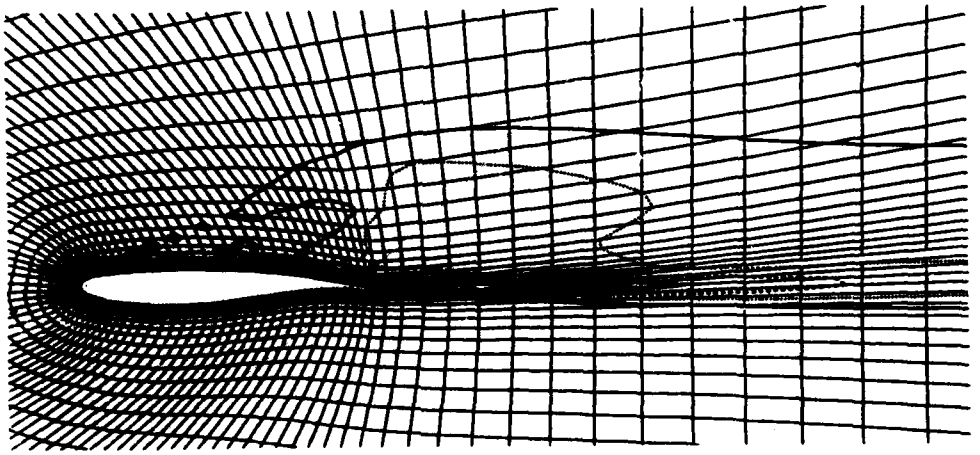

Fig. 6: Total pressure loss, streamwise direction
(3D Euler solution)

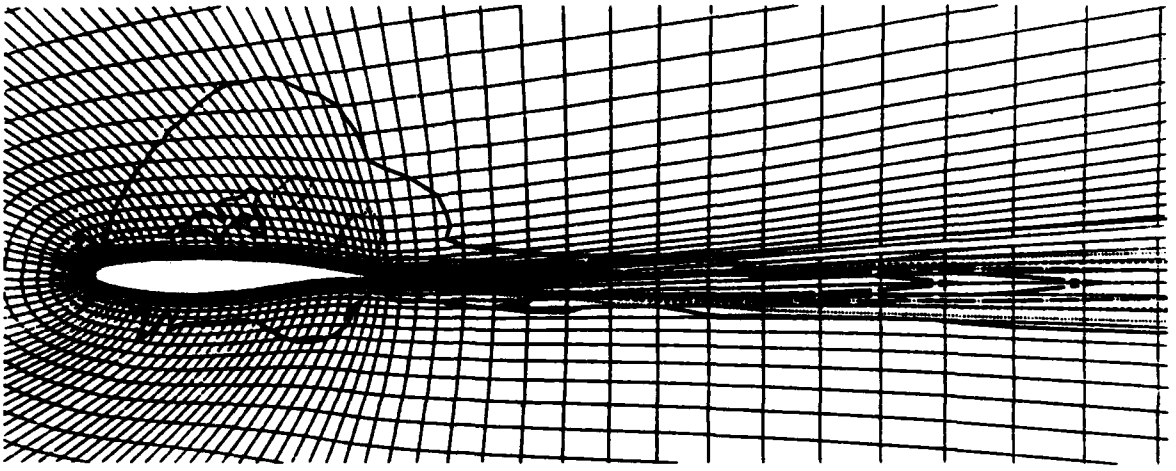

Fig. 7: Absolute value of vorticity, streamwise direction, (3D Euler solution)

Other very important problems to be solved are the interferencies caused by vortex systems. Euler and NS solvers should be able to capture this problem.

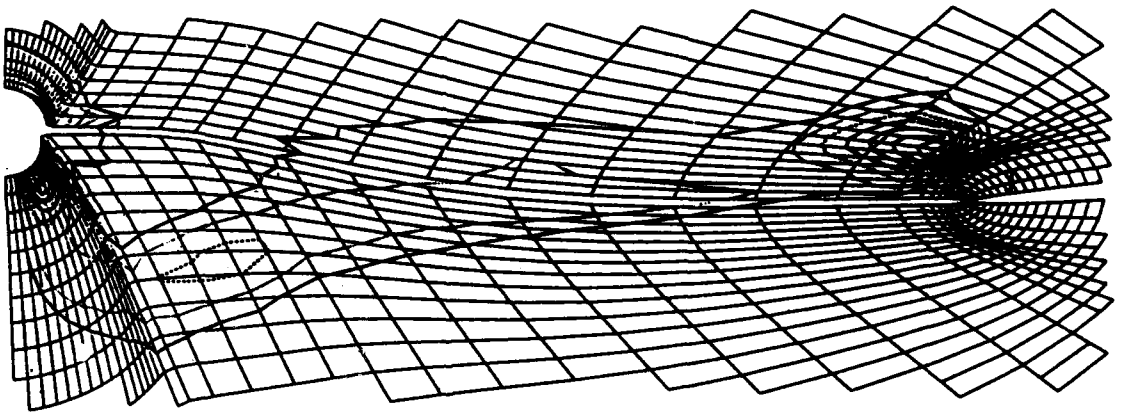

Fig. 8: Total pressure loss, wake behind wing (3D Euler solution)

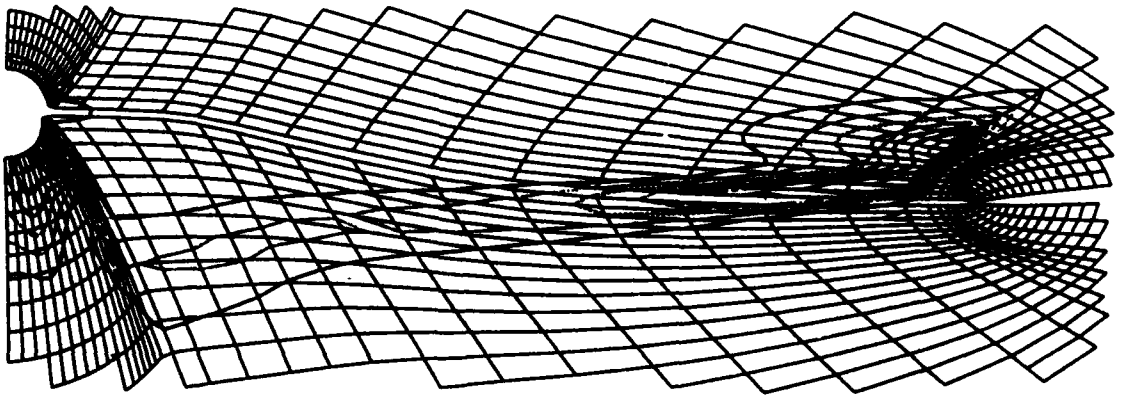

Fig. 9: Absolute value of vorticity, wake behind wing, (3D Euler solution)

Figs. 8/9 should show only the inviscid wake of an Euler solution. Partly vorticity occurs at the physically known places. But obviously, additional vorticity is generated by grid properties, is smeared out, and in the downstream direction the vorticity content [2] diminishes rapidly. So these codes are not yet helpful to solve this problem with the accuracy needed for aircraft design.

Looking at computing costs the Euler (and NS) codes are surprisingly expensive: This is mainly due to the fact that today's Euler codes need grid sizes comparable to those used with full potential codes. But to get the requested solution values (e.g. velocity or pressure) the potential function Φ has to be differentiated numerically with one order loss of accuray. In Euler equations, the requested values are directly obtained as solutions and therefore a much coarser mesh should give the same accuracy as for potential flow models. Moreover - because of the necessary degree of continuity - additional difficulties should be expected for full potential solvers in regions of strongly varying solutions. Therefore important accuracy and cost improvements of future Euler (and NS) codes can be expected.

The examples demonstrated here are Euler solutions. Real flow is viscous; so some people think that the difficulties will be overcome by the solution of the NS equations. But since the errors shown above are errors of the solution method rather than the Euler equations, they will not be overcome by using other equations but by other algorithms. Especially for high Reynolds number flows the Euler terms remain very important in the NS equations; they completely describe the outer flow field away from body surfaces or wakes. So a NS solution will only be possible with an accurate solution of the intrinsic Euler part. And as the important hyperbolic part of the flow equations are the Euler equations, their numerical solution by field methods will be discussed here.

It is well known, that the errors in numerical solutions are generated by numerical smearing, amplification and artificial damping, but it is difficult to localize the hidden sources of these effects. We will try to identify some of them and to show possibilities to overcome them. The presented facts are all known, but not yet respected in many numerical methods.

The construction of numerical field methods is done in five steps:
- Selection and analysis of the governing equations,
- Selection of a point distribution or grid to represent the flow field,
- Approximation of solution values between grid points,
- Formulation of the boundary conditions defining the special problem,
- Mathematical solution algorithm.

In the next sections only the first three points are discussed for the Euler equations as an example of systems of nonlinear hyperbolic equations.

Governing Equations

The well known Euler equations are

$$
\begin{aligned}
&\text{C} \quad \frac{D\varrho}{Dt} + \varrho \,\mathrm{div}\, \underline{v} = \frac{\partial \varrho}{\partial t} + \mathrm{div}\,(\varrho \underline{v}) = 0 \\
&\text{M} \quad \varrho \frac{D\underline{v}}{Dt} + \mathrm{grad}\, p = \underline{0} \qquad (1) \\
&\text{E} \quad \varrho \frac{De}{Dt} + p \,\mathrm{div}\, \underline{v} = \varrho \frac{De}{Dt} - \frac{p}{\varrho} \frac{D\varrho}{Dt} = \varrho T \frac{Ds}{Dt} = 0
\end{aligned}
$$

They have to be complemented by two equations describing the state of the gas.

A system of hyperbolic differential equations has a set of real directions with undefined derivatives. For the Euler equations (1) these directions are all the directions $\underset{\sim}{n}^*$ normal to the path lines and the directions normal to the Mach cone defined by the characteristic direction conditions

$$\begin{aligned} &\text{for the path line:} && \underset{\sim}{v}^* \cdot \underset{\sim}{n}^* = 0 , \\ &\text{for the Mach cone:} && \underset{\sim}{v}^* \cdot \underset{\sim}{n}^* = -a . \end{aligned} \tag{2}$$

All solutions of hyperbolic systems, except the trivial ones, are defined by jumps of (sometimes higher order) derivatives. The possible discontinuities in the shock free region are (depending on the selected set of dependant variables) e.g.

$$\begin{aligned} &\text{across the path line:} && \text{variables} && s, \rho, T, a, (h_o), \underset{\sim}{v}_t , \\ &\text{across the Mach cone:} && \text{1. derivatives of} && p, \ (\underset{\sim}{v} \cdot \underset{\sim}{n}) . \end{aligned} \tag{3}$$

In special cases the dependant variables themselves are discontinuous:

$$\begin{aligned} &\text{across wakes:} && \text{all variables except} && p, v_n , \\ &&& \text{(wakes consist of path lines)} \\ &\text{across shocks:} && \text{all variables except} && \underset{\sim}{v}_t . \end{aligned} \tag{4}$$

The path line and wake discontinuities are connected with vortices and occur even in steady subsonic flow.

In contrast to elliptic problems, where the polynomial order of the Taylor approximation is a quality measure for the discretization, for hyperbolic problems this is only true for regions with very smooth solutions. For the physically more interesting zones it is important to take care of the different kinds of discontinuities, because the solution cannot be expanded into Taylor series.

Corresponding to the directions $\underset{\sim}{n}^*$ normal to possible jumps there exist the directions of wave propagation with the associated wave operators

$$\begin{aligned} &\text{path line } \underset{\sim}{v}^* : && D_p \cdot := \frac{D \cdot}{Dt} := \frac{\partial \cdot}{\partial t} + (\underset{\sim}{v} \cdot \text{grad}) . \\ &\text{Mach cone } \underset{\sim}{v}^* + a \cdot \underset{\sim}{n} : && D_M \cdot := \frac{D \cdot}{Dt} + a \, (\underset{\sim}{n} \cdot \text{grad}) . \end{aligned} \tag{5}$$

The continuous part of the solution is defined by the set of compatibility conditions of characteristics theory, e.g. (depending on the selected set of dependant variables)

$$\begin{aligned} &\text{along path line:} && E && D_p \, s = 0 , \\ &&& \underset{\sim}{v} \cdot M && D_p \left(\frac{v^2}{2} \right) = - \frac{1}{\rho} \, \underset{\sim}{v} \cdot \text{grad} \, p , \\ &\text{along Mach cone:} && D_M (\underset{\sim}{v} \cdot \underset{\sim}{n}) + \frac{1}{\rho a} D_M \, p + a \, \text{div}_n \, \underset{\sim}{v} = 0 \\ &&& (\text{div}_n \, \underset{\sim}{v} : \text{ div } \underset{\sim}{v} \text{ taken in the plane normal to } \underset{\sim}{n}). \end{aligned} \tag{6}$$

These conditions are special combinations of the governing equations which are valid everywhere except across shocks and wakes. But only in the directions of the corresponding characteristics they describe continuous wave propagation although continuity is not required for each single term.

Along the path line entropy and stagnation enthalpy are convected without any continuity required in the transverse direction, even for subsonic flow. For simulation of vortical flows the correct calculation of vorticity transport is very important. It is described indirectly by transport equations along path lines, because Crocco's theorem

$$\underset{\sim}{v} \times \text{curl } \underset{\sim}{v} = - T \text{ grad } s + \text{grad } h_o + \frac{\partial \underset{\sim}{v}}{\partial t} \qquad (7)$$

defines vorticity by (mainly transverse) differentiation of entropy and stagnation enthalpy.

Important for numerical schemes is, that the hyperbolic solution is exclusively defined by derivative jumps across the characteristics and in certain cases as jumps of the solutions themselves, i.e. at wakes and shocks in the Euler equations.

Referring to the corresponding surface integral formulation instead of the differential equations,

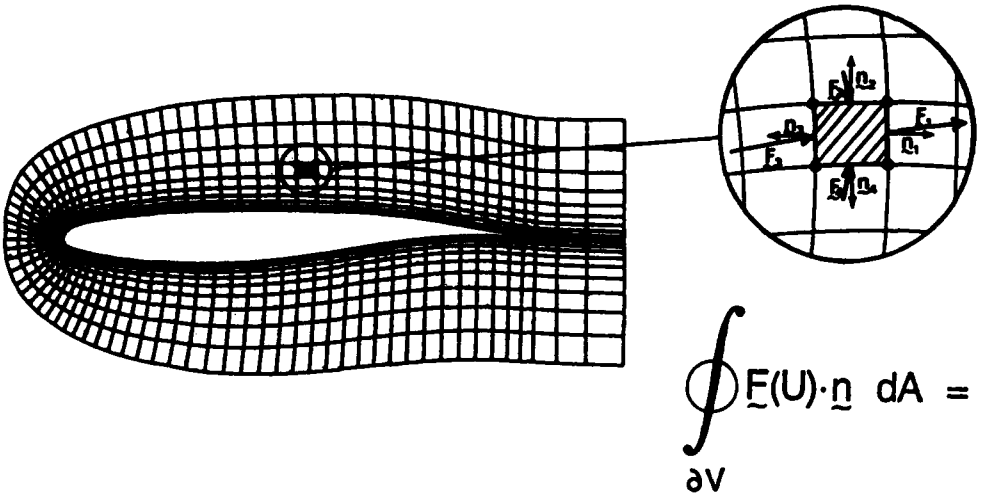

Fig. 10: Finite volume

$$\text{C} \qquad \int_V \frac{\partial \varrho}{\partial t}\, dV = - \oint_{\partial V} (\varrho\, \underset{\sim}{v}\cdot\underset{\sim}{n})\, dA$$

$$\text{M} \qquad \int_V \frac{\partial}{\partial t}(\varrho \underset{\sim}{v})\, dV = - \oint_{\partial V} [\varrho \underset{\sim}{v}\, (\underset{\sim}{v}\cdot\underset{\sim}{n}) + p\, \underset{\sim}{n}]\, dA \qquad (8)$$

$$\text{E} \qquad \int_V \frac{\partial}{\partial t}[\varrho(e+\frac{v^2}{2})]dV = - \oint_V [\varrho(e+\frac{v^2}{2} + \frac{p}{\varrho})(\underset{\sim}{v}\cdot\underset{\sim}{n})]\, dA$$

it is possible to capture all discontinuities within one cell for one-dimensional problems. The reason is that one can calculate the fluxes of the unknown solutions instead of the unknown solutions themselves. But this normally fails in multidimensional cases because the fluxes are tensors of one degree higher than the unknowns. For multidimensional problems it is impossible to get a sufficient number of equations for a direct solution of

the unknown fluxes. Therefore the fluxes are computed by integrating over the boundary where their values have to be calculated from a usual set of variables. But the values of these variables are only known at distinct points and not at the whole boundary. This must be overcome by interpolation assumptions which often are inconsistent with the discontinuities. Therefore a combination with other techniques is recommended which will be described later.

To achieve good numerical properties the selection of unknowns has a strong influence. For the Euler equations the so-called conservative variables yield shock capturing capability to finite difference schemes, but are normally working well only for one-dimensional cases. For finite volume schemes based on the boundary integral equations (8) instead of the differential equations, it is not necessary to use the conservative variables for shock capturing. Here the only important condition is, that the equations do not contain production terms.

Using the conservative variables or primitive variables the set of differential equations is strongly coupled. For numerical reasons and for consistency it is desirable to decouple the system of equations. This is at least partly possible by using an different set of variables. A complete decoupling is provided by Riemann invariants if they exist; unfortunately they usually do not exist. But often it is possible to construct a system of equations with weaker coupling and weaker nonlinearities, using the knowledge of Riemann properties of simpler cases. So choosing velocity, speed of sound and entropy as variables leads to a set of only mildly coupled and nearly linear compatibility conditions.

$$
\begin{aligned}
&\text{along path line:} \quad E \qquad D_p\, s = 0\,, \\
&\underset{\text{(transient)}}{\underset{\sim}{v}\cdot M} \qquad D_p \left(\frac{v^2}{2}\right) = \underset{\sim}{v}\cdot\left[T\ \text{grad}\ s - \frac{1}{\gamma-1}\ \text{grad}\ (a^2)\right]\,, \\
&\underset{\text{(quasi stat.)}}{\underset{\sim}{v}\cdot M} \qquad D_p\,(a_0^2) = \frac{\partial}{\partial t}(a^2) - (\gamma-1)T\,\frac{\partial s}{\partial t}\,, \\
&\text{along Mach cone:} \quad D_M \left(\frac{2}{\gamma-1}\,a + \underset{\sim}{v}\cdot\underset{\sim}{n}\right) = -\frac{a}{\gamma R}\,D_M\, s - a\ \text{div}_n\ \underset{\sim}{v}\,.
\end{aligned}
\tag{9}
$$

Wave transportation is described by the wave operators D. The nonlinearity is restricted to the determination of the differential operator's characteristic direction and the right hand terms. If we locally combine the wave variables velocity and speed of sound for each grid plane to plane Riemann invariants [6], as proposed by Moretti [4],

$$
\lambda(n) \;:=\; \frac{2}{\gamma-1}\,a + (\underset{\sim}{v}\cdot\underset{\sim}{n})\,, \quad \underset{\sim}{n}_1 = -\,\underset{\sim}{n}_2 \tag{10}
$$

we get the weakest possible coupling of the compatibility equations. As well known, for isentropic plane waves the equations are completely decoupled. This set, however, has no shock capturing capability.

Selection of Representative Points

In most numerical field methods the solution field is represented by a distinct number of grid points. Between the grid points the solution values are distributed by some kind of interpolation. Normally these interpolation functions are defined locally, changing definition at grid lines. Therefore grid lines introduce numerical discontinuities in the derivatives.

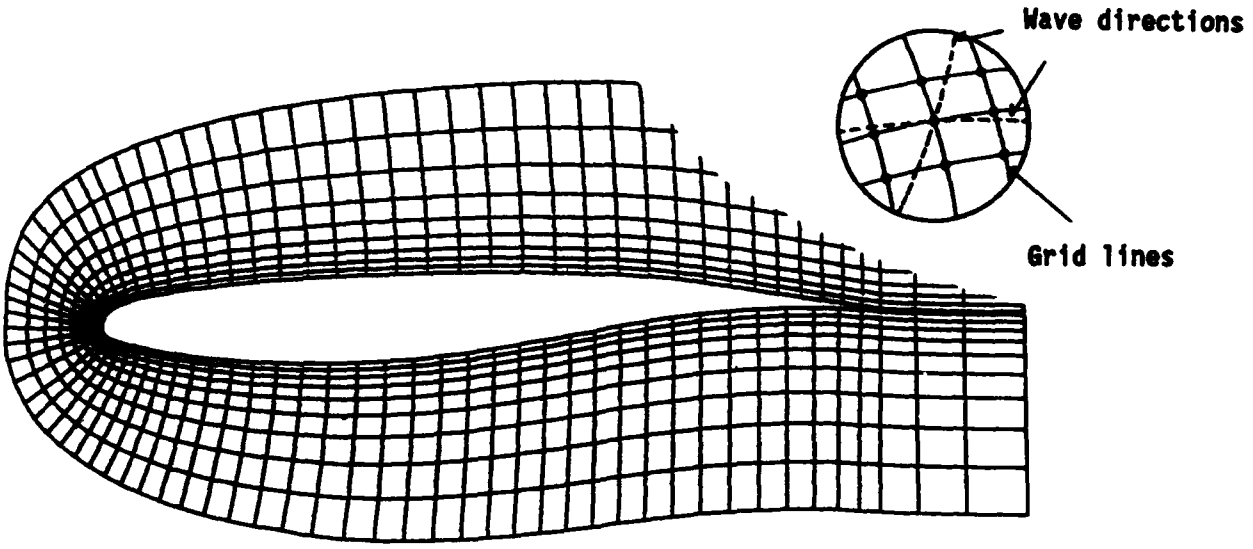

Fig. 11: Numerical grid

To obtain the best possible results the discontinuities generated by grid lines should coincide with the physical discontinuities, or at least with the most important physical discontinuities. Otherwise at each grid line the discontinuities will be redistributed and thus numerically dispersed.

For the Euler equations the most important discontinuities are:
- At shocks: shocks and path lines,
- In nonisentropic, shock-free regions: path lines and characteristics, especially "main characteristics" (The "main characteristic" is the downstream characteristic in the plane spanned by the boundary normal vector and the velocity vector.),
- In the isentropic region: characteristics, most important the "main characteristics",
- Steady subsonic vortex flow: path lines which here are stream lines.

It is not easy to fulfill this demand on grid construction, but it is the only way to get accurate solutions with a restricted number of grid points.

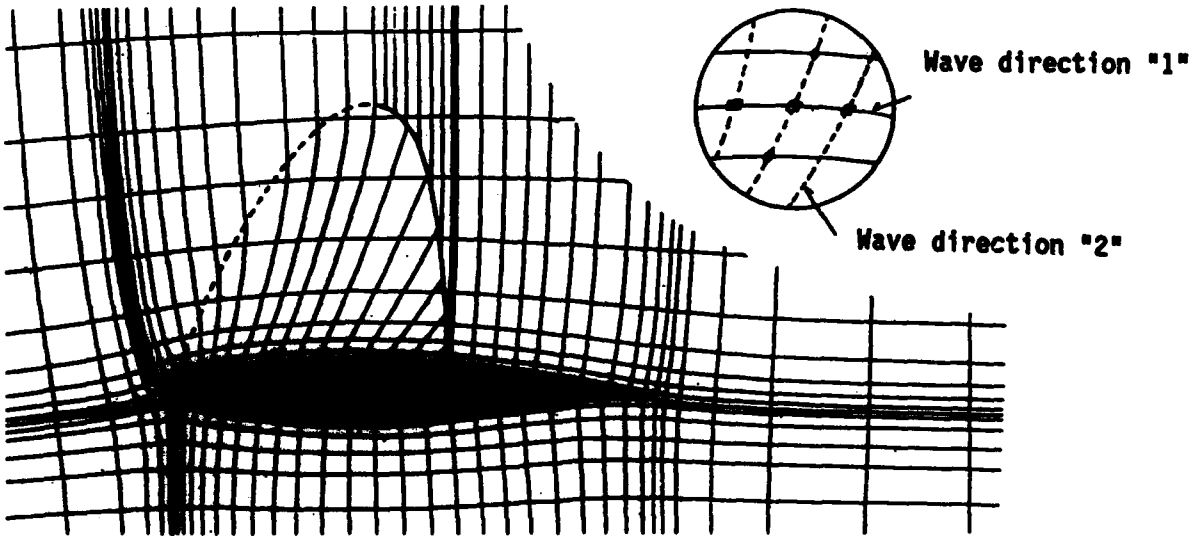

Fig. 12: Example of a physically motivated numerical grid

Approximation of Solution Values Between Grid Points

Most numerical field methods need some kind of solution distribution between grid points. As mentioned above, piecewise defined functions introduce numerical discontinuities. These discontinuities are generated along grid lines. If the grid lines do not coincide with the characteristics, part of the information transport changes direction from that of the characteristics to that of the grid line direction due to the redistribution of discontinuities. This produces numerical dispersion.

On the other hand, the interpolation functions often must be continuous across grid lines especially for difference and higher order schemes. So continuity is introduced numerically whereas physics can be discontinuous. This smears out solutions, amplifies disturbances and produces the well known wiggles [5].

Normally the interpolation of the different variables between the grid points is treated independent from each other, e.g. linear or quadratic for density, momentum and energy. But the equations are strongly coupled as well as the physical distributions of values. This becomes more obvious in the postprocessing, when other values like pressure, entropy or stagnation pressure are calculated. In the zones of strong gradients or even strongly varying gradients, the solution is affected by by the inconsistency of the interpolation. A subsequent computation, especially of sensitive functions as pressure, entropy or stagnation pressure, amplifies these errors due to the nonlinear combination of inconsistent values; spurious entropy often disappearing further downstream is generated. Moreover truncation errors increase with nonlinearity and stronger coupling of equations. So it becomes impossible to accurately calculate wave or induced drag by pressure integration, because the most important parts are the nose and trailing edge regions, both with strongly varying gradients producing large errors due to inconsistency and truncation errors.

Requirements for Numerical Field Methods

Most numerical schemes stay in the tradition of elliptic solvers or one-dimensional approximations, which are not compatible with hyperbolic problems describing three-dimensional wave propagation and the corresponding discontinuities. An accurate numerical scheme must be properly modelt. Therefore physical and numerical discontinuities should coincide as much as possible. The most convenient way is to select characteristic directions for grid construction, as the Massau construction [6] for two independent and two dependent variables. But for more than two variables it is necessary to select the most important directions. These wave and discontinuity lines transport the main information and the strongest discontinuities. When they cross over with grid lines, the information must be redistributed; physical discontinuities are smeared out and new numerical discontinuities are generated.

From the aircraft designer's view, a combination with a viscous solution is absolutely necessary. It is facilitated by the selection of grids well adapted to path or stream lines. To facilitate code construction, stream line adaption can be used as a construction principle of the code itself [1].

To achieve accurate solutions the scheme should be of second order in smooth regions, but at physical discontinuities it should introduce as little numerical smoothness as possible. Therefore interpolation or distribution functions should be restricted to one mesh or cell surface. Then numerical

inaccuracies introduced by approximation are not amplified and can be transported along the grid lines. If the grid lines coincide with a wave propagation direction, all the resp. approximation errors remain confined within the neighboring grid lines, with no further dispersion. A realization seems possible, for example, with characteristics oriented schemes or node oriented finite volume schemes using physically motivated grids.

To overcome the difficulties with inconsistent interpolation and truncation errors, it is possible to use a set of variables better decoupling the equations. These variable sets normally have no shock capturing capability. So they can only be used in a nearly converged state to improve accuracy; or shock fitting must be performed. Another possibility is to use better interpolation functions, based on local approximations of the flow field, e.g. based on a locally linearized potential solution combined with a vorticity approximation given by the entropy distribution.

The methods mentioned above will give the possibility of cost effective and accurate solutions. But programming work will be more arduous, especially when versatility is to be maintained. At comparable accuracy for Euler codes the goal is to achieve

- computing times in the order of full potential codes,

- with coarse grids as known from the method of characteristics.

References

[1] Agrawal, S.; Vermeland, R.E.; Verhoff, A.; Lowrie, R.B.: "Euler Transonic Solutions over Finite Wings", AIAA Paper 88-0009.

[2] Hirschel, E.H.: "On the Creation of Vorticity and Entropy in Solutions of the Euler Equations for Lifting Wings", MBB-LKE122-AERO-MT-716.

[3] Mertens, J.; Klevenhusen, K.-D.; Jakob, H.: "Accurate Transonic Wave Drag Prediction Using Simple Physical Models", AIAA Journal, June 1987

[4] Moretti, G.; Zanetti, L.: "A New and Improved Computational Technique for Two-Dimensional, Unsteady, Compressible Flows", AIAA Journal, Vol. 22, June 1984.

[5] Rizzi, A.; Viviand, H.: "Numerical Methods for the Computation of Inviscid Transonic Flows with Shock Waves", Notes on Numerical Methods in Fluid Mechanics 3, 1981.

[6] Sauer, R.: "Nichtstationäre Probleme der Gasdynamik", Springer, 1966.

[7] Wichmann, G.; Radespiel, R.; Leicher, S.: "Vergleich von Lösungen der vollständigen Potentialgleichung und der Eulergleichungen für die transsonsiche Umströmung des DFVLR-F4-Flügels", DFVLR-IB-85/39, 1985.

[8] "Accuracy Study of Transonic Flow Computations for Three Dimensional Wings", Study by GARTEUR AD(AG-05), August 1987.

SPONSORSHIP AND SUPPORT ACKNOWLEDGEMENTS

Host Organization

Rheinisch Westfälische Technische Hochschule Aachen

SUPPORTING ORGANIZATIONS - Assistance Gratefully Acknowledged

Control Data GmbH, Düsseldorf
Cray Research GmbH, München
Deutsche Forschungsgemeinschaft
Diehl GmbH & Co., Röthenbach
Digital Equipment GmbH, Köln
FAHO Gesellschaft von Freunden der Aachener Hochschule, Düsseldorf
IBM Deutschland GmbH, Stuttgart
Mathematisch Naturwissenschaftliche Fakultät der RWTH
Ministerium für Wissenschaft und Forschung des Landes Nordrhein - Westfalen
Office of Naval Research Branch, Office, London, England
Rheinmetall GmbH, Düsseldorf
Stadt Aachen
US Air Force EOARD
US Army European Research Office, London
Wegmann GmbH & Co., Kassel

Author Index

The decay of solutions to the equations of nonisentropic hydrodynamic flow as $t \to \infty$

Prof. Hans-Dieter Alber
Mathematisches Institut A
der Universität Stuttgart
Pfaffenwaldring 57

7000 Stuttgart 80

We study the initial value problem for the hydrodynamic equations of one-dimensional, compressible flow, prove that a global solution exists for initial values with small variation, and use this result to investigate the asymptotic behaviour of the solution for large times. Our main objective is to study the decay of the solution to initial values without compact support.

The initial value problem is given by the equations

$$\varrho_t + (\varrho v)_x = 0 \tag{1}$$

$$(\varrho v)_t + (\varrho v^2)_x + p_x = 0 \tag{2}$$

$$\varrho\left(\tfrac{1}{2} v^2 + e\right)_t + \left(\varrho v\left(\tfrac{1}{2} v^2 + e + \tfrac{1}{\varrho} p\right)\right)_x = 0 \tag{3}$$

and the initial conditions

$$\varrho(x,0) = \tilde{\varrho}(x),\ v(x,0) = \tilde{v}(x),\ e(x,0) = \tilde{e}(x) \tag{4}$$

for $x \in \mathbb{R}$ and $t \geq 0$. $\varrho(x,t)$, $v(x,t)$, $e(x,t)$, respectively, are the density, the velocity, and the initial energy of the medium at the point x at time t, and $p = p(\varrho,e)$ is the pressure. We assume that the medium is a polytropic gas, that is an ideal gas for which e is simply proportional to the temperature T. From the equation of state for an ideal gas we therefore obtain

$$p = (\gamma-1)\,\varrho e \tag{5}$$

with a constant $\gamma > 1$. We note that the entropy S is given by

$$S(\varrho,v,e) = c_v \ln\left(\frac{e}{\varrho^{\gamma-1}}\right) + S_0 \tag{6}$$

with constants c_v, S_0.

It is well known that global solutions exist to this problem if the variation of the initial values is sufficiently small. T.P. Liu proved in [2] for the equations of non-isentropic flow in the representation of Lagrange that a global solution exists if the variation of the initial data is bounded by $c/(\gamma-1)$. In [4] he studied the asymptotic behaviour of solutions to general conservation laws including the case where some of the fields are linearly

degenerate, if the initial data are constant on intervals $(-\infty,a)$ and (b,∞). It is proved that the genuinly nonlinear fields decay at the rate $t^{-1/2}$ to the constant state if the initial data have equal constant values on the intervals $(-\infty,a)$ and (b,∞). Moreover, it is shown that in the L_1-norm the genuinly nonlinear fields tend to N-waves. In [3] it is shown that the linearly degenerate fields converge to a constante state for general initial data with sufficiently small variation. Our aim is to derive decay estimates for the solution if the initial data $(\tilde{\varrho},\tilde{v},\tilde{p})$ with $\tilde{p} = (\gamma-1)\tilde{\varrho}\,\tilde{e}$ have sufficiently small variation and satisfy

$$\lim_{x\to-\infty} (\tilde{\varrho}(x),\ \tilde{v}(x),\ \tilde{p}(x)) = \lim_{x\to+\infty} (\tilde{\varrho}(x),\ \tilde{v}(x),\ \tilde{p}(x)) = (\varrho_o,\ v_o,\ p_o)$$

(7)

$$TV((\tilde{\varrho},\tilde{v},\tilde{p}) \mid (-\infty,-a] \cup [a,\infty)) \le C\, a^{-\beta}$$

for positive constants C,β, and all $a > 0$. To do this we first use the difference scheme introduced in [1] to prove the following global existence result:

Theorem 1: Let a compact subset $K \subseteq \mathbb{R}^+ \times \mathbb{R} \times \mathbb{R}^+$ be given such that for all $u_1 = (\varrho_1,v_1,e_1)$, $u_2 = (\varrho_2,v_2,e_2) \in K$ the inequality

$$|v_1-v_2| < 2\left(\frac{\gamma}{\gamma-1}\right)^{1/2} (e_1^{1/2} + e_2^{1/2})$$

holds. Then there exist constants $C_1,C_2 > 0$ such that to all initial data $\tilde{u} = (\tilde{\varrho},\tilde{v},\tilde{e}) : \mathbb{R} \to K$ with

$$TV(\tilde{u}) \le C_1$$

there exists a weak solution $u = (\varrho,v,e) : \mathbb{R} \times \mathbb{R}_0^+ \to \mathbb{R}^+ \times \mathbb{R} \times \mathbb{R}^+$ of (1) - (5) satisfying the entropy condition and

$$TV(u(\cdot,t)) \le C_2\ TV(\tilde{u}).$$

Here the total variation is understood in a generalized sense. A weak solution $u = (\varrho,v,e)$ is said to satisfy the entropy condition if

$$\partial_t(\varrho S(u)) + \partial_x(\varrho v S(u)) \ge 0$$

holds in the distributional sense for the entropy S defined in (6). To prove this theorem we construct a sequence of approximate solutions to (1) - (5), which consist out of solutions of Riemann problems, and prove that the total variation of these approximate solutions is uniformly bounded. Then we can select a subsequence converging to a weak solution of (1) - (5). By studying the asymptotic behaviour of the approximate solutions we prove the following theorem:

Theorem 2: Let K be defined as in theorem 1. Then to all $\varepsilon > 0$ there exist constants $C_1, C_2 > 0$ such that to all initial data $\tilde{u} = (\tilde{\varrho}, \tilde{v}, \tilde{e}) : \mathbb{R} \to K$ satisfying (7) and $TV(\tilde{u}) \leq C_1$ there exists a weak solution $u(\varrho, v, e)$ of (1) – (5), which fulfills the entropy condition and

$$(8) \qquad \begin{aligned} &\sup_{x \in \mathbb{R}} \left(|v(x,t) - v_0| + |p(x,t) - p_0| \right) \leq q(t, \beta, \varepsilon) \\ &TV(v(\cdot,t),\ p(\cdot,t)) \leq q(t; \beta, \varepsilon), \end{aligned}$$

where

$$q(t;\beta,\varepsilon) = \begin{cases} C_2\, t^{-\frac{\beta}{2+\beta} + \varepsilon}, & 0 < \beta \leq \frac{2}{3} \\ C_2\, t^{-\frac{1}{2} + \varepsilon}, & \frac{2}{3} < \beta, \end{cases}$$

with $p(x,t) = (\gamma - 1)\, \varrho(x,t)\, e(x,t)$.

Again, the total variation is meant in a generalized sense. This result means that the genuinly nonlinear fields in the solution decay with the rate given in (8). However, the best decay rate we get is $t^{-\frac{1}{2}+\varepsilon}$, which shows that our estimates are not optimal, because the decay rate for initial data with compact support is $t^{-\frac{1}{2}}$, as we already mentioned above.

References

1. H.D. Alber: Local existence of weak solutions to the quasi-linear wave equation for large initial values. Math. Z. 190 (1985), 249-276.
2. T.P. Liu: Solutions in the large for the equations of nonisentropic gas dynamics. Indiana Univ. Math. J. 26 (1977), 147-177.
3. T.P. Liu: Large-time behaviour of solutions of initial and initial-boundary value problems of a general system of hyperbolic conservation laws. Comm. Math. Phys. 55 (1977), 163-177.
4. T.P. Liu: Linear and nonlinear large-time behaviour of solutions of general systems of hyperbolic conservation laws. Comm. Pure Appl. Math. 30 (1977), 767-796.

A HYPERBOLIC (GENERALIZED) FLUID MODEL FOR RELATIVISTIC ELECTRON BEAMS.

A.M. Anile and S. Pennisi
Dipartimento di Matematica
Citta' Universitaria
Viale A. Doria 6
95125 Catania (Italy)

Relativistic intense charged particle beams are of great interest in several areas of plasma physics and technology (e.g. free-electron lasers) [1].
A fundamental description of these beams is usually based upon the Vlasov-Boltzmann equation. Calculations for specific situations are then performed by using numerical simulation techniques. A kinetic approach , however , has some drawbacks . In particular , within a kinetic framework , the actual calculation of equilibrium configurations in an arbitrary geometry is time consuming and very difficult. Furthermore a stability analysis of such equilibrium configurations is an almost impossible task except in very special cases. These drawbacks could be avoided , at least in part , by adopting a fluid model . Obviously a fluid model cannot provide an accurate microscopic description but could be adequate if one is mainly interested in the gross fearures of a configuration.
Relativistic fluid models can be constructed by considering the moment equations arising from the relativistic Vlasov equation and adopting a suitable closure approximation. For particle beams the closure approximation must be based on the assumption that the particle distribution function represents a warm fluid , i.e. the dispersion of the velocity about the mean is small. Based on this approximation models have been proposed by Siambis [2], Newcomb [3] ,Amendt and Weitzner [4] . The latter , according to our opinion , is the most satisfactory because it is fully covariant and complete (i.e. they provide a minimal set of field equations). The present work is based on the Amendt and Weitzner model and we believe that it represents a considerable improvement upon theirs. The Amendt and Weitzner relativistic covariant warm fluid model could be improved significantly in two points. The first point is related to the constraint equations which must be satisfied by the moments and which arise from the fact that the moments arise from a distributiopn function. In the Amendt and Weitzner model these constraints are satisfied only approximately . The second point is that the Amendt and Weitzner model can be shown to lead to a hyperbolic system but it is not known whether such a system is equivalent to a symmetric one (for symmetric hyperbolic systems one has a much more satisfactory mathematical theory [5]).
In this paper we present a fluid model which solves the above inconveniences of the Amendt and Weitzner one. More precisely ,

for our model the constraint equations are satisfied exactly and furthermore our model leads to a symmetric hyperbolic system.

REFERENCES

[1] R.B.Miller , Intense Charged Particle Beams (Plenum Press , N.Y. , 1982)

[2] J.G.Siambis , Phys.Flyuids 22 , 1372 (1979)

[3] W.A.Newcomb , Phys.Fluids 25 , 846 (1982)

[4] P.Amendt and H.Weitzner .Phys.Fluids 28 , 949 (1985)

[5] K.O.Friedrichs , Comm. Pure Appl. Math.,7 , 345 (1954).

NON-OSCILLATORY SCHEMES FOR

MULTIDIMENSIONAL EULER CALCULATIONS

WITH UNSTRUCTURED MESHES

Paul ARMINJON
University of Montreal, Dept de Mathematiques et Statistiques,
C.P.6128 Succ.A, Montreal, Quebec(CANADA), H3C3J7
Alain DERVIEUX
Loula FEZOUI
Herve STEVE
INRIA, 2004 Route des Lucioles, Sophia-Antipolis 1 et 2,
06565 VALBONNE (FRANCE)
Bruno STOUFFLET
AMD-BA, DGT-DEA, B.P.300, 78 Quai M.Dassault,
92214 SAINT-CLOUD (FRANCE)

The purpose of the paper is to present a synthesis of a set of recent (essentially unpublished) studies related to the design of multi-dimensional non-oscillatory schemes, with emphasis on those which apply to non-structured finite-element simplicial meshes (triangles, tetrahedra). While the direct utilization of 1-D concepts may produce robust and accurate schemes when applied to non-distorted structured meshes, it cannot when non-structured triangulations are to be used.

The subject of the paper is to study the adaptation of the so-called TVD methods to the above context. TVD methods have been derived for the design of hybrid first-order/second-order accurate schemes which present in simplified cases monotonicity properties (see, for example, the review [1]).

A various collection of first-order accurate schemes can be used, they are derived from an artificial viscosity model or from an approximate Riemann solver.

However, the main feature in the design is the choice of the second-order accurate scheme, this choice can rely either on central differencing or on upwind differencing.

CENTRAL DIFFERENCING

For central differencing, our work [2] extends S.Davis' approach (see also [8,9]). Two main features will be discussed :

-the viscosity model can be uniform, so that the first-order scheme is of Lax-Friedrichs type: we discuss its method of construction (see also [4]) ; another model can be derived from a flux-splitting : Osher's splitting has been used with some success.

- the construction of symmetric limiters (after [12]): it is geometrically based on segments, i.e. triangle sides in 2-D, edges in 3-D, joining adjacent nodes ; this enables one to derive conservative schemes. Four values of a sensor are then to be computed in order to perform a 1-D limiting process ; these values are obtained using a local representation of the flow variables, derived from a previous FEM-MUSCL scheme introduced in [6].

UPWIND SCHEMES

In the case of upwind differencing, the MUSCL approach of van Leer [11] is adapted ; the question whether the limiting step has to be done separately in each direction or as a multidimensional device is studied more precisely:

- 1-D limiting has been used in a scheme involving fully upwind derivatives together with central ones ; it produced nice results for the simulation of 3-D reentry supersonic flows [10].

- 2-D limiting proved also to be a very robust approach when limitation is applied to each element(not published).

ANALYSIS

The communication will involve :

- a theoretical discussion of two scalar linear multidimensional models, namely the advection model :

$$(1) \quad w_t + \vec{V}.\overrightarrow{gradw} = 0.$$

and the linear conservation law :

$$(2) \quad w_t + div(\vec{V}w) = 0 .$$

Then a numerical scheme will be declared monotonicity preserving if it satisfies the Maximum Principle (case of (1)) or preserves the positiveness of solutions (case of (2)). In the context of triangles, the study is a sequel of the work done by Baba and Tabata [3]: several ways to extend their first-order accurate schemes to TVD quasi second-order accurate schemes will be presented.

- a presentation of the various Euler schemes

- a comparison of the schemes with 2-D typical calculations; a recent GAMM workshop [13] presented several test cases (airfoil, blunt body flows)that are not easy to calculate from the point of view of robustness and/or accuracy.

- a few 3-D calculations using some among the best schemes presented.

CONCLUSION

Several schemes that we designed are interesting from the point of view of robustness and accuracy. At the present time, upwind TVD schemes seem to be more accurate, because the limiters introduce less first-order accurate numerical viscosity. However, since purely central differencing schemes involve no numerical viscosity, TVD schemes relying on these schemes have a chance to perform well in the future, when, for example, they are included in a Navier-Stokes solver.

REFERENCES

[1] ARMINJON P., Some aspects of high resolution numerical methods for hyperbolic systems of conservation laws with applications to gas dynamics, INRIA Report 520, (1986)

[2] ARMINJON P., DERVIEUX A., Schémas TVD en Eléments Finis triangulaires, in preparation.

[3] BABA K., TABATA M., On a conservative upwind finite element scheme for convective diffusion equations, RAIRO, Vol.15,1,pp 3-25(1981)

[4] BILLEY V., DERVIEUX A., FEZOUI L., PERIAUX J., SELMIN V., STOUFFLET B., Recent improvement of Galerkin and upwind Euler schemes and applications to 3-D transonic flow simulation in aircraft engineering, Eight Int. Conf. on Computing Methods in Applied Sciences and Engineering, Versailles (F), dec. 14-18 (1987)

[5] DAVIS S.F., TVD finite difference schemes and artificial viscosity, ICASE Report 84-20, (1984)

[6] FEZOUI F., Résolution des équations d'Euler par un schéma de van Leer en éléments finis, INRIA Report 358 (1985).

[7] OSHER S., CHAKRAVARTHY S., Upwind schemes and boundary conditions with applications to Euler equations in general geometries, J. of Comp. Physics, Vol. 50, 3, 447-81 (1983).

[8] SELMIN V., Finite Element solution of hyperbolic equations, II, two-dimensional case, INRIA Report to appear (1987)

[9] SELMIN V., Numerical simulation of 3-D flows with a finite element method, INRIA Report to appear (1987)

[10] STOUFFLET B., PERIAUX J., FEZOUI F., DERVIEUX A., Numerical simulation of 3-D Hypersonic Euler Flows around space Vehicles using adapted finite Elements, AIAA Paper 87-0560 (1987).

[11] VAN LEER B., Computational methods for ideal compressible flow, von Karman Institute for Fluid Dynamics, Lecture Series 1983-04.

[12] YEE H., Upwind and Symmetric Shock-capturing schemes, NASA TM 89464 (1987)

[13] GAMM Workshop on the numerical simulation of compressible Euler flows, Le Chesnay (F), June 10-13 (1986), proceedings to be published by Vieweg

a

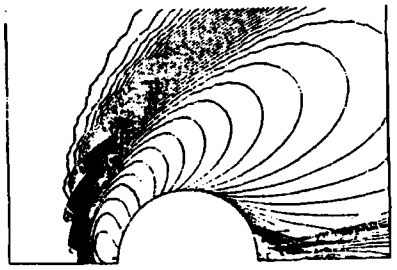

b

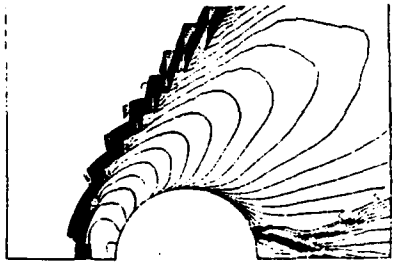

Construction of a high shock-resolution central-differencing scheme ; Mach-8 2-D flow past a cylinder :

a. First-order scheme (Osher's splitting)

b. TVD scheme, relying on the above scheme and a Richtmyer-Galerkin one.

The shock numerical thickness is in accordance with theoretical predictions.

Construction of a high shock-resolution upwind scheme ; Mach-8 2-D flow past a cylinder :

MUSCL-FEM scheme relying on Osher's splitting and on 2-D element-wise limiters.

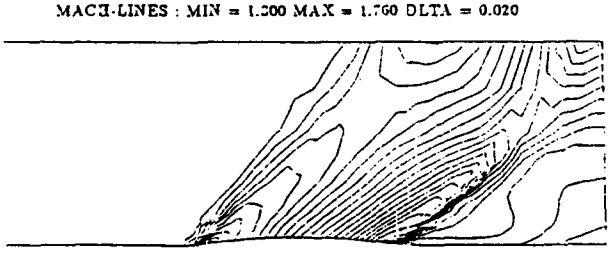

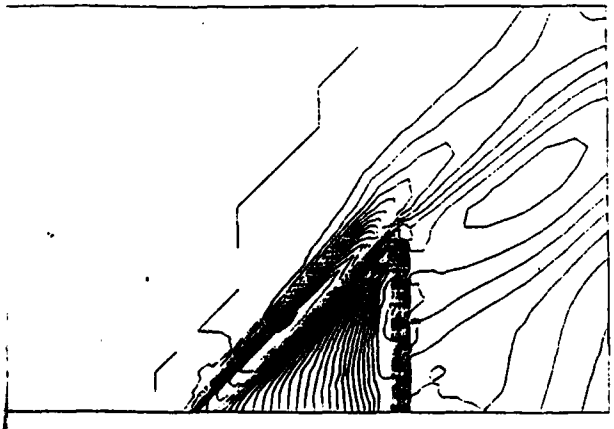

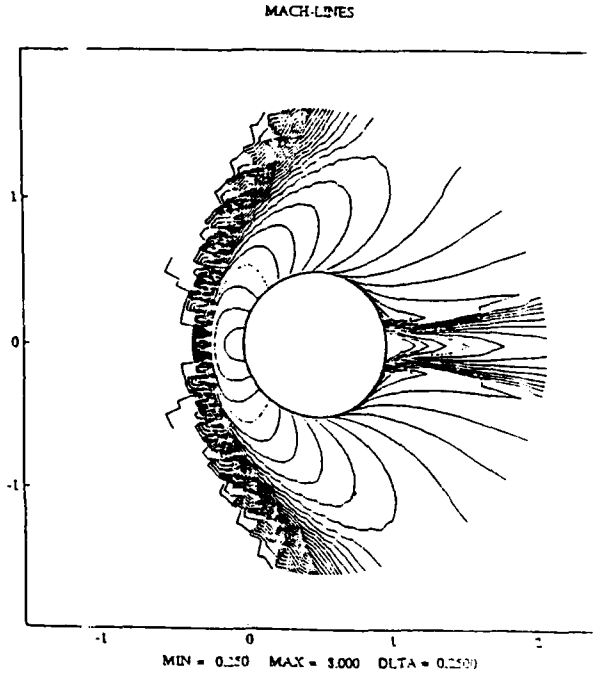

3-D calculation of a flow past a wing (Mach at infinity = 1.5), performed by applying a MUSCL-FEM scheme and a non-structured locally refined tetrahedrization.

Finite Domain Construction of TVD Schemes

TIMOTHY J. BARTH
CFD Branch, NASA Ames
M.S. 202A-1
Moffett Field, CA USA 94035

Introduction. The full paper will consider the construction of numerical solutions of the scalar initial-boundary-value problem (IBVP). The construction of total variation diminishing (TVD) schemes in periodic or infinite spatial domains with compact supported data has been considered by several authors in the literature (see [1],[2],[3],[4]). The construction of these schemes in finite domains has not been addressed. The proposed paper will discuss the construction of such schemes for the IBVP. The basic ideas parallel those used in the periodic/infinite domain case. The strategy for the full paper will be: (1) show that IBVP has an underlying integral constraint which relates solution variations in time and space, (2) consider this integral equation on a discrete mesh with appropriate Stieltjes sums (the "TVD" condition), (3) show that this provides Lax-Richtmyer stability in a maximum norm, (4) construct algebraic criteria for TVD schemes using standard arguments of positivity. In the following paragraphs, these ideas will be briefly discussed.

Preliminaries. The model nonlinear hyperbolic equation is given by

$$u_t + f(u)_x = 0, \quad -L/2 \le x \le L/2, \quad t > 0 \tag{1.0}$$

subject to initial data, $u(x,0) = u_0(x)$, and appropriate analytical boundary condition

$$u(-L/2,t) = g(t) \quad f' > 0, \quad u(L/2,t) = g(t) \quad f' < 0.$$

If u_0 and g are smooth, then unique local solutions for small time, $0 < t < \tau$, can be constructed. This may not be true for all time, i.e. discontinuities may form owing to the nonlinearity of (1.0). Whenever discontinuities do form, the viscous limit of (1.0) is considered which leads to the well-known Lax shock condition which provides that characteristics flow into discontinuities. For smooth initial/boundary data and small time the interior solution remains smooth and can be depicted in the $x-t$ plane by nonintersecting straight characteristics as shown in fig. 1.

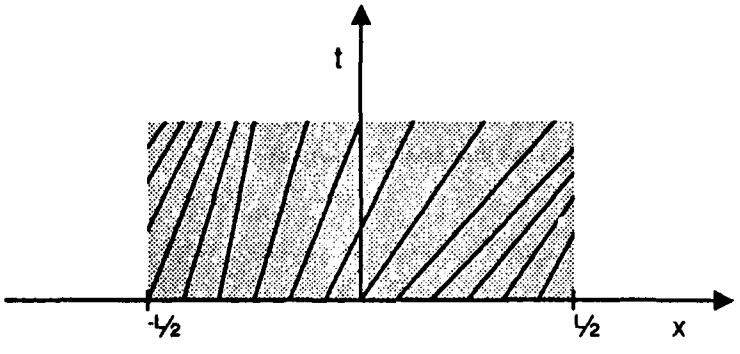

Figure 1.

In the full paper this will be shown to imply that the total variation is conserved in time and space, i.e. (assuming $f' > 0$)

$$\int_{-L/2}^{L/2} |du(x, T+\Delta t)| + \int_{T}^{T+\Delta t} |du(L/2, t)| = \int_{-L/2}^{L/2} |du(x, T)| + \int_{T}^{T+\Delta t} |du(-L/2, t)| \tag{1.1}$$

where $\int |du| = \pm \int du$ if u increasing/decreasing. This equation clearly shows the balance of inflowing and outflowing solution variation in the space-time domain. In the event that characteristics intersect, entropy increases, information is lost and the variation must decrease.

$$\int_{-L/2}^{L/2} |du(x, T+\Delta t)| + \int_{T}^{T+\Delta t} |du(L/2, t)| \leq \int_{-L/2}^{L/2} |du(x, T)| + \int_{T}^{T+\Delta t} |du(-L/2, t)| \tag{1.2}$$

Consider evaluating (1.2) on a discrete lattice of nodal values of the piecewise constant mesh function u_j^n approximating $u(x,t)$. In this notation, (j, n) denote spatial and temporal indices, $t = n\Delta t$, and $j = 0, 1, 2, 3, ..., J$. Evaluating (1.2) produces the following Stieltjes sums:

$$|u_j^{n+1} - u_j^n| + \sum_{j=1}^{J} |\Delta_{j-\frac{1}{2}} u^{n+1}| \leq |u_0^{n+1} - u_0^n| + \sum_{j=1}^{J} |\Delta_{j-\frac{1}{2}} u^n| \quad , \quad f' > 0 \tag{1.3a}$$

The solution total variation $\sum_{j=1}^{J} |\Delta_{j-\frac{1}{2}} u|$ is usually denoted by $TV(u)$ and (1.3a) is rewritten

$$|u_j^{n+1} - u_j^n| + TV(u^{n+1}) \leq |u_0^{n+1} - u_0^n| + TV(u^n) \tag{1.3b}$$

In the full paper, this equation will be shown to have the correct discrete extrema properties and provides a criteria for constructing discrete boundary schemes. For simplicity, in the next section stability will be demonstrated for the left quarter plane problem ($f' > 0$). This avoids complications present due to the possibility of extrema introduced because of time varying inflow conditions which will be considered in the full paper.

Stability Considerations. If an interior scheme and boundary condition valid in the left quarter plane satisfy

$$TV(u^{N+1}) + |u_J^{N+1} - u_J^N| \leq TV(u^N) \tag{1.4}$$

then the scheme is stable in the following maximum norm

$$\|\cdot\| = \|\cdot\|_\infty + TV(\cdot) \tag{1.5}$$

The resulting norm is identical to the periodic domain result. However consistency with the conservation law is used in the periodic domain proof. This bounds the arithmetic mean value of the solution (a constant dependant on the initial data). Here we have no such estimate and the balance is more delicate. Begin by rewriting (1.4) in terms of its original variation and boundary terms

$$TV(u^{N+1}) \leq TV(u^N) - |u_J^{N+1} - u_J^N| \leq TV(u^0) - \sum_{n=0}^{N} |u_J^{n+1} - u_J^n| \tag{1.6}$$

Also note that the total variation of a function must be greater than the difference between the maximum and minimum of the function in absolute value.

$$TV(u) \geq \max_j(|u_j|) - \min_j(|u_j|) = \|u\|_\infty - \min_j(|u_j|) \tag{1.7a}$$

Combining and rearranging these two results

$$\|u^{N+1}\|_\infty \le TV(u^0) - \sum_{n=0}^{N} |u_j^{n+1} - u_j^n| + \min_j(|u_j^{N+1}|) \tag{1.7b}$$

Using some elementary equalities/inequalities, we can bound the maximum norm by the original variation and maximum norm.

$$\begin{aligned}
\|u^{N+1}\|_\infty &\le TV(u^0) - \sum_{n=0}^{N} |u_j^{n+1} - u_j^n| + \min_j(|u_j^{N+1}|) \\
&\le TV(u^0) - \sum_{n=0}^{N} |u_j^{n+1} - u_j^n| + |u_j^{N+1}| \\
&\le TV(u^0) - \sum_{n=0}^{N} |u_j^{n+1} - u_j^n| + \sum_{n=0}^{N} (|u|_j^{n+1} - |u|_j^n) + |u|_j^0 \\
&\le TV(u^0) - \sum_{n=0}^{N} |u_j^{n+1} - u_j^n| + \sum_{n=0}^{N} |u_j^{n+1} - u_j^n| + |u|_j^0 \\
&\le TV(u^0) + |u|_j^0 \le TV(u^0) + \|u^0\|_\infty
\end{aligned}$$

With some final manipulations, a uniform norm is obtained

$$\begin{aligned}
\|u^{N+1}\|_\infty + TV(u^{N+1}) &\le TV(u^0) + \|u^0\|_\infty + TV(u^{N+1}) \\
&\le 2TV(u^0) + \|u^0\|_\infty \\
&\le 2\left[TV(u^0) + \|u^0\|_\infty\right] \\
\|u^{N+1}\| &\le 2\|u^0\|
\end{aligned}$$

TVD criteria: The development of sufficient conditions for constructing numerical schemes satisfying (1.3) parallels that developed for the periodic/infinite domain case. A simple example would again be the left quarter plane problem ($f' > 0$). For fully upwind schemes, the updating procedure for outflow boundaries is trivial since the interior scheme can be applied upto and including the outflowing boundary. For upwind biased schemes, this is not true and special boundary condition procedures are required.

Consider an explicit scheme in conservative form

$$v_j^{n+1} - v_j^n + \frac{\Delta t}{\Delta x}(h_{j+\frac{1}{2}}^n - h_{j-\frac{1}{2}}^n) = 0 \tag{1.8}$$

where the numerical flux h could be a function of $(p - r + 1)$ grid points, $h = h(u_{j-r}, ..., u_j, ...u_{j+p})$. In Harten's analysis, (1.8) is put in the form

$$v_j^{n+1} = v_j^n + C_{j+\frac{1}{2}}^+ \Delta_{j+\frac{1}{2}} v^n - C_{j-\frac{1}{2}}^- \Delta_{j-\frac{1}{2}} v^n \tag{1.9}$$

and shown to be TVD if

$$C^\pm \ge 0$$

$$(1 - C^- - C^+) \ge 0$$

To illustrate the basic ideas in constructing sufficient conditions for (1.4), we consider a simple 3-point numerical boundary scheme

$$v_j^{n+1} = v_j^n - \nu_{j-\frac{1}{2}} \Delta_{j-\frac{1}{2}} v^n + \nu_{j-\frac{3}{2}} \Delta_{j-\frac{3}{2}} v^n \tag{1.10}$$

This equation could represent a fully upwind form of (1.9) as well as various forms of space-time extrapolations depending on the choice of coefficients. Equation (1.10) is rewritten in the form

$$v_j^{n+1} = v_j^n - \nu_{j-\frac{1}{2}}\left(1 - \frac{\nu_{j-\frac{1}{2}}\Delta_{j-\frac{1}{2}}v^n}{\nu_{j-\frac{1}{2}}\Delta_{j-\frac{1}{2}}v^n}\right)\Delta_{j-\frac{1}{2}}v^n = v_j^n - D^-_{j-\frac{1}{2}}\Delta_{j-\frac{1}{2}}v^n \tag{1.11}$$

To find sufficient conditions for satisfying (1.4), we follow the technique used in the periodic/infinite domain case. First construct an interior equation for the evolution of spatial increments in v.

$$\Delta_{j-\frac{1}{2}}v^{n+1} = C^+_{j+\frac{1}{2}}\Delta_{j+\frac{1}{2}}v^n + (1 - C^- - C^+)_{j-\frac{1}{2}}\Delta_{j-\frac{1}{2}}v^n + C^-_{j-\frac{1}{2}}\Delta_{j-\frac{1}{2}}v^n \tag{1.12a}$$

with boundary equation

$$\Delta_{J-\frac{1}{2}}v^{n+1} = (1 - C^+ - D^-)_{J-\frac{1}{2}}\Delta_{J-\frac{1}{2}}v^n + C^-_{J-\frac{1}{2}}\Delta_{J-\frac{1}{2}}v^n \tag{1.12b}$$

Summing over the domain, applying the triangle inequality and requiring the coefficients of (1.12a-b) to be positive, we obtain

$$TV(u^{n+1}) + D^-_{J-\frac{1}{2}}|\Delta_{J-\frac{1}{2}}v^n| \le TV(u^n) \tag{1.13}$$

subject to

$$C^{\pm}_{j-\frac{1}{2}} \ge 0, \quad (1 - C^+ - C^-)_{j-\frac{1}{2}} \ge 0 \text{ for } j \ne J$$

and

$$(1 - C^+ - D^-)_{J-\frac{1}{2}} \ge 0$$

Imposing the additional condition that $D^-_{J-\frac{1}{2}} \ge 0$, we have from (1.11)

$$|v_j^{n+1} - v_j^n| = D^-_{J-\frac{1}{2}}|\Delta_{J-\frac{1}{2}}v^n|$$

and equation (1.4) is satisfied

$$TV(v^{n+1}) + |v_j^{n+1} - v_j^n| \le TV(v^n)$$

which is the desired result.

The full paper will expand on these topics and discuss the construction of numerical schemes with slope limiters.

References:

(1) Harten, A.: *High Resolution Schemes for Hyperbolic Conservation Laws*, J. Comput. Phys., 49 (1983),357-393.

(2) Harten, A.: *On a Class of High Resolution Total - Variation - Stable Finite - Difference - Schemes*, SIAM J. Numer. Anal., 21 (1984),1-22.

(3) Osher, S.; and Chakravarthy, S.: *Very High Order Accurate TVD Schemes*, ICASE Report 84-44, September 1984.

(4) Jameson, A. and Lax, P.: *Conditions for the Construction of Multi-Point Total Variation Diminishing Difference Schemes*, ICASE Report 178076, March 1986.

(5) Lax, P.: *Hyperbolic Systems of Conservation Laws and the Mathematical Theory of Shock Waves*, SIAM Regional Conf. Ser. Appl. Math., No. 11, Soc. Indust. Appl. Math, Philadelphia,Pa., 1973.

B

An "Optimal" Explicit Second-Order Scheme Joined to a Family of Flux-Splitting Applications to Steady and Unsteady Transonic Flows

Germain Billet

Office National d'Etudes et de Recherches Aérospatiales
29, Avenue de la Division Leclerc
92320 Chatillon Sous Bagneux

The recent appearance of the flux-splitting method [1] [2] used in solving the hyperbolic system of conservation laws $U_t + F(u)_x = 0$ has permitted the setting up of a class of flux-splitting explicit second-order finite difference $\mathcal{J}_{FS}$ schemes that depends on the single parameter α. These schemes are stable up to $CFL = 2$. The equivalent third-order system (ETOS) of this family has been obtained and the "optimal" value of α ($\alpha = 2.5$), that minimizes the amplitude of the peaks of the numerical solution near the shock, has been determined by using the numerical tests of shock-tube flow and moving shock in 1-D space [3]. The STEGER-WARMING splitting allows one to study the ETOS such as the ETOS associated with upwing schemes $\mathcal{J}_U$ and downwind schemes $\mathcal{J}_D$ defined in [4]. This study shows that the scheme $\mathcal{J}_{FS}$ with $\alpha = 2.5$ (noted $\mathcal{J}_{FS}{}^{OPT}$) is in fact more dissipative than with $\alpha = 1$ in the case of a compression wave or a shock. The scheme $\mathcal{J}_{FS}$ with this last value corresponds to the STEGER-WARMING scheme used in [1]. When van LEER flux splitting is used, the study of the ETOS appears more difficult because the jacobian matrices associated with the total flux and the partial fluxes have not the same eigenvalues and in this case the method taken into account above cannot be applied. Nevertheless, the ETOS has been studied for the one-dimensional isothermal flow and some interesting results concerning the dispersive and dissipative properties of $\mathcal{J}_{FS}$ schemes were brought to light.

In this paper, the $\mathcal{J}_{FS}$ schemes are joined to a family of flux-splitting. The partial fluxes F^+ and F^- of this family are defined by the following two essential conditions:

(a) $F = F^+ + F^-$

(b) All eigenvalues of dF^+/dU must be ≥ 0
All eigenvalues of dF^-/dU must be ≤ 0

and by four other conditions that define the class of flux-splitting that depends on the single parameter ε:

(c) F^+ and F^- must be continous
with $F^+ = F$ for the Mach number $M \geq 1$
$F^- = F$ for the Mach number $M \leq -1$

(d) $\frac{dF^\pm}{dU}$ must be continous everywhere only for $M = 0$ where it can be discontinous

(e) $\frac{dF^\pm}{dU}$ must have one eigenvalue that vanishes for $|M| < 1$

(f) $F^\pm$ must be a polynomial in M with the lowest possible degree.

Some van LEER conditions are taken up again (see [2]) and some other conditions are rewritten. In particular, we no longer suppose that $dF^\pm/dU$ must be continous for $M = 0$

or that all components of F^+ and F^- must mimic the symmetry of the components of F with respect to M. Van LEER has already shown the merit of the continuity of $dF^{\pm}/dU$ for $M = \pm 1$ at many times. But when the Mach number becomes small (≤ 0.5), van LEER splitting does not always represent the "optimal" decomposition. Respecting these conditions, we have sought to define the flux splitting with the greatest number of worthwhile properties (in particular near the sonic point) and which also gives a better representation of the numerical solution than van LEER or STEGER and WARMING splitting when the Mach number vanishes. To satisfy the conditions (a), (c), (d), (e) and (f), we have retained the following decomposition when the one-dimensional Euler equations are considered:

when $0 \leq M \leq 1$

$$(1)\ \begin{cases} F_1^- = -\frac{\rho c}{4}(1+\varepsilon)(M-1)^2 \\ F_2^- = -\frac{c}{\gamma}F_1^-[2-(\gamma-1)M] \\ F_3^- = \frac{\gamma^2}{2(\gamma^2-1)}\frac{F_2^{-2}}{F_1^-} \end{cases} \qquad (1')\ \begin{cases} F_1^+ = F_1 - F_1^- = \rho cM - F_1^- \\ F_2^+ = F_2 - F_2^- = \rho c^2(M^2+\frac{1}{\gamma}) - F_2^- \\ F_3^+ = F_3 - F_3^- = \frac{\rho c^3 M}{2(\gamma-1)}[2+(\gamma-1)M^2] - F_3^- \end{cases}$$

when $-1 \leq M \leq 0$

$$(2)\ \begin{cases} F_1^+ = \frac{\rho c}{4}(1+\varepsilon)(M+1)^2 \\ F_2^+ = \frac{c}{\gamma}\frac{(1-\varepsilon)}{(1+\varepsilon)}F_1^+[2-(\gamma-1)M] \\ F_3^+ = \frac{\gamma^2}{2(\gamma^2-1)}\left(\frac{1+\varepsilon}{1-\varepsilon}\right)^2\frac{F_2^{+2}}{F_1^+} \end{cases} \qquad \text{and} \quad F_i^- = F_i - F_i^+ \quad (i=1,2,3).$$

In these expressions, c, ρ and γ represent the sound speed, the density and the specific heat-ratio. It is difficult to show that the condition (b) is respected for the Euler equations because of the complexity of the calculations. Nevertheless, in the case of the isothermal flow ($\gamma = 1$), it is possible to demonstrate that this condition is respected for $0 \leq \varepsilon \leq 5/3$. It is thought that this result can be extended to the case $\gamma = 1.4$. When $\varepsilon = 0$, the parametric flux splitting degenerates to van LEER splitting. The evolution of the eigenvalues is drawn on fig. 1 for $\gamma = 1$ and $\varepsilon = 0.2$. The figures 2, 3 and 4 show the evolution of the components of F, F^+ and F^- with STEGER-WARMING and van LEER decompositions and with the parametric splitting ($\varepsilon = 0.2$).

It is relatively rare to have a Mach number that reaches the values -1 and 1 in a flow. Generally, we have a main flow where $0 \leq M \leq M_{sup}$ (M_{sup} can be greater than 1) with or without some secondary flows where the Mach number is limited in the lower values by M_{inf} such as $-1 < M_{inf}$. So, in a great number of applications, it is not useful to impose the condition of continuity of $dF^{\pm}/dU$ for $M = -1$. We can replace it by a condition of continuity of the same functions at $M = 0$ (in this case $dF^{\pm}/dU$ will be continous everywhere). We have carried out that by using only the flux splitting (1) (1') for $M_{inf} \leq M \leq 1$. The retained decomposition (1) (1') for the problems presented below must verify the following conditions:

for $M_{inf} \leq M < \infty$

(a') $F = F^+ + F^-$

(b') All eigenvalues of dF^+/dU must be ≥ 0
All eigenvalues of dF^-/dU must be ≤ 0

(c') F^+ and F^- must be continous
with $F^+ = F$ for the Mach number $M \geq 1$

(d') $dF^{\pm}/dU$ must be continuous everywhere

(e') $dF^{\pm}/dU$ must have one eigenvalue that vanishes for $M < 1$

(f') $F^{\pm}$ must be a polynomial in M with the lowest possible degree.

The new decomposition (1) (1') has been applied to shock-tube problem and compared with other methods:

$\alpha = 1, \quad \epsilon = 0$ (STEGER WARMING scheme with van LEER splitting)
$\alpha = 2.5, \quad \epsilon = 0$ ($\mathcal{J}_{FS}^{opt}$ scheme with van LEER splitting)
$\alpha = 2.5, \quad \epsilon = 0.3$ ($CFL = 1$)
or $\quad \epsilon = 0.2$ ($CFL = 1.6$) ($\mathcal{J}_{FS}^{opt}$ scheme with parametric splitting).

The pressure ratio that is equal to 13.5 makes it possible to have a Mach number varying between 0 and 1.14 and thus to test the new method in the case of a supersonic zone included in subsonic zones with different acoustic phenomena (expansion wave, contact discontinuity and shock wave). The figures 5 and 6 present the evolution of the pressure and the Mach number with respectively $CFL = 1$ and $CFL = 1.6$. The comparison between the fig. 5a and 5b of fig. 6a and 6b shows that the $\mathcal{J}_{FS}^{opt}$ scheme reduced the spikes at the shock appreciably. The solution is still improved when $\epsilon = 0.3$ ($CFL = 1$) or $\epsilon = 0.2$ ($CFL = 1.6$), especially in the region where the Mach number is weak (in front of the expansion wave and the shock) (see figs. 5c and 6c). The flux splitting method creates a discontinuity in the expansion wave at the sonic point. This phenomenon does not appear in the contact discontinuity that is spread out on five points.

We have also studied the shock-tube problem with a pressure ratio equal to 2.8 [5]. This case permits to have a contact discontinuity that moves more slowly and a Mach number that remains relatively weak ($0 \leq M \leq 0.4$). The numerical solution is presented in fig. 1 with $CFL = 1$. like in the previous problem, on one hand the solution is improved near the shock when $\alpha = 2.5$ (figs. 7a and 7b) because the scheme $\mathcal{J}_{FS}$ is more dissipative with this value. But on the other hand the solution of the expansion wave is lightly damaged for the opposite reason: when we adapt the value of α to have a more dissipative scheme for $u_x \leq 0$, automatically the scheme becomes more antidissipative when $u_x \geq 0$. In the present case, we solve this problem by using the couple of parameters (α, ϵ). The value of the first parameter α is adjusted to have a good solution when $u_x \leq 0$ (shock or compression wave) and the second parameter ϵ permits to have a correct representation of the expansion wave (fig. 7c). The contact discontinuity is not affected by the different treatments and spreads out on five points.

The conjoining of $\mathcal{J}_{FS}^{opt}$ scheme with parametric flux-splitting has been applied to 2-D flows too. A 2-D steady flow inside a nozzle has been studied and the result obtained with different values of ϵ are compared. Like in [6], some problems appear near the wall with $\epsilon = 0$, in particular strong oscillations of the numerical solution arise on the wall and the computation diverges rapidly. This is probably due to the strong gradient of the partial fluxes near the wall that are in this instance, sensitive to the different numerical treatments applied to the boundary mesh point and the following mesh points close to the wall. If the value of ϵ is adjusted so that the gradients become weaker, these problems are eliminated and the numerical solution becomes correct (fig. 8). This computation was realized for

$CFL = 2$, with a grid of 131 points over 21 points, and without artificial vscosity since the present method does not require the adjunction of such treatment. A 2-D flow past a biconvex profile in a channel with unsteady inlet conditions (sinusoidal pulsation of total pressure and total enthalpy) has been also studied. A movie has been made. This example makes it possible to see that this method is capable of understanding complex acoustic phenomena.

References

[1] Steger J.L. and Warming R.F., "Flux vector splitting of the inviscid gasdynamics equations with applications to finite difference methods". J. Comp. Phys. Vol 40, 1981, pp. 263–293.

[2] Van Leer B., "Flux vector splitting for the Euler equations". Von Karman Institute, Rhodes Saint Genèse, 1983.

[3] Billet G., "A class of flux-splitting explicit second-order finite difference schemes and application to inviscid gasdynamic equations". Eng. Comput. 1986 Vol 3, pp 312–316.

[4] Laval P. and Billet G., "Recent developments in finite difference methods for the computation of transient flows". In numerical methods for transient and coupled problems. Chapter 5, John Wiley and Sons Ltd, 1987.

[5] Lerat A. and Peyret R., "Propriétés dispersives et dissipatives d' une classe de schémas aux différences pour les systèmes hyperboliques non linéaires". La Recherche Aérospatiale n° 1975–2, p 61–79.

[6] Marx Y., "Etudes d'Algorithmes pour les équations de Navier-Stokes Compressible". thèse de Doctorat de l'Université de Nantes, Juillet 1987.

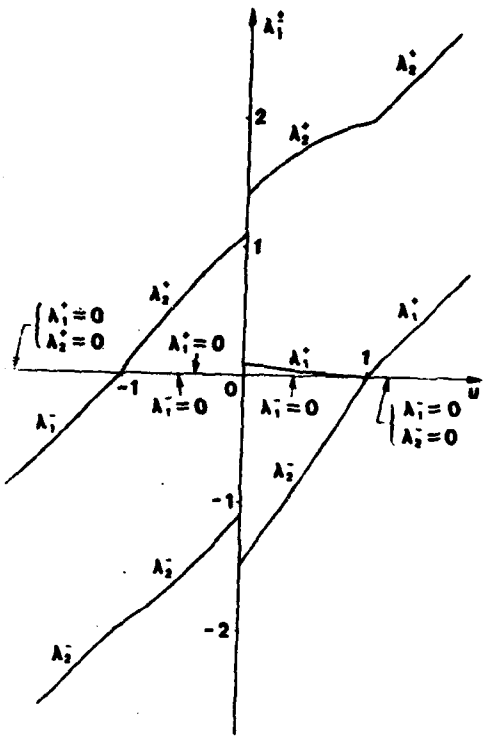

Fig. 1 - Eigenvalues of partial flux derivatives $\gamma = 1$
$\epsilon = 0,2$

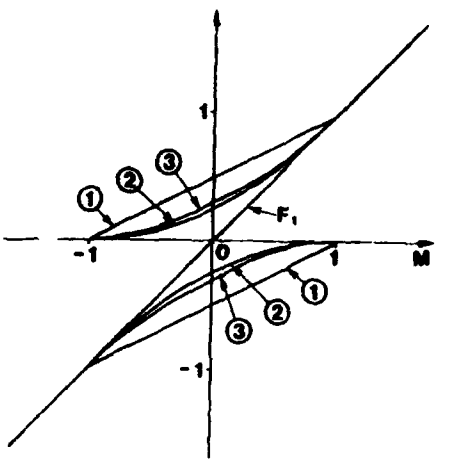

Fig. 2 - Evolution of F_1^+ and F_1^-
(1) Steger-Warming
(2) van LEER
(3) flux-splitting with parametrization ($\epsilon = 0,2$)

Fig. 3 - Evolution of F_2^+ and F_2^-
(1) van LEER
(2) with parametrization ($\epsilon = 0,2$)

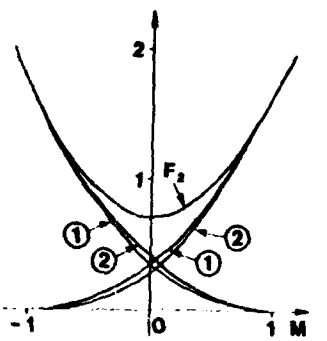

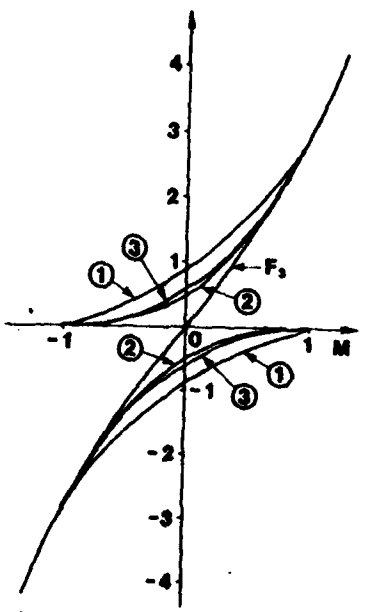

Fig. 4 - Evolution of F_3^+ and F_3^-
(1) Steger Warming
(2) van LEER
(3) with parametrization $\epsilon = 0,2$

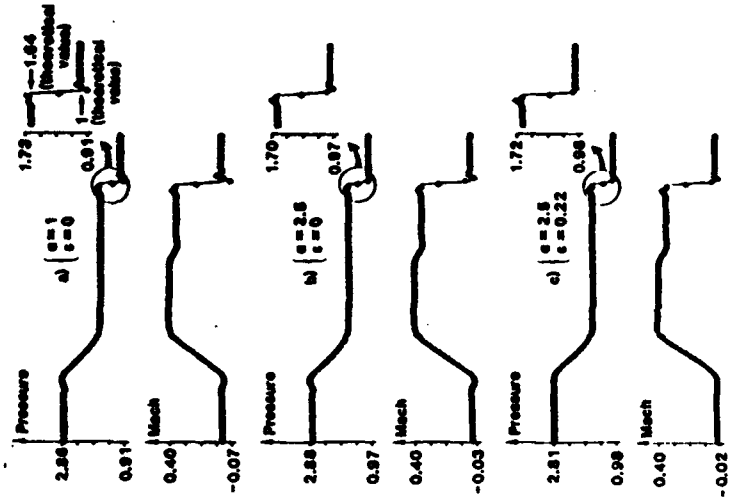

Fig. 4 - Shock tube problem $\Delta p = 13.5$ CFL = 1

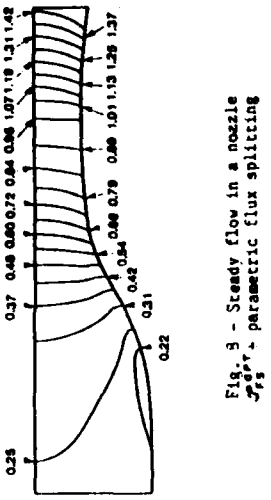

Fig. 3 - Steady flow in a nozzle
parametric flux splitting

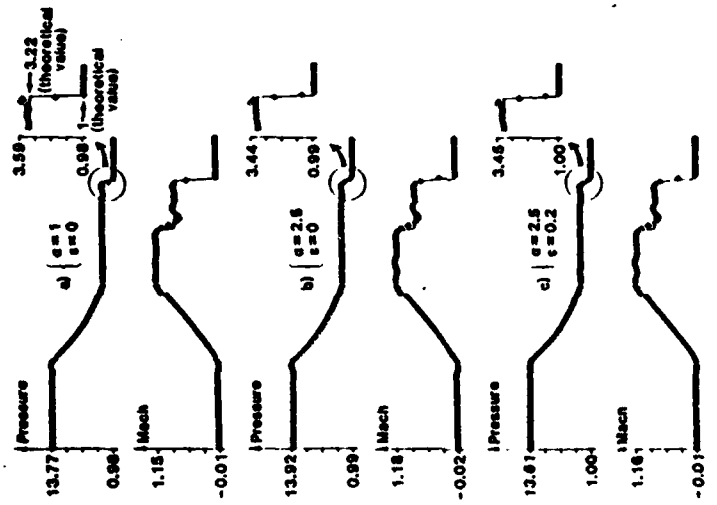

Fig. 6 - Shock tube problem $\Delta p = 13.5$ CFL = 1.6

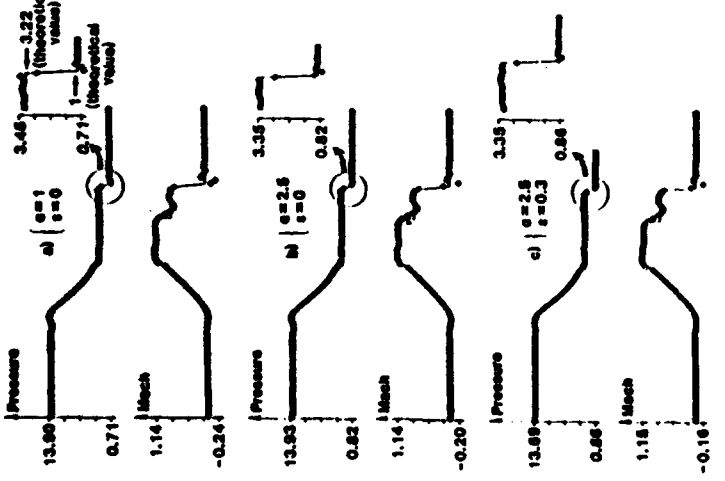

Fig. 5 - Shock tube problem $\Delta p = 13.5$ CFL = 1

Compution of Inviscid Vortical Flows in Piston Engines

B. Binninger, H. Henke, D. Hänel

Aerodynamisches Institut, RWTH Aachen

Two- and three-dimensional vortical flow in a cylinder of a piston engine is investigated by means of a finite-difference solution of the Euler equations.

The flow in a cylinder of a piston engine is characterized by complex vortical structures of large and small scales, resulting in turbulent behaviour in the shear layers. Therefore all the attempts to predict such flows have to rely on simplifying assumptions. A survey of such investigations is recently given by Heywood /1/.

In the present investigation interest is focused on the formation and development of large-scale vortices during the intake and compression stroke. The vortex structures are either generated by the jet-like flow when the air enters the cylinder, or by the shape of the piston. As far as the formation of the large vortices are concerned friction can be neglected and a description of the flow can be given by the Euler equations for compressible, time-dependent flow.

For the solution, the Euler equations are formulated for contour-fitted curvilinear, time-dependent coordinates

$$\xi = \xi(x,y,z,t), \quad \eta = \eta(x,y,z,t), \quad \zeta = \zeta(x,y,z,t), \quad \tau = t.$$

The equations then read

$$\bar{U}_\tau + \bar{F}_\xi + \bar{G}_\eta + \bar{H}_\zeta = 0.$$

In order to be able to compare with flow visualization studies through Mach-Zehnder interferometry and similar techniques, calculations were performed for

plane flow. Furthermore the investigations include axisymmetric and more recently three dimensional flows.

Spatial discretization was carried out with central differences. Artificial damping was introduced to suppress the high-frequency error components. The central differencing was chosen, because it seems to be better suited for the present low Mach number flows, than an upwind scheme as used in /2/. The Mach number is of the order of 0.1.

For the integration in time two time-consistent solution methods are used, namely the implicit factorized scheme of Beam and Warming /3/ with first order accuracy in time, and the explicit five-step Runge-Kutta scheme with second order accuracy in time for nonlinear equations /4/.

The difference of the two solutions will be discussed in the paper. Numerical experiments carried out in the frame of this investigation show the behaviour of the solution in the vicinity of tangential discontinuities which, as a part of the flow problem, are formed by the incoming jet flow during the early phase of the intake stroke.

The spatial and temporal development of the vortices in the cylinder as obtained by the solution will be demonstrated for the intake stroke and the compression stroke for several conditions.

The computational results are compared with experimental results obtained from Mach-Zehnder interferometry. Figure 1 shows computed lines of constant density with the corresponding interferograms for plane flow at different crank angles.

/1/ J. B. Heywood: Fluid Motion Within the Cylinder of Internal Combustion Engines - The Freeman Scholar Lecture, Journal of Fluids Engineering, March 1987, Vol. 109/3.

/2/ W. Schröder, D. Hänel: An Unfactored Implicit Scheme with Multigrid Acceleration for the Solution of the Navier-Stokes Equations, Computers & Fluids, Vol. 15, No. 3, pp. 313-336, 1987.

/3/ R. Beam, R. F. Warming: An Implicit Finite-Difference Algorithm for Hyperbolic Systems in Conservation-Law-Form, Journal of Comp. Physics, Sept. 1976, Vol. 22, pp. 87-110.

/4/ A. Jameson, W. Schmidt, E. Turkel: Numerical Solution of the Euler Equations by Finite Volume Methods Using Runge-Kutta Time-Stepping Schemes, AIAA-Paper 81-1259, 1981.

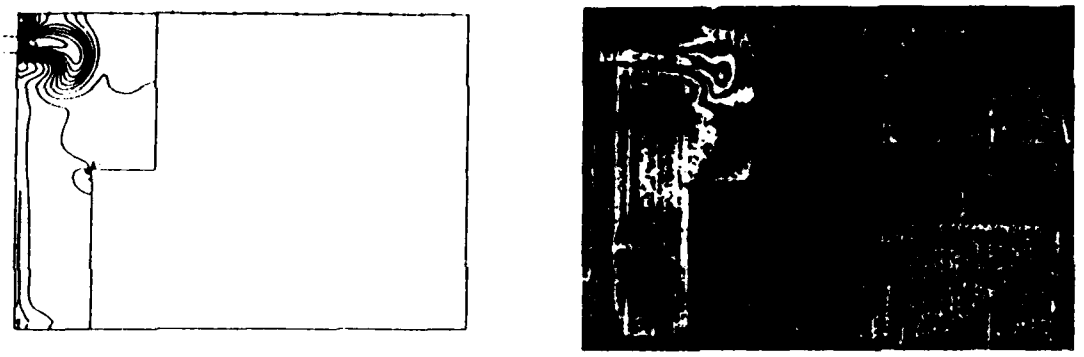

26^{o} crank angle

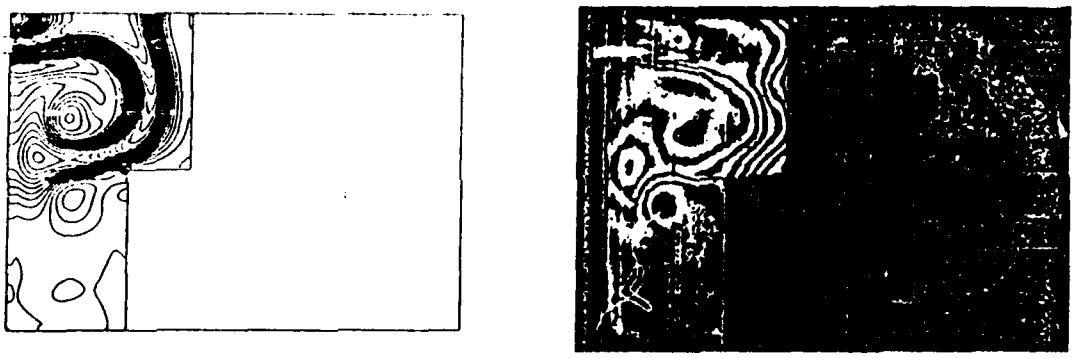

52^{o} crank angle

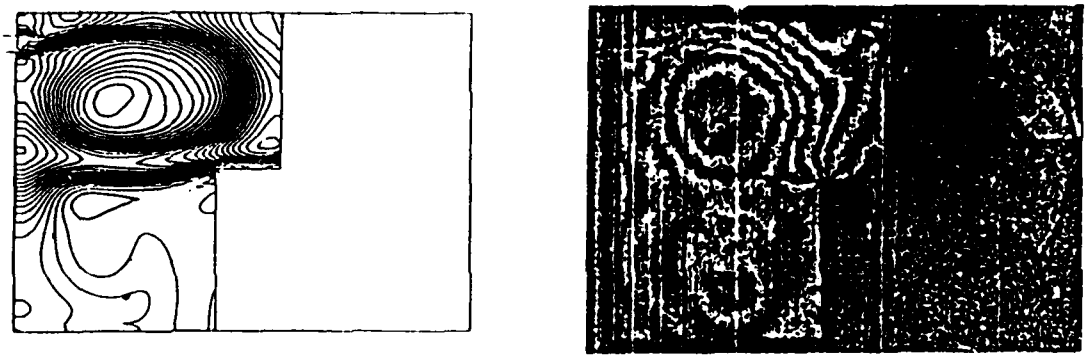

84^{o} crank angle

Fig. 1. Comparison of computed vortex pattern with experimental results obtained in the compressible flow of a two-dimensional model of a piston engine.

COMPUTATION OF AXISYMMETRIC WAVE PROCESSES IN VISCOPLASTIC SOLIDS WITH CURVED BOUNDARIES

C.D.Bisbos
Lehr- und Forschungsgebiet Mechanik,Templergraben 64
R.W.T.H. Aachen, D-51 Aachen, FRG

Some metals of technical interest, exhibiting nonlinear behaviour, can be modelled through an elasic/viscoplastic material law, within the small deformation theory, as the laws of PERZYNA(/1/,/2/) and BODNER-PARTOM (/3/,/4/) on the basis of the von MISES hypothesis.This paper presents a computational method for the numerical integration of the semilinear hyperbolic system of partial differential equations, which governs the propagation of axisymmetric acceleration waves in these materials (three independent variables :two space variables r,z and the time t).
The presented technique is based on the method of bicharacteristics and includes weigthed finite difference schemes for the various point types to treat irregular meshes (Fig.1). At every time step are imposed two boundary conditions as functions of the arc length of the boundary curve (Fig.2). The derivatives of these functions with respect to the arc length can be considered as given data of the problem. Through differentiation of the equations, connecting the boundary tractions(resp. velocities) with the stress tensor (resp.the velocity components along the coordinate axes),two new equations for the boundary schemes are obtained.This way the boundary curvature x is directly incorporated in the solution.FÖRSTER has proposed a similar idea for hyperbolic flow problems(/5/).

Denoting by v_i the velocities, by $\sigma_{ij},\varepsilon_{ij}$ the stress and strain tensor and by s_{ij},e_{ij} the related deviators we have the following system of partial differential equations :

$$\begin{aligned}
\rho\dot{v}_r - \sigma_{rr,r} - \sigma_{rz,z} - (\sigma_{rr} - \sigma_{ww})/r &= 0\\
\rho\dot{v}_z - \sigma_{rz,r} - \sigma_{zz,z} - \sigma_{rz}/r &= 0\\
\sigma_{kk} - (2\mu+3\lambda)\varepsilon_{kk} &= 0\\
(1/2\mu)\dot{s}_{ij} - \dot{e}_{ij} - (\gamma/2)F(J_2)s_{ij} &= 0
\end{aligned}$$

with:

$$J_2 = (1/2)s_{ij}s_{ij}$$

$$F_1 = 1/\sqrt{J_2} \qquad F_2 = \left(\sqrt{J_2}/\sigma_v - 1\right)^n$$

$F(J_2) = F_1F_2$ for the BODNER-PARTOM material

$F(J_2) = F_1\langle F_2\rangle$ for the PERZYNA material

$\langle A\rangle = \max(A, 0)$.

$\rho, \lambda, \mu, \gamma, n, \sigma_v$ are material constants.A comma between subcripts denotes partial differentiation with respect to the following subcript variable and a dot denotes partial diffentiation with respect to time.
Using the velocity-strain compatibility relations to eliminate the strains we obtain the governing system in the form:

$$\underline{L}(\underline{u}) = \underline{A}^t \underline{u}_{,t} + \underline{A}^r \underline{u}_{,r} + \underline{A}^z \underline{u}_{,z} + \underline{b}(\underline{u}) = \underline{0}$$

with unknown functions u :

$$\underline{u}^T = \{ v_r, v_z, \sigma_{kk}/3, (\sigma_{rr}-\sigma_{zz})/2, (\sigma_{rr}-2\sigma_{ww}+\sigma_{zz})/6, \sigma_{rz} \}$$

i.e. the two velocities, the trace of the stress tensor and the components of the stress deviator. The matrices $\underline{A}^t, \underline{A}^r, \underline{A}^z$ are constant and symmetric and $\underline{A}^t$ is positive definite. Since only the last three components of $\underline{b}(\underline{u})$ are non-linear functions of the last three components of $\underline{u}$, the system is partly linear and partly nonlinear. This fact is used later in the numerical schemes to reduce the number of iterations needed. The condition of characteristic surfaces : $\Phi(r,z,t)=\text{const.}$

$$\Phi_{,t}^2(\Phi_{,t}^2 - c_p^2(\Phi_{,r}^2+\Phi_{,z}^2))(\Phi_{,t}^2 - c_t^2(\Phi_{,r}^2+\Phi_{,z}^2)) = 0$$

$$c_p^2 = (\lambda+2\mu)/\rho\,, \qquad c_p^2 = \mu/\rho$$

and the corresponding MONGE cones (/6/,/7/,/2/.Fig.3a) are derived from :

$$\det(\underline{A})=0, \qquad \underline{A} = \Phi_{,t}\underline{A}^t + \Phi_{,r}\underline{A}^r + \Phi_{,z}\underline{A}^z$$

The left eigenvectors of $\underline{A}$ yield the compatibility equations, which involve derivatives along bicharacteristics and cross-derivatives in the characteristic surface elements:

$$\underline{l}^T \underline{L}(\underline{u}) = 0, \qquad \underline{l}^T \underline{A} = \underline{0}$$

By TAYLOR expansion and integration of a) the compatibility equations along the bicharacteristics and b) the equations of motion along the pathline, difference equations of second order accuracy are obtained for computing the solution at each mesh point at time $t=t_K$ from data in the dependency region of the point at time $t_K - \Delta t$. The data on the basis perimeters of the MONGE cones are determined from corresponding second order interpolation functions over the points belonging to the convex hull of the dependency region (CFL criterion). The coefficients of the interpolation functions are obtained through a local weigthed least-squares procedure. The weight of each point is related to its mass and to its distance from a circle, whose area is equal to the middle value of the base areas of the P- and the T- cones (Fig.3b). The final finite difference system has the form:

$$\begin{bmatrix} \underline{C}_{DD} & \underline{C}_{DL} & \underline{C}_{DN} \\ \underline{C}_{LD} & \underline{C}_{LL} & \underline{C}_{LN} \\ \underline{C}_{ND} & \underline{C}_{NL} & \underline{C}_{NN}+\underline{N}(\underline{u}_N) \end{bmatrix} \begin{bmatrix} \underline{f} \\ \underline{u}_L \\ \underline{u}_N \end{bmatrix} = \underline{d} \qquad \begin{aligned} \underline{u}^T &= \{\underline{u}_L^T, \underline{u}_N^T\} \\ \underline{u}_L^T &= \{u_1, u_2, u_3\} \\ \underline{u}_N^T &= \{u_4, u_5, u_6\} \end{aligned}$$

where $\underline{f}$ collects spatial derivatives of $\underline{u}$ at time t_K, $\underline{C}_{ij}$ are constant matrices and $\underline{N}$ a 3x3 matrix nonlinearly depending on the deviator components $\underline{u}_N$. Eliminating $\underline{f}$ and separating the linear part from the nonlinear one we obtain:

$$\begin{aligned} \underline{u}_L &= \underline{h}_L + \underline{G}\underline{u}_N \qquad (\underline{G}: \text{constant matrix}) \\ \underline{H}(\underline{u}_N)\,\underline{u}_N &= \underline{h}_N \qquad (\underline{H}: \text{nonconstant matrix}) \end{aligned}$$

The last system is iteratively solved for $\underline{u}_N$ by a NEWTON-RAPHSON procedure and then the first equation yields $\underline{u}_L$. The bicharacteristics used for an inner point are shown in Fig.3.c.

For boundary points a part of the bicharacteristics set is replaced by the boundary conditions and two of the following relations, selected according to

the boundary condition type (derivatives d/ds are boundary data), for boundary tractions S_N (normal), S_T (tangential):

$$(dS_N/ds) - 2\chi S_T = 0.5(\sigma_{rr}+\sigma_{zz})_{,r}\sin\omega + 0.5(\sigma_{rr}-\sigma_{zz})_{,r}\sin\omega\cos2\omega - 0.5(\sigma_{rr}+\sigma_{zz})_{,z}\cos\omega + 0.5(\sigma_{rr}-\sigma_{zz})_{,z}\cos\omega\cos2\omega + \sigma_{rz,r}\sin\omega\sin2\omega - \sigma_{rz,z}\cos\omega\sin2\omega$$

$$(dS_T/ds) + 2\chi(S_N - 0.5(\sigma_{rr}+\sigma_{zz})) = 0.5(\sigma_{rr}-s_{zz})_{,r}\sin\omega\sin2\omega + 0.5(\sigma_{rr}-\sigma_{zz})_{,z}\cos\omega\sin2\omega + \sigma_{rz,r}\sin\omega\cos2\omega - \sigma_{rz,z}\cos\omega\cos2\omega$$

for boundary velocities V_N(normal) ,V_T (tangential) :

$$-(dV_N/ds) - \chi V_T = 0.5(v_{r,r}-v_{z,z})\sin2\omega - 0.5(v_{r,z}+v_{z,r})\cos2\omega - 0.5(v_{r,z}-v_{z,r})$$
$$-(dV_T/ds) - \chi V_N = -0.5(v_{r,z}+v_{z,r})\sin2\omega - 0.5(v_{r,r}-v_{z,z})\cos2\omega + 0.5(v_{r,r}+v_{z,z})$$

The used bicharacteristics for various boundary conditions are shown in Fig.4. It is remarkable that the number of bicharacteristics varies from 4 (pure velocity contitions) to 6 (pure traction conditions),i.e. every von NEUMANN condition requires an addittional bicharacteristic.Similar schemes are devised for corner points and for points on the axis.

Two numerical examples ,concerning solids made from mild steel and aluminium,are discussed along with some similarities of the method proposed to mixed finite element formulations.

LITERATUR

1./PERZYNA,P., Proc.Vibr.Probl.,4,(1963),281-289.

2./NOWACKI,W.K.,Stress waves in non-elastic solids.Pergamon Press,Oxford,1978.

3./BODNER,G.R.,Y.PARTOM,J.Appl.Mech.,Trans. of ASME,39,(1972),751-757.

4./ZHOU,G.Q.,H.GHONEIN,Y.CHEN,Comp.and Struct.,18,(1984),591-601.

5./FOERSTER,K.,Archiv.Mech.,32,(1980),655-661.

6./COURANT,R.,D .HILBERT,Methods of Matemathical Physics,Vol.II,Interscience Publishers,N.York,1968.

7./CLIFTON ,R.J.,Quartl.Appl.Math.,25,(1967),97-116.

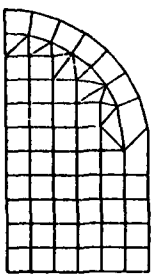

Fig.1:Axisymmetric solid with partly irregular mesh

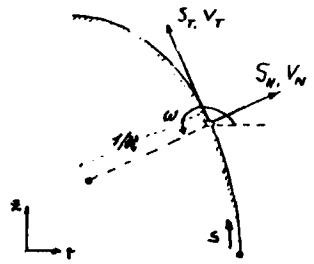

Fig.2:Conditions at the boundary:
a)boundary curve : r=r(s),z=z(s)
b)Traction conditions:$S_N=S_N(s)$,$S_T=S_T(s)$
c)Velocity conditions: $V_N=V_N(s)$,$V_T=S_T(s)$

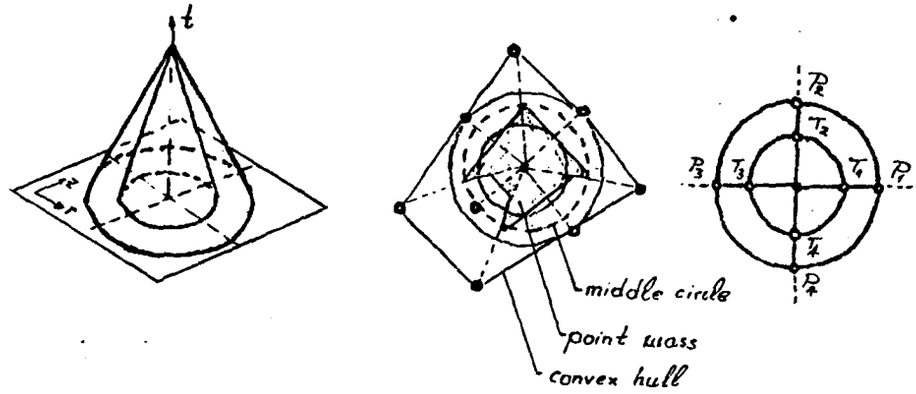

Fig.3.: a)MONGE cones
b)Convex hull of dependency region - mass weighting
c)Scheme for inner point

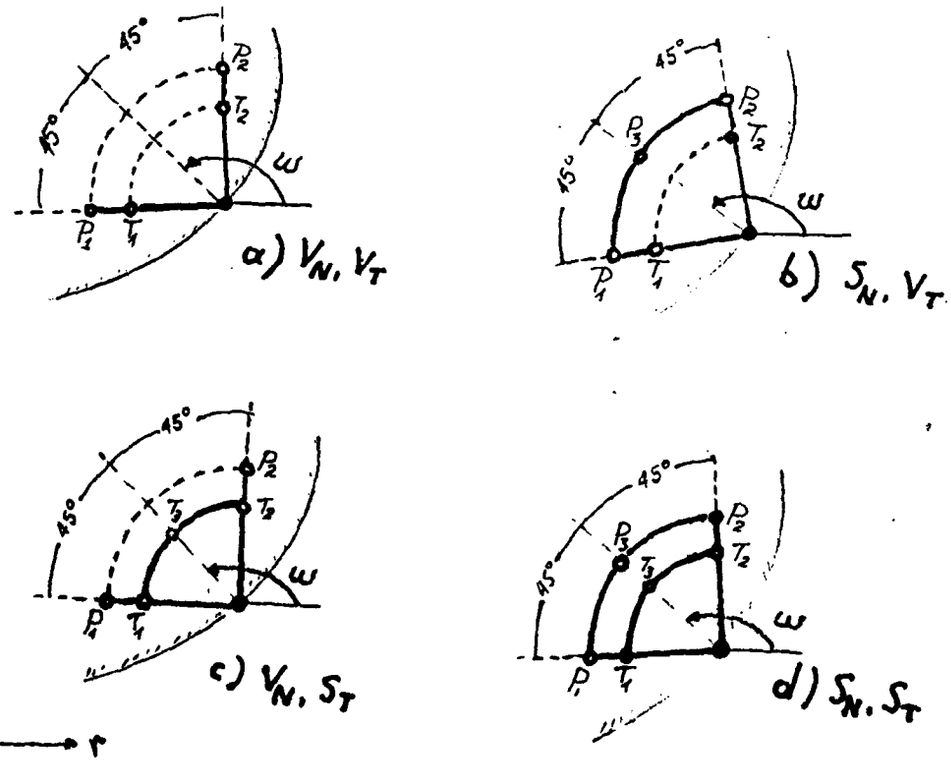

Fig.4:Used bicharacteristics for various boundary conditions

SOME QUESTIONS OF MATHEMATICAL SIMULATION IN THE PROBLEM OF SHOCK WAVE STABILITY

A. M. Blokhin
Novosibirsk
USSR

The talk is a survey of results obtained by the author ([1]) in the problem of shock wave structural stability.

In [1] this problem is interpreted as the investigation of correctness of the mixed problem for gas dynamics equations with boundary conditions on a shock wave. For a stable shock wave this problem has been set up correctly, for the unstable one it admits the construction of the incorrectness example, like the Hadamard example.

In the linear case the mixed problem is formulated as follows. For $t > 0, x > 0, |y| < \infty$ we search for the solution of acoustics system of equations

$$\begin{pmatrix} M^2 & 0 & 0 & 0 \\ 0 & M^2 & 0 & 0 \\ 0 & 0 & 1 & 0 \\ 0 & 0 & 0 & 1 \end{pmatrix} \cdot U_t + \begin{pmatrix} M^2 & 0 & 1 & 0 \\ 0 & M^2 & 0 & 0 \\ 1 & 0 & 1 & 0 \\ 0 & 0 & 0 & 1 \end{pmatrix} \cdot U_x + \begin{pmatrix} 0 & 0 & 0 & 0 \\ 0 & 0 & 1 & 0 \\ 0 & 1 & 0 & 0 \\ 0 & 0 & 0 & 0 \end{pmatrix} \cdot U_y = 0, U = \begin{pmatrix} u_1 \\ u_2 \\ u_3 \\ u_4 \end{pmatrix}, \quad (1)$$

which satisfies the following boundary conditions for $x = 0$:

$$u_1 + d \cdot u_3 = 0\,,\ u_4 + u_3 = 0\,,\ u_2 = \frac{\lambda}{\mu} \cdot F_y\,,\ F_t = \mu \cdot u_3 \quad (2)$$

and the initial data for $t = 0$:

$$U(0, x, y) = U_0(x, y)\,. \quad (3)$$

Here $M (0 < M < 1), d, \lambda, \mu$ are some constants ([1]).

Using the results of paper [2] on a plane d, λ one can single out a domain

$$K : \lambda < 0\,,\ d + M^2\lambda/\beta^2 > 0\,,\ \beta^2 = 1 - M^2\,,$$

in which exponential solutions of the mixed problem (1–3) do not increase with time. In [1] it is shown that if a point $(d, \lambda) \in K$, then the following a priori estimate

$$\|U(t)\|_{W_2^2(R_+^2)} \le C(T) \cdot \|U_0\|_{W_2^2(R_+^2)}, \qquad 0 < t \le T, \quad (4)$$
$$R_+^2 = \{(x, y) | x > 0, |y| < \infty\}$$

is valid. The existence of the a priori estimate (4) implies that the problem (1–3) is correctly set-up in the domain K which is called the domain of the shock wave stability. All estimates obtained for the problem with constant coefficients were also obtained for the case of variable coefficients. Then, by means of rather cumbersome methods the author managed to prove the local theorem of existence and uniqueness of the classical solution for quasilinear solutions of gas dynamics behind the curvilinear shock wave.

The talk discusses some problems of defining and investigation of difference schemes for gas dynamics equations. We propose to design and investigate difference schemes on the basis of the requirement of adequacy of the difference model to the initial differential problem. By adequacy we imply the following: a difference model is constructed so that by means of it one could prove the theorem of existence of a solution for the initial differential problem. Due to quasilinearity of a system of gas dynamics equations to prove the adequacy of a difference model to the initial differential problem is rather difficult. It can be done easily for the linear mixed problem(1–3).

A difference model for obtaining approximate solution of this problem is constructed so that it could admit the construction of difference analogy of the dissipative energy integral. The existence of such an analogy allows us to obtain energy estimate from which the stability of the proposed difference scheme follows. This would mean the adequacy of the difference model to the initial differential problem because in the presence of energy estimate the theorem of existence of smooth solution can be proved via standard calculations.

References

1. *Blokhin, A.M. Energy integrals and their Applications to the Problems of Gas Dynamic.– Novosibirsk, "Nauka",1986, 239 p. (In Russian).*
2. *Djakov, S.P. On shock wave stability. Z.experimental'noi i teoreticheskoi fizili, 1954, t.27, No 3/9/, 288–296. (In Russian).*

A TVD-PROJECTION METHOD FOR SOLVING IMPLICIT NUMERICAL SCHEMES FOR SCALAR CONSERVATION LAWS

A.Bourgeat* and B.Cockburn**

The stability of Newton's method applied to implicit numerical schemes for scalar conservation laws requires, in the general case, an upper bound on the size of the time steps. We introduce a simple locally defined projection , called "TVD-projection, and show how to use it to obtain an always stable extension of Newton's method.

We consider the problem of actually solving finite difference implicit schemes for the following boundary value problem

(1.1a) $\partial_t u + \partial_x f(u) = 0$ in $(0,T) \times (0,1)$,

(1.1b) $u(x=0) = b_0$ on $(0,T)$,

(1.1c) $u(x=1) = b_1$ on $(0,T)$,

(1.1d) $u(t=0) = u_0$ on $(0,1)$,

where $f \in C^1$,b_0 and $b_1 \in BV(0,T)$,and $u_0 \in BV(0,1)$. It is very well known that the main difficulty concerning the resolution of an implicit scheme is to solve at each time step the nonlinear equation defining the approximate solution. One of the most popular methods to do this ,is the Newton's method. Its quadratic convergence makes it very attractive; however ,its lack of global stability makes it useful only if a suitable initial guess can be obtained. A widely used practice is to take the approximate solution at time t^n, $u^n{}_h$,as the initial guess for the calculation of $u^{n+1}{}_h$:

$u_h^{(1)} = u_h^n$,

$u_h^{(m+1)} = \phi_h(u_h^{(m)})$ $m=1,\dots,M^n$.

---

* *Université St Etienne ,U.F.R. Sciences, 23 rue Dr P. Michelon, 42023 St Etienne Cedex 2, France*

** *IMA, University of Minnesota ,514 Vincent Hall,206 Church Street SE, Minneapolis,MN 55455,USA .*

But in this case the sufficient conditions for the convergence of this method given by the classical theorem of Kantorovich ,impose an upper bound on the time step $\Delta t^n = t^{n+1} - t^n$ .In this way ,the main advantage of using an implicit scheme is lost.

In practice, the number of inner iterations M^n is usually taken to be equal to 1, but some authors prefer to do a few inner iterations in order to improve the accuracy of the approximate solution. But it should be noted that in any case if the time step is too big the stability of the method is lost. For instance consider a problem of the form (1.1) with

$$f(u) = 20\, u^3 (20\, u^3 + (1-u)^3)^{-1} \quad ,$$

$$u_0(x) = 0 \qquad ,x \in (0,1) \quad ,$$

$$b_0(t) = 1 \qquad ,t \in (0,\ T=0.3) \quad ,$$

$$b_1(t) = 0 \qquad ,t \in (0,T=0.3) \quad ,$$

and consider the approximate solution obtained by discretising (1.1) with the implicit Godunov scheme. Then ,if we solve it with no limitation on M^n, it becomes unstable as the time step becomes greater or equal to 0.7 Δx. Note that the CFL-condition for the explicit Godunov scheme is in this case $\Delta t \leq 0.26\, \Delta x$!

Writing down the implicit Godunov's implicit scheme for (1.1) and its Newtonian iterations ,in a first section ,we stress the fact that the stability of Newton's iterations depends essentially on the size of $|f''|$ rather than the one of $|f'|$. In the case $f' > 0$ we make these statements precise by calculating explicitly the eigenvalues of the operator grad(ϕ^n_h) and the Kantorovitch convergence conditions. We then display sufficient conditions of convergence and a non-linear CFL-type condition involving only the quantity :

$$[\,\|f'\|_{L^\infty}]\,[\mathrm{disc}(\|f''\|_{L^\infty})\,] \quad ,$$

where disc(.) represents the maximum size of the discontinuities of the initial data. In particular ,it is shown that if the ratio

$$\|f\|_{L^\infty} / \|f'\|_{L^\infty}$$

is big enough the Newtonian iterations are stable .

In a second section we test numerically the stability of the Newtonian iterations in five different Riemann problems.The first three of them have a non-decreasing nonlinearity ;the last two have a non convex f , and their solution present a sonic point. Those tests allow to define a function that mesure the stability of Newtonian iterations and will serve as a reference for evaluating the performance of our proposed TVD projection method.

In the last section we introduce a new and very simple method for overcoming the Newtonian iteration difficulty. It consists in replacing the inner Newtonian iterations by the following modification

$$u_h^{(1)} = u_h^n \quad ,$$
$$u_h^{(m+1)} = P(u_h^{(m)})(\phi_h^n(u_h^{(m)})) \qquad m=1,\ldots,M^n \quad ,$$

where ϕ_h^n is the same as before,and the operator $P(v_h)$, called TVD-projection, is a locally defined projection verifying the stability property:

$$\|P(v_h)(w_h)\|_{BV} \le \|v^h\|_{BV} \quad .$$

With this new inner iterations procedure, no oscillations due to the linearization leading to the definition of ϕ_h^n appear anymore; and the method is then always $L^\infty \cap$ BV-stable regardless of the size of the time step. However the price that we have to pay for stability is a loss of total amount of mass , due to the projection $P(u^{(m)}_h)$,which is added to the loss of mass due to the standard Newtonian iterations. Nevertheless ,we

have to point out that when the step size Δt^n is small enough our method reduces to a Newtonian one. Our numerical experience indicates that this supplementary loss of mass tends to zero with the number of inner iterations and that once it becomes zero it stays equal to zero ,so that the method coincides with the Newton method after a certain number of inner iterations. Once this happens, convergence is achieved very quickly and it suffices to use a stopping criterion based on a control of the amount of mass lost by our projection .

Numerical tests, performed on the same test problems as in section 2, show that there is no more instability occuring under any time step; morover using the above stopping criterion allows a time stepping at least two orders of magnitude bigger than this one allowed by the standard Newtonian iterations.

A STABILITY ANALYSIS OF THE GLIMM ROE SCHEME

Yann Brenier
INRIA France

Let $w_t + f(w)_x = 0$ be a system of d conservation laws in one space dimension. It is assumed that, for each pair of states u, v in a neighborhood W of the origin in R^d, there exists a "Roe matrix" (see [3] for a review of this concept) A(u,v) satisfying the following requirements :

i) $A(u,v).(v-u) = f(v) - f(u)$ and $A(u,u) = f'(u)$;
ii) $A(u,v) = \sum_{k=1,m} \lambda_k(u,v)\, P_k(u,v)$

where $\lambda_1,\ldots, \lambda_m$ are its m ($m \le d$) real distinct eigenvalues of respective multiplicity $d_1,\ldots, d_m$ ($d_1+\ldots+ d_m=d$), and $P_1,\ldots, P_m$ are the corresponding eigenprojectors :
$P_k P_l = \delta_{kl} P_k$ for k,l = 1,...,m and $P_1+\ldots+ P_m$= Identity ;

iv) $\lambda_1,\ldots, \lambda_m$ and $P_1,\ldots, P_m$ are Lipschitz continuous with respect to u, v ;
v) multiplicities $d_1,\ldots, d_m$ do not depend on u and v ;
vi) the eigenvalues are globally separated :
$\lambda_k(u_1,v_1) < \lambda_{k+1}(u_2,v_2)$ for any u_1,v_1,u_2,v_2 in W and k = 1,...,m-1.

Under these assumptions (which include the case of many physical hyperbolic systems of conservation laws and *any* strictly hyperbolic system), it is shown that there exists a constant C=C(W) such that, for any initial data $w_0(x)$ of total variation no larger than C, the Cauchy problem has a global *weak* solution w(t,x), valued in W, of bounded total variation. Unfortunately, as it will be discussed below, this solution may not be physical.

The proof is based on a stability analysis of the "Glimm-Roe" scheme, that is a combination of Glimm's random choice method [1] and Roe's Riemann solver [2]. A total variation estimate is obtained in the same way as Glimm did in his famous paper. The analysis is somewhat simpler due to the extreme crudeness of Roe's approximate Riemann solver. Indeed, our estimates only need the Lipschitz continuity of the eigenprojectors, instead of the properties of the exact Riemann problem. This is why any assumption of genuine nonlinearity or linear degeneracy can be avoided.

Nevertheless, the main drawback of the method is that the so obtained weak solutions are not necessarily physical and may violate the entropy conditions because of the Roe Riemann solver ! It would be very interesting to prove the same existence result when the well known entropy modification of Roe's method [3] is used, but this has not be done so far. A different way would be to show that the non physical shocks *created* by the Glimm Roe scheme are not stable under L^1 perturbations, and therefore can be easily removed. Some results have been obtained in this direction, for the very simple case of *scalar* conservation laws. More precisely, it can be shown that the solution of the Cauchy problem is physical, provided there is no entropy violating discontinuities in the initial data, and either the flux function f is convex, or the initial condition $w_0(x)$ is monotone.

Another interest of the Glimm Roe scheme is the stability analysis of LeVeque's large time step method [4]. Indeed, in the same way as for the Godunov scheme, a large time step version of the Glimm Roe scheme can be easily designed, by "allowing waves to pass through one another with no change in strength and speed" [4]. This technique is closely related to the concept of averaged multivalued solutions [5], as well as Morton's characteristic Galerkin method [6]. In our case, it is shown that the large time step Glimm Roe scheme is total variation stable, provided the time step is limited in such a way that two waves of the *same* family cannot pass through one another. The resulting stability condition is much weaker than the usual CFL one (for which no waves of any kind are allowed to pass through one another). In the trivial case of a constant coefficient system, for example, the scheme is unconditionaly stable.

[1] J. Glimm, CPAM 18 (1965) 695.

[2] P.L. Roe, JCP 43 (1981) 357.

[3] A. Harten, P.D. Lax, B. Van Leer, SIAM Review 25 (1983) 35.

[4] R.J. LeVeque, in "Numerical methods for the Euler equations", INRIA Workshop, SIAM 1985.

[5] Y. Brenier, in "Numerical methods for the Euler equations", INRIA Workshop, SIAM 1985.

[6] P.N. Childs, K.W. Morton, Oxford University Computing Laboratory, 1986.

INRIA Rocquencourt, 78153 Le Chesnay Cedex, France

On some open questions related to MHD Riemann problem

Prof. Dr. Mosley Brio
Department of Mathematics
University of Arizona
Tucson, Arizona 85721 U.S.A.

We review briefly properties of the MHD equations as a hyperbolic system of conservation laws (derived about 30 years ago) and some recent numerical and analytical results by Brio and Wu (1985-87) which are in contrast with a popular view that the previous work makes MHD Riemann problem as well understood as, for example, similar problem in gas dynamics. In particular we show that MHD equations, due to their nonstrict hyperbolicity and nonconvexity, are much closer to some systems arising in combustion, elasticity and flow in a porous medium than they are to Euler equations of gas dynamics. We describe some techniques found to be useful for these problems, such as bifurcation from a double eigenvalue, global bifurcation, topological technique for traveling wave solutions, reductive perturbation technique, numerical methods and list open problem for stability of wave patterns, admissibility conditions, wave propagation and interaction which might be attacked by the above methods.

Qualitative Problems of Autonomous Hyperbolic Systems

M. Burnat
Warsaw University

The qualitative theory of autonomous ordinary systems

$$\frac{du}{dx} = f(u) \tag{1}$$

may be generalised is some naturale sense to hyperbolic autonomous P.D.S. of the following form

$$\sum_{i=1}^{n} A_i(u)\partial_{x_i} u = f(u) \tag{2}$$

where $A_i(u)$ are $l \times l$ matrices and solutions are mappings $u : D \subset \mathbb{R}^n \mapsto \mathbb{R}^l$ of some region D.

The basic facts for the qualitative theory of (1) are:

a. Simple available global existence theorems.
b. In order to obtain the solution of (1) it is sufficient to know its set of values $u(D)$, because one may then parametrise it simply.
c. One may obtain informations about $u(D)$ (for instance first integrals).

Because of the lack of global existence theorems for (2), the general qualitative problems for the partial differential case should be formulated as follows: 1. Assuming the global existence of the required solution u defined in some region D, construct the image $u(D)$ of the solution or at least obtain some information about it. 2. Knowing $u(D)$ ask about the parametrisation of $u(D)$ by the variables $x_1, \ldots, x_n$ giving the solution. 3. Find image manifolds $M \subset \mathbb{R}^l$ having the property, that for some infinite class of solutions we have if .

Knowing the image $u(D)$ of the solution of a given boundary problem we obtain a number of qualitative informations. Knowing how to parametrise $u(D)$ we may construct the required solution (the parametrisation may be simple or more complicate, for example it may require solutions of some nonlinear P.D.S.) or run into contradiction. In the last case we obtain a nonexistence theorem.

Our methods represent a fargoing development of those used in [1]. In the space of the matrices, we consider the planes

$$\chi(u) = \left\{ N : N = \sum_{i=1,j=1}^{n,l} A_i^{sj}(u) N_{ij} = f_s(u), \qquad s = 1, \ldots l \right\}$$

where $A_i(u) = \left(A_i^{sj}(u)\right), N = (N_{si}), f(u) = (f_1, \ldots, f_n)$. The C^1-mapping $u : D \subset \mathbb{R}^n \mapsto \mathbb{R}^l$ represents a solution of (2) if for $x \in D$:

$$Du(x) = (\partial_{x_i} u_j) = (N_{ij}) \in \chi(u(x))$$

For the manifolds $M \subset \mathbb{R}^l$ we introduce the notion of the equipment of M. This are planes $\chi'(u) \subset \chi(u)$ satisfying for $u \in M$ the following conditions

$$\dim \chi'(u) = \text{const}, \quad \text{for } N \in \chi'(u) \qquad N : \mathbb{R}^n \mapsto T_u(M) \subset \mathbb{R}^l$$

We seek for solutions

$$u : D \mapsto M, \qquad D(u(x)) \in \chi'(u(x))$$

We shall say, that the vectors $\lambda = (\lambda_1, \ldots, \lambda_n)$ and $\gamma = (\gamma_1, \ldots, \gamma_l)$ are adjoint at u, denoted $\lambda \rightharpoonup \gamma$ if $\left(\sum A_i(u)\lambda_i\right)\gamma = 0$. For the uniform hyperbolic systems ($f = 0$) we have

$$\chi^{\otimes}(u) = \left\{ N : N = \sum_{i=1}^{q} \overset{i}{\gamma} \otimes \overset{i}{\lambda}, \quad q < +\infty, \overset{i}{\gamma} \rightharpoonup \overset{i}{\lambda} \right\} = \chi(u) \tag{3}$$

(see [2]). This equality may be considered as the most general, geometric definition of the hyperbolicity. Because of (3) the image manifolds are tangent to vectors γ, what allows us the construction of this manifolds. We shall give two examples of concrete results.

EXAMPLE 1 (see [3]). Consider the hyperbolic system describing the steady plane flow of the ideal plastic material.

$$\begin{aligned}
\partial_{x_1}\sigma - 2k\,(\cos 2\vartheta\,\partial_{x_1}\vartheta + \sin 2\vartheta\,\partial_{x_2}\vartheta) &= 0 \\
\partial_{x_2}\sigma - 2k\,(\sin 2\vartheta\,\partial_{x_1}\vartheta - \cos 2\vartheta\,\partial_{x_2}\vartheta) &= 0 \\
(\partial_{x_2}v_1 + \partial_{x_1}v_2)\sin 2\vartheta + (\partial_{x_1}v_1 - \partial_{x_2}v_2)\cos 2\vartheta &= 0 \\
\partial_{x_1}v_1 + \partial_{x_2}v_2 &= 0
\end{aligned}$$

$$u = (v_1, v_2, \vartheta, \sigma), \qquad u : D \subset \mathbb{R}^2 \mapsto \mathbb{R}^4, \qquad n = 2,\ l = 4.$$

We have two characteristic vectors and the two corresponding kinds of characteristic curves $\overset{1}{C}, \overset{2}{C}$. From (3) we deduce:

Theorem 1. All two dimensional C^1-image manifolds $M_2 : u = \Psi(\mu_1, \mu_2)$ may be constructed by solving the following linear hyperbolic system

$$\begin{aligned}
\partial_{\mu_1}v_1 + \operatorname{tg}\vartheta\,\partial_{\mu_1}v_2 &= 0 \qquad & \partial_{\mu_2}v_1 - \operatorname{ctg}\vartheta\,\partial_{\mu_2}v_2 &= 0 \\
\partial_{\mu_1}\sigma - 2k\,\partial_{\mu_1}\vartheta &= 0 \qquad & \partial_{\mu_2}\sigma + 2k\,\partial_{\mu_2}\vartheta &= 0
\end{aligned}$$

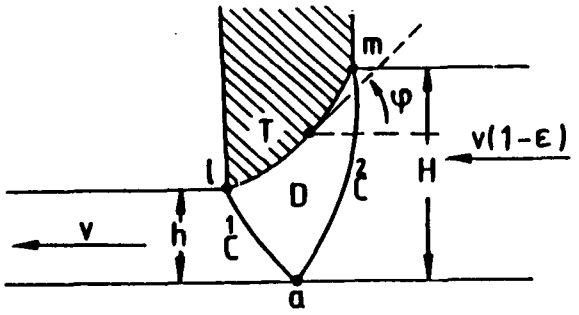

Consider the problem of drawing of a plate through the die. In the region D, which boundary consists of the curve T (the working part) and characteristic curves $\overset{1}{C}, \overset{2}{C}$, we seek for the solution satiesfying the following nonlinear boundary conditions

$$\text{on } T: \qquad v_1 \sin\varphi - v_2 \cos\varphi = 0 \qquad \varphi = \vartheta - \frac{\pi}{4}$$

$$\text{on } \overset{1}{C}: \qquad v_1 \sin\vartheta - v_2 \cos\vartheta = -V \sin\vartheta \qquad V = \text{const} > 0$$

$$\text{on } \overset{2}{C}: \qquad v_1 \cos\vartheta + v_2 \sin\vartheta = V(1-\varepsilon) \qquad \varepsilon = 1 - \frac{h}{H}$$

$$\text{in } a: \qquad \vartheta(a) = -\frac{\pi}{4}$$

We have to determine the solution and the region D knowing the curve T and numbers V, h, H. The solution may be singular in l, m. Let $Z = D \setminus \{l, m\}$ and $K(Z)$ be the class of mappings $u : Z \mapsto \mathbb{R}^4$ satiesfying the following conditions: 1. u is in Z of C^1-class with the exception of some weak discontinouities along characteristic curves.

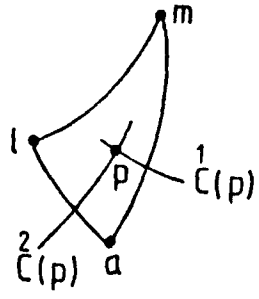

2. For $p \in D$ the characteristic curves $\overset{1}{C}(p), \overset{2}{C}(p)$ coming out of p meet the characteristic curves $(m, a), (l, a)$. Using the maximal equipments of the image manifolds $M_2 \subset \mathbb{R}^4$ we obtain, without any assumptions about the singularities at l, m the following

Theorem 2. For given $0 < \varepsilon < 1$, $V \neq 0$, there exists exactly one image manifold $M_2(\varepsilon, V)$ such that for each solution of our problem $u \in K(Z)$ and arbitrary working part $T : u(z) \subset M_2(\varepsilon, V)$. If T is given, then under assumption that the solution $u \in K(Z)$ exists, $u(Z)$ may be uniquely determined.

The uniqueness, a number of qualitative informations, and some nonexistence theorems are obtained.

Example 2. Consider the system describing the plane, non-steady isentropic gas flow.

$$\begin{aligned} &\partial_t c + v_1\, \partial_{x_1} c + v_2\, \partial_{x_2} c + kc \operatorname{div} v = 0 \\ &\partial_t v + v_1\, \partial_{x_1} v + v_2\, \partial_{x_2} v + \frac{c}{k} \operatorname{grad} c = 0 \end{aligned} \tag{4}$$

$$u = (c, v_1, v_2), \qquad u : D \subset \mathbb{R}^3 \mapsto \mathbb{R}^3, \qquad n = l = 3.$$

In the case of the one dimensional non-steady flow the conical solutions play an important role (see [4]). For the uniform hyperbolic systems (2) there often exist simple available conical solutions. Suppose that for the manifold $M_k \subset \mathbb{R}^l$, $k < n$, there exist functions $\overset{i}{\sigma}$: $M_k \mapsto \mathbb{R}^l$, $i = 1, \ldots, n-k$, $\overset{i}{\sigma}$ linearly independent, $\Pi^y(u) \subset \mathbb{R}^l$ denotes the plane including $y \in \mathbb{R}^n$, and tangent to $\operatorname{lin}\left[\overset{1}{\sigma}(u) \ldots \overset{n-k}{\sigma}(u)\right]$, so that the mapping $u_{\text{con}(x)} : D \subset \mathbb{R}^n \mapsto M_k$ given by the conditions $u_{\text{con}} = u$ for $x \in \Pi^y(u)$, $y = \text{const}$, represents in some domain D the solution. Image manifolds allowing this simple conical parametrisation we call conical image manifolds. Our problem is to find for (4) simple available conical manifolds $M_2 \subset \mathbb{R}^3$.

Using (3) we get the following answer (see [5],[6]):

$$M_2 : u = \dot{u} + \mu_1\gamma + g(\mu_2), \qquad (\mu_1, \mu_2) \in \mathbb{R}^2$$

where

$$\gamma = (\gamma_0, \gamma_1, \gamma_2) = (0, \bar{\gamma}) = \text{const}, \qquad \left(\frac{\gamma_0}{k}\right)^2 - \gamma_1^2 - \gamma_2^2 = 0$$

$$g(\mu_2) = (0, g_1(\mu_2), g_2(\mu_2)) = (0, \bar{g})$$

The functions $g_i(\mu_2)$ have to satisfy the conditions $\langle \bar{\gamma}, \dot{\bar{g}} \rangle \neq 0, \quad \dot{g}_1\ddot{g}_2 - \dot{g}_1\ddot{g}_2 \neq 0$. Assuming $\dot{g}_1 \neq 0$:

$$\sigma(u) = \left(\frac{k \left\langle \bar{\gamma}, \dot{\bar{g}} \left[g_1^{-1} \left(v_1 - \frac{\gamma_1}{\gamma_0} c \right) \right] \right\rangle}{\gamma_0 c}, \dot{g}_1 \left[g_1^{-1} \left(v_1 - \frac{\gamma_1}{\gamma_0} c \right) \right], \dot{g}_2 \left[g_1^{-1} \left(v_1 - \frac{\gamma_1}{\gamma_0} c \right) \right] \right)$$

Infinitely many other, more sofisticated conical manifolds may be constructed.

By means of our methods we may for (4) investigate the interactions of plane waves with and without shocks. For steady flows we may construct a wide new class of three dimensional nozzles, which transform one uniform flow into another one without shocks (see [7]).

References

[1] R. Courant, K.O. Friedrichs, Supersonic Flow and Shock waves. 1948.

[2] Z. Peradzyński, On Algebraic aspects of the generalised Riemann In-Variants Method. Bull. Acad. Polon. Sci. ser. Techn. 18, 4, 37–42, 1970.

[3] M. Burnat, Qualitative Problems of Autonomous Partial Differential Systems and Applications in Plasticity Theory (in russian). Din. Twerdogo Def. Tela, wyp. 6 Sib. Div. of A.Sc.USSR. Inst. of Hydrodynamics. 1984.

[4] B.L. Rozhdestvensky, N.N. Janenko, Systems of Quasilinear Equations (in russian) 1978.

[5] M. Burnat, The Conical Solutions for Quasilinear Systems, Bull. Acad. Polon. Sci. ser. Math. 24, 2, 101–105, 1976.

[6] M. Burnat, A.M. Grundland, Conical Solutions of the Autonomous Partial Differential Systems. Memorial Univ. of Newfoundland Dep. of Math. and Statistics, preprint 1987.

[7] M. Burnat, Supersonic Nozzles Without Shocks, Arch. Mech. 33, 1, 117–132, 1981.

HIGH RESOLUTION FINITE VOLUME SCHEMES AND COMPUTATIONAL AERODYNAMICS

by

D. M. Causon
Department of Mathematics and Physics
Manchester Polytechnic
Chester St
Manchester M1 5GD
U.K.

Over the past few years, substantial advances have been made in the numerical analysis of hyperbolic partial differential equations, especially those governing non-stationary gas dynamics. A popular approach is to solve numerically the time-dependent Euler equations which are of hyperbolic type. Shock waves and other discontinuities can be captured accurately without special treatment by employing a so-called "time-marching" numerical scheme. It is now possible to apply available computer codes to problems which involve complex physical phenomena including multiple shock waves, vortex sheets and combustion processes. Examples of methods in use are the flux-corrected transport (FCT) algorithms of Boris and Book (Ref. 1), the random choice method (RCM) of Chorin (Ref. 2) and Glimm (Ref. 3) and the total variation diminishing (TVD) schemes, of which Refs. 4-8 are representative. All of these methods stem, essentially, from a widespread dissatisfaction with the highly diffusive schemes of the early 1970's. These were characterised by the appearance of non-physical undershoots and overshoots around captured shock wave profiles and the need for large doses of artificial viscosity (numerical "smoothing") to ensure stability. The addition of artificial viscosity in large quantities causes a marked loss of resolution, particularly in cases where complex shock wave interactions occur.

This abstract concerns the development and application of a total variation diminishing finite volume method for computational gas dynamics. This method employs operator-splitting which enables a problem in three space dimensions to be solved by applying a sequence of one-dimensional operators. It also uses discretisation by finite volumes, rather than finite differences, in order more easily to map the complex geometries which arise in practice (Ref. 9). The classical MacCormack method is put into total variation diminishing form by appending to the right hand side of the corrector step, a specially devised artificial viscosity term. The ideas behind the design of this term import the theory of flux limiters (Refs. 4-6). Essentially, the term applies precisely the correction needed to limit overshoots or undershoots at each mesh cell. That is to say, it is a form of artificial viscosity which has a spatially varying coefficient. This is in strong contrast to the more classical methods which apply excesses of smoothing through the use of artificial viscosity terms having globally constant (and problem dependent) coefficients. Mathematically, it removes from the modified partial differential equation (the p.d.e. solved exactly by the numerical scheme) the term which is responsible for producing overshoots/undershoots. The result is a scheme which captures shock waves with high resolution and compares favourably with alternate schemes based on approximate Riemann solvers (see e.g Ref. 7), which are computationally more expensive. Clearly, the many production

codes used in industry, employing the MacCormack method, can be modified quickly and simply to yield a high resolution scheme.

Various different flux limiters can be used, some of which are more compressive than others (Ref. 10,11); or, artificial compression techniques can be applied explicitly, in conjunction with any particular limiter (Ref. 9). The paper will describe work which has been done to find the most suitable flux limiter for use within the TVD MacCormack scheme. Some results of our numerical experiments will be presented, together with results for practical applications of the method to high speed external aerodynamic flows. A sample of computed solutions are shown in Fig. 1.

References

1. Boris J P and Book D L, Flux Corrected Transport I SHASTA - A Fluid Transport Algorithm That Works, J Comp Phys v11 n38 1973.

2. Chorin A J, Random Choice Solutions of Hyperbolic Systems, J Comp Phys v22 pp517-533 1976.

3. Glimm J, Solution in the Large for Non-Linear Hyperbolic Systems of Equations, Comm Pure and Appl Math v18 pp697-715.

4. Davis S F, TVD Finite Difference Schemes and Artificial Viscosity, ICASE Report No 84-20 NASA CR 172373 1984.

5. Sweby P K, High Resolution Schemes Using Flux Limiters for Hyperbolic Conservation Laws, SIAM J Num Anal 1984.

6. Roe P L, Generalised Formulation of TVD Lax-Wendroff Schemes, ICASE Report No 84-53 NASA CR 172478 1984.

7. Harten A, High Resolution Schemes for Hyperbolic Conservation Laws J Comp Phys v49 p357 1983.

8. Causon D M and Kwong C M, Numerical Experiments With a TVD MacCormac Scheme, in Proc 6th GAMM Conf on Num Meth in Fl Mech Vieweg 1986.

9. Causon D M, Numerical Computation of External Transonic Flows, in Pro 7th GAMM Conf on Num Meth in Fl Mech Vieweg 1987.

10. Yee H C, Construction of Explicit and Implicit Symmetric TVD Scheme and Their Applications, J Comp Phys v68 pp151-179 1987.

11. Yee H C, Upwind and Symmetric Shock capturing Schemes, NASA TM 8946 1987.

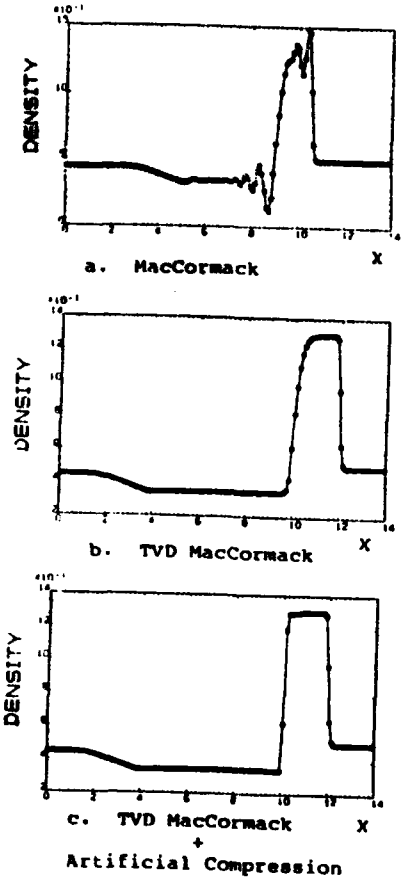

Fig. 1a 1-D RIEMANN PROBLEM

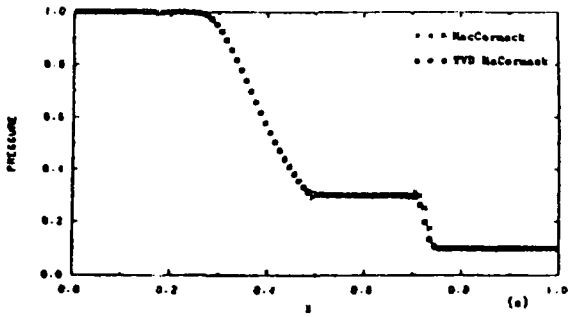

Fig. 1b 1-D shock tube solutions using M and TVDM schemes (a) Pressure and (b) Density

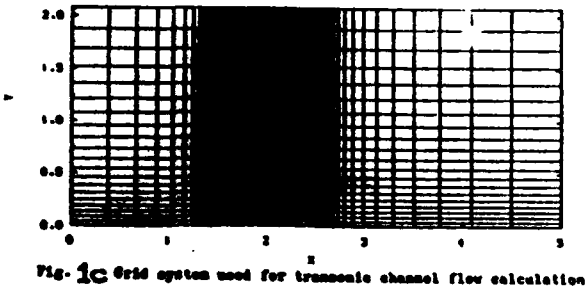

Fig. 1c Grid system used for transonic channel flow calculation

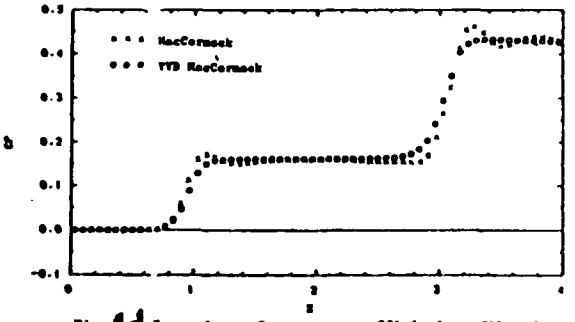

Fig. 1d Comparison of pressure coefficient profiles for shock reflection problem at y=0.5

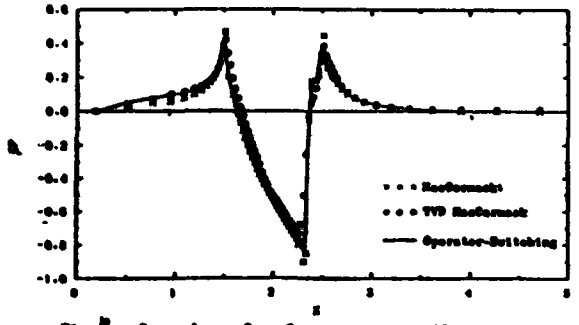

Fig. 1e Comparison of surface pressure coefficients for transonic channel flow using M, TVDM and OS schemes

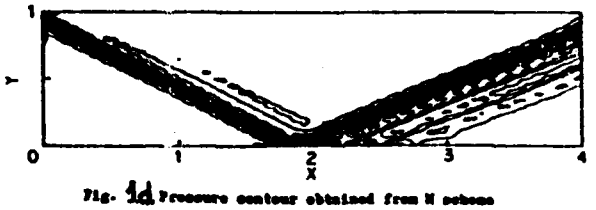

Fig. 1d Pressure contour obtained from M scheme

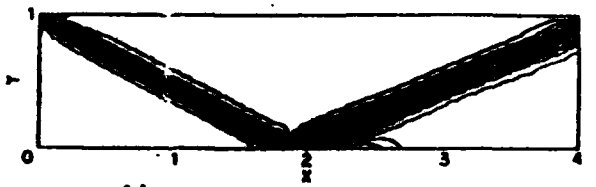

Fig. 1d Pressure contour obtained from TVDM scheme

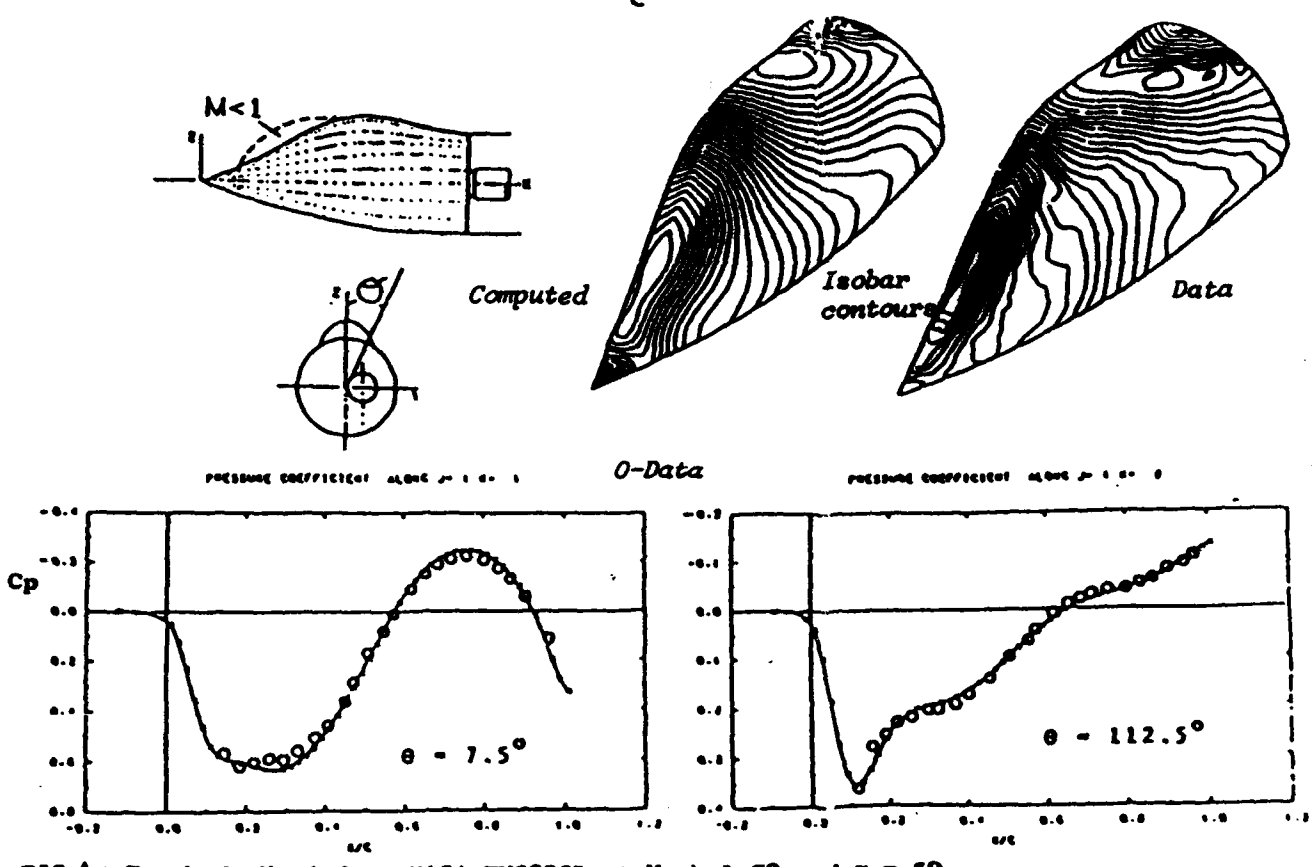

FIG 1e Forebody No 4 from NASA TM80062 at Mach 1.70 and α =-5°

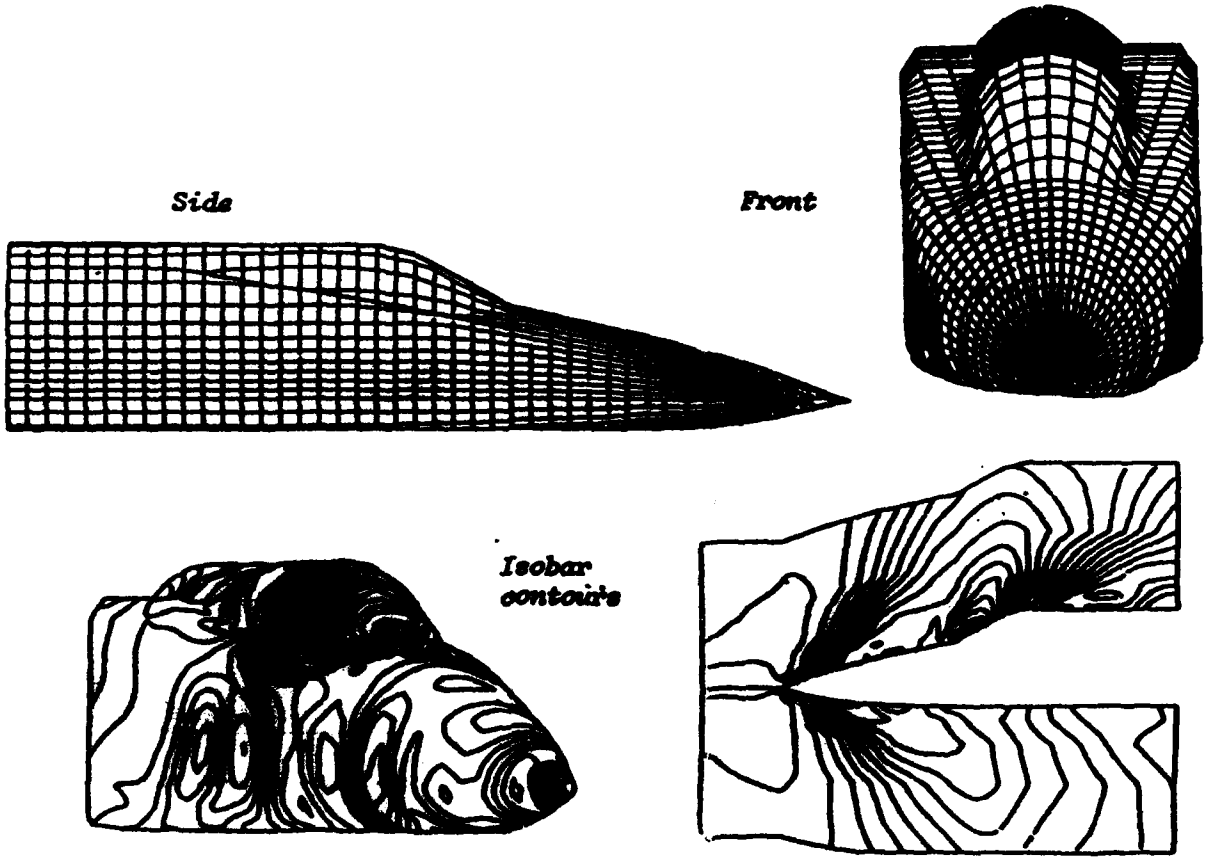

FIG 1f Realistic aircraft forebody at Mach 1.40 and α = -5°

BV discontinuous solutions of problems of the calculus of variations and of quasi linear hyperbolic differential equations

Lamberto Cesari
Department of Mathematics
University of Michigan
Ann Arbor, MI 48109, USA

1. **BV functions.** In 1936 I introduced [1] a concept of BV functions, or functions of bounded variation $f(x)$, $x = (x_1, \dots, x_\nu) \in G \subset \mathbb{R}^\nu$, $f \in L_1(G)$, $\nu \geq 1$, in a domain G of $\mathbb{R}^\nu$. I proved, among other results, that f is BV if and only if the nonparametric possibly discontinuous surface $S : z = f(x)$, $x \in G$, has finite generalized Lebesgue area $L(S)$.

Krickeberg in 1957 proved that f is BV if and only if $f \in L_1(G)$ and f has first order partial derivatives in the sense of distributions which are finite measures μ_j, $j = 1, \dots, \nu$. Thus, a BV function $f(x)$, $x = (x_1, \dots, x_\nu) \in G$, has distributional partial derivatives μ_j, $j = 1, \dots, \nu$, which are finite measures, as well as generalized partial derivatives $D^j f$ which are L_1-functions.

In 1966 Conway and Smoller considered the Cauchy problem for quasi linear hyperbolic equations (conservation laws)

$$u_x + \sum_{j=1}^{\nu} (F_j(u))_{y_j} = 0, \tag{0}$$
$$u(0, y) = w(y),$$

u scalar, $x \geq 0$, $y = (y_1, \dots, y_\nu) \in \mathbb{R}^\nu$, and other more general problems, and proved that whenever the Cauchy data are locally BV in $\mathbb{R}^\nu$, then the equation has exactly one scalar weak solution $u(x, y)$, $x \geq 0$, $y \in \mathbb{R}^\nu$, which is locally BV in $\mathbb{R}^+ \times \mathbb{R}^\nu$ and satisfies a suitable entropy condition.

2. **Calculus of variations in classes of BV functions.** In 1986 Cesari, Brandi, and Salvadori [5abc] considered integrals of the calculus of variations of the general form

$$I(u) = \int_G f_0(x, u(x), Du(x))\, dx, \tag{1}$$

$$x = (x_1, \dots, x_\nu) \in G \subset \mathbb{R}^\nu, \quad u(x) = (u_1, \dots, u_m), \quad \nu \geq 1, \quad m \geq 1,$$

and corresponding Serrin type functionals $\mathcal{J}(u)$, in classes of BV possibly discontinuous vector functions u. The Serrin functional $\mathcal{J}(u)$ is obtained as usual by taking lower limits on the values of I on AC, or $W^{1,1}(G)$ functions, process which is similar to the one with which Lebesgue area is defined. First, we obtained closure and lower closure theorems, hence theorems of lower semicontinuity in the L_1-topology, and finally existence theorems of the absolute minimum of $\mathcal{J}(u)$ in classes of BV vector functions $u(x) = (u_1, \dots, u_m)$,

$x \in G \subset \mathbb{R}^\nu$, whose total variations $V(u)$ are equibounded [5abc]. We proved also that $I(u) \leq \mathcal{J}(u)$, and that $\mathcal{J}$ is a proper extension of I in the sense that $\mathcal{J}(u) = I(u)$ for all u which are AC, or $W^{1,1}(G)$.

3.Existence of BV possibly discontinuous absolute minima for certain integrals without growth properties. Recently I considered [4a] multiple integrals of the form

$$
\begin{aligned}
&I(u) = \int_G \sum_{i=1}^{m} \Big| \sum_{j=1}^{\nu} [U_{ij}(x,u)]_{x_j} + V_i(x,u) \Big| \, dx, \\
&u(x) = (u_1, \ldots, u_m), \quad x = (x_1, \ldots, x_\nu) \in G \subset \mathbb{R}^\nu, \\
&u(x) = w(x), \quad x \in B \subset \partial G,
\end{aligned} \tag{2}
$$

and associated Serrin functionals $\mathcal{J}(u)$. I studied these integrals in classes of BV vector functions $u(x) = (u_1, \ldots, u_m)$, $x \in G$, with equibounded total variations. Here the U_{ij} are given functions of class C^1 and the V_i are given locally Lipschitzian functions. The existence theorems we mentioned in no. 2 above, and we had proved in [5c] do not apply directly to the integrals (2). However, I proved in [4a] that the same integrals $I(u)$ and $\mathcal{J}(u)$ can be transformed into integrals $H(v)$ and $\mathcal{H}(v)$ to which the existence theorems in [5c] apply. Thus, I could obtain the expected existence theorems for the absolute minimum $I(u)$ and $\mathcal{J}(u)$ for BV possibly discontinuous vector functions u, and of course $0 \leq I(u) \leq \mathcal{J}(u)$.

In [4b] and in [4c] I also studied a number of variants of the Serrin functional $\mathcal{J}(u)$ associated to the integral $I(u)$, namely, functionals $\mathcal{J}^*(u)$, $\mathcal{J}^{**}(u)$. I proved the needed properties of lower semicontinuity in the topology of L_1, and the basic relation $0 \leq I(u) \leq \mathcal{J}^{**}(u) \leq \mathcal{J}^*(u) \leq \mathcal{J}(u)$. It is clear that whenever we can prove that for the optimal solution u we have $I(u) = 0$, then u is a solution of the differential system $\sum_{j=1}^{\nu} [U_{ij}(x,u)]_{x_j} + V_i(x,u) = 0$, $i = 1, \ldots, m$, $x \in G$ (a.e.)

4. Rankin-Hugoniot type properties in terms of the calculus of variations and BV solution

For $m = 1$, $\nu = 1$, we are dealing with the original integral

$$
I(u) = \int_G |u_x + (F(u))_y| \, dx \, dy, \qquad G \subset \mathbb{R}^2 \tag{3}
$$

x, y, u, F scalars.

If u has a line $\Gamma : y = \ell(x)$, $a \leq x \leq b$, of class C^1 and of jump discontinuity, say

$$
u_2(x) = u(x, \ell(x)+), \qquad u_1(x) = u(x, \ell(x)-), \qquad a \leq x \leq b,
$$

then, under mild assumptions, the contribution of Γ on the value of the Serrin type functional $\mathcal{J}^*$ is ≥ 0, and such a contribution is zero if and only if

$$
[u_2(x) - u_1(x)] \, \ell'(x) = F(u_2(x)) - F(u_1(x)), \qquad a \leq x \leq b,
$$

along the line Γ (Cesari [4c]).

For $m = 1$, $\nu \geq 1$, we are dealing with the original integral

$$(4) \qquad I(u) = \int_G \Big| u_x + \sum_{j=1}^{\nu} (F_j(u))_{y_j} \Big| \, dx\, dy, \qquad G \subset \mathbb{R}^{\nu+1}, \quad dy = dy_1 \dots dy_\nu,$$

x, u scalar, $u(x,y) = u(x, y_1, \dots, y_\nu)$, $\quad F(u) = (F_1, \dots, F_\nu)$.

If $u(x,y)$ has a surface $\Gamma : x = L(y) = L(y_1, \dots, y_\nu)$, $y \in D$, of class C^1 and of jump discontinuity for u, say

$$u_2(y) = u(L(y)+, y), \qquad u_1(y) = u(L(y)-, y), \qquad y = (y_1, \dots, y_\nu) \in D,$$

then, under mild assumptions, the contribution of Γ on the value of the same Serrin type functional $\mathcal{J}^*$ is ≥ 0, and such a contribution is zero if and only if

$$u_2(y) - u_1(y) = \sum_{j=1}^{\nu} (L(y))_{y_j} \, [F_j(u_2(y)) - F_j(u_1(y))], \qquad y \in D,$$

on the surface Γ (Cesari [4c]).

For $m > 1$, $\nu = 1$, we are dealing with the original integral

$$(5) \qquad I(u) = \int_G \sum_{i=1}^{m} |u_{ix} + (F_i(u))_y| \, dx\, dy, \qquad G \subset \mathbb{R}^2,$$

$$x, y \text{ scalars}, \; u(x,y) = u(u_1, \dots, u_m), \quad F(u) = (F_1, \dots, F_m),$$

and in this situation we must use the Serrin type integral $\mathcal{J}^{**}$. Let us assume that for a given $i = 1, \dots, m$, the component $u_i(x,y)$ of u has a line $\Gamma : y = \ell(x)$, $\quad a \leq x \leq b$, of class C^1 and of jump discontinuity for u_i, say

$$u_{i2}(x) = u_i(x, \ell(x)+), \qquad u_{i1}(x) = u_i(x, \ell(x)-), \qquad a \leq x \leq b,$$

while the remaining components $u_h(x,y)$, $h = 1, \dots, m$, $h \neq i$, are continuous in a neighborhood of Γ. In this situation, let us take

$$u^{(i,2)}(x) = (u_i(x, \ell(x)+); u_h(x, \ell(x)), \qquad h \neq i, \quad h = 1, \dots, m),$$
$$u^{(i,1)}(x) = (u_i(x, \ell(x)-); u_h(x, \ell(x)), \qquad h \neq i, \quad h = 1, \dots, m), \quad a \leq x \leq b,$$

I proved in [4c], under mild assumptions, that the contribution of Γ on the value of the Serrin type integral $\mathcal{J}^{**}$ is ≥ 0, and such a contribution is zero if and only if

$$[u_{i2}(x) - u_{i1}(x)] \, \ell'(x) = F_i(u^{(i,2)}(x)) - F_i(u^{(i,1)}(x)), \qquad a \leq x \leq b,$$

along Γ (Cesari [4c]).

5. Existence of BV discontinuous solutions of the Cauchy problem for certain hyperbolic differential systems.

Let $m > 1$, $\nu = 1$, let $F(u) = (F_1, \dots, F_m)$ be of class C^1 in $\mathbb{R}^m$, and let the functions $w(y) = (w_1, \dots, w_m)$, $y \in \mathbb{R}$, be bounded and locally BV in $\mathbb{R}$, say $|w_i(y)| \le M$ in $\mathbb{R}$, and $V[w_i(y), -M \le y \le M] \le H$, $i = 1, \dots, m$. Let L be a Lipschitz constant for F in $[-M, M]^m$. Let R, T be arbitrary constants with $LT < R$, and let $G = [0 \le x \le T, -R + Lx \le y \le R - Lx]$. Then, there is a vector function $u(x, y) = (u_1, \dots, u_m)$, $(x, y) \in G$, with $|u_i(x, y)| \le M$, $V_y(u_i) \le HT$, $V_x(u_i) \le LHT$, satisfying

$$u_{ix} + (F_i(u))_y = 0, \qquad (x, y) \in G \text{ (a.e.)}, \qquad u(x, y) = (u_1, \dots, u_m),$$
$$u_i(0, y) = w_i(y) \text{ a.e. in } [-R, R], \qquad i = 1, \dots, m,$$

x, y scalars (Cesari and Pucci [6b]).

1. L. Cesari, Sulle funzioni a variazione limitata, Annali Scuola Norm.Sup.Pisa (2)5, 1936, 299–313.

2. L. Cesari, (a) Sulle funzioni di due variabili a variazione limitata e sulla convergenza delle serie doppie di Fourier, Rend. Sem.Mat.Univ.Roma 1, 1937, 277–294. – (b) Sulle funzioni di più variabili a variazione limitata e sulla convergenza delle relative serie multiple di Fourier, Pontificia Accad.Scienze, Commentationes 3, 1939, 171–197.

3. L. Cesari, Optimization - Theory and Applications. Problems with Ordinary Differential Equations, Springer Verlag 1983.

4. L. Cesari, (a) Existence of discontinuous absolute minima for certain multiple integrals without growth properties, Rend. Accad. Naz. Lincei, Roma, to appear. – (b) Existence of BV discontinuous absolute minima for modified multiple integrals of the calculus of variations, Atti Sem.Mat. Fis. Univ. Modena, to appear. – (c) Rankin-Hugoniot type properties in terms of the calculus of variations for BV solutions, Rend. Circolo Mat. Palermo, to appear.

5. L. Cesari, P. Brandi, and Anna Salvadori, (a) Discontinuous solutions in problems of optimization, Annali Scuola Norm.Sup.Pisa, to appear. – (b) Existence theorems concerning simple integrals of the calculus of variations for discontinuous solutions, Archive Rat.Mech.Anal. 98, 1987, 307–328. – (c) Existence theorems for multiple integrals of the calculus of variations for discontinuous solutions, Annali Matem. Pura Appl., to appear.

6. L. Cesari and Patrizia Pucci, (a) Remarks on discontinuous optimal solutions for simple integrals of the calculus of variations, Atti Sem.Mat.Fis.Univ. Modena, to appear. – (b) Existence of BV discontinuous solutions of the Cauchy problem for certain hyperbolic systems, Rend. Accad. Naz. Lincei Roma, to appear.

Convergence of the Lax-Friedrichs Scheme and Godunov Scheme for Isentropic Gas Dynamics

GUI-QIANG CHEN

Courant Institute of Mathematical Sciences, New York, USA
Institute of Systems Science of Academia Sinica, Beijing, PRC

We are concerned with the convergence of the Lax-Friedrichs scheme and Godunov scheme for the system of isentropic gas dynamics. The Cauchy problems in the Lagrangian coordinate and the Eulerian coordinate are respectively

$$\begin{cases} u_t + p(v)_x = 0, p'(v) < 0 \\ v_t - u_x = 0, \end{cases}$$

$$(u, v)|_{t=0} = (u_0(x), v_0(x)),$$

and

$$\begin{cases} \rho_t + (\rho u)_x = 0, \\ (\rho u)_t + (\rho u^2 + p(\rho))_x = 0, p'(\rho) > 0, \end{cases}$$

$$(\rho, u)|_{t=0} = (\rho_0(x), u_0(x)).$$

where $\rho_0(x), u_0(x)$ and $v_0(x)$ are bounded measurable functions. For polytropic gas, $p(v) = k^2 v^{-\gamma}$, where $\gamma > 1$ is the adiabatic exponent.

Nishida [1] established a global existence theorem with arbitrary data of bounded variation $\gamma = 1$ by using the Glimm scheme [2]. To the case $\gamma > 1$ which is of more importance, many studies have been made provided the data satisfy certain mandatory restrictions [3-6]. In 1983, DiPerna [7] established a large data existence theorem for $\gamma = 1 + \frac{2}{2m+1}, m \geq 2$ integers, by using the viscosity method and the theory of compensated compactness [8-11]. Since technical reasons, the results all were obtained provided that the initial density is away from the vacuum, namely, $\rho_0(x) \geq c_0 > 0$, or $v_0(x) \leq \frac{1}{c_0}$.

The Lax-Friedrichs scheme and Godunov scheme are finite difference schemes proposed by Lax [12] in 1954 and Godunov [13] in 1959 respectively. For scalar conservation law, Oleinik [14] and Conway and Smoller [15] proved that the Lax-Friedrichs difference approximations satisfy the Helly compactness principle and obtained the convergence of the scheme. For Cauchy problem of system of isentropic gas dynamics with the initial density containing the vacuum, it is plausible that one can't expect

to prove that the approximations, especially the Lax-Friedrichs and Godunov difference approximations, satisfy this compactness frame based on the analysis of Liu and Smoller [16]. One needs to find a new compactness frame which is satisfied by the Lax-Friedrichs and Godunov difference approximations and still ensures the existence of a subsequence converging pointwise a.e.. Recently, Ding Xia-Xi, Luo Pei Zhu and I [17-19] have found such a compactness frame satisfied by the Lax-Friedrichs and Godunov difference approximations for the Cauchy problem [3, 4] and, for $1 < \gamma \leq \frac{5}{3}$ and the initial density containing the vacuum, still ensures the existence of a subsequence converging pointwise a.e. on the basis of the work of DiPerna [7, 20] with the aid of the theory of compensated compactness [8-11]. Therefore, we obtained a global existence theorem with arbitrary data. Furthermore, we [21] have introduced a generalized Lax-Friedrichs scheme and Godunov scheme for the inhomogeneous equations of gas dynamics (with the sources) and established its convergence theorem.

References

[1] Nishida, T., Proc. Jap. Acad., 44 (1968), 642-646.

[2] Glimm, J., Comm. Pure Appl. Math., 18 (1965), 95-105.

[3] Zhang Tong and Guo Yu-Fa, Acta. Math. Sinica, 15 (1965).

[4] Ding Shia-Shi, Chang Tun, Wang Ching-hua, Hsia Ling and Li Tsai-Chung, Scientica Sinica, 16 (1973), 317-335.

[5] Nishida, T. and J. Smoller, Comm. Pure Appl. Math., 26 (1973), 183-200.

[6] Lin Longwei, Acta Scien. Nat. Jilin Univ., 1 (1978), 96-106.

[7] DiPerna, R. J., Comm. Math. Phys., 91 (1983), 1-30.

[8] Tartar, L., Compensated compactness and applications to partial differential equations. In: Research notes in mathematics, nonlinear analysis and mechanics: Heriot-Watt Symposium, Vol. 4. Knops, R.J. (ed.). New York: Pitman Press, 1979.

[9] Tartar, L., Compensated compactness method applied to systems of conservation laws. In: Systems of nonlinear partial differential equations, Ball, J.M. (ed.). NATO ASI Series, C. Reidel Publishing Co., 1983.

[10] Murat, F., Ann. Scuola Norm. Sup. Pisa 8, 69-102 (1981).

[11] Murat, F., J. Math. Pures et Appl. 60 (1981), 309-322.

[12] Lax, P., Comm. Pure Appl. Math., 7 (1954), 159-193.

[13] Godunov, S.K., Mat. Sb. 47 (89), 1959, 271-306.

[14] Oleinik, O., Usp. Mat. Nauk. (N.S.), 12, (1957), 3-73.

[15] Conway, E. and J. Smoller, Comm. Pure Appl. Math.. 19 (1966), 95-105.

[16] T.-P. Liu and J. Smoller, Adv. Appl. Math., 1 (1980), 345-359.

[17] Ding Xia-Xi, Chen Gui-Qiang and Luo Pei-Zhu, Acta Mathematica Scientia, 5 (1985), 4, 483-500, 501-540.

[18] Chen Gui-Qiang, Acta Mathematica Scientia, 6 (1986), 1, 75-120.

[19] Ding Xia-Xi, Chen Gui-Qiang and Luo Pei-Zhu, A supplement to the papers "Convergence of the Lax-Friedrichs scheme for isentropic gas dynamics (II)-(III)", Acta Mathematica Scientia, 7 (1987).

[20] DiPerna, R.J., Arch. Rat. Mech. Anal., 32 (1983), 27-70.

[21] Ding Xia-Xi, Chen Gui-Qiang and Luo Pei-Zhu, Convergence of the generalized Lax-Friedrichs scheme and Godunov scheme for isentropic gas dynamics. RR-NO. 1, 1986, Institute of Mathematical Sciences, Academia Sinica.

NUMERICAL SOLUTION OF STATIONARY EULER EQUATIONS WITH THE HELP OF THE SPLITTING UP METHOD

S.G. Cherny
Institute of Theoretical an Applied Mechanics
USSR Academy of Sciences
Novosibirsk 630090
USSR

Aerodynamics is one of the important fields of application of the theory of hyperbolic systems. The hyperbolic systems of quasilinear equations are widely adopted for predicting the unsteady and steady supersonic flows of compressible gases. The deriving of analytical solutions of these equations entails insuperable difficulties especially in three-dimensional problems. In this connection the use of numerical methods advances to the forefront. However, the construction of efficient numerical algorithms for solving the gas dynamics equations remains an urgent problem of computational aerodynamics.

The present study is devoted to the construction of a new efficient marching algorithm for solving the steady Euler equations.

Consider a system of three-dimensional equations of gas dynamics in cartesian coordinates

$$\sum_{l=1}^{3} B_l \frac{\partial f}{\partial x_l} = 0 \tag{1}$$

where $B_l = B_{l1} + B_{l2}$,

$$f = \begin{pmatrix} \varrho \\ v_1 \\ v_2 \\ v_3 \\ p \end{pmatrix}, \qquad B_{l1} = v_l \cdot I, \qquad B_{l2} = \begin{pmatrix} 0 & \delta_l^1 \varrho & \delta_l^2 \varrho & \delta_l^3 \varrho & 0 \\ 0 & 0 & 0 & 0 & \delta_l^1/\varrho \\ 0 & 0 & 0 & 0 & \delta_l^2/\varrho \\ 0 & 0 & 0 & 0 & \delta_l^3/\varrho \\ 0 & \delta_l^1 \varrho c^2 & \delta_l^2 \varrho c^2 & \delta_l^3 \varrho c^2 & 0 \end{pmatrix}$$

$$\delta_j^i = \begin{cases} 1, & i = j \\ 0, & i \neq j \end{cases}$$, c is the acoustic velocity.

Assume that $v_1 > c$. Then x_1 is the marching coordinate along which the numerical integration of equations (1) is carried out.

Approximate a system (1) by an implicit difference scheme

$$B_1^{n+1} \frac{f^{n+1} - f^n}{h_1} + \sum_{l=2}^{3} B_l^{n+1} \Lambda_l f^{n+1} = 0, \tag{2}$$

where n is cross-section number in the x_1 direction.

For implementing the nonlinear difference equations (2) we shall consider an iterative scheme

$$B_{11}^{\nu} \frac{f^{\nu+1} - f^n}{h_1} + B_{12}^{\nu} \frac{f^{\nu} - f^n}{h_1} + \sum_{l=2}^{3} B_l^{\nu} \Lambda_l f^{\nu+1} = 0. \tag{3}$$

Here ν denotes the iteration number in the $n+1$-th marching cross-section.

Write down the scheme (3) in a canonic form

$$C^{\nu} \frac{f^{\nu+1} - f^{\nu}}{h_1} = -W^{\nu}, \tag{4}$$

$$\text{where } C^\nu = (B_{11}^\nu + h_1 \sum_{l=2}^{3} B_l^\nu \Lambda_l),$$

$$W^\nu = (B_1^\nu \frac{f^\nu - f^n}{h_1} + \sum_{l=2}^{3} B_l^\nu \Lambda_l f^\nu).$$

After an approximate factorization of the operator C^ν:

$$C^\nu \approx (B_{11}^\nu + h_1 B_{21}^\nu \Lambda_2)(B_{11}^\nu)^{-1}(B_{11}^\nu + h_1 B_{22}^\nu \Lambda_2)(B_{11}^\nu)^{-1}(B_{11}^\nu + h_1 B_{31}^\nu \Lambda_3)(B_{11}^\nu)^{-1}(B_{11}^\nu + h_1 B_{32}^\nu \Lambda_3)$$

the scheme (4) is replaced by a scheme in fractional spets

$$\begin{aligned}
(B_{11}^\nu + h_1 B_{21}^\nu \Lambda_2)\,\xi^{\nu+1/4} &= -W^\nu \\
(B_{11}^\nu + h_1 B_{22}^\nu \Lambda_2)\,\xi^{\nu+2/4} &= B_{11}^\nu\,\xi^{\nu+1/4} \\
(B_{11}^\nu + h_1 B_{31}^\nu \Lambda_3)\,\xi^{\nu+3/4} &= B_{11}^\nu\,\xi^{\nu+2/4} \\
(B_{11}^\nu + h_1 B_{32}^\nu \Lambda_3)\,\xi^{\nu+1} &= B_{11}^\nu\,\xi^{\nu+3/4} \\
f^{\nu+1} &= f^\nu + h_1\,\xi^{\nu+1}
\end{aligned} \qquad (5)$$

Its solution at each fractional step is derived by scalar sweeps or a scheme of running calculation.

It is shown an absolute stability of the iterative scheme (5) and its convergence to the solution of the implicit scheme (2).

It is proposed a version of scheme possessing a conservativeness property and having a higher approximation order in x_1.

The accuracy and the efficiency of the proposed numerical method is examined on the problem on the interaction of an oblique shock wave and a plate. A good agreement of the numerical solution of the problem with an exact one and a fast convergence of iterations is demonstrated.

Analysis of Saw-Tooth Instabilities on Moving Gravity Surface Waves

Søren Christiansen
Laboratory of Applied Mathematical Physics
The Technical University of Denmark
DK-2800 Lyngby, Denmark

Surface water waves under gravity [W1] constitutes a hyperbolic, moving boundary problem. For the solution of such problems various methods are at disposal [Y2] . In some of them Laplace's equation (see below) is solved separately: (1) by differential equation methods [C1,C2,H3,K1,O1,P1,Y2] or (2) by integral equation methods [D2,H3,L3,L4,L5,L7,N1,N2,N3,S3,V1,Y2]. In [B1,C1,H1,H2,N3,O1,S2,S5] and notably in Longuet-Higgins & Cokelet [L7] it is reported that in the course of the computation, when the equations are integrated forward in time, a smooth surface curve may develop into a curve with a superimposed saw-tooth shape. The problem has been overcome by an artificial smoothing of the boundary curve. We shall here try to investigate the water wave problem, hoping to contribute to the clarification of the difficulties mentioned.

We consider a two-dimensional water problem, 2π-periodic in the (horizontal) x-direction, with horizontal bottom $y = 0$ with the y-axis pointing upwards (gravity $g = 1$) and with moving surface curve $y = \eta(x,t)$, where t is time. Inside the region a 2π-periodic potential $\phi = \phi(x,y,t)$ satisfies Laplace's equation $\Delta\phi = 0$, while $\phi_y = 0$ on $y = 0$. On $y = \eta$ the potential ϕ satisfies well known boundary conditions [S6], which make the problem non-linear. By introducing $\varphi(x,t) \equiv \phi(x,\eta(x,t),t)$, i.e., the potential ϕ evaluated on the moving boundary, the conditions on the moving surface can also be written

$$\eta_t = \phi_y(x,\eta,t) - \eta_x(x,t)\,\phi_x(x,\eta,t) \qquad (1a)$$

$$\varphi_t = H - \eta(x,t) - \tfrac{1}{2}\,\phi_x(x,\eta,t)^2 + \tfrac{1}{2}\,\phi_y(x,\eta,t)^2 - \eta_x(x,t)\,\phi_x(x,\eta,t)\,\phi_y(x,\eta,t) \quad . \qquad (1b)$$

where H is a constant.

For $x := x_i \equiv i\,2\pi/N$; $i = 1,2,\ldots,N$ (with N even) the functions $\eta_i(t) := \eta(x_i,t)$ and $\varphi_i(t) := \varphi(x_i,t)$ are to be found. These functions are combined into one 2N-vector $\underset{\sim}{\psi} = [\psi_1,\ldots,\psi_N,\psi_{N+1},\ldots,\psi_{2N}]^T \equiv [\eta_1,\ldots,\eta_N,\varphi_1,\ldots,\varphi_N]^T$. The potential ϕ is expressed by means of N terms, each 2π-periodic, satisfying Laplace's equation and the condition on $y = 0$, and each with an unknown coefficient. These coefficients are

determined in terms of $\underset{\sim}{\psi}$ by solving a system of linear algebraic equations [I4], while the derivative η_x is approximated in terms of $(\eta_i)_1^N$, e.g. by means of periodic splines [I3]. Hereby the quantities at the right hand side of (1) are expressed in terms of $\underset{\sim}{\psi}$, and we are therefore led to a system of 2N ordinary (autonomous) differential equations (ODE's) [L2]

$$\underset{\sim}{\psi}' = F(\underset{\sim}{\psi}) \quad . \tag{3}$$

For the analysis of such a system it is crucial to determine the Jacobi matrix $\underset{=}{J}$, with elements $J_{ij} = \partial F_i / \partial \psi_j$. In the special case where $\eta_1 = \eta_2 = \ldots = \eta_N =: \bar{\eta}$ (a horizontal surface curve) and $\varphi_1 = \varphi_2 = \ldots = \varphi_N =: \bar{\varphi}$ (a constant surface pressure) the 2N x 2N matrix $\underset{=}{J}$ has the form

$$\underset{=}{J} = \begin{array}{|c|c|} \hline \underset{=}{0} & \underset{=}{M} \\ \hline -\underset{=}{I} & \underset{=}{0} \\ \hline \end{array} \tag{3}$$

where each of the submatrices are N x N, and the matrix $\underset{=}{M}$ is circulant [D1] and symmetric.

The matrix $\underset{=}{J}$, (3), has the following N + 1 (imaginary) eigenvalues, with $\iota^2 = -1$,

$$\lambda^{(0)} = 0 \tag{4a}$$

$$\lambda^{(k)} = \pm \iota \sigma^{(k)} \quad ; \quad k = 1, 2, \ldots, \frac{N}{2}. \tag{4b}$$

where

$$\sigma^{(k)} = \sqrt{k \tanh(k\bar{\eta})} \quad . \tag{4c}$$

while $\underset{=}{J}$, (3), has only 2N - 1 (complex) eigenvectors, indicating that the matrix $\underset{=}{J}$ is defective [N4] . It is perhaps not surprising that the eigenvalues are expressed in terms of $\sigma^{(k)}$, (4c), which also enters in the formulas for infinitesimal waves on a horizontal surface [L1]. It is more important that the absolute largest eigenvalues are the two with k = N/2.

Systems of ODE can be integrated numerically using various numerical methods [L2] [Y1]: each method is characterized by a region of absolute stability [S4]. Let λ be an eigenvalue of $\underset{=}{J}$ and h be the time step, then if λh is outside the region, the solution will develop a growing component of the eigenvector corresponding to λ.

In the present case the eigenvalues $\lambda^{(N/2)} \pm = \pm \iota\sigma^{(N/2)}$ have eigenvectors which combine to a saw-tooth surface curve, described by $(\eta_i)_1^N$. With λ being purely imaginary the integration methods do not create saw tooths, provided that the step length h satisfy $0 \leq |\lambda| h \leq S$, or

$$0 \leq h \leq h_{max} := \frac{S}{\sigma(N/2)} = \frac{S}{\sqrt{\frac{N}{2}\tanh\left(\frac{N}{2}\eta\right)}} . \qquad (5)$$

where S depends upon the method used. For example: Adams-Bashforth-Moulton, 4th order (ABM4) in PECE mode [Y1; p. 458]: S = 0.92620161, cf. [S4; Fig. 24] [T1; Fig. 4.2] .(For a related problem [F1] it is found that $\Delta t \propto (\Delta x)^{1/2}$.)

Actual numerical calculations have been carried out using various methods, in particular the method ABM4 (which was used in [L7]), with N = 36. With $\bar{\eta} = 1$ then $h_{max} = 0.218308$ according to (5).

The initial functions

$$\eta = 1 + \varepsilon \sin x \qquad (6a)$$

$$\varphi = (\varepsilon/\sqrt{\tanh 1}) \cos x \qquad (6b)$$

correspond to a wave of permanent form travelling to the right with phase speed $c = \sqrt{\tanh 1}$, provided that $|\varepsilon|$ is infinitesimal [L1]. From (6) an initial vector can be derived by means of a sampling in x.

The value $\varepsilon = 0.01$ is small enough so that the numerically computed results follow what could be expected from the linear theory for a horizontal surface curve: If $h = 0.24 > h_{max}$ saw tooths will become visible with an amplitude which is independent of x, but grows with the number of timesteps as predicted, while for $h = 0.18 < h_{max}$ saw tooths apparently do not develop.

The value $\varepsilon = 0.1$ is so large that the above results are not applicable: If h = 0.24 the saw tooths again become visible, but now with a large amplitude near the crest and a small amplitude near the trough. This same feature is noticed from Figure 4 in Longuet-Higgins & Cokelet [L7]. From this coincidence it is - of course - not possible to conclude with certainty whether the saw tooths observed by Longuet-Higgins & Cokelet, and others, simply are due to an integration with a time step which is too large. (Professor Jean-Marc Vanden-Broeck, Math. Res. Center, Madison, WI, U.S.A., is thanked for discussions relating to that conclusion.)

The numerically computed evolution of a boundary curve may depend upon which integration rule is used, whereby some aspects of the problem under consideration may be blurred. Therefore it may be advantageous directly to compute the Jacobi matrix by numerical differentiation (e.g. by means of [I1]) at a prescribed boundary curve and boundary potential, and subsequently determine numerically [I2] the eigenvalues and eigenvectors for $\underline{J}$. (For a somewhat related problem [R1], where Laplace's equation is solved by means of a certain integral equation, a similar computation has been carried out.)

Actual numerical calculations can reproduce, with high accuracy, the results (4), including the double eigenvalues. For other boundary curves and/or boundary potentials, than those leading to (4), it is observed that two opposite, double, purely imaginary eigenvalues are split into a quadruple of simple eigenvalues, $\lambda = \pm\alpha \pm i\beta$, i.e. two with positive, and two with negative real part. (A similar splitting is reported in [R1].)

The theory for two-dimensional water wave problems states that waves can travel with a permanent form with a certain phase speed, and that the waves are stable to superharmonic perturbations provided that the waves are not too high compared to the wave length [L6,M1,S1,Z1]. The permanent form corresponds to certain functions η and φ, for t = 0. If however, for t = 0, such functions η and φ are chosen, which do not correspond to a permanent form, there will be a change of form, which may be obtained when some components are growing, corresponding to eigenvalues with positive real part. At a later stage the growing components may turn into

decaying components. Therefore, when waves of non-permanent form evolves, it may be accompanied by eigenvalues with positive real part. (Dr. Ulla Brinch-Nielsen is thanked for discussions leading to that conclusion.)

Therefore the following questions arise concerning the eigenvalues with positive real part:

(1) Do these eigenvalues indicate a genuine instability inherent in the system of ODE's?

(2) Do the original system of PDE's possess instabilities?

REFERENCES

[B1] Baker,Gregory R.; Daniel I. Meiron & Steven A. Orzag: Generalized vortex methods for free-surface flow problems. Jour. Fluid Mech. 123 (1982) 477-501.

[C1] Chan, Robert K.-C. & Robert L. Street: A Computer Study of Finite-Amplitude Water Waves. Jour. Computational Phys. 6 (1970) 68-94.

[C2] Cheng, S.I. & Yulin Lu: An Eulerian Method for Transient Nonlinear Free Surface Wave Problems. Jour. Computational Phys. 62 (1986) 429-440.

[D1] Davis, Philip J.: Circulant Matrices. John Wiley & Sons; New York, et al. (1979) 15+250 pp.

[D2] Dold, J.W. & D.H. Peregrine: Steep Unsteady Water Waves: An Efficient Computational Scheme. Proceedings 19th International Conference on Coastal Engineering, Houston, 1 (1984) 955-967. American Society of Civil Engineers; New York.

[F1] Fenton, J.D. & M.M. Rienecker: A Fourier method for solving nonlinear water-wave problems: application to solitary-wave interactions. Jour. Fluid Mech. 118 (1982) 411-443.

[H1] Haussling, H.J.: Two-dimensional linear and nonlinear stern waves. Jour. Fluid Mech. 97 (1980) 759-769.

[H2] Haussling, H.J. & R.M. Coleman: Nonlinear water waves generated by an accelerated circular cylinder. Jour. Fluid Mech. 92 (1979) 767-781.

[H3] Hume III, E.C.; R.A. Brown & W.M. Deen: Comparison of Boundary and Finite Element Methods for Moving-boundary Problems Governed by a Potential. Internat. Jour. Numerical Methods Engineering. 21 (1985) 1295-1314.

[I1] IMSL Library (International Mathematical & Statistical Libraries, Inc., 7500 Bellaire Blvd., Houston, Texas 77036, U.S.A.), Edition 9.2, November 1984; DRVTE (Calculate first, second or third derivative of a user supplied function).

[I2] Idem; EIGRF (Eigenvalues and (optionally) eigenvectors of a real general matrix in full storage mode).

[I3] Idem; ICSPLN (Cubic spline interpolation with periodic end conditions).

[I4] Idem; LEQT2F (Linear equation solution - full storage mode - high accuracy solution).

[K1] Kawahara, Mutsuto & Toshihiko Miwa: Finite Element Analysis of Wave Motion. Internat. Jour. Numerical Methods Engineering. 20 (1984) 1193-1210.

[L1] Lamb, Horace: Hydrodynamics. Dover Publications; New York. 6th Ed. (1945) 15+738 pp.

[L2] Lambert, J.D.: Computational Methods in Ordinary Differential Equations. John Wiley & Sons; Chichester et al. (1973) 15+278 pp.

[L3] Liggett, J.A.: Hydrodynamics calculations using boundary elements. pp. 889-896 in: Kawai, Tadahiko (ed.): Finite Element Flow Analysis. Proceedings of the Fourth International Symposium on Finite Element Methods in Flow Problems. Chuo University, Tokyo, 26-29 July 1982. University of Tokyo Press; North-Holland Publishing Company; Amsterdam, Oxford, New York. (1982) 16+1096 pp.

[L4] Liu, P.L.-F. & J.A. Liggett: Applications of Boundary Element Methods to Problems of Water Waves. pp. 37-67 (Chapter 3) in: Banerjee, P.K. & R.P. Shaw (Eds.): Developments in Boundary Element Methods - 2, Applied Science Publishers; London, New Jersey. (1982) 10+288 pp.

[L5] Liu, P.L.-F. & J.A. Liggett: Boundary Element Formulations and Solutions for Some Non-Linear Water Wave Problems. pp. 171-190 (Chapter 7) in: Banerjee, P.K. & S. Mukherjee (Eds.): Developments in Boundary Element Methods - 3, Elsevier Applied Science Publishers; London, New York. (1984) 11+313 pp.

[L6] Longuet-Higgins, M.S.: The instabilities of gravity waves of finite amplitude in deep water. I. Superharmonics. Proc. Roy. Soc., London A 360 (1978) 471-488.

[L7] Longuet-Higgins, M.S. & E.D. Cokelet: The deformation of steep surface waves on water. I. A numerical method of computation. Proc. Roy. Soc., London A 350 (1976) 1-26.

[M1] MacKay, R.S. & P.G. Saffman: Stability of water waves. Proc. Roy. Soc., London A 406 (1986) 115-125.

[N1] Nakayama, T.: Boundary Element Analysis of Nonlinear Water Wave Problems. Internat. Jour. Numerical Methods Engineering 19 (1983) 953-970.

[N2] Nakayama, T. & K. Washizu: The Boundary Element Method Applied to the Analysis of Two-dimensional Nonlinear Sloshing Problems. Internat. Jour. Numerical Methods Engineering 17 (1981) 1631-1646.

[N3] New, A.L., P. McIver & D.H. Peregrine: Computations of overturning waves. Jour. Fluid Mech. 150 (1985) 233-251.

[N4] Noble, Ben: Applied Linear Algebra. Prentice Hall, Inc.; Englewood Cliffs, New Jersey (1969) 16+523 pp.

[O1] Ohring, Samuel: Nonlinear Water Wave Generation Using the Method of Lines. Jour. Computational Phys. 39 (1981) 137-163.

[P1] Prosperetti, Andrea & Jeffrey W. Jacobs: Numerical Method for Potential Flows with a Free Surface. Jour. Computational Phys. 51 (1983) 365-386.

[R1] Roberts, A.J.: A Stable and Accurate Numerical Method to Calculate the Motion of a Sharp Interface Between Fluids. IMA Jour. Appl. Math. 31 (1983) 13-35.

[S1] Saffman, P.G.: The superharmonic instability of finite - amplitude water waves. Jour. Fluid Mech. 159 (1985) 169-174.

[S2] Saffman, Philip G. & Henry C. Yuen: A note on numerical computations of large amplitude standing waves. Jour. Fluid Mech. 95 (1979) 707-715.

[S3] Salmon, James R.; Philip L.-F. Liu & James A. Liggett: Integral Equation Method for Linear Water Waves. Jour. Hydraulics Division, ASCE 106, HY 12 (1980) 1995-2010.

[S4] Sand, Jørgen & Ole Østerby: Regions of Absolute Stability, Computer Science Department, Aarhus University, Denmark. DAIMI PB-102 (September 1979) 2+57 pp.

[S5] Soh, W.K.: A numerical method for non-linear water waves. Computers and Fluids 12 (1984) 133-143.

[S6] Stoker, J.J.: Water waves. Interscience Publishers, Inc.; New York (1957) 28+567 pp.

[T1] Thomsen, Per Grove & Zahari Zlatev: Two-Parameter Families of Predictor-Corrector Methods for the Solution of Ordinary Differential Equations. BIT; Nordisk Tidskr. Inform. 19 (1979) 503-517.

[V1] Vinje, T. & P. Brevig: Numerical simulation of breaking waves. Advances Water Res. 4 (1981) 77-82.

[W1] Wehausen, John W. & Edmund V. Laitone: Surface Waves. pp. 446-778 in: Flügge, S. (Ed.): Handbuch der Physik, IX, Strömungsmechanik III. Springer-Verlag; Berlin, Göttingen, Heidelberg (1960) 7+815 pp

[Y1] Young, David M. & Robert Todd Gregory: A Survey of Numerical Mathematics. I + II. Addison-Wesley Publishing Company; Reading, Massachusetts (1973) 51+63+1099 pp.

[Y2] Yeung, Ronald W.: Numerical Methods in Free-Surface Flows. Annual Rev. Fluid Mech. 14 (1982) 395-442.

[Z1] Zufiria, J.A. & P.G. Saffman: The Superharmonic Instability of Finite-Amplitude Surface Waves on Water of Finite Dept. Studies Appl. Math. 74 (1986) 259-266.

DISCONTINUOUS FINITE ELEMENT APPROXIMATIONS FOR NONLINEAR CONSERVATION LAWS

B.Cockburn†, J. Jaffré††, Veerappa Gowda††

† IMA, University of Minnesota, 206 Church Street S.E., Minneapolis, Minnesota 55455, U.S.A.
†† INRIA, B.P. 105, 78153 Le Chesnay Cédex, France.

Solutions of scalar nonlinear conservation laws are calculated by using discontinuous finite elements. First order schemes are obtained with piecewise constant approximations, while higher degree piecewise polynomial approximations give higher order schemes. On the boundary of the discretization cells, numerical fluxes are calculated by using one-dimensional Riemann solvers. Special attention is given to the piecewise linear case for which truely multidimensional slope limiters are defined.

1. Introduction

Recently there has been a large activity to design and analyze "high resolution" schemes for nonlinear hyperbolic conservation laws and one can find many references in the proceedings of this conference. In this paper we propose to use the discontinuous finite element method for such a purpose.

It is a finite volume method where the volumes considered for mass balance are the cells of the discretization themselves. Inside a cell polynomials of arbitrary degree can be used, and on the boundary the numerical flux is calculated by using Riemann solvers in the normal direction. Actually we consider only the case of piecewise constant and piecewise linear approximations. The latter yields a higher order scheme which has to be stabilized by a slope limiter that is a multidimensional extension of Van Leer's one [10].

The linear version of the discontinuous finite element method have been first analyzed in [8] and more recently in [7]. The nonlinear version has been used in reservoir simulation [2], [3] and is presented and analyzed in the one dimensional case in [1],[4]. It is also closely related to the MUSCL scheme analyzed in [9].

We consider here the scalar nonlinear conservation law

$$\partial u/\partial t + \operatorname{div} \vec{f}(u) = 0, \quad x \in \mathbb{R}^n, \tag{1.1a}$$

$$u(x,0) = u_0(x), \quad x \in \mathbb{R}^n, \tag{1.1b}$$

given $\vec{f}:[0,1] \to \mathbb{R}^n$ and $u_0: \mathbb{R}^n \to [0,1]$. The extension of the method to the Euler equation is under way using a field by field decomposition.

2. One-dimensional space approximation

Let us denote by $\ldots < x_{i-1/2} < x_{i+1/2} < \ldots$ and by $K(i) =]\, x_{i-1/2}, x_{i+1/2}\, [$, $i \in \mathbb{Z}$ the points and the intervals of the discretization of $\mathbb{R}$. The measure of $K(i)$ is $h_i = x_{i+1/2} - x_{i-1/2}$. We introduce the approximation space V^k of functions which are discontinuous at the discretization points and restrict to polynomials of degree k on each interval $K(i)$ and $v^L_{i+1/2}$, $v^R_{i+1/2}$ and $\bar{v}_i$ denote respectively the left-handed and the right-handed limits at $x_{i+1/2}$, and the mean value over $K(i)$ of a function v in V^k.

The approximation equation is obtained by multiplying equation (1.1) by test functions in V^k, by integrating over the intervals and by integrating by parts the term containing the derivative

with respect to space. Thus the approximate problem consists of seeking $u_h \in V^k$ solution of

$$(2.1)\quad \int_{K(i)} (\partial u_h/\partial t)\, v\, dx - \int_{K(i)} f(u_h)\, (\partial v/\partial x)\, dx + F_{i+1/2}\, v^L_{i+1/2} - F_{i-1/2}\, v^R_{i-1/2} = 0, \text{ for } v \in V^k,\ i \in \mathbb{Z},\ t > 0.$$

The numbers $F_{i+1/2}$, $i \in \mathbb{Z}$ are numerical fluxes which are functions of the two limit values at the discretization points and are calculated by means of exact or approximate Riemann solvers [5], [6].

Note that for $k = 0$ scheme (2.1) reduces to the first order finite difference scheme

$$du_i/dt + (F_{i+1/2} - F_{i-1/2}) / h_i = 0,\ i \in \mathbb{Z},\ t > 0,$$

and that, for $k > 0$, conservation equations are obtained by taking for v in (2.1) the characteristic functions of the intervals.

For $k > 1$ scheme (2.1) does not have good stability properties and the calculated solution oscillates. To stabilize them, we extend to the discontinuous finite element method the notion of slope limiters already introduced by Van Leer [10] for finite difference schemes. We now denote by $u^*_h(t)$ the function satisfying (2.1) and we impose on $u_h(t)$ to satisfy

$$(2.2)\quad \left(\int_{K(i)} u_h(t)\, dx\right) / h_i = \bar{u}_i(t) = \bar{u}^*_i(t),$$

in order to preserve mass balance, and

$$(2.3a)\quad (1-\alpha)\bar{u}_i(t) + \alpha \mathrm{Min}(\bar{u}_{i-1}(t), \bar{u}_i(t)) \leq u^R_{i-1/2}(t) \leq (1-\alpha)\bar{u}_i(t) + \alpha \mathrm{Max}(\bar{u}_{i-1}(t), \bar{u}_i(t)),$$

$$(2.3b)\quad (1-\alpha)\bar{u}_i(t) + \alpha \mathrm{Min}(\bar{u}_i(t), \bar{u}_{i+1}(t)) \leq u^L_{i+1/2}(t) \leq (1-\alpha)\bar{u}_i(t) + \alpha \mathrm{Max}(\bar{u}_i(t), \bar{u}_{i+1}(t)),$$

$$(2.3c)\quad 0 \leq \alpha \leq 1,$$

$$(2.4)\quad u_h(x) \equiv \bar{u}_i \text{ for } x \in K(i) \text{ if } \bar{u}_i > \mathrm{Max}(\bar{u}_{i-1}, \bar{u}_{i+1}) \text{ or } \bar{u}_i < \mathrm{Min}(\bar{u}_{i-1}, \bar{u}_{i+1}),$$

to limit the slope of u_h. Since $u_h(t)$ is not uniquely defined by (2.2-4), one can also impose for instance that $u_h(t)$ be as close as possible to $u^*_h(t)$ with respect to the L^2 norm.

The parameter α controls the slope limitations and the corresponding added numerical diffusion. In the case of a piecewise linear approximation ($k=1$), when $\alpha = 0$ the slope limited solution is piecewise constant so it is the strongest possible slope limitation; then we are taken back to a first order finite difference scheme and the added numerical diffusion is maximum. On the other hand, the larger α is the looser is the slope limitation and the smaller is the added numerical diffusion.

Note that in such a formulation, the slope limiting process is a step distinct from the finite element calculation. This makes it easier to design various time steppings - explicit, implicit, higher order [4],[11] - since they will affect only the latter, and to extend the method to the multidimensional case.

A crucial point for the method to be computationally efficient is to choose the adequate integration formulas in eq. (2.1). For example, in the case $k=1$ and of first order backward differencing in time, numerical experiments have shown that the trapezoidal rule for the integral containing the derivative with respect to time and the midpoint rule for the integral containing the derivative with respect to space is the best choice while more precise formulas give more costly and not as nice results.

3. Multidimensional space approximation

We consider a regular discretization of the domain Ω with n-simplices and n-rectangles $K \in \mathcal{T}_h$ of diameter less than or equal to h and we define the approximation space V^1 of functions which are discontinuous across the interelement boundaries and which restrict to P^1 polynomials on the n-simplices or Q^1 polynomials on the n-rectangles. The degrees of freedom of functions of V^1 are, element by element, their values at the vertices. We denote them $v_{K,A}$ with $K \in \mathcal{T}_h$ and A a vertex of K.

Another choice is possible in case of a structured mesh of rectangles: one can still take P^1 polynomials (instead of Q^1) in the definition of V^1. A convenient choice of the degrees of freedom is the average value of the function in the element and its slopes in the directions parallel to the axes. Then a multidimensional scheme is obtained by writing the one-dimensional scheme in the directions parallel to the axes. This is what is done usually in higher order finite difference schemes but this is not what we can call a truely multidimensional scheme.

As in one dimension, we calculate $u_h \in V^1$ in two steps: a finite element calculation giving a predicted solution $u^*_h \in V^1$ followed by a slope limitation yielding u_h. The finite element calculation consists in solving the following equation:

$$(3.1)\quad \int_K (\partial u^*_h/\partial t)\, v\, dx - \int_K \vec{f}(u_h)\, \vec{\mathrm{grad}} v\, dx + \int_{\partial K} F\, v\, d\gamma = 0, \quad \text{for } v \in V^1,\ K \in \mathcal{T}_h,$$

where the numerical flux F defined on the edges of the mesh is calculated as follows.

First we note that the integral over ∂K is the sum of integrals over three or four edges. Any integral over an edge E will be calculated by means of an integration formula

$$\int_E F\, v\, d\gamma \simeq \sum_{i=1,npi} \beta_i\, F(P_i)\, v(P_i),$$

where npi, β_i, P_i denote respectively the number of integration points, the weights and the points of the integration formula.

Then we note that the numerical flux F is an approximation on the edge E of the quantity $\vec{f}.\vec{\nu}$ where $\vec{\nu}$ is a unit normal to the edge E. Therefore it is legitimate to calculate $F(P_i)$ by solving the one-dimensional Riemann problem in the direction of $\vec{\nu}$, relative to the function $\vec{f}(P_i).\vec{\nu}$ and to the initial data the two limit values $u(P_i)^+$, $u(P_i)^-$ of u_h at the points P_i. Thus $F(P_i)$ is calculated by the same formulas as described in section 2.2 for the one-dimensional case with $u(P_i)^-$, $u(P_i)^+$, $\vec{f}.\vec{\nu}$ replacing respectively $u^L_{i+1/2}$, $u^R_{i+1/2}$, f.

We formulate now a multidimensional extension of the one-dimensional slope limiter (2.2-4). For any element $K \in \mathcal{T}_h$ and any $v \in V^1$ we introduce the following notations:

$nv(K)$ = number of vertices of K,

$\mathcal{T}(A) = \{ K \in \mathcal{T}_h \mid A \text{ is a vertex of } K \}$,

$\bar{v}_K = \left[\sum_{i=1}^{nv(K)} v_{K,A_i} \right] / nv(K)$ = average of v over K,

$v_K = (v_{K,A_i})_{i=1,nv(K)}$,

$$J_K(v_K) = \left[\sum_{i=1}^{nv(K)} (v_{K,A_i} - u^*_{K,A_i})^2 \right] / 2 .$$

J_K measures the distance between v and u^*_h inside the element K.

The slope limited function u_h must have the same cell averages as u^*_h to preserve mass balance and its degrees of freedom will satisfy inequalities similar to (2.3),(2.4). This can be achieved in the following way. Given u^*_h obtained from (3.1), we calculate for any vertex A of the discretization the minimum and the maximum of the averages in the cells surrounding A:

$$UMIN(A) = \min_{K \in T(A)} \overline{u}^*_K \quad , \quad UMAX(A) = \max_{K \in T(A)} \overline{u}^*_K .$$

Then u_h is obtained by solving the series of minimization problems:

Find $u_h \in V^1$ such that for all $K \in T_h$ $U_K \in P_K \cap Q_K$ and

$$J_K(U_K) = \min_{V_K \in P_K \cap Q_K} J_K(V_K),$$

where P_K and Q_K are respectively the following hyperplane and hypercube in $\mathbb{R}^{nv(K)}$:

$$P_K = \{ x \in \mathbb{R}^{nv(K)} \mid \sum_{i=1}^{nv(K)} x_i = nv(K)\, \overline{u}^*_K \},$$

$$Q_K = \prod_{i=1}^{nv(K)} [(1-\alpha)\, \overline{u}^*_K + \alpha\, UMIN(A_i) , (1-\alpha)\, \overline{u}^*_K + \alpha\, UMAX(A_i)].$$

It is easy to check that each minimization problem in K has a unique solution which can be calculated by dualizing the constraint $V_K \in P_K$ and solving the associated saddle point problem [2].

References

[1] G. Chavent, B. Cockburn, *The local projection P^0-P^1 discontinuous Galerkin finite element method for scalar conservation laws*, in preparation.

[2] G. Chavent, J. Jaffré, Mathematical Models and Finite Elements for Reservoir Simulation, (North Holland, Amsterdam,1986).

[3] G. Chavent, J. Jaffré, R. Eymard, D. Guérillot, L. Weill, *Discontinuous and mixed finite elements for two-phase incompressible flow*, paper SPE 16018 presented at the 9th SPE Symposium on Reservoir Simulation, San Antonio, Texas (Feb. 1-4, 1987).

[4] B. Cockburn,J. Jaffré, Veerappa Gowda, *Discontinuous finite elements for scalar nonlinear conservation laws* , in preparation.

[5] B. Engquist, S. Osher, *One sided difference approximations for scalar conservation laws*, Math. Comp. 36 (1981), pp. 321-351.

[6] S.K. Godunov, *Finite difference methods for numerical computation of discontinuous solutions of the equations of fluid dynamics*, Math. Sbornik 47 (1959), pp. 271-306.

[7] C. Johnson, J. Pitkaranta, *An analysis of the discontinuous Galerkin method for a scalar hyperbolic equation*, Math. Comp. 46 (1986), pp. 1-26.

[8] P. Lesaint, P.A. Raviart, *On a finite element method for solving the neutron transport equations*, in Mathematical Aspects of Finite Elements in Partial Differential Equations, Carl de Boor Ed. (Academic Press, New York, 1974), pp. 89-123.

[9] S. Osher, *Convergence of generalized MUSCL schemes*, SIAM J. Numer. Analysis 21 (1984), pp. 947-961.

[10] B. Van Leer, *Towards the ultimate conservative scheme : IV. A new approach to numerical convection*, J. Comp. Phys. 23 (1977), pp. 276-299.

[11] Veerappa Gowda, These de doctorat, Université Paris 9 (1988).

A METHOD TO GET CORRECT JUMP CONDITIONS FROM SYSTEMS IN NONCONSERVATIVE FORM

by J.F. Colombeau

Engineers use systems in nonconservative form to represent shock waves. Numerical experiments show that these systems have indeed such solutions; however, from the theoretical viewpoint, they do not have discontinuous solutions in the sense of distribution theory.

A theory of generalized functions which was developed to give a meaning to all products of distributions ([1,2], and [3,4] for more recent presentations), can be used to master mathematically discontinuous solutions of such systems. The equations have to be formulated in this theory. If one adopts the weakest formulation (corresponding to the concept of a weak solution in the distributional sense) then, in contrast with the conservative case, one gets in general an infinite number of possible jump conditions, depending on a parameter which has a physical significance.

To resolve the ambiguity this theory suggests to state the equations of physics in a way more precise than usual on the shocks: one postulates that the basic laws of physics still hold in a strong sense even in the infinitesimal space-time region in which the jump takes place, while the constitutive equations are not assumed to hold in this region. In basic cases this method gives nonambiguous jump conditions and then they agree with the results of experiments.

Unexpectedly this method can also be used for a new insight (offering new numerical methods) into classical conservative systems such as fluid dynamics: one can -within this mathematical theory- transform systems from a conservative form into an equivalent nonconservative form, whose numerical treatment can be easier (recall the well known fact that formal manipulations, which are valid in the case of smooth flows, can alter the jump conditions in the case of shocks ; therefore these transformations are not obvious).

The aim of this talk is to present this method very clearly on four examples: elasticity (system with density- velocity- stress given in nonconservative form), fluid dynamics (system with density- velocity - pressure- energy given in conservative form), elastoplasticity and shock waves in viscous media .

C

Formulas such as " $Y\delta=(1/2)\delta$ " (Y=Heaviside function) have been used since long time by physicists and mathematicians.They give correct results in some basic circumstances (in fact the simplest , and so ,the more important ones). The genuine difficulty lies precisely in finding the situations in which these formulas hold and, in general , in finding the correct conditions.

1 J.F.Colombeau: New generalized functions and multiplication of distributions. North-Holland 1984.
2 J.F.Colombeau: Elementary introduction to new generalized functions.North-Holland 1985.
3 E.E.Rosinger: Generalized solutions of nonlinear PDE. North-Holland (Math. Studies 144),november 1987.
4 H.A.Biagioni: Introduction to a nonlinear theory of generalized functions (200 p.) Preprint series Notas de Matematica .State University of Campinas UNICAMP, Campinas, Sao-Paulo ,Brazil.

Some results in the talk can be found in:

5 J.F.Colombeau,A.Y.LeRoux: Multiplications of distributions in elasticity and hydrodynamics.J.of Mathematical Physics ,to appear in february 1988.

Two related trends of works not developed in this talk:

This theoretical method leads to numerical methods;some of them are to be found in

J.F.Colombeau,A.Y.LeRoux:Numerical techniques in elastodynamics. Lecture Notes in Math.1270. Springer, 1987, p.103-114.
----------:Numerical methods for hyperbolic systems in non- conservative form .Advances in computer methods 6,IMACS 1987,p.28-37.

This mathematical context provides solutions of the Cauchy problem in cases in which there is no distribution solution:

J.J.Cauret,J.F.Colombeau,A.Y.LeRoux:Discontinuous generalized solutions of nonlinear nonconservative hyperbolic equations. J. of Math. Ana. and Appl.In press.

J.F.Colombeau,M.Oberguggenberger:Hyperbolic systems with a compatible quadratic term : generalized solutions, delta waves, and multiplication of distributions.
M.Oberguggenberger:Generalized solutions to semilinear hyperbolic systems. Monatshefte fur Math.103,1987,p.133-144.
----------:Hyperbolic systems with discontinuous coefficients; examples.Proceedings GFCA 1987. Plenum Pub. Comp. in press.
----------:----------; generalized solutions and a transmission problem in acoustics.

U.E.R. de Mathematiques et d' Informatique, Universite de Bordeaux 1, 33405 TALENCE , FRANCE.

UNIFORMLY HIGH ORDER CONVERGENT SCHEMES FOR HYPERBOLIC CONSERVATION LAWS.

F. COQUEL & J. CAHOUET
Research Group
Laboratoire National d'Hydraulique, E.D.F.
6, quai Watier 78400 CHATOU FRANCE.

Some years ago, Leonard ([1],[2]) derived a difference scheme using an original technique in order to combine monotonicy and high order accuracy. Based upon the attractive 5-point linear scheme Quick [3] without real theoretical frame, this scheme gives however remarkably sharp profile for the linear advection equation. It was the investigation of this scheme and associated ones ([4]) which prompted this work.

We consider numerical approximation of the weak entropy solution of the scalar equation :

$$(1) \qquad \begin{cases} u_t + f(u)_x = 0 & 0 \le t \le T \\ u(x,0) = u_0(x) \end{cases}$$

We present a systematic procedure to modify 5-points linear schemes such that convergence towards the weak entropy solution of (1) can be established while high order spatial accuracy is achieved even at non sonic critical points. Our method might be described as a simple modification of T.V.D. schemes which preserves $BV \cap L^\infty$ stability, entropy stability being achieved following Vila's ideas ([5],[6]). Having developed a suited procedure to check T.V.D. correction, we will state in a second part , precise results concerning the construction of uniformly high order accurate convergent schemes. Then, we derive several schemes based upon the Quick scheme which enligthen, in some extents, Leonard's approach. Details of proofs are provided in [12] .

1. T.V.D. AND ENTROPY CORRECTIONS OF 5-POINT LINEAR SCHEMES.

Let denote $h^n_{j+1/2}$ the numerical flux associated with a 5-point linear scheme. Restricting ourselves to E-schemes ([7]) which behave like the first order upwind scheme away from sonic points, we may write, before T.V.D. correction :

$$h^n_{j+1/2} = g^{E\,n}_{j+1/2} + a^n_{j+1/2}$$

In order to achieve $BV \cap L^\infty$ stability, we must "limit" the antidiffusive flux

$$a^n_{j+1/2} = \frac{1}{\lambda} \left| \nu^n_{j+1/2} \right| \frac{\varphi^n_{j+1/2}}{r^n_{j+1/2}} \Delta u^n_{j+1/2}$$

where

$$\varphi^n_{j+1/2} = \frac{h^n_{j+1/2} - f(u^n_j)}{\Delta f^n_{j+1/2}} \quad \text{and} \quad r^n_{j+1/2} = \frac{\Delta f^n_{j-1/2}}{\Delta f^n_{j+1/2}} \quad \text{if} \quad \nu^n_{j+1/2} > 0$$

$$\varphi^n_{j+1/2} = - \frac{h^n_{j+1/2} - f(u^n_{j+1})}{\Delta f^n_{j+3/2}} \quad \text{and} \quad r^n_{j+1/2} = \frac{\Delta f^n_{j+1/2}}{\Delta f^n_{j+3/2}} \quad \text{if} \quad \nu^n_{j+1/2} < 0$$

with the usual notation $\nu^n_{j+1/2} = \lambda \frac{\Delta f^n_{j+1/2}}{\Delta u^n_{j+1/2}}$

The reduced flux $\varphi^n_{j+1/2}$, thanks to the consistancy of $h^n_{j+1/2}$ with f(u), only depends on $r^n_{j+1/2}$ through a linear relation. This suggests to replace $\varphi^n_{j+1/2}$ by a suited function $\varphi(r)$ whose restriction to "smooth regions" is $\varphi^n_{j+1/2}$. Owing to the set of sufficient conditions derived by Harten ([8]) and Vila, ensuring the BV and L^∞ norms decay, we can prove :

Theorem 1 : Assume that $\varphi(r)$ satisfies :

$$(\exists (M,\mu) \in R_+^* \times [-1,0]) / (\forall r \in R ,\ \mu \le \varphi(r) \le M \quad \text{and} \quad -M \le \frac{\varphi(r)}{r} \le 1+\mu)$$

Then the corrected flux

$$\overline{h^n_{j+1/2}} = g^{E\,n}_{j+1/2} + \overline{a^n_{j+1/2}}$$

where

$$\begin{cases} \overline{a^n_{j+1/2}} = 0 & \text{near a sonic point} \\ \overline{a^n_{j+1/2}} = \dfrac{1}{\lambda} \left| \nu^n_{j+1/2} \right| \dfrac{\varphi(r^n_{j+1/2})}{r^n_{j+1/2}} \Delta u^n_{j+1/2} & \text{otherwise} \end{cases}$$

defines a T.V.D. scheme, which preserves L^∞ norm ∎

There is therefore, as the mesh size Δx tends to 0, a subsequence in L^1_{loc} converging towards a weak solution of (1).To achieve a good entropy production for the limit solution, we slightly modify the corrective antidiffusive flux according to Vila's ideas ([5],[6]). Thus if one enforces $a^n_{j+1/2}$ to vanish with the mesh size, we obtain

Theorem 2 : The following correction of the antidiffusive flux

$$a^n_{j+1/2} = \mathrm{sgn}\left(\overline{a^n_{j+1/2}}\right) \mathrm{Min}\ \left(C\Delta x^\alpha , \left|\overline{a^n_{j+1/2}}\right| \right) \qquad \text{with} \qquad (C,\alpha) \in R_+^* \times]\,0,1\,[$$

ensures the entropy convergence ∎

Notice that

$$(\forall A>0)\ (\exists C>0) / \left(a^n_{j+1/2} = \overline{a^n_{j+1/2}} \quad \text{in any region where} \quad |\Delta u^n_{j+1/2}| \le A\ \Delta x \right)$$

so that the resulting scheme is still high order accurate everywhere except at the critical points where T.V.D. property makes it necessarily degenerate into first order accuracy ([7]).This perpetual damping of local extrema leads the error to be $O(\Delta x)$ in L^∞ norm.

2. UNIFORMLY HIGH ORDER CONVERGENT SCHEMES.

To overcome this main drawback, Harten and al ([9], [10]) have introduced the E.N.O. schemes of globally high order accuracy in smooth regions. At this time, convergence estimates are unavailable but numerical experiments enlighten their extreme stability. Quite recently, Shu ([11]) has proposed a Total Variation Bounded (T.V.B.) modification of some existing T.V.D. schemes involving the classical min-mod function in such a way that high order spatial accuracy is achieved including at critical points.

We present here a systematic procedure to convert 5-point linear schemes into convergent schemes(i.e. $BV \cap L^\infty$ and entropy stable) of uniformly high order accuracy in space. As for Shu's approach, there is a price to pay for this extra-accuracy ; namely the loss of the monotonicity preserving property. However, the following estimates can be performed :

$$\begin{cases} \| u^n \|_{L^\infty} \le \| u_0 \|_{L^\infty} + O(\Delta x^2) \\ TV(u^n) \le TV(u_0) + O(\Delta x) \end{cases} \qquad \text{for} \quad 0 \le n\Delta t \le T$$

Theorem 3 : Assume that there exists $(a,b) \in R^{*2}_+$ such that the reduced flux $\varphi_{0,0}(r)$ (Fig.1) provides a scheme which preserves BV and L^∞ norm under the C.F.L. condition :

$$\mathrm{Max}\ |\nu^n_{j+1/2}| \le \beta$$

Then for any M' and M" > 0 , the scheme associated with the reduced flux $\varphi_{M',M''}$ (Fig. 2) is $BV \cap L^\infty$ stable in $0 \le t \le T$ under the same C.F.L. condition ∎

The main idea underlying the proof is to obtain , as Shu did , the following key estimate :

$h_{M',M'' j+1/2}^{n} = h_{0,0 j+1/2}^{n} + d_{j+1/2}^{n}$ where $|d_{j+1/2}^{n}| \leq B \Delta x^2$ for any n , j .

Then we ensure entropy stability as previously pointed out .

Theorem 4 : For any $D > 0$, there exist M' and M'' > 0 such that the scheme is high order spatial accurate in any region where derivatives of u are bounded by D (except at sonic points) ∎

3.APPLICATION TO QUICK SCHEME AND NUMERICAL RESULTS.

Under the latter guidelines, we present several convergent corrections of the attractive third order accurate Quick scheme ([3]).The formal extension of modified Exquisite scheme ([4]) to nonlinear hyperbolic scalar equations is shown to be T.V.D. Since its reduced flux suffers from a lack of symmetry $\{ \frac{\varphi(r)}{r} \neq \varphi(\frac{1}{r}) \}$, another T.V.D. correction is designed to get this property. Actually , Quick is modified in order to give a uniformly high order accurate scheme which justifies in some extent the Euler-Quick scheme ([1],[2]) .

For steady-state computations, a delta formulation ([13]) is used to speed up the convergence process. The implicit operator is discretized in space with the full Donor-Cell scheme and the explicit part uses previous schemes.

Theorem 5 : This implicit procedure preserves the total variation behaviour (decay or boundedness) of the underlying high order scheme ∎

Numerical experiments are performed in order to compare the uniformly high order convergent correction of the Quick scheme to the T.V.D. one. Numerical simulations of unsteady and steady fluid flows containing shocks will be shown at the conference. An approach allowing an easy extension to multidimensional system is described in ref [14] and applied to multiphase flow simulations.

- NOMENCLATURE -

$\Delta y_{j+1/2} = y_{j+1} - y_j$; $g_{j+1/2}^{E\,n} = g(u_{j+1}^{n}, u_j^{n})$; $\Delta f_{j+1/2}^{n} = f(u_{j+1}^{n}) - f(u_j^{n})$

Δx : Mesh size ; Δt : Time step ; $\lambda = \frac{\Delta t}{\Delta x}$

- REFERENCES -

[1] Leonard B. P. "A survey of finite differences with upwinding for numerical modelling of the incompressible convective diffusion equation" ,pp1-35, in Computational Techniques in Transient and Turbulent Flows edited by Taylor & Morgan (1981)

[2] Leonard B.P. "Locally Modified Quick scheme for highly convective 2D and 3D flows" Fifth International Conference in Numerical Methods in Laminar and Turbulent Flow, Montreal , Canada , (6-10 July ,1987)

[3] Leonard B.P. Comp. Methods Applied in Mech. Eng,19,59 (1979).

[4] Maekawa I & Murumatsu T. "High order differencing schemes in fluid flow analysis",5th IAHR Liquid Metal Working Group Meeting,Grenoble,France (June 23-27 , 1986).

[5] Vila J. P. Thesis Université PARIS VI (1986).

[6] Vila J.P. "High order schemes and entropy condition for nonlinear hyperbolic systems of conservation laws" C.M.A.P. report 111, Ecole Polytechnique Palaiseau France(1986).

[7] Osher S. & Chakravarty S. "High resolution schemes and the entropy condition",Siam J. Numer. Anal. Vol 21,N°5, pp955-983,(1984).

[8] Harten A. "High resolution schemes for hyperbolic conservation laws", J.Comp.Physics. Vol 49,pp357-393,(1983).
[9] Harten A. & Osher S."Uniformly high order accurate nonoscillatory schemes, I",SIAM J. Numer. anal., v.24,pp.279-309,(1987).
[10] Harten A., Enquist B., Osher S. & Chakravarty S. "Uniformly high order accurate essentially non-oscillatory schemes, III",J. Comput. Phys. , Vol 71, pp231-303,(1987).
[11] Shu C. "T.V.B. uniformly high order schemes for conservation laws", Math. Comp, Vol49, pp105,121,(1987).
[12] Coquel F. E.D.F. Report to be published.
[13] Peyret R. & Taylor C. "Computational methods for fluid flow" ,Spinger Verlag (1983).
[14] Cahouet J. & Aubry S. "A finite volume approch for 3D two phase flows".Submitted at this conference.

- FIGURES -

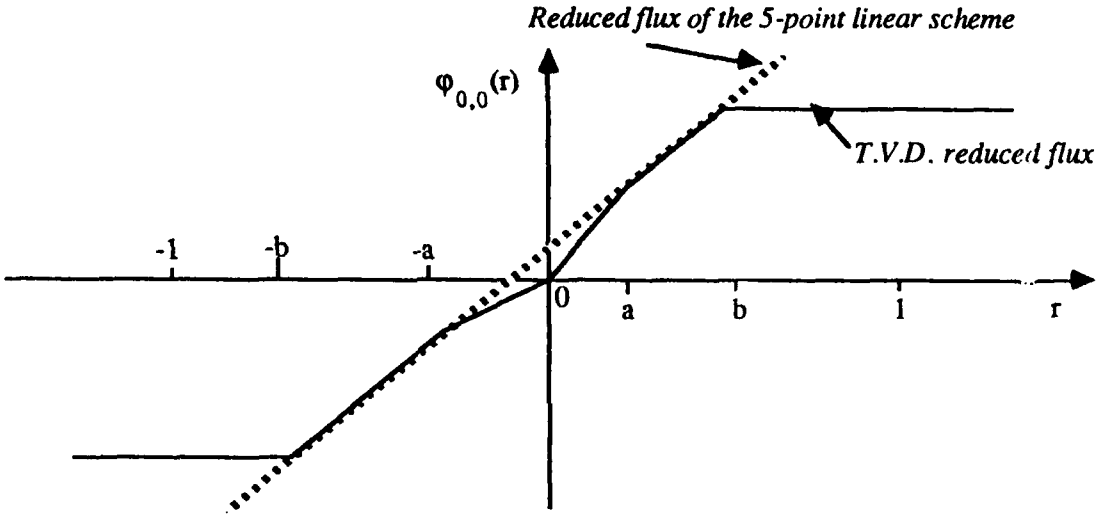

Figure 1 : T.V.D. reduced flux.

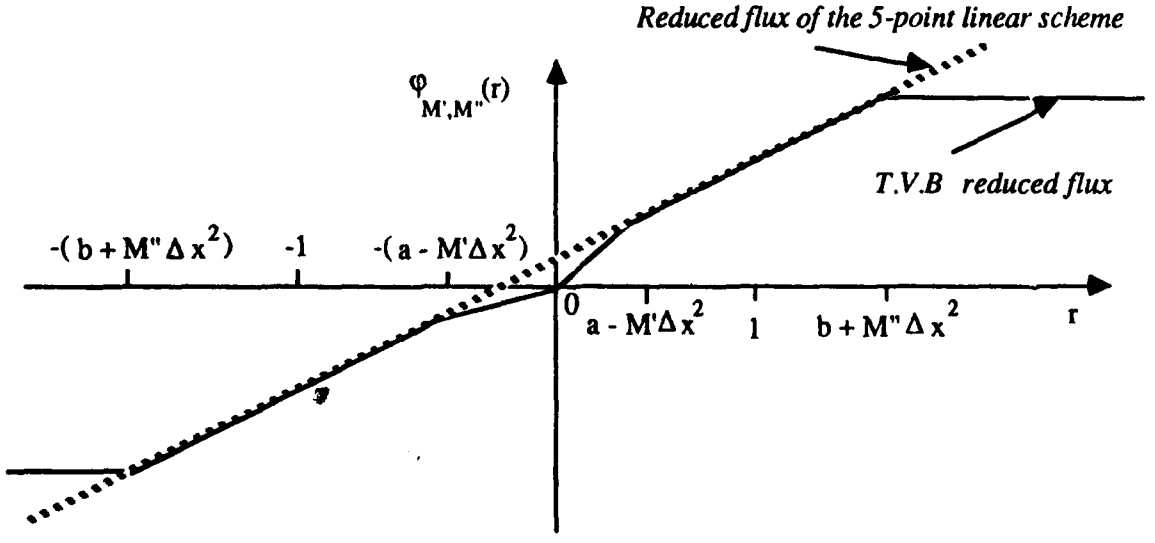

Figure 2 : T.V.B. reduced flux.

Grid Generation for General 2-d Regions Using Hyperbolic Equations

Jeffrey Q. Cordova
Sterling Federal Systems
Palo Alto, CA

Timothy J. Barth
NASA Ames Research Center
Moffett Field, CA

A method for applying a hyperbolic grid generation scheme to the construction of meshes in general 2-d regions has been developed. This approach is similar to that developed by Steger and Chaussee (1980) and represents a generalisation of their work. The equations used by Steger and Chaussee arise from imposing the constraints of orthogonality and volume distribution on the computed grid. These constraints can be relaxed by introducing an angle control source term and this leads to methods for solving the standard problems of hyperbolic grid generation. Novel applications of this approach include controlling the propogation of singularities, preventing shock formation (crossing grid lines), and the generation of internal grids.

INTRODUCTION

Over the past decade, the scope of finite difference methods has been extended to include equation sets posed on arbitrary geometries. This has been accomplished through the process of numerical grid generation wherein the geometry is mapped onto a simpler domain and the transformed equations solved there. For finite difference methods, the simplest domain is an n-rectangle (n = space dimension) and the grid generation problem consists of mapping an n-rectangle onto the domain of the equation set. Thus, the geometry is represented as a deformed n-rectangle and the numerically generated grid as a deformed n-lattice.

A variety of algorithms have been developed for numerical grid generation. Among these are algebraic methods, schemes based on solving partial differential equations and, optimization techniques. Many of the methods currently in use are documented in Thompson (1985). The discussion here will center on using hyperbolic equations to generate two dimensional grids.

The notion of using hyperbolic equations to construct grids was first proposed by Steger and Chaussee (1980). In this approach, an initial surface is propogated outward subject to spacing and orthogonality constraints. In practice, this technique suffers from three limitations: (1) discontinuities in the initial data are propogated, (2) shocks (crossing grid lines) may form and, (3) boundaries other than an initial surface may not be specified. The first two of these may be overcome by strictly numerical techniques as demonstrated by Kinsey and Barth (1984). The contributions of this research are to show how (3) may be overcome and to give another method for preventing (2). Both results follow as a consequence of including an angle control source term in the hyperbolic equations.

ANALYSIS

Let $(\xi, \eta) \rightarrow (x, y)$ denote the mapping from computational space to the domain of interest (Fig. 1). This mapping will be generated based on the following equations:

$$\frac{\mathbf{r}_\xi \cdot \mathbf{r}_\eta}{|\mathbf{r}_\xi||\mathbf{r}_\eta|} = cos\theta, \tag{1a}$$

$$|\mathbf{r}_\xi \times \mathbf{r}_\eta| = V. \tag{1b}$$

Here, $\mathbf{r} = (x, y)^t$ and θ, V are user specified angle and volume source terms respectively. These equations reduce to the Steger-Chaussee equations when $cos\theta = 0$.

The structure of these equations is obtained from a local linearization about a known state x^0, y^0. This results in the following 2x2 system:

$$A\mathbf{r}_\xi + B\mathbf{r}_\eta = \mathbf{f} \tag{2}$$

where

$$A = \begin{pmatrix} \frac{-cos\theta^0 x_\xi^0}{|\mathbf{r}_\xi^0|^2} + \frac{x_\eta^0}{|\mathbf{r}_\xi^0||\mathbf{r}_\eta^0|} & \frac{-cos\theta^0 y_\xi^0}{|\mathbf{r}_\xi^0|^2} + \frac{y_\eta^0}{|\mathbf{r}_\xi^0||\mathbf{r}_\eta^0|} \\ y_\eta^0 & -x_\eta^0 \end{pmatrix},$$

$$B = \begin{pmatrix} \frac{-cos\theta^0 x_\eta^0}{|\mathbf{r}_\eta^0|^2} + \frac{x_\xi^0}{|\mathbf{r}_\xi^0||\mathbf{r}_\eta^0|} & \frac{-cos\theta^0 y_\eta^0}{|\mathbf{r}_\eta^0|^2} + \frac{y_\xi^0}{|\mathbf{r}_\xi^0||\mathbf{r}_\eta^0|} \\ -y_\xi^0 & x_\xi^0 \end{pmatrix},$$

$$\mathbf{f} = (cos\theta - cos\theta^0, V + V^0)^t.$$

A brute force calculation shows that B^{-1} exists when $sin\theta \neq 0$ and that

$$\det(B^{-1}A) = -\frac{|\mathbf{r}_\eta|^2}{|\mathbf{r}_\xi|^2} = -\text{aspect ratio squared}$$

$$\mathrm{Tr}(B^{-1}A) = 0.$$

It follows that the eigenvalues of $B^{-1}A$ are $\pm$ aspect ratio. Hence, the system

$$\mathbf{r}_\eta + B^{-1}A\mathbf{r}_\xi = B^{-1}\mathbf{f} \tag{3}$$

is hyperbolic and the local solution consists of left and right running waves.

The mixed problem for this set of equations consists of specifying initial data on $\eta = 0$ and boundary data on $\xi = 0$ and $\xi = \xi_{max}$. For the Steger-Chausse equations ($cos\theta = 0$), this problem is typically ill-posed because the boundary curves $\eta \rightarrow [x(\bar{\xi}, \eta), y(\bar{\xi}, \eta)]$, $\bar{\xi} = 0$ or ξ_{max} need not intersect the initial curve orthogonally. From the geometrical nature of this problem, it is clear that angle terms can be chosen so that Eq. (1) is well-posed. An important detail in this matter concerns the specification of boundary conditions. As the solution is locally characterised by a left and right running wave, only one piece of data may be specificed on a ξ = constant boundary. The second condition is constrained to satisfy the characteristic relations.

ALGORITHM DEVELOPMENT

Following Kinsey and Barth (1984), we consider a one-parameter family of two-level methods for integrating Eq. (3), vis

$$\mathbf{r}_{k+1} - \mathbf{r}_k = (1-\alpha)\left(\frac{\partial \mathbf{r}}{\partial \eta}\right)_k + \alpha\left(\frac{\partial \mathbf{r}}{\partial \eta}\right)_{k+1} \tag{4}$$

where $\mathbf{r}_k = \mathbf{r}(k\Delta\eta)$. For $\alpha = 0$, $\frac{1}{2}$, and 1 this produces an Euler explicit, trapezoidal rule, and Euler implicit integration respectively. Substitution of Eq. (3) into Eq. (4) leads to

$$\mathbf{r}_{k+1} - \mathbf{r}_k = (1-\alpha)\left[B^{-1}(\mathbf{f} - A\mathbf{r}_\xi)\right]_k + \alpha\left[B^{-1}(\mathbf{f} - A\mathbf{r}_\xi)\right]_{k+1} \tag{5}$$

where B^{-1}, A, and f are evaluated at the known k level. Rewriting this in delta law form and adding fourth-order smoothing in ξ results in

$$\left[I + \alpha(B^{-1}A)_k\delta_\xi - \epsilon(\nabla\Delta)^2_\xi\right](\mathbf{r}_{k+1} - \mathbf{r}_k) = \left[B_k^{-1}(\mathbf{f} - A\delta_\xi) + \epsilon(\nabla\Delta)^2_\xi\right]\mathbf{r}_k \tag{6}$$

This discretisation differs from that presented by Steger and Chaussee in that a delta formulation is employed, implicit dissipation is added, and a variable integration scheme is used. The latter option is used to control shock formation while the other options are important in smoothing initial discontinuities. In each situation, a bad solution is avoided by introducing extra smoothing at the cost of losing orthogonality. This tradeoff between smoothing and orthogonality can be unacceptable for severe geometries. In that case, a better strategy is to control local departure from orthogonality via angle specification. For example, this technique prevents shock formation by forcing initial fronts straddling a concavity in the data to propogate away from each other. A more detailed analysis of these features as well as formulas for the source terms is given in the full paper.

The boundary conditions for the mixed problem are theoretically obtainable from the characteristic relations. In practice, these proved to be too complicated and were replaced by boundary conditions consistent with the local form of the solution. For a left boundary these are

$$\hat{t}\cdot(\Delta\mathbf{r}_{j=1} - 2\Delta\mathbf{r}_{j=2} + \Delta\mathbf{r}_{j=3}) = 0 \tag{7a}$$

$$\hat{t}\cdot\Delta\mathbf{r}_\perp = 0 \tag{7b}$$

here $\hat{t}$ is a unit vector tangent to the boundary curve and $\Delta\mathbf{r}_\perp$ is the vector perpendicular to $\Delta\mathbf{r}$. Note that these boundary conditions are exact on linear data.

APPLICATIONS

Three applications are presented to demonstrate the algorithm described above. Other applications as well as a more detailed discussion are presented in the full paper. The first example demonstrates the use of smoothing and angle specification to control the propogation of initial singularities. In the second example, grid lines are prevented from crossing by adjusting angle source terms at the initial surface. The last example shows an internal grid. This was generated by solving a mixed problem and shooting to the outer boundary.

CONCLUSIONS

A grid generation algorithm based on a 2x2 hyperbolic system of equations has been developed for constructing meshes in two dimensions. By adding an angle source term to the Steger-Chaussee equations and following the Kinsey-Barth algorithm, the standard objections to using hyperbolic systems for mesh generaton have been overcome. Novel applications of this approach include controlling the propogation of initial singularities, preventing shock formation (crossing grid lines), and the generation of internal grids.

REFERENCES

Kinsey, D. W., and Barth, T. J., *Description of a Hyperbolic Grid Generating Procedure for Arbitrary Two-Dimensional Bodies*, AFWAL TM 84-191-FIMM, Jul. 1984.

Steger, J. L. and Chaussee, D. S., *Generation of Body Fitted Coordinates Using Hyperbolic Partial Differential Equations*, SIAM J. Sci. Stat. Comput., Vol. 1, No. 4, Dec. 1980.

Thompson, J. F., Warsi, Z., and Mastin, C. W., *Numerical Grid Generation*, North-Holland, 1985.

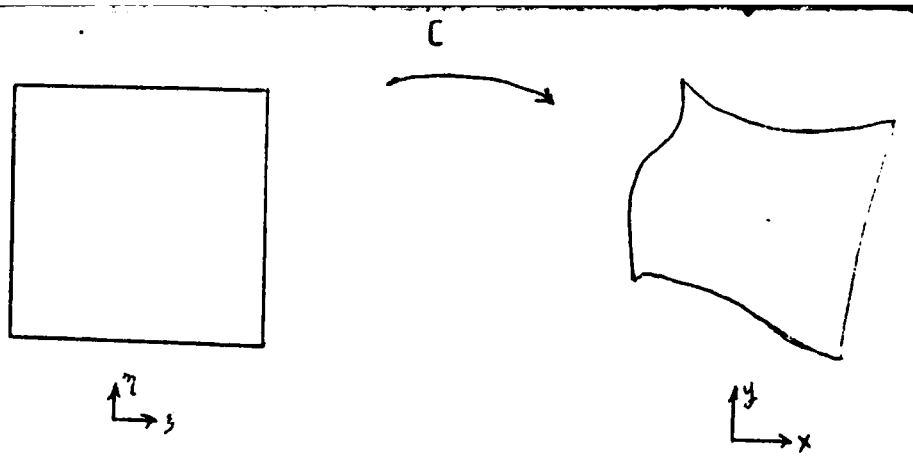

Fig. 1

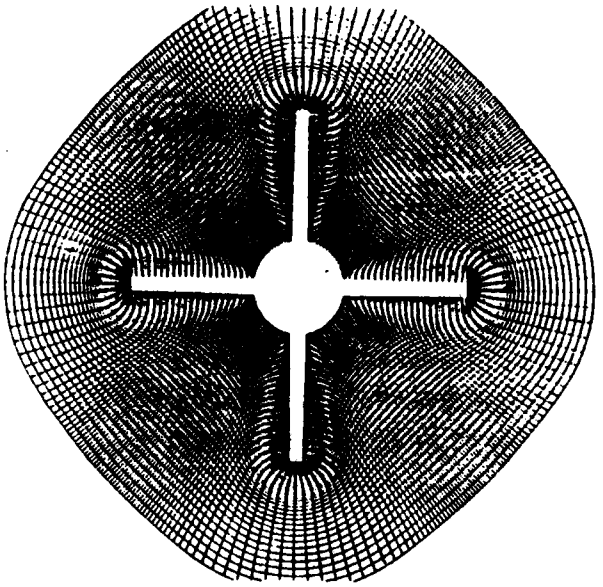

Fig. 2

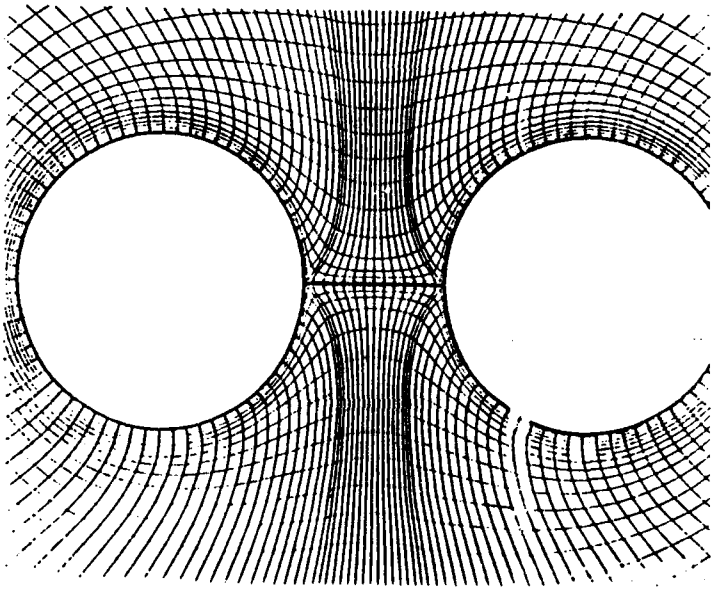

Fig. 3

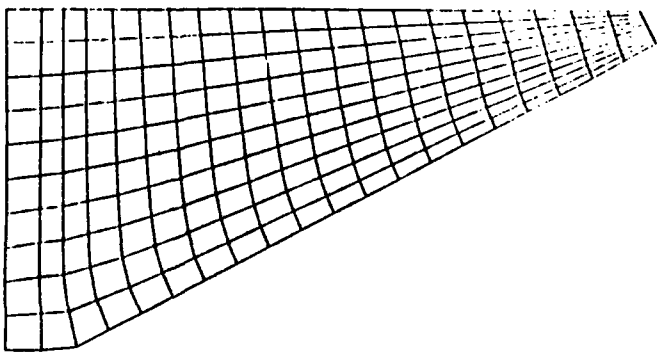

Fig. 4

A QUADRATURE APPROXIMATION OF THE BOLTZMANN COLLISION OPERATOR IN AXISYMMETRIC GEOMETRY AND ITS APPLICATION TO PARTICLE METHODS

P. DEGOND, F.J. MUSTIELES, B. NICLOT

Ecole Polytechnique, Centre de Mathematiques Appliquees
Unite de Rech. Associee Au CNRS-756, 91128 Palaiseau, France

This paper is devoted to a presentation of a new numerical method for the approximation of the non-linear Boltzmann equation.

In a first part, we present an explicit expression of the two-particle Boltzmann collision operator in an axisymmetric geometry (for distributions functions which are invariant under the group of rotations about a fixed axis), cf. [1]. Indeed, in numerous situations (study of shock layers in gas dynamics, homogeneous field formalism in semiconductor physics), such a geometric invariance is presented and seldom used to reduce the computational cost of the simulation. Our reduced expression of the collision operator in axisymmetric geometry involves an integral operator. The integration domain of which has a lower dimensionality than for the general Boltzmann operator.

We take advantage of this feature to propose a direct evaluation of the collision operator by quadrature formulae. This is in contrast to the usual numerical methods which always rely on a Monte-Carlo procedure [2]. We couple this new approximation method of the collision operator to a particle method for the approximation of the differential part of the Boltzmann equation, using the general ideas of P.A. Raviart and S. Mas-Gallic [3,4].

This numerical scheme has been applied to different test cases, with an emphasis on the verification of the momentum and energy conservation by the approximate collision operator (cf. figures). It has also been employed for a real case arising in semiconductor physics. Other tests are in progress. The conclusions of the tests are encouraging for the applicability of the method to other problems, cf [5].

References :

[1] B. Niclot, report N° 164, Centre de Mathématiques Appliquées, Ecole Polytechnique, 1987 (to be published)

[2] K. Nanbu, in Proceedings of the Fifteenth International Symposium on Rarefied Gas Dynamics, Grado, Italy, edited by V. Boffi and C. Cercignani (Teubner, Stuttgart, 1986), p. 369

[3] S. Mas-Gallic, Transport Theory and Statistical Physics 16, (1987), p. 855

[4] P.A. Raviart, in Lecture Notes in Mathematics, Vol. 1127, (Springer, Berlin, 1983), p. 243

[5] B. Niclot, thèse, Ecole Polytechnique, 1987.

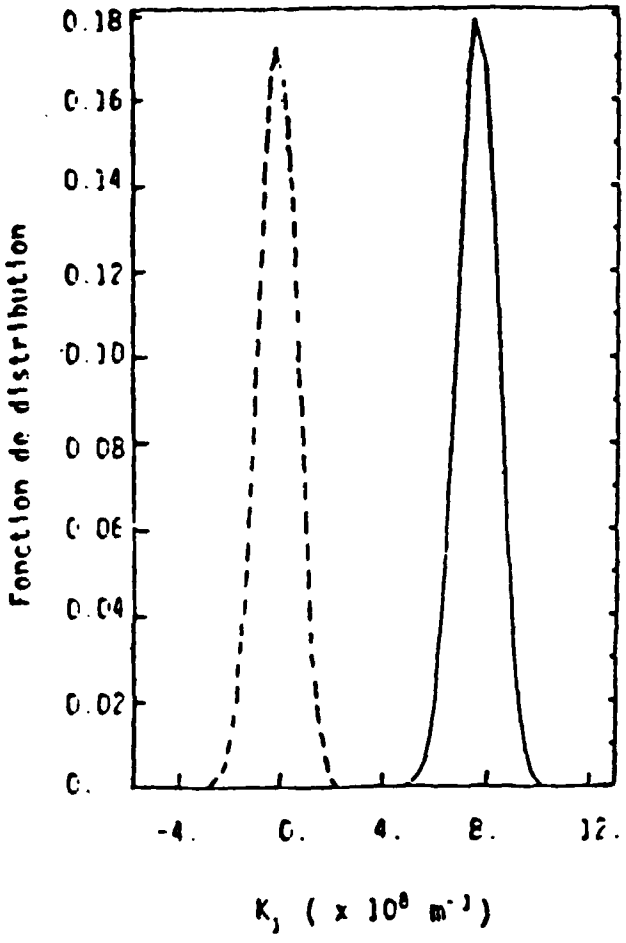

Fig. 1 Solution of the equation $(\partial f/\partial t) + (qE/m)(\partial f/\partial v_1) = Q(f)$ where $Q(f)$ is the two particle Boltzmann collision operator. The initial data (dashed line) is a Maxwellian distribution. The solid line is the solution after 200 time steps. We obtain a displaced Maxwellian by the action of the electric field ($E = 10^5$ vm^{-1}) with a relative error about 5 %.on the maximum.

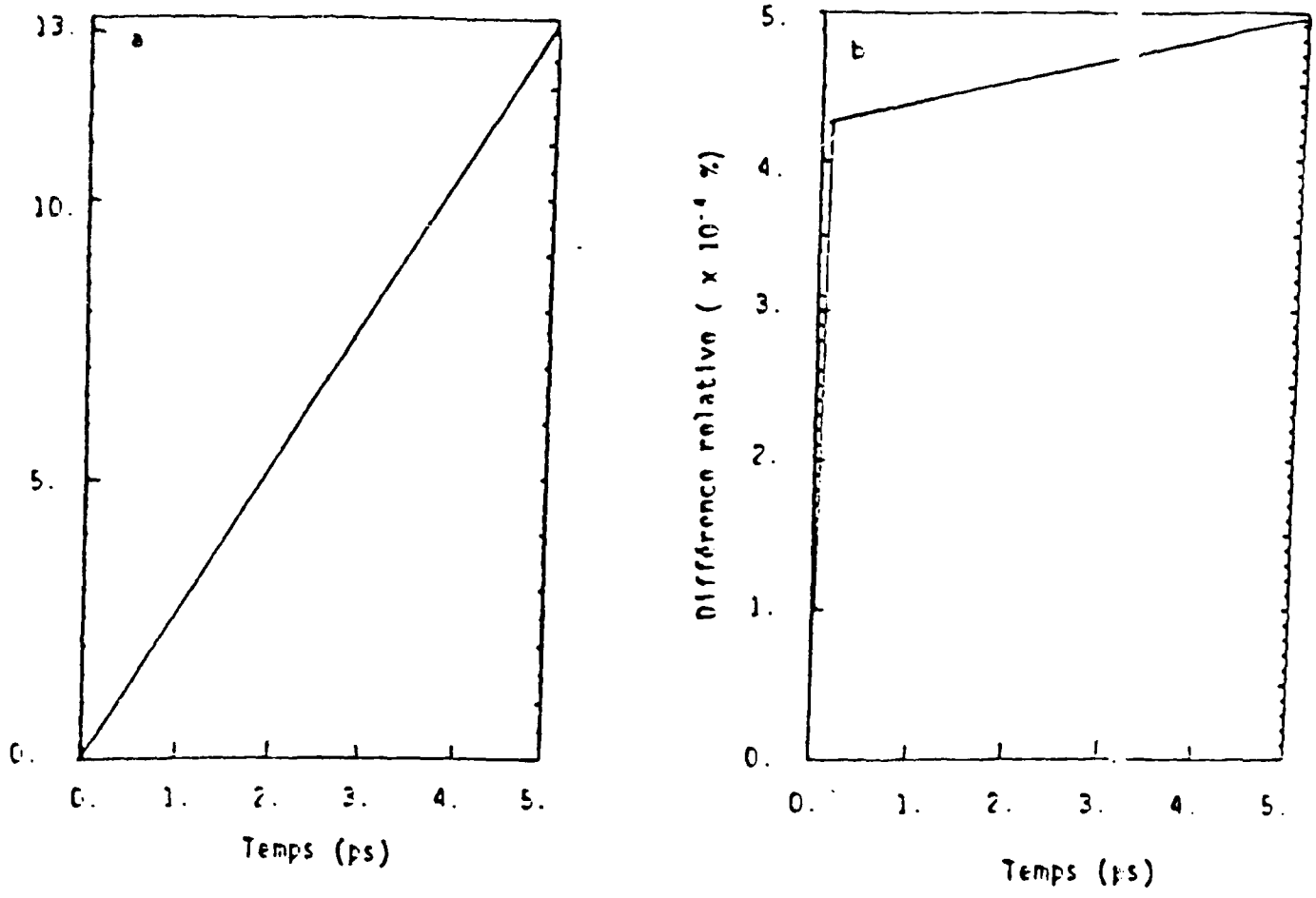

Fig 2 Mean velocity (figure a) and relative error (figure b) versus time for the equation $(\partial f/\partial t) + (qE/m)(\partial f/\partial v_1) = Q(f)$ where $Q(f)$ is the two particle Boltzmann collision operator and the initial data is a Maxwellian distribution. We obtain after 200 time steps a relative error lower than 0,001 %.

A Treatment of Discontinuities in Shock Capturing Finite Difference Methods

Mao De-kang
Department of Mathematics
Shanghai University of Science and Technology

1. The partial differential equation

We consider the following nonlinear hyperbolic equation of scalar conservation law

$$u_t + f_x(u) = 0 \tag{1}$$

with initial value $u(x,0) = u_0(x)$. Here f is a twice differentiable, convex function, i.e. $f'' > 0$. We would like to mention here that the treatment presented in this artical can be extended to the system of conservation laws. We have already applied this method to the system of isentropic flow (refer to [1]).

2. The principle idea

As we know, the so-called weak solution of (1) is a bounded measurable function $u(x,t)$ which satisfies

$$\int_{R\times]0,T[} (u\Phi_t + f(u)\Phi_x)dxdt + \int_R u_0(x)\Phi(x,0)dx = 0 \tag{2}$$

for all $\Phi \in C_0^2(R\times[0,T[)$. (2) means that the equality (1) is correct only in distribution sense. Hence if $u \in$ BV space, equation (1) is allowed to be nonvalid on a set of measure zero. In fact, such a measure zero set often corresponds to the discontinuities of solution.

To approximate equation (1), we can use a type of difference schemes

$$L_h u_h = 0. \tag{3}$$

Corresponding the fact that equation (1) can be nonvalid on a set of measure zero, we can add a grid function R_h to the right-side of (3), which can be nonzero on some grids. But in order to keep the consistency of discrete equation (3) with (1), we must make R_h approach zero in distribution sense as h,τ tends to zero. Here h and τ are mesh sizes. We shall call R_h the artificial terms.

3. The construction of artificial terms

For convenience we only consider (3) a general three point scheme

$$u_j^{n+1} = u_j^n + \sigma(h_{j+1/2}^n - h_{j-1/2}^n) \tag{4}$$

here $h_{j+1/2}^n = h(u_{j+1}^n, u_j^n)$, $h(u,u) = f(u)$, $\sigma = \tau/h$ is the mesh ratio. For clearity of the approach we start with a very special case, i.e. a Riemann problem which involves a shock facing to the right. Obviously, it is the simplest case of discontinuity. We consider in this case how to construct the artificial terms properly, and then extend the idea here to general case.

Riemann problem: The initial value is

$$u_0(x) = \begin{cases} u_l & x \le 0 \\ u_r & x > 0 \end{cases}$$

here $u_l > u_r$, and $s = (f(u_l) - f(u_r))/(u_l - u_r) > 0$. The shock divides the x-t plane into two parts. In the left part $u(x,t) \equiv u_l$ and in the right one $u(x,t) \equiv u_r$.

Now let us add an artificial term $-p^n_{j+1/2}/\sigma$ to the numerical flux $h^n_{j+1/2}$ in scheme (4). It is then reduced to

$$u^{n+1}_j = u^n_j - \sigma(h^n_{j+1/2} - h^n_{j-1/2}) + p^n_{j+1/2} - p^n_{j-1/2} \tag{5}$$

Because the weak solution of Riemann problem has the properties described above, naturally we consider constructing the artificial terms to make the solution also has a similar construction. We try to let the numerical solution u_h involve only one discrete shock, which on every time level is a jump occuping only two meshes. On its left $u_h \equiv u_l$, and on its right $u_h \equiv u_r$. It leads us to consider the following problem: suppose that on n level the numerical solution u^n_j has just a jump which is located on $j^* - 1 \sim j^* + 1$, then how to construct the artificial terms to make u^{n+1}_j keep the same properties, i.e. its jump is only over two meshes.

In order to make the artificial terms local, we only take $p^n_{j^*-1/2}$ and $p^n_{j^*+1/2}$ to be nonzero. Considering that the shock should face to right, we have two choices:

1) The jump of numerical solution on $n+1$ level is located on $j^* - 1 \sim j^* + 1$ (as shown in Fig. 1). Write the difference equations at points $j^* - 1$, j^*, and $j^* + 1$ respectively we get

$$\begin{aligned} u_l &= u_l - \sigma(h^n_{j^*-1/2} - f(u_l)) + p^n_{j^*-1/2} \\ u^{n+1}_{j^*} &= u^n_{j^*} - \sigma(h^n_{j^*+1/2} - h^n_{j^*-1/2}) + p^n_{j^*+1/2} - p^n_{j^*-1/2} \\ u_r &= u_r - \sigma(f(u_r) - h^n_{j^*+1/2}) - p^n_{j^*+1/2} \end{aligned} \tag{6}$$

Solve them to obtain

$$\begin{aligned} u^{n+1}_{j^*} &= u^n_{j^*} - \sigma(f(u_r) - f(u_l)) \\ p^n_{j^*-1/2} &= \sigma(h^n_{j^*-1/2} - f(u_l)) \\ p^n_{j^*+1/2} &= -\sigma(f(u_r) - h^n_{j^*+1/2}) \end{aligned} \tag{7}$$

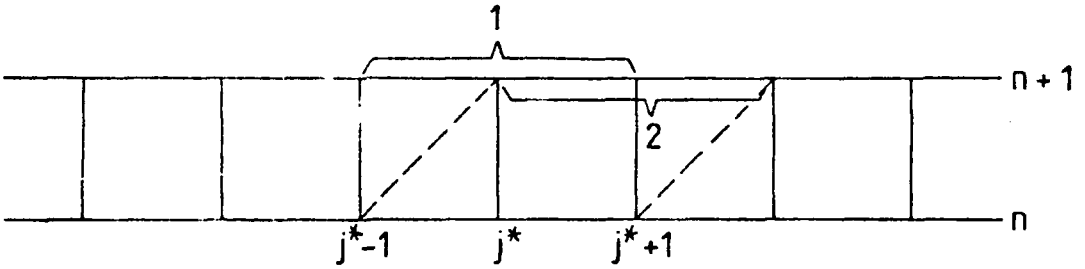

Fig. 1

2) The jump on $n+1$ level is located on $j^* \sim j^* + 2$ (also as shown in Fig. 1). This case is treated in a fashion analogue to the above situation.

Hence, there are essentially two different ways to construct the artificial terms. We cannot use only one way from the beginning to the end. So in a correct algorithm the two ways must be taken appropriately. Then a question arises: when should the first or second way be taken? We now consider it at a different angle. Multiplying equation (5) by $\Phi^n_j h = \Phi(jh, n\tau)h$, summing them by parts with respect to j and n, we arrive at

$$\sum_{n=0}^{\infty}\sum_{j=-\infty}^{\infty}\left[\frac{\Phi^{n+1}_j - \Phi^n_j}{\tau}u^{n+1}_j + \frac{\Phi^n_j - \Phi^n_{j-1}}{h}h^n_{j-1/2}\right]h\tau + \sum_{j=-\infty}^{\infty} h\Phi^0_j u^0_j$$

$$= \sum_{n=0}^{\infty}\sum_{j=-\infty}^{\infty}\frac{\Phi^n_j - \Phi^n_{j-1}}{\tau}p^n_{j-1/2}h\tau \tag{8}$$

When h, τ tend to 0, the left side of (8) approaches to the left side of (2). In order that the approximate solution tends to the weak solution, the right side of (8) must approach to zero as $h, \tau \to 0$. Notice that the numerical solution has only one jump on every time level. Assume that it is located on $j^n - 1 \approx j^n + 1$. Also notice that at every time level only two artificial terms, $p^n_{j^n-1/2}$ and $p^n_{j^n+1/2}$ are nonzero. Therefore, the right side of (8) is reduced to

$$\sum_{n=0}^{\infty}\left(\frac{\Phi^n_{j^n} - \Phi^n_{j^n-1}}{h} p^n_{j^n-1/2} + \frac{\Phi^n_{j^n+1} - \Phi^n_{j^n}}{h} p_{j^n+1/2}\right) h\tau\sigma^{-1} \tag{9}$$

If $\sigma \geq \delta > 0$, and $p^n_{j^n-1/2}$, $p^n_{j^n+1/2}$ are uniformly bounded with respect to h, τ and n, we can easily see that (9) tends to zero as $h, \tau \to 0$. The main consideration of our method is to keep the artificial terms $p^n_{j^n-1/2}$ and $p^n_{j^n+1/2}$ uniformly bounded. One finds that they will be uniformly bounded if $u^n_{j^n}$, the value of numerical solution at the middle point of the jump, is uniformly bounded.

We now still assume that the jump on n level is located on $j^* - 1 \sim j^* + 1$ (i.e. $j^* = j^n$). From (7) we find that in the first case, $u^{n+1}_{j^*}$, the value at middle point on $n+1$ level, increases by $\sigma(u_l - u_r)$ over $u^n_{j^*}$. In the second case, one finds that $u^{n+1}_{j^*+1}$, also the value at middle point on $n+1$ level, decreases by $(1-\sigma s)(u_l - u_r)$ down $u^n_{j^*}$, if CFL-condition, $|\sigma f'(u)| \leq 1$ holds. It is then easy to see that in order to keep $u^n_{j^n}$ uniformly bounded we should make the algorithm as follows: When $u^n_{j^n}$ becomes too small, the first way is taken, otherwize the second way is taken. In my papers I do this as follows: When

$$u^n_{j^n} < u_l + \sigma(f(u_l) - f(u_r)) \tag{10}$$

is true the first way is taken, otherwize the second way. In doing so, not only the artificial terms are kept uniformly bounded, but also the value of numerical solution at middle point, $u^n_{j^n}$, varies only between u_l and u_r.

4. General case

In general case we cannot apply this technique to all the meshes on which u^n_j decreases with respect to j. Because if doing so, we cannot make the artificial terms only exist locally. Therefore we choose a positive parameter $\alpha > 0$, and only apply the technique to the mesh sections on which the u^n_j decreases, and its jump is greater than α. We call these mesh sections on which the technique is applied the 'generated sections'. The generated section occupies at least two meshes. Then the computation on generated sections proceeds as follows: If, for example, the generated section occupies two meshes $j^* - 1 \sim j^* + 1$, then we use formula (5) to compute the u^{n+1}_j, with the artificial terms $p^n_{j^*-1/2}$, $p^n_{j^*+1/2}$ defined by (7) only in which u_l is replaced by $u^n_{j^*-1}$ and u_r by $u^n_{j^*+1}$.

The exact weak solution may involve many interactions of shocks. These cases may also occur in the numerical computation, i.e. discrete shocks meet and merge in a proper way. The algorithm handles all these cases.

5. The main theoretical results

a) Under certain conditions one can choose a convergent subsequence from the numerical solutions, and its limit is a weak solution of (1).

The so-called 'certain conditions' mentioned above contain mainly two parts. One is that the numerical solution u^n_j and its total variation respect to j are uniformly bounded. The other implies that the artificial terms exist only locally.

b) If we take the original scheme (4) to be TVD scheme (so-called after Harten [2]), i.e.

$$u^{n+1}_j = u^n_j + C^n_{+,j+1/2}(u^n_{j+1} - u^n_j) - C^n_{-,j-1/2}(u^n_j - u^n_{j-1}) \tag{11}$$

here

$$C^n_{\pm\, j+1/2} \geq 0, \quad 0 \leq C^n_{+,j+1/2} + C^n_{-,j+1/2} \leq 1$$

then the 'certain conditions' in a) can be satisfied by the algorithm. In fact we can prove the algorithm in this case also TVD in a slightly different sense.

c) If make some further improvement to the algorithm, then under certain conditions we can prove that the above weak solution satisfies entropy condition for any convex entropy $V(u)$, i.e.

$$\int_0^\infty \int_{-\infty}^{\infty} (\Phi_t V(u) + \Phi_x F(u)) dx dt \geq 0 \tag{12}$$

for all test functions $\Phi \in C^2$, $\Phi \geq 0$, with bounded support. Here $F(u) = \int V'(u) f'(u) du$.

As we know that the entropy violation in computation often occurs in the case when numerical solution increases with a great jump. In this case the numerical result may be not a rarefaction wave, but rarefaction shock. The above so-called 'some further improvement' is applied to these sections of numerical solution to avoid the entropy violation.

d) Also the 'certain conditions' can be satisfied by the algorithm if the original scheme (4) is taken to be TVD.

6. High resolution treatment of discontinuities

From the previous discussion we see that the evolution of a discrete shock is mainly determined by the value of numerical solution at the middle point of a generated section. Hence there must be some relation between the value at the middle point and the shock position at every time level. We therefore use this value to determine still further the shock position in the generated section at every time level. If the generated section occupies only two grids $j^n - 1 \approx j^n + 1$, we use the following formula

$$spos^n = jh - 0.5h + h\frac{u^n_{j^n} - u^n_{j^n+1}}{u^n_{j^n+1} - u^n_{j^n-1}} \tag{13}$$

to compute the coordinate of shock position $spos^n$. For generated sections of more than two grids, we also have a similar formular. In fact, if we use the above formula in previous Riemann problem involving a shock, we can find that the shock is just at the same position as the exact solution at every time level.

7. Numerical experiment

We take the $f(u) = \frac{1}{2}u^2$, the original scheme to be Lax-Wendroff scheme with a numerical viscosity which is very much like that of Majda ([3]), and we use the algorithm to compute many examples. Here we only present two of them.

Example 1. The initial value is

$$u_0(x) = \begin{cases} 2 & x < 0.205 \\ 0 & x \geq 0.205 \end{cases}$$

This problem involves a shock with speed of 1. Let $\alpha = 0.5$, $h = 0.01$, $\sigma = 0.45$. The numerical result is presented in Fig. 2.

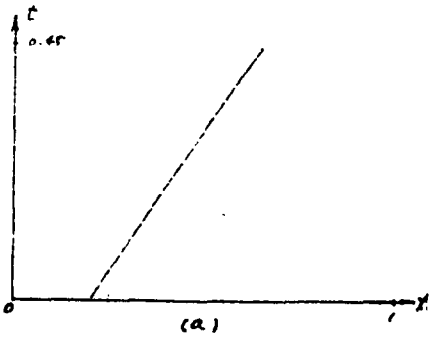

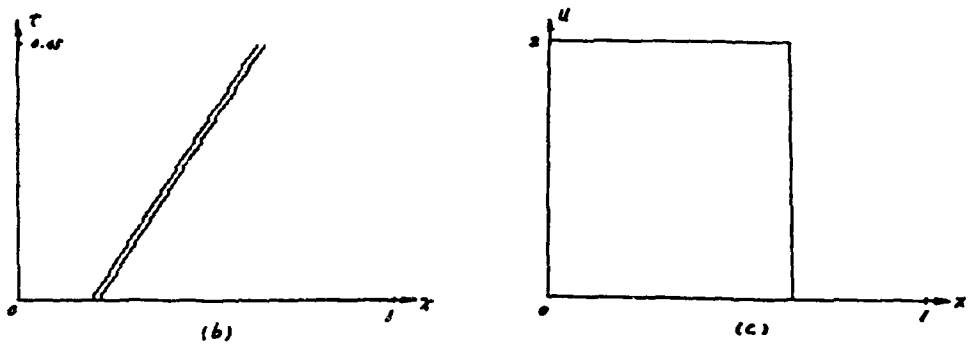

Fig. 2

Fig. 2-a shows a shock curve which is drawn by connecting all the *spos*^{n} on every time level successively. Fig. 2-b shows the discrete shock. Fig. 2-c shows the numerical solution on the 100th level. Fig. 2 indicates that the numerical solution obtained is almost an exact solution.

Example 2. The initial value is

$$u_0(x) = \begin{cases} 1 & x < 0.185 \\ -1 & 0.185 \le x < 0.2 \\ \frac{x-0.5}{0.3} & 0.3 \le x < 0.8 \\ 1 & 0.8 \le x \le 1 \end{cases}$$

This problem involves a shock with speed of 0, and a rarefaction wave. Let $\alpha = 0.1$, $h = 0.01$, $\sigma = 0.9$. The numerical result is presented in Fig. 3.

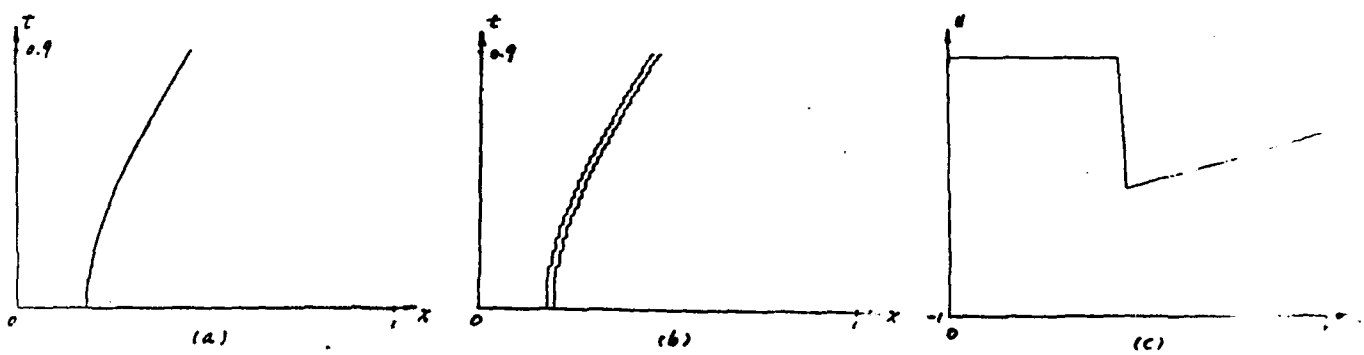

Fig. 3

Fig. 3-a shows the shock curve, Fig. 3-b shows the discrete shock, Fig. 3-c shows the numerical solutio the 100th level.

References

[1] Mao De-kang: A Difference Scheme for Shock Calculation
J. Computational Math. No. 3 (1985) 265 - 282 (in Chinese)

[2] A. Harten: High Resolution Schemes for Hyperbolic Conservation Laws
J. Comp. Phys. 49 (1983) 357 - 393

[3] A. Majda, S. Osher: Numerical Viscosity and the Entropy Condition
Comm. Pure Appl. Math. Vol. 32 (1979) 797 - 838

BOUNDARY CONDITIONS FOR NONLINEAR HYPERBOLIC SYSTEMS OF CONSERVATION LAWS.

François DUBOIS & Philippe LE FLOCH

Ecole Polytechnique
Centre de Mathématiques Appliquées
91128 Palaiseau Cédex - France

1. Introduction

We study initial-boundary value problems for non-linear hyperbolic systems of conservation laws. Recall that with strong Dirichlet boundary conditions the associated problem is not well posed. Generally there is neither existence nor uniqueness. Thus weaker conditions are necessary ; in the linear case by example we know that data are given only on incoming characteristics.

We consider two formulations of boundary conditions. A first approach is based on vanishing viscosity method and a second one is related to the Riemann problem.

Equivalence between these conditions is studied. The latter formulation is extended to treat numerically physically relevant boundary conditions. Monodimensional experiments will be presented.

2. Boundary entropy inequality (first formulation)

We consider a non-linear hyperbolic system of conservation laws in one space dimension :

$$(1) \qquad \frac{\partial u}{\partial t} + \frac{\partial}{\partial x} f(u) = 0 \quad ; \; u(x,t) \in \mathbb{R}^n \; , \; f(u) \in \mathbb{R}^n .$$

and we suppose that there exists at least a pair (η,q) of entropy-flux. The initial boundary value problem obtained by the viscosity method ($\epsilon > 0$)

$$(2) \qquad \begin{cases} \dfrac{\partial u^\epsilon}{\partial t} + \dfrac{\partial}{\partial x} f(u^\epsilon) = \epsilon \dfrac{\partial^2 u^\epsilon}{\partial x^2} & x > 0 \; , \; t > 0 \\ u^\epsilon (x,0) = v_0(x) & x > 0 \\ u^\epsilon (0,t) = u_0(t) & t > 0 \end{cases}$$

admits a unique solution u^ϵ and we study the behaviour of u^ϵ at the boundary as ϵ tends to zero. We have

Theorem 1 Suppose that u^ϵ is bounded in $W^{1,1}_{loc}(\mathbb{R}^+ \times \mathbb{R}^+, \mathbb{R}^n)$ and converges in L^1_{loc} to u as $\epsilon \to 0$. For each admissible pair (η,q) of entropy-flux we have :

$$(3) \quad q(u(0^+,t)) - q(u_0(t)) - \eta'(u_0(t)).(f(u(0^+,t)) - f(u_0(t))) \leq 0$$

between the taken value $u(0^+,t)$ and the prescribed value $u_0(t)$ at the boundary.

This result was obtained in [4] and the inequality (3) was independently proposed in [1,6] by other methods. Then given a state u_0, we may define a (first) set of admissible values at the boundary :

$$E(u_0) = \{ \, v \in \mathbb{R}^n \; , \; q(v) - q(u_0) - \eta'(u_0).(f(v) - f(u_0)) \leq 0$$

$$\forall (\eta,q) \text{ pair of entropy - flux} \, \}$$

Therefore the boundary condition is :

$$u(0^+,t) \in E(u_0(t)) \; , \; t > 0.$$

The set $E(u_0)$ is described in [4] in the cases of both linear systems and (non necessarily convex) scalar conservation laws. For instance, in the case of Burgers' equation we have :

Proposition 1 [5] $\quad u \in \mathbb{R}$, $f(u) = \frac{1}{2} u^2$

$$E(u_0) =]-\infty , -u_0] \cup \{u_0\} \qquad u_0 \geq 0$$
$$E(u_0) =]-\infty , 0] \qquad u_0 \leq 0$$

We enphasize that by the lack of entropy functions, there is no sufficiently information to explicit the E-sets in general cases.

3. Approach by the Riemann problem (second formulation)

For the second formulation of the boundary condition [3,4] we suppose that each Riemann problem $R(u_L, u_R)$ associated with (1) admits a unique entropy solution denoted by $w\left(\frac{x}{t} ; u_L , u_R\right)$. We define a second set of admissible values :

$$V(u_0) = \{ w(0^+ ; u_0 , u_R),\ u_R \text{ varying in } \mathbb{R}^n \}$$

we have the following result :

Theorem 2 Let v_0, u_0 be constant states. The problem

$$(4) \quad \begin{cases} \dfrac{\partial u}{\partial t} + \dfrac{\partial}{\partial x} f(u) = 0 & x > 0,\ t > 0 \\ u(x,0) = v_0 & x > 0 \\ u(o,t) \in V(u_0) & t > 0 \end{cases}$$

is well posed in the class of functions which consist of constant states separated by at most n elementary waves (rarefactions, shocks, contacts).

Proposition 2 In particular cases of strictly hyperbolic linear systems and (non necessarily convex) scalar conservation laws, we have

$$E(u_0) = V(u_0) \qquad \forall u_0 .$$

The advantage of the second formulation is that V can be easily computed. For the p-system, $V(u_0)$ is exactly the 1-wave containing u_0. And, in [3,4] we have given details on the V-sets in the case of barotropic Euler equations.

4. Nonlinear numerical boundary conditions for Euler equations

Classical boundary conditions for Euler equations are related to the theory of characteristics. As usual, we distinguish between four cases : the fluid may be sub or super-sonic at the in or out-flow and physical parameters can be associated with each case ([7]) :

(i)	supersonic inflow	:	a given state u_0
(ii)	subsonic inflow	:	total enthalpy and physical entropy
(iii)	subsonic outflow	:	static pressure
(iv)	supersonic outflow	:	none data.

We review briefly the main ideas of [2]. In a Godunov-type scheme the computation of a numerical flux ϕ at the boundary is just necessary to define the numerical evolution. In each case (i) - (iv) a partial Riemann problem P (M, z) can be posed between the above described manifold M associated with each condition, and the taken value near the boundary z . The flux ϕ is then computed thanks to 3 ; 2 ; 1 ; 1 or 0 waves respectively between M and z. Numerical 1D test cases on shock tube and nozzles involving the first order Osher scheme will be presented at the conference, showing the attractive convergence properties of the boundary conditions in evolution towards steady state.

References

1. J. AUDOUNET, Seminar, Toulouse III university, 1984-85
2. F. DUBOIS, to appear
3. F. DUBOIS, P. LE FLOCH, C.R.Ac.Sc. Paris, tome 304, serie 1, n°3, 198
4. F. DUBOIS, P. LE FLOCH, Internal Report n° 155, CMAP, Ecole Polytechnique, J. of Dif. Equations, 1987
5. P. LE FLOCH, Internal Report n°144, CMAP, Ecole Polytechnique, Math. Meth. in Appl. Sciences, 1988
6. P. MAZET, Internal Report, CERT, Toulouse 1987
7. H. VIVIAND, J.P. VEUILLOT, T.P. ONERA 1978-4

ON GODUNOV TYPE METHODS

by B. Einfeldt
RWTH Aachen, West Germany

In the last several years Godunov-type methods have been applied successfully for the calculation of inviscid compressible flow. In practice these methods are characterized by their robustness and their possibility of computing flows with very complicated shock structures.

Godunov [7] used the nonlinear Riemann problem as "building block" for his numerical method. This allows a self operating treatment of weak and strong shock waves. The numerical solution represents shocks nearly optimally thin, typical is a monotone profile over one to three computational cells without unphysical oscillations. From the theoretical point of view Godunov's method is an extension of the classical Courant-Isaacson-Rees scheme [8]. The underlying physical picture of Godunov's method is useful for the interpretation of certain schemes and to construct new ones.

The recent interest in Godunov-type methods was engendered by van Leer, who realized the importance of Godunov's method and invented a second-order extension. Further development along this line were made by Colella and Woodward [1], Colella [2], and Fryxell, Woodward, Colella, and Winkler [16]. A comparison of some of these Godunov-type methods with more classical methods can be found in [17].

The disadvantage of Godunov's method and its higher-order extensions is the difficulty of solving the nonlinear Riemann problem exactly, especially for materials with complex equations of state. The exact solution of the Riemann problem requires an iterative procedure, which leads to relatively complex and time consuming numerical codes. Since computational efficiency is a major requirement for applied numerical methods, this has restricted the extensive applications of Godunov-type methods.

To overcome this drawback, several approximations to the Riemann problem have been developed. For the ideal equation of state there are by now particular

approximate "Riemann solver" available, among them are the methods developed by Osher and Solomon [9], Roe [12] and Pandolfi [10]. These linear approximations are also of interest for the aerodynamic field where they provide a foundation for the construction of more elaborate schemes [13], [14]. More analytical effort is required if a general equation of state is considered. So far, only two Riemann solvers have been developed in this case. One iterative method by Colella and Glaz [3] and a second explicit method by Dukowicz [5].

In the presentation we describe a new approximate Riemann solver [5] for compressible gas flow. In contrast to previous Riemann solvers, where numerical approximations for the pressure and the velocity at the contact discontinuity are computed, we derive a numerical approximation for the largest and smallest signal velocities in the Riemann problem. Having obtained the numerical signal velocities we use theoretical results by Harten, Lax, and van Leer [8] to obtain the full approximation. A stability condition for the numerical signal velocities is given. We show that the addition of an artificial shock viscosity term of the van Neumann type is equivalent to the spreading of the numerical signal velocities. Thus we obtain a close relationship to artificial shock viscosity methods [11]. The great advantage of the Riemann solver is its simplicity. The approximation substantially reduces the program's complexity while retaining essential features of Godunov's method, especially the accurate approximation of shock waves. The computation of the signal velocities for a general equation of state will be discussed. We show a relation to the recent generalized Roe Average of Vinokur [15].

Numerical results for the focussing of a plane shock wave in air $\gamma = 1.4$ and a typical shock tube problem for some specimen equations of state are shown.

REFERENCES

[1] P. Colella and P. R. Woodward, "The piecewise-parabolic method (PPM) for gas-dynamical simultations", J. Compt. Phys. 54 (1984).

[2] P. Colella, "A direct Eulerian MUSCL scheme for gas dynamics", SIAM J. Sci. Statist. Compt. 6 (1985).

[3] P. Colella and H. M. Glaz, "Efficient Solution Algorithms for the Riemann Problem for Real Gases", J. Compt. Phys. 59 (1985).

[4] J. K. Dukowicz, "A General, Non-Iterative Riemann Solver for Godunov's Method", J. Compt. Phys. 61 (1985).

[5] B. Einfeldt, "On Godunov-Type methods for Gas Dynamics", to appear in SIAM Jou. Numer. Anal.

[6] B. Einfeldt, "On Godunov-Type methods for Euler's equation with a general equation of state", to appear in the Proceedings of the 16th International Symposium on Shock Tubes and Waves.

[7] S. K. Godunov, "A difference scheme for numerical computation of discontinuous solutions of equations of fluid dynamics", Mat. Sb. 47, (1959).

[8] A. Harten, P. D. Lax, and B. van Leer, "On upstream differencing and Godunov-type schemes for hyperbolic conservation laws", SIAM Review 25, (1983).

[9] S. Osher and F. Solomon, "Upwind difference schemes for hyperbolic systems of conservation laws", Math. Comp. 38, (1982).

[10] M. Pandolfi, "A contribution to the numerical prediction of unsteady flows" AIAA j. 22, (1984).

[11] R. D. Richtmyer and K. W. Morton, "Difference Methods for Initial Value Problems", Wiley Interscience, New York, (1967).

[12] P. L. Roe, "Approximate Riemann solvers, parameter vectors, and difference schemes", J. Compt. Phys. 43, (1981)

[13] P. L. Roe, "The use of the Riemann problem in finite-difference schemes", Lecture Notes in Physics 141, Springer Verlag, New York, (1981)

[14] P. L. Roe, "Some contributions to the modeling of discontinuous flows", Lecture Notes in Applied Mathematics 22, (1985)

[15] M. Vinokur, "Generalized Roe Averaging for Real Gas" , NASA Contractor Reaport, in preparation.

[16] P. Woodward, P. Colella, B. A. Fryxell, and K. W. Winkler, "An Implicit-Explicit Hybrid Method for Lagrangian Hydrodynamics", J. Compt. Phys., (1986)

[17] P. Woodward and P. Colella, "The numerical simulation of two-dimensional fluid flow with strong shock", J. Compt. Phys. 54, (1984)

Time-Marching Method to Solve Steady Incompressible Navier Stokes Equations for Laminar and Turbulent Flow

by

Peter Eliasson and Arthur Rizzi
FFA The Aeronautical Research Institute of Sweden
161 11 Bromma, Sweden
and
H.I. Andersson
Norwegian Institute of Technology
Trondheim, Norway

1 INTRODUCTION

Recently Müller and Rizzi developed a Navier Stokes solver based on an explicit Runge-Kutta finite volume method to simulate laminar compressible flows over wings [1]. In this paper we are concerned with incompressible flow. If we were to simply apply the compressible code to this problem we would find that it would not converge well at all because with decreasing Mach number sound waves travel at a speed much larger than the speed of convection and they dominate the system making it stiff. This increasing disparity in wave speeds causes the governing system of equations to be poorly conditioned, and the stability of the computation is greatly impaired. If, however, the interest is only the steady flow, artificial compressibility is one way round the difficulty, because this approach removes the sound waves from the system by prescribing a pseudotemporal evolution for the pressure through the continuity equation which is hyperbolic and which converges to the true steady state value.

Our purpose here is to prescribe a rather general numerical method that takes the artificial compressibility approach for solving the steady incompressible Navier Stokes equations. We show how it leads to a hyperbolic/parabolic system, carry

out a numerical study of its condition, set forth the CFL stability limit for the time integration, and develop a $k-\epsilon$ turbulence model. Appropriate numerical far-field and solid-wall boundary conditions are formulated also.

2 MATHEMATICAL MODEL

Since the continuity equation for incompressible flow contains no time dependent term, an artificial time dependent term is added to the continuity equation. This is done by using the method proposed by Chorin [1]. The Navier-Stokes equations governing an incompressible flow, using the above method for the continuity equation, can be stated in the following way:

$$\frac{1}{\rho_0}\frac{\partial p}{\partial t} + c^2\frac{\partial u_i}{\partial x_i} = 0 \tag{1}$$

$$\frac{\partial u_i}{\partial t} + \frac{\partial u_i u_j}{\partial x_j} + \frac{1}{\rho_0}\frac{\partial p}{\partial x_i} - \frac{\mu}{\rho_0}\frac{\partial}{\partial x_j}\frac{\partial u_i}{\partial x_j} = 0 \tag{2}$$

where ρ_0 is the constant density, u_i are the velocity components, μ is the viscosity coefficient and p the pressure. The viscosity coefficient μ is supposed to be constant, and c is an arbitrary parameter for optimal convergence. These equations have no physical meaning until steady state is obtained.

The incompressible Navier Stokes equations are spatially discretized by the finite-volume technique. The velocity gradients of the stress tensor are cell averaged [1]. Applying the gradient theorem, the volume integrals over the gradients are expressed by surface integrals over the cell boundary. At a cell interface, the velocity is approximated by the arithmetic average of their values in the two adjacent cells. Once the flux tensor is determined in each cell, its value at a cell interface is approximated similarly by arithmatic averaging. On a Cartesian grid, the present finite-volume approximation is equivalent to a second-order accurate central difference discretization involving 13 points opposed to the conventional 9 ones. For the viscous terms, the latter compact differencing is more accurate than the present approach, but our scheme offers a larger stability bound.

A linear stability condition is derived for explicit Runge-Kutta methods applied to the Navier Stokes equations. The condition is based on the scalar model equation obtained by linearizing the equations. The geometrical interpretation of the metric expression in transformed coordinates is used to apply the von Neumann analysis for finite-differences to finite-volumes. The resulting stability condition determines the local time steps of the present Runge-Kutta time integration scheme.

The $k-\epsilon$ turbulence model requires two extra equations to be solved. These equations are spatially discretized by the same finite volume technique, and a similar

stability condition is derived for the determination of the local time step.

3 RESULTS

Results have been obtained for both external and internal flows. Results for the external flow were obtained over a NACA0012 airfoil, and over a backward facing step for the internal flow.

The results for flow around the NACA0012 airfoil, Re=2880000, α=0 are shown on the 129 x 33 O-mesh after 3000 time steps. The flow becomes turbulent after the transition at $\bar{x}/\bar{L} = 0.5$ according to existing experimental data. In the pressure coefficient diagram (Fig. 1) there are comparisons between the incompressible Navier-Stokes solution, an Euler solution and the experimental data available. The two numerical results are almost identical, as they should be for such a high Reynolds number, except at a small region at the leading edge. The agreement between numerical prediction and experimental data for the pressure coefficient is very good even after the transition.

Results have also been obtained for internal flow, RE=50, 2:3 expansion, over a backward facing step, the problem of a 1984 GAMM workshop. The point of reattachment can be seen in the streamline plot (Fig. 2) and the wall shear stress plot (Fig. 3). It was calculated to $x/(H-h) = 2.83$. The experiments state 3.0 for the point of reattachment, though most of the participants of the workshop managed to predict the reattachment point between 2.7 and 2.9. The agreement between numerical results and experimental data is quite satisfying in the wall shear stress plot. The evolution of the maximum velocity (the maximum velocity along the y-axis in x-direction, Fig. 4) also shows a good agreement between numerical and experimental data.

Further details will be discussed and additional cases, both laminar and turbulent, will be computed in the complete paper.

4 REFERENCES

[1] Müller, B. and Rizzi A.: Navier Stokes Computation of Transonic Vortices Over a Round Leading Edge Delta Wing, AIAA Paper No. 87-1227, 1987.

[2] Chorin, A.J.: A Numerical Method for Solving Incompressible Viscous Flow Problems, J. Comp. Phys. 2, 12-26, 1967.

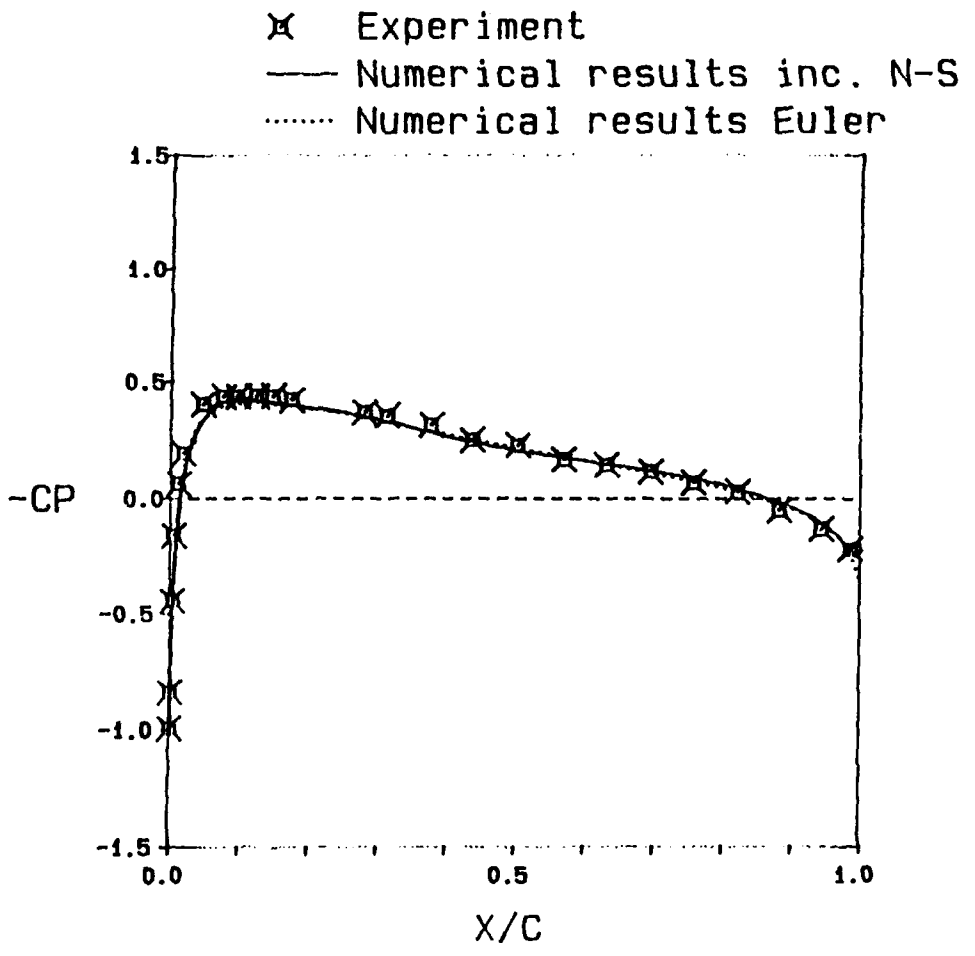

Figure 1: Pressure coefficient, Re=2880000, α=0

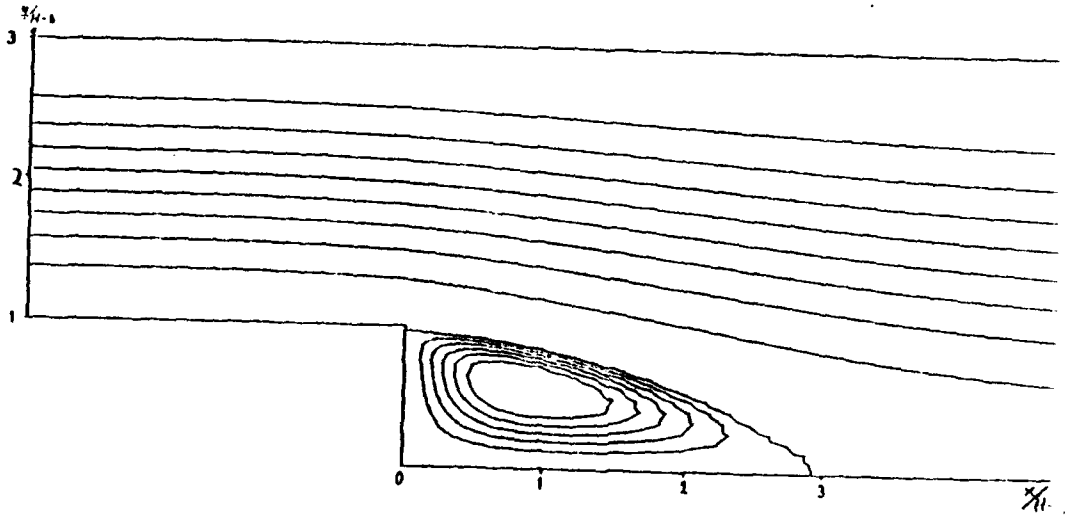

Figure 2: Streamline pattern, Re=50

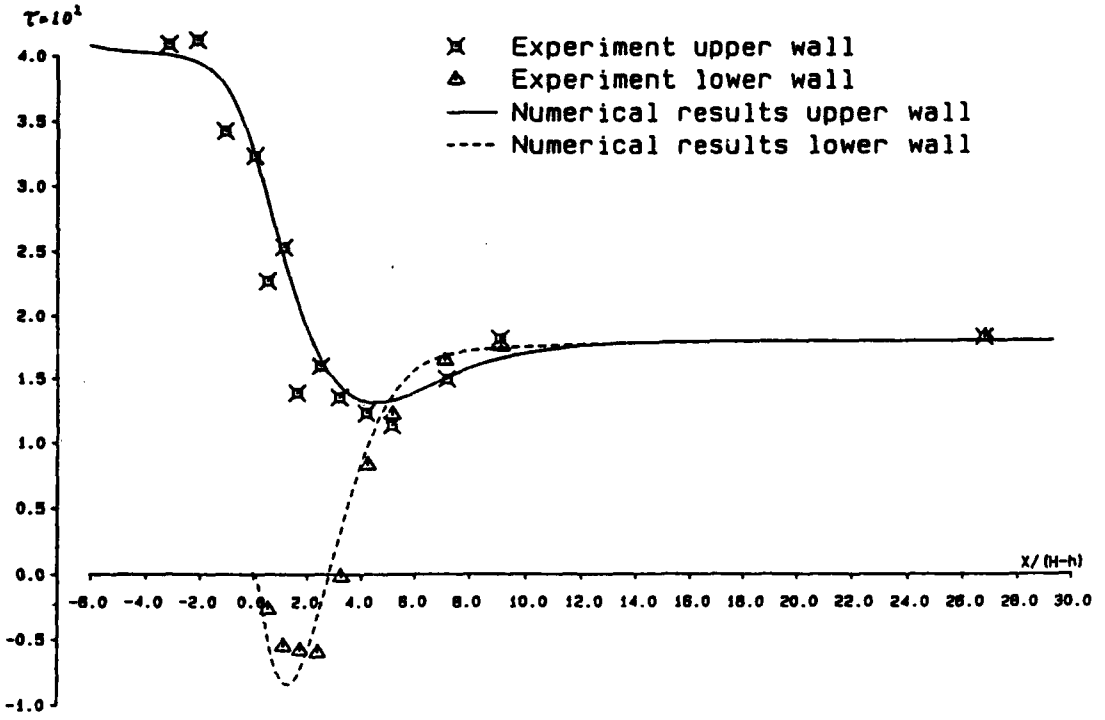

Figure 3: Wall shear stress distribution compared to experiments, Re=50

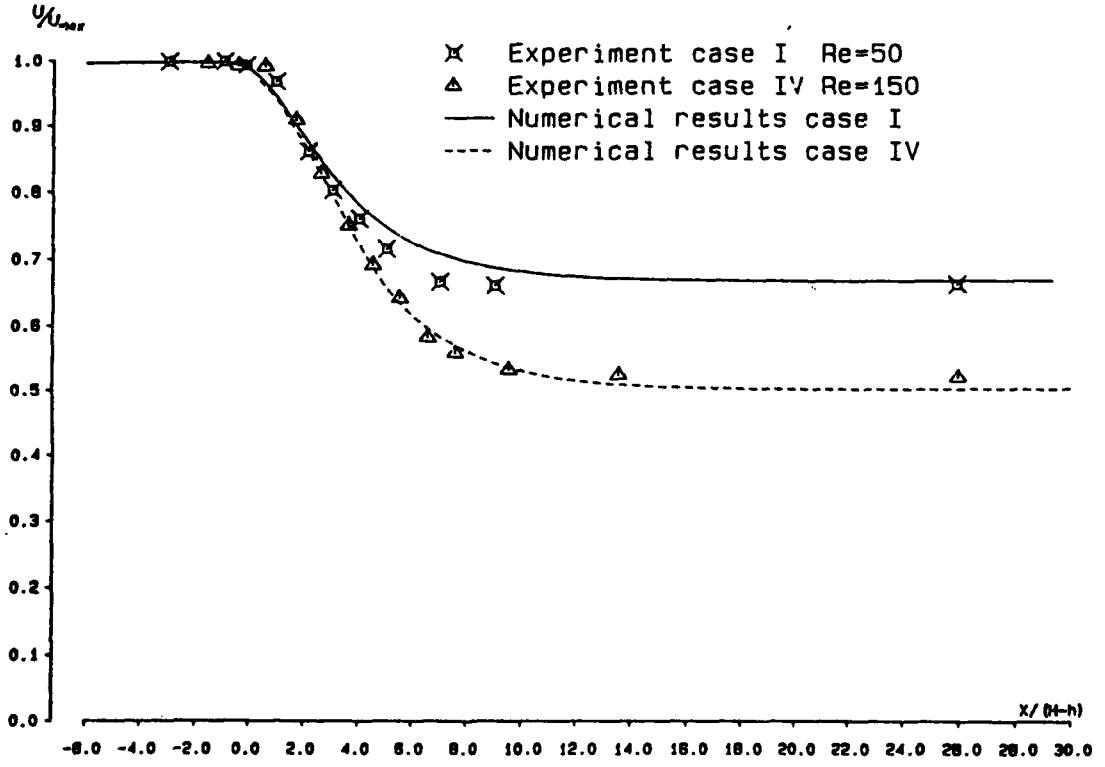

Figure 4: Evolution of maximum velocity compared to experiments, Re=50 and Re=150, expansion 2:3 and 1:2

ON THE FINITE VELOCITY OF WAVE MOTION MODELLED BY NONLINEAR EVOLUTION EQUATIONS

J. Engelbrecht
The Institute of Cybernetics, Estonian Academy of Sciences,
Akadeemia tee 21, Tallinn 200108, Estonia, USSR

Nonlinear evolution equations (EEs) used for describing the wave motion play an important role in contemporary mathematical physics. As a rule, the EEs give an approximate description of a process and their direct correspondence to the initial systems is quite often neglected. In the present talk, an attempt is made to analyse this correspondence.

The initial systems themselves may be divided into two classes [1]: hyperbolic and dispersive systems. It is clear that only the hyperbolic systems are directly based on the physics of wave motion, i.e. on the finite velocities. However, quite often the dispersive systems are derived from basic conservation laws by using certain asymptotic methods in order to emphasize certain physical effects and the concept of finite velocities may be lost. This way or another, the EEs are used for both cases. As shown by many authors [2-4], the moving frame used for deriving EEs, needs a finite velocity which is determined beforehand from the initial system. That is why the procedures of deriving EEs require full attention.

The details of general procedures are to be found elsewhere [5], here we shall outline only the general idea of the asymptotic method which is suitable to explain the problem of velocities.

Suppose a general system describing a certain wave motion is written in a form

$$L_g = \frac{\partial U}{\partial t} + A^k \frac{\partial U}{\partial x_k} + B^m_{pq} \frac{\partial^p}{\partial (x_m)^p} \frac{\partial^q}{\partial t^q} U = 0 \qquad (1)$$

with appropriate initial and boundary conditions. Here U is a

n-vector of field quantities. System (1) may beside the higher derivatives contain also the integral terms. An associated system to the $L_g = 0$ may be derived by using perturbation theory. Suppose it takes the form

$$L_a = \frac{\partial U}{\partial t} + A_0{}^k \frac{\partial U}{\partial x_k} + f(U) = 0. \tag{2}$$

If this associated system (2) is hyperbolic [2, 5], then the eigenvalues of $A_0{}^k$ are real and in the physical terms we have a set of velocities (for every wave n = 1, 2, ...). If the associated system describes dispersive waves then the correspondent group or phase velocities should be determined [3].

The EEs for every single wave $u_i \in U$ are derived using several approaches [2-5] in the form

$$\frac{\partial}{\partial \xi} R(u_i) = G(u_i) \tag{3}$$

written in a moving frame

$$\xi = t - c_i \varphi(x_k) \tag{4}$$

where c_i is a certain finite velocity determined from the associated system (2). Notice that in many cases $G(u_i) = 0$ which may yield

$$R(u_i) = 0. \tag{5}$$

This corresponds preferably to one-dimensional problems. The operator $R(u_i)$ itself is usually of the form

$$R(u_i) = \frac{\partial u_i}{\partial x_j} + u_i \frac{\partial u_i}{\partial \xi} + \frac{\partial^2 u_i}{\partial \xi^2} + \ldots \tag{6}$$

where x_j denotes the direction of the wave beam.

Beside the problems of distortion an important question arises - what is the real wave velocity (signal velocity) and how to determine it. In other words, the relation between the eigenvalues (or phase and group velocities) determined from the

associated hyperbolic (dispersive) system (2) and the real finite velocities of wave motion should be clearly stated for non-conservative processes.

Further, several specific cases are analysed, including the following:

(i) some rather well-known examples are briefly described in order to demonstrate various approaches; these examples include nonlinear waves in dispersive, thermoelastic and relaxing media;

(ii) a special non-conservative problem of wave motion in a dissipative medium with energy influx (an active medium) is analysed in more detail; the example under consideration is the nerve pulse propagation and two models - the classical one based on the diffusion equation as well as the evolution equation derived recently by the author - are compared.

As a conclusion, the full preference in analysis should be given to models based on the concept of finite velocities. The final governing equation, say EE written in a moving frame may not be strictly hyperbolic but then the real velocity, and/or the real wave number and frequency should be restored through a suitable transformation.

Numerical examples illustrating the talk are obtained by using an algorithm based on the FFT technique together with the leap-frog method [6].

References

1. Whitham G.B. Linear and Nonlinear Waves. John Wiley, New York e.a., 1974.
2. Jeffrey A. and Kawahara T. Asymptotic Methods in Nonlinear Wave Theory. Pitman, London, 1982.
3. Taniuti T. and Nishihara K. Nonlinear Waves. Pitman, London, 1983.
4. Engelbrecht J. Nonlinear Wave Processes of Deformation in Solids. Pitman, London, 1983.
5. Pelinovski J.N., Fridman V.E. and Engelbrecht J.K. Nonlinear Evolution Equations. Valgus, Tallinn, 1984 (in Russian, English edition to be published by Longman).
6. Peipman T. and Engelbrecht J. Two-dimensional evolution equations for transient waves - an algorithm by means of Fourier transform. Acta et comm. Universitatis Tartuensis, 1982, No. 627, pp. 107-112.

IMPLICIT UNFACTORED SCHEME FOR WEAK SOLUTIONS OF THE EULER EQUATIONS

B. Favini e F. Sabetta

Dipartimento di Meccanica e Aeronautica
Università di Roma " La Sapienza", Roma

A new non-linear finite difference scheme for the numerical approximation of the weak solutions of the Euler equations has been proposed in /1,2/. The flux vector of the Euler equations are homogeneous functions of degree one with respect to the conserved variables/3/. This property enables us to devise a non-linear scheme with shock-capturing property, but written in quasilinear form everywhere the solution is smooth. Let us consider for simplicity the one-dimensional case:

$$\underline{w}_t + \underline{F}(\underline{w})_x = 0 \qquad (1)$$

with

$$\underline{w} = \{ \rho , \rho u , e \} \qquad \text{and} \qquad \underline{F}(\underline{w}) = \{ \rho u , \rho u^2 , u(e+p) \}$$

As a consequence of the homogeneous property the flux vector is equal to the product of the iacobian matrix time the vector of the conserved variables:

$$\underline{F}(\underline{w}) = A\underline{w} \qquad \text{where} \quad A = \partial \underline{F}(\underline{w}) / \partial \underline{w} \qquad (2)$$

When the solution is smooth the system of equations (1) can be written in quasilinear form:

$$\underline{w}_t + A \underline{w}_x = 0 \qquad (3)$$

Consider now the discrete approximation of the flux derivative, for the homogeneous property:

$$\Delta \underline{F} = \Delta(A\underline{w}) = \hat{A} \Delta \underline{w} + \Delta A \hat{\underline{w}} \qquad (4)$$

where the hat means a suitable definition, e.g. the average value. If the solution is smooth the divergence and the quasilinear forms are equivalent, while if there is a discontinuity only the divergence form (1) is able to compute the correct weak solutions of the Euler equations /4/.The analysis of the expression

(4) shows that the second term in the right hand side is responsible of the shock capturing property of conservative schemes. But this term is also responsible of the great amount of numerical dissipation that affects the conservative schemes. Therefore when the solution is smooth the equations are discretized in quasilinear form, while, when a discontinuity is detected inside the field the divergence form is restored by simply adding the second term in the right hand side of expression (4).

By means of minor modification these technique can be incorporated in a non-conservative scheme to compute the correct weak solutions without the use of a shock-fitting procedure.

The technique has been tested by means of several one and two dimensional problems . The integration in time has been performed with a two-step explicit procedure. The space discretization is consistent with the sign of the characteristic and is second order accurate everywhere, except across a discontinuity where the first order accuracy is required to maintain the monotonicity of the solution.

In the present work we want improve the computational efficiency of the proposed scheme by the use of an implicit technique. The system of equations (1) is discretized in time by means of a two level implicit backward Euler scheme. The equation written in incremental form /5/, and linearized in time by neglecting terms of order Δ^2, are:

$$\{ I + \theta \lambda (\hat{A}^n \Delta\cdot + \Delta A^n\cdot) \} \delta\underline{w}^{n+1} = -(1-\theta) \lambda (\hat{A}^n \Delta\underline{w}^n + \Delta A^n \underline{w}^n) \qquad (5)$$

where $\lambda=\Delta t/\Delta x$, and the relation (4) has been substitute in (1). The left hand side operator is discretized in space by means a two point characteristic biased scheme. Therefore the incremental quantity $\delta\underline{w}$ is computed with a first order accuracy in time and space. Instead the right hand side is discrtized by means a three point characteristic biased scheme so that the final steady state solution is second order accurate. For the one-dimensional case a block tri-diagonal matrix is obtained and a direct inversion can been performed very efficiently.

In the two-dimensional case the matri results block penta-diagonal. In the present work the inversion of the matrix will be obtained by means of a n itera tive procedure/6/. In fact the use of an approximate factorization imposes a limitation on the size of the time step in order to reduce the numerical error introduced by the mixed derivative, whiwh is proportional to Δt^2. The parameter θ enables us to vary from a fully implicit to a fully explicit formulation. The accuracy and the convergence velocity of the scheme will be verified by means of one and two dimensional test cases.

References

1. B.Favini, L.Zannetti: On Conservation Properties and Non-Conservative Form of Euler Solvers. Proceedings of 10th ICNMFD, Beijing, China, 1986, Springer-Verlag.
2. B.Favini, L.Zannetti: A Difference Scheme for Weak Solutions of the Gasdynamic Equations. AIAA Paper 87-0537, AIAA 25th Aerospace Meeting, Reno, 1987.
3. J.L.Steger,R.F.Warming: Flux Vector Splitting of the Inviscid Gasdynamic Equations with Application to Finite Difference Methods. J. Comp.Phys., 40, 1981, 263-293.

4. P.D.Lax: Weak Solutions of Non-Linear Hyperbolic Equations and their Numerical Computation. Comm.Pure & Appl. Math.,7, 1954, 159-193.
5. R.M.Beam, R.F.Warming: An Implicit Factored Scheme for Compressible Navier-Stokes Equations. AIAA Journal, 6, April 1978, 393-402.
6. S.R.Chakravarty: Relaxation Methods for Unfactored Implicit Upwind Schemes. AIAA Paper 84-0165, 1984.

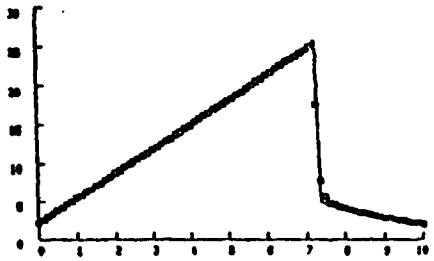

Fig. 1 - Mach distribution.

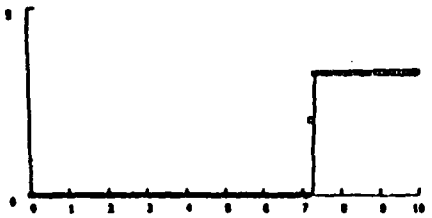

Fig. 2 - Entropy distribution.

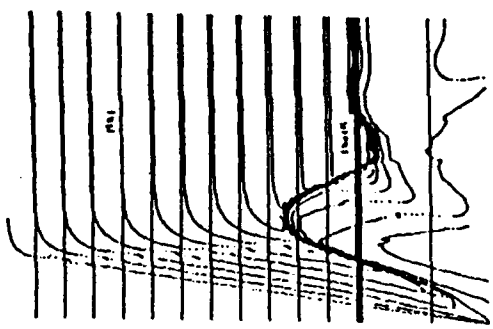

Fig. 3 - Time history of the isoMach lines.

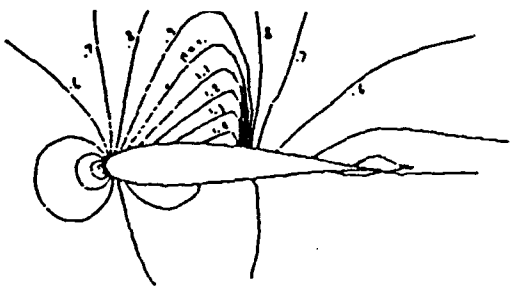

Fig. 4 - IsoMach lines.

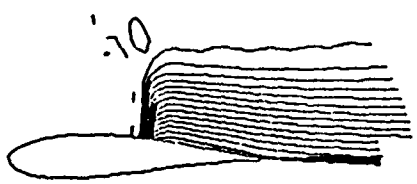

Fig. 5 - Constant entropy lines.

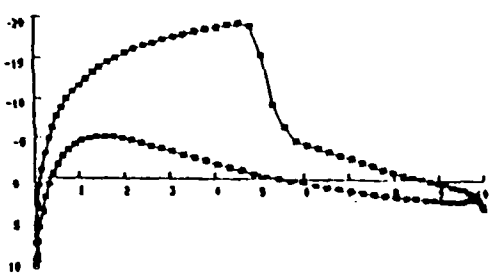

Fig. 6 - Pressure coefficient distribution.

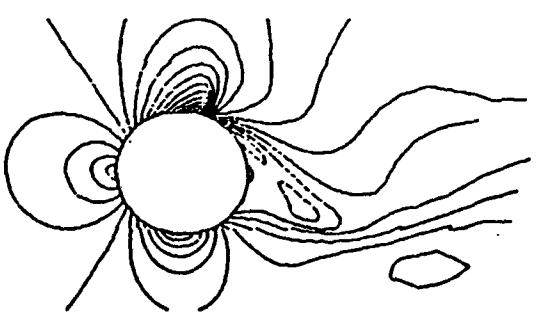

Fig. 7 - IsoMach lines.

Viscosity method in nonlinear systems of conservation laws for transonic flows

Miloslav Feistauer and Jindřich Nečas
Charles University Prague
Sokolovská 83
18600 Praha 8
Czechoslovakia

We prove that the solution of a compressible generally transonic flow of an ideal fluid can be obtained as a limit of viscous solutions, if the viscosity and heat conductivity tend to zero.

Let us consider a weak solution of a stationary, compressible, perfect, viscous, conductive gas flow in a bounded domain $\Omega \subset R^N$ ($N = 2$ or 3) with a Lipschitz-continuous boundary $\partial\Omega$, satisfying the conditions

$$(1) \qquad \varrho \in W^{1,2}(\Omega), \qquad 0 < \tilde{\varrho}_0 \le \varrho(x) \le \tilde{\varrho}_1 < +\infty,$$

$$(2) \qquad v \in W^{1,2}(\Omega, R^N), \qquad |v| \le K,$$

$$(3) \qquad g \in L^\infty(\partial\Omega), \qquad h \in L^1(\partial\Omega), \qquad \|g\|_{L^\infty(\partial\Omega)}, \qquad \|h\|_{L^1(\partial\Omega)} \le K,$$

$$(4) \qquad T \in W^{1,2}(\Omega), \qquad 0 < \tilde{T}_0 \le T(x),$$

$$(5) \qquad \left|\int_\Omega p\,dx\right| \le K \qquad p = R\varrho T, \qquad R = const > 0$$

with constants $\tilde{\varrho}_0, \tilde{\varrho}_1, K, T_0, R$ independent of the viscosity μ and heat conductivity k, and the equations

$$(7) \qquad \int_\Omega \varrho\, v_i \frac{\partial \varphi}{\partial x_i}\,dx = \int_{\partial\Omega} g\varphi\,ds \qquad \forall \varphi \in W^{1,2}(\Omega)$$

(continuity equation)

$$(8) \qquad \int_\Omega \varrho\, v_j \frac{\partial v_i}{\partial x_j}\varphi_i\,dx = \int_\Omega p\,\frac{\partial \varphi_i}{\partial x_i}\,dx + \frac{2}{3}\mu \int_\Omega \frac{\partial v_j}{\partial x_j}\,\frac{\partial \varphi_i}{\partial x_i}\,dx - 2\mu \int_\Omega e_{ij}(v) e_{ij}(\varphi)\,dx,$$

$$2e_{ij}(v) = \frac{\partial v_i}{\partial x_j} + \frac{\partial v_j}{\partial x_i}, \qquad \forall \varphi = (\varphi_1, \ldots, \varphi_N) \in W^{1,2}(\Omega, R^n),$$

$$v^0 \in W^{1,2}(\Omega, R^N) \cap L^\infty(\Omega, R^N), \qquad v = v^0 \text{ on } \partial\Omega,$$
$$\|v^0\|_{W^{1,2}(\Omega,R^N)} + \|v^0\|_{L^\infty(\Omega,R^N)} \le K$$

(Navier-Stokes equations),

$$
\begin{aligned}
&-\int_\Omega T\varrho S v_i \frac{\partial \varphi}{\partial x_i}\,dx + \int_{\partial\Omega} TSg\varphi\,ds - \int_\Omega \frac{\partial T}{\partial x_i}\varrho v_i S\varphi\,dx \\
&= -k\int_\Omega \nabla T\cdot\nabla\varphi\,dx + k\int_{\partial\Omega} h\varphi\,ds + \int_\Omega E(v)\varphi\,ds \qquad \forall\varphi\in W^{1,2}(\Omega)\cap L^\infty(\Omega)
\end{aligned} \tag{9}
$$

(energy equation),

where

$$
E(v) = 2\mu e_{ij}(v)e_{ij}(v) - \frac{2}{3}\mu\left(\frac{\partial v_i}{\partial x_i}\right)^2 \tag{10}
$$

and

$$
S = c_v \ln\frac{T}{\varrho^{\kappa-1}}\,. \tag{11}
$$

Here, we denote $v-$ velocity, $\varrho-$ density, $p-$ pressure, $T-$ temperature, $S-$ entropy, $E-$ dissipation; $c_v > 0$ and $\kappa > 1$ are constants.

Further, we consider the entropy control on the boundary

$$
\left|\frac{1}{\mu}\int_{\partial\Omega} Sg\,ds\right| \le K \qquad \forall\mu > 0 \tag{12}
$$

and assume that $k = \beta\mu$ with $\beta > 0$ independent of μ, k.

Let us consider a sequence $\{\mu_n\}$, $\mu_n \searrow 0$, $k_n = \beta\mu_n$ and a corresponding sequence of solutions $\{\varrho_n, p_n, v^n, T_n, S_n\}$ to (7)-(9) with properties (1)-(5). We derive estimates which allow to choose a subsequence (denoted again ϱ_n, p_n etc.) such that

$$
\begin{aligned}
&\varrho_n \rightharpoonup \varrho && \text{weakly in } L^2(\Omega),\\
&T_n \to T && \text{in } L^p(\Omega)\ \forall p\in[1,2),\\
&T_n \to T && \text{almost everywhere in } \Omega,\\
&v^n \rightharpoonup v && \text{weakly in } W^{1,4/3}(\Omega, R^N),\\
&v^n \to v && \text{in } L^p(\Omega)\ \forall p\in[1,\frac{4N}{3N-4}),\\
&v^n \to v && \text{almost everywhere in } \Omega.
\end{aligned} \tag{13}
$$

The main results [1] , [2] :

a) $\varrho_n \to \varrho$ in $L^2(\Omega)$.

b) If $S_n \to S_0$ in $L^1(\partial\Omega)$, then $\varrho, T, p = R\varrho T, v$ and $S = c_v \ln\frac{T}{\varrho^{\kappa-1}}$ form a weak solution of the conservation law equations of a nonviscous gas.

Under some special assumptions and with the use of the method of characteristics we prove that the limit flow is isentropic, adiabatic and potential.

The conditions (1)-(5) which lead in the limit to flows without strong shocks can be weakened in such a way that instead of (1) and (5) we consider ([2])

$$
0 \le \varrho \le \tilde{\varrho}_1 < +\infty, \qquad \varrho\in W^{1,2}(\Omega), \|\ln\varrho\|_{L^2(\Omega)} \le c < +\infty, \qquad \|T\|_{L^1(\Omega)} \le c < +\infty. \tag{14}
$$

Then

$$
\begin{aligned}
&\varrho_n \to \varrho && \text{in } L^2(\Omega),\\
&v_n \rightharpoonup v && *\text{-weakly in } BV(\Omega, R^N),\\
&\theta_n = \sqrt{T_n} \to \theta && \text{in } L^q(\Omega)\ \forall q\in[1,2),\\
&S_n \to S && \text{in } L^q(\Omega)\ \forall q\in[1,2),
\end{aligned} \tag{15}
$$

and the limit satisfies again the conservation laws for a nonviscous gas in a weak sense. The fact that $v \in BV(\Omega, R^N)$ permits also strong shocks in the flow.

Finally, if instead of (1) and (5) we assume that

$$0 < \tilde{\varrho}(\mu, k) \le \varrho(x) \le \tilde{\varrho}_1 < +\infty, \qquad \varrho \in W^{1,2}(\Omega) \tag{16}$$

and

$$\int_{\partial\Omega} \ln \frac{T}{T_0}\, ds \le K, \tag{17}$$

then the limit flow can have cavitations on a set of positive measure ([3]).

References:

1. *M. Feistauer, J. Nečas: On the solution of transonic flows with weak shocks. CMUC 27,4 (1986), 791–804.*
2. *M. Feistauer, J. Nečas: Viscosity method in a transonic flow. Comm. on PDE (to appear).*
3. *M. Feistauer, J. Nečas: Remarks on the solvability of transonic flow problems. Manuscripta Mathematica (submitted).*

HYPERBOLIC SCHEMES FOR MULTI-COMPONENT EULER EQUATIONS

G. Fernandez , H. Guillard , B. Larrouturou

INRIA, Sophia Antipolis, 06560 Valbonne, FRANCE

1 Introduction

Our purpose is to build efficient conservative schemes for the computation of multi-species (possibly reactive) flows. On this way we consider simplified models in which the governing equations include Euler's hyperbolic terms for several species. Even in the case where the different species have different molecular weights and specific heat ratios, the model is shown to remain hyperbolic. We present several preliminary numerical results obtained by extending to this multi-component Euler system some classical flux-splitting schemes.

2 Multi-component Euler equations

For sake of simplicity, we first write the model in one space dimension, with only two species Σ_1 and Σ_2. Neglecting diffusive and reactive terms in a first step, we consider the following "multi-component Euler equations":

$$W_t + F_x = 0, \tag{1}$$

with:

$$W = \begin{pmatrix} W_1 \\ W_2 \\ W_3 \\ W_4 \end{pmatrix} = \begin{pmatrix} \rho \\ \rho u \\ E \\ \rho Y \end{pmatrix}, \qquad F = \begin{pmatrix} \rho u \\ \rho u^2 + p \\ u(E+p) \\ \rho u Y \end{pmatrix}. \tag{2}$$

The notations for the density ρ, velocity u, pressure p and total energy E are classical; moreover, Y is the mass fraction of the first component Σ_1 [i.e. ρY (resp: $\rho(1-Y)$) is the separate density of Σ_1 (resp: Σ_2)]. To close the system (1), we need to express the pressure as a function of the dependent variables W_i. Assuming that the two species behave as constant gases, and using classical thermodynamical relations, such as Dalton's law and Mayer's relation, we get:

$$p = (\gamma - 1)(E - \frac{1}{2}\rho u^2), \tag{3}$$

with:

$$\gamma = \frac{Y\alpha_1\gamma_1 + (1-Y)\alpha_2\gamma_2}{Y\alpha_1 + (1-Y)\alpha_2} = \frac{W_4\alpha_1\gamma_1 + (W_1 - W_4)\alpha_2\gamma_2}{W_4\alpha_1 + (W_1 - W_4)\alpha_2}, \tag{4}$$

where $\alpha_1^{-1} = M_1(\gamma_1 - 1)$, $\alpha_2^{-1} = M_2(\gamma_2 - 1)$; the subscripts 1 and 2 refer to the two species and M denotes the molar weight.

BLANK PAGE

Thus $\gamma = \gamma(W)$ is an homogeneous function of degree 0, and $F = F(W)$ is homogeneous of degree 1, as in the single component case. Setting $F(W) = \mathcal{F}(W, \gamma(W))$, we can write the Jacobian matrix as:

$$A(W) = \frac{dF}{dW} = \frac{\partial \mathcal{F}}{\partial W} + \frac{\partial \mathcal{F}}{\partial \gamma}\frac{\partial \gamma}{\partial W},$$

with the properties:

$$A(W)W = F(W)\ , \quad \frac{\partial \gamma}{\partial W}W = 0\ .$$

A remarkable result is that the matrices A and $\frac{\partial \mathcal{F}}{\partial W}$ have the same real eigenvalues:

$$\lambda_1 = u\ ,\ \lambda_2 = u + c\ ,\ \lambda_3 = u - c\ ,\ \lambda_4 = u\ , \tag{5}$$

where the sound speed still has the classical expression $c = \sqrt{\frac{\gamma p}{\rho}}$. The corresponding eigenvectors

$$\vec{e}_1 = \begin{pmatrix} 1 \\ u \\ \frac{u^2}{2} - X \\ 0 \end{pmatrix}, \quad \vec{e}_2 = \begin{pmatrix} 1 \\ u + c \\ H + uc \\ Y \end{pmatrix}, \quad \vec{e}_3 = \begin{pmatrix} 1 \\ u - c \\ H - uc \\ Y \end{pmatrix}, \quad \vec{e}_4 = \begin{pmatrix} 0 \\ 0 \\ X \\ Y \end{pmatrix}$$

with $H = \frac{E+p}{\rho}$, $X = \frac{p}{(\gamma-1)}\frac{\partial \gamma}{\partial W_1}$, are linearly independant, which shows that the system (1)-(4) is hyperbolic (although non strictly hyperbolic since $\lambda_1 = \lambda_4$).

There is no difficulty in checking that these results also hold in several space dimensions or if the number of species is greater than two.

3 Numerical approach

Following previous studies on the numerical simulation of perfect gas flow or reactive gas flow, we use for the approximation of system (1) a finite-volume approach on a (possibly unstructured) finite-element mesh (see [1], [3]). Our goal is therefore to investigate how the classical flux-splitting hyperbolic schemes perform when applied to the full system (1) with the species equations added.

The numerical results presented below have been obtained with Roe's numerical flux function (written here for the one-dimensional system (1)):

$$\Phi(W_1, W_2) = \frac{F(W_1) + F(W_2)}{2} + \frac{1}{2} \mid A(\tilde{W}) \mid (W_1 - W_2) \tag{6}$$

where $\tilde{W}$ is defined by:

$$\sqrt{\tilde{\rho}} = \frac{\sqrt{\rho_1} + \sqrt{\rho_2}}{2}\ ,\ \tilde{u} = \frac{\sqrt{\rho_1}u_1 + \sqrt{\rho_2}u_2}{2\sqrt{\tilde{\rho}}}\ ,\ \tilde{H} = \frac{\sqrt{\rho_1}H_1 + \sqrt{\rho_2}H_2}{2\sqrt{\tilde{\rho}}}\ ,\ \tilde{Y} = \frac{\sqrt{\rho_1}Y_1 + \sqrt{\rho_2}Y_2}{2\sqrt{\tilde{\rho}}}\ .$$

Concerning this last scheme, it is of interest to notice that the fundamental property of Roe's scheme $F(W_1) - F(W_2) = A(\tilde{W})(W_1 - W_2)$ is still satisfied when $\gamma_1 = \gamma_2 = \gamma$, but no longer holds if $\gamma_1 \neq \gamma_2$.

Figure 1 shows how the above scheme performs when applied to a Riemann problem for system (1). We consider Sod's shock tube problem, with two different components on both sides of the discontinuity at $t = 0$, and with $\gamma_1 = \gamma_2 = 1.4$. The species profile obtained with the scheme (6) can be compared to the profile obtained by combining the usual Roe's scheme for the Euler equations with a donor-cell approximation of the species equation $(\rho Y)_t + (\rho u Y)_x = 0$.

Figure 2 represents mass fraction profiles across a planar premixed flame with one-step chemistry (in this case, diffusive and reactive terms are added to the energy and species equations in (1)). The scheme (6) is now compared to a scheme combining Roe's scheme for the Euler equations and a centered approximation for the species equation (see [2]). Using as a reference the results obtained with the "combined scheme" and 401 mesh points, we observe that the error in the flame location obtained with the "combined scheme" operating on a coarse grid is considerably reduced with the global flux-splitting (6).

Lastly, we show in Figure 3 the two-dimensional interaction of two supersonic gaseous jets; the impinging jets are made up of two different species, with $M_1 \neq M_2$ and $\gamma_1 \neq \gamma_2$; the system of governing equations simply is the two-dimensional analogue of (1)-(4), with no diffusive and reactive terms. Although the diffusive effect of the scheme clearly appears when observing the mass fraction contours (obtained on a uniform non adaptive mesh), the scheme behaves in a very promising fashion.

4 Conclusion

For the solution of (possibly reactive) systems including the multi-component Euler equations, it appears that the results of calculations in which the usual Euler terms and the added continuity equations are treated separately can be substantially improved by using a global flux-splitting approach similar to (6).

REFERENCES

[1] A. Habbal, A. Dervieux, H. Guillard, B. Larrouturou, "Explicit calculation of reactive flows with an upwind hydrodynamical code", INRIA Report 690, (1987).

[2] P. L. Roe, "Approximate Riemann solvers, parameters vectors and difference schemes", J. Comp. Phys., **43**, pp. 357-372, (1981).

[3] B. Stoufflet, J. Periaux, F. Fezoui, A. Dervieux, "Numerical simulation of 3-D hypersonic flow around space vehicle using adapted finite elements", AIAA paper 87-0560, (1987).

ACKNOWLEDGEMENTS: We thank A. Dervieux for his helpful suggestions.

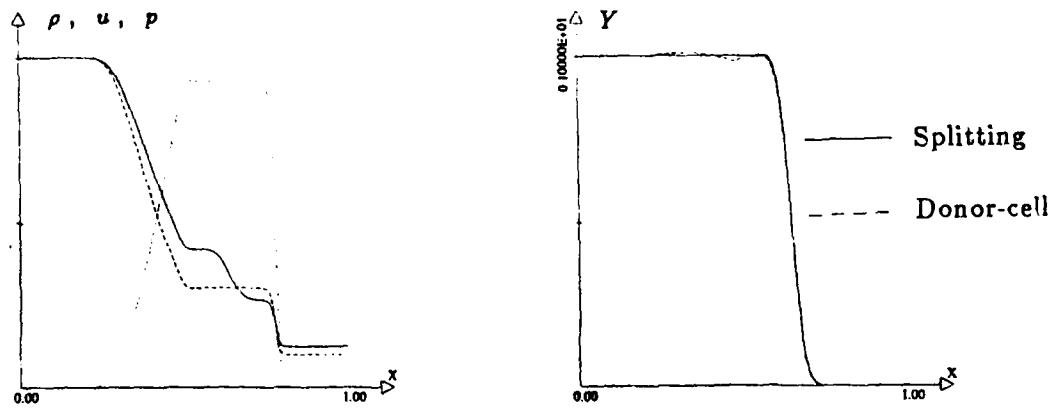

Figure 1: Density, pressure, velocity and mass fraction profiles for a two-component shock tube problem.

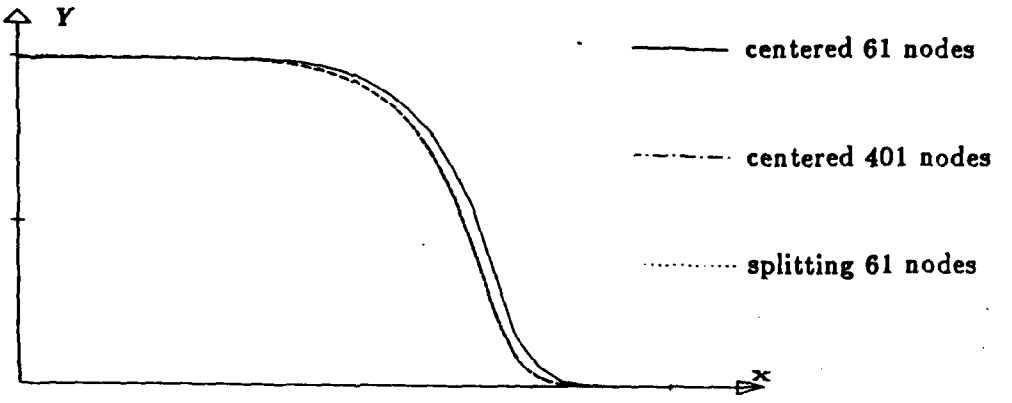

Figure 2: Mass fraction profiles across a planar premixed flame (the dashed curve and the dotted curve coincide on the figure).

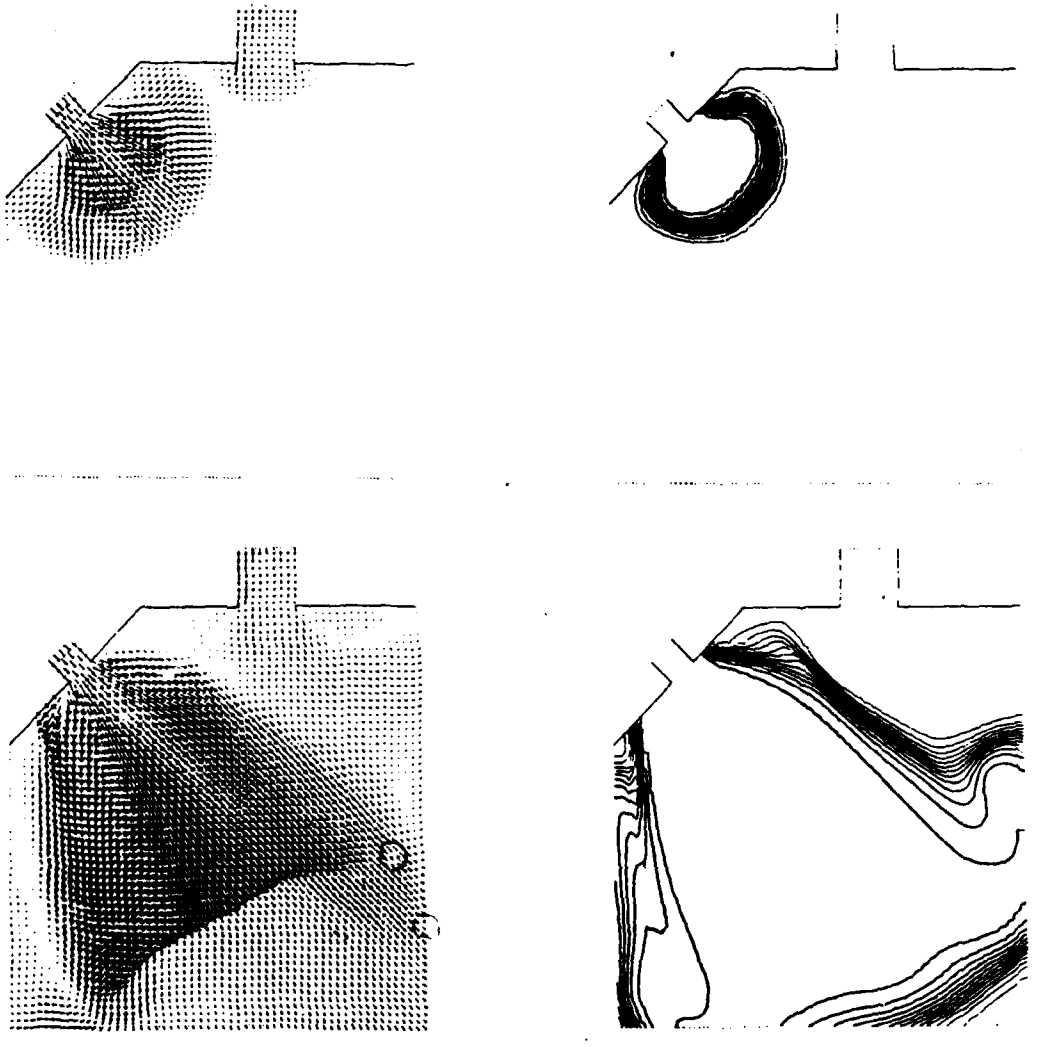

Figure 3: Gaseous jets interaction: velocity field and mass fraction contours.

Multigrid Methods for the Solution of Porous Media Multiphase Flow Equations

by

T. W. Fogwell and F. Brakhagen *

For flow in a porous medium Darcy discovered that a good method to calculate the superficial velocity was to use the pressure gradient as the driving force and regard the properties of the medium as a transmission factor. The velocity was inversely proportional to the viscosity and the pressure could be due to gravity effects. For each phase ℓ, then, we have the velocity

$$v_\ell = -\frac{K_\ell}{\mu_\ell}(\nabla P_\ell + \rho_\ell g) \tag{1}$$

where μ is the viscosity, K is the permeability, P is the pressure, ρ is the density, and g is the gravity vector.

The volumetric fraction (saturation) of phase ℓ is denoted by S_ℓ, so that $\sum S_\ell = 1$. It was discovered that for multiphase flow the permeability tensor could be more accurately split into two parts so that $K_\ell = k_{r\ell}K$ where $k_{r\ell}$ is a scalar depending on the saturations and K is a tensor depending on the spatially varying structure of the medium. Mass conservation is represented by the continuity equation

$$\frac{\partial(\phi\rho_\ell S_\ell)}{\partial t} = -\nabla\cdot(\rho_\ell v_\ell) - q_\ell \tag{2}$$

where q_ℓ is a production (sink) term and ϕ is porosity (fraction void space).

In order to solve the equations boundary and initial conditions must be specified together with the parameters in the equation. Usually the boundary conditions are no-flow Neumann type conditions. For constant temperature, the following are specified: $\phi(P)$, $\rho_\ell(P_\ell)$, $\mu_\ell(P_\ell)$, and $k_{r\ell}(S_1,\ldots,S_n)$. Another relationship is then needed. This is usually taken to be the capillary pressure P_c defined to be the difference in pressure between a wetting and a non-wetting phase, and is considered an emperical function of the saturations.

The Darcy's law equation is combined with the continuity equation to eliminate the velocity and gives

$$\frac{\partial(\phi\rho_\ell S_\ell)}{\partial t} = -\nabla\cdot[\frac{\rho_\ell k_{r\ell}K}{\mu_\ell}(\nabla P_\ell + \rho_\ell g)] - q_\ell. \tag{3}$$

The unknowns are then the P_ℓ and S_ℓ. For incompressible flow this becomes

$$\phi\frac{\partial S_\ell}{\partial t} = \nabla\cdot[\frac{k_{r\ell}K}{\mu_\ell}(\nabla P_\ell + \rho_\ell g)] - Q_\ell \tag{4}$$

where $Q_\ell = q_\ell/\rho_\ell$. In order to eliminate the saturations we can sum the above equations to give

$$\nabla\cdot\sum_\ell[\frac{k_{r\ell}K}{\mu_\ell}(\nabla P_\ell + \rho_\ell g)] - Q_t = 0 \tag{5}$$

where Q_t is the total production. This is an elliptic equation and demonstrates why one might expect multigrid methods to work.

If just two phases, o and w, are present, then capillary pressure $P_c = P_o - P_w$. If the capillary pressure is taken to be zero, then $P_o = P_w = P$. If the flow is horizontal, then $\rho_\ell g = 0$, and we have $v_\ell = -(k_{r\ell}K/\mu_\ell)\nabla P$ for each phase ℓ. Also, $v_w = (k_{rw}\mu_o/k_{ro}\mu_w)v_o$. Let $v_t = v_o + v_w$ and $f_\ell = (k_{r\ell}/\mu_\ell)/(k_{rw}/\mu_w + k_{ro}/\mu_o)$ for $\ell = o$ or w. Then $v_\ell = f_\ell v_t$ and the equation for phase ℓ becomes

$$\phi\frac{\partial S_\ell}{\partial t} = -\nabla\cdot(f_\ell v_t) - Q_\ell.$$

If we look at the places where there is no source or sink term, then $Q_\ell = 0$. Expanding the right side, we get

$$\phi\frac{\partial S_\ell}{\partial t} = -f_\ell\nabla\cdot v_\ell - v_t\cdot\nabla f_\ell.$$

For incompressible flow this becomes

$$\phi\frac{\partial S_\ell}{\partial t} = -v_t\frac{df_\ell}{dS_\ell}\cdot\nabla S_\ell$$

which has the form of a first order hyperbolic equation. The discontinuities in the initial conditions are then propagated. This is why one might expect multigrid methods not to work so well.

The discontinuities in the solution are not the only problems. There are large discontinuities in the coefficients as well. K can have discontinuous jumps of several orders of magnitude due to changes in the medium's geological

* Schloß Birlinghoven, 5205 Sankt Augustin

features. These are aggravated by large discontinuous changes in $k_{r\ell}$ as a result of the sudden changes in the saturations.

The equations we solve are those for incompressible two phase flow in two dimensions. We use two general techniques, both using multigrid, one called IMPES (implicit pressure, explicit saturation) and the other called the simultaneous solution (SS) method. The general equations for both methods are

$$\phi\frac{\partial S_w}{\partial t} = \nabla\cdot[\frac{k_{rw}K}{\mu_w}(\nabla P_w + \rho_w g)] - Q_w \tag{6}$$

$$-\phi\frac{\partial S_w}{\partial t} = \nabla\cdot[\frac{k_{ro}K}{\mu_o}(\nabla P_o + \rho_o g)] - Q_o. \tag{7}$$

For the IMPES method we add the two above equations to obtain a "pressure equation," as follows,

$$\nabla\cdot[(\lambda_o+\lambda_w)\nabla P_o - \lambda_w\nabla P_c - (\lambda_o\rho_o+\lambda_w\rho_w)g] = Q_o + Q_w \tag{8}$$

where $\lambda_\ell = k_{r\ell}K/\mu_\ell$ for $\ell = o$ or w. This equation is elliptic. All saturation related terms are taken at the old time level and equation (8) is solved for P_o at the new time. Once P_o is known, equation (7) is solved explicitly for the new saturation S_w. From this P_c is known and the process is started again.

The problem is discretised by the standard finite difference method with reflection boundary conditions. The standard multigrid method will fail because of the large jump discontinuities in the coefficients λ_ℓ. The difference operator itself is used for the interpolation operator as originally proposed by Alcouffe, Brandt, Dendy, and Painter. This more closely follows the continuity of the $\lambda_\ell\nabla P_\ell$ terms rather than attempting to interpolate the discontinuous ∇P_ℓ terms. The restriction operator is taken to be the transpose of the interpolation operator. The coarse grid operator is taken to be the Galerkin approximation derived from the fine grid operator together with the restriction and interpolation operators. If L^{h-1} is the coarse grid operator, L^h is the fine grid operator, and I is the interpolation operator, then $L^{h-1} = I^T L^h I$. Although the finite difference operator on the finest grid has a five point star, the operators on the coarser grids all have nine point stars.

For relaxation steps we use point, line and alternating line Gauss Seidel methods. With the W–cycles we use, the algorithm exhibits the usual multigrid efficiency. The average reduction factor per work unit ranges from 0.25 to 0.6, where one work unit is the work required for one relaxation step on the finest grid. Because of the explicity treatment of saturation, the following restriction on the sise of the time step, as was given by Azis and Settari, is imposed for stability:

$$\Delta t < \min_i \frac{\Delta x\Delta y\phi}{K_x\frac{\Delta y}{\Delta x} + K_y\frac{\Delta x}{\Delta y}} \min_{i,S_w} \frac{\frac{\mu_w}{k_{rw}} + \frac{\mu_o}{k_{ro}}}{|P_c'|}.$$

If the mesh sizes are very small or P_c' is very large, then the sizes of the time steps required for stability are unacceptably small. In this case the simultaneous solution method preferable.

The system we use in the simultaneous solution method is symmetric. The equations (6) and (7) are transformed into

$$\nabla\cdot[\lambda_o(\nabla P_o - \rho_o g)] = -\phi S_w'(\frac{\partial P_o}{\partial t} - \frac{\partial P_w}{\partial t}) + Q_o \tag{9}$$

$$\nabla\cdot[\lambda_w(\nabla P_w - \rho_w g)] = \phi S_w'(\frac{\partial P_o}{\partial t} - \frac{\partial P_w}{\partial t}) + Q_w \tag{10}$$

by taking $S_w' = \partial S_w/\partial P_c$, on the assumption that $P_c(S_w)$ is invertible and S_w' exists. The equations are solved simultaneously for P_o and P_w. The new saturations are then found by $S_w(P_c)$. The finite difference discretization of the system leads to a symmetric, block–pentadiagonal system where the blocks are 2x2 submatrices. The off–diagonal blocks are diagonal matrices. The discretisation is backward in time with explicit mobilities λ_o and λ_w. The scheme is unconditionally stable.

Again the difficulties in a multigrid scheme are the discontinuities in the coefficients λ_ℓ. We use a generalization of the interpolation procedure we use for the IMPES method applied to systems, which was originally proposed by Dendy. The coarse grid operator is still the Galerkin approximation derived from the interpolation operator $L^{h-1} = I^T L^h I$. The interpolation and restriction operators, however, consist of submatrices. The relaxation is done by collective point, line or alternating line Gauss Seidel methods. The convergence of this multigrid method seems to be about the same as for the IMPES method. Because of the large accumulation term which appears on the coarser grids (not found with the IMPES method), the coarsest grid must be taken fine enough to assure that the operator equation is nonsingular. This seems to impose no practical restriction on the method. We are currently testing different more efficient methods of obtaining the coarse grid operators. These promise to save much computational effort over the Galerkin approximation, particularly in three dimensions.

CENTRAL DEGENERACY OF ROTATIONALLY SYMMETRIC HYPERBOLIC SYSTEMS OF CONSERVATION LAWS

H.Freistühler
Institut für Mathematik, RWTH Aachen

1. Outline

Theorem: Assume the flux function of a hyperbolic system of conservation laws displays a generic rotational symmetry. Then, locally near any point that belongs to the center of symmetry, the Riemann problem has a unique stable solution, which depends continuously on the data. -

The assumption is wide enough to cover interesting cases from continuum mechanics, so nonlinear elasticity of an isotropic body near the ground state and magnetohydrodynamics with magnetic field nearly parallel to the direction of wave propagation.

The difficulty lies in a loss of strictness at the center: the usual construction of *Lax* and *Liu* is not directly applicable; we adapt it to the degenerate situation by giving an appropriate less (but enough) regular parametrization of the elementary waves.

There are many interesting papers on non-strictly hyperbolic systems (see *Keyfitz*'s survey) that do however not touch the rather natural problem considered here. E.g. the classification by *Schaeffer & Shearer* in the frequently useful model class of 2×2 systems accidentally avoids rotational symmetry by its restriction to quadratic flux functions. The only rotationally symmetric systems whose RP has been studied rigorosly in previous literature, that of the elastic string and intimately related models (*Keyfitz & Kranzer, Liu & Wang, Shearer*), have their state space bounded away from the center, so that the central degeneracy does not appear there. Examples of centrally degenerate rotationally symmetric 2×2 and 3×3 systems have recently been given by *Freistühler*.

2. Details

2.1. Stable solutions of Riemann problems

As usual we look for weak solutions that are centered, piecewise smooth and have discrete discontinuities. Let $f:U\to\mathbb{R}^n$ describe the system. For $(u,s)\in U\times\mathbb{R}$, write $R^{\pm}(u,s) := \sum_{\lambda \gtrless s} \ker(Df(u)-\lambda)$.

Def 1. $(u^-,u^+,s)\in U\times U\times\mathbb{R}$ represents a linearly stable discontinuity $:\Leftrightarrow$

(RH) $f(u^+)-f(u^-)=s(u^+-u^-)$ and

(LS) $R^+(u^-,s)+R^-(u^+,s)\subset R^-(u^-,s)\oplus R^+(u^+,s)\oplus\mathbb{R}(u^+-u^-)$. -

Def 2. A linearly stable solution of a RP is one with all its discontinuities linearly stable; any weak limit of linearly stable solutions is called a stable solution. -

Actually, with rotationally symmetric systems, weakly (= not linearly) stable solutions occur naturally. Some of these are associated by a continuous version of structural lability in the sense of discontinuous changes of constant states in solutions.

For this concept of stability compare *Jeffrey & Taniuti* and *Majda*.

2.2. Rotational symmetry

Def 3. For $m,k,n=m+k\in\mathbb{N}$, decompose $u\in\mathbb{R}^n$ as $u=(x,y)\in\mathbb{R}^m\times\mathbb{R}^k$; to any $O\in\mathcal{O}(m)$ define $\bar{O}\in\mathcal{O}(n)$ by $\bar{O}(x,y)=(Ox,y)$. $f:U\to\mathbb{R}^n$ is rotationally symmetric (with respect to x) $:\Leftrightarrow$ $f\circ\bar{O}=\bar{O}\circ f$ for all $O\in\mathcal{O}(m)$. -

Cor. 1. Then $f=(X,Y)$ with $X(x,y)=\hat{X}(|x|,y)x$, $X:\mathbb{R}\times\mathbb{R}^k\to\mathbb{R}$,
$Y(x,y)=\hat{Y}(|x|,y)$, $Y:\mathbb{R}\times\mathbb{R}^k\to\mathbb{R}^k$.

$$Df(x,y)=\begin{pmatrix}\hat{X}_{\hat{X}}|x|^{-1}xx^T+\hat{X}I_m & x\hat{X}_y\\ \hat{Y}_{\hat{X}}|x|^{-1}x^T & \hat{Y}_y\end{pmatrix}\text{ at }(|x|,y);\quad Df(0,y)=\begin{pmatrix}\hat{X}(0,y)I_m & 0\\ 0 & \hat{Y}_y(0,y)\end{pmatrix}$$

$\lambda^a:=\hat{X}(|.|,.)$ is an eigenvalue of Df. -

Cor. 2. For the corresponding radial system $\hat{f}:=(\hat{X}\hat{X},\hat{Y})$,

$$D\hat{f}=\begin{pmatrix}\hat{X}_{\hat{X}}\hat{X}+\hat{X} & \hat{X}\hat{X}_y\\ \hat{Y}_{\hat{X}} & \hat{Y}_y\end{pmatrix}\text{ has a continuous eigenvalue }\hat{\lambda}\text{ with }\hat{\lambda}(0,y)=\hat{X}(0,y).$$

$\lambda^r:=\hat{\lambda}(|.|,.)$ is an eigenvalue of Df. -

Def 4. Let $u_o=(0,y_o)\in\mathcal{C}:=\{(0,y)\in U\}$. f is generic at u_o $:\Leftrightarrow$

(i) $\hat{f}$ is strictly hyperbolic and

(ii) $D^2_{\hat{X}}\hat{\lambda}(0,y_o)\neq 0$ and

(iii) Each eigenvalue of $D\hat{f}$ different from $\hat{\lambda}$ is genuinely nonlinear or linearly degenerate. -

2.3. Parametrization of the stable transverse waves

Def. 5. Near u_o: transverse waves :⇔ elementary waves with speeds s near $\hat{X}(0,y_o)$. -

Main lemma: Near u_o, all combinations of stable transverse waves can be parametrized by a map S^t, defined in $U\times\mathbb{R}^m$ near $(u_o,0)$, where $S^t(u_l,\varepsilon^t)=u_r$ means that u_l,u_r are left and right hand states of a sequence of stable transverse waves of increasing speeds. S^t is continuous and piecewise smooth and fulfils

(i) $S^t(.,0)=id$

(ii) $D_{u,\varepsilon^t}S^t(u,\varepsilon^t)=(I_n+\Delta)(I_n,(I_m,0)^T)$ with $\Delta=O(|u-u_o|+|\varepsilon^t|)$. -

3. Literature

LAX, P.: Hyperbolic systems of conservation laws II, Comm. Pure Appl. Math. 10 (1957)

LIU, T.-P.: The Riemannproblem for general systems of conservation laws, J. Diff. Eqs. 18 (1975)

JEFFREY,A. and T. TANIUTI: Nonlinear wave propagation (1964)

MAJDA, A.: Stability of multidimensional shockfronts, AMS Mem. No. 275 (1983)

DAFERMOS, C. M.: Hyperbolic systems of conservation laws, in: Systems of nonlinear partial differential equations (ed. J. M. Ball,1983)

KEYFITZ, B.: A survey of nonstrictly hyperbolic conservation laws, in: Nonlinear hyperbolic problems, Proc. 1st Int. Conf. on Hyperbolic Problems held at St. Etienne 1986 (1987)

KEYFITZ, B. and H. KRANZER: A system of nonstrictly hyperbolic conservation laws arising in elasticity theory, Arch. Rat. Mech. Anal. 72 (1980)

LIU, T.-P. and C. H. Wang: On a nonstrictly hyperbolic system of conservation laws, J. Diff. Eqs. 57 (1985)

SHEARER ,M.: The Riemann problem for the planar motion of an elastic string, J. Diff. Eqs. 61 (1986)

SCHAEFFER, D. and M. SHEARER: Classification of 2x2 systems of nonstrictly hyperbolic conservation laws, with application to oil recovery, Comm. Pure Appl. Math. (1987)

FREISTÜHLER, H.: Stabile Lösungen von Riemannproblemen und die Geometrie der Rankine-Hugoniot-Bedingungen (1987)

ON A HODOGRAPH-LIKE TRANSFORMATION FOR QUASILINEAR HYPERBOLIC NON REDUCIBLE SYSTEMS OF FIRST ORDER

D. FUSCO

Dipartimento di Matematica e Applicazioni
Università di Napoli, Via Mezzocannone 8
80134 Napoli, Italy

Let us consider a quasilinear nonhomogeneous hyperbolic system of first order

$$\underline{U}_t + A(\underline{U})\,\underline{U}_x = \underline{B}(\underline{U}) \qquad (1)$$

where x and t are, respectively, space and time coordinates and

$$\underline{U} = \begin{Vmatrix} u \\ v \end{Vmatrix}; \qquad A(\underline{U}) = \begin{Vmatrix} a_{11} & a_{12} \\ a_{21} & a_{22} \end{Vmatrix}; \qquad \underline{B}(\underline{U}) = \begin{Vmatrix} b_1 \\ b_2 \end{Vmatrix}; \qquad \underline{U}_t = \frac{\partial \underline{U}}{\partial t}; \qquad \underline{U}_x = \frac{\partial \underline{U}}{\partial x}.$$

The hodograph transformation is no longer useful to reduce the governing model to linear form. However, along with the lines suggested in [1] , we introduce the following variable transformation

$$\bar{x} = x - \xi(u,v) \qquad \bar{t} = t - \tau(u,v) \qquad (2)$$

where $\xi(u,v)$ and $\tau(u,v)$ are differentiable functions such that $\dfrac{\partial(\xi,\tau)}{\partial(u,v)} \neq 0$ and satisfying the pair of equations

$$\begin{Vmatrix} -\xi_v \\ \xi_u \end{Vmatrix} + A(\underline{U}) \begin{Vmatrix} \tau_v \\ -\tau_u \end{Vmatrix} = \frac{\partial(\xi,\tau)}{\partial(u,v)}\, \underline{B}(\underline{U}). \qquad (3)$$

Hence the transformation (2) can be considered hodograph-like.

Under the change of variables (2) the system (1) transforms into a similar system of the form

$$\underline{U}_{\bar{t}} + A(\underline{U})\,\underline{U}_{\bar{x}} = \underline{B}(\underline{U}). \qquad (4)$$

The transformation (2) can be useful to solving physical problems only when the transformed system is in a form whose properties are well known.

Occasionally, the transformation (2) may be used also to link certain quasilinear systems like (1) to linear canonical forms.

We characterize the most general class of models of the form (1) which can be linearized directly through the use of (2).

More general than the direct requirement of linearity to the transformed system is the case where the model (4) can be reduced to linear canonical form via a further Bäcklund transformation.

Apart from its own theoretical value, the afore-mentioned reduction procedure either to linear or to nonlinear canonical forms can be used also as a mathematical vehicle for characterizing functional forms to the material response functions involved in the basic governing system (1) (model constitutive laws).

Physical contexts where the present approach can be applied are given, for instance, by hyperbolic models for heat conduction, river flows, nonlinear transmission lines.

Such an analysis can be used:

i) for solving certain classes of nonlinear hyperbolic boundary value problems;

ii) for constructing exact progressive wave solutions;

iii) for investigating simple wave interactions in nonlinear hyperbolic dissipative media.

References

[1] B. Seymour & E. Varley, Studies Appl. Math., 72, 241-262 (1985).

Algebraic Solutions of Benney's Equations

J. Gibbons
Department of Mathematics
Imperial College
London
U.K.

Y. Kodama

Department of Physics
Nagoya University
Nagoya 464
Japan.

and

Department of Mathematics
Ohio State University
Columbus, OH 43210
U.S.A.

The first two equations of the Benney hierarchy [1],

$$\begin{aligned}\frac{\partial A_n}{\partial t_2} &= \frac{\partial A_{n+1}}{\partial t_1} + n\,A_{n-1}\frac{\partial A_1}{\partial t_1} \\ \frac{\partial A_n}{\partial t_3} &= \frac{\partial A_{n+2}}{\partial t_1} + A_0\frac{\partial A_n}{\partial t_1} + (n+1)\,A_n\frac{\partial A_0}{\partial t_1} + n\,A_{n-1}\frac{\partial A_1}{\partial t_1}\end{aligned} \tag{1}$$

are the simplest members of an infinite family of commuting flows [2], the n-th of which is parameterised by a 'time' t_n. They possess an infinite number of conserved densities, which are polynomial in the 'moments' A_n.

One of the most interesting physical applications of these equations arises from the fact that A_0 satisfies the autonomous equation [3]:

$$\frac{\partial^2 A_0}{\partial t_3 \partial t_1} = \frac{\partial^2 A_0}{\partial t_2^2} + \frac{1}{2}\frac{\partial^2 \left(A_0^2\right)}{\partial t_1^2} \tag{2}$$

which arises in the theories of transonic flow [4] and nonlinear acoustics [5]. Some special solutions of this equation can be found by looking for solutions independent of t_2 or t_3; in these cases, respectively, only one and two of the moments A_n are independent. By restricting to solutions invariant under higher equations of the hierarchy, we obtain nonlinear systems of higher order, which lead to solutions of (2). Algebraic solutions of these N-th order systems can be found by looking for expressions for the times $t_1, \ldots, t_N$ as polynomials

in the variables $A_0, \ldots, A_{N-1}$, a procedure which can be carried out systematically. This procedure is the natural generalisation of the hodograph transformation [6].

The transformation is carried out by first writing down the equations for the dependence of $A_0 \ldots A_{n-1}$ on the variables $x, t_2, t_3 \ldots t_n$, where all the A_i are required to be invariant under t_{n+1} translation. Then we write theses equations in terms of differential forms, and obtain a consistency condition between them, which is a *linear* p.d.e. for the minors of the Jacobian matrix $\partial(t_1, \ldots, t_n)/\partial(A_0, \ldots, A_{n-1})$. Solving this linear equation, we then may integrate once, to obtain equations for differential forms of order one less; this gives an over-determined system in general, but for these equations we have found (at least for n=3) a construction for the solutions. It is then possible to continue the process, until explicit formulae for the t_i as functions of the A_ℓ are obtained [7].

There seems to be a remarkable and largely unexplained relationship between these functions and the conservation laws of the restricted system; it seems that the polynomial for t_n is always a conserved density of (1), provided $\frac{\partial A_\ell}{\partial t_{n+1}} = 0$, while the other t_i are the corresponding fluxes. It is expected that these techniques can be extended to other systems of completely integrable dispersionless p.d.e.'s, of which the most important examples are perhaps the modulation equations for slowly varying KdV wavetrains of genus g [8,9]. These have a similar structure to Benney's equations, although they are much more complicated; for instance, the conserved densities are no longer polynomials, but may be expressed as hyperelliptic integrals (elliptic if $g = 1$). Since even the genus 1 case has not been solved explicitly, this problem is well worth pursuing.

References

[1] Benney D.J., Stud. Appl. Math. 52, 45 (1973).

[2] Kupershmidt, B.A., and Manin, Yu.I., Funct. Anal. Appl. **11**, 188 (1978) and **12**, 20 (1978).

[3] Gibbons J., Dynamical Problems in Solition Systems, ed. S. Takeno, p.36 (Springer-Verlag, Berlin 1985).

[4] Timman R., Symposium Transsonicum, ed. K. Oswatitsch, p.394, (Springer-Verlag, Berlin 1964).

[5] Zabolotskaya E.A., Khokhlov R.V. Sov. Phys. Acoustics **15**, 35 (1969).

[6] Riemann, Werke, 2te Auflage., p.157 (Leipzig 1892).

[7] Gibbons J., Kodama Y., in preparation.

[8] Whitham G.B., Linear & Nonlinear Waves, p. 565, (Wiley-Interscience 1974).

[9] Flaschka H., Forrest G., McLaughlin D.W., Comm. Pure Appl. Math. **33**, 739 (1979).

GLIMM SCHEME AND CONSERVATION LAWS OF MIXED TYPE

H. GILQUIN
CNRS UA 04-740 and University of Saint-Etienne

We investigate the numerical resolution of problems modelized by conservation laws of mixed type. Many phenomena in elasticity are governed by such equations; i.e. :

A) Longitudinal (or pure shearing) motions of a material admitting phase changes:

$$1\text{-}1 \quad \begin{cases} u_{tt} = \sigma(u_x)_x \\ u(x,t) : \mathbb{R} \times \mathbb{R}^+ \longrightarrow \mathbb{R} \\ \text{with } \sigma'(u) > 0 \quad \text{if } u \notin [\alpha,\beta] \\ \text{and } \sigma'(u) \leq 0 \quad \text{if } u \in [\alpha,\beta] \end{cases}$$

One phase of the material can be distinguished from another using intervals where $\sigma'(u_x)$ stays of constant sign.

System 1-1 is hyperbolic if $\sigma' < 0$ and elliptic if $\sigma' > 0$. The same basic system is obtained when we study the motion of an isentropic Van der Waals gas [HS].

B) The motion of an elastic string :

$$1\text{–}2 \qquad y_{tt} = \left(T(|y_s|) \frac{y_s}{|y_s|} \right)_s$$

$y(s,t) : \mathbb{R}^2 \times \mathbb{R}^+ \longrightarrow \mathbb{R}^2$ is the location at time t of the string at rest's point of reference s. The stress T satisfies :

$$1\text{–}3\text{–}a \qquad \begin{cases} T(1) = 0 \\ T'(r) > 0 \quad \text{for } r > 0 \end{cases}$$

and for sake of simplicity, we will assume :

$$1\text{–}3\text{–}b \qquad \begin{cases} \text{either } T''(r) > 0 \\ \text{or } T''(r) < 0 \ \text{ and } \ T'(r) > rT(r) \quad \forall\, r > 0 \end{cases}$$

The system 1–2 is strictly hyperbolic if $y \in H = \{ y / r = |y_s| > 1 \}$ and of mixed type if $r < 1$. It has been studied in [Sh], [KK] and [CRS].

The difficulty of the numerical approximation of such systems arises from :

I) Classical schemes (Godunov, Glimm, Van Leer ...) are mainlybased on solving Riemann problems, resolution which is not always possible if the solution leaves the hyperbolic domain.

II) These systems are ill-posed when the solution leaves the hyperbolic domain and numerical approximations are very unstable (Hadamard instabilities).

Our goal is not to predict unstable states, but the search of stable states, particularly when the solution comes back in the hyperbolic domain after having left it.

For system 1-1 and system 1-2 under assumptions 1-3, it has been proved ([Sh], [CRS]) that the hyperbolic domain is stable by Riemann problem solution and therefore by Glimm's scheme. A theoretical study of approximated solutions of 1-1 and 1-2 by Glimm's scheme [Gl] has been done in [PS] and it is proved that weak convergence and hence strong convergence cannot occur in some cases where the solution leaves the hyperbolic domain.

We restrict our investigation to system 1-2 because it is too expensive to solve the Riemann problem for system 1-1. We show in this talk that the original version of Glimm's scheme [Gl] is sufficiently robust to allow computations even when the solution leaves the hyperbolic domain.

An elastic string which is a circle and for which the exact solution is known, is analysed as a two-dimensional (2D) test-case and we investigate numerical approximations of system 1-2 computed using two versions of Glimm's scheme. According to the results of [PS], the first version of Glimm's scheme does not allow the computation of the solution when it leaves the hyperbolic domain to enter the mixed one because the numerical solution is not kinematically admissible. The second version of Glimm's scheme (the original one) allows to reconstruct a numerical solution which is kinematically admissible and dynamically admissible on an average but not locally.

The presentation is organised as follows. In the first section, the test-problem is analysed and we define the numerical cases studied. In the second section, we summarize the two versions of Glimm's scheme and we recall a result given in [PS]. The numerical solutions obtained with the first version of Glimm's scheme are presented in section 3 and those obtained with the original version in section 4; the section 5 is devoted to a discussion about the results.

REFERENCES

[CRS] C. Carasso, M. Rascle et D. Serre, Etude d'un modèle hyperbolique en dynamique des câbles, M^2AN 19 (1985) 573-599.

[Gi] H. Gilquin, Une famille de schémas numériques T.V.D. pour les lois de conservation hyperboliques, M^2AN 20 (1986) 429-460.

[Gl] J. Glimm, Solutions in the large for nonlinear hyperbolic systems of equations, Communications on pure and applied mathematics 18 (1965) 697-715.

[Go] S.K. Godounov, A finite difference method for the numerical computation of discontinuous solutions of the equations of fluid dynamics, Mat. Sb. 47 (1959) 271-290.

[HS] R. Hagan & M. Slemrod, The viscosity-capillarity admissibility criterion for shocks and phase transitions. Arch. Rat. Mech. Anal. 83 (1983) 333-361.

[KK] B.L. Keyfitz & H.C. Kranzer, A system of non-stricly hyperbolic conservation laws arising in elasticity theory , Arch. Rat. Mech. Anal. 72 (1980) 219-241.

[Liu] T.P. Liu, The deterministic version of the Glimm scheme, Comm. Math. Phys. 57 (1977) 135-148.

[PS] R.L. Pego & D. Serre, Instabilities in Glimm's scheme for two systems of mixed type. Preprint.

[Sh] M. Shearer, The Riemann problem for a class of conservation laws of mixed type, J. Diff. Eqns 46 (1982) 426-443.

A NUMERICAL METHOD FOR A CLASS OF EQUATIONS MODELLING ONE-DIMENSIONAL MULTIPHASE FLOW

-G-

Tore Gimse
Matematisk Institutt
Universitetet i Oslo
P.B. 1053 Blindern
0316 OSLO 3
NORWAY

The general system of hyperbolic conservation laws governing multiphase flow in one spatial dimension :

$$u_{i,t} + f_i(u)_{,x} = 0 \; ; \; i=1,2,,,N$$

is modified in the following way :
We assume that the function f_i is a function of the components u_1 , u_2 ,,,,, u_i only. Hence we obtain the equation system :

$$\begin{aligned} & u_{1,t} + f_1(u_1)_{,x} = 0 \\ (*) \qquad & u_{2,t} + f_2(u_1,u_2)_{,x} = 0 \\ & \vdots \\ & u_{N,t} + f_N(u_1,u_2,,,,u_N)_{,x} = 0 \end{aligned}$$

Existence and uniqueness of the solution of this kind of equation system (where the derivative of the flux function df , is a lower triangular matrix) is recently shown by Holden and Høegh-Krohn (HH). In their proof they bring forth ideas of a method for constructing the solution explicitly. These ideas are here developed as a numerical method. They are closely related to concepts of polygonal approximations (e.g. Dafermos (Da)) and convex-envelope tracking (as presented in (HHH)).
With assumptions of 3-phase flow (N=2) of oil,gas and water, we also obtain stability and convergence results for the numerical method.

The equations (*) are solved by solving one equation at the time, starting out with the first equation, which is, of course, an ordinary scalar equation. The solution, for any initial value function, gives us, by the methods mentioned above, a finite number of shocks, that is, a finite number of u_1 - values to be considered in equation nr. 2. These values of u_1 give rise to $f_2(u_1, \;)$ - functions, upon which the solution of eq.2 is constructed. Passing

from one function $f_2(u_1^i, \ )$ till another $f_2(u_1^{i+1}, \ )$ should be shocks coinciding with the u_1-shock from u_1^i to u_1^{i+1}. In between these shocks we use the simple scalar algorithm for a single equation : $u_{2,t} + f_2(u_1^i, u_2) = 0$. Then, the solution of equations no. 1 and 2 gives us a finite number of u_2 -shocks - some of them coinciding with u_1 -shocks. All these shocks give a sequence of f_3 - functions which should be treated as the previous f_2 - sequence and so on.

Turning away from the general system of equations, we now consider a system for three-phase flow :

$$(**) \qquad \begin{aligned} u_t + f(u)_x &= 0 \\ v_t + g(u,v)_x &= 0 \end{aligned}$$

If u is the gas-saturation, v the oil-saturation then the water-saturation is determined by $w = 1 - u - v$. The simplification from a general 2x2-system is based upon an assumption that the gas-flow (Eq.1) is independent of whatever it takes place in oil or water, while the oil-flow (Eq.2) is sensitive to the amount of gas present.

With no gravitational effects involved we may assume (as is commonly done) that the flux-functions f and g have an S-shaped form:

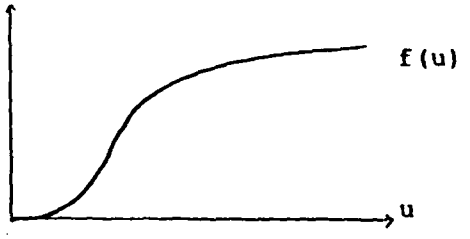

Furthermore that $g(\ ,v)$ is strictly decreasing :

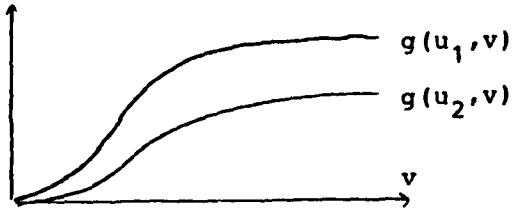

if $u_1 < u_2$.

Treating the Riemann-problem for (**) (a general initial value problem is decomposed into a finite number of Riemann-problems), that is :

$$(u,v)(x,0) = \begin{cases} (u_-, v_-) & \text{if } x < 0 \\ (u_+, v_+) & \text{if } x > 0 \end{cases}$$

where u_-, v_-, u_+ and v_+ are constants.
We develope a numerical method that is well-defined (the solution is inside the phase-space : $u + v < 1$), and stable. By stability we will mean that by making the polygonal approximation better than a certain limit, no additional information is gained, nor does variation increase (as has been a problem with finite difference methods, e.g. (Te)).
The solution (as a curve in phase-space) also depends L_1 - continuosly upon the initial data.

Numerical examples are shown, also with some comparision to finite difference methods.

References (from the Abstract) :

(Da) Dafermos C.M. Polygonal Approximations of Solutions of the Initial Value Problem for a Conservation Law. Jour. Math.Anal. and Appl. (38) 1972

(HH) Holden L. and Høegh-Krohn R. A nxn class of systems of hyperbolic conservation laws. Preprint, Univ. of Oslo, 1986.

(HHH) Holden H., Holden L. and Høegh-Krohn R. A numerical method for first order non-linear scalar hyperbolic conservation laws in one dimension. Preprint, Univ. of Oslo, 1986.

(Te) Temple B. Global Solution of the Cauchy Problem for a Class of 2 x 2 nonstrictly Hyperbolic Conervation Laws. Adv. in Appl. Math. (3) 1982

THE INTERACTION OF NONLINEAR WAVES

J. Glimm

Courant Institute of Mathematical Sciences

New York University

New York, N. Y. 10012

Nonlinear hyperbolic waves interact in distinctive patterns. The systematic study of nonlinear wave interactions leads to Riemann solutions and elementary waves, which are solutions of a hyperbolic conservation law with one or two extra continuous symmetries respectively: scale invariance and time invariance (in some frame). Striking and qualitative new wave interaction phenomena have been discovered in conservation laws having natural motivations from science. The general feature of this phenomena is a strong qualitative departure from linearity in the wave interactions. Resonance, or coinciding wave speeds typically give rise to such phenomena, as do anomalies in the equation of state such as phase transitions or exothermic reactive chemistry.

Two theoretical problems of a very fundamental nature will be emphasized. They are uniqueness (entropy conditions) and length scales. Both of these problems require stepping outside of the conservation law, the entropy condition by restricting the class of allowed weak solutions and the length scales by breaking the scale invariance of the equation through modifications of the equation itself.

The use of Riemann solutions in numerical computations by the front tracking method will be presented. Our main conclusion is that this method has succeeded in cases in which complex wave interactions occur.

Convenient Stability Criteria for Difference Approximations of Hyperbolic Initial-Boundary Value Problems

Moshe Goldberg
Department of Mathematics
Technion—Israel Institute of Technology
Haifa 32000, Israel

Consider the first order system of hyperbolic partial differential equations

$$\partial u(x,t)/\partial t = A\partial u(x,t)/\partial x + Bu(x,t) + f(x,t), \quad x \geq 0, \quad t \geq 0,$$

where $u(x,t)$ is the unknown vector, A a diagonal matrix of the form $A = A_1 \oplus A_2$ with $A_1 > 0$ and $A_2 < 0$, B an arbitrary matrix, and $f(x,t)$ a given vector. The problem is well posed in $L_2(0,\infty)$ if initial values

$$u(x,t) = u_0(x) \in L_2(0,\infty), \quad x \geq 0,$$

and boundary conditions

$$u_1(0,t) = Su_2(0,t) + g(t), \quad t \geq 0,$$

are prescribed. Here u_1 and u_2 are the inflow and outflow parts of u corresponding to the partition of A, and S is a coupling matrix.

This talk describes a recent and joint effort with E. Tadmor (*Math. Comp.* 48 (1987), 503-520), in which we sharpened and extended our 1985 results in order to achieve more versatile, convenient stability criteria for a wide class of finite difference approximations to the above initial-boundary value problem.

In our work the difference approximations consist of a general difference scheme — explicit or implicit, dissipative or not, two-level or multilevel — and boundary conditions of a wider type than discussed by us before. As in the past, we restrict attention to the case where the outflow components of the principal part of the boundary conditions are *translatory*, i.e., determined at all boundry points by the same coefficients. In many cases this is not a severe limitation since such boundary conditions are commonly used in practice; and in particular, when the numerical boundary consists of a single point, the boundary conditions are translatory by definition.

Throughout our work we assume that the basic scheme is stable for the pure Cauchy problem, and that the other assumptions which guarantee the validity of the Gustafsson-Kreiss-Sundström stability theory, hold. With this in mind we raise the question of stability for the given difference approximation.

The first step in our stability analysis is to prove that the approximation is stable if and only if the scalar outflow components of its principal parts are stable. Thus, our global stability question is reduced to that of a scalar, homogeneous approximation associated with the elementary initial value problem

$$\partial u/\partial u = a\partial u/\partial x, \quad a = \text{constant} > 0, \quad x \geqslant 0, \quad t \geqslant 0.$$

$$u(x,0) = u^0(x), \quad x \geqslant 0.$$

The stability criteria obtained by us for the reduced problem depend both on the basic difference scheme and on the boundary conditions, but very little on the interaction between the two. Such criteria eliminate the need to analyze the intricate and often complicated interaction between the basic scheme and the boundary conditions; hence providing in many cases a convenient alternative to the well known stability criteria of Kreiss (1968) and of Gustafsson, Kreiss and Sundström (1972).

Having the new criteria, we establish all our previous examples, as well as new ones. This includes a host of dissipative and nondissipative cases that incorporate and generalize most of the examples studied in recent literature. To mention some of our examples, we prove stability for:

(a) Arbitrary two-level schemes, with boundary conditions generated by either the explicit or implicit one-sided Euler schemes.

(b) Arbitrary two-level schemes, with boundary conditions generated by either horizontal extrapolation or by the one-sided three-level Euler scheme.

(c) Arbitrary dissipative schemes, with boundary condition generated by oblique extrapolation or by the Box scheme.

(d) The Crank-Nicolson, Backward-Euler, Leap-Frog and Lax-Friedrichs schemes (all nondissipative), with boundary conditions generated by either oblique extrapolation or by the one-sided Weighted Euler scheme.

Hyberbolic Heat Transfer Problems with Phase Changes

J. M. Greenberg*

This talk will focus on hyperbolic models of heat transfer capable of supporting both "superheating" and "undercooling". These are obtained as limits of "phase-field" models as a small parameter tends to zero. The principal motivation for this work is to obtain a formula for the speed of propagation of the free boundary (either a melt or freezing interface) which depends on the temperature ahead of the interface and the interface curvature. Such a formula is required as a closure relation for the limiting hyperbolic system of partial differential equations in order to have a well posed problem.

The theory of the limiting hyperbolic systems will be discussed and qualitative properties of solutions to the hyperbolic models will be compared with solutions to classic melt problems modelled by parabolic partial differential equations.

* Department of Mathematics
The University of Maryland
Boltimore County Campus
Cantonsvill, Maryland 21228
USA

Unsymmetric hyperbolic systems and almost incompressible flow.

Bertil Gustafsson*

We consider systems

$$u_t + Au_x + Bu_y = 0$$

where the coefficient matrices A, B are very unsymmetric. One example of such a system is almost incompressible flow, which is characterized by low Mach-numbers ε. We take $1/\varepsilon$ as the degree of unsymmetry for general systems. If T is a matrix which symmetrizes A and B, the L_2-norm fulfills

$$\| u(t) \| \leq \text{cond}(T) \| u(0) \|$$

where

$$\text{cond}(T) = |T| \cdot |T^{-1}| \ .$$

If the system has a high degree of unsymmetry, the condition number is large, and some transformation must be applied. We shall discuss this symmetrization procedure. In general it is not sufficient to do a direct scaling of the dependent variables. For smooth solutions it is possible to express the solution as an asymptotic expansion in ε, and by subtracting the first term, a symmetric system can be obtained. We demonstrate how this procedure can be generalized to the non-linear Euler equations.

The transformed system can be used as a basis for computation of almost incompressible flow, or for incompressible flow which corresponds to the limit $\varepsilon = 0$. In this case a semiimplicit method is used which is such that the divergence is kept low automatically. The method requires the solution of a linear system in each step, but the coefficient matrix is constant and the LU-decomposition can be made once and for all. We shall present an analysis of this method, and also discuss another class of methods based on splitting of the differential operator.

* Department of Scientific Computing
Uppsala University
Sturegatan 4B
S-752 23 UPPSALA
SWEDEN

For the Navier-Stokes equations the same principles can be applied, and the system can be made symmetric by using the same transformation as above. We shall present numerical experiments where the difference scheme uses the Euler backwards method for the large hyperbolic part, the leap-frog method for the remaining hyperbolic part and the Euler forwards method for the parabolic part.

For singular perturbation problems of the type discussed here, the form of the boundary conditions play an important role. Even if the problem is well posed for any fixed ε, the solution is of little use if the problem is not well posed also for $\varepsilon = 0$. In other words, the estimates of the solution must be independent of ε.

For the symmetrized Euler equations such boundary conditions can be easily constructed. However, for the Navier-Stokes equations a fundamental difficulty arises. For an inflow boundary the two-dimensional compressible equations require three conditions, while the incompressible equations require only two. We shall show how this difficulty can be overcome. By introducing the divergence $u_x + v_y$, the extra boundary condition becomes the incompressibility condition $u_x + v_y = 0$ in the limit. In this way there is no undue restriction imposed on the limit solution.

The assumption that the fast time scale is not present in the solution can be interpreted as an assumption of smoothness.

If the derivatives are bounded independently of ε initially, they remain bounded on any finite time interval. We shall prove that our boundary conditions are such that this is the case.

Numerical results are presented, including some recent computations for the incompressible Navier-Stokes equations.

Multi-Grid Methods for Hyperbolic Problems

W. Hackbusch
Praktische Mathematik
Christian-Albrechts-Universität Kiel
D-2300 Kiel 1

Abstract. As well-known the multi-grid methods consists of two parts, the smoothing procedure and the coarse-grid correction. While the coarse-grid correction seems to be applicable independent of the kind of problem, the smoothing process is closely connected with *elliptic* problems. Therefore, multi-grid programmes cannot be expected to run for hyperbolic equations without difficulties.

Indeed, it is kwown that singular perturbation problems like the convection diffusion equation

(1) $$- \varepsilon \, \Delta u + c \, \mathbf{grad} \, u = f$$

require an appropriate choice of the smoothing procedure in order to achieve fast convergence. In particular for $\varepsilon = 0$, when Eq (1) becomes an hyperbolic problem, the smoothing process must be adapted carefully to the problem.

Often the difficulties are tried to be avoided by adding *artificial viscosity or ellipticity.* Here, one has to define clearly, what is meant by ellipticity. If the additive term is Lu with an elliptic Operator L, the term *ellipticity* makes sense. However, then one-sided differences do not nessecarily add (numérical) ellipticity. E.g. the backward difference for u_x adds a term $Lu=u_{xx}$, where L is *not* elliptic (in 2D or 3D). This difference is essential for the behaviour of usual smoothing iterations. The more ellipticity is added the less critical is the choice of the smoothing process. On the other hand the only harmless additive term is a non-elliptic 2nd order derivative with respect to the characteristic direction.

In this contribution a multi-grid method is constructed, whic works also for (of course stable) hyperbolic discrete problem without any ellipticity in the sense defined above. As consequence the usual smoothing procedures may be inefficient Instead of proposing sophisticated smoothing iterations, we appl a completely different procedure for the *coarse-grid correction* In 2D a fine grid is the union of four different coarse grids Each coarse grid is combined with a special prolongation into th fine grid and a restriction from the fine grid. Most of thes prolongations and restrictions are completely different from th usual ones, in order to approximate also *high* frequencies Since each of the coarse grids applies to a special part of th

spectrum, this method is called the *frequency decomposition multi-grid method.*

The features of the proposed method are as follows. The smoothing iteration can be chosen to be a very simple one. On the other hand the coarse-grid correction becomes more complicated. The V-cycle can still be performed with O(n) operations, where n is number of unknowns. Instead, the usual W-cycle results in an operation count of O(n*log n). The method is restricted to uniform grid structures, i.e. it does not work for a discrete problem in a general unstructured triangulation. However, the method is independent of the number of dimension, therefore the treatment of 3D equations causes no further difficulties.

Accurate Boundary Conditions for Exterior Problems in Gas Dynamics

Thomas Hagstrom

Department of Applied Mathematics and Statistics
SUNY at Stony Brook
Stony Brook, NY 11794
and
S. I. Hariharan
Department of Mathematical Sciences
University of Akron
Akron, OH 44325

Abstract

Interesting and important problems in gas dynamics are often posed in exterior domains. Examples include the explosion of gas bubbles in various media and flows external to aircraft. An approach to the numerical solution of such problems is to restrict the computational domain to a finite region through the introduction of an artificial boundary. For large time computations interactions between the solution and the artificial boundary can strongly influence the results. The focus of this paper is the development of an accurate treatment of these conditions.

A variety of authors have invoked a principle of no reflection [2,5,6]. However, as pointed out by Gustafsson and Kreiss [3], conditions satisfied by the exact solution may involve reflections. The current study involves spherical waves which exhibit coupling between incoming and outgoing Riemann variables. One expects this coupling to result in natural reflections which should be accounted for in an efficient numerical treatment. Our procedure is to develop approximate solutions to the appropriate weakly nonlinear initial boundary value problem in the region exterior to the computational domain. A condition is thus obtained which includes appropriate reflections at the computational boundary. (It is, in some sense, a generalization of the results for the linear wave equation given in [1].) Related

works using asymptotic techniques in the derivation of numerical boundary conditions for hyperbolic systems include [8-10] for steady state problems and [11,12] for time dependent solutions.

The particular equations under consideration are the Euler equations for spherically symmetric, isentropic fluid flow;

$$\frac{\partial R}{\partial t} + \left(\frac{z}{\rho} + \sqrt{f'(\rho)}\right)\frac{\partial R}{\partial r} = -\frac{2\sqrt{f'(\rho)}z}{\rho r},$$

$$\frac{\partial S}{\partial t} + \left(\frac{z}{\rho} - \sqrt{f'(\rho)}\right)\frac{\partial S}{\partial r} = \frac{2\sqrt{f'(\rho)}z}{\rho r}.$$

Here, R and S are the Riemann variables;

$$R = \frac{z}{\rho} + G(\rho),$$

$$S = \frac{z}{\rho} - G(\rho).$$

We also assume that the computational boundary is located at $r = L$ and that the initial momentum and density satisfy $z = 0$ and $\rho = \rho_\infty$ for $r \geq L$.

To derive the boundary conditions, we consider the initial boundary value problem on the exterior domain $r \geq L$ with boundary condition

$$R(L,t) = g(t).$$

Solving this problem yields

$$S(L,t) = \mathcal{F}[g(\cdot)].$$

The equations above represent an exact boundary condition at $r = L$. Following the construction presented by Whitham [7, Ch.9], we find approximate representations for $\mathcal{F}$. Three asymptotically equivalent representations of these are:

$$\frac{\partial S}{\partial t}(L,t) = \begin{cases} \frac{\sqrt{f'(\rho_\infty)}(R(L,t)-R_0)}{2L} & or \\ \frac{z(L,t)\sqrt{f'(\rho_\infty)}}{L\rho(L,t)} & or \\ \frac{(G(\rho(L,t))-G(\rho_\infty))\sqrt{f'(\rho_\infty)}}{L}. \end{cases}$$

Nonlinear energy estimates are established for the resulting finite domain problem and numerical experiments are presented for an idealized weak explosion problem. Our technique is shown to yield the correct steady state for values of L significantly smaller than those required by the nonreflecting conditions.

Finally we propose extensions of our conditions for the truly three dimensional case. This involves the assumption that the primary direction of propagation is the radial one. Additional conditions are required whenever the artificial boundary is an inflow boundary. Then we suggest augmenting the relations above with:

$$\frac{\partial m}{\partial t} + \frac{1}{L^2}\frac{\partial f}{\partial \theta} = 0,$$

$$\frac{\partial q}{\partial t} + \frac{1}{L^2 \sin\theta}\frac{\partial f}{\partial \phi}.$$

Here, m and q are the angular momenta.

Details of this work may be found in [4]. The first author was partially supported by ICOMP, NASA Lewis Research Center and the second by National Science Foundation grant No. DMS-8604047

References

[1] Bayliss, A. and E. Turkel, "Radiation Boundary Condition for Wave-like Equations", *Comm. Pure Appl. Math.*, Vol. 33, (1980), pp. 707-723.

[2] Engquist, B. and A. Majda, "Absorbing Boundary Conditions for the Numerical Simulation of Waves", *Math. Comp.* Vol. 31, (1977), pp. 629-651.

[3] Gustafsson, B. and H.-O. Kreiss, "Boundary Conditions for Time Dependent Problems with an Artificial Boundary", *J. Comp. Phys.* Vol. 30, (1979), pp. 333-351.

[4] Hagstrom, T. and S. I. Hariharan, "Accurate Boundary Conditions for Exterior Problems in Gas Dynamics", *Math. Comp.* submitted for publication.

[5] Hedstrom, G.W., "Non-Reflecting Boundary Conditions for Nonlinear Hyperbolic Systems", *J. Comp. Phys.* Vol. 30, (1979), pp. 222-237.

[6] Thompson, K.W.,"Time Dependent Boundary Conditions for Hyperbolic Systems", *J. Comp. Phys.* Vol. 68, (1987), pp. 1-24.

[7] Whitham, G.B., *Linear and Nonlinear Waves,* (1974), Wiley, New York.

[8] Ferm, L., "Open Boundary Conditions for External Flow Problems", Uppsala University, Dept. of Sci. Comp., rep. 108, (1987).

[9] Ferm, L. and B. Gustafsson, "A Down-Stream Boundary Procedure for the Euler Equations", *Computer and Fluids* Vol. 10, (1982), pp. 261-276.

[10] Ferm, L. and B. Gustafsson, "Far Field Boundary Conditions for Steady State Solutions to Hyperbolic Systems", *Nonlinear Hyperbolic Problems; Proceedings St. Etienne 1986*, Lecture Notes in Math. 1270.

[11] Gustafsson, B., "Inhomogeneous Conditions at Open Boundaries for Wave Propagation Problems", *Appl. Num. Math.*, (1988) to appear.

[12] Gustafsson, B., "Far Field Boundary Conditions for Time-Dependent Hyperbolic Systems", *SIAM J. Sci. Stat. Comp.*, (1988) to appear.

H

ON NUMERICAL METHODS FOR VISCOUS PERTURBATIONS OF HYPERBOLIC CONSERVATION LAWS

Eduard Harabetian *

We consider the numerical approximation of solutions to viscous perturbations of genuinely nonlinear conservation laws:

$$(1) \qquad u_t + f(u)_x = \varepsilon(a(u)u_x)_x\,, \quad a>0, \quad f''>0$$

When ε is small, the solution develops viscous shock layers, i.e., thin ($O(\varepsilon)$) regions where the derivative is large ($O(1/\varepsilon)$). It is plausible that for an accurate resolution of such layers, one should not take h/ε too large, where h is the spacial mesh width. Our results are the following:

a) We construct a three-point explicit scheme in conservation form:

$$u_j^{n+1} = u_j^n + (\nu_{j+1/2}^n - \nu_{j-1/2}^n),$$

which can be written in incremental form (see[1]):

$$u_j^{n+1} = u_j^n + C_{j+1/2}\Delta_{j+1/2}u^n - D_{j-1/2}\Delta_{j-1/2}u^n,$$

where

$$C_{j+1/2} = C(h/\varepsilon, \delta t/h, u_j^n, u_{j+1}^n),$$

$$D_{j-1/2} = D(h/\varepsilon, \delta t/h, u_{j-1}^n, u_j^n), \text{ and } \Delta_{j+1/2}u^n = u_{j+1}-u_j.$$

Let

$$a_1=\sup_u(a(u)),\ a_0=\inf_u(a(u))$$

$$\lambda=\frac{\delta t}{h}\cdot\sup_u(f'(u)),\ R=\frac{h}{\varepsilon}\cdot\sup_u(f'(u)).$$

We show that this scheme is second order accurate with the equation (1) (in a precise sense), and Total Variation Diminishing (T.V.D. [1]) if

$$\frac{R}{a_0F(a_1/a_0)} \le 1,$$

and the following CFL condition

$$\lambda\left(2a_1\frac{F(a_0/a_1)}{R}+1\right)\le 1$$

are satisfied. Here, $F(x)=x(1+g^{-1}(x))$, $g(x)=\frac{1}{x}\log(1+x)$. In particular, F is decreasing, $F(1)=1$, so if $a(u)\equiv 1$, we get:

* Dep. of Mathematics, University of Michigan, Ann Arbor MI, USA

$R \leq 1$, and

$$\lambda(2/R + 1) \leq 1.$$

Our scheme uses the travelling wave solutions of (1) as approximating tools. The approach is similar to the one introduced by Godunov for the hyperbolic problem [2]. Our construction also yields the following interesting corollary:

b) Given any three-point, second order accurate scheme which is TVD in the sense introduced by Harten [1] then the pair (R, λ) associated with it must satisfy the following constraints:

$$0 \leq \frac{R(1-\lambda)}{2a_1} \leq 1, \text{ and}$$

$$2\lambda a_0/R + \lambda^2 \leq 1.$$

If $a \equiv 1$, then

$$\frac{2\lambda}{1-\lambda^2} \leq R \leq \frac{2}{1+\lambda}, \quad \lambda < 1$$

Bellow we computed a viscous profile for Burger's equation, with $R=1$, $\lambda=1/3$, $h=.05$. The computed error indicated better than second order convergence.

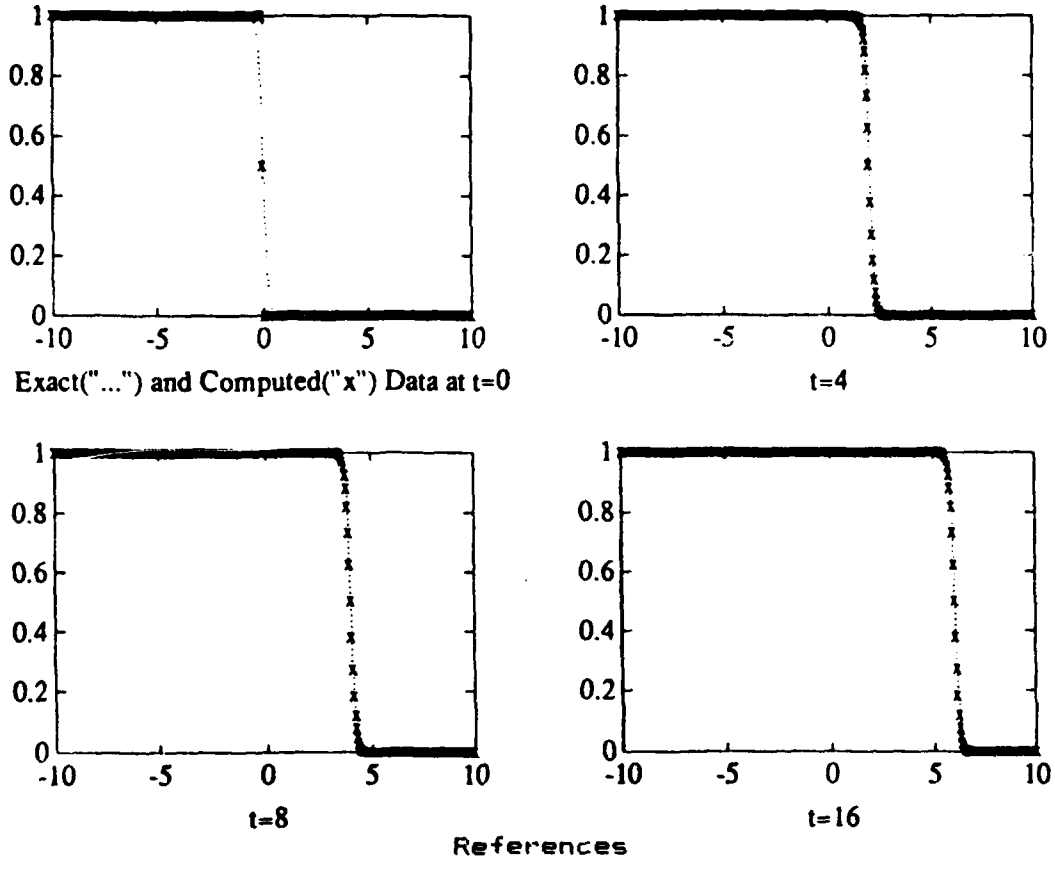

References

[1] Harten A., *J. Comput. Phys., v.49, 1983, pp. 357-393*
[2] Godunov S. K., *Math. Sb., v. 47, 1959, pp.271-295 (Russian)*

Solution of the Euler Equations for Unsteady, Two-Dimensional, Transonic Flow by the Approximate-Factorization Method

H. Henke

Messerschmitt-Bölkow-Blohm GmbH
Bremen, FRG

Introduction

The numerical simulation of the aerodynamic forces acting on an oscillating wing section in transonic flow by solving the Euler equations is described. The method of solution is the approximate-factorization method of Beam und Warming /1/. Since time-dependent calculations should be performed, an implicit algorithm was developed because it allows considerably larger time-steps than explicit schemes, and calculations must be carried out over several periods of oscillation on airfoils. In this paper several calculations for for steady and unsteady transonic flow cases were carried out.

Governing Equations and Method of Solution

For the present investigation the Euler equations are written in curvilinear coordinates (ξ,η,τ):

$$\bar{U}_\tau + \bar{F}_\xi + \bar{G}_\eta = 0 \qquad (1)$$

where $\bar{U} = \frac{1}{J}\begin{bmatrix} \rho \\ \rho u \\ \rho v \\ e \end{bmatrix}$; $\bar{F} = \frac{1}{J}\begin{bmatrix} \rho\tilde{U} \\ \rho u\tilde{U} + \xi_x p \\ \rho v\tilde{U} + \xi_y p \\ (e+p)\tilde{U} - \xi_t p \end{bmatrix}$; $\bar{G} = \frac{1}{J}\begin{bmatrix} \rho\tilde{V} \\ \rho u\tilde{V} + \eta_x p \\ \rho v\tilde{V} + \eta_y p \\ (e+p)\tilde{V} - \eta_t p \end{bmatrix}$

In the above relations $\tilde{U}$ and $\tilde{V}$ are the contravariant velocities and J is the Jacobian of the coordinate transformation.

The method of approximate factorization of Beam and Warming /1/ was used for solving the Euler equations

$$(I + \Delta\tau \frac{\partial}{\partial\xi}\bar{A}^n + D_{I\xi})(I + \Delta\tau \frac{\partial}{\partial\eta}\bar{B}^n + D_{I\eta})\Delta\bar{U}^n = -\Delta\tau(\frac{\partial\bar{F}}{\partial\xi} + \frac{\partial\bar{G}}{\partial\eta})^n + D_E = RHS \qquad (2)$$

$$\Delta\bar{U}^n = \bar{U}^{n+1} - \bar{U}^n$$

where $\bar{A}$ and $\bar{B}$ are the Jacobian matrices, and D_I and D_E are implicit and explicit nonlinear damping terms defined in /2/.

The spatial derivatives were approximated by central differences of second order accuracy, so that a 4x4 block-tridiagonal system results. The solution of this system of equations requires relatively long computational time.
A substantial reduction of the computing time is obtained by diagonalizing the matrices $\bar{A}$ and $\bar{B}$ with the similarity transformatio of the form /3,4/

$$\bar{A} = T_\xi \Lambda_\xi T_\xi^{-1} \qquad \bar{B} = T_\eta \Lambda_\eta T_\eta^{-1}$$

$$\text{where} \quad \Lambda_\xi = \begin{bmatrix} \tilde{U} & 0 & 0 \\ 0 & \tilde{U} & 0 \\ 0 & 0 & \tilde{U}+k_\xi c \\ & & \tilde{U}-k_\xi c \end{bmatrix} \quad , \quad \Lambda_\eta = \begin{bmatrix} \tilde{V} & 0 & 0 \\ 0 & \tilde{V} & 0 \\ 0 & 0 & \tilde{V}+k_\eta c \\ & & \tilde{V}-k_\eta c \end{bmatrix} \qquad (3)$$

yielding a system of 4 scalar equations /4,5/

$$T_\xi^n \left(I + \Delta\tau \frac{\partial}{\partial\xi} \Lambda_\xi^n + D_{I_\xi}\right) N^n \left(I + \Delta\tau \frac{\partial}{\partial\eta} \Lambda_\eta^n + D_{I_\eta}\right) \left(T_\eta^{-1}\right) \Delta\bar{U}^n = RHS \qquad (4)$$

he latter method is nonconservative in unsteady transonic flow and as therefore only used for the calculation of steady flow with embedded shocks. For unsteady flow calculations scheme (2) was used.

he boundary condition at the body surface is given for $\eta=0$ by the condition of impermeability $\tilde{V}=0$. The density and the tangential component of the velocity is obtained by linear extrapolation. The pressure on the body contour is calculated by the normal momentum equation. In the far-field, characteristic compatibility relations based on the one-dimensional characteristics similar to that given in /6/ are employed. Additionally a vortex-correction formulation /7,8/ must be taken into account, so that there is no or little change in lift due to the extend of the computational domain.

he linear stability analysis shows unconditional stability for the approximate-factorization method, but the amplification factor approaches unity for large Courant numbers, as a result of the factorization error. The consequence is a decreasing rate of convergence with increasing time step, and in practice the Courant number is restricted to O(10). This restriction is not so weighty for unsteady flow computation because the physical aspects must be taken into account.

Results

For all calculations carried out a C-type grid, given for transonic test problems in /9/ with 141x21 points was used. The response characteristics of the airfoil surface pressure to the airfoil motions can be depicted using Fourier representation. If the unsteady angle of attack is expressed as $\alpha(t)=\alpha_\infty+\mathrm{Im}(\alpha_0 e^{i\omega t})$, the Fourier series representation of the pressure coefficient can be written as $c_p(x,t)=c_{p_\infty}(x)+\Sigma\,\mathrm{Im}(c_{p,\alpha_0}^n(x)\alpha_0 e^{in\omega t})$.
In Fig. 1 the pressure distribution is given for several time points for a harmonically oscillating profile at a Mach-number of 0.80. For the same profile the steady pressure distribution for M=0.85 is given in Fig. 2a, and in Fig. 2b the first mode harmonic components of the pressure on the lower and upper side of the profil are shown. For the same case in Fig.3 the L_2-Norm in the change of the density ($\Delta\rho/\Delta t$) as a function of the time steps for steady and unsteady flow is presented. In Fig. 4 the steady pressure distribution and the lines of constant Mach-number for a MBB A3 profile in transonic flow is shown. In Fig. 5a the corresponding unsteady pressure distribution for the oscillating wing section, and in Fig. 5b the number of supersonic points as a function of the time-steps is used as a crude indication of convergence (for the steady case); for the number of time-steps n>400 the change of supersonic points for the oscillating airfoil can be seen.

Conclusion

In this paper a method has been developed for calculating aerodynamic forces on a wing-section oscillating harmonically in transonic inviscid flow. The Euler equations are taken as governing flow equations. They are solved by the approximate-factorization method of Beam and Warming. Results have been presented for steady and unsteady flow cases for an oscillating airfoil.

References

/1/ Beam, R., Warming, R.F., J. Comp. Physics, 22, (1976), 87
/2/ Henke, H., Hänel, D.: N. Numer. Fluid Mech., 13, (1986), 137
/3/ Warming, R.F., Beam, R., Hyett, B.J., Math. Comput., 29, (1975), 1037
/4/ Pulliam, T.H., Chaussee, D.S., J. Comp. Phys., 39, (1981), 347
/5/ Henke, H., Hänel, D., Lecture Notes Phys., 218, (1985), 267
/6/ Whitfield, D.L., Janus, J.M., AIAA Paper 84-1552
/7/ Thomas, J.L., Salas, M.D., AIAA J., 24, (1986), 1074
/8/ Pulliam, T.H., Steger, J.L., AIAA Paper 85-0360
/9/ Rizzi, A., Viviand, H., (Eds.), N. Numer. Fluid Mech., 3, (1981)

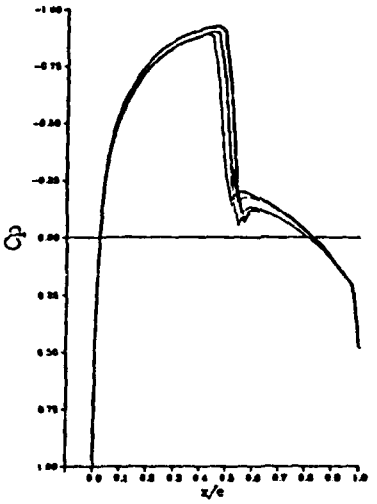

Fig. 1: Pressure distribution for several times for a pitching airfoil-section, NACA 0012, M_∞=0.80, α_m=0°, α_0=0.5°

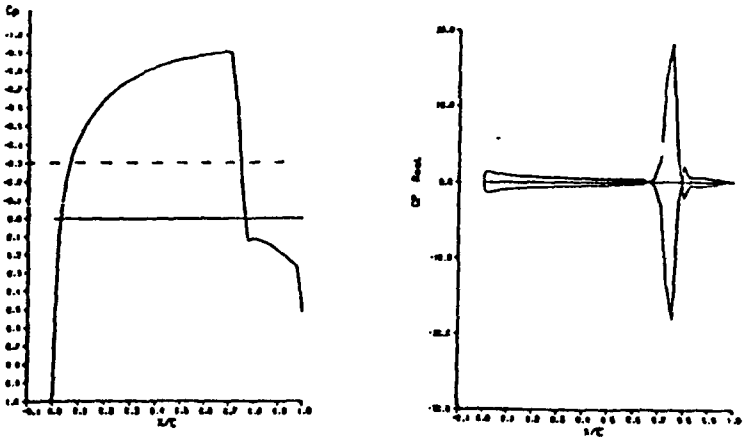

Fig. 2: Pressure distributions for a NACA 0012 profil, M_∞=0.85, α_∞=0°

a) steady pressure

b) unsteady pressure: $c_{p_{real}}$ for upper and lower side

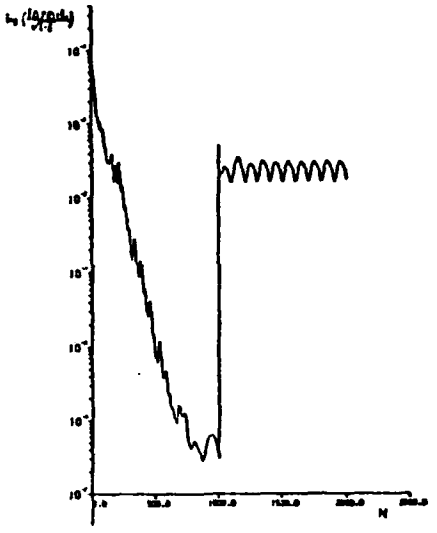

Fig. 3: L_1-Norm of the density ($\Delta\rho/\Delta t$) as a function of the number of time steps
Steady flow: n<1000, Unsteady flow: n>1000 with 200 time-steps/period

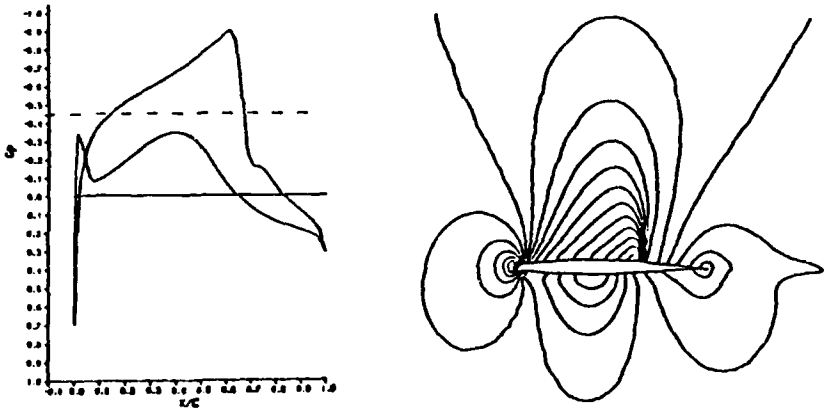

Fig. 4: Steady pressure distribution for a MBB A3 profil and lines of constant Mach-numbers, M_∞=0.80, α_∞=-0.20°

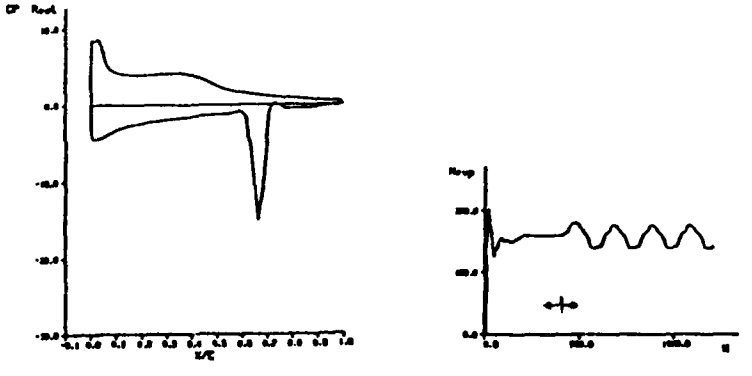

Fig. 5: Unsteady pressure distribution and number of supersonic points as function of the time steps

a) c_p for upper and lower side

b) NSUP: n<400 - steady flow
n>400 - unsteady flow

ON SOME RECENT RESULTS FOR CONSERVATION LAWS IN ONE DIMENSION

Helge Holden

Matematisk institutt, Universitetet i Trondheim, N-7034 Trondheim-NTH, Norway

1. The equations

Here we will give a very short introduction to some properties of the initial value problem

$$z_t + F(z)_x = 0$$
$$z(x,0) = z_0(x) = \begin{cases} z_L, & x < 0 \\ z_R, & x > 0 \end{cases} \tag{1.1}$$

($\frac{\partial z}{\partial t} = z_t$ etc.) where $z = z(x,t) = (u(x,t),v(x,t)) \in \mathbf{R}^2$, $F(z) = (f(z),g(z))$ and $x \in \mathbf{R}$, $t \geq 0$. With this particular choice of initial value (with z_L and z_R constants, $z_L, z_R \in \mathbf{R}^2$) (1.1) is called the Riemann problem for the conservation law $z_t + F(z)_x = 0$. (1.1) expresses a conservation law since, formally

$$\frac{d}{dt} \int_{x_1}^{x_2} z(x,t)dx = F(z(x_1,t)) - F(z(x_2,t)). \tag{1.2}$$

Basic in the analysis is the 2×2 matrix $dF(z) = \begin{bmatrix} f_u & f_v \\ g_u & g_v \end{bmatrix}$. If $dF(z)$ has two real eigenvalues $\lambda_1(z),\lambda_2(z),\lambda_1(z) \leq \lambda_2(z)$, with corresponding right eigenvectors $r_1(z)$ and $r_2(z)$ respectively, (1.1) is said to be hyperbolic, if $\lambda_1(z) < \lambda_2(z)$ (1.1) is strictly hyperbolic, while (1.1) is said to be elliptic if $dF(z)$ has no real eigenvalues. A fundamental property of (1.1) is that even for $z_0 \in C^\infty$ the solution $z = z(x,t)$ will in general develop singularities in finite time [1], hence one has to look for weak solutions which again raises uniqueness questions. In the context of (1.1) one imposes additional entropy conditions to select the correct physical solution.
The solution of the Riemann problem consists of combinations of two elementary solutions, namely shocks and rarefaction waves. A shock solution to (1.1) is

$$z(x,t) = \begin{cases} z_L, & x < st \\ z_R, & x > st \end{cases} \tag{1.3}$$

where the shock speed s satisfies the Rankine-Hugoniot relation

$$s(z_R - z_L) = F(z_R) - F(z_L) \tag{1.4}$$

A rarefaction wave solution to (1.1) is

$$z(x,t) = \begin{cases} z_L & , \quad x < \lambda_j(z_L)t \\ \eta(\frac{x}{t}) & , \quad \lambda_j(z_L)t \leq x \leq \lambda_j(z_R)t \\ z_R & , \quad x > \lambda_j(z_R)t \end{cases} \tag{1.5}$$

where η satisfies

$$\dot{\eta}(\xi) = r_j(\eta(\xi)), \quad \eta(\lambda_j(z_L)) = z_L, \quad \eta(\lambda_j(z_R)) = z_R \tag{1.6}$$

and the eigenvector r_j is normalized such that $\nabla\lambda_j(z)\cdot r_j(z) = 1$. Observe that the shock solution is a weak solution of (1.1) while the rarefaction is an "ordinary" solution. As a basic reference for the theory of conservation laws we refer to [1].

2. Applications

A simple conservation law like (1.1) has of course a multitude of applications. We cannot here discuss any of them in detail, but we mention that (1.1) has been applied e.g. to traffic flow [2], van der Waal fluids [3], elastic bars [4], ultra-relativistic heavy ion collisions [5], three phase flow in a porous medium (enhanced oil recovery) [6].

3. Mathematical theory demanded by the applications

With applications ranging from traffic flow to elementary particle physics, one would expect considerable variation in the demands of mathematical results for systems (1.1). However this is not the case. We will here only discuss in some detail the case of three phase flow in a porous medium based on a recent numerical analysis [7]. It was found that (1.1) had a small, compact elliptic region. In addition one had to handle complicated behavior of the

so-called inflection loci (the set where $\nabla\lambda_j(z)\cdot r_j(z) = 0$, i.e. where genuine nonlinearity fails) near the elliptic region. In spite of this the solution of the Riemann problem seemed to be surprisingly stable and wellbehaved for physically relevant values of z_L and z_R. One can of course argue that the existence of an elliptic regions is a result of bad modelling. However as far as we know there is nothing in the laws that determine the flux function F which a priori rules out elliptic regions. Ellintic regions also occur in [2], [3] and [4].

4. Existing mathematical theory

The first fundamental result is due to Lax [8] giving a local existence and uniqueness theorem for (1.1) provided (1.1) is strictly hyperbolic and genuinely nonlinear. Existence here means the existence of a shock and/or rarefaction solution, uniqueness means uniqueness within the class of functions satisfying an entropy condition, and local means for z_L and z_R close. Liu [9] extended this to a global result for strictly hyperbolic systems with the assumption of genuine nonlinearity replaced by strong monotonicity conditions on the flux function.

The analysis was only recently extended to the case where $dF(z)$ is allowed to have degenerate eigenvalues at a single isolated point. In this situation it has been shown that it suffices to study flux functions F which are qudratic polynomials in u and v.

With such F the Riemann problem can be classified into four distinct classes [6]. By now a complete solution to the Riemann problem has been given [10], uncovering new and surprising structures.
But the mathematical understanding of the entropy conditions involved in terms of say travelling waves is still rather incomplete, depending on

subtle global properties of systems of ordinary differential equations. For problems of mixed type there is no general mathematical theory, but rather some examples where the problem can be analyzed rigorously in detail [11], [12]. In [12], where the elliptic region is compact, it is found that the Riemann problem always posesses a solution. However the solution is very complicated near the elliptic region where both uniqueness and continuity in data fail. This example sheds some light on the example studied in [7].

We will in the talk discuss some new results for the solution of the mixed type Riemann problem corresponding to class II and IV.

References

[1] Smoller, J. Shock Waves and Reaction-Diffusion Equations Springer-Verlag, Berlin-Heidelberg-New York 1983.

[2] Bick, J.H., Newell, G.F. Quart. J. Appl. Math. 18 (1961) 191-204.

[3] Slemrod, M. Arch. Rat. Mech. Anal. 81 (1983) 301-315.

[4] James, R.D. Arch. Rat. Mech. Anal. 13 (1980) 125-128.
Shearer, M. Proc. Roy. Soc. (Edinburgh) 93A (1985) 233-244.

[5] Plohr, B.J., Sharp, D.H. Los Alamos preprint 1986, to appear in Proc. IAMP Conference, Marseille 1986.

[6] Shearer, M., Schaeffer, D.G. Comm. Pure Appl. Math., to appear.

[7] Bell, J.B., Trangenstein, J.A., Shubin, G.R. SIAM J. Appl. Math. 46 (1986) 1000-1017.

[8] Lax, P. Comm. Pure Appl. Math. 19 (1957) 537-566.

[9] Liu, T.P. Trans Amer. Math. Soc. 199 (1974) 89-112.

[10] Isaacson, E., Marchesin, D., Plohr, B., Temple, B. Preprints, MRC, University of Wisconsin 1985, 1986.
Shearer, M., Schaeffer, D.G., Marchesin, D., Paes-Leme, P.J. Arch. Rat. Mech. Anal., to appear.
Schaeffer, D.G., Shearer, M. Trans. AMS, to appear.

[11] Shearer, M. J. Diff. Eqn. 46 (1982) 426-445.

[12] Holden, H. Comm. Pure Appl. Math., to appear.

Admissible weak solution for nonlinear system of conservation laws in mixed types

L. Hsiao
Academia Sinica, Institute of Mathematics, Beijing, China

Consider a strictly hyperbolic system of conservation laws, it is well-known that the classical solution of initial value problem exists only locally in time, in general, and one has to extend the concept of classical solution to weak solution or discontinuous solution in order to obtain a globally defined solution. Since weak solutions are not unique, one has to use admissibility condition or sometimes called entropy condition to pick out an admissible weak solution which is physically reasonable. There has been a general theory about the existence, uniqueness, asymptotic behavior of the admissible weak solution of Cauchy problem for the one-space dimensional strictly hyperbolic system of conservation laws. Moreover, there are different kinds of admissibility criteria proposed from either physical point of view or mathematical consideration and there are certain results about the equivalence among these different forms of entropy conditions.

However, what will take place if the strict hyperbolicity fails. Parabolic degeneracy will arise which can be found in the literature in connection with various models in applied sciences (c.f.[1] and the reference there). Furthermore, elliptic domain may occur in the phase space, in other words, the system of conservation laws is of mixed type. For instance, the following quasilinear system is the simplest model of mixed type which can be used as the equations of motion for dynamic elastic bar theory where the stress-deformation relation is not monotone or used as the equations governing isothermal motion of a Van der Waals fluid.

$$\begin{cases} u_t - K(v)_x = 0 \\ v_t - u_x = 0 \end{cases} \tag{1}$$

where $K(v)$ is given by a nonmonotone function and the elliptic domain is a strip $\{v_\alpha < v < v_\beta\}$ on the (u, v) plane because the eigenvalue is defined by $\lambda^2 = K'(v)$.

Another system of mixed type which arises in modelling certain nonlinear advection processes has more complicated structure of the elliptic domain

$$\begin{cases} u_t + [u(1-v)]_x = 0 \\ v_t + [v(a+u)]_x = 0 \end{cases} \tag{2}$$

where u, v as the space derivatives of nonnegative quantities which represent the dens s of two populations, the fugitives U and pursuers V. The case $a \neq 1$ leads to an interes g example of a general class of equation that changes type from hyperbolic to elliptic as he state variable crosses a parabolic manifold of codimension one. The elliptic domain for a 1 is defined by $\Delta(u, v) \equiv (v - u + a - 1)^2 + 4(a-1)u < 0$

and the eigenvalues of (2) are given as

$$\lambda_1 = \frac{1}{2}\{u - v + a + 1 - [\Delta(u,v)]^{1/2}\}$$
$$\lambda_2 = \frac{1}{2}\{u - v + a + 1 + [\Delta(u,v)]^{1/2}\}$$

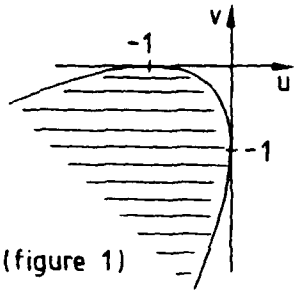

(figure 1)

wherever $\Delta(u,v) \geq 0$.

It is an open problem to determine the extent to which the Cauchy problem is meaningful for such kind of nonlinear system of mixed type. For a first step, we study the simplest Cauchy problem --- Riemann problem, namely

$$(u,v)(x,o) = \begin{cases} (u_-, v_-) & x < 0 \\ (u_+, v_+) & x > 0 \end{cases} \tag{3}$$

where $(u_\mp, v_\mp)$ are arbitrary constant states.

Since both the system ((1) or (2)) and the initial data (3) are invariant under the transformation $x \to \alpha x$, $t \to \alpha t$, we look for similarity solutions $u = u(\xi)$, $v = v(\xi)$, $\xi = \frac{x}{t}$ for which the condition (3) becomes into the boundary condition

$$(u(\xi), v(\xi)) \to (u_\mp, v_\mp) \qquad \text{as} \quad \xi \to \mp\infty.$$

It is easy to show that any similarity solution consists of constant states, rarefaction waves and discontinuities. A discontinuity is defined by Rankine-Hugoniot condition which takes the form (4)

$$\begin{aligned} \sigma[u] &= [(1 - v)u] \\ \sigma[v] &= [(a + u)v] \end{aligned} \tag{4}$$

for the system (2). Where $[w] = w_r - w_l$ denotes the jump of the quantity W across the discontinuity with speed σ. For any given (u_0, v_0), the state which can be joined to (u_0, v_0) by a discontinuity defines the shock wave curve S_i with $\sigma_i \quad i = 1, 2$ from (4). It can be shown that S_1 (S_2) is a single-valued function of u (v) but is not necessary to be connected. For instance, for any given (u_0, v_0) such that $v_0 \geq 0$, $-(a-1) < u_0 < 0$, the curves S_1 and S_2 for the system (2) are shown in the figure where the location of the ending points can be calculated.

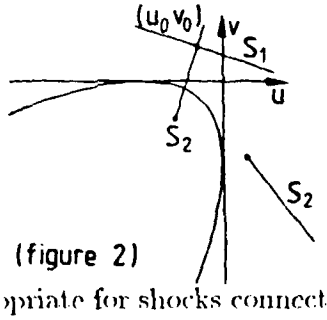

(figure 2)

An essential feature of mixed type nonlinear systems is the possibility of shocks between values one of which is in the elliptic region and the other in the hyperbolic region. Such discontinuities are routinely observed in transonic flow, but are not described by linear system of mixed type or by purely hyperbolic nonlinear systems. It is obvious that in order to determine which shocks are admissible on physical grounds the classical entropy condition is not appropriate for shocks connecting states in elliptic domain with states in hyperbolic domain. For handling the elliptic domain we need to introduce a generalized entropy condition instead of the classical entropy condition.

Definition of generalized entropy condition (denoted by G.E.C.)
For any given (u_-, v_-), (u_+, v_+) is said to be satisfied with the G.E.C. if either

I. when u varies from u_- to u_+, excluding u_+ itself, the corresponding σ_1 is decreasing wherever it is defined, or

II. for any u between u_- and u_+ where σ_1 is defined, it holds that

$$\sigma_1(u; u_-, v_-) \geq \sigma_1(u_+; u_-, v_-)$$

It is similar for σ_2.

For any given (u_-, v_-), the state $(u_+, v_+) \in S_i(u_-, v_-)$ which satisfies the G.E.C. can be determined. For the above example, it is shown in figure 3.

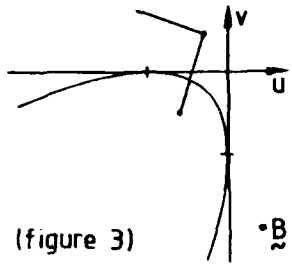

(figure 3)

It is ready now to define an admissible weak solution.

Definition.
A single-valued function $(u(\xi), v(\xi))$ is called an admissible weak solution of (1)(3) or (2)(3) if

I. It satisfies the boundary condition $(u, v) \to (u_\mp, v_\mp)$ as $\xi \to \mp\infty$

II. It is either a rarefaction wave or a constant state wherever it is smooth.

III. Any discontinuity satisfies the Rankine-Hugoniot condition and the above generalized entropy condition.

IV. The image in the phase plane takes the minimum variation among all possible single-valued function $(u(\xi), v(\xi))$ satisfying (I) -(III).

By using this definition of admissible weak solution, we are able to prove that there exists an unique similarity admissible weak solution of the problem (1) (3) (c.f.[2]) or (2) (3) (c.f.[3]) for any given states $(u_\mp, v_\mp)$ on the whole plane (u, v).

Remark 1 It fails to ensure the uniqueness for the problem (1)(3) or (2)(3) without the item IV. in our definition which is a global condition. For a pure hyperbolic system of conservation laws our G.E.C. becomes into the well-known entropy condition (E) and the last item in the definition of an admissible weak solution disappear automatically.

Remark 2 The number of the elementary waves in the solution can be any number from 1 to 4 and it is possible to occur 3 shocks in the solution for the system (1) and 4 shocks for the system (2). However, it is impossible to have such kind of discontinuity for which the both of values are in elliptic domain. The only way to join two states both of which are in elliptic domain is through a sequence of waves in which there is at least one shock connecting one side of its value in elliptic domain and the other in hyperbolic domain.

Remark 3 The above framework seems to be able to work with other systems of mixed type if the elliptic domain is of the following property: there is at least one direction on (u, v) plane such that for any given straight line, parallel to this direction, the intersection of the line with the elliptic domain is finite in the length.

Reference

[1]. L. Hsiao and P. de Mottoni, Quasilinear Hyperbolic system of conservation laws with parabolic degeneracy. (to appear)

[2]. L. Hsiao, Admissible weak solution for nonlinear system of conservation laws in mixed type. (to appear)

[3]. L. Hsiao and P. de Mottoni, Existence and uniqueness of Riemann problem for nonlinear system of conservation laws of mixed type. (to appear)

H

On Convergence of a Second Order TVD Scheme

Xiaoping Hu
Dept. of Mathematics
Nanjing Aeronautical Institute
Nanjing
P.R.C.

In his paper [1] Harten presented a class of second order accurate, high-resolution TVD schemes for hyperbolic conservation law

$$u_t + f(u)_x = 0 \qquad x \in I\!R,\ t \in I\!R^+$$
$$u(x,0) = u_0(x) \qquad x \in I\!R$$

When taking $Q(x) \equiv 1$, Harten's Scheme reads

$$u_j^{n+1} = u_j^n - \lambda(f_{j+\frac{1}{2}}^n - f_{j-\frac{1}{2}}^n)$$
$$f_{j+\frac{1}{2}}^n = \frac{1}{2}(f_j^n + f_{j+1}^n - \frac{1}{\lambda}\Delta_{j+\frac{1}{2}}u)$$
$$f_j^n = f(u_j) + \frac{1}{\lambda}g_j$$

with

$$g_j = s_{j+\frac{1}{2}} \max[0, \min(|\bar{g}_{j+\frac{1}{2}}|, s_{j+\frac{1}{2}}\bar{g}_{j-\frac{1}{2}})]$$
$$\bar{g}_{j+\frac{1}{2}} = \frac{1}{2}(1 - v_{j+\frac{1}{2}}^2)\Delta_{j+\frac{1}{2}}u$$
$$s_{j+\frac{1}{2}} = \mathrm{sgn}(\bar{g}_{j+\frac{1}{2}})$$
$$v_{j+\frac{1}{2}} = \lambda(f(u_{j+1}) - f(u_j))/\Delta_{j+\frac{1}{2}}u$$
$$\Delta_{j+\frac{1}{2}}u = u_{j+1} - u_j$$

In this paper we consider only those initial value problems which have monotone initial value function $u_0(x)$.

First, we show the stability of the scheme under the C.F.L. condition. Thus one can deduce the existence of convergent subsequence of approximate solutions by using compactness arguments since the total variation is uniformly bounded.

Then, we show that the limit solutions satisfy the Kruzkov's entropy condition under the more restrictive condition

$$\lambda\|f'\|_\infty \leq 3 - 2\sqrt{2}$$

hence, by the uniqueness of solutions, one can conclude the convergence of the whole approximate solution family.

The method we used can be regarded as a generalization of the method developed by Le Roux.

[1] Ami Harten "High Resolution Schemes for hyperbolic conservation laws" J.Comp.Phys. vol 49(1983) PP.357–393.

[2] A.Y.Le Roux "A Numerical Conception of Entropy for Quasi-linear Equations" Math. Comp. vol 31 (1977), pp.848–872.

STRONGLY NONLINEAR HYPERBOLIC WAVES

John K. Hunter
Deptartment of Mathematics
Colorado State University
Ft. Collins
CO 80523 USA

We shall describe an asymptotic theory for solutions to hyperbolic conservation laws, with large amplitude, rapidly varying inital data. In a short initial layer the solution is described by a constant coefficient system of conservation laws in one space dimension. The solution develops shocks and quickly decays. For longer times, the solution is described by weakly nonlinear ray methods. The theory is most complete for compactly supported initial data. Then, the initial data splits up into a number of small amplitude N–waves, and the evolution of these N–waves for longer times is governed by a generalised Burgers' equation. In certain situations, the theory also applies to initial data which consists of a modulated high frequency periodic wave.

THE STRUCTURE OF ASYMPTOTIC STATES IN A SINGULAR SYSTEM OF CONSERVATION LAWS

Eli Isaacson
Department of Mathematics
University of Wyoming
Laramie, Wyoming

Blake Temple
Department of Mathematics
University of California, Davis
Davis, California

We consider the 2x2 system of conservation laws which model the polymer flood of an oil reservoir. These equations are strictly hyperbolic everywhere except along a curve in state space where the wave speeds in the problem coincide. The Riemann problem and Cauchy problem for this system were solved by the first and second authors respectively. The Lax characteristic condition was used as the admissibility criterion for solutions of the Riemann problem, and the Cauchy problem was solved by demonstrating the convergence of the Random choice method. Here we describe the noninteracting waves to which solutions of the Cauchy problem decay asymptotically as $t \to +\infty$. In contrast to the strictly hyperbolic case, the waves in the asymptotic solution are essentially different from the waves in the solution of the Riemann problem with left state $u_L = u_0(-\infty)$ and right state $u_R = u_0(+\infty)$. (Here $u_0(x)$ denotes the initial data for the Cauchy problem.) Indeed, the asymptotic state can have strong nonlinear waves even when the solution of the Riemann problem for the states at $\pm\infty$ is identically zero. In fact, the asymptotic solution, which is determined by u_L, u_R and the initial maximum value of c (the concentration of polymer), is in fact an inadmissible solution of the Riemann problem $[u_L, u_R]$. An immediate consequence of the analysis is that although the admissible solutions of the Riemann problem depend continuously on u_L and u_R, and although each solution of the initial value problem is L^1–Lipshitz continuous in time, the initial value problem is not well–posed in L^1. In fact, continuous dependence on initial values fails in every L^p for this one–dimensional hyperbolic problem. This lack of continuous dependence parallels the presence of a Rayleigh–Taylor instability in the higher dimensional problem. We imagine that continuous dependence is recovered in two dimensions (because of "fingering") and also when diffusion is not neglected. However, to our knowledge, this is the first time such a lack of well–posedness has been observed in a purely hyperbolic problem. In particular, this example violates the stability result proved by Temple for strictly hyperbolic systems.

The analysis also highlights the role of the Lax admissibility criterion in

this.nonstrictly hyperbolic problem. In contrast to the classical rarefaction shocks which violate the Lax condition, the asymptotic solutions of the Riemann problem for this system are not unstable solutions which never appear, but rather are solutions which are incompatible with the Riemann data in that they spontaneously introduce polymer into the problem. We can improve the convergence of the random choice method by replacing the admissible solution of the Riemann problem in each cell by the asymptotic solution determined by the right and left cell states together with the maximum value of c in each cell. In this case, a previous analysis of the authors can be applied essentially unchanged to obtain convergence of this modified method – and since both the original and modified methods conserve polymer, we expect that both methods generate the same weak solution. From this point of view, the admissible solution of the Riemann problem is unique among all solutions of the Riemann problem which generate the polymer conserving solutions in the random choice method, in that it depends only on left and right cell states, and not on the additional information of the c–values in each cell. We wonder whether this perspective can be of help in determining admissibility criterion for problems with more complicated hyperbolic singularities.

We note that not all the steps in the construction of the asymptotic solutions are obtained rigorously.

SHOCKCAPTURING STREAMLINE DIFFUSION FINITE ELEMENT METHODS FOR HYPERBOLIC CONSERVATION LAWS

Claes Johnson, Anders Szepessy and Peter Hansbo

Mathematics Department
Chalmers University of Technology
412 96 Göteborg , Sweden

We report on our recent theoretical and computational work on streamline diffusion finite element methods for hyperbolic conservation laws.These methods combine good stability with high accuracy and promise to find extensive applications in computational fluid mechanics. We give a new interpretation of the shock-capturing term as an artificial viscosity with viscosity coefficient depending on the residual of the finite element solution and we show how the shock-capturing term may be used in the theoretical analysis to obtain improved results. For example, for the shock-capturing streamline diffusion method applied to the Burgers' equation one can prove an a priori bound in the maximum norm, and thus obtain a complete convergence proof in this case using compensated compactness. We discuss the implementation of the method and give computational results for the time dependent compressible Euler equations in one and two space dimensions, in the latter case with also automatic adaptivity of the finite element mesh.

K

A UNO-based Scheme for the Euler Equations of Gasdynamics with an Arbitrary Equation of State

James R. Kamm
Science Applications International Corporation
San Diego, California, USA

We present a high resolution, characteristic-based algorithm for calculating solutions of the Euler equations of gasdynamics with a general equation of state. The numerical flux function we employ uses a preprocessed approximate Riemann solver based on a cell-centered flow representation obtained with the uniformly non-oscillatory (UNO) approximation of Harten & Osher[1]. The temporal integration of the resulting semi-discrete numerical conservation law is performed with a second-order Runge-Kutta scheme. This combined method, while neither as accurate nor as elaborate as higher-order, reconstruction-based essentially non-oscillatory (ENO) schemes[2] or Harten's one-dimensional sub-cell resolution technique[3], resolves the salient phenomena of discontinuous solutions that the Euler equations admit and extends easily to two-dimensional cartesian and cylindrical geometries.

A fundamental requirement of all methods that contain approximate Riemann solvers is the accurate representation of the flow within adjoining grid cells. This information is used to calculate the values of the interface fluxes, which are used to advance the solution forward in time. The UNO approximation uses the flow values in the adjoining cells to interpolate an "optimal" cell-centered quadratic representation of the solution. Although the solution obtained by using this interpolant does not possess the total variation diminishing (TVD) property, it does retain nominal second-order accuracy at extrema, a property that is particulary desirable, e.g., in computing two-dimensional flows with vortical structure. One difficulty with these methods is often the resolution of contact

discontinuities (slipstreams). We address this concern by adding a version of the compression enhancement of Yang[4]. This compression, augmenting the linear characteristic fields, is based on the difference of the flow variables in adjoining cells, limited in such a way as to inhibit unphysical under- or overshoot.

As our interests are in computing flows of real (i.e., non-polytropic) materials, in the following discussion we assume only that the general (convex) equation of state can be represented by the pressure as a function of density and internal energy. This generalization complicates the expressions for the eigenvalues and eigenvectors of the Jacobians of the fluxes, thereby precluding the use of Roe-averaging in the Riemann solver. In certain high pressure, high temperature regimes, an approximation used in some equation of state models is that the derivative of pressure with respect to density or internal energy vanish. While these simplifications can lead to non-physical results (e.g., zero soundspeed) and must therefore be used with care, we provide a discussion of how to incorporate these approximations into our scheme.

Lastly, we compare some of our computed results with those of a preprocessed TVD schemes for the one-dimensional shock tube and a two-dimensional shock-wedge interaction problem for both polytropic and real gas equations of state.

References

1. A. Harten & S. Osher [1987] Uniformly High-order Accurate Nonoscillatory Schemes. I, *SIAM J. Numer. Anal.* **24**, 279-309.

2. A. Harten, B. Engquist, S. Osher & S. Chakravarthy [1987] Uniformly High Order Accurate Essentially Non-oscillatory Schemes, III, *J. Comput. Phys.* **71**, 231-303.

3. A. Harten [1987] ENO Schemes with Subcell Resolution, UCLA Computational and Applied Mathematics Report 87-13.

4. H. Yang [1988] Ph. D. Thesis, UCLA (to appear).

Detonation Initiation due to Shockwave-Boundary Interactions

R. Klein

Institut für Allgemeine Mechanik
RWTH Aachen

The ignition of an explosive gas within the L-shaped duct, as it is depicted in Fig. 1, is investigated by means of numerical simulations. A plane, initially inert shock wave enters the configuration from the open side and eventually ignites the mixture. This model problem is related to knock damage in internal combustion engines. We believe, that shock waves, which may be initiated by autoignition within the unburnt end gas, can penetrate into the narrow gap between the piston and the cylinder wall, as is sketched in Fig. 1b. If there is a combustible mixture within the gap, then after interactions of the shock with the boundary walls the temperatures locally become high enough to ignite the mixture and to lead to coupled shockwave-reaction structures.

Neglecting molecular transport and real gas effects, we describe the gasdynamic properties of the system by means of the two-dimensional Euler equations for an ideal gas with constant specific heats. We account for the chemical heat release by supplying a source term to the conservation equation for thermal and kinetic energy. The reaction progress is controlled by means of an additional balance equation for a reaction progress variable. With an appropriate choice of the reaction rate expression and of the relation between the source terms of the energy- and of the reaction progress equations it is possible to simulate different types of model chemistry.

In particular a two-reaction model, similar to that of Korobieinikov et al. /1/ can be realized, for which usually two separate reaction progress equations are employed (see Taki and Fujiwara /2/). By prescribing suitable initial conditions it is possible to reduce this system to a one-step irreversible reaction with Arrhenius kinetics.

The numerical scheme used here is an extended two-step Godunov-type scheme for the one-dimensional Euler equations with source terms. After introduction of limited piecewise linear distributions within the cells of the numerical grid, an advance in time by half a time step is performed using the characteristic form of the governing equations. This approach is nearly analogous to that of Colella and

Glaz /3/. With the pair of thermodynamic states, obtained at each cell interface in this way, we calculate numerical fluxes using Einfeldt's /4/ approximate Riemann-solver. In order to account for the source terms within the balance equations a second order 'source wave splitting' approach is employed, which is based on a suggestion of Roe /5/. The scheme is extended to two dimensions by means of directional operator splitting applied on a cartesian numerical grid. In order to avoid extensive numerical dissipation in the vicinity of the convex corner, which would provoke artificial ignition due to unphysical temperature increases, we impose special corner flow boundary conditions. These were presented recently in /6/ together with the construction of the 'source wave splitting' method.

The results of an example calculation, obtained with the one-step Arrhenius model on a /60x20/+/30x80/-cell grid are given in Figs. 2. They show sequential plots of pressure contour lines for a typical ignition process. The sequence starts a short time after the incident shock has been reflected at the opposite wall. In the present regime of the chemical model parameters the gas is ignited rapidly after this first reflection. Correspondingly Fig. 2a shows the leading reflected shock wave as well as the strong pressure gradients, which indicate a thermal runaway next to the wall. In Fig. 2b the reaction zone has catched up the inert shock and the resulting coupled shock-reaction front is seen as it runs back towards the open side of the duct and towards the convex corner. In Figs. 2c,d this wave is partially reflected again and, where it meets the leading shock at the wall, a very high pressure peak is formed. This peak develops into a typical triple wave configuration. An inert transverse shock within the burnt gas, which traverses the channel and is re-reflected between the walls, devides the leading reacting shock front into a weak and a strong section, corresponding to the temperature and pressure increases that appear across this transverse wave. The triple shock structure is maintained while the whole configuration propagates down the duct (Figs. 2e,f). It is believed, that the very high pressures and temperatures, which appear when the triple wave hits the walls, are an important ingredient of the mechanisms of knock damage.

The typical pattern of shock-reaction fronts described here was also observed experimentally within plane, two-dimensional detonation waves by Strehlow and Fernandez /7/ and they were obtained by means of numerical simulations by Taki and Fujiwara /2/, Oran et al. /8/ and recently by Schoeffel /9/. Thus our results reveal an interesting mechanism for the detonation initiation due to shockwave boundary interactions. However, it depends on the relations between the characteristic detonation cell sizes and the width of the duct, whether a fully

developed detonation could establish or whether the wave structures would decay, when they were followed over longer travelling distances within a continued straight channel (see e.g. Williams /10/).

In the presentation at first a brief summary of the corner flow boundary conditions and of the 'source-wave-splitting' scheme will be given together with the results of some test calculations. The emphasis will then be posed on the complete model problem and on the discussion of different patterns of the ignition processes within the L-shaped duct.

References

/1/ Korobieinikov, V.P., Levin, V.A., Markov, V.V. and Chernyi, G.G.
"Propagation of Blast Wave in a Combustible Gas", Acta Astronautica, Vol. 17, 529 (1972).

/2/ Taki, S. and Fujiwara, T.
"Numerical Analysis of Two-Dimensional Nonsteady Detonations", AIAA Journal 16, 73 (1978).

/3/ Colella, P. and Glaz, H.M.
"Efficient Solution Algorithms for the Riemann Problem for Real Gases", Journal of Computational Physics 59, 264-289 (1985).

/4/ Einfeldt, B.
"On Godunov Type Methods for Gasdynamics", to appear in SIAM, J. Numer. Anal.

/5/ Roe, P.L.
"Upwind Differencing Schemes for hyperbolic Conservation Laws with Source Terms", A. Dold, B. Eckmann (Eds.), Lecture Notes in Mathematics, 1270 (1987).

/6/ Klein, R.
"Shock Initiated Ignition in a L-Shaped Duct, Two Aspects of its Numerical Simulation", to appear in Proc. of the 7th GAMM Conference on Numerical Methods in Fluid Mechanics, Belgium, Sept. 1987.

/7/ Strehlow, R.A. and Fernandez, F.D.
"Transverse Waves in Detonations", Combustion and Flame 9, 109 (1965).

/8/ Oran, E.S., Boris, J.P., Young, T., Flanigan, M., Burks, T. and Picone, M.
"Numerical Simulations of Detonations in Hydrogen-Air and Methane-Air Mixtures", Proc. of the 18th Symp. on Combustion, The Combustion Institute (1981).

/9/ Schoeffel, S.U.
"Numerical Analysis Concerning the Spatial Dynamics of an Initially Plane Gaseous ZND-Detonation", to appear in Proc. of the 11th ICODERS, Warsaw, Poland (1987).

/10/ Williams, F.A.
"Combustion Theory", (2nd ed.), Benjamin/Cummings Publishing Company, Inc., Memlo Park, California (1985).

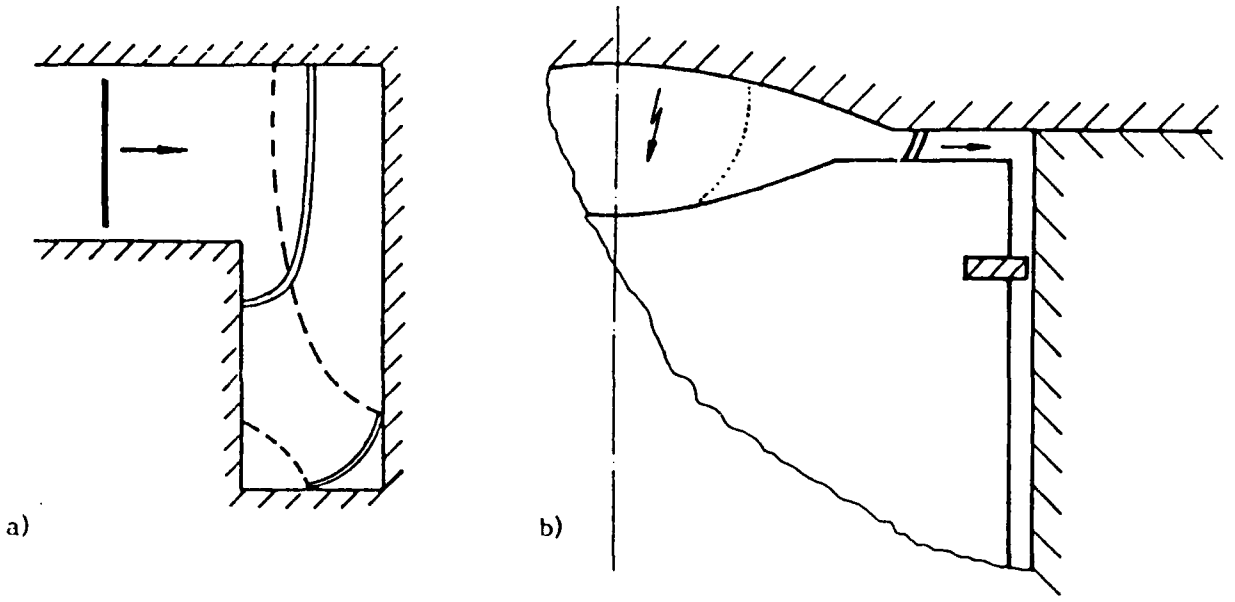

Fig. 1 : The L-shaped duct a) and its counterpart in an internal combustion engine b)

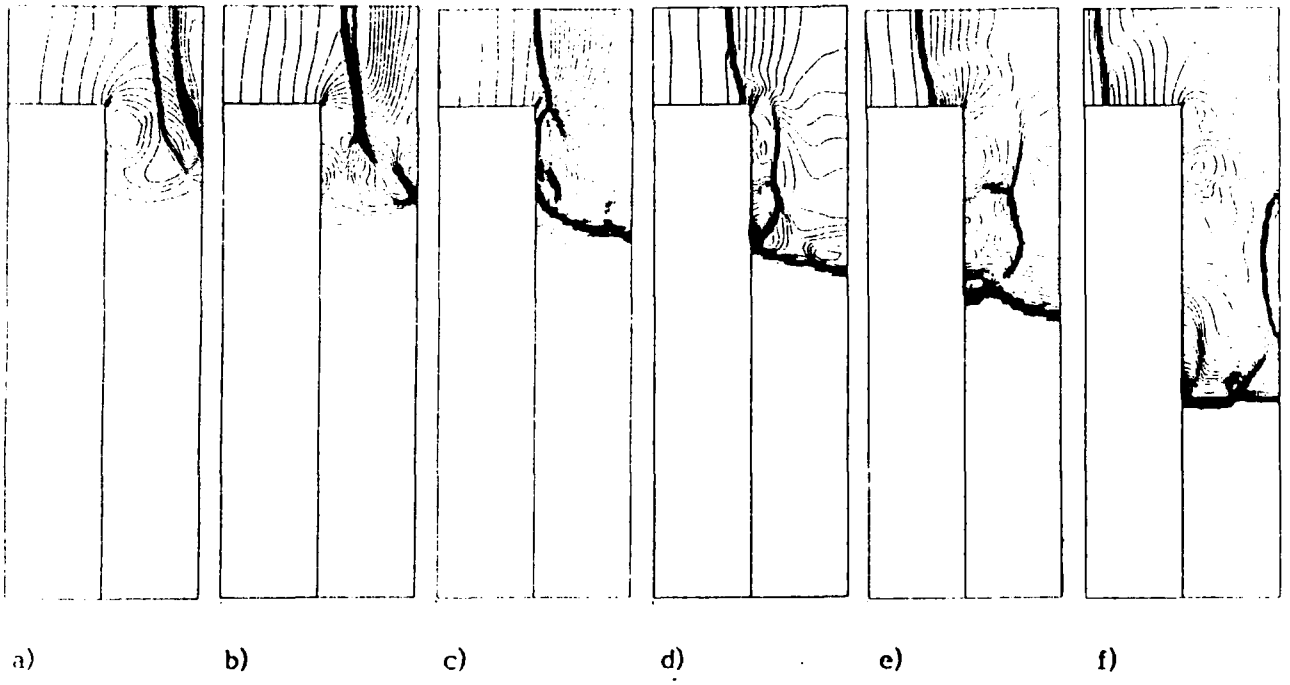

Fig. 2 : Development of a cellular detonation due to shockwave-boundary interactions.

TWO DIMENSIONAL RIEMANN PROBLEMS AND ITS APPLICATIONS: A CONFERENCE REPORT

CHRISTIAN KLINGENBERG
Dept. of Applied Mathematics, University of Heidelberg
Im Neuenheimer Feld 294, 6900 Heidelberg, W. GERMANY

We shall consider nonlinear hyperbolic equations in conservation form

$$(1) \qquad u_t + \nabla . f(u) = 0$$

$$u(0,x,y) = u_o \quad .$$

Even for smooth initial data u_o the solution to (1) in general will lead to jump discontinuities in the solution.

We are interested in the stucture of the solution. The set of jump discontinuities may become quite complicated without any apriori assumptions on the flux function f and initial data.

This is of some importance, when solving (1) numerically. I shall give two examples.

a) One can obtain high resolution by using the method of front tracking. There one marks the jump discontinuities (the front) in the solution by special grid points, which evolve dynamically with the front. From one time step to the next first the front gets moved and the states next to the front get updated. The time step gets finished by solving initial/boundary value problems in the smooth regions between the jump discontinuities using standard finite difference methods. Clearly it is necessary for this approach to qualitatively understand the structure of the jump discontinuities, see [GK].

b) When using finite difference schemes in more than one space dimension, one time step usually consists of sequentially applying a one dimensional scheme in each time direction. This has disadvantages. Roe's [R1] work indicates that the more accurate the one dimensional scheme is, the less accurate the two dimensional split scheme will be. Currently the development of methods which are not relying on the direction of the space axes is under way, e.g. following Roe [R2]. Again a knowledge about the geometry of the jump discontinuities is helpfull for this approach.

In this note we shall consider selfsimilar solutions of (1), this then reduces the number of independent variables by one. In particular we shall consider Riemann problems:

Definition: If (1) together with initial data u_o is invariant under

$$(cx, cy, ct) \longrightarrow (x, y, t) \quad , \quad c > 0$$

then it is called a Riemann problem. Thus initial data which is piecewise constant in sectors meeting at the origin together with (1) constituts a Riemann problem.

Definition: A Riemann solution which is invariant under the group action

$$(x , y , t) \longrightarrow (x + \sigma_1 \tau, \; y + \sigma_2 \tau, \; t + \tau)$$

is an elementary wave with velocity $\vec{\sigma} \in \mathbb{R}^2$.

We believe that the solution to Riemahn problems are described

qualitatively by the following picture: it consists of elementary waves, moving apart each with their own distinct velocity. These elementary waves are then connected by jump surfaces. We mention in passing that one can give a short list of these generic types of such intersection points for two dimensional gas dynamics, [K], [GK].

For two dimensional Riemann Problems for scalar conservation laws

$$u_t + f(u)_x + g(u)_y = 0$$

we have explicitly constructed the solution [HK] for generic cases. We found that the solution is piecewise smooth. In Fig. 1 we give a list of pieces that this solution is made of. We believe that this constitutes a complete list for polynomial flux functions f and g. In Fig. 2 we give an example of a solution to illustrate how it is composed of the pieces mentioned above.

These constructions lead us to a numerical two dimensional Riemann solver for a certain class of Riemann problems. Suppose we have two shock waves approaching each other, see Fig. 3. At their time of intersection they approximately give rise to a two dimensional Riemann problem, Fig. 4. We think of this as two waves giving rise to a wave fan. Thus in analogy to the time dependent one dimensional case of two waves crossing, there the "timelike" direction corresponds here to a "direction of causality", say ξ. In such a way we introduce new coordintes ξ, η. These transform our system (1) to the problem

$$\frac{\partial P(u)}{\partial \xi} + \frac{\partial Q(u)}{\partial \eta} = 0$$

$$P = P(u-), \quad \eta < 0$$
$$P = P(u+), \quad \eta > 0 \quad .$$

For scalar equations and assuming that $dP/du > 0$, we have implemented a numerical Riemann solver by constructing numerically the Oleinik convex hull, see Fig. 5. The solution then gets transformed back to the x - y plane to give a two dimensional Riemann solution. This constituts a helpful tool for a front tracking algorithm, [KZ].

References:

[GK], Glimm, Klingenberg, McBryan, Plohr, Yaniv, "Front Tracking and Two Dimensional Riemann Problems", Adv. Appl. Math. 6, (19)

[HK], Hsiao, Klingenberg, "Constructing the solution to a noncon x two dimensional Riemann problem", Preprint

[K], Klingenberg, "Hyperbolic Conservation Laws in Two Space Dimensions", Report Institut Mittag-Leffler 2, (1986)

[KZ], Klingenberg, Zhu, "A front tracking algorithm including tw dimensional Riemann solvers", manuscript

[R1], Roe, "Discontinuous solutions to hyperbolic systems under operator splitting", manuscript

[R2], Roe, "Discrete models for the numerical analysis of time d penden multidimensional gas dynamics", J. Comp. Physics, 63, (986)

Fig. 1 The solution to $u_t + f(u)_x + g(u)_y = 0$ with initial data constant in the wedges we believe is genericaly made up of the following pieces in the x - y plane:

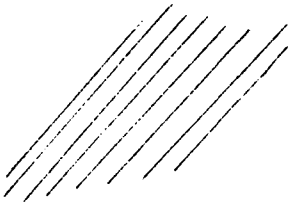

Parallel charactertistics, with the constant state as a special case.

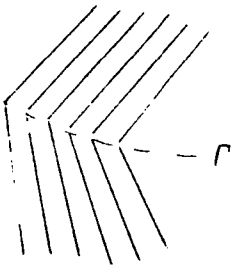

Characteristics meet along $\Gamma = (f'(u) , g'(u))$.

Contanct discontinuities (c.d.), with one sided c.d. as a special case or jumps with constant states on both sides.

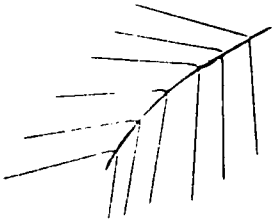

Curved jumps with rarefactic waves impinging on both side The characteristics may be tangential on one side or ma represent constant states.

Two jumps meet along $\Omega = \left(\frac{[f]}{[u]} , \frac{[g]}{[u]} \right)$

Jump triple points.

Fig. 2 The solution to $u_t + (u-u^3)_x + (u^3-u)_y = 0$ with initial data given in i) is shown in ii).

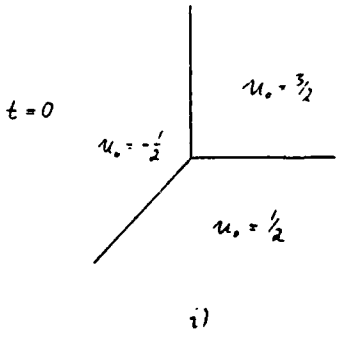

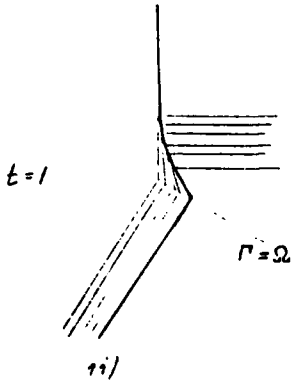

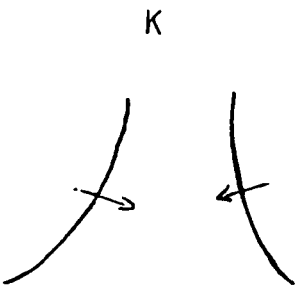

Fig. 3 Two shock waves approaching each other.

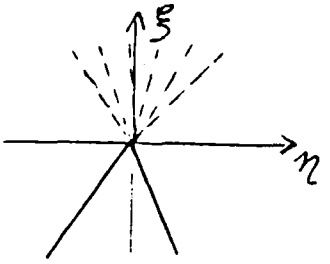

Fig. 4 The two dimensional Riemann problem which arises from Fig. 3 after the intersection of the waves.

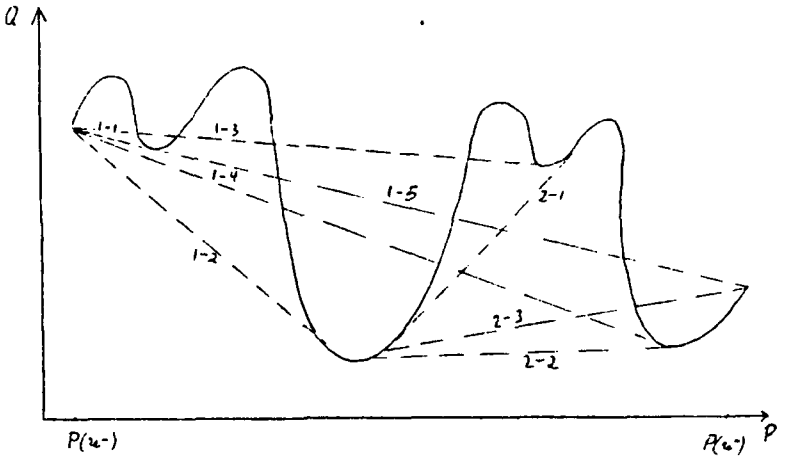

Fig. 5 The numerical construction of the convex hull to the graph of Q versus P, which gives the solution to the Riemann problem. In this case, we first determine the minimum of lin 1-1, 1-2, 1-3, 1-4, 1-5. After having found this to be line 1-2, we continue our search with minimizing slopes of 2-1, 2-2, 2-3, which in this case is 2-2. This then gives the convex hull.

Upwind Schemes for the Navier-Stokes Equations

Barry Koren
Centre for Mathematics and Computer Science
P.O. Box 4079, 1009 AB Amsterdam, The Netherlands

Introduction

A computational method is presented for the steady, 2D, compressible Navier-Stokes equations. The method is hybrid in the sense that it can also be used for the Euler equations. It is based on a method developed for steady Euler flows [4]. In this Euler flow method an upwind finite volume technique was used. The same technique appears to be suitable for the convective terms in the Navier-Stokes equations. The discretization used for the diffusive terms is the central finite volume technique outlined in [13].
To solve the nonlinear system of discretized equations, symmetric point Gauss-Seidel relaxation is used in which one or more Newton steps are used for the collective relaxation of the four unknowns in each finite volume. Point Gauss-Seidel relaxation is simple and robust but needs an acceleration. A suitable acceleration technique is found in nonlinear multigrid [7]. The difficulty in inverting a 2nd-order accurate operator is by-passed by introducing defect correction as an outer iteration for the nonlinear multigrid cycling. The defect correction process may be either standard, damped or mixed with an additional smoother [8].
In the present paper the emphasis lies on the upwind discretization of the convective terms in the Navier-Stokes equations.

Discretization of convective terms

The steady, 2D, compressible Navier-Stokes equations are discretized in the form

$$\frac{\partial f(q)}{\partial x} + \frac{\partial g(q)}{\partial y} - \frac{1}{\mathrm{Re}}\left\{\frac{\partial r(q)}{\partial x} + \frac{\partial s(q)}{\partial y}\right\} = 0\,, \tag{1}$$

with q the state vector of conservative quantities, $f(q)$ and $g(q)$ the convective flux vectors, and $r(q)$ and $s(q)$ the diffusive flux vectors. To allow Euler flow ($1/\mathrm{Re} = 0$) solutions with discontinuities, the equations are discretized in the integral form. A straightforward and simple discretization of the integral form is obtained by subdividing the integration region Ω into finite volumes $\Omega_{i,j}$, and by requiring that the conservation laws hold for each finite volume separately :

$$\int_{\partial\Omega_{i,j}} (f(q)n_x + g(q)n_y)ds - \frac{1}{\mathrm{Re}} \int_{\partial\Omega_{i,j}} (r(q)n_x + s(q)n_y)ds = 0, \forall i,j. \tag{2}$$

For convection dominated flows, our objective, a proper evaluation of the convective flux vectors is of paramount importance. Based on previous experience [2, 3, 4, 5, 6, 9, 16], for this we prefer an upwind approach. Along each finite volume wall we assume the convective flux vector to be constant, and to be determined by a constant left and right state only.

Approximation of left and right state

The approximation of the left and right state determines the accuracy of the convective discretization. First- and higher-order accurate discretizations can be made [2]. Considering for instance the numerical flux function $(f(q))_{i+\frac{1}{2},j} = f(q^l_{i+\frac{1}{2},j}, q^r_{i+\frac{1}{2},j})$, where the superscripts l and r refer to the left and right side of volume wall $\partial\Omega_{i+\frac{1}{2},j}$ (fig. 1), first-order accuracy is obtained by taking

$$q^l_{i+\frac{1}{2},j} = q_{i,j}, \text{ and} \tag{3a}$$

$$q^r_{i+\frac{1}{2},j} = q_{i+1,j}\,. \tag{3b}$$

Higher-order accuracy can simply be obtained with the κ-schemes as introduced by van Leer [10]:

$$q^l_{i+\frac{1}{2},j} = q_{i,j} + \frac{1+\kappa}{4}(q_{i+1,j} - q_{i,j}) + \frac{1-\kappa}{4}(q_{i,j} - q_{i-1,j}), \text{ and} \tag{4a}$$

$$q^r_{i+\frac{1}{2},j} = q_{i+1,j} + \frac{1+\kappa}{4}(q_{i,j} - q_{i+1,j}) + \frac{1-\kappa}{4}(q_{i+1,j} - q_{i+2,j}), \tag{4b}$$

with $\kappa \in \mathbf{R}$ ranging from $\kappa = -1$ (fully one-sided upwind) to $\kappa = 1$ (central).

An optimal value for κ is found by giving an error analysis, using as model equation

$$\frac{\partial u}{\partial x} + \frac{\partial u}{\partial y} - \epsilon\left(\frac{\partial^2 u}{\partial x^2} + \frac{\partial^2 u}{\partial x \partial y} + \frac{\partial^2 u}{\partial y^2}\right) = 0. \tag{5}$$

On a grid with constant mesh size h, a finite volume discretization which uses the κ-approximation for the convective terms and which is second-order central for the diffusive terms, yields as modified equation

$$\frac{\partial u}{\partial x} + \frac{\partial u}{\partial y} - \epsilon\left(\frac{\partial^2 u}{\partial x^2} + \frac{\partial^2 u}{\partial x \partial y} + \frac{\partial^2 u}{\partial y^2}\right) + h^2 \frac{\kappa - 1/3}{4}\left(\frac{\partial^3 u}{\partial x^3} + \frac{\partial^3 u}{\partial y^3}\right) + \tag{6}$$

$$+ h^3\left(\frac{\kappa - 1}{8} - \frac{1}{12}\frac{\epsilon}{h}\right)\left(\frac{\partial^4 u}{\partial x^4} + \frac{\partial^4 u}{\partial y^4}\right) +$$

$$+ O(h^4) = 0.$$

Assuming the reliability of the underlying Taylor series expansion, the modified equation clearly shows that the highest accuracy (third-order) is obtained for $\kappa = 1/3$ (upwind biased), and the lowest false diffusion for $\kappa = 1$ (central). Euler flow computations [6] have shown that for stability reasons the upwind biased approximation is to be preferred above the central approximation.
To avoid spurious non-monotonicity, a new limiter is constructed for the $\kappa = 1/3$ approximation. Let $q_{i+\frac{1}{2},j}^{l(k)}$ and $q_{i+\frac{1}{2},j}^{r(k)}$ be the *kth* component ($k = 1,2,3,4$) of $q_{i+\frac{1}{2},j}^{l}$ respectively $q_{i+\frac{1}{2},j}^{r}$. Then a limited left and right state can be written as

$$q_{i+\frac{1}{2},j}^{l(k)} = q_{i,j}^{(k)} + \frac{1}{2}\psi(R_{i,j}^{(k)})(q_{i,j}^{(k)} - q_{i-1,j}^{(k)}), \text{ and} \tag{7a}$$

$$q_{i+\frac{1}{2},j}^{r(k)} = q_{i,j}^{(k)} + \frac{1}{2}\psi(1/R_{i+1,j}^{(k)})(q_{i+1,j}^{(k)} - q_{i+2,j}^{(k)}), \tag{7b}$$

with $\psi(R)$ the limiter considered, and $R_{i,j}^{(k)}$ the ratio

$$R_{i,j}^{(k)} = \frac{q_{i+1,j}^{(k)} - q_{i,j}^{(k)}}{q_{i,j}^{(k)} - q_{i-1,j}^{(k)}}. \tag{8}$$

Using this notation, the limiter constructed for the $\kappa = 1/3$ approximation reads

$$\psi(R) = \frac{R + 2R^2}{2 - R + 2R^2}. \tag{9}$$

Solution of 1D Riemann problem
Osher's scheme [12] has been preferred so far for the approximate solution of the standard 1D Riemann problem thus obtained. Osher's scheme has been chosen because of: (i) its continuous differentiability, and (ii) its consistent treatment of boundary conditions. (The continuous differentiability guarantees the applicability of a Newton type solution technique, which is what we make use of.) The question arises whether it is still a good choice to use Osher's scheme when diffusion also has to be modelled. Another, more widespread upwind scheme used in Navier-Stokes codes is van Leer's flux splitting scheme [10, 14, 15, 18]. Reasons for its popularity are: (i) its likewise continuous differentiability, and (ii) its simplicity. The latter property is generally believed to be in contrast with Osher's scheme. (Recent work may help to reduce this difference, see e.g. [17].) A detailed error analysis is given for both schemes. The analysis is confined to the steady, 2D, isentropic Euler equations for a perfect mono-atomic gas:

$$\frac{\partial f(q)}{\partial x} + \frac{\partial g(q)}{\partial y} = 0, \quad \text{with} \tag{10}$$

$$f(q) = \begin{bmatrix} \rho u \\ \rho(u^2 + c^2) \\ \rho u v \end{bmatrix}, \quad g(q) = \begin{bmatrix} \rho v \\ \rho u v \\ \rho(v^2 + c^2) \end{bmatrix}. \tag{11}$$

(Notice that for an isentropic, perfect and mono-atomic gas c is a constant.) For a subsonic flow and a first-order accurate finite volume discretization on a grid with constant mesh size h, the system of modified equations is derived for both Osher's and van Leer's scheme. For both systems we consider a subsonic shear flow (the new element) along a flat plate. For this Lamb's approximate solution is used. Substitution of Lamb's solution into the modified equation yields at the boundary layer edge a discretization error ratio as given in fig. 2. In this figure, M_δ denotes the Mach number at the boundary layer edge. The analysis gives some evidence for the superiority of Osher's scheme above van Leer's scheme, when dealing with shear flows. Results are presented which show this superiority for the Navier-Stokes equations indeed.

Results

Subsonic flat plate flow

To compare Osher's and van Leer's scheme, we consider a subsonic flat plate flow with known solution (the Blasius solution). With the first-order approximation, we perform for both schemes an experiment with h- (mesh size) and Re-variation. In all computations we use grids composed of square finite volumes. Results obtained are given in fig. 3. They clearly show the superiority of Osher's scheme under hard conditions (1st-order approximation, high value of Reh).

Supersonic flat plate flow

A standard test case for Navier-Stokes codes is the flat plate shock wave - boundary layer experiment performed by Hakkinen et al. at $Re = 2.96\ 10^5$ [1]. A nice feature of the present code is its possibility to optimize a grid for convection separately. For this test case this leads via the grid shown in fig. 4a to the one in fig. 4b. The corresponding inviscid surface pressure distributions as obtained with Osher's scheme, and with successively the first-order, the non-limited and the limited $\kappa = 1/3$ approximation, are given in fig. 5. Navier-Stokes results obtained on the oblique grid are given in fig. 6. Clearly visible here is the good agreement of the (limited) second-order results with the experimental results.

References

1. R.J. Hakkinen, I. Greber, L. Trilling and S.S. Abarbanel (1958). *The Interaction of an Oblique Shock Wave with a Laminar Boundary Layer.* NASA-memorandum 2-18-59 W.
2. P.W. Hemker (1986). *Defect Correction and Higher Order Schemes for the Multi Grid Solution of the Steady Euler Equations.* Proceedings of the 2nd European Conference on Multigrid Methods, Cologne, 1985, Springer, Berlin.
3. ——— and B. Koren (1987). *A Non-linear Multigrid Method for the Steady Euler Equations.* Proceedings GAMM-Workshop on the Numerical Solution of Compressible Euler Flows, Rocquencourt, 1986. Notes on Numerical Fluid Mechanics xx, Vieweg, Braunschweig (to appear).
4. ——— and S.P. Spekreijse (1986). *Multiple Grid and Osher's Scheme for the Efficient Solution of the Steady Euler Equations.* Appl. Num. Math. 2, 475-493.
5. B. Koren (1988). *Euler Flow Solutions for a Transonic Wind Tunnel Section.* Proceedings V-Aerodynamic Seminar, Aachen, 1987 (to appear).
6. ——— (1988). *Defect Correction and Multigrid for an Efficient and Accurate Computation of Airfoil Flows.* J. Comput. Phys. (to appear).
7. ——— (1988). *First-Order Upwind Schemes and Multigrid for the Steady Navier-Stokes Equations.* CWI report NM-R88xx, Amsterdam (to appear).
8. ——— (1988). *Higher-Order Upwind Schemes and Defect Correction for the Steady Navier-Stokes Equations.* CWI report NM-R88yy, Amsterdam (to appear).
9. ——— and S.P. Spekreijse (1987). *Multigrid and Defect Correction for the Efficient Solution of the Steady Euler Equations.* Proceedings of the 25th Meeting of the Dutch Association for Numerical Fluid Mechanics, Delft, 1986. Notes on Numerical Fluid Mechanics 17, Vieweg, Braunschweig.
10. B. van Leer (1982). *Flux-Vector Splitting for the Euler Equations.* Proceedings of the 8th International Conference on Numerical Methods in Fluid Dynamics, Aachen, 1982. Lecture Notes in Physics 170, Springer, Berlin.
11. ——— (1985). *Upwind-Difference Methods for Aerodynamic Problems governed by the Euler Equations.* Proceedings of the 15th AMS-SIAM Summer Seminar on Applied Mathematics, Scripps Institution of Oceanography, 1983. Lectures in Applied Mathematics 22, AMS, Providence, Rhode Island.
12. S. Osher and F. Solomon (1982). *Upwind-Difference Schemes for Hyperbolic Systems of Conservation Laws.* Math. Comp. 38, 339-374.
13. R. Peyret and T.D. Taylor (1983). *Computational Methods for Fluid Flow.* Springer, Berlin.
14. W. Schröder and D. Hänel (1987). *An Unfactored Implicit Scheme with Multigrid Acceleration for the Solution of the Navier-Stokes Equations.* Computers and Fluids 15, 313-336.
15. G. Shaw and P. Wesseling (1986). *Multigrid Solution of the Compressible Navier-Stokes Equations on a Vector Computer.* Proceedings of the 10th International Conference on Numerical Methods in Fluid Dynamics, Beijing, 1986. Lecture Notes in Physics 264, Springer, Berlin.
16. S.P. Spekreijse (1987). *Multigrid Solution of Monotone Second-Order Discretizations of Hyperbolic Conservation Laws.* Math. Comp. 49, 135-155.
17. ——— (1987). *Multigrid Solution of the Steady Euler Equations.* Ph.D.-thesis, CWI, Amsterdam.
18. J.L. Thomas and R.W. Walters (1985). *Upwind Relaxation Algorithms for the Navier-Stokes Equations.* AIAA-paper, 86-1501.

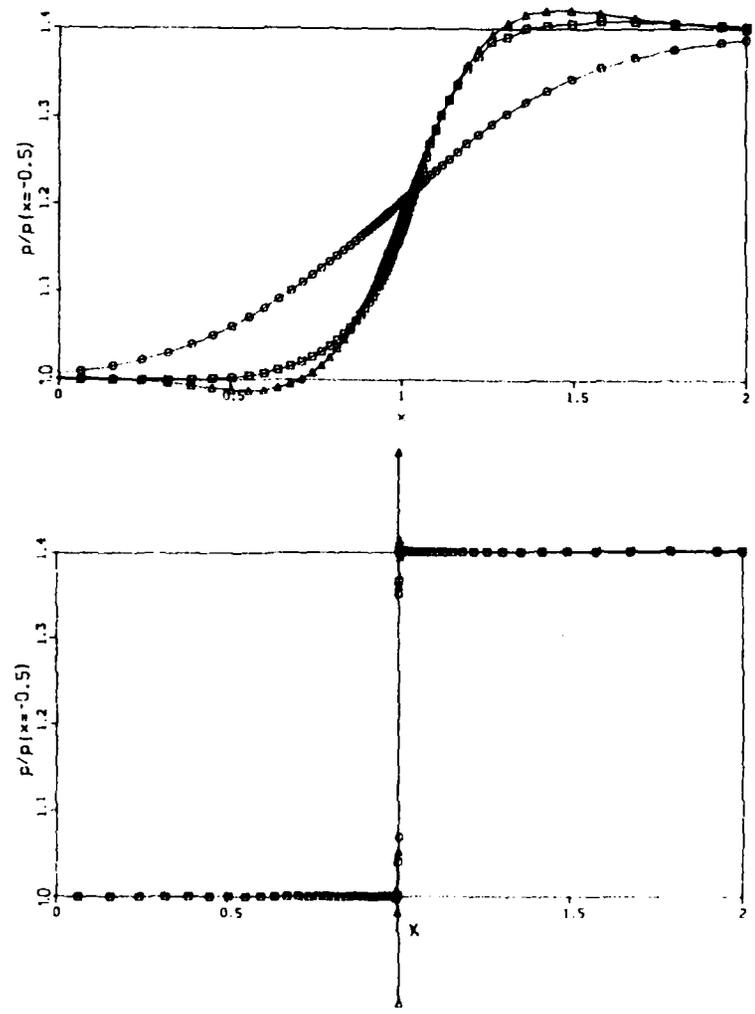

a. On rectangular grid.

b. On oblique grid.

Fig. 5. Inviscid surface pressure distributions supersonic flat plate flow
(O: first-order, △: non-limited higher-order, □: limited higher-order).

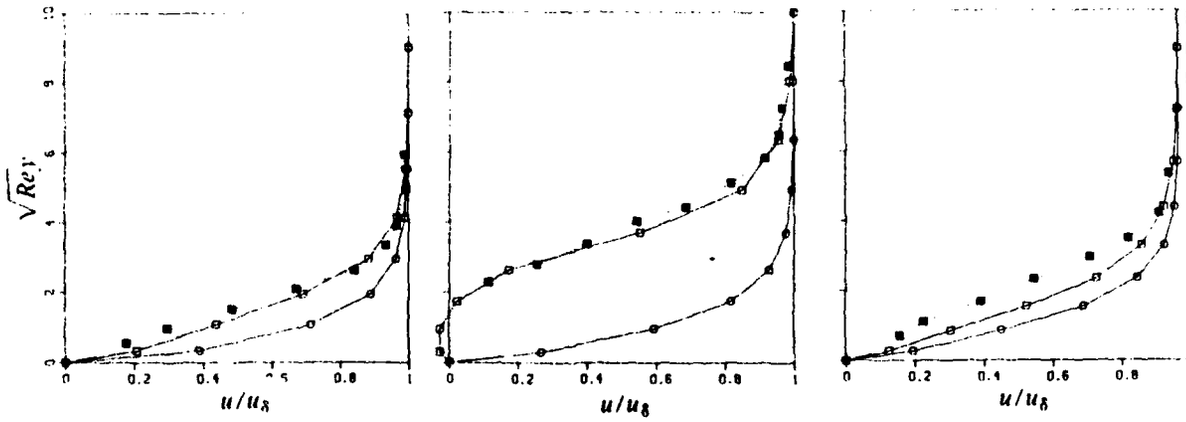

a. $x = 2.27\ 10^5/Re$ b. $x = 2.87\ 10^5/Re$ c. $x = 3.62\ 10^5/Re$

Fig. 6. Velocity profiles supersonic flat plate flow
(O: first-order, □: limited second-order, ■: measured).

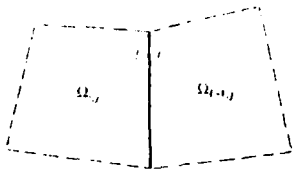

Fig. 1. Volume wall $\partial\Omega_{i+1/2,j}$.

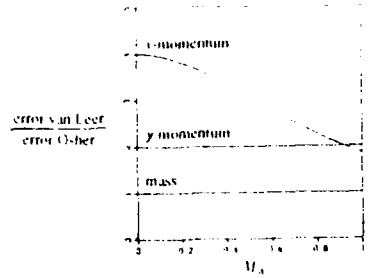

Fig. 2. Ratio of discretization errors at boundary layer edge.

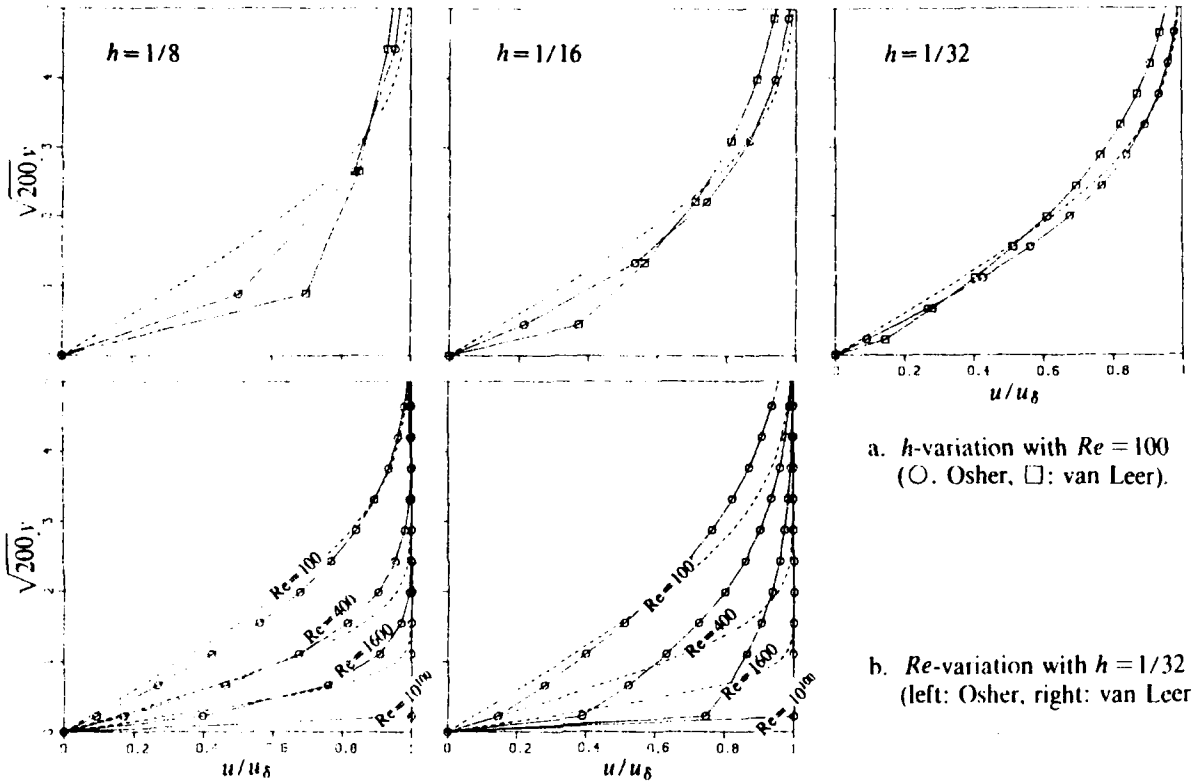

a. h-variation with $Re = 100$ (○. Osher, □: van Leer).

b. Re-variation with $h = 1/32$ (left: Osher, right: van Leer).

Fig. 3. Velocity profiles subsonic flate plate flow (- - - - : Blasius solution).

a. Rectangular grid (-----: shock wave).

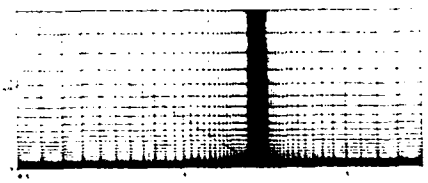

b. Oblique grid.

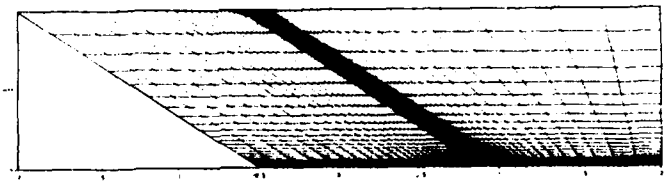

Fig. 4. Finest grids supersonic flat plate flow.

NORMAL REFLECTION-TRANSMISSION OF SHOCK WAVES ON A PLANE INTERFACE BETWEEN TWO RUBBER-LIKE MEDIA.

Sławomir KOSIŃSKI
Technical University Łódz, POLAND

Using a semi-inverse method proposed by Wright [1] a normal reflection and transmission of a finite elastic plane shock wave, at a plane interface of two rigidly coupled rubber-like elastic solids is examined. In this method the incident shock wave is given a priori.

Consider an unbouded medium consisting of two elastic half-spaces of different material properties, joined along the plane $x_2 = 0$. Suppose that a plane shock wave of strength m_o, unit normal $\underset{\sim}{N}_o$ and polarisation vector $\underset{\sim}{d}_o$ propagates in the half-space $x_2 > 0$ with speed V_o (Fig.1). It is assumed that the material solids in front of the shock are unstrained and at rest. Such a wave has displacement components in the x_3 direction only.

Both material solids are isotropic incompressible and are defined by the constitutive equation in the form

$$(1) \qquad W(I_1,I_2) = \varrho\sigma(I_1,I_2) = C_1(I_1 - 3) + C_2(I_2 - 3) + C_3(I_1^2 - 9)$$

where I_1, I_2 - invariants of the left Cauchy-Green strain tensor $\underset{\sim}{B}$, ϱ - density C_1, C_2, C_3 - elastic constants.

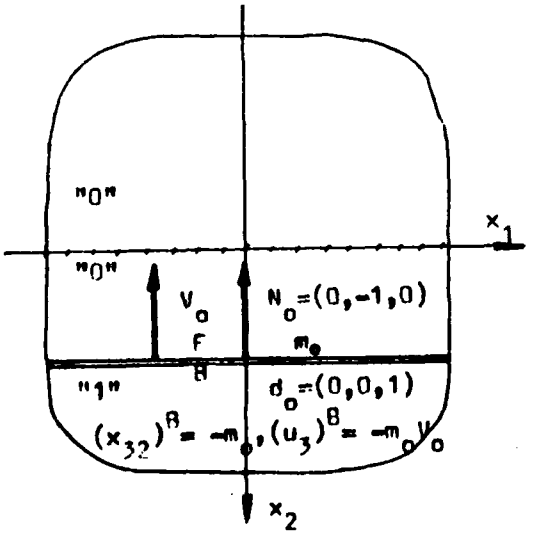

Fig.1 Incident shock wave

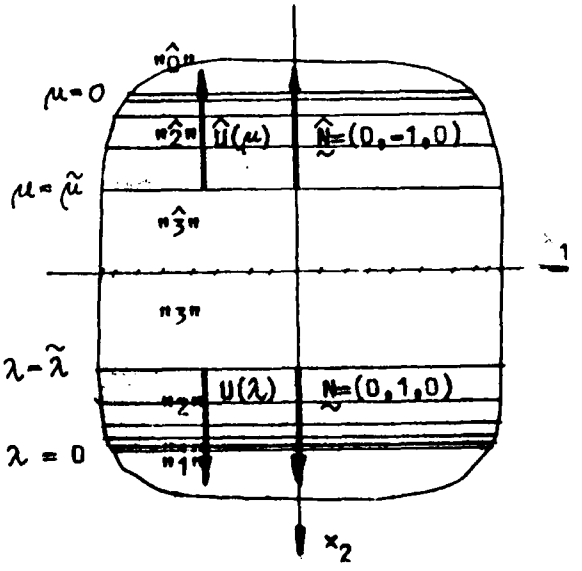

Fig. 2 Assumed shock reflection-transmission pattern.

It is assumed ([1]), that the constant state behind the incident shock (ahead of the transmitted wave) and the state at the interface and below "3" (above "$\hat{3}$") compatible with the interface conditions, are connected by means of a sequence of one parameter families of reflected (transmitted) simple waves and constant state regions (Fig.2).

The equation of motion (propagation condition) and the compatibility condition in the region of the simple wave take the form ([1] , [3])

$$(2) \qquad (Q^{*}_{ij} - \rho U^2 \delta_{ij})\, u_j' = 0 \quad , \quad U x'_{j\beta} + u_j' N_\beta = 0$$

where $Q^{*}_{ij} = \tilde{Q}_{ij} - \tilde{Q}_{kj} n_k n_i$, $\tilde{Q}_{ij} = \mathcal{G}_{i\alpha j\beta} N_\alpha N_\beta$, $\mathcal{G}_{i\alpha j\beta} = \dfrac{\partial^2 \mathcal{G}}{\partial x_{i\alpha} \partial x_{j\beta}}$ $\tilde{Q}_{ij}$, Q^{*}_{ij} are the components of the acoustic tensor and the reduced acoustic tensor respectively, the prime indicates differentiation with respect to λ - simple wave parameter, $x_{i\alpha}$, u_i are components of the deformation gradient, and particle velocity. U denotes the speed of propagation. The constraint of incompressibility restricts the propagating waves to transverse waves only. In general, the reflection-transmission problem may have no solution in terms of simple waves, as there are at most possible two families of reflected (transmitted) simple waves in such a case ; this means that there are four free parameters, with six interface conditions to be meet (particle velocity vector and stress vector must be continuous from one medium to the other). However solutions may exist for some types of incompressible materials, with particular deformation, symmetry and interface conditions. In this paper we examine such special case.

Since the motion is restricted to one dimension we assume that the incident plane shock wave generates at the interface a single (instead of two) reflected and single transmitted simple wave with a direction of propagation perpendicular to the interface. The propagation condition for single reflected and single transmitted simple wave $(2)_1$ is reduced to a single equation

$$(3) \qquad (\mathcal{G}_{3232} - U^2)\, u_3' = 0 \quad \text{or} \quad (\hat{\mathcal{G}}_{3232} - \hat{U}^2)\, \hat{u}_3' = 0$$

respectively. The symbol "$\wedge$" serves here to label the field quantities connected with the transmitted wave. The characteristic root U ($\hat{U}$) is a real single valued function of the component x_{32} ($\hat{x}_{32}$) and it represent the speed of simple wave. The reflection-transmission problem then reduces to an initial boundary value problem for ordinary differential equations governing the variation of the deformation gradient (x_{32}) and particle velocity (u_3) in the region of reflected (transmitted) wave. We assume $u_3' = -U$ and $\hat{u}_3' = \hat{U}$, and from $(2)_2$ we obtain $x'_{32} = 1$, $\hat{x}'_{32} = 1$.

These equations can be integrated directly. Substitution of solution for x_{32} ($\hat{x}_{32}$) into expression for σ_{3232} ($\hat{\sigma}_{3232}$) gives the reflected (transmitted) wave speed as a function of the wave parameter.

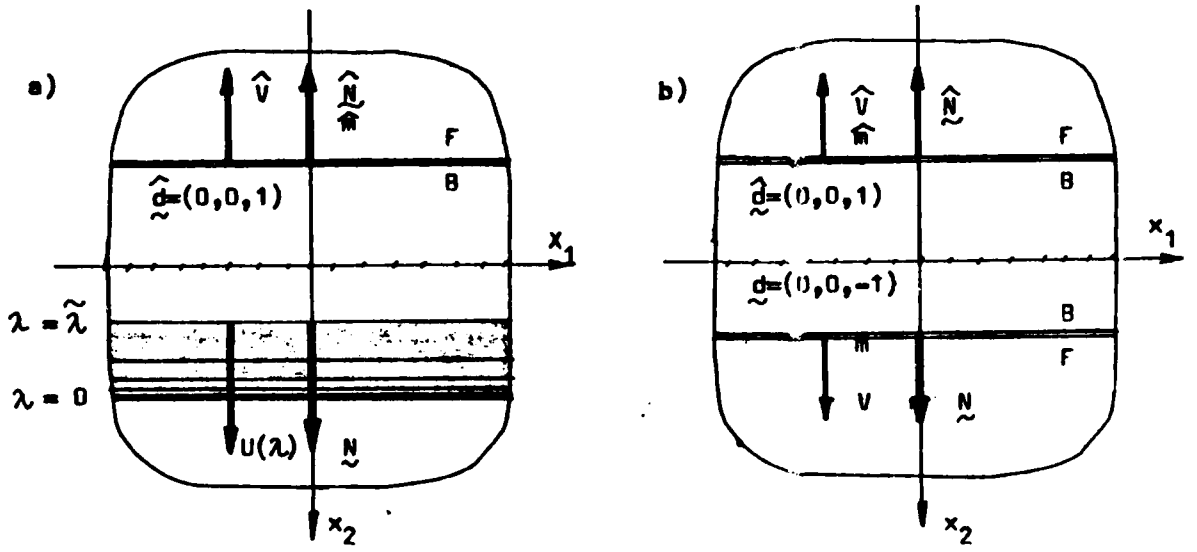

Fig. 3 Shock reflection-transmission patterns

However for $U(\lambda)$ and $\hat{U}(\mu)$ to define a simple wave it must be a decreasing function of the wave parameter λ (μ) varying from 0 to the terminal value $\lambda=\tilde{\lambda}$ ($\mu=\tilde{\mu}$). If U ($\hat{U}$) were an increasing function of λ (μ), the following wavelets would travel faster than the preceding ones and in due course a shock wave would be formed, [1] , [2] . Equation of motion are now replaced by jump conditions. In all cases the reflection solution is depending on the properties of the both material solids, either a single simple wave or a shock wave, when the transmitted wave is always the single simple wave (Fig.3). The conditions of continuity of the velocity and stress field at the interface give us a system of two nontrivial independent nonlinear algebraic equations for the transmitted shock wave strength $\hat{m}$ and the reflected shock wave strength m (or the final value $\tilde{\lambda}$ of the parameter λ in the reflected simple wave).

The numerical analysis shows that for two different pairs of materials can exist the reflected (transmitted) wave having the same parameters, while the parameters of the transmitted (reflected) wave are different. The wave reflection pattern : shock or simple wave depends on the elastic properties of both joined materials and their succesion. The main part of energy of the incident shock wave is used to formation of the transmitted wave. Simply condition for optimal transmission, when the reflected wave is absent, is derived.

The analogous but linearized boundary value problem is considered in 4 by using the Toupin-Bernstein's equations of motion for analysing small but finite amplitude waves.

References

[1] T.W. Wright , Reflection of oblique shock waves in elastic solids. Int. J. Solids Structures , vol. 7 , 161-181, (1971).

[2] P. Lax , Hyperbolic systems of conservation laws II. Comm. Pure Appl. Math. 10 , 537-566, (1957).

[3] B.Duszczyk, S.Kosiński, Z.Wesołowski , Reflection of oblique shock waves in incompressible elastic solids. J. Austral. Math. Soc. Ser B 27 , 31-47 , (1985).

[4] S. Kosiński , Normal reflection and transmission of plane shock waves in nonlinear elastic material. Engineering Transactions , 34 , 4 , 483-502, (1986).

Uniqueness of weak solutions to hyperbolic dissipative systems of balance laws

Witold Kosiński, Polish Academy of Sciences, IPPT, Warsaw

Balanace laws are common features of individual theories of continuum physics. The laws are supplemented with constitutive relations which charcterize the particular medium in question by relating the values of the main vector field $\mathbf{U}$ to the flux $\mathbf{f}$ and the supply term $\mathbf{B}$. We assume the relations are smooth functions and the balance laws lead to a system of 1-st order PDE's:

$$\frac{\partial}{\partial t}\mathbf{U} + \mathrm{Div}\,\mathbf{f}(\mathbf{U}) = \mathbf{B}(\mathbf{U},t,x), \quad (t,x)\in \mathcal{P} \subset E^4. \tag{1}$$

Solutions to the system are restricted by the unilateral constraint, which expresses the second law of thermodynamics [cf.1,2,6],

$$\frac{\partial}{\partial t}\eta(\mathbf{U}) + \mathrm{Div}\,\mathbf{k}(\mathbf{U}) \geq r(\mathbf{U},t,x), \tag{2}$$

where η represents the entropy function, $\mathbf{k}$ - the entropy flux vector and r - the entropy supply term. The terms $\mathbf{B}$ and r appearing in (1) and (2) manifest existing in the medium of non-differential viscous effects. Viscosity due to nonhomogeneity of equations is typical in the thermodynamics with hidden (internal state) variables which have to describe viscous, dissipative properties of matter [cf.3,Sec.20].

In the paper we confine ourself to the case when η is a strictly concave function on a convex set $\mathcal{D}$ in the hodograph space E^m. Then (1) can be written as a symmetric system in the new variable $\mathbf{U}'$ given by the Legandre transformation of η [1]. Moreover, because of the constraint (2), the system (1) possesses the supplementary balance law for entropy

$$\frac{\partial}{\partial t}\eta(\mathbf{U}) + \mathrm{Div}\,\mathbf{k}(\mathbf{U}) = \nabla\eta(\mathbf{U})\,\mathbf{B}(\mathbf{U},t,x). \tag{3}$$

To establish the uniqueness and continuous dependence results for weak, distributional, solutions of Cauchy problem governed by (1) and (2), the class $BV(\mathcal{P})$ is introduced, which is the subset of regular distributions whose first order derivatives

are zero order distributions, i.e. distributions represented by regular, locally finite, Borel measures [4]. In this class a weak solution is defined with the help of the function

(4) $$S(U,V) := K(V) - K(U) + \eta(V)\,(F(U) - F(V)),$$

where $K(U) := (\eta(U), k(U))$, $F(U) := (U, f(U))$.

A function $U \in BV(\mathcal{P}, E^m)$ is called a *weak* solution to (1-2) if is H^n-a.e.bounded and for any constant vector $C \in \mathcal{D}$ and a bounded set $\mathcal{X}$ with finite perimeter the inequality

(5) $$\operatorname{div} S(U,C)(\mathcal{X}) \le \int_{\mathcal{X}} (\nabla\eta(C) - \nabla\eta(U))\cdot B(U,y)\,d\lambda^{n+1}(y)$$

holds, where $y = (t,x)$, H^n denotes the n-D Hausdorff measure on E^{n+1} in which the Lebesgue measure λ^{n+1} is defined. Here div is a divergence operator (identyfied with a Borel scalar measure) in E^{n+1}. It is proved that ineq.(5) is equivalent to eqs (1) and (2), which have to be satisfied in the sense of measure, and to the Rankine-Hugoniot and entropy increase conditions - at points of jumps of U. By the *admissible* weak solution to (1-2) we understand that weak solution to (1-2) which is a limit of a boundedly and a.e.convergent sequence $\{V_k\}_0^\infty$ of regular (smooth) solutions to the parabolized version of (1), in which $f(U)$ is replaced by

(6) $$f'(V_k, \operatorname{Grad} V_k)) := f(V_k) - \varepsilon_k \operatorname{Grad} V_k, \qquad \lim_{k\to\infty} \varepsilon_k = 0.$$

By a *weak* solution to the Cauchy problem

$$\operatorname{div} F(U) = B(U,y), \quad U(0,x) = g(x), \qquad y = (t,x),\ x \in E^n,\ t \in (0,T)$$

we mean a weak solution to (1-2), which satisfies the initial condition in the sense of means, i.e. $\lim_{t\to 0+} \hat{U}(t,x) = g(x)$, λ^n-a.e.on E^n. Here $\hat{U}$ denotes the symmmetric mean value of U [4].

The general strategy of the proof of the continuous - dependence theorem is the same as in [2] and was inspired by [5]. The assumptions on η are essential for the derivation of an evolutionary inequality in terms of the measure div $S(U,V)$, when U is a weak solution to the primitive hyperbolic problem while V is a regular solution to the parabolized one. Integrating the inequality over a space-time frustum we end up with a Gronwall type inequality, already discussed and used in

[2,6]. It is proved that an admissible weak solution of the Cauchy problem is unique in $BV(\mathcal{P},E^m)$, provided $\{\varepsilon_k{}^p\Delta V_k\}_o^\infty \subset$ bounded set of $L^2(\mathcal{P},E^m)$ and the spacial gradients of V_k are in $L^\infty_{loc}(\mathcal{P},E^m)$. The last condition is related to the method used in the proof and it may be released, according to our conjecture .

References

1.Ruggeri, T. and Strumia, A.:Main field and convex covariant desity for quasi-linear hyperbolic systems.Relativistic fluid dynamics, Ann.Inst. H. Poincare, **34**, 65-84 (1981).

2.Dafermos, C.M. and Kosiński, W.:Continuous dependence results for quasi-linear hyperbolic equations, SFB 72-Preprint no.666, Universität Bonn, 1984.

3.Kosiński, W.:Field Singularities and Wave Analysis in Continuum Mechanics, Ellis Horwood Ltd. Chichester and PWN-Polish Scientific Publishers, Warsaw, 1986.

4.Vol'pert, A.I. and Chudaiev, S.I.:Analysis in Class of Discontinuous Functions and Equations of Mathematical Physics (in Russian), Izdatelstwo "Nauka", Moskwa, 1975.

5.DiPerna, R.J.:Uniqueness of solutions to hyperbolic conservation laws, Indiana U.Math.J.,**28**, 137-188 (1979).

6.Dafermos, C.M.:The second law of thermodynamics and stability, Arch.Ration.Mech.Anal.,**70**(3), 167-179 (1979).

Numerical Solution of the Euler Equations Used for Simulation of 2D and 3D Steady Transonic Flows

K. Kozel*, N. Nhac, M. Vavřincová***

The work deals with numerical solution of the system of Euler equations for the case of 2D steady transonic flows in a channel or through a cascade and 3D steady transonic flows in a channel.

I. 2D steady transonic flows in a channel and through a cascade

Consider 2D system of Euler equations in conservation form

$$W_t + F(W)_x + G(W)_y = 0, \tag{1}$$

where $W = \mathrm{col}\,\|\rho, \rho u, \rho v, e\|$; (u, v) is velocity vector, ρ is density, e is energy per unit volume. Weak solution of (1) is based on fulfilling following relation

$$\iint_D W\Big|_{t_1}^{t_2} dx\, dy = -\int_{t_1}^{t_2} \Big\{ \oint_{\partial D} F\, dy - G\, dx \Big\}\, dt \tag{2}$$

for every suitable Jordan curve $\partial D \subset \Omega$, $D = \mathrm{Int}\,\partial D$, $\forall t_1, t_2 > 0$ and $W(t, x, y)$ piecewise smooth for every $t > 0$. Consider finite volume form of numerical solution. Difference scheme is fulfilling integral relation (2) for each computational cell $D_m \equiv D_m^{(1)} D_m^{(2)} D_m^{(3)} D_m^{(4)}$, $D_m^{(k)} = [x_k^m, y_k^m]$, rewritten in the form

$$\mu_m = \iint_{D_m} dx\, dy, \qquad \Delta t = t_2 - t_1 = t^{n+1} - t^n$$

$$W_m^{n+1} - W_m^n = -\frac{\Delta t}{\mu_m} \oint_{\partial D_m} \mathcal{F}\, dy - \mathcal{G}\, dx, \tag{3}$$

where W_m is mean value of W in computational cell D_m, $\mathcal{F}$, $\mathcal{G}$ are approximations of $F(W)$, $G(W)$ along ∂D_m. Steady state is considered to fulfil integral relation (3) for $W_m^{n+1} - W_m^n = 0$.

For numerical solution we use time dependent method, steady state is considered for $t \to \infty$ and steady boundary conditions. Mac Cormack explicit difference scheme [2] in

* Dept. of Comp. Techniques and Informatics, Faculty of Mech. Eng. TU Prague
** Dept. of Mathematics, Faculty of Nuclear Eng. TU Prague

finite volume form is used with artificial disipative terms that are in (x, y) coordinate system difference approximations of the terms

$$\varepsilon_1 \frac{\Delta t}{\Delta x} \frac{\partial}{\partial x} (|W_x| W_x) + \varepsilon_2 \frac{\Delta t}{\Delta y} \frac{\partial}{\partial y} (|W_y| W_y), \qquad \varepsilon_2 \sim \varepsilon_1/2 = O(\Delta t\, \Delta x^2). \tag{4}$$

Boundary conditions along a profile surface are considered using following formula (a case of lower boundary)

(5)

pressure $p_{i,j-1/2}$ is extrapolated by double quadratic extrapolation and relation (5) is then used for deriving other special difference formula for boundary computational cell in predictor step as well as in corrector step. Periodical conditions are considered by usual way. For steady state computation of channel flows we use 1D theory to fulfil upstream and downstream boundary conditions, for 2D cascade flows all components of vector W are considered along upstream boundary; along downstream boundary first three components of W are extrapolated and energy e is computed using given downstream pressure p_2 and extrapolated values ρ, ρu, ρv. Governing system of Euler equations is considered in dimensionless form.

Presented 2D numerical results of transonic channel flows are compared with numerical results of Ron-Ho-Ni, $M_\infty = 0.675$. Interferometric measurements of Institute of Thermomechanics of Czechoslovak Academy of Sciences [5] of 2D transonic flows through 8% DCA cascade for upstream Mach numbers $M_\infty < 1$ as well as $M_\infty > 1$ are compared to our numerical results using lines M=const (see fig. 1,2).

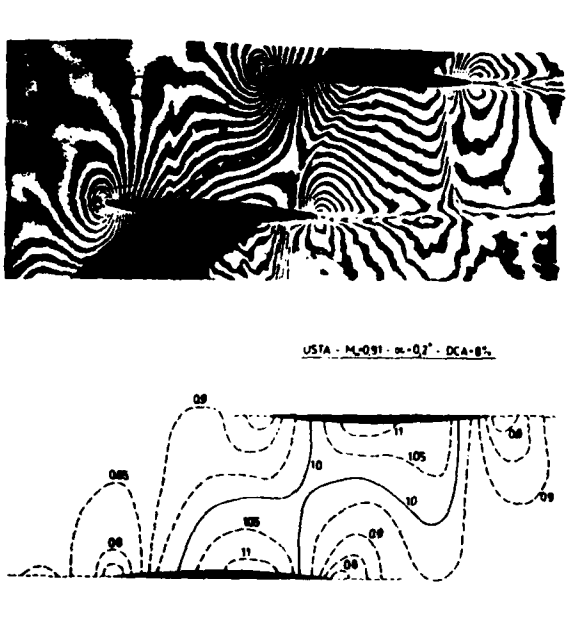

Fig 1.

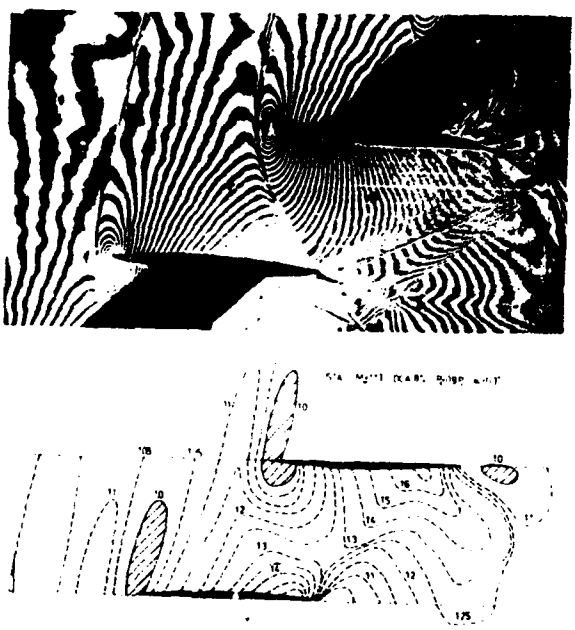

Fig 2.

II. Numerical solution of 3D transonic flows in a channel

Consider 3D system of Euler equations in conservation form

$$W_t + F(W)_x + G(W)_y + H(W)_z = 0, \tag{6}$$

$W = \mathrm{col}\,\|\rho, \rho u, \rho v, \rho w, e\|$, (u, v, w) is velocity vector. In this case finite difference method is used for numerical solution. Cross-section of considered 3D channel is oblong and we use transformation of equation (6) to (x, s, z) coordinate system; s is approximatelly streamline direction. Then (6) is transformed to

$$W_t + F(W)_x + G(W)_s + H(W)_z = 0, \tag{7}$$

and for numerical solution Mac Cormack explicit predictor-corrector conservative difference scheme is used. Grid points are not considered on the walls. Boundary conditions on the walls are fulfilled by the similar way as in 2D case of finite volume form using extrapolated pressure p. Downstream and upstream boundary conditions are fulfilled also by the way similar to 2D numerical solution.

Presented 3D numerical results of transonic flows in a channel are compared to numerical results computed by 1D theory and 2D theory.

References

1. Kozel, K., Vavřincová, M., Finite Volume Solution of the Euler Equations, Proceedings of 2. ISNA Conference, Prague, August 1987
2. Mac Cormack, R.W., The Effect of Viscosity in Hypervelocity Impact Cratering, AIAA Paper 69–354, 1969
3. Lerat, A., Implicit Method of Second-Order Accuracy for the Euler Equations AIAA Journal, Vol. 23, No 1. 1985
4. Ron-Ho-Ni, A Multiple-Grid Scheme for Solving the Euler Equations, AIAA Journal, Vol. 20, No 11, 1982
5. Dvořák, R., On the Development and Structure of Transonic Flow in Cascades, Symposium Transsonicum II, Göttingen, 1975
6. Thomkins, W.T.Jr., Analysis of Pseudo-Time-Marching Schemes for Applications to Turbomachinery Cascade Calculations, in Advances in Computational Transonics, Vol. 4, Pineridge Press, 1985, ed. W.G. Habashi

THE INITIAL-BOUNDARY VALUE PROBLEM FOR THE TRANSONIC EQUATION IN THE UNBOUNDED DOMAIN

Lar'kin N.A.
The Institute of Theoretical and Applied Mechanics
630090 Novosibirsk
USSR

While studying the transonic flow, model equations governing the development of perturbations near a known solution widely are used. These equations are derived under various assumptions from Navier-Stokes equations for a compressible heatconducting gas. The Lin-Reissner-Tsieghn equation

$$u_{xt} + u_x u_{xx} - \Delta_y u = 0 \quad , \tag{1}$$

where $\Delta_y = \partial^2/\partial y_1^2 + \partial^2/\partial y_2^2$ simulates the development of perturbations in nonsteady nonviscous transonic flows near a slender body, [1]. It is easy to verify that (1) is hyperbolic for all finite values of u_x. Equation (1) is considered in the unbounded domain $G = (0,T) \times D$, $D = \Omega \times I\!R^1$, $y \in \Omega \subset I\!R^2$, $t \in (0,T)$, T is a finite number. The boundary $\partial\Omega$ of Ω is smooth enough. On $\partial\Omega$ Neuman's condition is given

$$\left.\frac{\partial u}{\partial N}\right|_{\partial\Omega \times I\!R^1} = \varphi(x,y) \tag{2}$$

Here N is an outward normal on $\partial\Omega$. The function φ is equal to zero for $|x| \geq R$, R is a finite number. The decay of perturbations at $|x| \to \infty$ is given:

$$\lim_{|x|\to\infty} u_x = 0 \qquad \lim_{|x|\to\infty} \frac{\partial u}{\partial y}(-\infty, y, t) = 0 \tag{3}$$

At $t = 0$ the initial data are given

$$u(x,y,0) = u_0(x,y) \tag{4}$$

Theorem 1.

$$\text{If } \varphi \in W_2^{4\frac{1}{2}}(\partial\Omega \times I\!R^1), \qquad u_0 \in W_2^6(D), \qquad \left.\frac{\partial u_0}{\partial N}\right|_{\partial\Omega} = \varphi, \qquad \int_{-\infty}^{x} u_0(\xi,y)d\xi \in W_2^6(D)$$

then such $T_0 \in (0,T)$ can be found that there exists a unique (accurate to the constant) solution of (1)–(4) in $G_0 = (0,T_0) \times D$:

$$\partial_t^j u_x \in L_\infty(0,T_0; W_2^{3-j}(D)) \qquad (j = 0,1,2)$$
$$\partial_t^i \Delta_y u \in L_\infty(0,T_0; W_2^{2-i}(D)) \qquad (i = 0,1)$$

Theorem 1 is proved by approximation of (1)–(4) by a sequence of problems:

$$v_{xt} - \mu v_{xxx} + v_x v_{xx} - \Delta_y v = 0 \tag{5}$$

$$\left.\frac{\partial v}{\partial N}\right|_{\partial\Omega \times I\!R^1} = \varphi_\mu(x,y),$$

$$\lim_{|x|\to\infty} v_x = 0, \qquad \lim_{|x|\to\infty} \frac{\partial v}{\partial y} = 0, \qquad v(x,y,0) = v_{0\mu}(x,y) \tag{6}$$

Here $\varphi_\mu, v_{0\mu}$ are smooth approximations for φ and v_0 respectively, μ is a positive parameter. Equation (5) is a physical one, it describes nonsteady perturbations in viscous heatconducting transonic flows [2]. Unlike (1) equation (5) is not hyperbolic but a nonclassical one.

Theorem 2.

$$\text{If } \varphi_\mu \in W_2^{4\frac{1}{2}}(\partial\Omega \times I\!R^1), \qquad v_{0\mu} \in W_2^6(D), \qquad \left.\frac{\partial v_{0\mu}}{\partial N}\right|_{\partial\Omega\times I\!R^1} = \varphi_\mu, \qquad \int\limits_{-\infty}^{x} v_{0\mu}(\xi, y)d\xi \in W_2^6(D)$$

then for any $\mu > 0$ such a $T_0 \in (0, T)$ can be found, that there exists a unique solution of (5),(6) (accurate to the constant):

$$\partial_t^j v_x \in L_\infty(0, T_0; W_2^{3-j}(D)) \quad (j = 0, 1, 2); \qquad \mu\partial_t^i v_{xxx} \in L_\infty(0, T_0; W_2^{3-i}(D)),$$
$$\partial_t^i \Delta_y v \in L_\infty(0, T_0; W_2^{2-i}(D)) \quad (i = 0, 1),$$

which tends to the solution of (1)-(4) as μ tends to zero. Theorem 2 is proved by approximation of (5),(6) by a sequence of steady problems using a discretization in time. Then steady problems are approximated by problems in bounded domains, which are solved by Galerkin's method.

Literature:

1. *Lin C., Reissner E., Tsieghn. On two-dimensional non-steady motion of a slender body in a compressible fluid. J. of Mathematics and Physics. v27, n3, 1948.*
2. *Ryzov O., Shefter G. O vliyanii vyazkosti i teploprovodnosti na strukturu szimaemych techenij. Prykladnaya Matematika i Mechanika. (Russian). t.28, v6. 1964.*

ON THE "MULTI-ZONAL-MARCHING" METHOD FOR THIN-LAYER VISCOUS-DEFECT HYPERBOLIC PROBLEMS IN AERODYNAMICS

M. LAZAREFF and J.C. LE BALLEUR

ONERA - BP 72 - 92322 Chatillon Cedex (France)

1. The 'Thin-Layer Viscous-Defect' (TLVD) hyperbolic problem

The Defect Formulation [3,4,5] of the Navier-Stokes equations allows the viscous terms to be isolated in a "Viscous Defect" problem. In the Thin Layer approximation, this leads to a 'TLVD' boundary-layer like problem. In two dimensions, this Defect thin-layer problem is of parabolic type and is amenable to a space-marching method of solution (we consider the steady case). In three dimensions, the same TLVD problem becomes of hyperbolic type in space and is to be solved in general curvilinear coordinates (ξ^1, ξ^2) on a curved surface. Moreover, the corresponding discrete grid is specified a priori and cannot be adjusted nor interpolated, from numerical precision considerations.

2. The ideas for the Multi-Zonal Marching (MZM) method

In numerical steady aerodynamics, hyperbolic systems of equations generally appear in the computation of compressible flows (Euler equations is an example). The corresponding characteristic directions usually lie in the dominant direction of the general flow, meaning that their angular excursion is not great and allowing for a simple space-marching method of solution.

From the mathematical point of view, the peculiarity of the hyperbolic system representing the TLVD problem (or any kind of boundary-layer like formulation) is that the angular excursion of the characteristic directions may be very large. As this prevents the use of a simple space-marching method (except in the most trivial cases), and as the numerical difficulties associated with the 'exact' characteristic method seem forbidding to us, we have resorted to developing a specific method of space-marching solution.

The Multi-Zonal (Multi-) Marching method (MZM) [1,2] is meant to save the advantages of the space-marching method while allowing for the solution to proceed in the general case.

(*i*) - multi-marching method :
The first, natural, idea is to use all four possible marching directions of the grid, namely $+\xi^1$, $-\xi^1$, $+\xi^2$, $-\xi^2$, locally selecting whichever one is most appropriate.
The second, more powerful one, is to alternate general sweeps of the solution domain along these four marching directions, updating the solution only on newly accessible nodes. This constitutes the multi-marching method, which is in principle sufficient to cover by iteration the domain of influence of the initial conditions (i.e. stagnation-point).

(*ii*) - multi-zonal method :
The idea is to use available information on the expected general flow topology (of the kind that is useful for grid generation) for the definition of a system of "zones" which are to be solved in successive order, with expected increase of numerical efficiency.

(*iii*) - multi-zonal multi-marching method :
The combination of the previous ideas leads to the present "MZM" method, which combines repeated sweeps along the four ξ directions, for each successive element of a system of zones covering the solution domain, with possible overlap whenever deemed efficient. This system is automatically predefined (expert-system like) according to the expected general flow topology of the

given type of configuration.

This in principle provides a general method of solution on the whole domain of influence of the Cauchy data (stagnation point), given that the grid is not too highly distorted and the characteristic cone angle does not come near nor exceeds that of the local grid lines. Thus it cannot be proven that the method will work on an arbitrary grid, or if the magnitude of the characteristic cone angle exceeds 90°.

But it is reasonable to expect few difficulties, except perhaps on certain configurations near points of closed separation. In this neighbourhood, the TLVD problem may lead to cone angles nearing 90°, depending on its (direct or inverse) formulation.

3. The numerical method of solution

The hyperbolic system of equations of the TLVD problem in integral formulation consists, in tensor form [2], of one vector equation for the Defect momentum balance :

$$(1)\; div\left[\rho q^2 \underline{\ell} + \rho q(\underline{u} \bigcirc \underline{\delta})\right] = \rho \underline{u} w - \overline{\rho}\,\overline{\underline{u}}\,\overline{w} + \frac{\rho q^2}{2} C_f$$

one scalar equation for the entrainment (collocation equation for momentum):

$$(2)\; div\left[\rho \underline{u}\delta - \rho q \underline{\delta}\right] = \overline{\rho}\,\overline{w} + \rho q E$$

and one scalar equation for the Defect mass balance :

$$(3)\; div\left[\rho q \underline{\delta}\right] = \rho w - \overline{\rho}\,\overline{w}$$

where :

$\rho, \underline{u}$ pseudo-inviscid density and velocity fields

$\overline{\rho}, \overline{\underline{u}}$ real (viscous) " " " "

$q = ||\underline{u}||_0$ pseudo-inviscid velocity modulus at the surface

$$\underline{\delta} = (\rho q)^{-1} \int_{0}^{\infty} (\rho \underline{u} - \overline{\rho}\,\overline{\underline{u}})\, dn$$

$$\underline{\ell} = (\rho q^2)^{-1} \int_{0}^{\infty} (\rho \underline{u} \bigcirc \underline{u} - \overline{\underline{\rho}} \bigcirc \overline{\underline{u}})\, dn - q^{-1} \underline{u} \bigcirc \underline{\delta}$$

n field coordinate locally normal to the (ξ^1, ξ^2) surface

$w = \underline{u}_0^n$ normal component of pseudo-inviscid velocity at the surface

$\overline{w} = \overline{\underline{u}}_0^n$ " " real (viscous) " "

$C_f = (\tau_0/\rho q^2)^{1/2} \cdot (\underline{\tau}_0/||\underline{\tau}_0||)$

$\underline{\tau}_0$ wall shear stress in the real (viscous flow)

δ boundary - layer thickness scale parameter

Equations (1)-(3) are written on the (ξ^1, ξ^2) surface for vectors and tensors defined in two-dimensional space. These can be written in projection on the local holonomic (ξ_1, ξ_2) vector basis computed from the (ξ^1, ξ^2) curvilinear coordinate set.

Taking into account a physical modelling based on the three-dimensional velocity profiles of Le Balleur [5,6], this yields a closed system of rank-4 hyperbolic type. It can be written, for solution by a marching procedure in the x^1 direction (where $x^1 = +\xi^1, -\xi^1, +\xi^2, -\xi^2$) :

$$\frac{\partial \mathcal{L}}{\partial x^1} = -\frac{\partial \mathcal{G}(\mathcal{L})}{\partial x^2} \quad ; \quad \mathcal{L} \in \mathbb{R}^4$$

(i) - local integration scheme (x^1-marching):

The resulting set of four scalar equations is discretized on the discrete grid $\xi^1(i)$, $\xi^2(j)$ using the explicit MacCormack scheme, and solved by space-marching in the ξ direction which is instantaneously chosen as x^1, subject to two stability criteria. One is the linear CFL criterion mandatory with explicit integration. The other is a non-linear criterion based on the boundary-layer displacement thickness.

(ii) - global integration method ($+\xi^1, -\xi^1, +\xi^2, -\xi^2$ - marching):

The progressive development of the local integrations generates the characteristic directions and automatically guides the increasing coverage of the solution domain with successive sweeps on each predefined zone, until no further grid node can be accessed.

4. Numerical results

The method allows the computation to proceed in presence of rather complex viscous-flow topologies, such as those which develop on slender bodies at both incidence and yaw conditions. While a unique integration direction might suffice for a prolate ellipsoid at 10° of incidence, the same one at 30°, or the flattened type with both incidence and yaw, will exhibit a complex flow topology in the nose region, and also around the predicted separation line (open and/or closed separation). This will require to sweep away from the stagnation point at the nose and towards the accumulation line at the rear.

An example is given for a 6:1:1 ellipsoid at 15° of incidence (fig. 1), showing the accumulation line, and the stagnation point region on a slender body at incidence 30° and yaw 10° (fig. 2), showing the four integration directions which radially diverge from the stagnation-point cell.

5. Conclusion

The technique of iterative sweeps along the four grid directions (multi-marching method) solves the difficulties associated with space-marching methods for hyperbolic problems when the characteristic directions are widely varying in the computational domain, as it is usual for TLVD equations.

The corresponding numerical efficiency is augmented by decomposition of the computational domain into a system of possibly overlapping zones, which are expected to be solved in successive order (multi-zonal method).

The resulting "MZM" method provides an efficient means of space-marching computation for hyperbolic problems with highly contorted characteristic line patterns.

References

[1] - LE BALLEUR J.C., LAZAREFF M. - A "Multi-Zonal-Marching" integral method for 3D-boundary layer with viscous-inviscid interaction. Proceed. 9th ICNMFD, Saclay (France), 1984, Lecture Notes in Physics, 218, p. 351-356, Springer-Verlag 1985 (or ONERA-TP 1984-67).

[2] - LAZAREFF M., LE BALLEUR J.C. - Computation of three dimensional flows by viscous-inviscid interaction using the "MZM" method. Proceed. AGARD-CP 412, paper 25 (or ONERA TP 1986-29).

[3] - LE BALLEUR J.C. - Computation of flows including strong viscous interactions with coupling methods. AGARD-CP-291, General introduction, Lecture 1, Colorado-Springs, 1981 (or ONERA-TP 1980-121).

[4] - LE BALLEUR J.C. - Strong matching method for computing transonic viscous flows including wakes and separation. Lifting airfoils. La Recherche Aérospatiale, 1981-3, p. 21-45, English edition, 1981.

[5] - LE BALLEUR J.C. - Numerical viscid-inviscid interaction in steady and unsteady flows. Proceed. 2nd Symp. Numerical and Physical Aspects of Aerodynamic flows, Long Beach, 1983, Springer Verlag, T. Cebeci ed., chapt. 13, p. 259-284, 1984 (or ONERA-TP 1983-8).

[6] - LE BALLEUR J.C. - Numerical flow calculation and viscous-inviscid interaction techniques. Recent Advances in Numerical Methods in Fluids, vol. 3 : Computational methods in viscous flows, p. 419-450, W. Habashi ed., Pineridge Press, 1984.

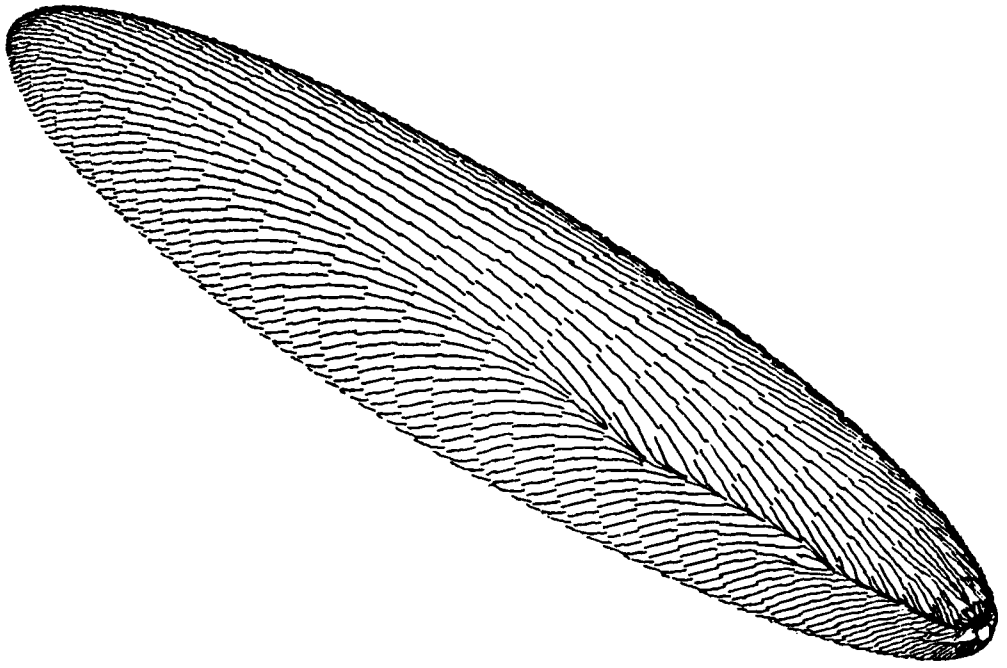

Fig. 1 : 6:1:1 prolate ellipsoid α=15°
Skin-friction directions showing the accumulation line at the rear

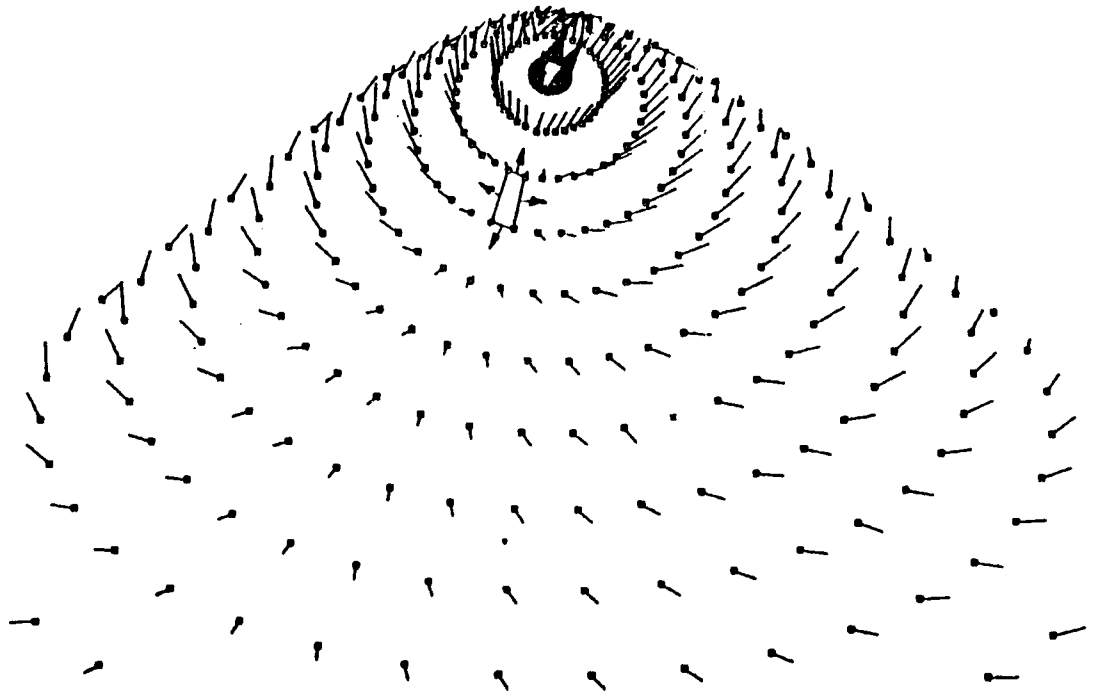

Fig. 2 : Slender lifting body α=30° β=10°
Skin-friction directions with outward integration from the stagnation cell

ENTROPY WEAK SOLUTIONS TO NONLINEAR HYPERBOLIC SYSTEMS UNDER NONCONSERVATIVE FORM

Philippe Le Floch
Centre de Mathématiques Appliquées, Ecole Polytechnique,
91128 Palaiseau Cédex, France.

1.Introduction.

For nonlinear hyperbolic systems under nonconservative form, we consider weak solutions in the class of bounded functions of bounded variation in the sense of Volpert A generalized global entropy inequality is proposed and studied. In this framework, we solve the Riemann problem and prove, for the Cauchy problem, the consistancy of a corresponding random choice method. Our theory is applied to nonconservative systems issued from Elasticity and Hydrodynamics.

2. A definition of entropy weak solutions for nonconservative systems:

Let us consider nonlinear hyperbolic systems under nonconservative form

$$(1) \qquad A_0(u)\,\partial_t u + A(u)\,\partial_x u = 0,\ u(x,t) \in \mathbf{U},\ x \in \mathbb{R},\ t > 0.$$

Here, $\mathbf{U}$ is an open subset of $\mathbb{R}^p$, A_0 and A are continuously differentiable functions defined from $\mathbf{U}$ to the space of $p\times p$ matrix. For each u in $\mathbf{U}$, we assume that $A_0(u)$ is invertible, and for the sake of simplicity the matrix $A_0(u)^{-1}A(u)$ has p distinct eigenvalues. Each i-characteristic field is supposed to be globally either genuinely nonlinear or linearly degenerate.

Generally, the nonlinear hyperbolic system (1) is not an usual system of conservation laws, because the matrix A_0 and A may be not Jacobian matrix. The theory of conservation laws does not apply: the notions of weak solutions and entropy conditions have no sense for (1). Nevertheless such nonconservative systems appear in some applications of Elasticity or Hydrodynamics as recently shown by Colombeau and Leroux [6]. Thus a mathematical theory of weak solutions for (1) is needed. Here we define a notion of entropy weak solution for (1) in the space of bounded functions of (locally) bounded variation. Let us recall that the relevance of the space BV for studying systems of conservation laws is recognized by many authors as Glimm [3], DiPerna [1], Diperna-Majda [2],... Our results will establish that the BV space yields also a suitable framework even for systems under nonconservative form.

• First to define in which weak sense must the equations be understood, we follow Volpert [7] and seek weak solutions to (1) in the space $L^\infty \cap BV(\mathbb{R}\times\mathbb{R}^+)$ of bounded functions u of (locally) bounded variation. Let us recall some regularity properties of BV functions. For an element u in $L^\infty \cap BV(\mathbb{R}\times\mathbb{R}^+;\mathbb{R}^p)$, it turns out that -with the possible exception of a set with zero 1-dimensional Hausdorff measure -each point $\mathbb{R}\times\mathbb{R}^+$ is regular, that is : either a point of

approximate continuity ($u=u_-=u_+$) or a point of approximate jump (where u admits two limit values u_- and u_+). Henceforth, we will consider representants of BV-functions modulo 1-dimensional Hausdorff measure. And following [7], we define the superposition of a fonction as follows. Consider a continous function f in $C^0(\mathbb{R}^p;\mathbb{R})$ and an element u in $L^\infty \cap BV(\mathbb{R}\times\mathbb{R}^+;\mathbb{R}^p)$. The fonctional superposition of u by f, denoted by $\hat{f}(u)$, is the function of $L^\infty \cap BV(\mathbb{R}\times\mathbb{R}^+;\mathbb{R}^p)$ given by the formula

$$(2) \qquad \hat{f}(u)(y) = \int_0^1 f(u_-(y) + \alpha(u_+(y) - u_-(y)))\, d\alpha,$$

valid for each y in $\mathbb{R}\times\mathbb{R}^+$ without a set of zero 1-dimensional measure. If A is a matrix valued function, $\hat{A}(u)$ is defined similarly. Volpert [7] proves that the fonction $\hat{f}(u)$ given by (2) is measurable and locally integrable with respect to the Borel measure defined by a partial derivative $\partial v/\partial t$ (or $\partial v/\partial x$) of an arbitrary bounded BV-function v. Thus the product $\hat{f}(u).\partial v/\partial t$ makes sense as a locally finite Borel measure. Indeed, for systems of conservation laws, this concept of superposition is very useful as noted by many authors (DiPerna-Majda [2]...). Now using this notion of functional superposition, we propose to set [5]:

DEFINITION 1: A function u in $L^\infty \cap BV(\mathbb{R}\times\mathbb{R}_+;U)$ is a weak solution to the nonconservative nonlinear hyperbolic system (1) if the equality

$$(3) \qquad \hat{A}_0(u)\,\partial_t u + \hat{A}(u)\,\partial_x u = 0$$

holds in the sense of the Borel measures.

Let us apply this definition to special discontinous functions and get a practical formula for computing jump relations for (1).

THEOREM 1: The discontinous function u given by: $u(x,t) = u_L$ for $x-\sigma t<0$, u_R for $x-\sigma t>0$, **with u_L and u_R in U, σ in $\mathbb{R}$, is a weak solution to the system (1) if and only if the following generalized Rankine-Hugoniot relation holds**

$$(4) \qquad \int_0^1 \{ -\sigma A_0(u_L+\alpha(u_R-u_L)) + A(u_L+\alpha(u_R-u_L)) \}\, d\alpha\ (u_R-u_L) = 0.$$

Second, for the sake of uniqueness, we define a generalized notion of (global) entropy inequality [5]:

DEFINITION 2: A p-vector valued function $\phi : U \to \mathbb{R}^p$ of C^1-class is an admissible function for the nonconservative system (1) if it is increasing and satisfies the compatibility property

$$(5) \qquad D\phi^T A_0 = A_0{}^T D\phi \ , \qquad D\phi^T A = A^T D\phi .$$

And we propose the following definition of entropy weak solutions [5]:

DEFINITION 3: Suppose there exists an admissible function ϕ for (1). Then a weak solution to (1) (in the sense of Definition 1) is an entropy weak solution to (1) (with respect to the admissible function ϕ) if the generalized entropy inequality

$$(6) \qquad (\phi^T A_0)\hat{}(u)\,\partial_t u + (\phi^T A)\hat{}(u)\,\partial_x u \le 0$$

holds in the space of measures.

The (nonconservative, in general) inequality (6) is a generalization of the usual entropy inequality [4] derived for conservation laws by the viscosity method. When A_0 and A are Jacobian matrix, (1) is a system of conservation laws and we prove [5] that our notion of entropy weak solution reduces exactly to the usual notion of Glimm [3] and Volpert [7]. Examples of admissible functions for nonconservative systems are presented in [5].

3. Riemann problem and random choice method.

We are concerned with the existence of entropy weak solutions of the Cauchy problem for the nonconservative system (1). We begin by considering the Riemann problem for (1), which is a Cauchy problem with a piecewise constant initial data u_0 of the form:

$$(7) \qquad u_0(x) = u_L \text{ if } x<0, \quad u_R \text{ if } x>0, \quad \text{with } u_L \text{ and } u_R \text{ in } \mathbf{U}.$$

For (1), the usual notion of rarefaction waves is still valid And, we note that the Lax admissibility criterion [4] makes also sense for (1). Using our jump formula (4), we are able to define a generalized notion of shock waves and contact discontinuities for a nonconservative system. Then, we get [5]:

THEOREM 2: For $|u_R - u_L|$ small enough, there exists one self similar solution of the Riemann problem (1)(7), which is composed of (at most) p rarefaction waves, generalized shock waves or contact discontinuities.

And a main result concern the equivalence between the two entropy conditions.

THEOREM 3: For weak shock waves, our generalized entropy inequality (6) is equivalent to the Lax admissibility criterion for the nonconservative system (1).

Then,given a random sequence a, approximate solutions $\{ u^h \}$ of the Cauchy problem for (1) are constructed by glueing together solutions of different Riemann problems as in the random-choice method of Glimm [3]. It is a simple matter to prove that this family is uniformly bounded in norms L^∞ and BV, and thus it (or a subsequence) converges almost everywhere with respect to the Lebesgue measure to a bounded BV-function $u = u(x,t)$. Finally, we get [5]:

THEOREM 4: The family of approximate solutions $\{ u^h \}$ is consistent with the nonconservative system (1) in the following sense. There exists a subsequence $(h_n)_{n\in\mathbb{N}}$ tending to zero, such that

$$(8) \qquad \int\int_{\mathbb{R}\,\mathbb{R}_+} \theta \{ \hat{A}_0(u^h)\,\partial_t u^h + \hat{A}(u^h)\,\partial_x u^h \}\,dx\,dt \to 0, \quad h = h_n \to 0,$$

for every function θ in $C^0(\mathbb{R}\times\mathbb{R}^+, \mathbb{R})$ with compact support and almost every sequence a. Moreover when (1) admits an admissible function ϕ and all the characteristic fields are genuinely nonlinear, the family of approximate solutions $\{u^h\}$ is also consistant with the generalized entropy inequality (6):

$$(9) \qquad \lim \int_{\mathbb{R}} \int_{\mathbb{R}_+} \theta \{ (\phi^T A_0)(u^h)\, \partial_t u^h + (\phi^T A)(u^h)\, \partial_x u^h \}\, dx\, dt \le 0, \quad (h=h_n \to 0)$$

4. Nonconservative systems issued from Hydrodynamics and Elasticity.

As an application of our theory, we study in particular a system of 3 equations introduced by [6] and issued from Elasticity. In Euler coordinates, the density ρ, the velocity u, the stress deviator σ of an one dimensional homogenous elastic medium satisfy

$$(10) \quad \partial_t \rho + \partial_x(\rho u) = 0, \qquad \partial_t(\rho u) + \partial_x(\rho u^2 - \sigma) = 0, \qquad \partial_t \sigma + u\partial_x \sigma - k^2 \partial_x u = 0,$$

where k is a positive constant. As noted in [6], the third equation in (10) is nonconservative and corresponds to the Hooke's law. For this model, we solve the Riemann problem without restriction on the size of the initial data, and we find the generalized entropy inequalities (6).

We have also considered the system of conservation laws of Gaz Dynamics. Following some previous ideas of [6], we derive an equivalent nonconservative form of this system [5]:

THEOREM 5: For the sake of simplicity, assume an equation of state of a polytropic perfect gas. The usual system of gas dynamics in Lagrangian coordinates is equivalent to the following nonconservative system with the unknown (v,u,p):

$$(11) \qquad \partial_t v - \partial_x u = 0, \qquad \partial_t u + \partial_x p = 0, \qquad v\,\partial_t p + \gamma p\, \partial_x u = 0,$$

where the unknown are the volume v, the velocity u and the pressure p; $\gamma \ge 1$.

5. References.

[1] DiPerna, R.J., Uniqueness of solutions of hyperbolic conservation laws, Ind. Univ. Math. J., 28 (1979), 137-188.

[2] DiPerna, R.J., Majda, A., The validity of nonlinear geometric optics for weak solutions of conservation laws, Comm. Math. Phys. 98 (1985), 313-347.

[3] Glimm, J., Solutions in the large for nonlinear hyperbolic systems of equations, Comm. Pure Appl. Math. 18 (1965), 697-715.

[4] Lax, P.D., Hyperbolic systems of conservation laws and the mathematical theory of shocks waves, CBMS Monograph N°11, SIAM (1973).

[5] Le Floch, Ph., Nonlinear hyperbolic systems under nonconservative form, to appear in Comm. in P.D.E. (1988); and Thesis of the Ecole Polytechnique (France) (1987).

[6] LeRoux, A.Y., Colombeau, J.F., Techniques numériques en élasticité dynamique, Communication to the First International Conference on Hyperbolic Problems, Saint-Etienne (France), January 1986.

[7] Volpert, A.I., The space BV and quasilinear equations, Math. USSR Sb.2, 257-267 (1967).

A velocity pressure model

for elastodynamics

by A.Y. Le Roux

Mathématiques, Université de Bordeaux 1

F-33405 TALENCE

The dynamical problems in elasticity and elastoplasticity used to be modelized by the classical conservation laws, involving the density, the momentum and the total energy. These laws need to be completed by adding a state law, which expresses the pressure as a function of the density and the internal energy, and some equations ruling the the non isotropic part of stress tensor. These equations and the state law are deduced from experimental measures.

The use of such a state law may be very unstable in some computations, for some materials such as copper or iron. As a matter of fact, for such materials, a tiny variation of the density leads to a big variation of the pressure. Thus one can see, in a numerical computation, some oscillations of the pressure near a contact discontinuity, though the pressure must be theoretically a constant.

The equations ruling the non isotropic part of the stress are usually deduced from a Hooke law which has not a conservative form in Eulerian coordinates. Moreover, by making the Lamé coefficient depending on the state of the material (density, stress, pressure or internal energy), one puts some non conservative terms into the model.

We can get rid of the numerical drawback on the pressure by introducing a new equation for the pressure in place of the conservation law of the total energy and the state law. This is a rigorous computation in the absence of shocks, which leads to an equation of the same (non conservative) type as for the stress. Then the whole difficulty of the problem has not increased since, in any case, non conservative terms are already occuring for the stress. This difficulty lies into the handling of the products of distributions. By performing them in a right way, one can find the same shocks as given by the experimental data.

Our aim here is to show how one can solve such a difficulty for a very simple problem involving only the velocity and the pressure, in the one dimension case. These two parameters are of high interest in practice, for the shocks polars which are deduced from the experimental data, are drawn in fact on a diagram involving tle velocity and the pressure (see [4]).

The first section recalls the experimental technique which leads to the construction of this shock polar. This curve corresponds exactly to the shock curve, that is the Hugoniot curve, of the model to be written. This curve is in practice very close to the Riemann invariant or the isentropic curve, and the difference used to be neglected by experimenters.

The model is built in the second section. One needs three basic physical hypotheses to build it. The first one expresses that the velocity and the pressure are varying "in phase" on a given shock wave. The second one deals with the sound celerity in the material, which is assumed to be independant of the material velocity. The last one corresponds to neglect the variations of the specific volume with respect to the variations of the pressure; this is only done in order to get a simplified model. The phase hypothesis means that, on a shock wave, the velocity and the pressure can be shaped with jump functions corresponding to the same equivalenve class of an algebra wider than the classical distribution space (see [1]), but where the multiplication is suitable as for the C^∞ functions. It was shown in [2] and [3] that

for perfect gas, the phase hypothesis is really fulfilled by the velocity and the pressure together, since in this way one gets the right solutions with shocks. This property is not true for another couple of parameters, such as the momentum and the velocity for example, which can lead to shocks with a wrong velocity or a wrong intensity. From the phase hypothesis, one can obtain a shock condition to be identified with the experimental shock polar. In this way we get the expression of the sound celerity with respect to the pressure, as expected from the second hypothesis. Thus we are now certain to have the discontinuities of the solutions of this model corresponding exactly with the shocks which have been observed experimentally.

Now the model has been written and we want to solve it by making numerical computations. This will be performed by mean of a numerical scheme of the "transport projection" type as the Godunov scheme for example. The third section is concerned with the transport part of the scheme, which is in fact reduced to the construction of a Riemann solver. This solver uses the phase hypothesis that we have done by writing the model and then we can be sure that the shocks will be the right ones. From a technical point of view, this corresponds to solve a system of two nonlinear algebraic equations. This is performed through a very fast iterated process which uses the dynamical impedance (which is defined as the product of the density by the sound celerity) as the linearization parameter.

This Riemann solver allows to build an approximate solution for a short time interval, from constant piecewise data. We have now to project this solution on a space of constant piecewise functions in order to be able to start again for the next time step. The fourth section deals with a discussion on several kinds of possible projections which can lead to different numerical results, more particular for gas or light materials. Some numerical results are reported in this section.

We give also a few comments and generalizations, such as the introduction of a variable density in the computation. We notice in this case a good behaviour of the pressure and of the velocity near a contact discontinuity, and by applying this scheme to gas dynamics, we get results similar to those given by the Godunov scheme with the classical conservation laws. Thus the scheme described in section 3 and 4 is not of high interest for gas dynamics since its performances are not better than many other methods, though it always gives the entropy solution. We find its full interest by applying to stronger materials and in its capability to be generalized to more complex systems in elastodynamics or in dynamical elastoplasticity, even for several space dimensions.

References

[1] J.F. Colombeau - *Elementary introduction to new generalized functions*, North Holland - 1978.

[2] J.F.Colombeau, A.Y.Le Roux - Numerical method for hyperbolic systems in non conservative form using product of distributions, *Advances in computer methods for partial differential equations VI*- R.Vichnevetsky and R.S. Stepleman ed, Publi. IMACS, 1987.

[3] J.F.Colombeau, A.Y.Le Roux, B.Perrot - Multiplication de distribution et ondes de choc élastiques ou hydrodynamiques en dimension un. Note aux Comptes Rendus de l'Académis des sciences, to appear (1987).

[4] M.Desfourneaux - Théorie et mesure des ondes de choc dans des solides, Cours CP32, ENSTA Paris-1973.

Linearized Wave Interactions for Nonlinear Conservation Laws

Randall J. LeVeque
University of Washington

The basic idea discussed in this talk is the use of linear superposition to generate approximate solutions of nonlinear hyperbolic systems of conservation laws.

The application that motivates this work is the extension of Godunov-type numerical methods to situations in which the Courant number is greater than one. This means that waves from neighboring Riemann problems may interact, and it is this interaction that is approximated by linear superposition. This can be useful in efficiently dealing with nonuniform grids where some grid cells are orders of magnitude smaller than others due to irregular boundaries, shock tracking, mesh refinement, etc. For mildly nonlinear problems it can also be advantageous to use uniformly large Courant numbers.

Let U_j represent an approximate solution in the jth cell (x_j, x_{j+1}) and let $u_j(x,t)$ be the solution to the Riemann problem with a single discontinuity at x_j, i.e.,

$$u_j(x,0) = \begin{cases} U_{j-1} & x < x_j \\ U_j & x > x_j. \end{cases}$$

For a strictly hyperbolic system $u_t + f(u)_x = 0$ of m equations, u_j is a similarity solution that typically consists of m waves. Denote the wave strengths by vectors $R_p^{(j)}$, $p = 1, 2, \ldots, m$, i.e.,

$$U_j - U_{j-1} = \sum_{p=1}^{m} R_p^{(j)}. \tag{1}$$

Then we can define an approximate solution $\tilde{u}(x,t)$ for all $t \geq 0$ with the piecewise constant initial data

$$\tilde{u}(x,0) = U_j \text{ for } x_j < x < x_{j+1}$$

by setting

$$\tilde{u}(x,t) = \tilde{u}(x,0) + \sum_j (u_j(x,t) - u_j(x,0)). \tag{2}$$

For t sufficiently small that no wave interaction occurs, this is in fact the true solution. For a constant coefficient linear system $u_t + Au_x = 0$ it is the true solution for all t. For nonlinear problems it is an approximation in which the waves interact by passing through one another with no change in speed or strength.

A large time step generalization of Godunov's method is obtained by averaging $\tilde{u}(x,t)$ to obtain a new piecewise constant function at the end of a time step of arbitrary length. This method has been studied in [2] and [4]. It is also possible to obtain second order accurate methods in a similar vein by using piecewise linear approximations[3].

To show second order accuracy of such a method it is necessary to demonstrate that this linearization is compatible with second order accuracy in time. This can be done by considering the continuous analogue of this linearization. If $u(x,0)$ is a smooth function then as the mesh width goes to zero the decomposition (1) approaches a (scaled) decomposition of $u_x(\xi,0)$ at each point ξ into eigenvectors $r_p(\xi)$ of the Jacobian matrix $J(\xi) = f'(u(\xi,0))$. These vectors satisfy

$$u_x(\xi,0) = \sum_{p=1}^{m} r_p(\xi).$$

Corresponding to the Riemann solutions $u_j(x,t)$ used above we define $z(x,t;\xi)$ for each ξ as the solution of the constant coefficient linear equation

$$z_t + J(\xi)z_x = 0$$

with data

$$z(x,0;\xi) = H(x-\xi)u_x(\xi,0)$$

where H is the Heaviside function. These solutions are then combined by linear superposition to give the continuous analogue of the approximate solution (2):

$$\tilde{u}(x,t) = u(x,0) + \int_{-\infty}^{+\infty} [z(x,t;\xi) - z(x,0;\xi)]d\xi.$$

This approximation was originally introduced by Brenier[1] to give a unified view of several finite difference methods, including Boltzman and particle methods. It is also similar to nonlinear geometrical optics approximations.

If we hope to achieve second order accuracy from a numerical method based on this approach, we need

$$\tilde{u}(x,t) = u(x,t) + O(t^3)$$

as $t \to 0$. This has been shown to hold for sufficiently smooth initial data[5].

At the other end of the spectrum one can investigate the effect of linearizing highly nonlinear interactions, for example of strong shocks. Some results in this direction indicate a surprising degree of long-time structural stability of solutions under this type of approximation.

The talk will contain both numerical and theoretical results related to the above questions.

REFERENCES

[1] Y. Brenier, *A time discretization for conservation laws*, in Numerical Methods for the Euler Equations of Fluid Dynamics, F. Angrand et al., eds., INRIA Workshop, SIAM, 1985, pp. 108–120.

[2] R. J. LeVeque, *Convergence of a large time step generalization of Godunov's method for conservation laws*, Comm. Pure Appl. Math., 37 (1984), pp. 463–477.

[3] ———, *High resolution finite volume methods on arbitrary grids via wave propagation*, J. Comput. Phys., (to appear).

[4] ———, *A large time step generalization of Godunov's method for systems of conservation laws*, SIAM J. Num. Anal., 22 (1985), pp. 1051–1073.

[5] ———, *Second order accuracy of Brenier's time-discrete method for nonlinear systems of conservation laws*, SIAM J. Num. Anal., (to appear).

L

A MULTIGRID TECHNIQUE FOR THE LAMBDA FORMULATION

A. Lippolis and A. Dadone
University of Bari, Italy

Multigrid techniques for accelerating convergence are widely applied to elliptic equations and their efficiency has been established from a theoretical point of view as well as in practical applications. These techniques have been extended to the Euler equations by Ni /1/; since this pioneer work, many multigrid techniques have been proposed, the most popular being those developed by Jameson /2/ and Hall /3/, which also use other accelerating devices such as local and multistage time stepping, residual averaging, enthalpy damping. The physical interpretation of these two methods is different: Hall figures out the multigrid technique as a faster propagation of errors to the computational boundaries, while Jameson considers the use of multiple grids an efficient damping of different frequency components, according to the original "elliptic" interpretation of this technique.

The authors of the present paper are strong supporters of the lambda formulation proposed by Moretti /4/, because of its desirable features. The time dependent compressible Euler equations are recast in terms of compatibility conditions for characteristic (Riemann) variables along characteristic lines and discretized by means of upwind differences, which correctly take into account the direction of wave propagation. In this way a numerical technique is obtained, which combines the coding simplicity of finite difference methods with the intrinsic accuracy and physical soundness of the method of characteristics. Since its first appearance as a working tool for computing unsteady as well as steady flows, many contributions for improving the convergence rate of the lambda formulation have been provided: implicit formulations (see, e.g., Ref. 5), fast solvers for one-, two- and three-dimensional flows /6; 7; 8/. In these last references, transonic flow computations have been performed by taking advantage of the shock fitting procedure suggested by Moretti /9/.

The first application of multigrid techniques to the lambda formulation is due to Favini and Sabetta /10/, who presented interesting results limited to one-dimensional flows using an explicit scheme as basic solver.

Aim of the present paper is to present a multigrid technique for the lambda formulation apt to compute one- and two-dimensional subsonic as well as transonic flows. The main features of the suggested multigrid technique are the following:

- the fast sovers due to Moretti /6/ and Dadone-Moretti /7/ are used as basic solvers for the one- and two-dimensional flows, respectively; these solvers incorporate a shock fitting technique for dealing with transonic flows;
- four and five different grid levels are used;
- the shock position is updated only at the finest mesh level, while its position is frozen for the computations at the other grid levels;
- the interpolation procedure is applied to the time increment of the variables;
- the multigrid cycle starts from the finest grid, moves to the coarsest mesh and returns gradually to the finest one.

At first the technique has been applied to quasi one-dimensional convergent, divergent, and convergent-divergent nozzles; subsonic as well as transonic flow cases have been considered. The results have shown a substantial gain in the work required to reach a machine-zero convergence; this gain ranges from one to two orders of magnitude with respect to Moretti's fast solver /6/, which presents a fast convergence by itself. As a sample, for the subsonic flow in a converging nozzle computed by means of 128 mesh intervals and five mesh levels, 30 multigrid cycles bring the logarithm (base 10) of the residual to -13, while 60 cycles are required to compute the transonic flow in a convergent-divergent nozzle. The suggested technique has been also applied to the computation of subsonic flows around airfoils and the first results obtained have shown a work gain of the order of three with respect to Dadone-Moretti's fast solver /7/. Plots of the results are unavailable at present because of temporary plotting problems, but they will be inserted in the camera-ready abstract.

Work is in progress with reference to transonic flows around airfoils and the results will be presented at the conference. Work is also in progress with reference to a simple subsonic three-dimensional flow case in an elbow duct, using the fast solver technique suggested in /8/ as basic solver, but the authors are not so confident to be able to present the final results at the conference.

References

1. *Ni R.H., "A Multiple Grid Scheme for Solving the Euler Equations", AIAA Journal, Vol. 20, n. 11, 1982, pp. 1565–1571.*
2. *Jameson A., "Numerical Solution of the Euler Equations for Compressible Inviscid Fluids", MAE Rept. 1643, Princeton University, 1984.*
3. *Hall M.G., "Cell-Vertex Multigrid Schemes for Solution of the Euler Equations", Numerical Methods for Fluid Dynamics II, ed. Morton & Baines, Clarendon Press, Oxford, 1985.*
4. *Moretti G., "The Lambda Scheme", Computers and Fluids, Vol 7, 1979, pp. 191–205.*
5. *Dadone A. and Napolitano M., "An Efficient ADI Lambda Formulation", Computers and Fluids, Vol 13, 1985, pp. 383–395.*
6. *Moretti G., "Fast Euler Solver for Steady One-Dimensional Flows", Computers and Fluids, Vol 13, 1985, pp. 61–81.*
7. *Dadone A. and Moretti G., "Fast Euler Solver for Transonic Airfoils", to appear in the AIAA Journal.*
8. *Dadone A., Fortunato B. and Lippolis A., "A Fast Euler Solver for Two and Three Dimensional Internal Flows", Symposium on Physical Aspects of Numerical Gas Dynamics, Farmingdale, NY, August 1987.*
9. *Moretti G., "A Technique for Integrating Two-Dimensional Euler Equations", Computers and Fluids, Vol 15, 1987, pp. 59–75.*
10. *Favini B. and Sabetta F., "On Multigrid Solution of Euler Equations", Symposium on Physical Aspects of Numerical Gas Dynamics, Farmingdale, NY, August 1987.*

HIGHER ORDER KINETIC FLUX VECTOR SPLITTING METHOD FOR EULER EQUATIONS

J. C. Mandal and S. M. Deshpande
Department of Aerospace Engineering
Indian Institute of Science
Bangalore, India

A new upwind scheme called Kinetic Flux Vector Splitting (KFVS) method has been developed for the solution of Euler equations of gas dynamics, which relies on the well known fact that the Euler equations are the moments of Boltzmann equation when the velocity distribution function F is a Maxwellian. Defining the Maxwellian F by

$$F = F(v,I) = (\rho/I_o\sqrt{2\pi RT})\ \exp[(-(v-u)^2/2RT)-I/I_o]$$

and a moment function vector ψ by

$$\psi = [1 \quad v \quad I+v^2/2]^T \ *$$

the moment of the Boltzmann equation

$$< \psi\ ,\ \partial F/\partial t\ +\ v\ \partial F/\partial x\ = 0 >$$

yields the Euler equations in strong conservation law form

$$\partial W/\partial t\ +\ \partial G/\partial x\ = 0$$

Here v is molecular velocity, I is the internal energy variable corresponding to nontranslational degrees of freedom, ρ is mass density, u is fluid velocity, T is temperature, R is the gas constant per unit mass, $I = (3-\gamma)/2RT(\gamma-1)$, γ is the ratio of specific heats, and the inner product $<\psi,F>$ is defined by

$$<\psi,F> = \int_{-\infty}^{+\infty} dv \int_{0}^{\infty} dI\ \psi F$$

$$W = <\psi,F> = [\rho \quad \rho u \quad \rho e]^T$$

$$G = <v\psi\ ,F> = [\rho u \quad p+\rho u^2 \quad (\rho e+p)u]^T$$

In case of one-dimensional unsteady flows, the Maxwellian is split into two parts corresponding to $v>0$ and $v<0$ in order to apply upwind differencing on the split flux derivatives. The splitting essentially amounts to writing the Boltzmann equation in the following form

$$\partial F/\partial t\ +\ [(v+|v|)/2]\ \partial F/\partial x\ +\ [(v-|v|)/2]\ \partial F/\partial x\ = 0 \qquad (1)$$

and then to take the moment of the Courant-Isaacson-Rees(CIR) differenced equation (1). We then obtain the first-order accurate

* T is the transpose of a matrix

KFVS scheme

$$W^{n+1}_j = W^n_j - (\Delta t/\Delta x)[(G^{+n}_j - G^{+n}_{j-1}) + (G^{-n}_{j+1} - G^{-n}_j)] \qquad (2)$$

where

$$G^{\pm} = \langle \psi, [(v \pm |v|)/2]F \rangle$$

and superscript n denotes the time level and subscript j denotes values of variables at the mesh point j.

Now a question may arise whether such splitting which is equivalent to CIR scheme at Boltzmann level will remain upwind after the moments are taken. It is seen that in the flux vector split Euler equations

$$\partial W/\partial t + \partial G^+/\partial x + \partial G^-/\partial x = 0 \qquad (3)$$

the Jacobians $\partial G^+/\partial W$, $\partial G^-/\partial W$ have complex eigenvalues having real positive and real negative parts respectively. This raises a further doubt whether KFVS is truly an upwind scheme. But using the theory given in [1],[2] it can be shown that the kinetic flux vector split Euler equations (3) can be transformed to the following symmetric hyperbolic form

$$P\ \partial q/\partial t + B^+ \partial q/\partial x + B^- \partial q/\partial x = 0 \qquad (4)$$

where q is a transformed vector, P is a positive symmetric matrix, B^+ and B^- are positive and negative matrices respectively. In [2] $P^{-1}B^+$ and $P^{-1}B^-$ have been shown to have respectively real positive and real negative eigenvalues. Since eigenvalues are invariant under such transformations, it is immediately confirmed that the upwinding based on this splitting is justifiable. It is also observed that the eigenvalues show all necessary features such as there are no sonic glitches which are present in Steger and Warming flux splitting[3]. The eigenvalues of $P^{-1}B^-$ (see Fig.1) decrease to very small values as Mach number $M \to 1$ and gradually tend to zero as M becomes increasingly supersonic. While the eigenvalues of $P^{-1}B^+$ (see Fig.2) gradually tends to those of $P^{-1}B$ (see Fig.3) as $M \to 1$. It is interesting to note that though this splitting also leads to split fluxes whose Jacobians (in symmetric hyperbolic form) have positive and negative eigenvalues, it has been perfomed in a completely different manner compared to that of Steger and Warming[4]. Also unlike Steger and Warming's flux splitting the present method is not dependent on the property that nonlinear flux vectors of Euler equations have to be homogeneous functions of degree one in the conserved variable for the splitting to be performed.

First-order KFVS scheme given by (2) can also be cast in the flux difference split form

$$\partial W/\partial t + (G_{j+1/2} - G_{j-1/2})/\Delta x = 0 \qquad (5)$$

where

$$G_{j+1/2} = (G_{j+1} + G_j)/2 + (DG^-_{j+1/2} - DG^+_{j+1/2})/2$$

$$= \text{EFS(Expression for First-order Scheme)} ,$$

and

$$DG^{\pm}_{j+1/2} = \langle \psi, [(v \pm |v|)/2](F_{j+1} - F_j) \rangle$$

Thus extension of the first-order KFVS scheme to higher-order schemes can be done according to the analysis of Chakravarthy and Osher[5], that is, define flux vector $G_{j+1/2}$ at the interface j+1/2 as

$$G_{j+1/2} = EFS + [(1+\phi)(DG^{+}_{j+1/2} - DG^{-}_{j+1/2}) + (1-\phi)(DG^{+}_{j-1/2} - DG^{-}_{j+3/2})]/4 \qquad (6)$$

where, -1 and 1/3 are the corresponding values ϕ for second- and third-order accurate schemes respectively.

As higher-order accurate schemes are known to have wiggles in their solutions, modified differences can be used in (6) to suppress them. These modified differences[5] are given by

$$\tilde{DG}^{\pm}_{j+1/2} = \text{minmod}[\, DG^{\pm}_{j+1/2},\ R \cdot DG^{\pm}_{j-1/2} \,]$$

$$\tilde{\tilde{DG}}^{\pm}_{j+1/2} = \text{minmod}[\, DG^{\pm}_{j+1/2},\ R \cdot DG^{\pm}_{j+3/2} \,]$$

where

$\text{minmod}[a,b] = 0.5[\text{sign}(a)+\text{sign}(b)]\ \min[\,|a|, |b|\,]$ and

$0 \leq R \leq (3-\phi)/(1-\phi)$

The final modified expression for $G_{j+1/2}$ to be used in (4) is

$$G_{j+1/2} = EFS + [(1+\phi)(\tilde{DG}^{+}_{j+1/2} - \tilde{\tilde{DG}}^{-}_{j+1/2}) + (1-\phi)(\tilde{\tilde{DG}}^{+}_{j-1/2} - \tilde{DG}^{-}_{j+3/2})]/4$$

which gives wiggle-free solutions.

Shock-tube problem has been solved using the KFVS schemes. Results of the higher-order accurate schemes with the use of modified differences show progressive improvement over first-order result and have excellent agreement with the exact one (see Fig.4).

REFERENCES :

[1] Deshpande S. M. : On the Maxwellian distribution, symmetric form and the entropy conservation for the Euler equations. NASA TP-2583, 1986.

[2] Deshpande S. M. and Mandal J. C. : Kinetic Flux Vector Splitting(KFVS) for the Euler equation. Fluid Mech. Report No. 87FM2, Dept. of Aerospace Engineering, Indian Institute of Science, Bangalore, April 1987.

[3] Van Leer B. : Flux Vector Splitting for the Euler equations. ICASE Report No.82-30, Sept. 1982.

[4] Steger J. L. and Warming R. F. : Flux Vector Splitting of the inviscid Gasdynamic equations with application to Finite-difference methods. J. Computational Physics, Vol. 40, 1981, 263.

[5] Chakravarthy S. R. and Osher S. : High resolution applications of the Osher upwind scheme for the Euler equations. AIAA Paper No. 83-1943, 1983.

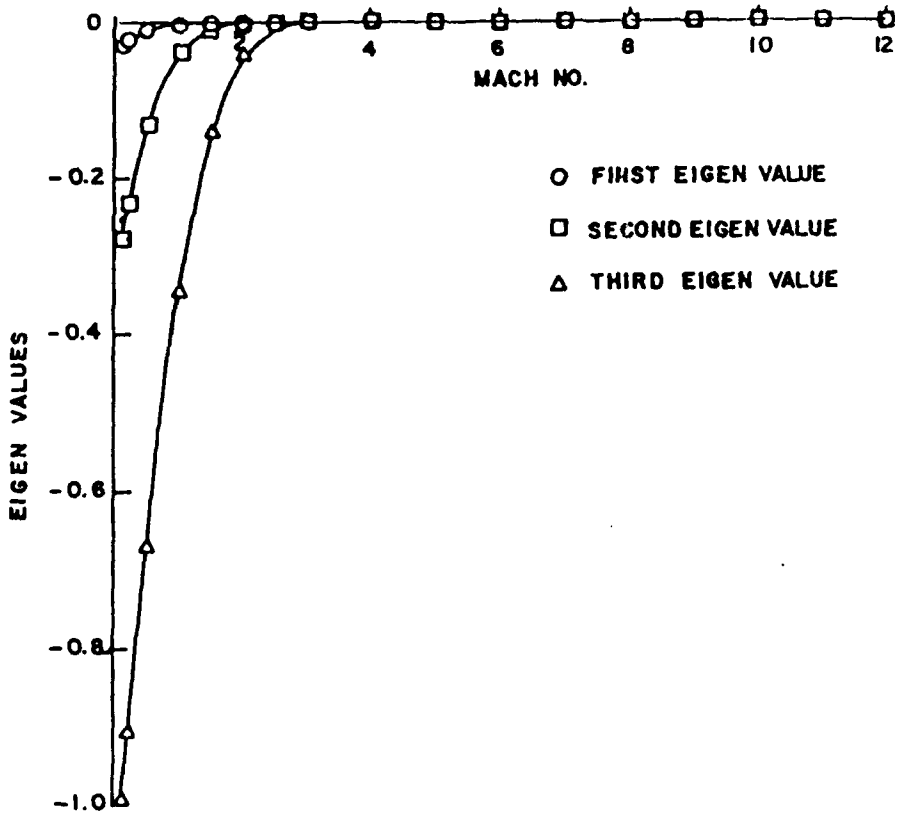

FIG. 1 NORMALIZED (with respect to wave speed) EIGENVALUES OF $P^{-1}B^{-}$ MATRIX

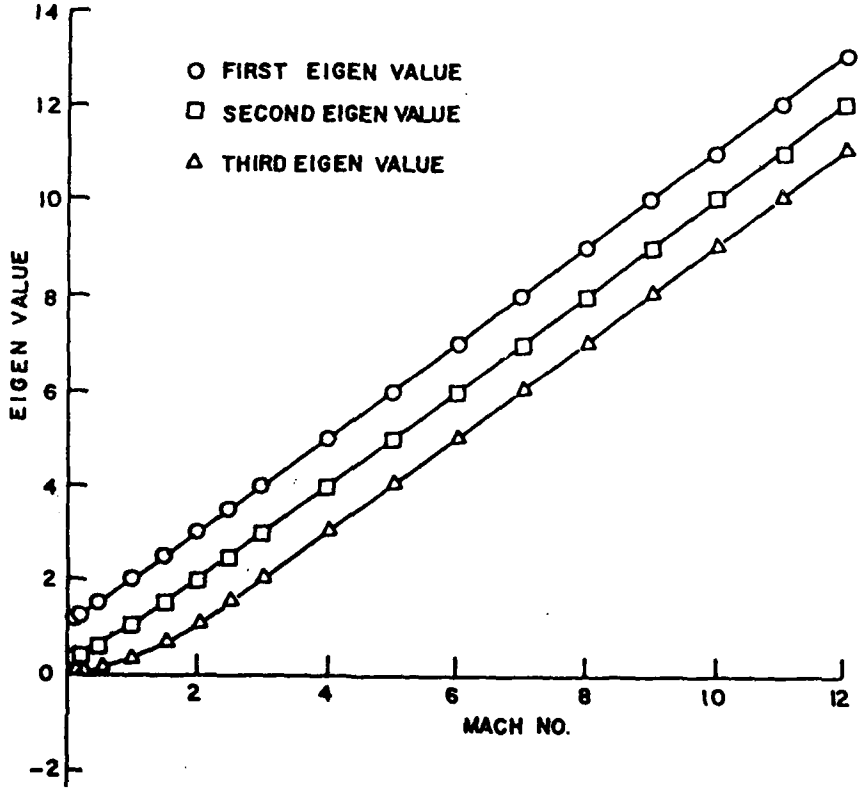

FIG. 2 NORMALIZED (with respect to wave speed) EIGENVALUES OF $P^{-1}B^{+}$ MATRIX

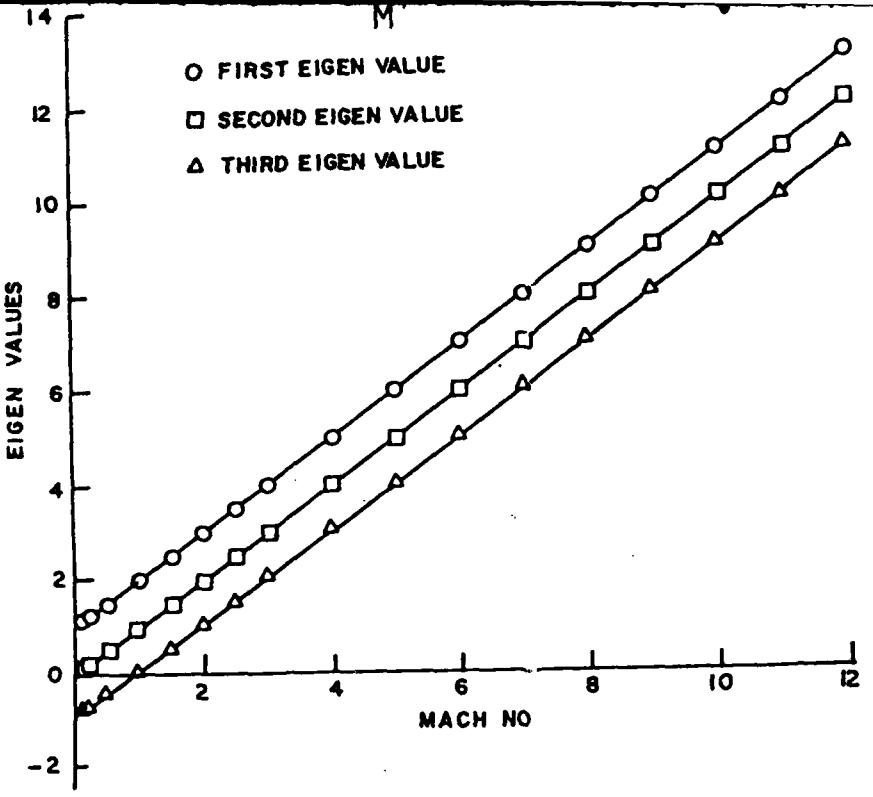

FIG. 3 NORMALIZED (With respect to wave speed) EIGENVALUES OF $P^{-1}B$ MATRIX

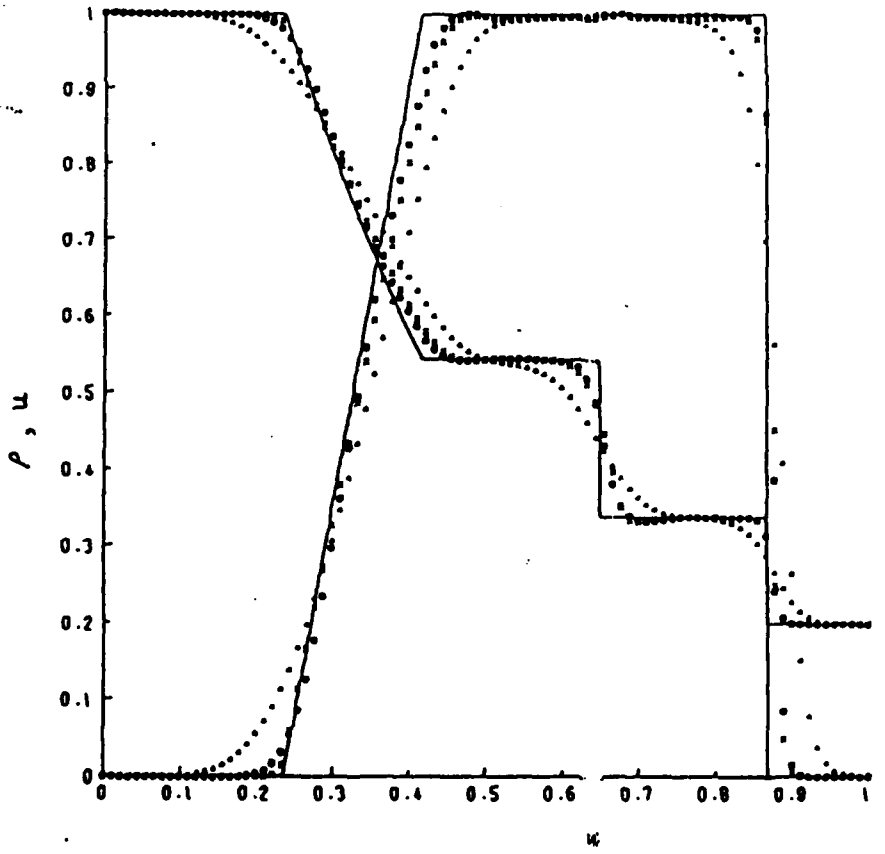

FIG. 4 COMPUTED ρ, u AND EXACT(-) PROFILES FOR SHOCK TUBE PROBLEMS FOR KFVS, FIRST-ORDER(Δ), SECOND-ORDER(x) AND THIRD-ORDER(o), J = 91

RIEMANN PROBLEMS FOR NON-STRICTLY HYPERBOLIC CONSERVATION LAWS

Dan Marchesin

IMPA and PUC

Rio de Janeiro

Brazil

Two essential elements in the classical construction of Lax (1) of the Riemann solution for systems of strictly hyperbolic conservation laws are a local "coordinate system" in state space, and a criterion for the choice of physically meaningful shocks. The local "coordinate system" allows one to construct the solution of the Riemann problem in state space through a succession of wave curves of a given family "i", each one consisting of rarefaction and shock curves. The correct choice of shocks based on entropy consideration is essential to obtain unique solutions; Lax's entropy inequalities may be obtained by allowing only shocks which are limits of traveling waves for the conservation law with small parabolic terms (2).

The above mentioned construction is generic for small data with the proviso that we consider "strictly nonlinear" systems. This theory has been generalized in some directions by Oleinik (3) and Tai Ping Liu. (4)

For a number of years, we have been trying to find the Riemann solution for a 2X2 system of conservation laws, arising from a simplified model for the flow of water, oil and gas in porous media. The importance of such problem has been pointed out in 1941 by Leverett and Lewis. The solution for the two phase problem was found in 1942 in the classical work of Buckley and

Leverett who established the formation of shocks as the mechanism responsible for oil recovery in petroleum reservoirs.

The one dimensional system, which represents the conservation of mass of oil, water and gas with appropriate boundary conditions and neglecting compressibility and capillary pressure effects is

$$\begin{cases} u_t + f(u,v)_x = 0 \\ v_t + g(u,v)_x = 0 \end{cases}$$

with $f = U/D$, $g = V/D$ and $D = U+V+D$.

Here $U = U(u)$, $V = V(v)$, $W = W(w)$ are the "permeabilities" of oil, water and gas, respectively, functions of u, v, w, the saturations of these three fluids.

These are numbers between 0 and 1 which add to 1, so that we take $w = 1-u-v$. Laboratory measurements are consistent with taking $U = u^2/a$, $V = v^2/b$, $W = w^2/c$ where a, b, c are the viscosities of the fluids.

The novel feature of this model is that it has an umbilic point $(a/(a+b+c), b/(a+b+c))$ interior to the region of physical space of interest, where the characteristic speeds are equal.

At this point the jacobian of the system $\begin{pmatrix} f_u & f_v \\ g_u & g_v \end{pmatrix}$ becomes a multiple of the identity and the characteristic directions are indefinite. As a result, the "local coordinate" system does not exist anymore. In fact the rarefaction curves, integrals of the characteristic vectors $\vec{r}i$ in the neighborhood of the umbilic look like the figure.

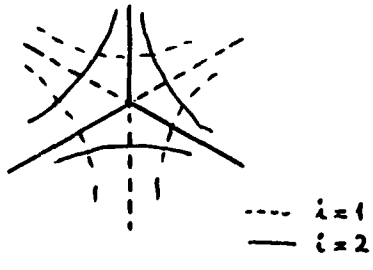

This fact introduces all sort of new difficulties and features. One would think that these problems are peculiar to the model considered. They are not. One can prove that generic perturbations of (f,g) near umbilic points generate compact

"elliptic" regions where the characteristic values are complex (5). In the last work a nice geometrical analysis is presented for the nature of rarefaction curves.

For models in actual use in oil reservoir engineering, the existence of elliptic regions has been established based on numerical studies (6) and topological considerations (7).

The Hugoniot curve, which represent the jump relation afross shocks

$$s\begin{pmatrix} u - u_L \\ v - v_L \end{pmatrix} = \begin{pmatrix} f(u,v) - f(u_L,v_L) \\ g(u,v) - g(u_L,v_L) \end{pmatrix}$$

has new features due to the existence of umbilics:

While its classical shape in the (u,v)plane is

it may have self intersection or disconnected branches.

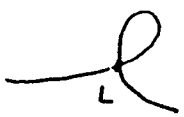

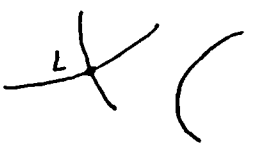

The study of these curves falls naturally in the framework of bifurcation theory. We are currently trying to obtain a global geometric picture describing the Hugoniot curves.

Putting together rarefaction and shock curves possessing these non trivial topological features has been a challenging endeavor in our design of a computer code to solve 2X2 Riemann problems. There are new kinds of wave curves, not associated with any particular family, which we call transition waves.

To insure that we use meaningful shocks, we have used those originating from "viscous profiles", namely traveling wave solutions of type $Z = Z(\frac{x-st}{\epsilon})$, $Z(-\infty) = Z_L$, $Z(+\infty) = Z_R$ of the 2X2 system modified by the addition of a viscous term, due in multiphase flow to capillary pressure effects:

$$Z_t + F(Z)_x = \epsilon(H(Z)Z_x)_x$$

in the limit when ϵ tends to zero.

For $H = I$, this gives rise to the dynamical system

$$\dot{Z} = F(Z) - F(Z_L) - s(Z-Z_L).$$

The existence of a traveling wave solution is equivalent to the existence of an orbit connecting the singularities Z_L, Z_R of the ODE's above. Lax weak shocks are connections between saddles and attractors or repellers (2). We have encountered examples where Lax strong shocks are non admissible. To guarantee existence of Riemann solutions, "crossing shocks", which are saddle-saddle connections are necessary. We believe that other kinds of connections may be relevant. We are investigating spirals occuring within elliptic regions.

An important point is that considering only shocks which are viscous profiles does not guarantee uniqueness of the Riemann solution.

Thus other "entropy conditions" have to be invoked, possibly stability criteria for fronts in two space dimensions. This is one of many issues which remain to be established.

REFERENCES

(1) Lax P.P., "Hyperbolic Systems of Conservation Laws II", Comm. Pure Appl. Math. Vol. X, 537-566, 1957.

(2) Conley C.C., Smaller I.A., "Shock Waves as Limits of Progressive Wave Solutions of Higher Order Equations", Comm. Pure Appl. Math. Vol. XXIV, 459-472, 1971.

(3) Oleinik O.A., "On the Uniqueness of Generalized Solution of Cauchy Problem for Non Linear System of Equations Occuring in Mechanics, Uspeki Mat. Nauk (Russian Math. Surveys) 12, 169-176, 1957.

(4) Liu T.P., "Existence and Uniqueness Theorems for Riemann Problems", Trans. Am. Math. Soc., Vol. 212, 375-382, 1975.

(5) Schaeffer D.C., Shearer M., "Riemann Problem for Non-strictly Hyperbolic 2X2 Systems of Conservation Laws", Appendix Including Isaacson E., Marchesin D., Trans. AMS, to appear.

(6) Bell J.B., Trangenstein J.A., Shubin G.R., "Conservation Laws of Mixed Type Describing Three-Phase Flow in Porous Media", Exxon Production Research, preprint 1985, SIAM J. Appl. Math., to appear.

(7) Shearer M., "Loss of Strict Hyperbolicity in the Buckley-Leverett Equations of Three Phase Flow in a Porous Medium", in Proceeding of IMA Workshop in Oil Reservoir Simulation, ed. M. Wheeler, to appear.

(8) Isaacson E., Marchesin D., Plohr B. and Temple B.. "The Classification of Solutions of Quadratic Riemann Problems(I)" MRC Report #2891, 1985.

A MONTE CARLO FINITE DIFFERENCE SCHEME FOR HYPERBOLIC EQUATIONS

Guillermo Marshall
EPFL, GASOV,
1015 Lausanne, Switzerland.

A probabilistic model related to a differential equation is any procedure which involves the use of sampling devices based in probabilities to approximate its solution. A probabilistic model uses stochastic processes, that is, a sequence of states whose transition is governed by random events.
Stochastic methods for hyperbolic equations can be subdivided into Random Choice Methods (RCM) and Monte Carlo Methods (MCM). The RCM is a numerical technique which in essence consists in sampling local exact solutions of Riemann problems. The RCM was introduced by Chorin, 1976, and is based on a fundamental existence proof due to Glimm, 1965. The main problem with the RCM is the difficulty associated with constructing the Riemann solver. To circumvent it an approximate Riemann solver was introduced by Harten and Lax,1981 and by Cohen and Lavita, 1986, these methods however, are only valid for scalar conservation laws. The advantages of RCM are that they are grid free, unconditionally stable and give high resolution near sharp fronts without over shooting. The MCM is a numerical technique which consists in sampling local exact solutions of finite difference schemes. In the context of this work is somehow located between the RCM and plain deterministic finite difference schemes, in a more general context is an extension of the MCM applied to parabolic and elliptic equations. The idea of the method dates back to Polya, 1938 who introduced a random walk method for an hyperbolic equation studied by Albert Einstein Junior. In this work we generalize the idea of Polya extending the MCM to hyperbolic equations and systems. The MCM shares many of the advantages of the RCM.

We introduce the MCM with a simple example. Consider the hyperbolic equation

$$u_t + F(u)_x = 0, \quad 0 \le x \le 1, \quad t > 0 \qquad (1)$$

with $F(u) = U_0(x)u$, $U_0(x) > 0$, and with initial and boundary conditions: $u(x,0)=g(Q)$, $0\le x\le 1$, $t>0$, $u(x,t)=f(Q)$, $x=0,1$, $t>0$. Discretizing the domain with a rectangular grid of size h and k for the space and time coordinates and denoting a generic node by P_0, and by P_1 and P_2 the corresponding left and right neighbours, a deterministic explicit finite difference analogue of (1) reads

$$u^{n+1}(P_0) = \sum_{i=0}^{i=2} a_i(P_0)\, u^n(P_i) \qquad (2)$$

where the coefficients $a_i(P_0)$ depend on the particular scheme being chosen. For the Lax scheme, for instance, $a_0(P_0)=0$, $a_1(P_0)=(1+p_0/2)$, $a_2(P_0)=(1-p_0/2)$, where $p_0=U_0k/h$. If the CFL condition is satisfied, stability and thus convergence of the method is assured. Similar expressions can be obtained with the Godunov or Wendroff implicit schemes.

We now consider the stochastic model for (1) (stochastic in space, deterministic in time). For this we impose the following restrictions

$$\sum_{i=0}^{i=2} a_i(P_0) = 1 \quad \text{and} \quad a_i(P_0) \geq 0 \tag{3}$$

These restrictions are necessary for probability assignment. We can now associate the set of states S_i of a finite Markov chain with nodes in the domain on which the finite difference is defined, the internal nodes corresponding to transient states and boundary nodes to absorbing states. The coefficients $a_i(P_0)$ of the difference equation (2) can be associated with transition probabilities P_{ij} in the Markov chain. Consider now the following random walk procedure. Let P_0 at time t_{n+1} be the current state of an hypotetical particle and P_i, i=1,2, the next possible states at t_n,reached in the unit time. The transition from P_0 at t_{n+1} to P_i at t_n occurs with probability $a_i(P_0)$ given by (2). This random step process is repeated until a boundary or absorbing state is reached and the corresponding random walk terminates. If $u(P_0,Q_j)$ denotes the probability of ending a random walk at a boundary Q_j having started at P_0, the expectation of the boundary values reached is given by

$$V(P_0) = \sum_{j=1}^{j=s} u(P_0,Q_j)\ f(Q_j) \tag{4}$$

where s is the total number of boundary nodes. It can be shown that $V(P_0)$ satisfies the finite difference equation (2) with boundary conditions given by (1). For estimating $u(P_0,Q_j)$ we simulate N times the random walk starting at P_0 and counting the number of times in which a boundary node Q_j is reached. An approximation of (4) reads

$$V^{n+1}(P_0) \cong \sum_{j=1}^{j=s} n_j/N\ f(Q_j) = 1/N \sum_{j=1}^{j=s} n_j\ f(Q_j) \tag{5}$$

The last summation is the average of all the boundaries reached after N random walks. It can be shown that the expectation of this average is $u(P_0)$ and that by the law of large numbers this average converges to the exact solution of the difference equation (2) for increasing values of N.

The main advantages of the method just described are: the solution at a point can be estimated independently of the solution at other points, the algorithm is extremely simple, it is easily extendable to higher dimensions and the dependency of the computing time on the dimensionality is weak, and it can be solved simultaneously for several set of boundary conditions with almost no extra computing time. The main disadvantages are: it is limited to linear problems for which an associated finite Markov chain can be found (the

matrix of the resulting algebraic system should be a stochastic matrix) and the solution estimate converges slowly to the exact solution. Because of this last statement, the method requires much computing time when implemented in serial computers. Improvements can be made using variance reducing techniques and a floating random walk introduced by Haji-Sheikh and Sparrow, 1966. However, the simplicity and intrinsic parallel properties of the Monte Carlo method is ideally suited for parallel environment arquitectures. At present, the advent of massively parallel processors greatly stimulated the application of Monte Carlo methods, see for instance, Kalos, 1986, or Solum, 1985.

In nonlinear problems the transition probabilities are unknown apriori since they are function of the unknown solution, thus we are forced to estimate the latter to calculate the former. A simple example illustrates the matter. Consider Burgers inviscid equation given by (1) with $f(u)=u^2/2$, $u > 0$, and with appropriate initial and boundary conditions. A consistent explicit finite difference scheme is given by (2)where now for the Godunov scheme, for instance, $a_0(P_0)=1-P_0$, $a_1(P_0)=P_0$, $a_2(P_0)=0$ and $P_0=0.5(u_0^n+u_1^n)k/h$.

For the construction of the stochastic model we proceed in the same way as for the linear case but rather than starting at any position on the grid, the random walk begins at a node P_0 of a time level t_{n+1} for which the solution, at the previous time level and for all grid nodes, is known. Here a random walk consists in one random step since after it a boundary node or absorbing state is inevitably encountered. The Monte Carlo finite difference scheme for (1) is given by

$$u^{n+1}(P_0)=\begin{cases} u^n(P_1) & \text{if} \quad 0 \le \xi_i \le a_1(P_0) \\ u^n(P_0) & \text{if} \quad a_1(P) \le \xi_i \le a_1(P_0)+a_2(P_0) \\ u^n(2) & \text{if} \quad a_1(P_0)+a_2(P_0) \le \xi_i \le 1 \end{cases} \qquad (6)$$

where a point fall at random in the interval [0,1] with coordinate ξ_i picked from a uniform distribution in the range [0,1]. Implicit in this procedure is the fact that the unknown transition probabilities had been estimated using the solution at the previous time level; obviously the solution is calculated for all nodes at each time level.

To reduce the variance we have used the following strategy due to Chorin, 1976. The interval [0,1] is subdivided into m_2 subintervals, ξ_1 is picked in the first subinterval, ξ_2 in the second, etc., ξ_{m_2+1} in the first subinterval, i.e., $\xi_i^* = (\xi_i+\eta_{i+1})/m_2$. The subinterval ordering is obtained with $\eta_{i+1}=(\eta_i+m_1) \bmod m_2$, where m_1, m_2, $m_1<m_2$ are prime integers, $\eta_0<m_2$ and η_0 given. It is clear that since only one ξ_i^* is picked per random walk, after m_2 random walks, m_2 random coordinates ξ_i^* have

been picked and each one on a different subinterval. With this procedure the sequence of samples ξ_i^* reach approximate equidistribution over [0,1] at a faster rate. Numerical experiments show a significant improvent using this technique as compared with the simple previous one.

The Monte Carlo method for systems of hyperbolic equations can be applied in various ways using primitive or characteristic forms. For instance, the shallow water equations in characteristic form are described by (1) where now $f(u)_x = A\, u_x$, $u=(r,s)$, $A=\mathrm{diag}((3r+s)/4,(r+3s)/4)$, r and s are the Riemann invariants, $r=v+2C$, $s=v-2C$, $C=\sqrt{gh}$, v and h are the velocity and height of the water (see details in Marshall and Menendez, 1982). An explicit finite difference scheme is given by (2) where now $u_i=(r_i,s_i)$ and, assuming an upstream scheme and supercritical flow, $a_0(P_0)=I-k/2\ A(P_0)$, $a_1(P_0)=k/2\ A(P_0)$ and $a_2(P_0)=0$.

For obtaining an stochastic matrix similar restrictions as given by (3) but for vectors must be satisfied. Thus a Monte Carlo finite difference scheme for (1) is given by (6) but now taking into account the non scalar character of the algorithm, that is,

$\xi_i=(\xi_{1_i},\xi_{2_i})$ and ξ_1 and ξ_2 are picked from a uniform distribution in the range [0,1].

Stochastic methods for the numerical solution of hyperbolic equations have been analyzed and a new method based on exact solutions of finite difference schemes and sampling techniques has been introduced. The MCM has been applied to the Burgers equation, the Buckley-Leverett equation and to the shallow water equations, using a VAX 780 and a CRAY 1 computer. The preliminary numerical results demonstrating the convergence of the method are encouraging.

REFERENCES

J. S. Cohen and J. A. Lavita, SIAM J. Sci. Stat. Comput., 7, No. 4, 1986, p. 1350.
A. J. Chorin, J. Comput. Phys.,22, 1976, p.517.
J. Glimm, Comm. Pure Appl. Math., 18, 1965, p. 697.
A. Haji-Sheikh and E. M. Sparrow, SIAM J. Appl. Math., 14, 1966, p.370.
A. Harten and P. Lax, SIAM J. Numer. Anal., 18, 1981, p. 289.
M. H. Kalos,Monte Carlo Methods and the Computers of the Future, NYU Ultracomputer Project, Internal Report, 1986.
G. Marshall and A. Menendez, J. Comput. Phys. 44, 1981, p. 167.
G. Polya, Actualites Scientific et Industrielles No.734, Paris, 1938, p. 25.
J. C. Solem, MECA:A Multiprocessor Concept Specialized to Monte Carlo, in Monte Carlo Methods and Applications in Neutronics, Photonics and Statistical Physics, Ed. B. Mercier, Springer, 1985.

A "NATURAL" FLUX SPLITTING METHOD FOR A CLASS OF NON LINEAR HYPERBOLIC PROBLEMS

P.-A. MAZET*, Ph. DELORME**, F. BOURDEL*
Centre d'Etudes et de Recherche de Toulouse, Complexe Aerospatial
2 Avenue Edouard Belin - B.P. 4025, 31055 Toulouse Cedex, France

The systems we are dealing with are non linear, hyperbolic, pluridimensionnal, symmetrizable systems

- m is the number of equations
- n+1 is the time-space dimension :

$i \in \{0,1,\ldots n\}$ and index $i = 0$ means time.

Such a system can be written as :

$$(1) \quad \partial_i f^i(\varphi) = 0 \qquad \text{in the distributional sense}$$

where φ, the so-called entropic variables, are values of functions from R^{n+1} into R^m. It is well known that for any $i \in \{0,\ldots n\}$, there exists a scalar function, S^{i*}, of φ, such that :

$$\text{grad}_\varphi S^{i*}(\varphi) = f^i(\varphi)$$

and

$-S^{o*}(\varphi)$ is strictly convex in φ.

Then : $w = \text{grad}_\varphi S^{o*}(\varphi)$ are the conservative variables ;
we have : $\varphi = \text{grad}_w S^o(w)$
where $S^o(w)$, the Legendre transform of $S^{o*}(\varphi)$, is the Lax entropy of system (1), associated with the fluxes :

$$S^i(w) = w.f^i(\text{grad}_w S^o(w)) - S^{i*}(\text{grad}_w S^o(w))$$

and of course : $f^o(\text{grad}_w S^o(w)) = w$.

One can notice that such a system is fully determinated by the n+1-vector :

$$(S^{o*}(\varphi), \ldots S^{n*}(\varphi))$$

---

*CERT, 2 av. E. Belin, B.P. 4025, 31055 - TOULOUSE CEDEX
**ONERA, B.P. 72, 92322 - CHATILLON CEDEX

or identically by the scalar function :

$$\Sigma^*(\varphi,u) = S^{i*}(\varphi).u_i$$

where $(u_i)_{i=0,\dots n}$ are the components of any unit (time-space) vector u in R^{n+1}.

DEFINITION

We say that system (1) is k-diagonalizable if there exists a regular function k from $E \times R^n$ into R^m, and a scalar convex function L^* such that :

$$\forall u \in R^{n+1} \; : \; \Sigma^*(\varphi,u) = \int_{E \times R^n} L^*(k(\eta,u).\varphi)(u^i u_i) d_\eta \; du_1 \dots du_n$$

(with the convention $u_o = 1$)

Let we define : $\theta : E \times R^n \times R^{n+1} \longrightarrow R$ by

$$\theta(\eta,u,x) = L^{*/}(k(\eta,u).\varphi(x))$$

Then we have :

$$\partial_i f^i(\varphi) = \int_{E \times R^n} k(\eta,u).(u^i \partial_i \theta(\eta,u,x)) \, d\eta \; du_1 \dots du_n$$

and system (1) appears as a k-weighted mean of the scalar linear equation :

$$(2) \quad u^i \partial_i \theta = 0 .$$

The i^{th} scalar entropy flux is given by :

$$\forall x \in R^{n+1} \quad S^i(w(x)) = \int_{E \times R^n} u^i L(\theta) \, d\eta \; du_1 \dots du_n$$

L being the polar function of L^*,
$(L(\theta), u^i L(\theta))$ is of course the vector (entropy, entropy fluxes) for (2).

Some comments can be made :

*) For the linear symmetric system :
$\partial^i A^i \varphi = 0$ with $A^i = P \Lambda^i P^t$ for $i \in \{0,\dots n\}$
Λ^i a diagonal matrix $(\Lambda^0 = I)$

We have only m vectors u and :

(2) $u^i \partial_i \theta = 0$ are the equations verified by the Riemann invariants.

*) For Euler equations for γ-polytropic gases, we have a k-diagonalization with :

$$E = R^+ \quad \text{and} \quad k(\eta,u) = (1,u_1,\ldots u_n, \frac{1}{2} \sum_{i=1}^{n} u_i^2 + \eta^\delta)$$

where $\delta + \frac{n}{2} = \frac{1}{\gamma-1}$

*) The "hidden" statistichal meaning of such a diagonalization leads us to hope that we could find it again in many physical systems.

From a numerical point of view, this allows us to suggest a discretization of system (1) as a k-weighted mean of a discretization of equations (2).

For instance, if we choose the discontinuous Galerkin method to approximate (2), we obtain the following finite element formulation of system (1) :

$$(3)\ \forall\, \Psi_h : \int_{\Omega_e} \partial_i f^i(\varphi_h).\Psi_h + \int_{\partial\Omega_e} \Psi_h(\text{grad}_\varphi\, \Sigma^{*-}(\varphi_h^e,\upsilon)-\text{grad}_\varphi\, \Sigma^{*-}(\varphi_h^d,\upsilon)) = 0$$

where

. the approximation space V_h is componed of functions which are discontinuous across inter-element boundaries,

. Ψ_h is a basis function of V_h,

. $\varphi_h \in V_h$

. υ is the outwards unit normal vector to a time-space element Ω_e,

. φ_h^e , φ_e^d are the exterior and interior values of φ_h on the boundary $\partial\Omega_e$ of Ω_e,

and

$$\Sigma^{*-}(\varphi,\upsilon) = \int_{E \times R^n} \min\,(u^i n_i, 0)\ .\ L^*(k(\eta,u).\varphi)\ d\eta\ .\ du_1 \ldots du_n$$

One can notice that this approximation involves a flux splitting, given by the decomposition of $\Sigma^*(\varphi,\upsilon) = \Sigma^{*-}(\varphi,\upsilon) + \Sigma^{*+}(\varphi,\upsilon)$ into its convex (Σ^{*+}) and concave (Σ^{*-}) parts relatively to φ.

The local convexity in φ of $\Sigma^*(\varphi,\upsilon)$ has very significant interpretations.

For instance, the convexity inequality :

$$\Sigma^*(\varphi^d,\upsilon) - \Sigma^*(\varphi^e,\upsilon) - \text{grad}_\varphi \Sigma^*(\varphi^d,\upsilon).(\varphi^d - \varphi^e) \leq 0$$

can be proved equivalent to the following :

$$S^i(w^e).\upsilon_i - S^i(w^d)\upsilon_i - \text{grad}_w S^o(w^e).(f_e^i - f_d^i).\upsilon_i \leq 0$$

where w^e, w^d, f_e^i, f_d^i are the conservative variables and fluxes associated with φ^e, φ^d.

This latter inequality is very useful in the study of both boundary conditions, and dissipation.

Numerically, we have tested functions Ψ_h constant on every element Ω_e (and discontinuous on the element boundaries).

It has been proved that if $\tilde{\varphi}_h \longrightarrow \varphi$ in some sense (for instance : in $(B.V._{loc})^m$), then φ satisfies both the conservation equations and the entropy inequality.

In the case of Euler equations, the explicitation of $\Sigma^{*-}(\varphi,\upsilon)$ is easy ; an explicit scheme obtained through this approximation has given good results as well in quality as in CPU time.

HYPERSONIC BLUNT BODY COMPUTATIONS INCLUDING REAL GAS EFFECTS

J.-L. Montagné†
ONERA, B.P. 72, 92322 Chatillon Cedex, France

H.C. Yee‡
NASA Ames Research Center, Moffett Field, CA 94035 USA

G.H. Klopfer*
NEAR Inc., Mountain View, CA 94043 USA

and

M. Vinokur**
Sterling Software, Palo Alto, CA 94030 USA

I. Motivation and Objective

The recently developed second-order explicit and implicit total variation diminishing (TVD) shock-capturing methods of the Harten and Yee [1,2], Yee [3,4], and van Leer [5,6] types in conjunction with a generalized Roe's approximate Riemann solver of Vinokur [7] and the generalized flux-vector splittings of Vinokur and Montagné [8] for two-dimensional hypersonic real gas flows are studied. A previous study [9] on one-dimensional unsteady problems indicated that these schemes produce good shock-capturing capability and that the state equation does not have a large effect on the general behavior of these methods for a wide range of flow conditions for equilibrium air. The objective of this paper is to investigate the applicability and shock resolution of these schemes for two-dimensional steady-state equilibrium real gas flows.

The main contribution of this paper is to identify some of the elements and parameters which can affect the convergence rate for high Mach numbers or real gases but have negligible effect for low Mach number cases. In order to investigate these different points, two kinds of flows are considered. The blunt body calculations at Mach number higher than 15 allow significant real gas effects to occur, while the case of an impinging shock provides a test on the treatment of slip surfaces and complex shock structures.

---

†Research Scientist, *Theoretical Aerodynamics Division*, currently on leave as an Ames Associate at NASA Ames Research Center, Moffett Field, CA 94035 USA.

‡Research Scientist, Computational Fluid Dynamics Branch

*Research Scientist

**Principal Analyst

The current study on the shock resolution of the various schemes for two-dimensional steady-state blunt-body computations indicates similar trends as the one dimensional study. The main issue appears to be their relative efficiency. Due to extra evaluations per dimension in the curve fitting between the left and right states in a real gas for the van Leer formulation, additional computation is required for the van Leer type schemes than the Harten and Yee, and Yee types of TVD schemes. Here van Leer type schemes refer to the use of the MUSCL approach in conjunction with Roe type approximate Riemann solver [10] or flux-vector splittings [6,11]. Moreover, for steady-state applications, implicit methods are preferred over explicit methods because of the faster convergence rate. In addition, it is easier to obtain a noniterative linearized implicit operator for the Harten and Yee type schemes than for the van Leer type schemes. For these reasons, the linearized implicit versions of Harten and Yee [12] and Yee [3] are preferred over the van Leer type schemes.

In the following section, the generalized Roe's approximate Riemann solver and flux-vector splittings for real gases are reviewed. Due to space limitation, only the ADI linearized conservative implicit version of the Harten and Yee schemes [12,3] is reviewed here since most of the illustrations are computed with this particular algorithm. The findings concerning the various aspects in improving the convergence rate and numerical examples are discussed in the subsequent sections.

II. Description of the Numerical Algorithm

The conservation laws for the two-dimensional Euler equations can be written in the form

$$\frac{\partial U}{\partial t} + \frac{\partial F(U)}{\partial x} + \frac{\partial G(U)}{\partial y} = 0. \tag{1}$$

where $U = \left[\, \rho,\ m,\ n,\ e \,\right]^T$, $F = \left[\, \rho u,\ mu + p,\ nu,\ eu + pu \,\right]^T$, and $G = \left[\, \rho v,\ mv,\ nv + p,\ ev + pv \,\right]^T$. Here ρ is the density, $m = \rho u$ is the x-component of the momentum per unit volume, $n = \rho v$ is the y-component of the momentum per unit volume, p is the pressure, $e = \rho[\epsilon + \frac{1}{2}(u^2 + v^2)]$ is the total internal energy per unit volume, and ϵ is the specific internal energy.

A generalized coordinate transformation of the form $\xi = \xi(x, y)$ and $\eta = \eta(x, y)$ which maintains the strong conservation-law form of equation (1) is given by

$$\frac{\partial \hat{U}}{\partial t} + \frac{\partial \hat{F}(\hat{U})}{\partial \xi} + \frac{\partial \hat{G}(\hat{U})}{\partial \eta} = 0, \tag{2}$$

where $\hat{U} = U/J$, $\hat{F} = (\xi_x F + \xi_y G)/J$, $\hat{G} = (\eta_x F + \eta_y G)/J$, and $J = \xi_x \eta_y - \xi_y \eta_x$, the Jacobian transformation. Let $A = \partial F/\partial U$ and $B = \partial G/\partial U$. Then the Jacobians $\hat{A} = \partial \hat{F}/\partial \hat{U}$ and $\hat{B} = \partial \hat{G}/\partial \hat{U}$ can be written as

$$\hat{A} = (\xi_x A + \xi_y B) \tag{3a}$$

$$\hat{B} = (\eta_x A + \eta_y B). \tag{3b}$$

2.1. Riemann Solvers

Here the usual approach of applying the one-dimensional scalar TVD schemes via the so called Riemann solvers for each direction in multidimensional nonlinear systems of hyperbolic conservation laws (see for example reference [2]) is used. The eigenvalues and eigenvectors of the Jacobian matrices $\hat{A}$ and $\hat{B}$ are used in approximate Riemann solvers. Given two states whose difference is ΔU, Roe [10] obtained an average $\overline{A}$ in the ξ-direction, for example, satisfying $\Delta \hat{F} = \overline{A} \Delta U$ for a perfect gas.

The generalization by Vinokur [7] for an arbitrary gas involves the pressure derivatives $\chi = (\partial p/\partial \rho)_{\tilde{\epsilon}}$ and $\kappa = (\partial p/\partial \tilde{\epsilon})_{\rho}$, where $\tilde{\epsilon} = \rho\epsilon$. The relation $c^2 = \chi + \kappa h$ then gives the speed of sound, where $h = \epsilon + p/\rho$. Introducing $H = h + (u^2 + v^2)/2$, Vinokur found the same expressions for $\bar{u}, \bar{v}$ and $\bar{H}$ as for the perfect gas, and that $\bar{\chi}$ and $\bar{\kappa}$ must satisfy

$$\bar{\chi}\Delta\rho + \bar{\kappa}\Delta\tilde{\epsilon} = \Delta p. \tag{4}$$

Unique values of $\bar{\chi}$ and $\bar{\kappa}$ are obtained by projecting the arithmetic averages of the values for the two states into this relation (see references [7] and [2] for the exact formulas).

Flux-vector splitting methods divide the flux $\hat{F}$ into several parts, each of which has a Jacobian matrix whose eigenvalues are all of one sign. The approach by Steger and Warming [11] made use of the relation $F = AU$, valid for a perfect gas. Van Leer [6] constructed a different splitting in which the eigenvalues of the split-flux Jacobians are continuous and one of them vanishes leading to sharper capture of transonic shocks. Vinokur and Montagné [8] showed that the expressions for both these splittings can be generalized to an arbitrary gas by using the variable $\gamma = \rho c^2/p$, and adding to the split energy flux a term equal to the product of the split mass flux and the quantity $\epsilon - c^2/[\gamma(\gamma - 1)]$ (see references [8] and [2] for the exact formulas).

2.2 Description of the Implicit TVD schemes

Let Δt be the time step and let the grid spacing be denoted by $\Delta\xi$ and $\Delta\eta$ such that $\xi = j\Delta\xi$ and $\eta = k\Delta\eta$. An implicit second-order in space, first-order in time TVD algorithm in generalized coordinates of Yee and Harten for two-dimensional systems (1) [2-4] can be written as

$$\hat{U}^{n+1}_{j,k} + \frac{\Delta t}{\Delta\xi}\left[\tilde{F}^{n+1}_{j+\frac{1}{2},k} - \tilde{F}^{n+1}_{j-\frac{1}{2},k}\right] + \frac{\Delta t}{\Delta\eta}\left[\tilde{G}^{n+1}_{j,k+\frac{1}{2}} - \tilde{G}^{n+1}_{j,k-\frac{1}{2}}\right] = \hat{U}^{n}_{j,k}. \tag{5}$$

The functions $\tilde{F}_{j+\frac{1}{2},k}$ and $\tilde{G}_{j,k+\frac{1}{2}}$ are the numerical fluxes in the ξ- and η-directions evaluated at $(j+\frac{1}{2},k)$ and $(j,k+\frac{1}{2})$, respectively. Typically, $\tilde{F}_{j+\frac{1}{2},k}$ can be expressed as

$$\tilde{F}_{j+\frac{1}{2},k} = \frac{1}{2}\left(\hat{F}_{j,k} + \hat{F}_{j+1,k} + R_{j+\frac{1}{2}}\Phi_{j+\frac{1}{2}}\right). \tag{6}$$

Here $R_{j+\frac{1}{2}}$ is the eigenvector matrix for $\partial\hat{F}/\partial U$ evaluated at some symmetric average of $U_{j,k}$ and $U_{j+1,k}$ (for example, Roe average [10] for a perfect gas and generalized Roe average of Vinokur [7] for real gases). Similarly, one can define the numerical flux $\tilde{G}_{k+\frac{1}{2}}$ in this manner.

Second-order Symmetric TVD Scheme: The elements of the $\Phi_{j+\frac{1}{2}}$ in the ξ-direction denoted by $(\phi^l_{j+\frac{1}{2}})^S$ for a spatially second-order symmetric TVD scheme [3,4] are

$$(\phi^l_{j+\frac{1}{2}})^S = -\psi(a^l_{j+\frac{1}{2}})\left[\alpha^l_{j+\frac{1}{2}} - \phi^l_{j+\frac{1}{2}}\right]. \tag{7a}$$

The value $a^l_{j+\frac{1}{2}}$ is the characteristic speed a^l for $\partial\hat{F}/\partial U$ evaluated at some average between $U_{j,k}$ and $U_{j+1,k}$. The function ψ is

$$\psi(z) = \begin{cases} |z| & |z| \geq \delta_1 \\ (z^2 + \delta_1^2)/2\delta_1 & |z| < \delta_1 \end{cases}. \tag{7b}$$

Here $\psi(z)$ in equation (7b) is an entropy correction to $|z|$ where δ_1 is a small positive parameter. For steady-state problems containing strong shock waves, a proper control of the size of δ_1 is very

important, especially for hypersonic blunt-body flows. See reference [2] or section III for a discussion. An example of limiter function $\widehat{Q}^l_{j+\frac{1}{2}}$ used in calculations is:

$$\widehat{Q}^l_{j+\frac{1}{2}} = \text{minmod}\left[\alpha^l_{j-\frac{1}{2}}, \alpha^l_{j+\frac{1}{2}}, \alpha^l_{j+\frac{3}{2}}\right]. \tag{7.c}$$

The minmod function of a list of arguments is equal to the smallest number in absolute value if the list of arguments is of the same sign, or is equal to zero if any arguments are of opposite sign. Here $\alpha^l_{j+\frac{1}{2}}$ are elements of

$$\alpha_{j+\frac{1}{2}} = R^{-1}_{j+\frac{1}{2}}(U_{j+1,k} - U_{j,k}). \tag{8}$$

Second-Order Upwind TVD Scheme: The elements of the $\Phi_{j+\frac{1}{2}}$ in the ξ-direction denoted by $(\phi^l_{j+\frac{1}{2}})^U$ for a spatially second-order upwind TVD scheme [12,2] are

$$(\phi^l_{j+\frac{1}{2}})^U = \frac{1}{2}\psi(a^l_{j+\frac{1}{2}})(g^l_{j+1} + g^l_j) - \psi(a^l_{j+\frac{1}{2}} + \gamma^l_{j+\frac{1}{2}})\alpha^l_{j+\frac{1}{2}}. \tag{9a}$$

where

$$\gamma^l_{j+\frac{1}{2}} = \sigma(a^l_{j+\frac{1}{2}}) \begin{cases} (g^l_{j+1} - g^l_j)/\alpha^l_{j+\frac{1}{2}} & \alpha^l_{j+\frac{1}{2}} \neq 0 \\ 0 & \alpha^l_{j+\frac{1}{2}} = 0 \end{cases}. \tag{9b}$$

An example of limiter function g^l_j used in calculations is

$$g^l_j = \text{minmod}\left[\alpha^l_{j-\frac{1}{2}}, \alpha^l_{j+\frac{1}{2}}\right]. \tag{9c}$$

A Conservative Linearized ADI Form for Steady-State Applications: A conservative linearized ADI form of equation (5) used mainly for steady-state applications as described in detail in references [3,12], can be written as

$$\left[I + \frac{\Delta t}{\Delta\xi}H^{\xi}_{j+\frac{1}{2},k} - \frac{\Delta t}{\Delta\xi}H^{\xi}_{j-\frac{1}{2},k}\right]E^* = -\frac{\Delta t}{\Delta\xi}\left[\tilde{F}^n_{j+\frac{1}{2},k} - \tilde{F}^n_{j-\frac{1}{2},k}\right] - \frac{\Delta t}{\Delta\eta}\left[\tilde{G}^n_{j,k+\frac{1}{2}} - \tilde{G}^n_{j,k-\frac{1}{2}}\right], \tag{10a}$$

$$\left[I + \frac{\Delta t}{\Delta\eta}H^{\eta}_{j,k+\frac{1}{2}} - \frac{\Delta t}{\Delta\eta}H^{\eta}_{j,k-\frac{1}{2}}\right]U = E^*, \tag{10b}$$

$$\widehat{U}^{n+1} = U^n + E, \tag{10c}$$

where

$$H^{\xi}_{j+\frac{1}{2},k} = \frac{1}{2}\left[\widehat{A}_{j+1,k} - \Omega^{\xi}_{j+\frac{1}{2},k}\right]^n, \tag{10d}$$

$$H^{\eta}_{j,k+\frac{1}{2}} = \frac{1}{2}\left[\widehat{B}_{j,k+1} - \Omega^{\eta}_{j,k+\frac{1}{2}}\right]^n. \tag{10e}$$

The nonstandard notation

$$H^{\xi}_{j+\frac{1}{2},k}E^* = \frac{1}{2}\left[\widehat{A}^n_{j+1,k}E^*_{j+1,k} - \Omega^{\xi}_{j+\frac{1}{2},k}E^*\right]^n \tag{10f}$$

is used, and $\Omega^{\xi}_{j+\frac{1}{2},k}$, $\Omega^{\eta}_{j,k+\frac{1}{2}}$, can be taken as

$$\Omega^{\xi}_{j+\frac{1}{2},k} E^{*} = R_{j+\frac{1}{2},k}\,\mathrm{diag}\left[\psi(a^{l}_{j+\frac{1}{2}})\right] R^{-1}_{j+\frac{1}{2},k}\,(E^{*}_{j+1,k} - E^{*}_{j,k}) \tag{10g}$$

$$\Omega^{\eta}_{j,k+\frac{1}{2}} E = R_{j,k+\frac{1}{2}}\,\mathrm{diag}\left[\psi(a^{l}_{k+\frac{1}{2}})\right] R^{-1}_{j,k+\frac{1}{2}}\,(E_{j,k+1} - E_{j,k}). \tag{10h}$$

Here $\widehat{A}_{j+1,k}$ and $\widehat{B}_{j,k+1}$ are (3) evaluated at $(j+1,k)$ and $(j,k+1)$, respectively. The nonconservative linearized implicit form suitable for steady-state calculations [2] is also considered. Numerical study indicated that the latter form appears to be slightly less efficient in terms of convergence rate than the linearized conservative form.

III. Enhancement of Convergence Rate for Hypersonic Flows

The current study indicated that the following three elements can affect the convergence rate at hypersonic speeds: (a) the choice of the entropy correction parameter δ_1, (b) the choice of the dependent variables on which the limiters are applied, and (c) the prevention of unphysical solution during the initial transient stage.

(a). For blunt-body steady-state flows with $M > 4$, the initial flow conditions at the wall are obtained using the known wall temperature in conjunction with pressures computed from a modified Newtonian expression. Also, for implicit methods, a slow startup procedure from free stream boundary conditions is necessary. Most importantly, it is advisable to use δ_1 in equation (7b) as a function of the velocity and sound speed. In particular

$$(\delta_1)_{j+\frac{1}{2}} = \tilde{\delta}(|u_{j+\frac{1}{2}}| + |v_{j+\frac{1}{2}}| + c_{j+\frac{1}{2}}) \tag{11a}$$

$$(\delta_1)_{k+\frac{1}{2}} = \tilde{\delta}(|u_{k+\frac{1}{2}}| + |v_{k+\frac{1}{2}}| + c_{k+\frac{1}{2}}) \tag{11b}$$

with $0.05 \le \tilde{\delta} \le 0.25$ appears to be sufficient for the blunt-body flows for $4 \le M \le 25$. Equation (11) is written in Cartesian coordinates. In the case of generalized coordinates, the u and v should be replaced by the contravariant velocity components, and one half of the sound speed would be from the ξ-direction and the other half would be from the η direction. For implicit methods, it is very important to use (11) in $\psi(z)$ on both the implicit and explicit operators. For the implicit operator, numerical experiments showed that the linearized conservative form (10) converges slightly faster than the linearized nonconservative form [12]. It seems also that when the freestream Mach number increases, the convergence rate of the linearized conservative form (10) is slightly better than a simplified version which replaces $\Omega^{\xi}_{j+\frac{1}{2},k}$ and $\Omega^{\eta}_{j,k+\frac{1}{2}}$ of (10g,h) by $\max_l \psi(a^{l}_{j+\frac{1}{2}})$ and $\max_l \psi(a^{l}_{k+\frac{1}{2}})$ times the identity matrix.

(b). Higher-order TVD schemes in general involve limiter functions. However, there are options in choosing the types of dependent variables in applying limiters for system cases, in particular for systems in generalized coordinates. The choice of the dependent variables on which limiters are applied can affect the convergence process. This point will be addressed more fully in the final paper. In particular, due to the nonuniqueness of the eigenvectors $R_{j+\frac{1}{2}}$, the choice of the characteristic variables on which the limiters are applied play an important role in the convergence rate as the Mach number increases. For moderate Mach numbers, the different choice of the eigenvectors have negligible affect on the convergence rate. However, for large Mach number cases, the magnitudes of all the variables at the jump of the bow shock are not the same. In general, the jumps are much larger for the pressures than for the densities or total energy. Studies indicated that employing the

form $R_{j+\frac{1}{2}}$ such that the variation of the α are of the same order of magnitude as for the pressure would be a good choice for hypersonic flows. The form similar to the one used by Gnoffo [13] or Roe and Pike [ ] can improve the convergence rate over the ones used in references [4,15].

(c). Due to the large gradients and to the fact that the initial conditions are far from the steady-state physical solution, the path used by the implicit method can go through states with negative pressures if a large time step is employed. A convenient way to overcome the difficulties is to fix a minimum allowed value for the density and the pressure. With this safety check, the scheme allows a much larger time step and converges several times faster.

IV. Numerical Results

Resolution of First- and Second-Order schemes: For problems containing complex shock structures, first-order upwind TVD schemes are too diffusive unless extremely fine grids are used. For a blunt-body flow containing a single steady bow shock only, the shock-capturing capability of a first-order upwind TVD schemes seems to be quite adequate if one is interested in the shock resolution only. However, a careful examination of the overall flow field of the density and Mach number contours of the first- and second-order TVD schemes compared with the exact solution reveals the inaccuracy of the first-order scheme. Figure 1 compares the resolution of the first-order (setting $g_j^l = 0$) and second-order upwind TVD schemes (10) using the Roe approximate Riemann solver [10], with the "exact solution" for a perfect gas ($\gamma = 1.4$) at a freestream Mach number of 10. The computations are performed on a 61 x 33 adapted grid for the full (half) cylinder, which yields a fairly good bow shock resolution by both schemes. However, the contour levels near the body are significantly shifted with the first-order scheme, while the second-order scheme reproduces almost identical results as the exact solution.

Convergence Rate of Explicit and Implicit TVD Schemes at Hypersonic Speed: The five different second-order TVD methods previously studied [9] in one dimension yield very similar shock-resolution for the blunt-body problem. In particular, for an inviscid blunt-body flow in the hypersonic equilibrium real gas range, the explicit second-order Harten and Yee, and Yee-Roe-Davis type TVD schemes [2-4] using the generalized approximate Riemann solver [7] produce similar shock-resolution but converge slightly faster than an explicit second-order van Leer type scheme using the generalized van Leer flux-vector splitting [8].

The freestream conditions for the current study are M_∞ = 15 and 25, $p_\infty = 1.22 \times 10^3\ N/m^2$, $\rho_\infty = 1.88^{-2}\ kg/m^3$, and $T_\infty = 226°K$. The grid size is 61 x 33 for the full (half) cylinder (figure 2). For the $M_\infty = 25$ case, the shock stand off distance is at approximately fourteen points from the wall on the symmetry axis. The relaxation procedure for the explicit methods employs a second-order Runge-Kutta time-discretization with a CFL of 0.5. The parameter $\tilde{\delta}$ is set to a constant value of 0.15. Pressure and Mach number contours converge and stabilize after 3000-4000 steps but the convergence rate is much slower for the density (with a 2-3 order of magnitude drop in L_2-norm residual). The bow shock is captured in two to three grid points. The curve fits of Srinivasan et al. [16] are used to generate the thermodynamic properties of the gas.

The same flow condition was tested on the implicit scheme (10). The convergence rate is many times faster. Figures (3) and (4) show the Mach number, density, pressure and κ contours computed by the linearized conservative ADI form of the upwind scheme (10) for Mach numbers 15 and 25. Figure 5 shows the slight advantage of the convergence rate of the linearized conservative implicit TVD scheme (10) over the linearized nonconservative implicit TVD scheme suggested in reference [12]. The convergence rate and shock resolution for the symmetric TVD scheme (10,7) behave

similarly. For $M_\infty = 15$ case, the L_2-norm residual stagnated after a drop of four orders of magnitude. In general, for a perfect gas with $10 \leq M_\infty \leq 25$ and not highly clustered grid, steady-state solutions can be reached in 800 steps with 12 orders of magnitude drop in the L_2-norm residual. However, the convergence rate is at least twice as slow for the real gas counter part. An important observation for the behavior of the convergence rate for the Mach 15 real gas case is that the discontinuities of the thermodynamic derivatives exist in the curve fits of Srinivasan et al. [16] might be the major contributing factor. This is evident from figures (3d) and (4d) and from comparing with the convergence rate for the perfect gas result.

Computations of impinging shocks: Figure (6) shows the Mach contours computed by the implicit upwind TVD scheme (10) of an inviscid shock on shock interaction on a blunt cowl lip in the low hypersonic range. Extensive study on flow fields of this type were reported in references [17-19] for the viscous case. This flow field is typical of what will be experienced by the inlet cowl of the National Aerospace Plane (NASP). The freestream conditions for this flow field are $M_\infty = 4.6$, $p_\infty = 14.93\ \mathrm{N}/m^2$, $T_\infty = 167°\mathrm{K}$, $T_w = 556°\mathrm{K}$, and $\gamma = 1.4$ for a perfect gas. An oblique shock with an angle of 20.9° relative to the free stream impinges on the bow shock. Various types of interactions occur depending on where the impingement point is located on the bow shock. As shown by the Mach contours, the impinging shock has caused the stagnation point to be moved away from its undisturbed location at the symmetry line. The surface pressures at the new stagnation point can be several times larger than those at the undisturbed location of the stagnation point. In addition, a slip surface emanates from the bow shock and impinging shock intersection point and is intercepted by a shock wave which starts at the upper kink of the bow shock. The interacting shock waves and slip surfaces are confined to a very small region and must be captured accurately by the numerical scheme if the proper surface pressures and heat transfer rates are to be predicted correctly. The 77×77 grid used and the convergence rate computed by the implicit scheme (10) are shown in figure (6). Though the pattern of the flow is significantly more complicated than for the previous cases, the convergence rate remains quite satisfactory.

IV. Concluding Remarks

Some numerical aspects of the TVD schemes that can affect the convergence rate for hypersonic Mach numbers or real gas flows but have negligible effect on low Mach number or perfect gas flows are identified. Improvements have been made to the various TVD algorithms to speed up the convergence rate in the hypersonic flow regime. Even with the improvement though, the convergence is in general slightly slower for the real gas than for the perfect gas. The nonsmoothness in the curve fits of Srinivasan et al. may be a major contributing factor in slowing down the convergence rate. Due to extra evaluations per dimension in the curve fitting between the left and right states in a real gas for the van Leer formulation, more computation is required for the van Leer type schemes than for the Harten and Yee, and Yee types of TVD schemes.

Aside from the difference in convergence rate, the numerical results confirm the findings of the one dimensional study. The different methods yield very similar shock-resolution on the blunt body problem with freestream Mach numbers up to 25, and the state equation does not have a large effect on the general behavior of these methods. Further improvements on the ADI relaxation algorithm could speed up the convergence rate even more.

References

[1] A. Harten, On a Class of High Resolution Total-Variation-Stable Finite-Difference Schemes,

SIAM J. Num. Anal, **21**, 1-23 (1984).

[2] H.C. Yee, Upwind and Symmetric Shock-Capturing Schemes, NASA TM-89464, May 1987; also to appear, proceedings of the "Seminar on Computational Aerodynamics," Dept. Mech. Engin., University of Calif., Davis, Spring Quarter, 1986.

[3] H.C. Yee, Construction of Explicit and Implicit Symmetric TVD Schemes and Their Applications, J. Comput. Phys., **68**, 151-179 (1987); also NASA TM-86775, July 1985.

[4] H.C. Yee, Numerical Experiments with a Symmetric High-Resolution Shock-Capturing Scheme, Proc. 10th Int. Conf. on Numerical Methods in Fluid Dynamics, June 1986, Beijing, China; also NASA TM-88325, June 1986.

[5] B. van Leer, Towards the Ultimate Conservation Difference Scheme V, A Second-Order Sequel to Godunov's Method, J. Comp. Phys., **32**, 101-136 (1979).

[6] B. van Leer, Flux-Vector Splitting for the Euler Equations, ICASE Report 82-30; Sept., 1982.

[7] M. Vinokur, Generalized Roe Averaging for Real Gas, NASA Contractor Report, in preparation.

[8] M. Vinokur and J.-L. Montagné, Generalized Flux-Vector Splitting for an Equilibrium Gas, NASA contractor report, in preparation.

[9] J.-L. Montagné, H.C. Yee and M. Vinokur, Comparative Study of High-Resolution Shock-Capturing Schemes for Real Gas, NASA TM-86839, July 1987.

[10] P.L. Roe, Approximate Riemann Solvers, Parameter Vectors, and Difference Schemes, J. Comp. Phys., **43**, 357-372 (1981).

[11] J.L. Steger and R.F. Warming, Flux-Vector Splitting of the Inviscid Gasdynamic Equations with Application to Finite Difference Methods, J. Comput. Phys., 40, 263-293 (1981).

[12] H.C. Yee, Linearized Form of Implicit TVD Schemes for Multidimensional Euler and Navier-Stokes Equations, Computers and Mathematics with Applications, **12A**, 413-432 (1986).

[13] P.A. Gnoffo, R.S. McCandless and H.C. Yee, Enhancements to Program LAURA for Efficient Computation of Three-Dimensional Hypersonic Flow, AIAA Paper 87-0280, Jan. 1987.

[14] P.L. Roe and J. Pike, Efficient Construction and Utilisation of Approximate Riemann Solutions, Computing Methods in Applied Sciences and Engineering, ed. R. Glowinski, North-Holland, Amsterdam, J.-L. Lions, 499-518 (1984).

[15] S. Chakravathy and K.Y. Szema, An Euler Solver for Three-Dimensional Supersonic Flows with Subsonic Pockets, AIAA Paper 85-1703, June 1985.

[16] S. Srinivasan, J.C. Tannehill, K.J. Weilmunster, Simplified Curve Fit for the Thermodynamic Properties of Equilibrium Air, ISU-ERI-Ames 86401; ERI Project 1626; CFD15.

[17] T.L. Holst and J.C. Tannehill, "Numerical Computation of Three-Dimensional Viscous Blunt Body Flow Fields with an Impinging Shock," ERI Rept. 75169, 1975, Iowa State University, Ames, Iowa.

[18] J.C. Tannehill, T.L. Holst and J.V. Rakich, "Numerical Computation of Two-Dimensional Viscous Blunt Body Flows with an Impinging Shock," AIAA J., Vol. 14, No. 2, 1976, pp. 204-211.

[19] J.C. Tannehill, T.L. Holst and J.V. Rakich, "Comparison of a Two-Dimensional Shock Impingement Computation with Experiment," AIAA J., Vol. 14, No. 4, 1976, pp. 539-541.

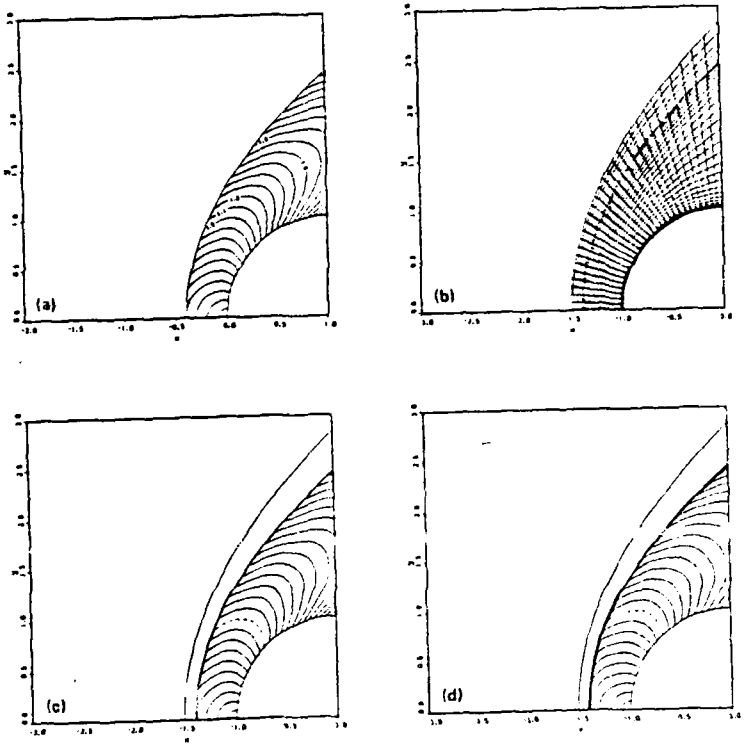

Fig. 1 Comparison among the Mach contours of a second-order implicit upwind TVD scheme (c), a first-order TVD scheme (d) and the shock fitting "exact" solution (a) using the adapted grid (b) for a perfect gas at $M_\infty = 10$.

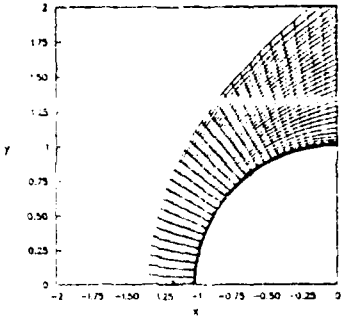

Fig. 2 The 31 × 33 grid.

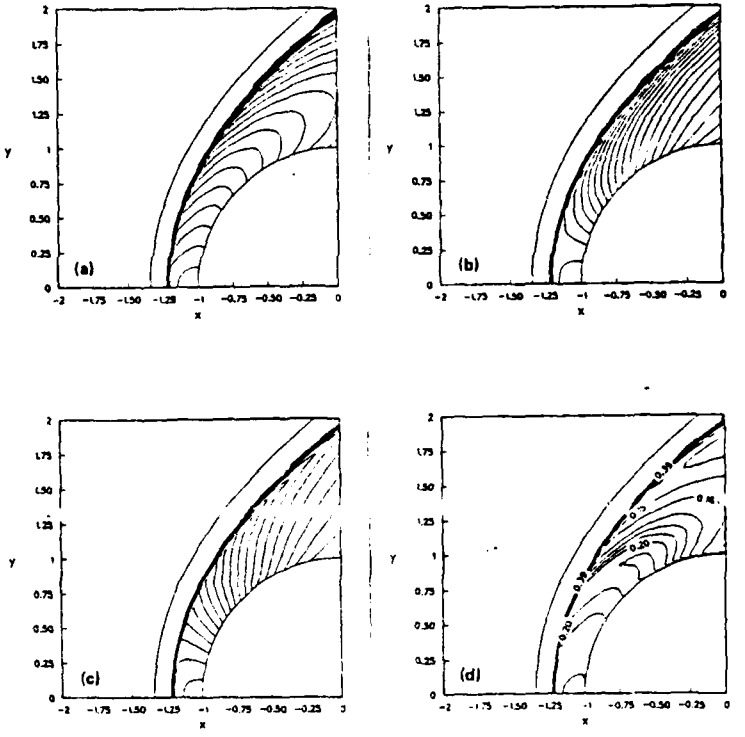

Fig. 3 The Mach contours (a), density contours (b), pressure contours (c) and κ (d) computed by a second-order implicit TVD scheme for an equilibrium real gas at $M_\infty = 15$.

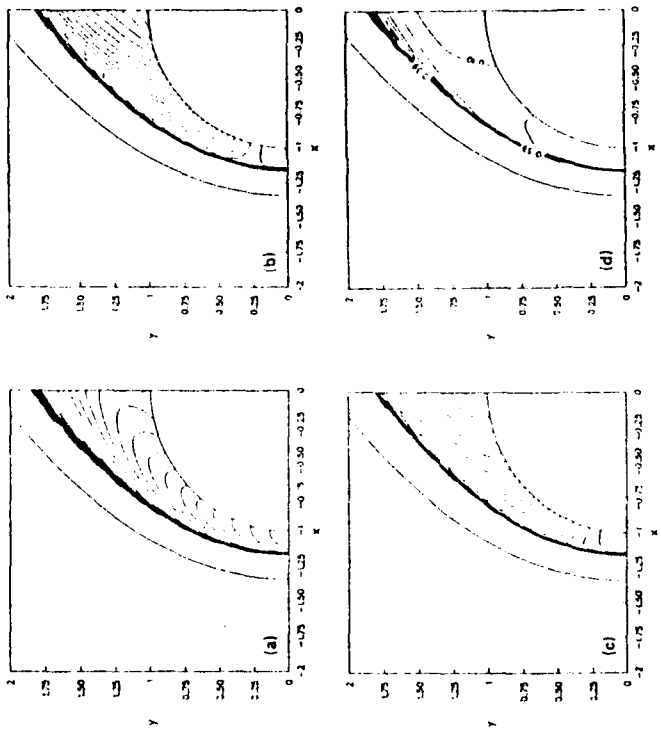

Fig. 4 The Mach contours (a), density contours (b), pressure contours (c) and κ (d) computed by a second-order implicit TVD scheme for an equilibrium real gas at $M_\infty = 25$.

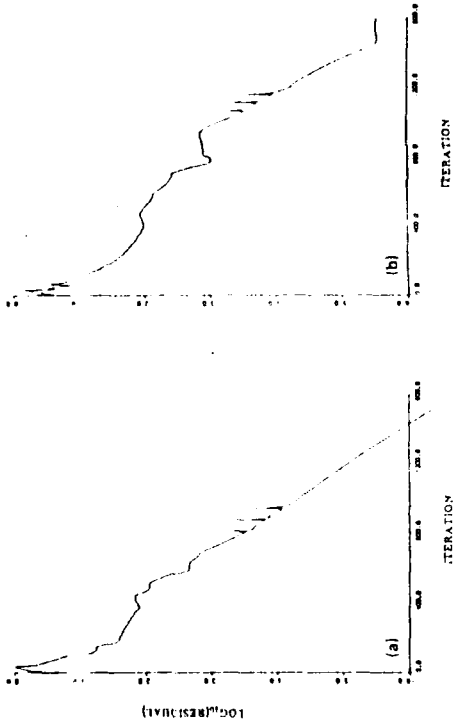

Fig. 5 Comparison of the L_2-norm residual of a linearized conservative implicit operator (a) and a linearized nonconservative implicit operator (b) for an equilibrium real gas at $M_\infty = 25$.

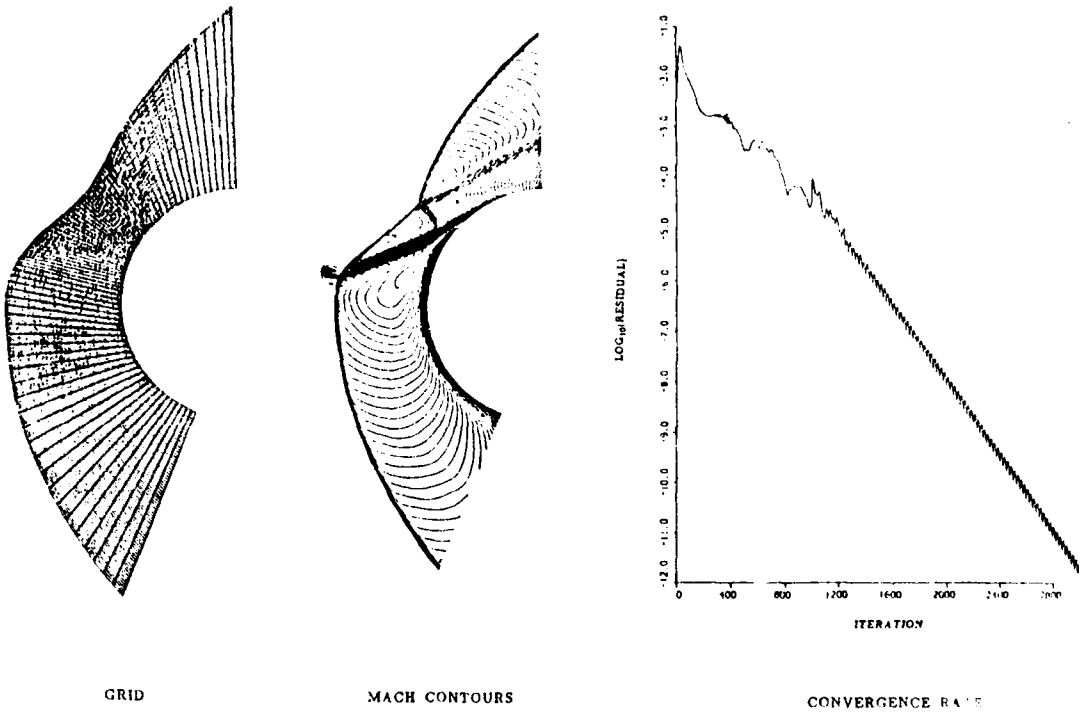

GRID MACH CONTOURS CONVERGENCE RATE

Fig. 6 Two-dimensional inviscid blunt-body flow computed by a second-order implicit scheme for a perfect gas at $M_\infty = 4.6$.

M

AIRFOIL CALCULATIONS IN CARTESIAN GRIDS

Gino Moretti
G.M.A.F., Inc., Freeport, NY, USA
and
Andrea Dadone
University of Bari, Italy

Numerical analysis of Euler equations is generally performed using computational grids which are chosen to be as close to orthogonal as possible, and to have all rigid boundaries on grid lines. Orthogonality of the grid enhances accuracy. The handling of boundary conditions is simplified if boundaries coincide with grid lines.

Generation of suitable grids, however, becomes a major problem when the geometry of the bodies is complicated, when there are many bodies in the field, and in three-dimensional problems.

In the light of recent improvements, both in computing machines and in numerical techniques, the importance of a choice of a grid can be challenged and the possibility of using a Cartesian grid all throughout has already been explored. Successful attempts have been made using a finite volume method as the basic integration technique [1]. Here we present and discuss results obtained using the λ-scheme and shock-fitting. The reason for our attempt is that the latter technique has been proved to be accurate and efficient in all cases analyzed so far and we want to see whether its good qualities can be retained when a Cartesian grid is used to compute the flow about an arbitrary body.

In all problems, the boundary condition on rigid bodies determines the entire flow field. Accuracy in enforcing such a condition is crucial. In using upwind schemes, particularly the λ-scheme, on an orthogonal grid wrapped around a body, the procedure does not introduce arbitrary elements; accuracy is not impaired. The crucial problem of our new attempt consists of maintaining spirit and accuracy of the above approach. We focus our attention on all grid points in the immediate vicinity of the body (such as points A, B, and C in Fig. 1). The boundary condition is easily enforced at A and B. At point A, according to the rules of the λ-scheme, there is only one quantity which cannot be evaluated from grid values, i.e. the forward difference approximating one of the x-derivatives. Similarly, at point B, only the backward difference approximating one of the y-derivatives cannot be evaluated. In either case, however, one boundary condition is available, i.e. the direction of the velocity vector at point D or point E. To use such a condition at A or B, the direction of the velocity vector at A or B is interpolated from F or G (where it has been computed) and D or E. At C, where

none of the two above differences is computable, arbitrariness seems to be unavoidable, but there are ways to circumvent the difficulty. In brief, one has to express derivatives in the directions normal and tangential to the body as functions of derivatives along Cartesian lines, without violating the domains of dependence. This can be accomplished in different ways, two of which have been explored in the present work.

As a side issue, in view of extensions to complicated geometries and three-dimensional flows, we use a number of rectangular regions, of increasing sizes, contained inside one another. One of the regions contains the rigid body. For example, in the airfoil calculation we use a maximum of four regions, as shown in Fig. 2. Each region is covered by a Cartesian grid. The fineness of the mesh varies from region to region, increasing toward the body. In going from one region to the surrounding one, the mesh intervals can be doubled, tripled or quadrupled.

In each region, the basic calculation is performed according to the λ-scheme [2] in Cartesian coordinates. The coding is obviously simpler and faster than with any other coordinate system; it is also more accurate, due to the absence of Christoffel symbols. Vectorization of the computation is straightforward. Accuracy is enhanced by using the COIN (Compressible Over INcompressible) technique [3,4].

Matching of regions is performed as follows (Fig. 3). Rows of values used in the λ-scheme (Riemann variables) are linearly interpolated along AB and CD from the outer (coarse) mesh, and used to generate certain normal derivatives along EF and FG, when needed. The integration of the inner region is performed including the lines EF and FG, but not along AB, CD. The values in the outer region along EF and FG are transferred from the inner region. This procedure is correct for a first-order accurate calculation. If a two-level scheme is used (to achieve second-order accuracy), some additional manipulation is needed, which we will not outline here.

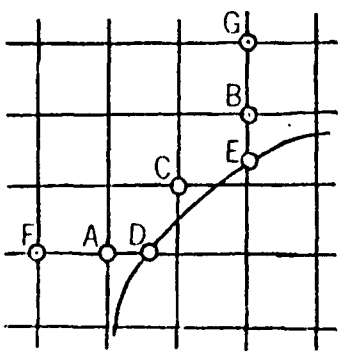

Fig. 1

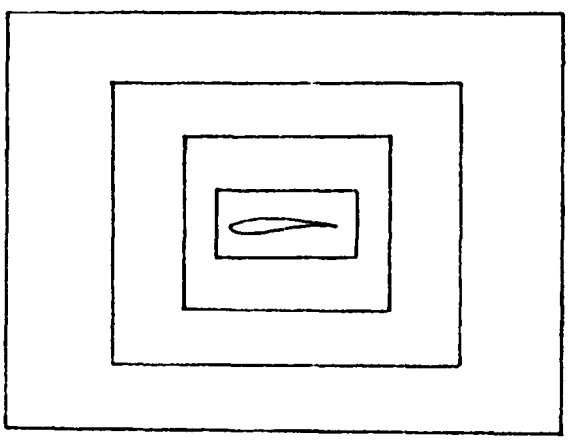

Fig. 2

We ran preliminary tests for a circle. The circle is centered in a square, the side of which is twice the diameter of the circle. This square, in turn, is contained within another square, the side of which is 12 times the diameter. The inner square is covered by a 30x30 mesh, the outer square by a 60x60 mesh. Both meshes are Cartesian, with equal spacing in x and y. The spacing in the outer mesh is three times the spacing in the inner mesh. The Mach number at infinity is 0.4. At convergence, the maximum Mach number is 0.989. This result compares well with results obtained by other Authors [5]. It is important to note that the total number of points on the circle is only 44. A plot of isobars is presented in Fig. 4.

Calculations have been made for a NACA 0012 profile, and results for the case of free stream Mach number equal to .72 at no incidence are presented. Four grids have been used, testing effects of different mesh sizes and different overall sizes. The results shown in Figs. 5 (isobar plot in the innermost region), 6 (Mach number distribution on the profile), and 7 (C_p distribution on the profile) prove that an accuracy comparable with that of the most reliable codes can be reached. Indeed, the mesh used around the body is still coarse in the leading edge region, when compared with current C-grids or O-grids. A fair comparison can be made between the present results and results obtained using our fast solver code [4] with a 64x16 mesh; they are identical.

We intend to present calculations of transonic flows past airfoils at the meeting. Such calculations are made by combining the present technique with the shock-fitting subroutine of [4].

References

1. Clarke, D.K. et al., Euler calculations for multielement airfoils using Cartesian grids, AIAA J. 24:353-58, 1986
2. Moretti, G., A technique for integrating two-dimensional Euler equations, Comp.Fl., 15:59-75, 1987
3. Dadone, A., A quasi-conservative COIN lambda formulation, Lect. Notes in Phys. 264:200-4, 1986
4. Dadone, A. and Moretti, G., Fast Euler solver for transonic airfoils, to appear in the AIAA J.
5. Salas, M.D., Recent developments in transonic Euler flow over a circular cylinder, Math. and Comp. in Simulation XXV:232-6, 1983.

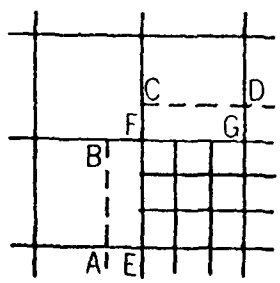

Fig. 3

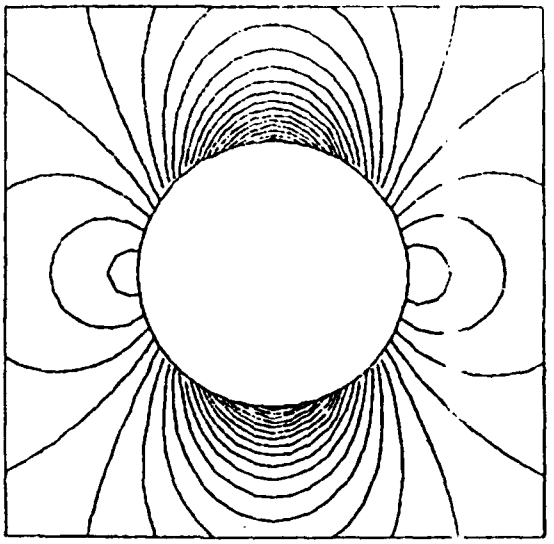

Fig. 4

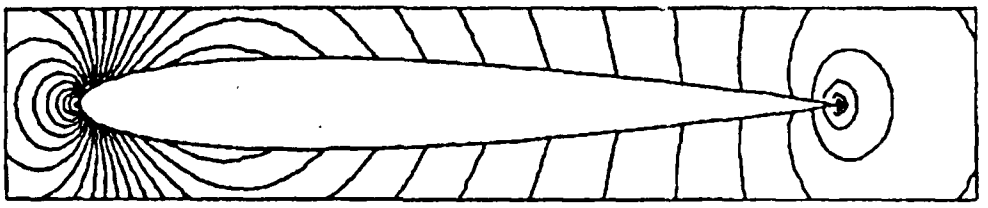

Fig. 5

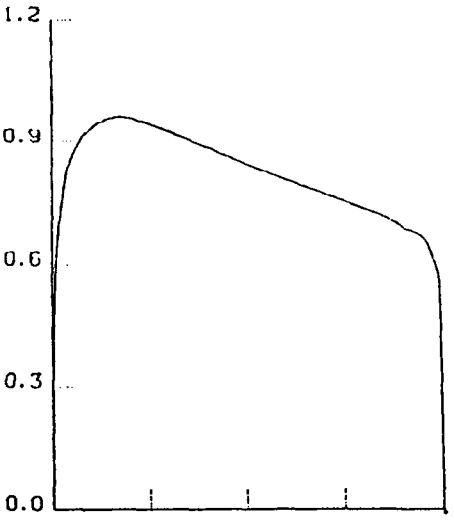

Fig. 6

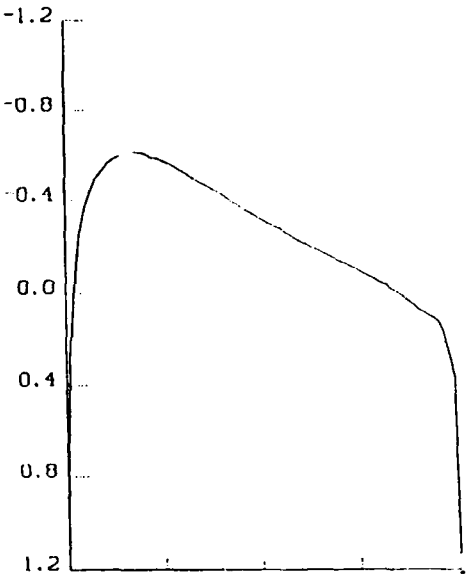

Fig. 7

Characteristic Galerkin Methods for Hyperbolic Systems

K.W. Morton and P.N. Childs

(ICFD, Oxford University Computing Laboratory
8-11 Keble Road, Oxford OX1 3QD)

1. Introduction

The idea of combining the use of characteristics with the Galerkin projection is one that has occurred to many people in the early 1980s, including Benqué and Ronat [1981], Bercovier et al. [1982], Douglas and Russell [1982], Morton and Stokes [1982] and Pironneau [1982].

A piecewise constant approximation space, with explicit time-stepping, then gives the familiar first order upwind scheme in one dimension, and a genuinely two-dimensional scheme which on a rectangular mesh has an interesting cross-derivative term. Piecewise linear approximations with the same time-stepping can give third order accuracy, which is maintained on non-uniform meshes.

For linear, constant coefficient advection this sequence is continued with splines of order s giving schemes of order of accurary $2s - 1$: and with centred time-stepping the order becomes $2s$. Moreover, there are several ways of generating the same scheme, and schemes of intermediate accuracy can also be generated. Thus suppose U^n is the approximation at time level n using splines of order s, with the basis $\{\phi_i : i = 1,2,\ldots\}$. Suppose further that the spline approximation $\tilde{u}^n$ using splines of order $s+p$ is recovered from U^n by means of the projection equations

$$\langle \tilde{u}^n - U^n, \phi_i \rangle = 0 \quad i = 1,2,\ldots . \qquad (1)$$

Then if the characteristic Galerkin procedure is continued at each time step by using $\tilde{u}^n$ rather than U^n, the resulting scheme has accuracy of order $2s + p - 1$. For example, recovery with quadratic splines from piecewise constant approximations gives the third order scheme obtained using piecewise linears with no recovery step. On the other hand recovery with piecewise linears gives a second order scheme (see Childs and Morton [1986]).

The advantage of introducing the recovery step is the degree of adaptivity that can be introduced. For example, monotonicity may be preserved or the scheme made TVD, as with various flux-limited difference schemes (see Morton and Sweby [1987] for a comparison of the two approaches).

2. Scalar conservation laws

We have developed such adaptive finite element algorithms in one dimension, using piecewise constants with recovery by piecewise linears, where the linear section replaces the jump between pairs of elements but may not entirely remove the constant section in each element (Morton [1985], Morton and Sweby [1987], Childs and Morton [1986]). For problems with shocks, the shock may be recognised and explicitly taken account of at the recovery stage: that is, the shock appears in the interior of an element and the recovered $\tilde{u}^n$ is continuous, piecewise linear (and piecewise constant) on either side.

A convenient way to write the algorithm for some purposes is as follows:

$$\left\langle U^{n+1} - U^n, \phi_i \right\rangle + \Delta t \left\langle \partial_x f(\tilde{u}^n), \Phi_i^n \right\rangle = 0, \quad i = 1,2,\ldots; \qquad (2)$$

here the special test function in the spatial term is the average of the basis function ϕ_i over the distance moved by the characteristics $dx/dt = a(\tilde{u}^n)$ in one time-step

$$\Phi_i^n(x) := \frac{1}{a(\tilde{u}^n(x))\Delta t} \int_x^{x+a(\tilde{u}^n)\Delta t} \phi_i(z)dz. \qquad (3)$$

This is the easiest starting point for making comparisons with Petrov-Galerkin and Taylor-Galerkin methods.

However, the algorithms are best programmed by considering in turn each contribution to the update from a linear section of $\tilde{u}^n$, and allocating some proportion to the appropriate elements reached by the characteristics. It is clear that an arbitrary non-uniform mesh may be used and the only limit on the time-step arises from considerations of accuracy.

To put the procedure in a rigorous framework, it has been found best to use the formalism of Brenier [1984, 1985]. Then convergence can be proved under suitable conditions even with the shock recovery stage.

3. Systems of conservation laws

The Brenier formalism can be extended to systems if flux-difference splitting is used, which we have found to be more accurate than flux-vector splitting. To extend our algorithm, the jump in the recovered solution $\tilde{\underline{u}}$ over each linear segment is decomposed by the flux-difference splitting method into jumps corresponding to each characteristic field of the system. Corresponding to each of these characteristic jumps, the appropriate updates are effected by using a form similar to (2), where $\tilde{\Phi}_j^n$ must now be computed for that characteristic field using an appropriate characteristic speed determined from the decomposition. This yields an adaptive second order method. We prefer to use the splitting due to Roe [1981], through which we obtain results comparable with flux-limited difference methods.

Again, we place no restriction on the mesh and therefore a number of adaptive grid strategies may be employed. With the use of Godunov's splitting and for the scheme based on piecewise constant elements, the large timestep scheme due to LeVeque [1985] is reproduced.

4. References

1. J.P. Benqué & J. Ronat, Quelques difficultés des modéles numérique en hydraulique, 5th Int. Symp. on Comp. Meths. in Appl. Sciences and Engng., (1981), INRIA, Versailles, France.

2. M. Bercovier, O. Pironneau, Y. Hasbani & E. Livne, Characteristic and finite element methods applied to the equations of fluids, Proc. MAFELAP 1981, J.R. Whitemen, ed., Academic Press, London (1982), pp. 471-478.

3. Y. Brenier, Average multivalued solutions for scalar conservation laws, SIAM J. Numer. Anal., 21 (1984), pp. 1013-1037.

4. Y. Brenier, Averaged multivalued solutions and time discretization from conservation laws, SIAM/AMS Lectures in Applied Math., 22 (1985), pp. 41-55.

5. P.N. Childs & K.W. Morton, Characteristic Galerkin methods for scalar conservation laws in one dimension, Oxford University Computing Laboratory, Report 86/5 (1986).

6. J. Douglas & T. Russell, Numerical methods for convection dominated diffusion problems based on combining the method of characteristics with finite element or finite difference procedures, SIAM J. Numer. Anal., 19 (1982), pp. 871-885.

7. R.J. LeVeque, A large timestep generalisation of Godunov's method for systems of conservation laws, SIAM J. Numer. Anal., 22 (1985) pp. 1051-1073.

8. K.W. Morton, Characteristic Galerkin methods for hyperbolic problems, in Proc. 5th GAMM Conference on Numerical Methods in Fluid Mechanics, Rome, M. Pandolfi & R. Riva eds., F. Vieweg & Sohn, Wiesbaden (1983), pp. 213-250.

9. K.W. Morton & A. Stokes, Generalized Galerkin methods for hyperbolic problems, in Proc. MAFELAP 1981, J.R. Whiteman, ed., Academic Press, London (1982), pp. 421-431.

10. K.W. Morton & P.K. Sweby, A comparison of flux-limited difference methods and characteristic Galerkin methods for shock modelling, J. Comput. Phys., 73 (1987), p.203.

11. O. Pironneau, On the transport-diffusion algorithm and its application to the Navier-Stokes equations, Numer. Math., 38 (1982), pp. 302-322.

12. P.L. Roe, Approximate Riemann solvers, parameter vectors and difference schemes, J. Comp. Phys., 43 (1981), pp. 357-372.

M

ON SOME NUMERICAL SCHEMES FOR TRANSONIC FLOW PROBLEMS

by Marco Mosché Mostrel #

Recently a number of new shock capturing finite difference approximations for solving scalar conservation law nonlinear partial differential equations in several space dimensions have been constructed and applied to solve numerically the equations of inviscid compressible flows of aerodynamics. Those partial differential equations are, in the time-independent (steady) case, of mixed-type, i.e. their type changes from elliptic to hyperbolic as the flow regime changes from subsonic to supersonic and vice-versa.

In this paper, we present some new shock capturing finite difference approximations for solving scalar conservation laws. Our new schemes have the following properties:

(i) second order accuracy throughout the computational domain;

(ii) global linear stability in all elliptic and all hyperbolic regions;

(iii) sharp steady discrete shock solutions;

(iv) total variation non-increasing property of the approximate solutions;

(v) entropy stability, at least in some cases, i.e. the approximate solutions satisfy a discrete entropy condition consistent with the differential entropy condition of the p.d.e.; this property ensures that the approximate solutions are admissible on physical grounds.

A model 2D conservation law equation is constructed and the above properties are proven for this model. This model can serve to represent two commonly used equations for simulating inviscid, isentropic potential flow problems at transonic speeds: the Transonic Small Disturbance (TSD) equation and the Full Potential (FP) equation.

The new schemes are studied first in their semi-discrete (method of lines) versions. A new Alternate Direction Implicit (ADI)-like time discretization is also presented for the particular application to the low-frequency, unsteady, two-dimensional TSD equation; the results of the numerical implementation of this implicit scheme on a variable computational mesh proved satisfactory.

In [1], [7], [6], [4] and [2], a number of shock capturing finite difference approximations for solving the TSD and the FP equations have been proposed. These schemes satisfy

This work was partially supported under grants ONR N00014-86-K-0691 and NASA NAG-270. Some of the analytical calculations presented in this paper were obtained with the aid of Macsyma, a symbolic manipulation program developed at the M.I.T. Laboratory for Computer Science and supported by Symbolics, Inc. The author's current addresses are: Department of Mathematics, University of California, Los Angeles, CA 90024 and Department of Mathematics and Computer Science, California State University, Long Beach, CA 90840. Send electronic mail to *marco@math.ucla.edu*.

properties (iii) & (v), and with the inclusion of flux limiters, property (iv) as well. Properties (i) & (ii) are usually satisfied in all elliptic regions; in hyperbolic regions, only first order accuracy is attained and the linear stability of the method is typically limited to values of the Mach number in $[0, M_c]$ where M_c is large enough to include the transonic regime. These schemes have a four-point bandwith and are type-dependent, i.e. they use *different* formulas for the difference approximations in the elliptic and the hyperbolic regions. They use *central* differencing in the elliptic regions and *upwind* differencing in the hyperbolic regions. The upwinding is designed to take into account the correct region of influence and to keep the shock front sharper. For the TSD equation, since the flow is quasi-unidirectional, the upwinding is performed in that direction ([2]). For the FP equation, the upwinding can be performed separately for the x-dependent term and the y-dependent term. This approach was labeled directional flux biasing in [4]. Recently this approach was refined by introducing the method of streamwise flux biasing (see [5]) in which the upwinding is performed in a direction close to that of the actual flow. Unfortunately, the method hence obtained is only first order accurate (see [3], section 8, for a review of the schemes based on this method).

Our new method does not use flux biasing but a special kind of upwinding *uniformly* in all regions. The resulting stencil, the same in all regions, is of 7-point bandwidth, with 4 points upwind and 2 points downwind.

The format of this paper is as follows.

In Section 1, we introduce our new second order accurate numerical schemes for a class of 2D conservation law nonlinear p.d.e.'s which includes the TSD equation and the FP equation. We prove a convergence result à la Lax-Wendroff.

In Section 2, we prove the linear stability of these schemes for the most commonly used numerical fluxes for the TSD equation and the FP equation.

In Section 3, we present an extended version of these schemes which makes use of flux limiters to keep the total variation non-increasing.

In Section 4, we prove a discrete entropy inequality satisfied by our finite difference approximation in the case of the low-frequency, unsteady TSD equation and we show that this inequality is consistent with the differential entropy inequality of the problem.

In Section 5, we describe a time-splitting algorithm for solving the unsteady TSD equation.

In Section 6, we present the numerical results obtained by implementing our finite difference method for the TSD equation for the flow over a thin airfoil.

REFERENCES

1. Engquist, B. and Osher, S., "One-sided difference approximations for nonlinear conservation laws," *Math. Comp.*, vol. 6, no. 154, pp. 321-351, 1981.
2. Engquist, B. and Osher, S., "Stable and entropy satisfying approximations for transonic flow calculations," *Math. Comp.*, vol. 34, no. 149, pp. 45-75, 1980.
3. Mostrel, M.M., "On some numerical schemes for transonic flow problems," *Ph.D. Thesis*, University of California, Los Angeles, 1987.
4. Osher, S., Hafez, M.M., and Whitlow, W.Jr., "Entropy condition satisfying approximations for the full potential equation of transonic flow," *Math. Comp.*, vol. 44, no. 169, pp. 1-29, 1985.
5. Shankar, V., Ide, H., Gorski, J., and Osher, S., "A fast, time-accurate unsteady full potential scheme," AIAA Paper no. 85-0165, 1985.
6. Shankar, V., "Implicit treatment of the unsteady full potential equation in conservation form," AIAA Paper no. 84-0262, 1984.
7. Shankar, V. and Osher, S., "An efficient, full-potential implicit method based on characteristics for supersonic flows," *AIAA J.*, vol. 21, no. 9, pp. 1262-1270, 1982.

Numerical Simulations of Compressible Hydrodynamic Instabilities with High Resolution Schemes

Claus-Dieter Munz
Kernforschungszentrum Karlsruhe

Lutz Schmidt
Universität Karlsruhe

Interface instabilities arise in a wide variety of physical contexts. In this paper, we will examine the numerical simulation of the large-scale motion of two-dimensional interfacial instabilities. We will show numerical results for the instability of interfaces separating two domains of the same compressible fluid which move at different velocities, namely the Kelvin-Helmholtz instability, the Rayleigh-Taylor instability and the instability of a jet. Our calculations are based on the direct simulation of the instabilities by numerical solution of the equations of compressible fluid flow, usually called Euler equations. There are two different formulations of these equations. Numerical methods based on the Lagrangean formulation use a computational mesh traveling with the fluid. Hence these methods seem to be ideal for solving problems which involve interfaces between two fluids. However, these calculations can typically be carried out for short times only. Then severe mesh distortion or mesh tangling will occur and rezoning must be performed in which all computational quantities are transferred to a new computational mesh. Because this procedure calls for much computational effort, the Lagrangean methods are not favourable for dealing with large-scale computations. On the other hand, Eulerian methods, in which the mesh is fixed, are ideal for treating flows with large deformations. But interfaces are smeared out over some grid zones and the movement of the interfaces can hardly be seen. We will present a combined method: The flow field is calculated by a Eulerian method, while the interfaces are moved in a Lagrangean fashion according to the Eulerian flow field. This means that we discretize the interface and then within each time step we calculate the new position of the discretized interface from the Eulerian flow field. This may also be considered as a marker particle algorithm which is used to visualize the movement of the interface.

We consider a class of high resolution schemes for solving the two-dimensional Euler equations

$$U_t + f(U)_x + g(U)_y = q(U)$$

which, after van Leer /4/ are usually called MUSCL-type schemes. U denotes the vector of the conserved variables ρ, ρu, ρv, e and f, g denote the fluxes

$$f(U) = (\rho u, \rho u^2+p, \rho uv, u(e+p))^T, \quad g(U) = (\rho v, \rho uv, \rho v^2+p, v(e+p))^T,$$

q is a source term, e.g. due to gravitational forces. As usual ρ is the density, $(u,v)^T$ is the velocity, e is the energy and p is the pressure. The numerical schemes are based on the one-dimensional MUSCL-type schemes formulated in a two-step format (see /4/) and on dimensional splitting. In the first step of the MUSCL-type scheme a piecewise linear approximation of the solution is calculated from the approximative values at the grid points. This piecewise linear representation is determined by calculating slopes in each grid zone by means of interpolation. Contrary to the schemes of van Leer /4/ and Colella /1/ we calculate the slopes in terms of characteristic values based on the method of Roe /7/. By that we can apply different slope calculations on the genuinely nonlinear and linearly degenerate characteristic fields which gives sharp resolution of shock waves as well as contact discontinuities /6/. Slope calculations which have been indicated and analyzed for scalar conservation laws (see e.g. /5/) are used. To obtain second-order accuracy as regards the time t the piecewise linear representation is advanced a half time step. Then an upwind scheme is applied to these data to calculate the fluxes between the grid zones which gives new approximative values at the next time level. Within this algorithm each upwind scheme as reviewed in /3/ may be used.

The two-step algorithm can be implemented efficiently on vector computers. We will add some remarks about it and present a comparison of computer times of fully vectorized MUSCL-type schemes based on different upwind schemes and on different slope calculations. Together with the tracking algorithm for interfaces the schemes have been fully optimized for vector computers. Very fast schemes are based on the upwind scheme of Einfeldt /2/ and van Leer (see /3/). Fig. 2 shows an example of our calculations. A diagram of the initial values for this jet is sketched in Fig. 1. A fluid to the left is separated by a small band of gas flowing into the opposite direction. The interfaces between the different fluids are sinusoidally perturbed. The perturbations grow and the shear layers start to roll up into a Karman vortex street. These calculations have been performed on a uniform grid with 100 x 100 grid zones. About 1000 time steps have been computed within 3 minutes of computer time on vector computer Cyber 205. Because the roll-up of a shear layer depends on viscosity, large scale computations of interfacial instabilities may be used to measure and to compare the numerical viscosity which is inherent in each scheme. We will present a comparison of several schemes.

References

/1/ Collela, P: A direct Eulerian MUSCL scheme for gas dynamics, SIAM J. Sci. Stat. Comput 6 (1985), 104-117.

/2/ Einfeldt, B.: On Godunov-type methods for gas dynamics, to appear in SIAM J. Numer. Anal.

/3/ Harten, A., Lax, P.D. and van Leer, B.: On upstream differencing and Godunov-type schemes for hyperbolic conservation laws, SIAM Rev. 25 (1983), 35-62.

/4/ Leer, B. van: On the relation between the upwind-differencing schemes of Godunov, Engquist-Osher and Roe, SIAM J. Sci. Stat. Comput 5 (1984), 1-21.

/5/ Munz, C.D.: On the numerical dissipation of high resolution schemes for nonlinear hyperbolic conservation laws, to appear in J. Comput. Phys.

/6/ Munz, C.D.: On the construction and comparison of two-step schemes for the Euler equations, in Finite Approximations in Fluid Mechanics 14, Vieweg 1986, 195-217.

/7/ Roe, P.L.: Approximate Riemann solvers, parameter vectors and difference schemes, J. Comput. Phys. 43 (1981), 357-372.

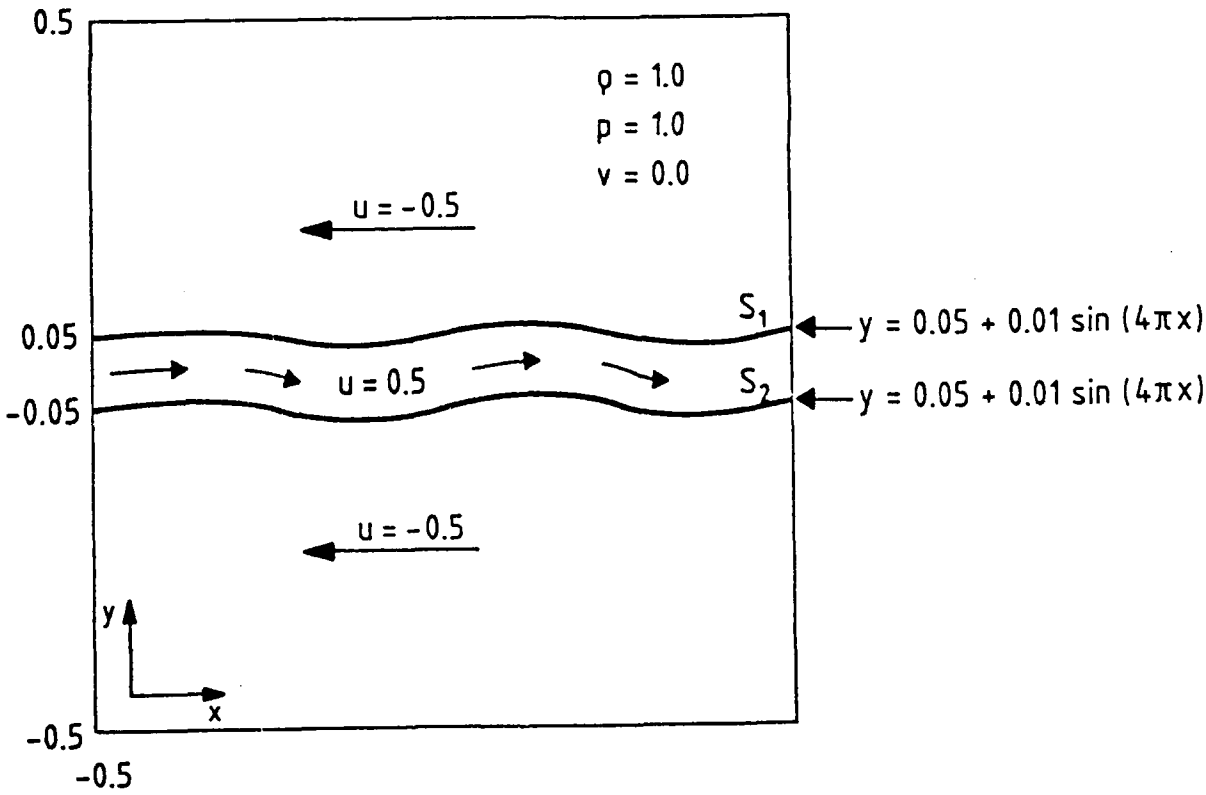

Fig. 1: Initial values for a jet

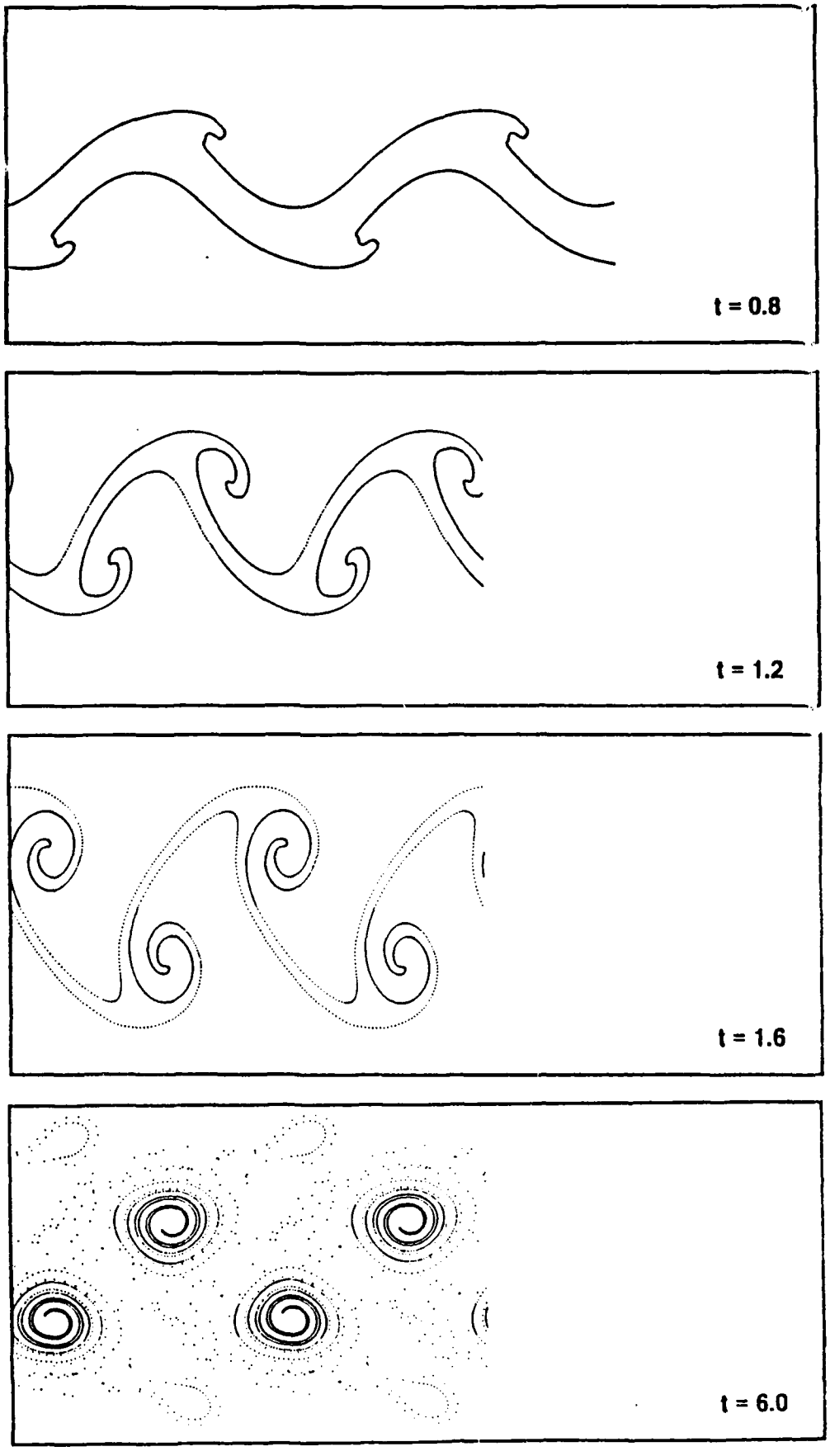

Fig. 2: Numerical simulations of a jet

P

ON THE "FLUX-DIFFERENCE SPLITTING" FORMULATION

Maurizio Pandolfi.
Dipartimento di Ingegneria Aeronautica e Spaziale.
Politecnico di Torino, Torino, Italy.

++

The Euler equations describe inviscide compressible flows. In the case of unsteady flows, we deal with a hyperbolic problem, where the time is playing the role of the "hyperbolic" coordinate. Also for the steady flows we may have a hyperbolic problem, provided that a fully supersonic flow is developed: in this case any space coordinate along which the velocity component is supersonic can be the "hyperbolic" coordinate.

The Euler equations are founded on the three basic laws of the physics which account for the conservation of the mass, the equilibrium between the inertial forces and the pressure gradient, and the respect of the first principle of the thermodynamics. The so called "centered schemes" methods are operating directly on this original form of the governing equations. No reference is done to the hyperbolic nature of the problem, except, for some methodologies, in the definition of the step of integration and/or in the numerical treatment of the boundaries.

The hyperbolic character hidden in the original equations can be put in evidence by a proper rearrangement of them. We refer to this work as to the formulation. There are different formulations, but each of them is more or less related to the basic ideas developed in the old method of the characteristics. It is in the formulation that the wave-like nature of the problem is emphasized, and it is recognized that the evolution of the flow at a given point is determined by the merging of signals there, after they have been propagating along characteristic rays. For these reasons these approaches are generally known in the literature as "upwind" methodologies.

Different upwind formulations have been proposed. Some of them are founded on the quasi linear form of the governing equations (lambda formulation, split coefficient method,..), other are based on the conservative form of them (flux-vector splitting, flux-difference splitting,....) They only differ each other because the problem is not linear. For a linearized version of the Euler equations, all of them turn out to coincide perfectly. The main feature common to all these formulations is the attempt of extracting, from the usual thermodynamic properties and the velocity, informations about the corresponding waves or signals travelling there.

The present lecture refers to the "flux-difference splitting" (FDS) formulation and is addressed to the presentation of some different forms in which such upwind formulation has been proposed in the literature. The attention will be mainly pointed toward the unsteady flows (the time is the "marching" coordinate), since almost all the contributions refer to these problems. However we stress that all the following concepts can be easily extended to the steady supersonic flows, whereas the same kind of extension does not look feasible for other formulations such as the flux-vector splitting.

The FDS formulation is based upon an interpretation of the initial data (given at a discrete set of computational points) over the intervals of the computational grid. Constant or variable distributions of the flow properties can be assumed in the neighboring of each computational point. Therefore a discontinuity of the flow properties will generally occur at the middle of an interval. Godunov (1959) has proposed to look at the evolution of this discontinuity along the hyperbolic coordinate and to draw informations on how to split the difference of the flux over each computational interval. Such a splitting determines which part of this difference is going to affect, through the governing equations, the flow evolution at points located on one side of the interval, and which parts will act on the opposite side. The prediction of the evolution of the discontinuity is known as the solution of a Riemann problem. Once these splittings have benn operated, we can proceed to the numerics and plug the terms, in which the difference of the flux has been split, into a numerical approximation. The approximation can be characterized by the assumed kind of discretization (finite differences, finite volumes, finite elements,...) and by the numerical scheme (explicit, implicit, order of accuracy,...)

In his original presentation, Godunov was pointing out two shortcomings in his procedure. The first was represented by the too large computational effort needed in achieving the exact solution of the Rieman problem (the possibility of shocks brings to tedious and time consuming multiple

iterations). The second shortcoming was represented by the unsatisfactory accuracy of the numerical results, since he was using the plain first order scheme. In fact the very brilliant idea of Godunov was not performing so well because he was looking at the exact solution of the Riemann problem (with the related penalty in the computations), without getting any profit from this expensive work in the following numerical scheme, which was the simplest one (with the related penalty in the accuracy).

Therefore the following research efforts have been addressed in two directions. On one side the search for efficient solvers of the Riemann problems, even approximate solvers. On the other side more sophysticated interpretation of the initial data and more suitable definition of the Riemann problems in order to increase the level of the accuracy.

Iterative time consuming procedures are needed for solving a Riemann problem, because of the non linear and non isentropic behaviour of the shocks. To overcome this problem, Roe (1980) has proposed to replace the original non linear problem with a linear one (chosen in some convenient way in oreder to meet some positive requirements). Now the linear problem is solved exactly and quickly. A completely different approach has been proposed by Osher (1980). He suggested to neglect the jump of entropy generated by the shocks originated in the Riemann problem. The resulting approximated non linear problem has now an immediate and exact solution, based on the properties of the Riemann Invariants in omoentropic flows. A variation of this solver has been also proposed by the present author (1983). Here we want to stress that the above approximated solutions of the Riemann problem only affect slightly the splitting, but do not touch the wholeness of the Euler equations which will be integrated in their full form.

In order to improve the accuracy of the numerical integration, one can use numerical schemes more elaborated than the original first order scheme proposed by Godunov (which was not performing at the best level of accuracy, but was, and is still now, very cheap in terms of computer memory and time and very robust without violating any monotonicity criterium in the numerical capturing of shocks).

A different approach for improving the accuracy is based on interpretations of the initial data more sophysticated than the piecewise constant value distribution proposed originally by Godunov. Remarkable contributions have been given by the MUSCL method (Van Leer and Woodward, 1979) and the PPM procedure (Colella and Woodward, 1984). Here the attention is wholly focused on the interpretation of the initial data in

terms of linear or parabolic distributions around a computational point. The resulting Riemann problems are solved through an almost exact algorithm and provide the terms in which each difference of the flux is split. The following integration of the full Euler equations is carried out with the plain first order scheme. However the final accuracy turns out to be at much higher levels, owing to the previous sophysticated interpretation of the initial data.

The above different contributions to the FDS formulations will be presented in a uniform manner, in order to put in evidence the different features. For this reason the physics will be described under the eulerian point of view, whereas in some contributions has been originally considered under the lagrangian one. Finally the extension to the steady supersonic flow problems will be shown to be straightforward.

A FULLY IMPLICIT SCHEME FOR MULTIPHASE FLOW IN ONE DIMENSIONAL POROUS MEDIA

Jorge G.S. Patiño

Department of Mathematics
Pontificia Universidade Católica do Rio de Janeiro
22453 Rio de Janeiro-RJ, Brasil

We show that a system of equations (cf. Eq.1) appearing in multiphase flow in porous media has a global solution in time. The method of the proof is based on the random choice method. As a result we also obtain a fully implicit numerical scheme for the solution of these equations.

1. Statement of the problem

Consider the following system of differential equations

$$
\begin{aligned}
& u_t + v\, f_x(u) = 0 && x \in [a,b],\ t \geq 0 \\
(1) \qquad & v_x = 0 && \\
& v = -k(u)p_x && u \in \mathbb{R}^n,\quad v \in \mathbb{R}
\end{aligned}
$$

which arises in the study of incompressible, inmiscible, no capillarity, multiphase flow in porous media [1] . In (1) the components of u are the saturations (or volumetric concentrations), v is the velocity, p is the pressure, k is the permeability and f is the flux function defined in terms of the individual permeabilities. Equations (1a), (1b) and (1c) represent the individual mass balances, the imcompressibility condition and Darcy's law respectively.

Suppose that the Jacobian matrix df has real and distinct eigenvalues λ_j on a region R of the u space, then(1a)is an hyperbolic system of conservation laws which is coupled to the elliptic equation

$$(2) \qquad (k(u)p_x)_x = 0$$

obtained by substituting(1c) in(1b).

We shall show below that system (1), interpreted in the weak sense, has a global solution in time for continuous boundary conditions $p_a(t) = p(a,t)$, $p_b(t) = p(b,t)$, $u_a(t)$, $u_b(t)$, and initial data $u_0(x)$ with small variation provided $k(u)$ is continuous and $M>k(u)>\varepsilon$ for some ε,M. The proof of this result, based on the random choice method , will provide an implicit scheme for the numerical solution of (1). In the scheme, v at time t_{j+1} is calculated using the approximate solution u at time t_{j+1}, but the invariance properties of equation (1a) will permit us to actually obtain an explicit formula for $v(t_{j+1})$. In [3] Marchesin showed that the scalar analogue to (1) has a global solution in time using a somewhat different approach that does not yield an efficient computational scheme.

ON OVERDETERMINED HYPERBOLIC SYSTEMS

Zbigniew Peradzynski
Institute of Fundamental Technological Research
Polish Academy of Sciences
Swietokrzyska 21, 00-049 Warszawa, Poland

We consider an overdetermined ($m \geq 1$) quasilinear first order system of PDE's

$$\sum_{\nu,j} A_j^{s\nu}(u,x)\,\frac{\partial u^j}{\partial x^\nu} = f^s(u,x). \qquad \begin{matrix} s = 1,\ldots,m \\ j = 1,\ldots,l \\ \nu = 1,\ldots,n \end{matrix}$$

The Maxwell equations (with extra constrains div E = 0, div B = 0) or the vorticity equations in hydrodynamics can be viewed as prototypes of such system.

For any u_o, x_o we define a linear space $I(x_o,u_o)$ of integral elements as composed of all $l \times n$ matrices (p_ν^j) satisfying

$$\sum_{\nu,j} A_j^{s\nu}(u_o,x_o)\; p_\nu^j = 0.$$

Special role is played by the characteristic elements which are the matrices of rank 1, i.e. they are of the form $p_\nu^j = \gamma^j \lambda_\nu$.

The system is said to be hyperbolic at (x_o,u_o) if and only if:

1° The space of integral elements $I(x_o,u_o)$ is generated (as a linear space) by the characteristic elements;

2° It is an involutive system (i.e. it is compatible).

General properties of such system (solubility, restrictions appearing for possible boundary conditions etc.) are considered. In certain cases the existence can be proved.

Theory of overdetermined systems can be helpfull in investigating the structure of the solution set of the well-determined systems (l = m). For example, the characteristic determinant of such a system

$$\det |A_j^{\alpha\nu}\lambda_\nu| = 0$$

defines a cone of characteristic vectors. This cone, in general, consists of a number of branches. Let us take a simple branch. It turns out that there is a system of PDE's associated with this branch - the overdetermined system consisting of all modes from this branch only. If this system is compatible then one says that the interaction of modes from this selected branch do not involve other modes. In this way the interaction of modes can be investigated. There is a number of results conserning this question.

Runge-Kutta Split-Matrix Method for the Simulation of Real Gas Hypersonic Flows

M. Pfitzner

Messerschmitt-Boelkow-Blohm GmbH
Ottobrunn , FRG

In recent years there has been growing interest in the possible development of hypersonic aircraft and reentry bodies in the US and in Europe. The construction of these configurations requires an accurate prediction of the flow about three-dimensional bodies at Mach numbers ranging from $0 <= M_\infty <= 30$.

In the regime of hypersonic flow ($M_\infty > 4$) very strong gradients and shocks appear in the flowfield, which have to be resolved on relatively coarse meshes for 3-D calculations. Because of the strong compression ($p_{max}/p_\infty > 1000$ at $M_\infty = 30$) in the hypersonic regime high temperatures occur and air cannot be treated as an ideal gas. For a realistic simulation of the flow a robust and accurate algorithm including real gas effects is mandatory.

We integrate the instationary Euler equations in quasi-conservative form in generalized coordinates:

$$Q_\tau + A^+Q_\xi{}^+ + A^-Q_\xi{}^- + B^+Q_\eta{}^+ + B^-Q_\eta{}^- + C^+Q_\zeta{}^+ + C^-Q_\zeta{}^- = 0 \qquad (1)$$

The matrices $A^\pm, B^\pm, C^\pm$ are split according to the sign of their eigenvalues /1,2,8/. The space derivatives of Q are calculated with a third order accurate upwind-biased formula /3/.

$$Q^+\xi\big|_m = \frac{1}{6\Delta\xi}(Q_{m-2} - 6Q_{m-1} + 3Q_m + 2Q_{m+1})$$
$$Q^-\xi\big|_m = -\frac{1}{6\Delta\xi}(Q_{m+2} - 6Q_{m+1} + 3Q_m + 2Q_{m-1}) \qquad (2)$$

The bow shock can be captured or fitted /4/, whereas imbedded shocks are always captured. Owing to the simple geometry of reentry vehicles and the strong bow shocks encountered there, the shock fitting option is preferred in this case. For hypersonic flows, where real gas effects are important, the pressure of the gas is a general function of the density and the internal energy. The flux matrices A,B,C can be calculated with their eigenvectors and eigenvalues for arbitrary pressure $p(\rho,\varepsilon)$ and the shock fitting algorithm can be generalized for this case /5/.

The time-stepping towards the stationary state between time levels n and (n+1) is done with an explicit three-step Runge-Kutta method /6/:

$$Q^{(1)} = Q^n - a_1\,CFL\,P(Q^n)$$
$$Q^{(2)} = Q^n - a_2\,CFL\,P(Q^{(1)}) \qquad (3)$$
$$Q^{n+1} = Q^n - a_3\,CFL\,P(Q^{(2)})$$

where the operator P contains the space derivatives. Second order accuracy requires $a_3=1$ and $a_2=1/2$. The coefficient a_1 cannot be chosen such that the algorithm becomes third order accurate but serves to increase the stability region of the algorithm. We have done a von Neumann stability analysis of the Runge-Kutta scheme (3) for the 1-d linear advection equation for second order central and third order upwind-biased space discretisations. For central differences $a_1>1/4$ is needed for stability and for $a_1=1/2$ CFL numbers up to 2 may

be used. In contrast, for the upwind-biased space discretisation $a_1=1/4$ maximizes the stability region with $CFL_{max} \approx 1.77$. Fig. 1 shows a comparison of the square of the modulus of the amplification factor g as a function of the CFL number and $s=\sin^2(k\Delta x/2)$ for the one-step and the three-step Runge-Kutta time-stepping schemes. The big square hiding part of the plot of the function $|g|^2(CFL,s)$ denotes the stability limit $g=1$.

The one step algorithm is only weakly unstable at wave numbers $k \to 0$ for small CFL numbers. It can be used in practical calculations of 2-d and 3-d inviscid flows provided the cell aspect ratio is not extremely small. At a fitted bow shock a global time step must be used even if the rest of the field is calculated with a local timestep. For many configurations a fully converged result may be achieved with the one step algorithm depending on the configuration and the Mach numbers involved. The weak instability normally does not blow up the code but leads to small instationary disturbances in the flowfield, which do not die out and prevent a true stationary solution.

For the iterative Runge-Kutta scheme one additional storage of an intermediate value of the flow variables is needed (in contrast to three values with the classic four step Runge-Kutta scheme /7/), but a larger time step can be used and the linear stability of the algorithm is guaranteed.

Fig. 2 shows a comparison of lines of constant temperature in flow about a hemisphere-cylinder at $M_\infty=11$, $\alpha=0$, H=50 km ($T_\infty=271$ K) for ideal gas ($\gamma=1.4$) and equilibrium real gas. A local time step with CFL=1.5 was used and the calculation was converged after 500 time steps. The standoff distance of the shock is smaller for the real gas case and the temperature near the stagnation point is much lower. The wiggle in one of the real gas temperature isolines is a result of inaccuracies of the curve-fit routine used for the calculation of the real gas temperatures/9/. It is not visible in the flow variables.
The temperature isolines on the HERMES forebody in ideal gas and real gas flow with $M_\infty=10$, $\alpha=30$, H=50 km are displayed in fig.3. Fig.4 shows the pressure and the temperature distribution on the body in the symmetry plane. It reveals the small influence of the real effects on the pressure. The stagnation point temperature (5700 K for ideal gas) is lowered to 3120 K by the real gas effects.

REFERENCES

[1]: Chakravarthy S.R.: The Split-Coefficient Method for Hyperbolic Systems of Gas Dynamic Equations, AIAA paper 80-0268 (1980)

[2]: Weiland C.: A Split Matrix Method for the Integration of the Quasi-Conservative Euler Equations, Notes on Numerical Fluid Mechanics, Vol.13, Vieweg 1986

[3]: Weiland C. and Pfitzner M.: 3-D and 2-D Solutions of the Quasi-Conservative Euler Equations, Lectures Notes in Physics, Vol. 264, pp. 654-659, Springer Verlag (1986)

[4]: Weiland C.: Numerical Integration of the Governing Equations for the Domain of Pure Supersonic Flow, ESA TT-380 (1977)

[5]: Pfitzner M. and Weiland C.: 3-D Euler Solutions for Hypersonic Mach Numbers, AGARD-CP 428, Paper No. 22, Bristol - U.K. (1987)

[6]: Turkel E. and Van Leer B.: Flux Vector Splitting and Runge-Kutta Methods, Lecture Notes in Physics, Vol. 218, pp. 566-570, Springer Verlag (1985)

[7]: Jameson A., Schmidt W. and Turkel E.: Numerical Solutions of the Euler Equations by Finite Volume Methods Using Runge-Kutta Time-Stepping Schemes, AIAA paper 81-1259 (1981)

[8]: Whitfield D.L. and Janus J.M.: Three-Dimensional Unsteady Euler Equations Solution Using Flux Vector Splitting, AIAA paper 84-1552 (1984)

[9]: Tannehill J.C. and Mugge P.H.: Improved Curve Fits for the Thermodynamic Properties of Equilibrium Air Suitable for Numerical Computation Using Time-dependent or Shock-capturing Methods, NASA CR-2470 (1974)

Fig.1 : Comparison of the square of the modulus of the amplification factor g of the third order upwind-biased space discretisation

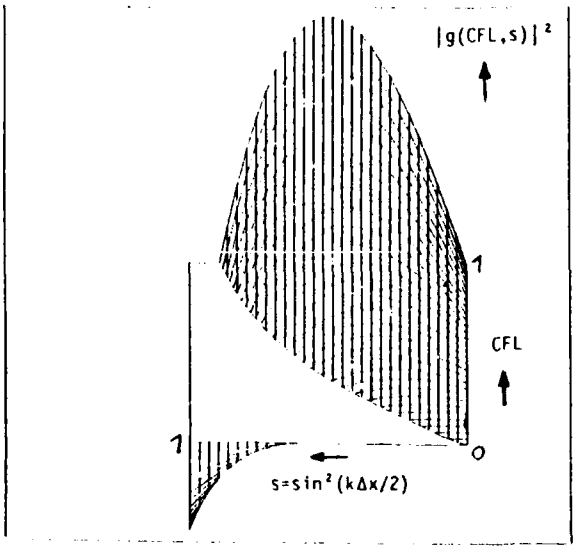

Fig.1a : one step algorithm

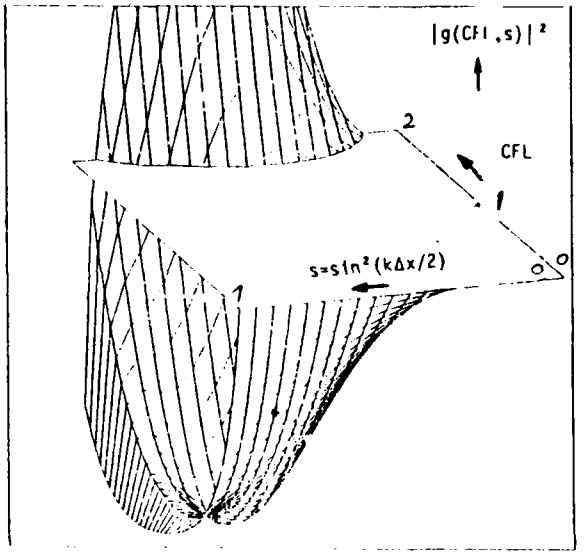

Fig.1b : three step Runge-Kutta algorithm

Fig.2 : Comparison of temperature isolines of flow about a hemisphere-cylinder at M_∞ = 11, α = 0, H = 50 km for ideal gas and real gas (ΔT = 100 K)

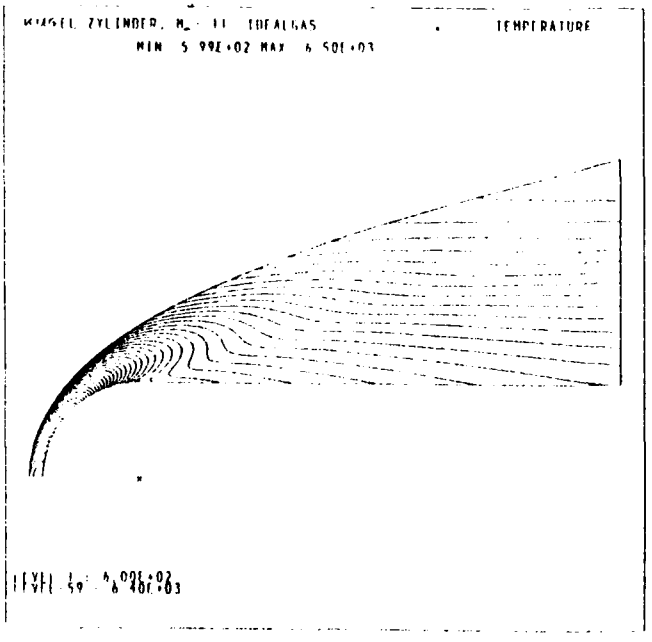

Fig.2a : ideal gas

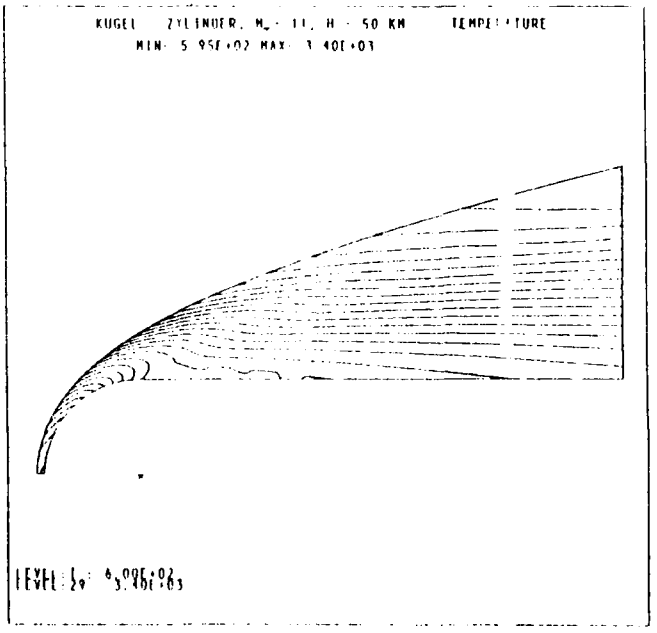

Fig.2b : equilibrium real gas

Fig.3 : temperature isolines on the Hermes forebody at M_∞ = 10, α = 30, H = 50 km for ideal gas and real gas (ΔT = 100 K)

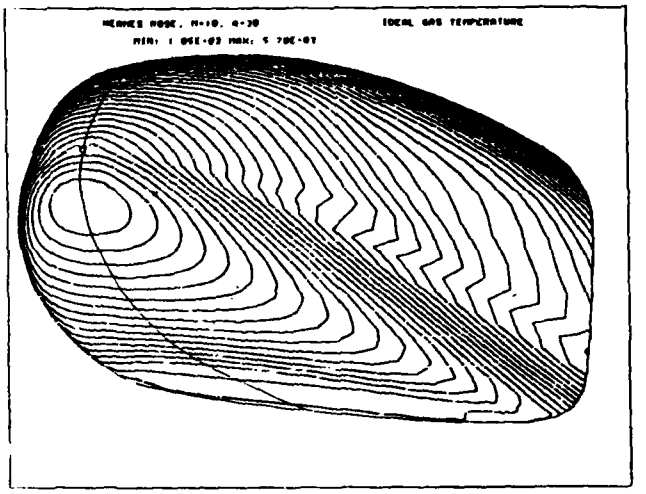

Fig.3a : ideal gas

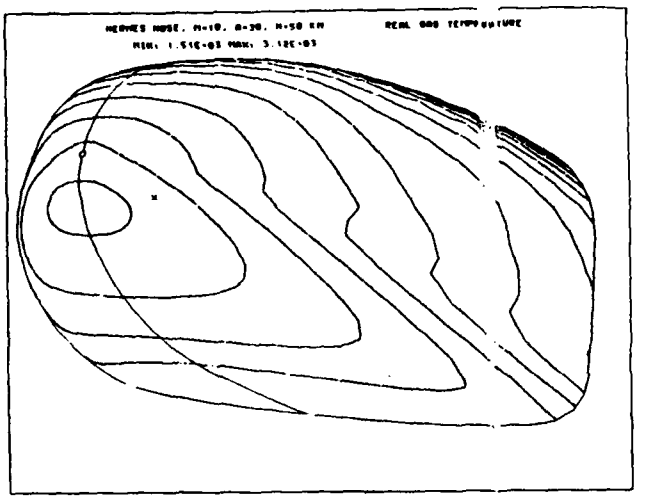

Fig.3b : equilibrium real gas

Fig.4 : comparison of the pressure and temperature distribution on the HERMES forebody in the symmetry plane for real gas and ideal gas (z coordinate in [1/450 mm])

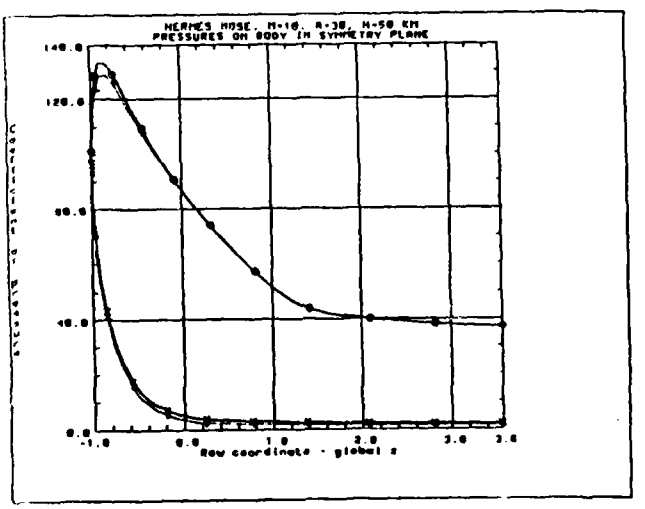

Fig.4a : pressure distribution
+ : ideal gas luv side
* : ideal gas lee side
o : real gas luv side
x : real gas lee side

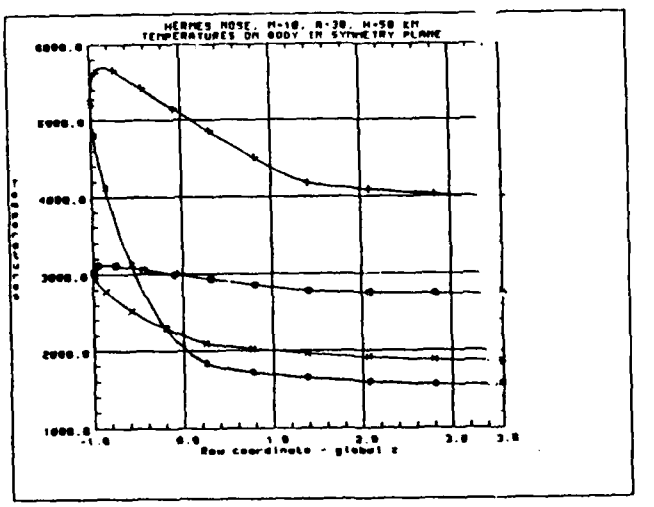

Fig.4b : temperature distribution
+ : ideal gas luv side
* : ideal gas lee side
o : real gas luv side
x : real gas lee side

A.Pham Ngoc Dinh
Université d'Orléans
Département de Mathématiques - B.P.6759
45067 ORLEANS CEDEX 2

Dang Dinh Ang
Department of Mathematics
Dai Hoc Tong Hop
HO CHI MINH City University

" ON SOME VISCOELASTIC STRONGLY DAMPED NONLINEAR WAVE EQUATIONS "

We study the problem of existence, uniqueness and asymptotic behaviour for $t \to \infty$ of (weak or strong) solutions of equations in the form

$$u_{tt} - \lambda \Delta u_t - \sum_{i=1}^{N} \partial / \partial x_i \, \sigma_i(u_{x_i}) + f(u, u_t) = 0 \qquad (1)$$

$$\lambda \geq 0, \quad (x,t) \in \Omega \times]0,T[, \quad u_t = \partial u / \partial t, \quad u_{x_i} = \partial u / \partial x_i$$

with various boundary and initial conditions on $u(x,t)$.
In (1) Ω is a bounded domain in $\mathbb{R}^N$ with a sufficiently smooth boundary $\partial\Omega$, σ_i $(i=1,\ldots N)$ are continuous functions satisfying certain monotonic and other conditions.
The case $\lambda > 0$ corresponds to a nonlinear Voight model (for σ_i nonlinear). The case $\lambda = 0$, $N=1$ and $f(u,u_t) = |u_t|^{\alpha} \operatorname{sgn}(u_t)$, $0 < \alpha < 1$ with nonhomogeneous boundary conditions corresponds to the motion of a linearly elastic rod in a nonlinearly viscous medium. Equations of the type (1) with $f=0$, were given the first systematic treatment by Greenberg, Mac Camy and Mizel [4] in the case of space dimension $N=1$.

We studied (1) with $\lambda > 0$ and $f(u_t) = |u_t|^{\alpha} \operatorname{sgn}(u_t)$, $0 < \alpha < 1$, $u(x,0) = \tilde{u}_0(x)$ $u_t(x,0) = \tilde{u}_1(x)$ [1]. For $\tilde{u}_0$ in $H_0^1(\Omega)$, $\tilde{u}_1$ in $L^2(\Omega)$ and σ_i in $C(\mathbb{R},\mathbb{R})$ non decreasing, $\sigma_i(0) = 0$ and inducing mappings of $L^2(\Omega)$ into itself, taking bounded sets into bounded sets, the problem admits a global weak solution. If in addition the σ_i's are assumed locally Lipschitzian, then the solution is unique. For $N=1$, $\tilde{u}_0$ in $H_0^1(\Omega) \cap H^2(\Omega)$, $\tilde{u}_1$ in $L^2(\Omega)$, σ_i in $C^1(\mathbb{R},\mathbb{R})$ with $\sigma_i' > 0$ and locally Hölder continuous, there exists a unique strong solution $u(t)$ of the initial and boundary value problem i.e. $t \to u(t)$ is continuous on $t \geq 0$ to $H_0^1(\Omega) \cap H^2(\Omega)$ and twice continuously differentiable on $t > 0$ to $L^2(\Omega)$.

If we consider the problem with $\lambda > 0$, the function f being a function of u : $f(u)$, then for $\tilde{u}_0$ in $H_0^1(\Omega)$, u_1 in $L^2(\Omega)$ and a certain local Lipschitzian condition on f, a local existence and uniqueness theorem is proved [2], using the method of successive linearizations. If we strengthen the above hypotheses and assume that $1 \leq N \leq 3$, $\tilde{u}_0 \in H_0^1(\Omega) \cap H^2(\Omega)$ and $\tilde{u}_1 \in L^2(\Omega)$ while f is to satisfy no other condition than $f' \geq -c$ for $c > 0$, then, the unique solution $u(t)$ exists for all $t \geq 0$, with the property that $u_t'(t)$ and $\Delta u(t)$ decay exponentially to 0 as $t \to \infty$, more pre-

cisely we have the result

$$\|\Delta u(t)\| + \|u_t(t)\| \leq Me^{-\gamma t},\ \gamma>0\ ,\ \text{for all } t\geq 0$$

(here $\|\cdot\|$ stands for the $L^2(\Omega)$-norm)

This last result generalizes a result of Webb[9] .

In the case N=1, $\lambda=0$, $\sigma(x)=x$ and $f(u_t)=|u_t|^{\alpha}\operatorname{sgn}(u_t)$, $0<\alpha<1$, we study the equation (1) with a nonhomogeneous condition namely

$$u_x(0,t)= g(t),\quad u(1,t)= 0 \qquad (2)$$

Then the global existence and uniqueness of the initial and boundary value problem (1),(2) with $\tilde{u}_0 \in H_0^1(\Omega)$ and $\tilde{u}_1 \in L^2(\Omega)$ can be proved by using a Volterra nonlinear integral equation and the monotonicity generated by the nonlinear term[3] .

Note that for the equation of the form

$$u_{tt} - \Delta u = \varepsilon f(t,u,u_t)\quad ,\ (x,t)\in]0,1[\times]0,T[\qquad (3)$$

associated to Dirichlet conditions , a theorem on local existence is proved[8] and an asymptotic expansion of order 2 in ε ($\varepsilon>0$) is obtained, for ε sufficiently small and $f\in C^1([0,\infty[\times R^2)$.
The linear recursive schemes developped in[2] enables us to use a perturbation technique based on the ideas of best uniform approximation by polynomials, which considerably extends the classical Tau method of Lanczos. This Tau method has been developped by Ortiz[5] and computational procedures for the numerical treatment for partial differential equations with polynomial coefficients have been discussed by Ortiz and Samara[7]. Ortiz and Pham Ngoc Dinh[6] have discussed the numerical solution of a semi-linear hyperbolic problem of the following type

$$u_{tt} - \Delta u = f(t,u) \qquad (4)$$

and sufficient conditions for the quadratic convergence are given in this paper. By using this best approximation technique and these linear recursive schemes we effectively produce numerical solutions of a high accuracy.

[1] Dang Dinh Ang and A.Pham Ngoc Dinh - Strong solutions of a quasilinear equation with nonlinear damping. To appear in SIAM J. on Math.Analysis(1987)

[2] Dang Dinh Ang and A.Pham Ngoc Dinh - On the strongly damped wave equation : $u_{tt} - \Delta u - \Delta u_t + f(u) = 0$. To appear

[3] Dang Dinh Ang and A.Pham Ngoc Dinh - Mixed problem for some semi-linear wave equation with a nonhomogeneous condition. To appear in Nonlinear Analysis T.M.A. (1987)

[4] J.M.Greenberg,R.C.Mac Camy and V.Mizel - On the existence, uniqueness and stability of solutions of the equation : $\sigma'(u_x)u_{xx} + u_{xtx} = \rho_0 u_{tt}$ J.Math.Mech.17(1968)pp.707-728

[5] E.L.Ortiz - The Tau method. SIAMJ.Numer.Analysis 6(1969) pp. 480-492

[6] E.L.Ortiz and A.Pham Ngoc Dinh - Linear recursive schemes associated with some nonlinear partial differential equations in one dimension and the Tau method. SIAM J. on Math. Analysis 18(1987) pp.452-464
[7] E.L.Ortiz and H.Samara - Numerical solution of partial differential equations with variable coefficients with an operational approach to the Tau method . Comp.Math.Appls.10(1984) pp.5-13
[8] A.Pham Ngoc Dinh and Nguyễn Thanh Long - Linear approximation and asymptotic expansion associated to the nonlinear wave equation in 1 dim. Demostratio Mathematica 19(1986) pp.45-63
[9] G.F.Webb - Existence and asymptotic behavior for a strongly damped nonlinear wave equation .Can.J.Math.32(1980) pp.631-643

The Cauchy problem in three-dimensional thermoelasticity

Reinhard Racke

Institut für Angewandte Mathematik der Universität Bonn
Wegelerstr. 10 , D-5300 Bonn

We consider the Cauchy problem in three-dimensional nonlinear thermoelasticity for a medium which is homogeneous and initially isotropic. The governing equations for the displacement vector U and the temperature difference θ represent a hyperbolic-parabolic coupled system. The interesting question which arises is if the behaviour will be dominated by the hyperbolic part - mainly equations for U plus coupling terms - or by the parabolic one - mainly an equation for θ plus coupling terms. In the case of pure elasticity one knows that there exist global smooth solutions for small data if the nonlinearity degenerates up to order 2 (see (4) below) (cf. [K]). In the genuine nonlinear case there occurs a blow up for sufficiently small radially symmetric data with compact support (cf. [Jo]. This raises the question wether the dissipation effect induced by the internal damping through heat conduction is strong enough to prevent smooth solutions from blowing up for large data or at least for small data.

For a one-dimensional model the latter is true as was shown in [Z&S], cf. also the similar result for the initial boundary value problem in [S]. For large data already in one dimension a blow up occurs as was proved in [D&H].

The one-dimensional behaviour is dominated by the heat conduction equation in some sense which elucidates these results, e.g. no transversal waves can appear. In higher dimension the behaviour relies on conjectures up to now which stress the influence of the hyperbolic part.

Our contribution in this lecture will be to demonstrate that global smooth solutions exist for small data if the nonlinearity degenerates up to order 2. The method of proof is based on that developed by S. Klainerman and G. Ponce (cf. [K&P], [Po], similarly by J. Shatah [Sh]) and simultaneously yields the time-asymptotic behaviour and the scattering behaviour of the solution. More precisely we show the following:
The system for the displacement U and the temperature difference reads as follows:

$$(1)\quad \frac{\partial^2 U_i}{\partial t^2} = \sum_{m,j,k=1}^{3} C_{i,m,j,k}(\nabla U,\theta)\,\frac{\partial^2 U_j}{\partial x_m \partial x_k} + \sum_{m=1}^{3} \tilde{C}_{im}(\nabla U,\theta)\,\frac{\partial \theta}{\partial x_m}\,,\quad i=1,2,3$$

(2) $a(\nabla U,\theta)\frac{\partial\theta}{\partial t} = \frac{1}{f(\theta)}\operatorname{div} q(\nabla U,\theta,\nabla\theta) + \operatorname{tr}((\tilde{C}_{im}(\nabla U,\theta))_{i,m}\cdot(\frac{\partial}{\partial t}\frac{\partial U}{\partial x_m})_{i,m})$

(3) $U(t=0) = U^0,\ \frac{\partial U}{\partial t}(t=0) = U^1,\ \theta(t=0) = \theta^0$,

with known coefficients C_{imjk}, $\tilde{C}_{im}$, a, f, q and data U^0, U^1, θ^0. The nonlinearity shall degenerate up to order 2 near the origin, e.g.

(4) $|C_{imjk}(\nabla U,\theta) - C_{imjk}(0,0)| = O(|\nabla U|^2 + |\theta|^2)$

(and similar for the remaining terms). Then we prove under the assumption (4):

Theorem : *There are integers* s_0, s_1, s_2 *and a* $\delta > 0$ *such that if*

$$(SDU^0,\ U^1,\ \theta^0) \in W^{s_0,2}\cap W^{s_1,6}$$

with

$$\|(SDU^0,\ U^1,\ \theta^0)\|_{s_0,} + \|(SDU^0,\ U^1,\ \theta^0\|_{s_2,6/5} < \delta\ ,$$

there exists a unique smooth solution (U,θ) *of (1), (2), (3) with*

$$SDU,\ \frac{\partial U}{\partial t} \in C_1([0,\infty],\ W^{s_0-1,2}\cap C_0([0,\infty),\ W^{s_0,2})\ ,$$

$$\theta \in C_1([0,\infty],\ W^{s_0-2,2})\cap C_0([0,\infty),\ W^{s_0,2})\ ,$$

and

$$\|(SDU,\ \frac{\partial}{\partial t}\ U,\ \theta)(t)\|_{s_1,6} = O(t^{-2/3}) = \|(SDU,\ \frac{\partial}{\partial t}\ U,\ \theta)\|_\infty\ ,$$

$$\|(SDU,\ \frac{\partial}{\partial t},\ \theta)(t)\|_{s_0,2} = O(1) \quad as\ t\to\infty.$$

(SDU are certain combinations of first-order derivatives of U). Moreover there is a solution $(U_\infty,\ \theta_\infty)$ *of the associated linear problem for data* $(U^0_\infty,\ U^1_\infty,\ \theta^0_\infty)$ *such that the scattering behaviour is described by*

$$\lim_{t\to\infty}\|(SDU,\ \frac{\partial t}{\partial t},\ \theta)(t) - (SDU_\infty,\ \frac{\partial U_\infty}{\partial t},\ \theta_\infty)(t)\|_{s_1,6} = 0$$

$$= \lim_{t\to\infty}\|(SDU,\ \frac{\partial U}{\partial t},\ \theta)(t) - (SDU_\infty,\ \frac{\partial U_\infty}{\partial t},\ \theta_\infty)(t)\|_{\infty,0}$$

The method of proof is the following:

1. A suitable transformation to a first-order system is given:

   $V_t + AV_t = \tilde{F}(V,\nabla V,\ \nabla^2 V)$, $V(0) = V^0$, where $-A$, being a differential operator with constant coefficients, generates a contraction semigroup.

   (4) will imply:

   (5) $|\tilde{F}(W)| = O(|W|^3)$ near the origin.

2. The time-decay of the associated linear problem is analyzed and it is proved that

(6) $\|V(t)\|_{q,\sigma} \leq \text{const}(1+t)^{-(1-2/q)} \|V^0\|_{N_p,p}$, $\frac{1}{q} + \frac{1}{p} = 1$, $q \geq 2$.

3. A local existence result for (1), (2), (3) in $W^{s,2}$-spaces is yielded by S. Kawashima [Ka].

4. A high energy estimate of the type

(7) $\|V(t)\|_{s,2} \leq \text{const } \|V^0\|_{s,2} \cdot \exp \int_0^t (\|V\|_\infty^2 + \|V_t\|_\infty^2 + \|\nabla V\|_\infty^2 + \|\nabla^2 V\|_\infty^2)$

is proved as well as

5. a weighted a priori-estimate:

$\sup_{0\leq t\leq T} (1+t)^{2/3} \|V(t)\|_{s_1,6} \leq M_0 < \infty$, M_0 being independent of T, for small ($\|V^0\|_{s_2,6/5} + \|V^0\|_{s_0,2}$).

6. This yields an a-priori-estimate for $\|V(t)\|_{s_0,2}$ and thus allows to apply the usual continution argument.

The procedure indicated above has been developed and succesfully applied by S. Klainerman and G. Ponce (cf. [K&P], [Po], similarly in [Sh]) e.g. for nonlinear wave equations, nonlinear heat equations, nonlinear Schrödinger equations or the equations of compressible viscous and heat-conductive fluids. This works whenever one has sufficiently strong estimates in 1. and 2. - especially a semigroup structure of the solutions of the linear problems - and of course a local existence theorem.

The lecture is organized as follows: In section 1 we give a short derivation of the equations, section 2 presents the formulation as a first-order system (which is in some sense crucial), section 3 presents the main theorems. In section 4 the time-decay of the associated linear problem is analyzed and in section 5 we prove the main theorems.

References:

[D&H] Dafermos, C.M., Hsiao, L.: Development of singularities in solutions of the equations of nonlinear thermoelasticity. Quart. Appl. Math. 41 (1986), 463-474.

[Jo] John, F.: Formation of singularities on elastic waves. Trends and Applications of Pure Mathematics to Mechanics. Proceedings Palaiseau (1983). Ed. P.G. Ciarlet, M. Roseau, Lec. Notes Phys. 195 (1983), 194-210.

[Ka] Kawashima, S.: Systems of a hyperbolic-parabolic composite type, with applications to the equations of magnetohydrodynamics. Thesis: Kyoto University (1983).

[Kl] Klainerman, S.: Long-time behavior of solutions to nonlinear evolution equations. Arch. Rat. Mech. Anal. 78 (1982), 73-98.

[K&P] Klainerman, S., Ponce, G.: Global, small amplitude solutions to nonlinear evoultion equations. Comm. Pure Appl. Math. 36 (1983), 133- 141.

[Po] Ponce, G.: Global existence of small solutions to a class of nonlinear evolution equations. Nonlinear Anal. T.M.A. 9 (1985), 399-418.

[Sh] Shatah, J.: Global existence of small solutions to nonlinear evolution equations. J. Diff. Equ. 46 (1982), 409-425.

[Sl] Slemrod, M.: Global existence , uniqueness, and asymptotic stability of classical smooth solutions in one-dimensional non-linear thermoelasticity. Arch. Rat. Mech. Anal. 76 (1981), 97-134.

[Z&S] Zheng, S, Shen, W.: Global solutions to the Cauchy problem of a class of quasilinear hyperbolic parabolic systems. Submitted to: Scientia Sinica.

ON THE POSSIBILITY AND THE STRUCTURE OF OSCILLATING SOLUTIONS TO SOME NONLINEAR SYSTEMS OF CONSERVATION LAWS.

Michel RASCLE
Département de Mathématiques,Université de Nice,Parc Valrose
06034 NICE CEDEX,FRANCE

We study the structure of the Young's measure associated to a sequence of approximate solutions to some 2x2 hyperbolic systems of conservation laws.This family of probability measures,which depend on x,t describes the possible oscillations which can (or can't) propagate.We show that oscillations can't propagate except if the system is linearly degenerate,and that even in this case,no oscillation can develop if it was not present in the initial data.This study uses(and is in the spirit of)previous results of R.DI PERNA,M.RASCLE,D. SERRE AND L.TARTAR.

A NUMERICAL SCHEME FOR COMPUTING HYPERSONIC VISCOUS FLOWS ON UNSTRUCTURED MESHES.

Philippe ROSTAND * and Bruno STOUFFLET **

* INRIA-MENUSIN Domaine de Voluceau Rocquencourt BP 105 78153 Le Chesnay Cedex FRANCE
** AMD-BA 78 Quai Marcel Dassault 92214 Saint Cloud FRANCE

Computing hypersonic viscous flows requires both oscillation-free,for strong shock-capturing,and accurate,for boundary layer representation,approximation of the Navier Stokes equations.The use of second order upwind schemes for the convective part,combined with centerly discretized diffusive terms,seem to be a good approach,although added visosity must be carefully controlled. In a recent paper,Van Leer et al [1] showed the influence of the choice of the numerical flux formula on the added diffusion.

We derive here an extension of an existing code for inviscid gas,based on approximate Riemann solvers on unstructured meshes (see [2]),to the case of viscous fluids.We analyse the slope limiting procedure in terms of added viscosity, our goal beeing to take into account in its definition the physical diffusion.

1 Spatial Approximation

Our scheme relies on a finite volume formulation,using unstructured triangular (tetrahedral) meshes.We upwind the convection terms through Osher's Riemann solver (see[3]),extended to second order by a MUSCL type method (see[4] for the MUSCL method,[2] for its extension to unstructured meshes).We give the formulation in two dimensions for simplicity. The adimensionalized Navier-Stokes equations are :

$$\frac{\partial \rho}{\partial t} + div(\rho u) = 0 \tag{1}$$

$$\frac{\partial (\rho u)}{\partial t} + div(\rho u \otimes u) + \nabla P = \frac{1}{Re} div(D(u)) \tag{2}$$

$$\frac{\partial E}{\partial t} + div((E+P)u) = \frac{1}{Re}(div(u(D(u)) + \frac{\gamma}{Pr}\Delta T) \tag{3}$$

where: ρ is the density, u $\in R^2$ is the speed , E is the total energy , $D(u) = \nabla u + \nabla u^t$ - $\frac{2}{3}\nabla$.u I , T = $\frac{E}{\rho} - \frac{1}{2}u^2$ is the internal energy, P = $(\gamma - 1)\rho T$ is the pressure , Re is the Reynolds number , Pr is the Prandtl number ,

with boundary conditions: on a wall

$$u = 0 \quad , \quad T = T_{wall} \tag{4}$$

at infinity :

$$u = (cos\alpha, sin\alpha) \quad , \quad \rho = 1 \quad , \quad T = \frac{1}{\gamma(\gamma-1)M_\infty^2} \tag{5}$$

where M_∞ is the free stream mach number and α the angle of attack .

In fact, we enforce the four boundary conditions (5) at the inflow,but only three of them at the outflow in the supersonic case.

We denote by F^c the convection flux,by F^d the diffusion flux,so that the Navier Stokes equations are:

$$\frac{\partial W}{\partial t} + div(F^c(W)) + div(F^d(W)) = 0 \tag{6}$$

where W is the vector of the conservation variables.

We take a piecewise linear (P1) approximation of the conservation variables,and use control volumes (cells) limited by the medians of the triangles.

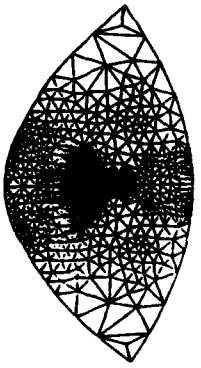

example of the unstructured meshes used

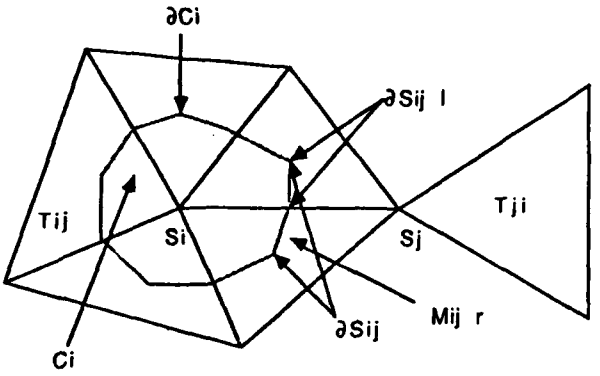

definition of the geometrical quantities

For every vertex S_i,we define the cell C_i surrounding it, ∂C_i its boundary, K(i) the set of the neighboring nodes, ν_i the outward unit normal to ∂C_i ; for j∈ K(i),we define T_{ij} and T_{ji} the downstream and upstream triangles of S_iS_j, ∂S_{ij} the segment of ∂C_i separating S_i from S_j, ∂S_{ij}^r its right half, ∂S_{ij}^l its left half, M_{ij}^r the middle of ∂S_{ij}^r, M_{ij}^l the middle of ∂S_{ij}^l, $t_{ij}$the set of triangles containing both S_i and S_j , $F_{ij}^c(W)$, $F_{ij}^{dr}(W)$, $F_{ij}^{dl}(W)$ by

$$F_{ij}^c(W) = F^c(W).\int_{\partial S_{ij}} \nu_i dl \quad , \quad F_{ij}^{dr}(W) = F^d(W).\int_{\partial S_{ij}^r} \nu_i dl \quad , \quad F_{ij}^{dl}(W) = F^d(W).\int_{\partial S_{ij}^l} \nu_i dl$$

W_{ij} and W_{ij} by

$$W_{ij} = W_i + \frac{s_i}{4}((1-\kappa)\nabla_{ij}W + (1+\kappa)\nabla W).S_iS_j$$

$$W_{ji} = W_j - \frac{s_j}{4}((1-\kappa)\nabla_{ji}W + (1+\kappa)\nabla W).S_iS_j$$

where $\nabla_{ij}W$ and $\nabla_{ji}W$ are the gradients of W on T_{ij} and T_{ji} while ∇W is the gradient on the triangles containing both S_i and S_j, $\kappa \in [-1,1]$,s_i and s_j are the slope limiters,$s \in [0,1]$, s_i (resp.s_j) is a decreasing function of $|\nabla_{ij}W - \nabla W|$, (resp.$|\nabla_{ji}W - \nabla W|$).

Osher's flux is defined by:

$$\Phi_{F_{ij}^c}^{OSHER}(U,V) = \frac{F_{ij}^c(U) + F_{ij}^c(V)}{2} - \frac{1}{2}\int_U^V |F_{ij}^{c'}(W)|dW \tag{7}$$

The finite volume formulation is:

$$Area(C_i)\frac{\partial W_i}{\partial t} + \Sigma_{j\in K(i)}\Phi_{F_{ij}^c}^{OSHER}(W_{ij},W_{ji}) + \Sigma_{j\in K(i)}(F_{ij}^{dl}(W(M_{ij}^l)) + F_{ij}^{dr}(W(M_{ij}^r))) = 0 \tag{8}$$

2 Relation with Finite Elements and error analysis

To examine what numerical viscosity is produced,we apply this discretization to a linear advection diffusion equation:

$$\frac{\partial W}{\partial t} + A\frac{\partial W}{\partial x} + B\frac{\partial W}{\partial y} - \nu\Delta W = 0 \tag{9}$$

+ boundary and initial conditions.

It is easy to check that that a centered finite volume scheme,namely the preceeding formulation with κ=1 and s=1,is strictly equivalent to the P1 centered Galerkin approximation,which is well known to be second order accurate for this parabolic equation.So we can symbolically write our scheme as:

$$F.V. = F.E.M. + R$$

with:

$$R = \Sigma_{j \in K(i)} [\Pi_{ij}^{+} (\frac{1-\kappa}{4} s_i (\nabla_{ij} W - \nabla W) + \frac{s_i - 1}{2} \nabla W).S_i S_j$$

$$+ \Pi_{ij}^{-} (\frac{1-\kappa}{4} s_j (\nabla_{ji} W - \nabla W) + \frac{s_j - 1}{2} \nabla W).S_i S_j] \quad (10)$$

with $\Pi_{ij} = (\int_{\partial S_{ij}} \nu_{ix} dl) \quad A + (\int_{\partial S_{ij}} \nu_{iy} dl) \quad B$

and $\Pi_{ij}^{+} = \frac{\Pi_{ij} + |\Pi_{ij}|}{2} \qquad \Pi_{ij}^{-} = -\frac{\Pi_{ij} - |\Pi_{ij}|}{2}$

We analyze this remaining term, to isolate the added viscosity as a function of the slope limiters,and consequently to chose the most adapted limiting procedure,in a way similar to that defined by Hughes and Mallet in [5].

3 Time discretization

A classical Fourrier analysis on the linear equation (9) shows that the stability of an explicit scheme requires that $\Delta t \leq \frac{\alpha \Delta x^2}{\nu + (U+C)\Delta x}$, α beeing a constant lower than 1.This condition can be very restrictive for fine meshes.

For this reason,we introduce an implicit linearized algorithm,defined in [2] for the inviscid case,and extended here to the Navier Stokes equations. If R is the discrete non linear operator associated to the steady Navier Stokes equation,and M an approximate jacobian of R,the scheme is:

$$(I + \Delta t M)(W_h^{n+1} - W_h^n) = -\Delta t R(W_h^n) \quad (11)$$

4 Numerical results

We first compare our scheme with a centered Galerkin like code with no artificial viscosity [6], on a weakly transonic flow over a Naca 0012 airfoil (Mach = 0.85 , Re = 500).The use of the implicit scheme divides the needed cpu time by more than 8 on an IBM 3090.We present the comparison of the skin friction and drag coefficients.

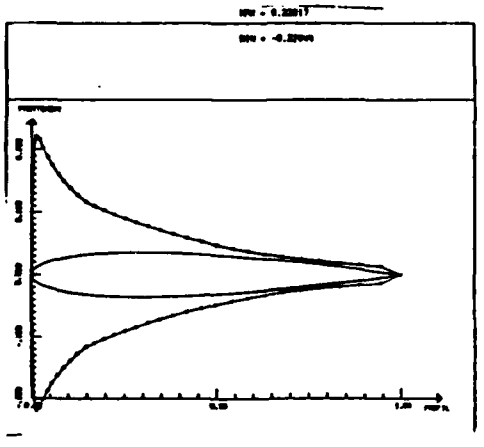

centered F.E.M. code : CD = 0.214

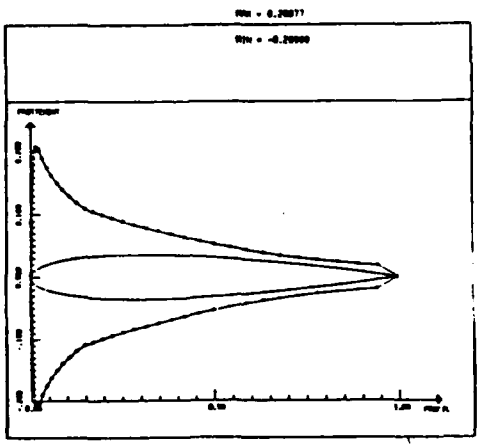

upwind F.V. code:CD = 0.226

Flow over a cylinder : Mach = 8 , Re = 1000.

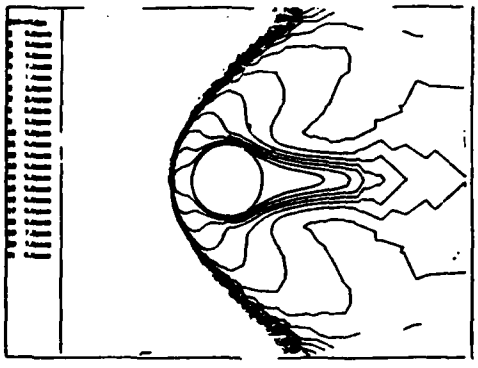

Iso Mach lines

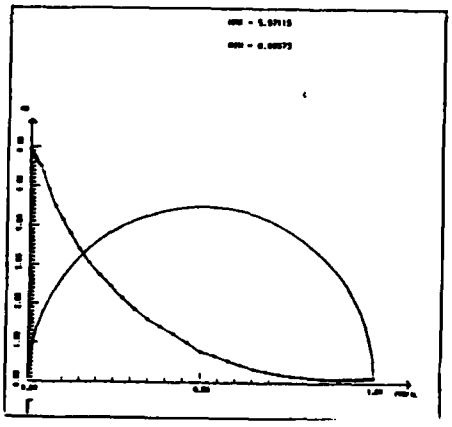

density on the body

Flow over an ellipse : Mach = 20 , Re = 1000.

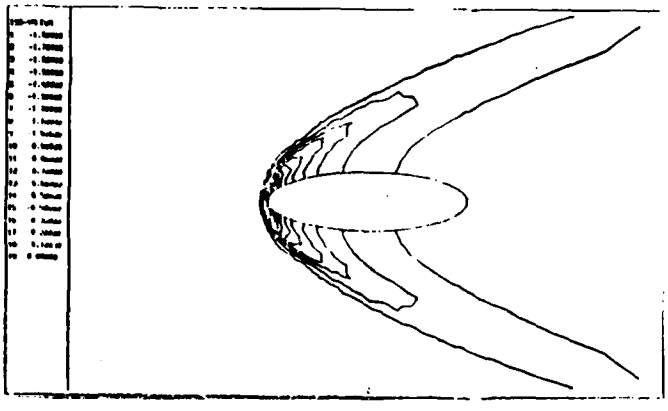

Pressure contours

References :

[1] B.Van Leer,J.L.Thomas,P.L.Roe,R.W.Newsome,A Comparison of Numerical Flux Formulas for the Euler and Navier Stokes Equations,proceedings of the AIAA Honolulu meeting,1987,p 36-41.

[2] B. Stoufflet,J.Periaux,L.Fezzoui,A.Dervieux,Numerical Simulations of 3-D Hypersonic Euler Flows Around Space Vehicles Using Adapted Finite Elements ,AIAA paper 87 0560 Reno 1987.

[3] S.Osher,S.Chakravarthy,Upwind difference schemes for the hyperbolic systems of conservation laws, Mathematics of Computation,April 1982.

[4] B.Van Leer,Computational Methods for Ideal Compressible Flow,Von Karman Institute for fluid dynamics,lecture series 1983-04,Computational Fluid Dynamics, March 7-11 1983.

[5] T.J.R.Hughes,M.Mallet,A New Finite Elements Formulation for Computational Fluid Dynamics:III The Generalized Streamline Operator for Multidimensional Advective-Diffusive Systems,Computer Methods in Applied Mechanics and Engineering,n_o 58,1986,p 305-328.

[6] F.Angrand,Numerical Simulations of Compressible Navier Stokes Flows , GAMM Workshop , M.O.Bristeau R.Glowinski, J.Periaux , H.Viviand (eds),Friedr. Vieweg und Sohn,1987,p 69-85.

A NEW NUMERICAL TECHNIQUE FOR INTEGRATING THE NAVIER-STOKES EQUATIONS

B.L.Rozhdestvensky and M.I.Stoynov
Keldysh Institute of Applied Mathematics
USSR Academy of Sciences
Miusskaya sq., 4
Moscow 125047
USSR

The incompressible viscous fluid flows are described by solutions of the Navier-Stokes equations, and the incompressible inviscid fluid flows by solutions of the Euler equations. The both systems of equations are not of a hyperbolic type. Nevertheless these models are used to describe approximately the poorly compressible "inviscid" fluid or gas flows.

In this report a new numerical technique is considered for integrating some boundary value problems involving the Navier-Stokes equations and suitable for simulating the 3D nonstationary incompressible low-viscosity fluid flows (including turbulent) flows. For correct simulation of turbulent flows the technique used must satisfy the following very stringent requirements:

(a) the solutions allowed by the numerical algorithms must describe sufficiently accurately the time evolution of small perturbations of stationary flow regimes (stationary flows, pulsating flows, etc.);

(b) the algorithms must have the conservativeness property: the allowed solutions must satisfy the discrete analogs of the mass, impulse and energy conservation laws.

The computation experience shows that unsatisfaction of conditions (a) and (b) may lead to the abrupt growth of solutions and overfilling of the CPU or to incorrect simulation of turbulence.

The numerical technique was constructed for simulating the fluid flows in an infinite plane channel $K = \{(x,y,z) : (x,y) \in R^2, |z| \leq 1\}$ with fixed walls – the planes $z = \pm 1$.

The Galerkin method and trigonometrical polynomials are used for a spatial discretization of the problem with respect to the variables x, y (the flow velocity field is approximated by the functions with a finite number of degrees of freedom). The collocation method and the Jacobi polynomials are used for the problem discretization with respect to the variable z.

For the time discretization the implicit second order Crank-Nicolson type scheme is employed. It was shown that the integration scheme obtained in the linear approximation is absolutely stable and the discrete analogs of the nonlinear conservation laws are satisfied. From the energy conservation law analog it follows that the scheme has the so called "nonlinear stability" property.

The technique described was used to carry out a considerable number of computations of **2D and 3D laminar and turbulent flows. The turbulent Poiseuille flows, the pulsating turbulent** flows and the Couette flows in a plane channel were simulated. The computations showed a high efficiency and reliability of the technique proposed.

The results and the scheme properties are discussed, and the possibilities of using the technique for computations of compressible media, both viscous and inviscid are considered.

APPENDIX

In our algorithm the approximate fluid velocity $\vec{V}(t,x,y,z)$ is represented in the form

$$\vec{V}(t,x,y,z) = (1-z)^2 \sum_{m=-M}^{M} \sum_{n=-N}^{N} \sum_{q=0}^{Q} \vec{V}_{m,n,q}(t) \cdot P_q^{(1,1)}(z) \exp\{im\alpha_0 x + in\beta_0 y\} ,$$

where $\vec{V}_{-m,-n,q}(t)$ are complex-conjugate to $\vec{V}_{m,n,q}(t)$ and $P_q^{(1,1)}(z)$ are Jacobi's polynomials. This representation is used for spatial discretization of the problem.

The numerical scheme for time advancement of the Crank-Nicolson type is

$$(\vec{V}^{j+1} - \vec{V}^{j})/\tau = -\nabla p^{j+1/2} + \nu\Delta\vec{V}^{j+1/2} + \vec{F}(\vec{V}^{j+1/2}) ,$$

$$\text{where } \vec{V}^{j+1/2} = 0.5 \cdot (\vec{V}^{j+1} + \vec{V}^{j}) , \; p^{j+1/2} = 0.5 \cdot (p^{j+1} + p^{j}) ,$$

$$\vec{V}^{j} = \vec{V}(j\tau, x, y, z) \qquad \text{and } \vec{F}(\vec{V}) = -(\vec{V}\nabla)\vec{V}$$

are the nonlinear terms of the Navier-Stokes eqns. This implicit scheme is solved by iteration method.

The Discrete Shock Waves in Numerical Solutions of Hyperbolic Problems

V.V. Rusanov
Keldysh Institute of Applied Mathematics
USSR Academy of Sciences
Moscow, USSR

Consider the hyperbolic system

$$u_t + [F(u)]_x = 0, \quad u = \{u_1, u_2, \ldots, u_r\}^T, \quad F(u) = \{F_1, F_2, \ldots, F_r\}^T \tag{1}$$

where vector-function $F(u)$ is such that the system of equations

$$F(u) - D\,u = F(u^{(1)}) - D\,u^{(1)} \tag{2}$$

has for vector u besides $u = u^{(1)}$ one and only one other solution $u = u^{(2)}$ if

$$\mathrm{Det}\,\{F'(u) - D \cdot E\}_{u=u^{(1)}}, \quad F'(u) = \frac{dF}{du}, \quad E = \{\delta_i^k\}_{i,k=1}^r$$

For (1) we consider the difference scheme on a floating grid with steps $\triangle x = h$ and $\triangle t = \tau$, $\kappa = \tau/h$

$$\begin{gathered} u_x^{n+1} = u_x^n - \frac{\kappa}{2}\left[F(u_{x+h}^n) - F(u_{x-h}^n)\right] + \phi_{x+h/2}^n - \phi_{x-h/2}^n \\ u_x^n = u^n(x), \quad \phi_{x+h/2}^n = \Omega\left(\sigma_{x+h/2}\right)\left(u_{x+h}^n - u_x^n\right)/2 \\ \sigma_{x+h/2} = \kappa\, F'\left(u_{x+h/2}\right) \qquad u_{x+h/2} = (u_{x+h} + u_x)/2 \end{gathered} \tag{3}$$

Let u^-,u^+ and D satisfy the Hugoniot conditions

$$F(u^+) - F(u^-) = D(u^+ - u^-), \quad \kappa\, D = \delta$$

A discrete stationary shock wave DSW is the vector-function which satisfies the equations:

$$\begin{gathered} v_{x-\delta h} = v_x - \frac{\kappa}{2}\left[F\left(v_{x+h}\right) - F\left(v_{x-h}\right)\right] + \phi_{x+h/2} - \phi_{x-h/2} \\ \phi_{x+h/2} = \Omega\left(\sigma_{x+h/2}\right)\left(v_{x+h} - v_x\right)/2 \\ \sigma_{x+h/2} = \kappa\, F'\left(v_{x+h/2}\right) \end{gathered} \tag{4}$$

and the boundary conditions

$$\lim_{x \to \pm\infty} v_x = u^{\pm} \tag{5}$$

The problem is to find the function v_x and study its properties. In this communication the solution of this problem is considered for a rational value $\delta = p/q$ and some special vector-function $F(u)$.

Assuming without loss of generality $h = q$ we fix a certain value of $x = x_0$. Then the points $x_l = x_0 + l$ where l is any integer, form a grid, and v_{x_0+l} are values of a grid function $w_l(x_0)$ on this grid. We obtain for $w_l(x_0)$ the system of an infinite number of nonlinear difference equations:

$$
\begin{aligned}
w_{l-p} &= w_l - \frac{\kappa}{2}\left[F(w_{l+q}) - F(w_{l-q})\right] + \phi_{l+q/2} - \phi_{l-q/2} \\
\phi_{l+q/2} &= \Omega\left(\sigma_{l+q/2}\right)\left(w_{l+q} - w_l\right)/2
\end{aligned}
\tag{6}
$$

If (4) has a continuous solution on the interval $(-\infty, +\infty)$ then (6) should have an one-parameter family of solutions $w_l(x_0)$ such that $w_l(x_0 + 1) = w_{l+1}(x_0)$. The existence of the solution of (6) is proved for the scalar equation (1) and for the monotonic scheme [1]. Numerical experiments show that in scalar case system (6) has a solution for a nonmonotonic scheme too. In this case the grid function w_l is also nonmonotonic. It proves that for a special function $F(w)$ system (6) is equivalent to a nonlinear system with a finite number of unknowns and for that system the direct method of solution may be shown applicable to both monotonic and nonmonotonic schemes.

Consider the scalar equation (1) and determine $F(w)$ as

$$
F(w) = \begin{cases} g^- w + f^- & |w - w^-| \le \varepsilon_L \\ G(w) & \{|w - w^-| > \varepsilon_L \quad \wedge \quad |w - w^+| > \varepsilon_R\} \\ g^+ w + f^+ & |w - w^+| \le \varepsilon_R \end{cases}
$$

where ε_L, ε_R are some small numbers.

By assuming the existence of w_l satisfying (6) and the boundary conditions at $\pm\infty$, we obtain that there exist l_L and l_R such that $|w_l - w^-| \le \varepsilon_L$ for $l \le l_L$, $|w_l - w^+| \le \varepsilon_R$ for $l \ge l_R$. Then for $l \le l_L - q$ and $l \ge l_R + q$ we have, respectively,

$$
\begin{aligned}
w_{l-p} &= a^{\pm} w_{l+q} + b^{\pm} w_l + c^{\pm} w_{l-1}, \\
a^{\pm} &= (w^{\pm} - \sigma^{\pm})/2, \quad b^{\pm} = 1 - w^{\pm}, \quad c^{\pm} = (w^{\pm} + \sigma^{\pm})/2
\end{aligned}
\tag{7}
$$

where $w^{\pm} = \Omega(\sigma^{\pm})$, $\sigma^{\pm} = \kappa\, g^{\pm}$. The sign $-$ stands for $l \le l_l - q$ and the sign $+$ for $l \ge l_R + q$.

A general solution of (7) may be written in the form

$$
w_l^{\pm} = \sum_{k=1}^{K^{\pm}} A_k^{\pm} \left(\xi_k^{\pm}\right)^l + w^{\pm} \tag{8}
$$

where $\xi_k^{\pm}$ are roots of the equations

$$
\xi^{q-p} = a^{\pm}\xi^{2q} + b^{\pm}\xi^q + c^{\pm} \tag{9}
$$

For the simplicity of presentation only we suppose that $a^{\pm} \neq 0$ and $c^{\pm} \neq 0$. Only the $\xi_k^{\pm}$ satiesfying the conditions $|\xi_k^+| < 1$, $|\xi_k^-| > 1$ should be included in (8).

Analysing equation (9) and applying the Kreiss theorem [2] enable us to find that there are exactly $q - p = K^+$ roots of $|\xi_k^+| < 1$ and exactly $q + p = K^-$ roots of $|\xi_k^-| > 1$.

Now we consider the equations of system (6) for l from $l_L - q + 1$ to $l_R + q - 1$, and call this set of equations the system S_0. We add to S_0 equations (9) namely the S_+ with the sign $-$ for $l_L - 2q + 1 \le l \le l_L$ and the S_- with $+$ for $l_R \le l \le l_R + 2q - 1$. We obtain a system S of $l_R - l_L + 2q - 1$ equations for the same number of unknowns $w_{l_L+1}, \ldots, w_{l_R-1}$, $A_1^-, \ldots, A_{q+p}^-$, $A_1^+, \ldots, A_{q-p}^+$. A direct check shows that these equations are dependent and have an one-parametric set of solutions, as it should be.

A specific character of the system S allows rather simple algorithms for its solution providing high accuracy. A particularly simple algorithm may be obtained if $q - p = 1$. In this case there is only one root ξ_1^+ and the coefficient A_1^+ may be taken as a parameter. By giving it we may successively calculate from right to left all by using equations (6), and then calculate A_k^- from (8).

In a general case the quantity α_w determining 'the middle point' of the profile may be taken as a parameter [1].

Let $\alpha^\lambda(l_1, l_2) = \sum_{l=l_1}^{l_2}(\lambda + lq + q/2)(w_{\lambda+lq+q} - w_{\lambda+lq})$. Then $\alpha_w^\lambda = \alpha^\lambda(-\infty, \infty)$, $\lambda = 1, 2, \ldots, q$. It has been proved [3] that for the stationary solution the α_w^λ does not depend on λ. It is easy to found that

$$\alpha_w^\lambda = \sum_k A_k^- \Psi_k^-(\xi_k^-, q, \lambda) + \alpha^\lambda(l_L, l_R) + \sum_k A_k^+ \Psi_k^+(\xi_k^+, q, \lambda) \tag{10}$$

The solution of system S for given α_w could be found using the following iterative process.

1) Let the value of w_l at iteration j be w_l^j, $l_L - 2q + 1 \le l \le l_R + 2q - 1$;
2) w_l^{j+1} for these l is computed using the difference scheme (3);
3) the predicted $\tilde{A}_k^\pm$ are determined solving equations (8);
4) the value of coefficients $A_k^\pm$ are corrected using (10) for the given value of α_w and some fixed λ.

It could be shown that for non-monotonic scheme the solution of (4), (5) is not unique and (4), (5) have an infinite number of solutions. But numerical experiment shows that only one of them is stable with respect to iterative process which always converge to this solution.

The structure of the DSW for hyperbolic system is much more complicated. Instead of one equation (9) we have of them for all characteristics of equation (1). By means of the modified Kreiss theorem it is proved that the full number of roots of (9) is not $2qr$ but $2qr - (r - 1)$. The full number of equations in system S is $r\{l_R - l_L + 2q - 1\}$ and the full number of unknowns w_l and coefficients $A_k^\pm$ is $r\{l_R - l_L + 2q - 1\} - (r - 1)$. The missing $(r - 1)$ parameters arise from relative differences $\alpha_{w,j} - \alpha_{w,i}$, $i, j = 1, \ldots, r$, which correspond to the relative shifts of the profiles for different components of w_l.

Analysis of the roots $\xi_k^\pm$ for hyperbolic system shows that for all schemes (including 'monotonic' ones) the components of w are asymptotically (as $x \to \pm\infty$) non-monotonic.

References

1. V.V. Rusanov, and I.V. Bezmenov. 1981, Proceeding of the Mathematical Steklov Institute Ac.Sci.USSR, v.157, 178–190 (in Russian).
2. H.O. Kreiss. 1968, Math. Comp., v.22, 703–714.
3. V.V. Rusanov. 1975, Lecture Notes in Physics, v.35, 270–278.

On Nonstationary Shock Wave Generation in Droplet-Vapour Mixtures

Peter Schick and Klaus Hornung

Fakultät für Luft- und Raumfahrttechnik, Universität der Bundeswehr München, D-8014 Neubiberg, W.-Germany

If a piston is accelerated into a tube filled with gas, shock waves will be generated. A mixture of droplets and their own vapour will show the same behaviour, if the fraction of the liquid phase is small. But when the fraction of the droplets becomes greater, a significant shock damping may occur.

The process has been investigated numerically by a method of characteristics, simultaneously taking into account mass- momentum-, and energy transfer between the phases. The system consists of seven differential equations, describing the conservation of mass, nomentum, energy and particle number. The contribution of the droplet`s volume to the pressure terms is included. The interfacial pressure forces between the droplets and vapour are considered using the detailed description of Stuhmiller /1/. By additionally including particle-particle interaction, the set of equations shows real eigenvalues in a local linear stability analysis, according to Ramshaw and Trapp /2/.

The whole description uses dimensionless variables, normalized to the critical point and a generalized fluid model, fitted to a large class of substances by means of corresponding states arguments. The results presented here are for H_2O with an upstream state of T_o = 293 K, p_o = 20 mbar.

The piston is driven with a constant acceleration and then remains at constant velocity. The time of acceleration is 40 µs, which leads to shock formation times within up tc 100 µs for the example chosen, which compares to the value for pure gases (Oertel /3/).

As an example, the following figures show results for a final piston velocity of 1.9 c_o, where c_o ist the velocity of sound in the upstream vapour phase.

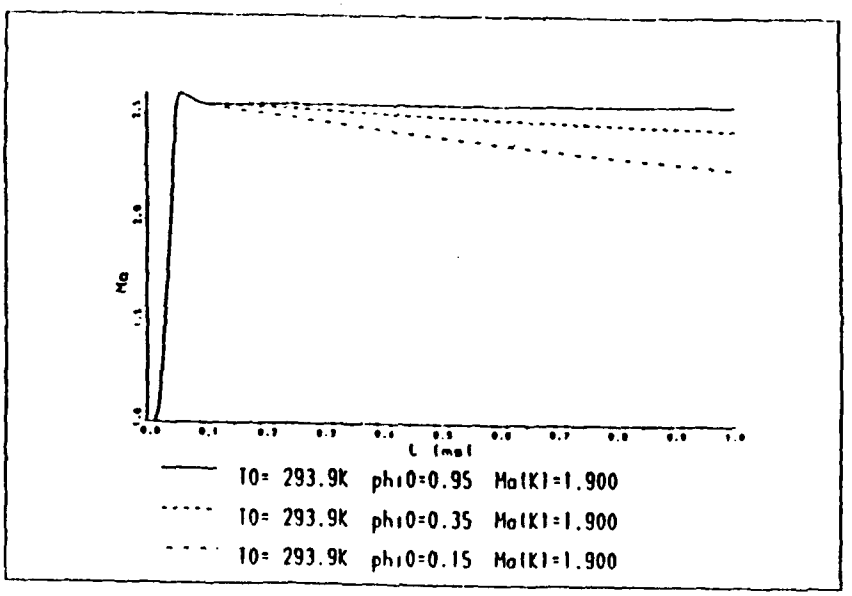

Fig. 1: Shock Mach number in dependence on time for three values of the initial vapour mass fraction.

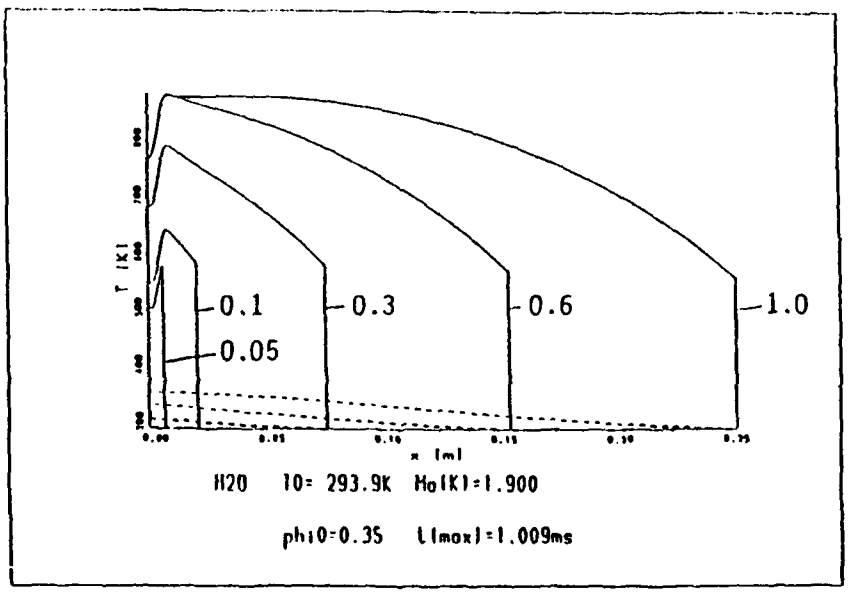

Fig. 2: Temperature profiles at different times (msec). x= 0 indicates the position of the driving piston (—— vapour ---- droplets).

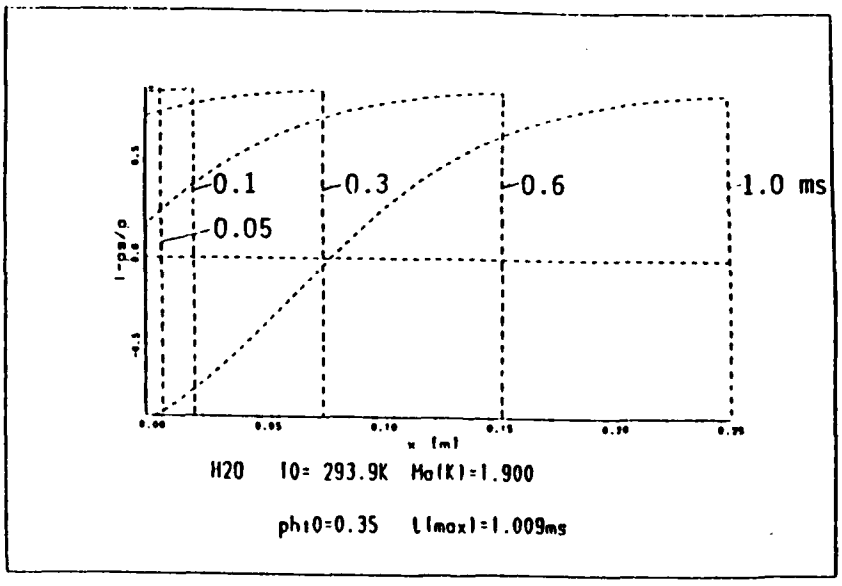

Fig. 3: Profiles of the quantity $1-p_s/p$, which indicates the direction of the mass transfer (positve: condensation, negative: vaporization, p : gas pressure, p_s: saturation pressure of the droplets).

Above an initial vapour mass fraction of 0.15, shock wave generation is not influenced by the liquid phase (Fig.1). Up to about 100 µs, shock wave propagation is the same as in a pure gas. Then the shock velocity decreases with decreasing vapour mass fraction. As the velocity of the driving piston is reduced, the shock wave propagation is influenced at earlier times. The decrease of the shock Mach number is also known for solid particle-gas mixtures (Sommerfeld /4/). For larger times, the gas temperature profiles become similar to stationary profiles (Fig. 2). For t = 1 ms, it first rises in the shock front and then increases smoothly in the relaxation zone due to the droplet-vapour frictional dissipation. At the piston it is limited by an isentropic boundary condition. Within the first 20 cm of the relaxation zone, the droplet temperature rises by condensation and related release of latent heat. Afterwards it increases by heat conduction alone (the location of condensation and evaporation regions is shown in Fig. 3). Fig. 4 shows that the velocity relaxation occurs in the same region.

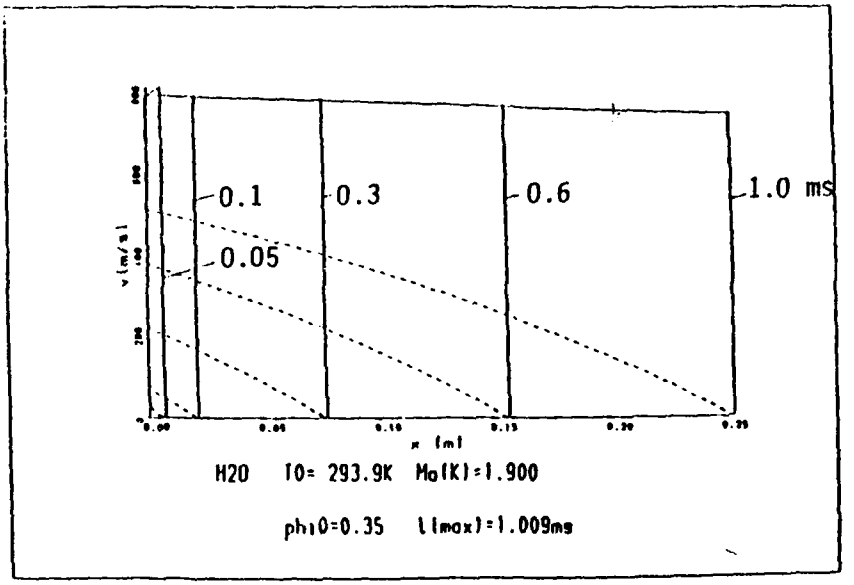

Fig. 4: Velocity profiles at different times (——— vapour, ----- droplets).

The two-phase shock problem with mass exchange has been treated previously by Marble /5/ using a stationary approach. His main results were, that the fastest process behind the shock front is condensation, followed by droplet acceleration and subsequent heating by conduction with evaporation being the slowest process. The present investigation shows that this type of wave is generated after some time. Furthermore it is an example for the simultaneous treatment of nonstationary and nonequilibrium processes in fluids.

/1/ J.H. Stuhmiller, Int. J. Multiphase Flows, 3, 551 (1977).

/2/ J.D. Ramshaw, J.A. Trapp, Nuclear Science and Eng. 66, 93 (1978).

/3/ H. Oertel, Stoßrohre, Springer (1966).

/4/ M. Sommerfeld, Experiments in Fluids 3, 197 (1985).

/5/ F.E. Marble, Astronautica Acta 14, 585 (1969).

S

NONLINEAR RESONANCE PHENOMENA FOR THE EULER - EQUATIONS COUPLED WITH CHEMICAL REACTION KINETICS

by STEFAN U. SCHÖFFEL

Mechanische Verfahrenstechnik und Strömungsmechanik

Fachbereich Maschinenwesen, Universität Kaiserslautern
Postfach 3049, D - 6750 Kaiserslautern, West Germany

Combustion phenomena occurring in jet propulsion systems, particularly in closed combustion chambers and afterburners are known to be associated with self-excited nonlinear oscillations. A particularly intimate coupling between the heat released by chemical reactions and the created pressure waves occurs for detonative combustion. The most important dynamic detonation-parameter constitutes the cell-size of a detonation limit-cycle. The detonation cell-size indicates the sensitivity of a reactive mixture to undergo a transition from a high-speed deflagration to a shock-induced detonation.

It was shown by St. Schöffel and F. Ebert in /1/ by comparison of characteristic time- and length-scales that a hyperbolic mathematical model which ignores dissipative transport processes is appropriate in order to describe the cellular, dynamic detonation structure. The detonation-dynamics may therefore be described by the gasdynamic EULER - equations together with balance-equations for the exothermic chemical reaction-kinetics.

In the last few years a wealth of papers were devoted to construction principles of monotonous, non-oscillatory, entropy-satisfying numerical methods for solving nonlinear hyperbolic conservation laws. One class of this methods are the high-resolution schemes presented first by A. Harten, which possess the so-called Total-Variation-Diminishing (TVD) property. Without additional remedies the nonlinear flux-limiters of these schemes are usually not able to prevent instabilities in the linearly degenerated field. Therefore contact-discontinuities or flame-fronts cannot be resolved accurately. Moreover symmetric TVD - schemes are in contrast to upwind-oriented methods unstable at flow stagnation points or sonic points.

The development of the cellular detonation-structure from a steady ZELDOVICH - DÖRING - V.NEUMANN equilibrium structure is according to /1/ an ill-posed problem, since the transverse wave-structure does not depend continuously on the initial ZDN - data. K.W. Morton

& R.D. Richtmyer mention in /2/, p.59 that any ill-posed initial-value problem can only be solved by an unstable difference-scheme, which is consistent with the conservation law. Fig.1 - 3 shows three-dimensional pressure distributions and corresponding contour-plots as computational results of a numerical simulation of a dynamic detonation-process in a shock-fixed, GALILEI - transformed frame of reference. The numerical scheme applied is a symmetric two-step LAX - WENDROFF - method, whose flux is modified in order to achieve the TVD - property. This scheme proves to be unstable because of sonic flow in the Chapman-Jouguet plane at the end of the reaction-zone. In contrast to all previous numerical studies of the cellular detonation - structure in a laboratory frame of reference the author of this abstract got a spontaneous development of a transverse wave-strucure in a shock-oriented coordinate system without perturbing the global reaction progress.

The cell-sizes obtained from my numerical calculation compare nicely with the values obtained from soot-tracks in Strehlow's experiments (see /1/ and /3/ for further reference).

In fig. 1-3 the condition of nonlinear resonance between the heat-release due to chemical reactions and the transverse pressure-modes is fulfilled. The number of modes in figure 1-3 is equal to 2.5 for a channel-width of 24 induction-reaction lengths.

In contrast fig.4 shows a more irregular pressur listribution for a channel-width of 34 induction-reaction lengths. In this case the mode-number is not unique and changes in the course of a number of detonation-cycles between mode 4 and mode 4.5. By holding all system-parameters as constant the author could also show that for certain channel-widths a chaotic pressure distribution developes. In the latter case no resonance could be obtained.

Conclusions:

Explosion and detonation phenomena can be modelled adequately by non-strict hyperbolic conservation laws. The consideration of reaction-chemistry results in nonlinear source-terms appearing in the balance-equations. T.-P. LIU mentioned already in /4/ (1982) that instabilities and resonance-phenomena appear, if the propa-

gation velocity of the source corresponds with one of the Eigen - values of the JACOBIAN of an hyperbolic system.
For a dynamic detonation-process the present author applied the ideas of LIU in order to derive criteria for the occurrence of nonlinear resonance phenomena.

Acknowledgement:
The work of St. Schöffel and F. Ebert is sponsored by the Deutsche Forschungsgemeinschaft in the priority research-project ´Finite Approximations in Fluid Mechanics´ since June 1984.

Literature:

/1/ St. Schöffel & F.Ebert: Numerical Analyses Concerning the Spatial Dynamics of an Initially Plane Gaseous ZDN - Detonation, 11th International Conference on Dynamics of Explosions and Reactive Systems, p. 35, Warschaw (Poland), August 3-7 (1987)

/2/ R.D. Richtmyer & K.W. Morton: Difference Methods for Initial-Value Problems, Wiley-Interscience, N.Y. (1967)

/3/ St. Schöffel & F. Ebert: A Numerical Investigation of the Reestablishment of a Quenched Gaseous Detonation in a Galilei-Transformed System, 16th. International Symposium on Shock Tubes & Waves, Aachen, July 26-30 (1987)

/4/ T.-P. LIU: Resonance for quasilinear hyperbolic equation, Bulletin Amer. Math. Soc., Vol.6, N 3, pp. 463-465 (1982)

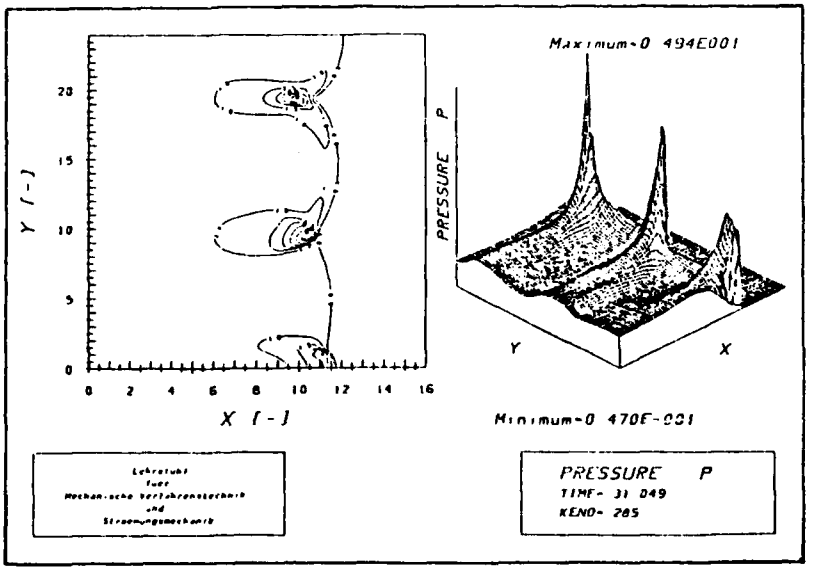

Fig. 1

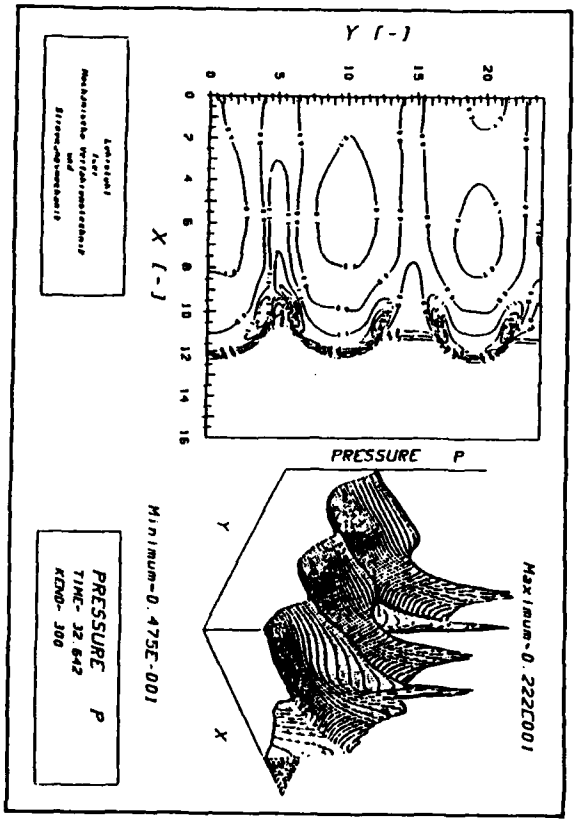

Fig. 2

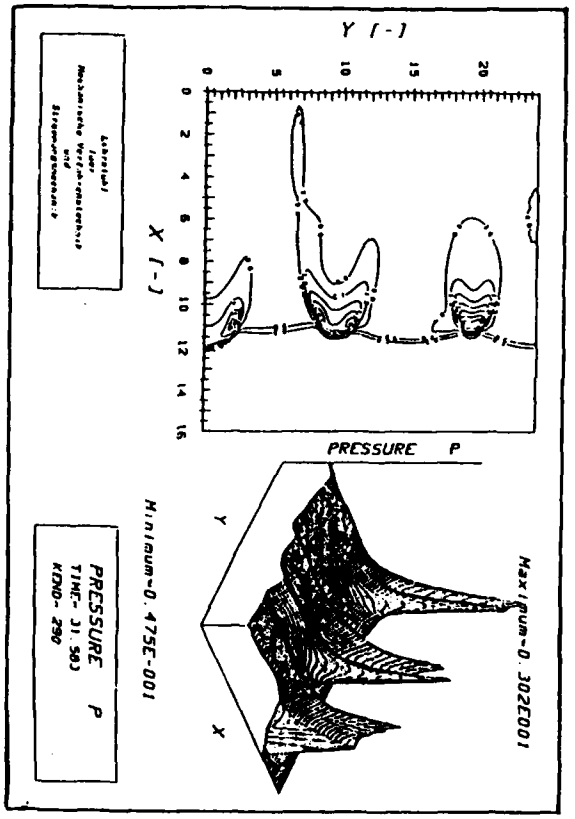

Fig. 3

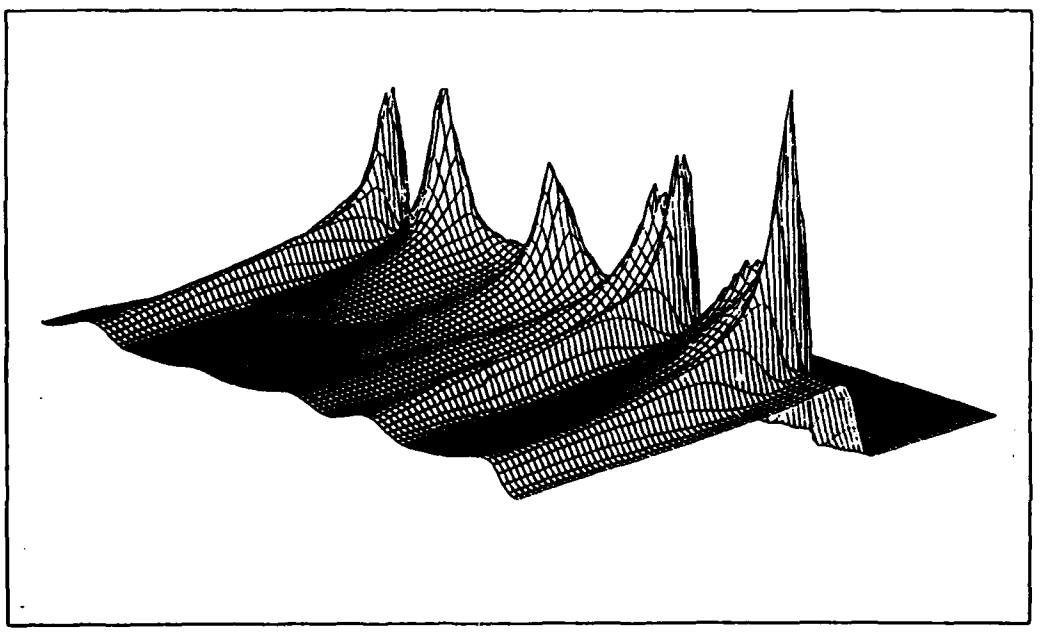

Fig. 4

Nonlinear Maxwell's equations: global existence of plane waves.

Denis Serre
Laboratoire de Mathématiques
Ecole Normale Supérieure de Lyon
46, allée d'Italie
F-69364 Lyon Cédex 07

Electromagnetism is described by means of four vector fields E, D (electric field and induction) and B, H (magnetic field and induction). Two universal laws link them, trough partial differential equations

$$B_t + \operatorname{curl} E = 0, \quad D_t - \operatorname{curl} H = 0. \tag{1}$$

For this system to be closed, one needs a so called state law, consisting on six relations. These shall depends on the material inside which the phenomena are studied. In the vacuum, these are $B = \mu_0 H$, $D = \varepsilon_0 E$. Such linear laws are rather general and are usually admitted in the most of materials. But extreme ranges may involve nonlinear relations, as in ferromagnetic materials, or in plasma physics.

Colleman and Dill[1] have given a general settling, which unify the both cases, trough the equalities

$$E_j = \partial W/\partial D_j, \quad H_j = \partial W/\partial B_j. \tag{2}$$

The function W(B, D) is the electromagnetic energy density. It is required to be a strictly convex function, which ensures that the Maxwell's system is of hyperbolic type. Moreover one recovers the Poynting's theorem, namely the conservation law for energy:

$$W_t + \operatorname{curl} E \wedge H = 0. \tag{3}$$

Actually, there are some important differences with the usual linear isotropic case. Firstable, the speed of propagation is no longer unique, nor constant. One cannot speak about *the ligth speed.* Secondly, as in gas dynamics or elasticity, shocks may develop even for analytical data. Thus the nonlinear system of Maxwell's equations lies in a class for which we do not know any global existence theorem.

Nevertheless, one can study an important simplified problem: the propagation of plane waves. The fields B and D will depend only on one space variable, and two of them six components will vanish. For such solutions, the problem reduces to four one-dimensionnal conservation laws. Our main result is that for any bounded measurable initial data, there exists a bounded solution, globaly in time. Actually, it will not satisfy (3), but the entropy inequality

$$W_t + \operatorname{curl} E \wedge H \leq 0. \tag{4}$$

This theorem is submitted to fairly reasonnable hypotheses: the energy W is assumed to depend on $r = \{B.B + D.D\}^{1/2}$, as in the linear isotropic case, and to satisfy some differential inequalities. Among the convenient state laws, one find the simplest ones:

$$W(r) = r^k, \; k > 2.$$

The plan of the proof is as follow. Firstable, the system of four equation splits into a 2x2 system and two transport equations. The first one is solved using positively invariant regions of the phase plane[2] and the compensated compactness theory[3,4].Each of these both steps needs an aforementioned differential inequality. Secondly, one write the transport equations as infinite sets of compatible conservation laws. This allows us to handle bounded measurable coefficients, given by the previous system. These infinite sets can be solved by a new idea, which unfortunately cannot be generalized to multidimensionnal transport equation.

The second of our results about the plane waves deals with the propagation of oscillations. Actually, the 2x2 sub-system does not allow such a propagation of its components, due to genuine nonlinearity, but the transport equations do. Thus, instead of the linear case, the half of the initial oscillations are killed, and the other half propagate with speeds $\pm r^{-1}W'(r)$. A fundamental consequence of this study is that the nonlinear system of plane waves is ill-posed, with respect to the weak-star topology of L^∞, the one which is involved by oscillatory data.

[1]B.D.Colleman, E.H.Dill: Z. Angw. Math. Phys. 22, (1971), p 691-702.

[2]C.Chuey, D.Conley, J.Smoller: Ind. U. Math. J. 26, (1977), p 373-392.

[3]L.Tartar: NATO Series C, n°111, (1983), J.Ball Ed., Reidel Dordrecht, Holland.

[4]R.DiPerna: Arch. Rat. Mech. Anal. 82, (1983), p 27-70.

S

The Design of Algorithms For Hypersurfaces Moving with Curvature-Dependent Speed

James Sethian
Department of Mathematics
University of California
Berkeley, California 94720

The need to follow fronts moving with curvature-dependent speed arises in the modeling of a wide class of physical phenomena, such as crystal growth, flame propagation and secondary oil recovery. In this paper, we show how to design numerical algorithms to follow a closed, non-intersecting hypersurface propagating along its normal vector field with curvature-dependent speed. The essential idea is an Eulerian formulation of the equations of motion into a Hamiton-Jacobi equation with parabolic right-hand side. This is in contrast to marker particle methods, which are rely on Lagrangian discretizations of a moving parameterized front, and suffer from instabilities, excessively small time step requirements, and difficulty in handling topological changes in the propagating front. In our new Eulerian setting, the numerical algorithms for conservation laws of hyperbolic systems may be used to solve for the propagating front. In this form, the entropy-satisfying algorithms naturally handle singularities in the propagating front, as well as complicated topological changes such as merging and breaking. We demonstrate the versatility of these new algorithms by computing the solutions of a wide variety of surface motion problems in two and three dimensions showing sharpening, breaking and merging.

I. Introduction: Equations of Motion

We wish to follow the evolution of an intial surface $\gamma(0)$ propagating along its gradient field with speed $F(K)$ a given function of the curvature K (either mean or Gaussian). The key idea, as derived in [5], is to view the evolving front $\gamma(t)$ as the level set of a higher-dimensional function ϕ. To be more precise, let the initial surface $\gamma(0)$ be a closed, non-intersecting hypersurface of dimension $N-1$. We construct the function ϕ by letting $\phi(\bar{x},0) = (1 \pm d) \quad \bar{x} \in R^N$ where g is the distance from $\bar{x}$ to $\gamma(0)$, with the plus (minus) sign chosen if $\bar{x}$ is inside (outside) $\gamma(0)$. Then, at $t=0$, the level set $\left\{ \bar{x} \mid \phi(\bar{x},0) = 1 \right\}$ gives $\gamma(0)$. We now require a time-dependent differential equation for ϕ corresponding to the evolution of $\gamma(t)$. If the family of level sets $\phi=C$, where C is a constant, flow such that each level surface propagates with speed fiven by $F(K)$, then it can be shown (see [5]), that

$$\phi_t = F(K)\,\nabla\phi \tag{1}$$

$$\phi(\bar{x},0) = \text{given}$$

Equation (1) specifies the complete intial value partial differential equation. Note that

1) ϕ is a function in $R^N x[0,\infty)\rightarrow R$, thus we have added an extra dimension to the problem.

2) At any time t, the position of the front $\gamma(t)$ is just the level set $\left\{ \bar{x} \mid \phi(\bar{x},t) = 1 \right\} = \gamma(t)$

Note that Eqn. (1) is an Eulerian formulation of the front propagation problem. Furthermore, the level surface ϕ=1 may change topology as it moves, either breaking into multiple parts or fusing together. For any fixed t, slicing ϕ by the level plane at height 1 retrieves the position of the front.

II. Hamilton-Jacobi Equations: The role of curvature as viscosity

To see the effect of curvature on a propagating front, consider a propagating closed curve in R^2 and special speed function $F(K)$=1–εK. Using the expression for the mean curvature in terms of ϕ, we substitute into Eqn. (1) to produce

$$\phi_t - H(\nabla\phi) = \varepsilon\left[\frac{\phi_{xx}\phi_y^2 - 2\phi_x\phi_y\phi_{xy} + \phi_{yy}\phi_x^2}{(\phi_x^2+\phi_y^2)^{3/2}} \right] \tag{2}$$

where $H(\nabla\phi) = (\phi_x^2+\phi_y^2)^{1/2}$. Eqn. (2) is a Hamilton-Jacobi equation with parabolic right-hand-side, which has a type of "viscosity" solution discussed in [1]. Thus, the role of curvature (εK) is to smooth propagating fronts so that sharp corners do not develop. In the limit as $\varepsilon\rightarrow 0$ (curvature term vanishes and $F(K)$=1), corners develop, and a weak solution is obtained from an appropriate entropy condition (see [6,7,8]). Thus the role of curvature in this Hamilton-Jacobi formulation for propagating fronts is identical to the the role of viscosity in hyperbolic conservation laws: it inhibits the formation of corners, that is, shocks in the tangent vector.

III. Numerical Algorithms Based on Hyperbolic Conservation Laws

Our goal is to approximate the solution to the initial value problem given in Eqn. (1). In [5], a class of non-oscillatory, upwind, entropy-satisfying algorithms of arbitrary order were given to solve this equation, based in part on ideas in [3,4]. The central idea behind these algorithms is to exploit the conservation form of theses schemes directly into the initial value Hamiton-Jacobi equation. As a motivation to

understand the scheme, consider the initial value Hamilton-Jacobi equation

$$\psi_t - F(K)(1+\psi_x^2)^{1/2} = 0 \tag{3}$$

where $x \in R$ and $\psi: R \times [0,\infty) \to R$. This is a simplified version of Eqn. (1), and applies when the propagating curve $\gamma(0)$ can be written as a function $\psi(x,t)$ for all time. Furthermore, in the simple case $F(K)=1$, we have

$$\psi_t - (1+\psi_x^2)^{1/2} = 0 \tag{4}$$

Eqn. (4) is a Hamilton-Jacobi equation. If we differentiate with respect to t, and let $u=\psi_x$, we have

$$u_t + [G(u)]_x = 0 \tag{5}$$

where $G(u) = -(1+u^2)^{1/2}$. Eqn. (5) is hyperbolic conservation law which maybe solved by a variety of methods. The key lies in an adequate numerical flux function $g_{j+1/2} = g(u_{j-p+1},.....,u_{j+q+1})$ which approximates the flix $G(u)$. Rather than differentiate the numerical flux function to achieve an approximation to Eqn. (5), we work directly with Eqn. (4) and write

$$\psi_j^{n+1} = \psi_j^n - \Delta t g \tag{6}$$

A wide class of flux functions are described in [5], leading to a collection of upwind, non-oscillatory, entropy-satisfying algorithms in several space dimensions for the original Hamilton-Jacobi initial value problem (Eqn. 1). The upwind nature of these schemes is crucial in the formulation of far-field boundary conditions. Finally, parabolic right-hand-sides (resulting from the curvature component of $F(K)$) are approximated by straight-forward central differences.

IV. Examples

A. Level Curve, Burning out, Development of Corners

We consider a seven-pointed star

$$\gamma(s) = (.1+(.065)\sin(7\cdot 2\pi s)(\cos(2\pi s),\sin(2\pi s))$$

$$s \in [0,1]$$

as the initial curve and solve the initial equations with speed function $F(K) = 1$. The computational domain is a square centered at the origin of side length 1/2. We use 300 mesh points per side and a time step

Δt=.0005.

At any time $n\Delta t$, the front is plotted by passing the discrete grid function ϕ_{ij} to a standard contour plotter and asking for the contour ϕ=1. The initial curve corresponds to the boundary of the shaded region, and the position of the front at various times is shown in Fig. 1. The smooth initial curve develops sharp corners which then open up as the front burns, asymptotically approaching a circle.

B. Level Curve, Motion Under Curvature

We consider the initial wound spiral

$$\gamma(s) = (.1e^{(-10y(s))} - (.1-x(s))/20)(\cos(a(s)), \sin(a(s)))$$

where $a(s) = 25\tan^{-1}(10y(s))$ and

$$x(s) = (.1)\cos(2\pi s)+.1 \quad y(s) = (.05)\sin(2\pi s)+.1 \quad s \in [0,1].$$

and let $F(K)=-K$, corresponding to a front moving in with speed equal to its curvature. It has recently been shown (see [2]), that any non-intersecting curve must collapse smoothly to a circle under this motion. With N_{point}=200 and Δt=.0001, Figure 2 shows the unwrapping of the spiral from t=0 to t=0.65. In Figures 2a-d we show the collapse to a circle and eventual disappearance at t=.295 (The surface vanishes when $\phi_{ij} < 1$ for all ij.)

C. Level Surface, Torus, $F(K) = 1-\varepsilon K$

We evolve the toroidal initial surface, described by the set of all points (x,y,z) satisfying

$$z^2 = (R_0)^2-((x^2+y^2)^{1/2}-R_1)^2$$

where R_0=.5 and R_1=.05. This is a torus with main radius .5 and smaller radius .05. The computational domain is a rectangular parallelpiped with lower left corner (-1,-1,-.8) and upper right corner (1.,1.,.8). We evolve the surface with $F(K) = 1-\varepsilon K$, ε=.001, Δt=.01, and N_{point}=90 points per x and y side of the domain and the correct number in the z direction so that the mesh is uniform. Physically, we might think of this problem as the boundary of a torus separating products on the inside from reactants outside, with the burning interface propagating with speed $K=1-\varepsilon K$. Here, K is the mean curvature. In Figure 3, we plot the surface at various times. First, the torus burns smoothly (and reversibly) until the main radius collapses to zero. At that time (T=0.3), the genus goes from 1 to 0, characteristics collide, and the entropy condition is automatically invoked. The surface then looks like a sphere with deep inward spikes at the top and bottom.

These spikes open up as the surface moves, and the surface approaches the asymptotic spheroidal shape. When the expanding torus hits the boundaries of the computational domain, the level surface $\psi=1$ is clipped by the edges of the box. In the final frame (T=0.8), the edge of the box slices off the top of the front, revealing the smoothed inward spike.

REFERENCES

1) Crandall, M.G., and Lions, P.L., Math. Comp., **43**, 1, (1984).

2) Grayson, M. "The heat equation shrinks embedded plane curves to round points, J. Diff. Geom., to appear.

3) Harten, A., Engquist, B., Osher, S., Chakravarthy, S., Uniformly high order accurate essentially non-oscillatory schemes III, J. Comput. Phys., to appear.

4) Osher, S., Siam J. Num. Anal., **21**, 217, (1984).

5) Osher, S., and Sethian, J.A., Front Propagating with Curvature-Dependent Speed: Algorithms Based on Hamilton-Jacobi Formulations, CPAM 380, Univ. Of Cal., Berkeley, 1987, submitted to J. Comp. Phys.

6) Sethian, J.A.: An analysis of flame propagation. Ph.D. Dissertation, University of California, Berkeley, California, June 1982; CPAM Rep. 79.

7) Sethian, J.A.: Curvature and the Evolution of Fronts. Comm. Math. Phys, **101**, 487, (1985).

8) Sethian, J.A.: Numerical Methods for Propagating Fronts, in *"Variational Methods for Free Surface Interfaces"*, edited by P. Concus and R. Finn, (Springer-Verlag, New York, 1987).

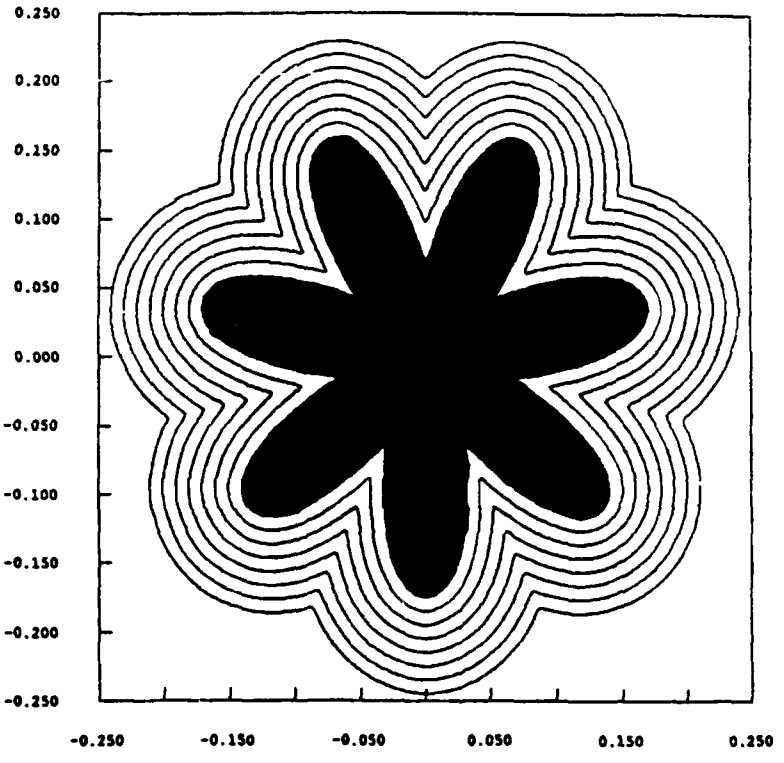

Fig. 1. F(K)=1 T= 0.0, 0.07 (.01)

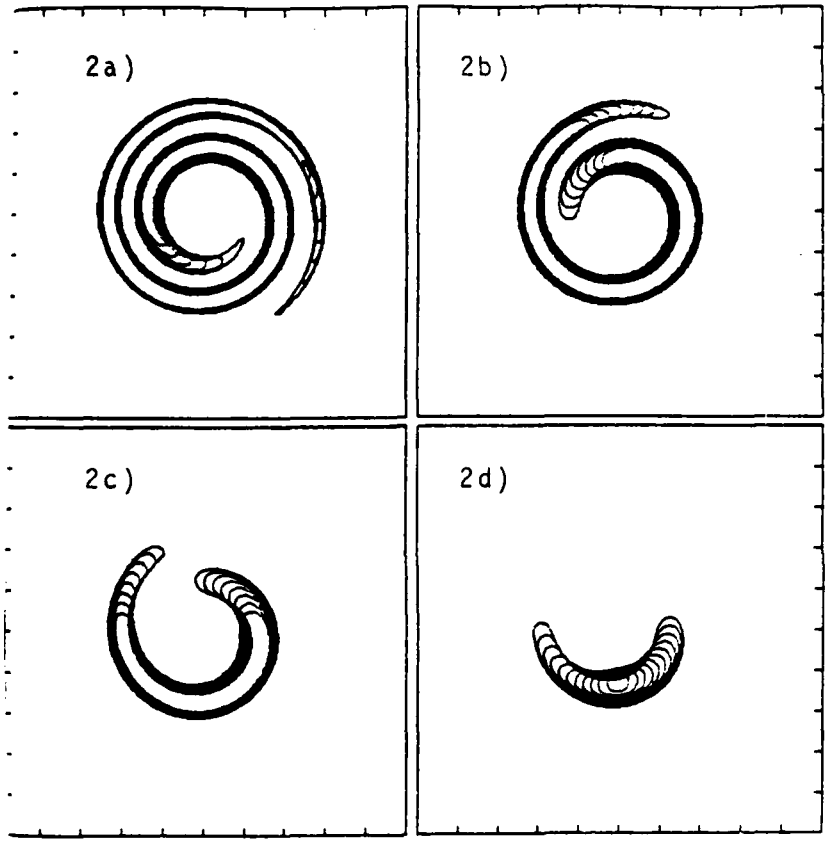

Fig. 2a) F(K) = K T = 0.0, 0.065 (.01)

Fig. 2b) F(K) = 1 T = 0.065, .130 (.01)

Fig. 2c) F(K) = K T = 0.130, 0.195 (.01)

Fig. 2d) F(K) = K T = 0.195, 0.295 (.01)

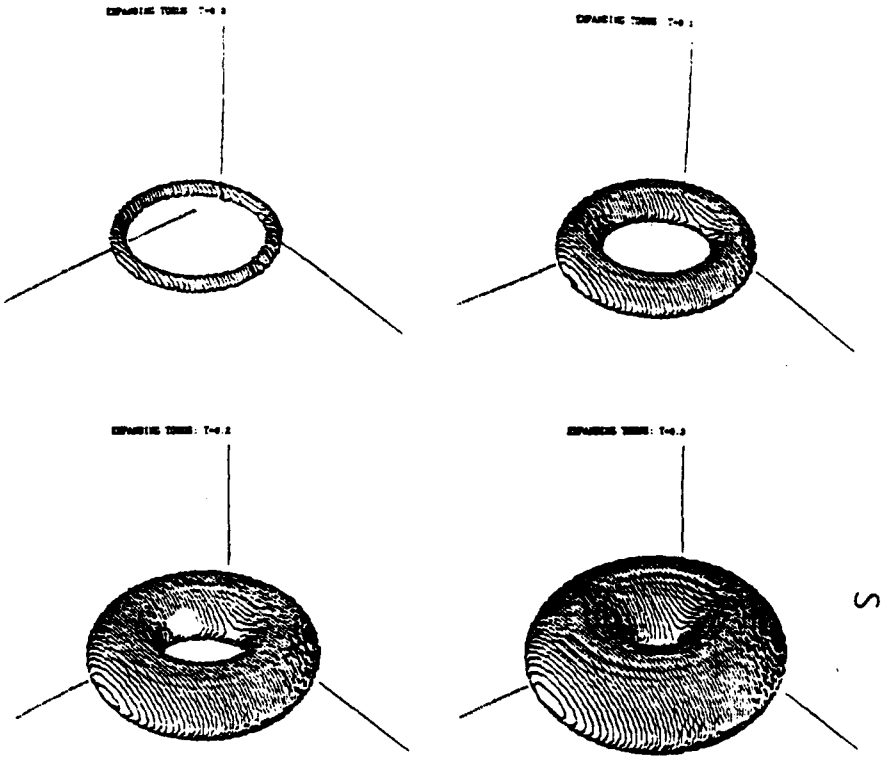

Figure 3a: F(K)=1- ϵ K , ϵ = .01, Surface at T=0.0, 0.1, 0.2, 0.3

FIGURE 3: BURNING TORUS

Prediction of Dispersive Errors in Numerical Solution of the Euler Equations

Richard A. Shapiro
Computational Fluid Dynamics Laboratory
Department of Aeronautics and Astronautics
Massachusetts Institute of Technology

1 Introduction

Any numerical PDE solution method introduces some numerical error. In many cases, this error appears as dispersion. In the Euler equations for flow of a compressible, inviscid, ideal gas, these dispersive errors can give rise to undesirable oscillations near discontinuities such as shocks. The purpose of this paper is to point out some of these errors, examine their origins, and attempt to predict the effect of dispersion on solution quality.

The analytic work will include analyses of the exact Euler equations, Cell-Vertex method [1], Central Difference method (finite volume method) [2], and a Galerkin Finite Element method [3].

To demonstrate the predictive ability of the analysis, I show some numerical results for test problems using the above schemes. The problems include a 1/2 degree compression corner at Mach 2 and a series of flows over 1/2 degree wedges using the Finite Element method on grids with differing cell aspect ratios and Mach numbers. In these cases, the flow is linear enough to permit comparison with analytic theory.

2 Analytic Results

This section shows the basic analysis of dispersion, using a method suggested to me by Michael Giles [4]. The 2-D Euler equations can be written:

$$\frac{\partial U}{\partial t} + \frac{\partial (AU)}{\partial x} + \frac{\partial (BU)}{\partial y} = 0 \tag{1}$$

where A and B are the flux Jacobians. If one linearizes this equation and assumes a steady-state, this can be written:

$$(A_L s_x + B_L s_y) U = 0 \tag{2}$$

where s_x and s_y are the x and y derivative operators and A_L and B_L are "frozen" flux Jacobians. This requires that U be an eigenfunction for Eq. (2), because we would like a non-trivial solution. Let

$$r = \frac{s_x}{\sqrt{s_x^2 + s_y^2}} \tag{3}$$

$$s = \frac{s_y}{\sqrt{s_x^2 + s_y^2}} \tag{4}$$

then the characteristic equation is

$$(ru + sv)^2 \left[c^2 (r^2 + s^2) - (ru + sv)^2 \right] = 0 \tag{5}$$

where c is the speed of sound and u and v are velocities in the x and y directions. If we write

$$\vec{s} = \begin{bmatrix} r \\ s \end{bmatrix} \qquad \vec{u} = \begin{bmatrix} u \\ v \end{bmatrix}$$

the solution to Eq. 5 is just

$$\vec{s} \cdot \vec{u} = \begin{cases} 0 \\ \pm c \end{cases} . \tag{6}$$

Since $\vec{s}$ has unit norm, the non-zero solution will exist only if the flow is supersonic, that is, when the system is hyperbolic in space.

Moving now to the discrete domain, assume a state vector of the form

$$U_{j\Delta x, k\Delta y} = U' \exp i(j\phi + k\theta)$$

where ϕ is a scaled wave number in the x direction, θ is a scaled wave number in the y direction and U' is some eigenvector. Here, ϕ and θ are scaled into the interval $[-\pi, \pi]$.

To get some idea of the consequences of this relation, I considered a flow in which $u = Mc$, $v << u$. Then, neglecting v, Eq. (6) becomes

$$\frac{s_x}{\sqrt{{s_x}^2 + {s_y}^2}} = \pm \frac{1}{M}. \tag{7}$$

This equation holds for the exact Euler equations as well as the discrete appoximations. After some more algebra, the above relation gives rise to a family of curves relating ϕ and θ, parameterized by a similarity parameter $\kappa = \mathcal{R}\sqrt{M^2 - 1}$, where $\mathcal{R} = \Delta y / \Delta x$. Thus, I expect problems with similar values of κ to have similar dispersive properties for any given method. Figure 2 shows these curves for various methods for $\kappa = 1.732$ (to correspond with the numerical cases below). The slope of a curve represents a spatial group velocity, or the *angle* at which wave packets propagate. Note that for the Central Difference and Finite Element cases, the curves bend such that one would expect oscillations downstream of a feature, while the Cell-Vertex predicts oscillations upstream of the feature. Also note that the curves for the Central Difference and Finite Element methods are multivalued.

3 Numerical Experiments

Figure 1 shows the geometry for the numerical test cases. A test case with inflow Mach number 2 on a grid with cell aspect ratio 1 was computed for each method. This corresponds to a value of $\kappa = 1.732$. Figure 3 shows the Mach number at mid-channel for a 1/2 degree compression using the three methods. There are several things to note here. First, the correct spatial frequencies appear at the places predicted by the dispersion curves above. Note that the oscillations appear on the side of the shock predicted above. Also note that the Finite Element method has a sharper shock than the other two methods, corresponding to the fact that, for the Euler equations on a nearly uniform grid, the Finite Element method is fourth order accurate [5].

Figure 4 shows the Mach number at mid-channel for flow over a 1/2 degree wedge with $\kappa = 1.732$. The three cases are $M = 2$, $\mathcal{R} = 1$; $M = 1.323$, $\mathcal{R} = 2$; and $M = 3.606$, $\mathcal{R} = .5$ using the Finite Element method. The figure shows Mach number normalized by free stream Mach number (so that all the plots fit on the same axes). Note that the solution *shapes* are very much alike, even though the shock amplitude varies. Note especially that the frequency of the post-shock oscillations is identical. This is as expected from the analysis.

Preliminary experiments indicate that the linear analysis is still useful for predicting the dispersive behavior for flows over wedges with angles as great as 7-10 degrees.

The final paper will contain a more detailed demonstration of the predictive ability of the linear analysis. It will demonstrate that the oscillation in the x and y directions are of differing frequency, and that the frequencies are as predicted by the dispersion curves.

References

[1] K. Powell, *Vortical Solutions of the Conical Euler Equations*, Technical Report CFDL-TR-87-8, MIT Computational Fluid Dynamics Laboratory, July 1987.

[2] A. Jameson, W. Schmidt, and E. Turkel, "Numerical Solutions of the Euler Equations by a Finite Volume Method Using Runge-Kutta Time Stepping Schemes," AIAA Paper 81-1259, June 1981.

[3] R. Shapiro and E. Murman, "Cartesian Grid Finite Element Solutions to the Euler Equations," AIAA Paper 87-0559, January 1987.

[4] M. B. Giles, personal communication.

[5] S. Abarbanel, personal communication.

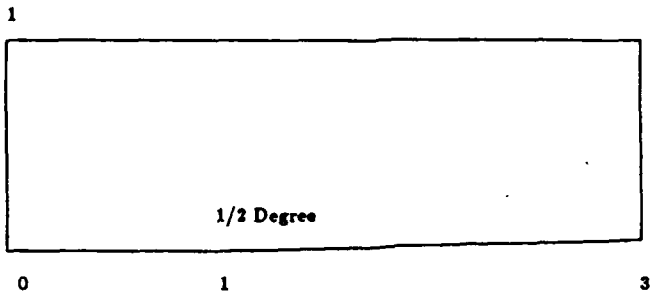

Figure 1: Geometry for Test Cases

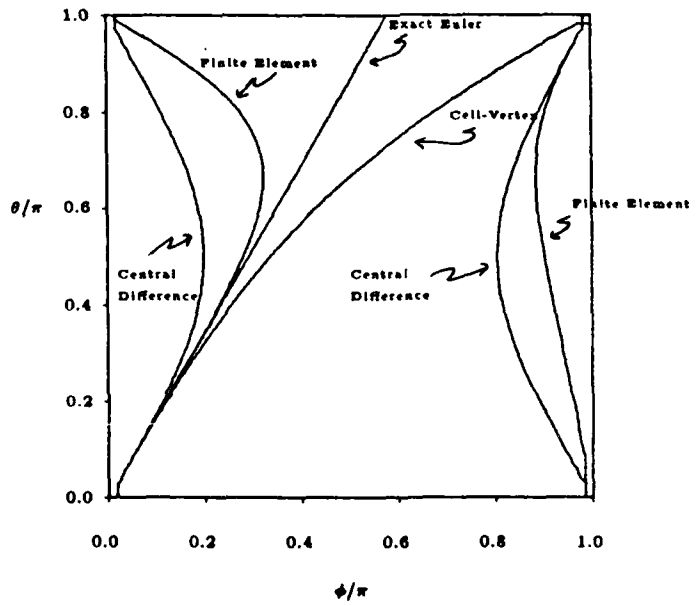

Figure 2: Dispersion Plots for Various Methods

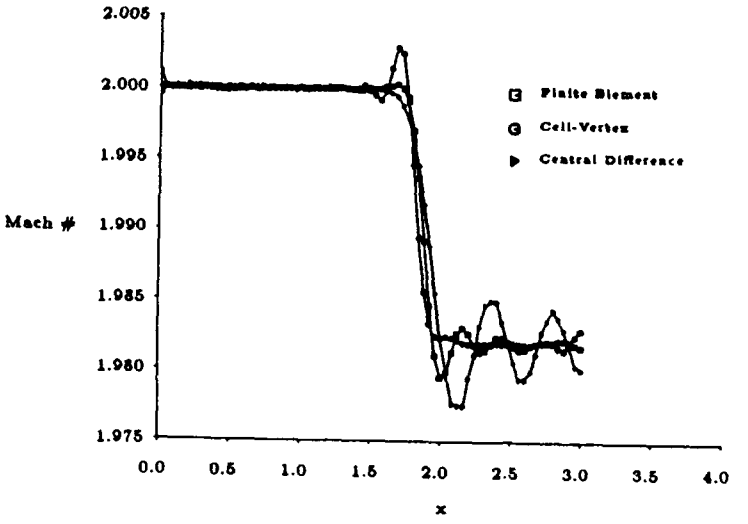

Figure 3: Mid-Channel Mach Number, Compression Corner

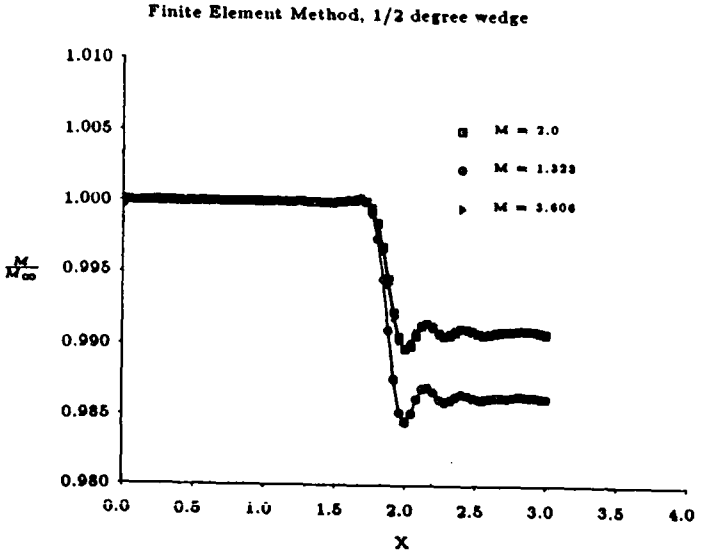

Figure 4: Effect of Changing M and $\mathcal{R}$ with Constant κ

NUMERICAL PREDICTION OF SHOCK WAVE FOCUSING PHENOMENA IN AIR WITH EXPERIMENTAL VERIFICATION

by

Martin Sommerfeld

Lehrstuhl für Strömungsmechanik
Universität Erlangen-Nürnberg
Egerlandstr. 13, D-8520 Erlangen

INTRODUCTION

In recent years shock wave focusing by means of different types of concave reflectors has received increasing attention /1 - 5/. The reason for this increasing interest is the use of converging focusing shock waves for the non invasive treatment of kidney stones. Recently, a second order extension of Goudunov's method, called piecewise linear method /6/, was applied to the numerical prediction of the shock wave focusing process in air /5, 8/ and water /7/. The numerical results for water however showed some problems in predicting the maximum peak pressure in the focal region /7/; by decreasing the mesh size, it was also seen that there was still some difference between experiment and calculation. The experiments for the shock focussing in air conducted by Nishida et al. /5/ showed a rather low pressure amplification in the focal region and, therefore, only poor agreement with the calculations could be obtained for the shock pressure distribution along the reflector axis.

In order to verify the ability of the piecewise linear method to predict the shock wave focusing process and the obtained peak pressure in air, numerical computations were performed and compared with the experiments performed by Sturtevant und Kulkarny /1/.

Results of numerical calculation

To prove the grid independence of the numerically calculated peak pressure, the shock wave focussing process in air was computed using several different mesh sizes utilizing the boundary conditions of the experiments (Fig. 1).

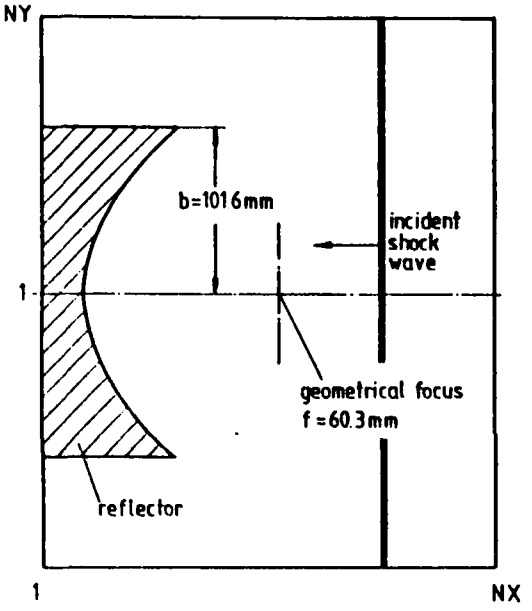

Fig. 1: Reflector configuration

mesh size $\Delta x/b$	peak pressure ratio
0.01471	0.915
0.0098	0.97
0.00735	1.0

Table

Using a rather course mesh, a high peak pressure was obtained, which increased only slightly by halving the mesh size (see Table). Due to the limited computer storage, the number of nodes for the finest mesh was limited to 180 by 150.

For optimizing the number of grid points above the reflector edge which are necessary (Fig. 1) to guarantee the appropriate prediction of the expansion eminating from this edge, a number of computations were performed and the distribution of the maximum pressure on the axis of symmetry was compared (Fig. 2). When increasing the number of nodes in y-direction from 75 to 90, no considerable difference in the pressure distribution is observed.

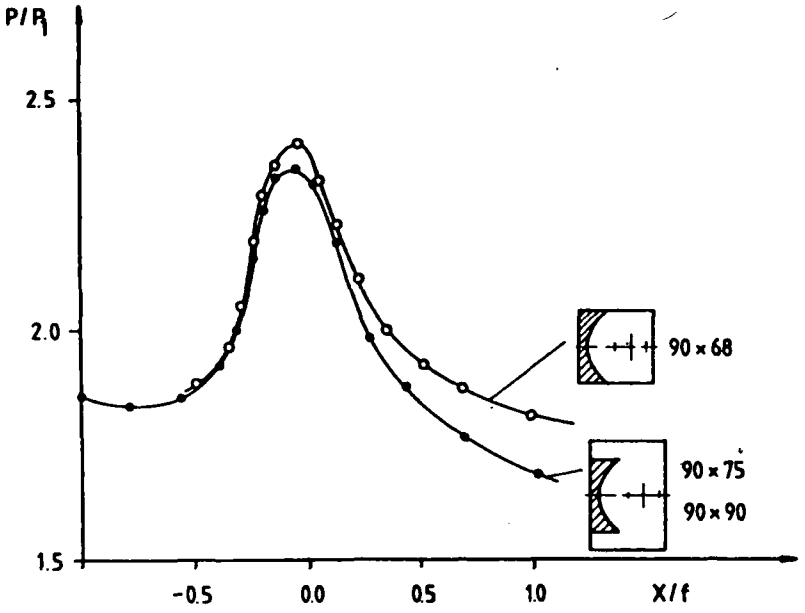

Fig. 2: Pressure distribution along the axis of symmetry for different computational domains

The computations carried out for the purpose of comparison with the experiments, were finally performed on a mesh of 180 by 150 in the x- and y-direction, respectively. Computational results agreed reasonably well with experimental ones (Fig. 3).

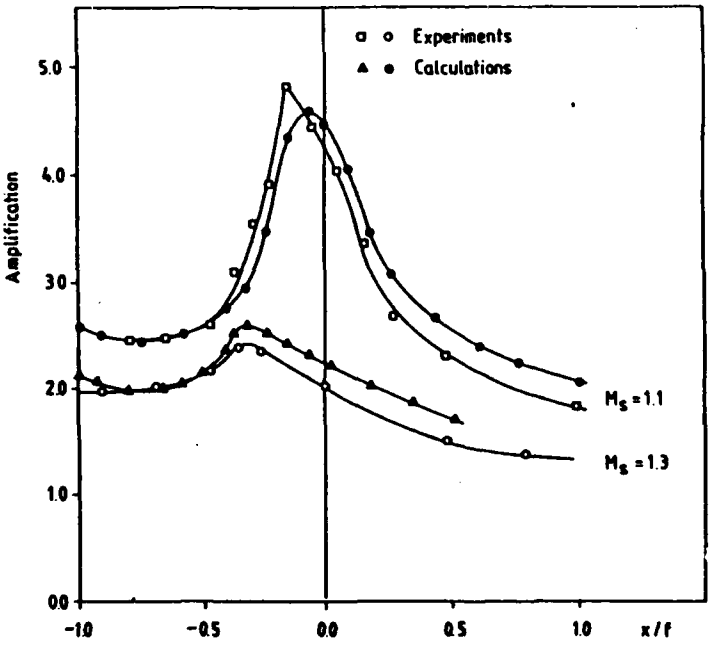

Fig. 3: Pressure amplification along the axis of symmetry (the pressure jump is normalized with the pressure jump of the reflected shock as it leaves the reflector surface).

Slightly higher pressures than those found in the experiments are predicted by the computations in the region behind the focal area, which may be due to boundary layer effects. Since also the comparison of the computed wave patterns at different instants and the pressure history at different locations showed a good agreement with the shadowgraphs and the measured pressure traces, it can be concluded, that the piecewise linear method is an appropriate method for the calculation of the shock focusing phenomenon, even for weak shock waves.

References

/1/ Sturtevant, B. and Kulkarny, V.A.: The focusing of weak shock waves, J. Fluid Mech., 73, 651-671 (1976).

/2/ Holl, R.: Wellenfokussierung in Fluiden, Dissertation, RWTH Aachen (1982).

/3/ Müller, H.M. and Grönig, H.: Experimental investigations on shock wave focusing in water, Proc. 12th Int. Congr. on Acoustics, Vol. III, H3-3, Toronto (1986).

/4/ Takayama, K., Esashi, H. and Sanada, N.: Propagation and focusing of spherical shock waves produced by underwater microexplosions, In: Proceedings of the 14th Int. Symp. on Shock Tubes and Shock Waves (eds. Archer, R.D., Milton, B.E.), pp. 553-562, Kensington/Australia: New South Wales University Press (1983).

/5/ Nishida, M., Nakagawa, T., Saito, T. and Sommerfeld, M.: Interaction of weak shock waves refelcted on concave walls, In: Proceedings of the 15th Int. Symp. on Shock Waves and Shock Tubes (eds. Bershader, D., Hanson, R.), pp. 211-217, Stanford/CA: Stanford University Press (1985).

/6/ Colella, P. and Glaz, H.M.: Efficient solution algorithms for the Riemann problem for real gases, J. Comp. Phys., 59, 264-289 (1985).

/7/ Sommerfeld, M. and Müller, H.M.: Experimental and numerical studies of shock wave focusing in water, Experiments in Fluids, 6 (1987), in print.

/8/ Nishida, M. and Kishige, H.: Numerical simulation of focusing process of reflected shock waves, Presented at the 16th Int. Symp. on Shock Tubes and Waves, Aachen (1987), Abstracts.

FUNDAMENTAL ASPECTS OF NUMERICAL METHODS FOR THE PROPAGATION OF MULTIDIMENSIONAL NONLINEAR WAVES IN SOLIDS

M. STAAT, J. BALLMANN
Lehr- und Forschungsgebiet Mechanik of RWTH Aachen,
D-5100 Aachen, FRG

For the solution of hyperbolic problems with more than two independent variables (two- and three-dimensional wave propagation) many characteristic-based methods have been devised. Most of them (e.g. GODUNOV-Type-Methods and Random-Choice-Methods) use schemes developed for one-dimensional wave propagation by operator splitting techniques. May be this is the reason why promising results are only known for nonlinear media with scalar constitutive equations so far.

In solids only physically one-dimensional problems can be modelled by scalar laws, whereas tensor constitutive equations describe the material behaviour in multidimensional problems. Thereby a strong coupling of the different spatial directions may result and, if the material is nonlinear, local effects of anisotropy may occur. Such effects are best known from magnetohydrodynamics and for optical and mechanical waves in linear anisotropic solids |1|. Due to the dependence on the solution, the situation is even more complicated for nonlinear elastic and plastic waves in solids.

For a numerical treatment of these nonlinear problems, methods of near-characteristics have been devised, which become methods of bicharacteristics if the local scheme uses the axis of symmetry of the local wave fronts of point disturbances |2,3|.

For a uniform treatment of the PDEs in space and time, it is helpful to introduce a material gradient in space and time in dyadic notation (quantities in space and time will be

marked by an asterix *)

$$\nabla^* f := \frac{\partial f}{\partial \xi^\alpha} \circ g^\alpha \qquad \text{with } \xi^o := c\tau \ ; \quad \alpha=1,2,3 \ . \tag{1}$$

ξ^λ ($\lambda=1,2,3$) are the spatial coordinates of a material point in the reference configuration, τ is the time and c a chosen speed (arbitrary but constant to give ξ^o the physical dimension of space). The following notations are used: ϱ mass density in the reference configuration, v velocity of a material point, f density of body forces, E unit tensor, F deformation gradient, H=F-E material gradient of displacement ($\delta H=\delta F$ their variations), σ first PIOLA-KIRCHHOFF-stress, $\bar{\mathbf{Q}}$ acoustic tensor, q eigenvector of $\bar{\mathbf{Q}}$, v solution of characteristic condition (wave speed). Multiple dots denote multiple transvection.

The local balance of momentum in material formulation is

$$\mathbf{l}^* = \mathbf{o} \ , \quad \mathbf{l}^* := \varrho c(\nabla^* \bar{v}) g_o - \mathbf{A} \vdots \nabla^* \mathbf{H}^T - \varrho \bar{f}. \tag{2}$$

In addition, SCHWARZ's lemma on the second covariant derivatives of the displacements holds. If one seperates the purely spatial derivatives, it reads

$$\mathbf{L}^* = \mathbf{0} \quad , \quad \mathbf{L}^* := (\nabla^* \bar{v})\mathbf{E} - c(\nabla^* \mathbf{H}) g_o, \tag{3a}$$

$$(\nabla^* \mathbf{H}) : (g_k o g^l - g_l o g^k) = \mathbf{0} \ , \qquad k,l=1,2,3. \tag{3b}$$

The fourth order elasticity A,

$$\mathbf{A} := \frac{\partial \sigma}{\partial \mathbf{F}} \tag{4a}$$

can be derived from a stored energy density U for hyperelastic materials

$$\delta \mathbf{F} : \mathbf{A} : \delta \mathbf{F} = \varrho \delta^2 U \ . \tag{4b}$$

For materials which are infinitesimally stable in statics (elliptic BVP of place and traction), the dynamic equations turn out to be hyperbolic. This results in undetermined derivatives in certain normal directions $\mathbf{n}^*$ in space and time, associated with singular hypersurfaces (so-called characteristic manifolds). With the ansatz

$\mathbf{n}^* = -\frac{v}{c}\,\bar{\mathbf{g}}_o + \mathbf{n}$ and the arbitrary choice of the spatial unit normal $\mathbf{n}$ in a material point, one obtains the appropriate time-like component v of $\mathbf{n}^*$ from the characteristic condition

$$0 = \frac{1}{\varrho^2}\, v_o^2 \det(\bar{\mathbf{Q}}(\mathbf{n}) - \varrho v_\varepsilon^2(\mathbf{n})\mathbf{E}) \quad \text{with } \varepsilon = L, T_1, T_2 \,. \tag{5}$$

Besides $v_o = 0$, one obtains solutions $v_\varepsilon(\mathbf{n})$ of (5) from the eigenvalue problem of the acoustic tensor $\bar{\mathbf{Q}}(\mathbf{n})$,

$$\bar{\mathbf{Q}}(\mathbf{n}) := (\bar{\mathbf{g}}_\lambda \circ \mathbf{n} : \mathbf{A} : \bar{\mathbf{g}}^\mu \circ \mathbf{n})\, \bar{\mathbf{g}}^\lambda \circ \bar{\mathbf{g}}_\mu \,. \tag{6}$$

At a given material point the components of $\mathbf{A}$ are determined by the local deformation. There is a proper eigenvalue at the point for any choice of $\mathbf{n}$. In three-dimensional space $\mathbf{n}$ has two independent parameters. If one varies these parameters at the point, the vectors

$\mathbf{n}_o^* = \mathbf{n}$, $\mathbf{n}_\varepsilon^* = -\frac{v_\varepsilon}{c} + \mathbf{n}$ generate the normal hypercones N_o, N_ε. The according local characteristic hyperplanes envelope the local MONGE-hypercones M_o, M_ε. The lines of tangency are given by the bicharacteristics $\mathbf{m}_o^*$, $\mathbf{m}_\varepsilon^*$ (generators of M_o, M_ε). The local characteristic hyperplanes represent plane wave fronts of point disturbances in space.

In the characteristic manifolds there hold so-called compatibility equations. These are linear combinations of the original PDEs (2),(3a) retaining continuous derivatives only. Eq. (3a) holds on M_o and has already the form of a compatibility equation. With eq. (5) the compatibility equations on M_ε are

$$0 = \bar{\mathbf{q}}_\varepsilon(\mathbf{n})(v_\varepsilon(\mathbf{n})\mathbf{1}^* - \mathbf{A} \vdots (\mathbf{n} \circ \mathbf{L}^*)). \tag{7}$$

If (3b) is satisfied in the initial value space, a solution of the system (2), (3a) is obtained by integration of (7), (3a) in the domain of dependence, represented analytically by the backward MONGE-hypercones emanating from the solution point in space and time and given by

$$\mathbf{m}_o^* \quad , \quad \mathbf{m}_\varepsilon^* = \mathbf{m}_o^* + \frac{1}{2\varrho v_\varepsilon}\, \bar{\mathbf{q}}_\varepsilon \circ \bar{\mathbf{q}}_\varepsilon : \frac{\partial \bar{\mathbf{Q}}}{\partial n} \quad . \tag{8a}$$

In the nonlinear case, the M_ε are only local linear approximations of MONGE-conoids. These may show anisotropy and torsion in finite time due to inhomogeneous deformation. The anisotropy may lead to self-intersections of the cones and to crunodes and cusps on their conics. These phenomena result in gaps which are called lacunae and lie like islands in the domain of dependence |1|. To take the torsion of M_ε into account, one has to integrate the PDEs

$$(\nabla^* \mathbf{n})\mathbf{m}_\varepsilon^* = (\mathbf{n} \circ \mathbf{n} - \mathbf{E})\, (\nabla^* v_\varepsilon(\mathbf{n}))\, \mathbf{E} \tag{8b}$$

additionally.

The torsion may be neglected in a second order numerical scheme for plane problems |3|. Based on |2,4| and on the above analysis a second order method of bicharacteristics has been developed for acceleration waves in plates |3|. It reproduces the local anisotropy very well and has been applied to the steepening and focussing of waves. Numerical results will be shown.

|1| R.G. PAYTON: Elastic Wave Propagation in Transversely Isotropic Media. Martinus Nijhoff, The Hague 1983.

|2| J. BALLMANN, H.J. RAATSCHEN, M. STAAT: High Stress Intensities in Focussing Zones of Waves. In P. LADEVESE (Ed.): Local Effects in the Analysis of Structures. Elsevier, Amsterdam 1985.

|3| M. STAAT: Nichtlineare Wellen in elastischen Scheiben. Dr.-Ing. Thesis, RWTH-Aachen 1987.

|4| R.J. CLIFTON: A Difference Method for Plane Problems in Dynamic Elasticity. Quart. of Appl. Math. **25** (1967) 97-116.

ON A NONLINEAR TELEGRAPH EQUATION WITH A FREE BOUNDARY.

Ivan Straškraba, Praha

In the present contribution we study the following problem: For given functions f_o, f_1, Q_o, Q_1 to find functions $Q = Q(x,t), \xi = \xi(t)$, $(x \in [0,\ell]$, $t \in [0,T]$, $\ell > 0$, $T > 0)$ such that

$$(1) \qquad Q_{tt} - c^2 Q_{xx} + f_o(Q)_t = 0 \ , \ 0 < x < \xi(t) \ ,$$

$$(2) \qquad Q_{tt} - c^2 Q_{xx} + f_1(Q)_t = 0, \ \xi(t) < x < \ell, \ t \in (0,T) \ ,$$

$$(3) \qquad Q(\xi(t)-,t) = Q(\xi(t)+,t), Q_x(\xi(t)-,t) = Q_x(\xi(t)+,t) \ ,$$
$$Q_x(0,t) = Q_x(\ell,t) = 0 \ , \quad t \in [0,T] \ ,$$

$$(4) \qquad Q(x,0) = Q_o(x) \ , \ Q_t(x,0) = Q_1(x), \ x \in [0,\ell]$$

$$(5) \qquad \xi(t) = G\left(\frac{1}{S}\int_0^t Q(\xi(\tau),\tau)\,d\tau\right) \ ,$$

where c and S are positive constants and

$$G(y) = \min\{\ell, \max\{0,y\}\} = \begin{cases} 0, & y \le 0 \\ y, & 0 < y < \ell \\ \ell, & y \ge \ell. \end{cases}$$

Motivation for this problem is given in [1] . It is filling a cylindric compartment with a suspension which drives out the original content of the pipe (water). In this engineering problem we seek for a rate of flow Q , a pressure and a free boundary $x = \xi(t)$ between the two fluids, x being longitudinal coordinate of the pipe. Original Euler equations for a barotropic fluid flow are simplified, the pressure excluded, which gives rise to the problem (1) - (5) . Here c is the sound speed which is supposed to be almost the same in both fluids, $f_o(Q)$, $f_1(Q)$ are the friction terms, Q_o, Q_1 initial distribution for the rate of flow Q and its time-derivative

Q_t respectively, S the cross section of the pipe. The form of the equation (5) is due to the fact that the free boundary $x = \xi(t)$ must not leave the pipe and so it may slip along $x = 0$ or $x = \ell$. The boundary conditions (3) mean that Q and the pressure are continuous across the free boundary and the pressure is constant at the ends of the pipe.

DEFINITION: *By a weak solution of the problem* (1) - (5) *on* $[0,T]$ *we call the couple* $(Q,\xi) \in W_2^1((0,\ell)\times(0,T))\times C^{(0)+1}([0,T])$ *satisfying*

$$(6)\quad \int_0^T\int_0^\ell (c^2 Q_x\phi_x - Q_t\phi_t)\,dxdt + \int_0^T\int_0^{\xi(t)} f_o(Q)_t\,\phi dxdt +$$

$$+ \int_0^T\int_{\xi(t)}^\ell f_1(Q)_t\,\phi dxdt - \int_0^\ell Q_1(x)\phi(x,0)\,dx = 0$$

for all $\phi \in C^1([0,\ell]\times[0,T])$, $\phi(x,T) = 0$, $x \in [0,\ell]$.

Let the following assumptions be fulfilled:

(i) f_o, f_1 are continuous in R with locally Lipschitz continuous derivatives f_o', f_1' ;

(ii) there exists an $\alpha \in R$ such that

$$f_o'(u),\ f_1'(u) \geq \alpha \quad \text{for all } u \in R\ ;$$

(iii) there exist nonnegative constants c,d and a $p \geq 1$ such that

$$\max_{i=0,1}\{|f_i(u)|,|f_i'(u)|\} \leq c + d|u|^p\ ,\ u \in R\ ;$$

(iv) $Q_o \in W_2^1\ (0,\ell)$, $Q_1 \in L_2(0,\ell)$.

EXISTENCE THEOREM: *Let the functions* f_o, f_1, Q_o, Q_1 *satisfy the assumptions* (i) - (iv). *Then there exists at least one weak*

solution of the problem (1) - (5) .

Sketch of the proof: A complete presentation of the proof is given in [2] and will be published in [3] . We determine Faedo-Galerkin approximations (Q^n,ξ_n) from the equations

$$Q^n(x,t) \equiv P_n Q\,(.,t)(x) = \sum_{j=0}^{n} q_j^n(t)\, v_j(x),$$

$$(x,t) \in \Omega = [0,\ell] \times [0,T] ,$$

$$(7)\quad \ddot{q}_k^n(t) + \lambda_k\, q_k(t) + \int_0^{\xi_n(t)} f_o'\Big(\sum_{j=0}^{n} \dot{q}_j(t)\, v_j(x)\Big) \cdot \sum_{j=0}^{n} \dot{q}_j(t)\, v_j(x)\, v_k(x)\, dx +$$

$$+ \int_{\xi_n(t)}^{\ell} f_1'\Big(\sum_{j=0}^{n} q_j(t)\, v_j(x)\Big) \sum_{j=0}^{n} \dot{q}_j(t)\, v_j(x) v_k(x) dx = 0 ,$$

$$k = 0,1,\dots,n, \quad t \in [0,T] ,$$

$$(8)\quad q_k(0) = \int_0^{\ell} Q_o(x)\, v_k(x) dx , \quad \dot{q}_k(0) = \int_0^{\ell} Q_1(x) v_k(x) dx , \quad k = 0,1,\dots,n,$$

$$(9)\quad \xi_n(t) = G\Big(\frac{1}{S} \int_0^t \sum_{j=0}^{n} q_j(\tau)\, v_j(\xi_n(\tau),\tau)\, d\tau\Big), \quad t \in [0,T];$$

$$n = 0,1,\dots,$$

where $v_o(x) = \ell^{-1/2}$, $v_j(x) = \left(\frac{2}{\ell}\right)^{1/2} \cos\left(\frac{j\pi}{\ell} x\right)$,

$j = 1,2,\dots, x \in [0,\ell]$, $\lambda_j = c^2 \pi^2 \ell^{-2} j^2$, $j = 0,1,2,\dots$.

First, we establish the local existence theorem for the integro-differential system (7) - (9) . Then we derive apriori estimates

$$(10)\quad \sup_{t,n} \int_0^{\ell} [Q_t^n(x,t)^2 + c^2 Q_x^n(x,t)^2] dx < \infty$$

(11) $$\sup_{t,n} |\xi_n(t)| < \infty$$

which imply the global existence of a solution (7) - (9). Further using (10), (11) we show that

(12) $$\sup_{t_1 \neq t_2, n} \frac{|\xi_n(t_1) - \xi_n(t_2)|}{|t_1 - t_2|} < \infty .$$

From (10) - (12) we get compactness of the sequences $\{Q^n\}_{n=0}^{\infty}$, $\{\xi_n\}_{n=0}^{\infty}$ in sufficiently strong topologies and some limit functions Q, ξ. The rest of the argument is a tedious work with the limiting process in an integral identity which is a finite dimensional analogue of (6).

REMARK: Although we are not able to prove the uniqueness of the weak solution, it seems that the uniqueness can be obtained for more regular (strong) solutions, namely for $Q \in H^2(\Omega)$, $\xi \in W_\infty^1(0,\ell)$. Unfortunately, we are not able to show the existence of a strong solution. We are going to solve some of these and related questions in [3].

References

[1] Kolarčík, V.: Formulation of the problem "filling the compartment by a mixture". (Czech) VÚ Sigma, Olomouc 1986.

[2] Straškraba, I.: An existence result for a nonlinear telegraph equation with a free boundary. Preprint No. 27, MÚ ČSAV, Praha 1987.

[3] Straškraba, I.: On a telegraph equation with a free boundary. To appear in Czech. Math. J.

"TVD" Schemes for Inhomogeneous Conservation Laws.

P.K. Sweby

Department of Mathematics,

University of Reading,

England.

Recent years have seen the development of a variety of high resolution Total Variation Diminishing (TVD) schemes for hyperbolic conservation laws (see e.g. [1],[2],[3],[4]) as well as the related Essentially Non-Oscillatory (ENO) schemes [1],[5]. These have all had the aim of producing solutions giving high resolution to discontinuities whilst being devoid of the spurious oscillations generated by the more classical high order schemes, such as Lax-Wendroff. All of these schemes have mimicked (at least approximately) the analytic property of solutions to the scalar homogeneous conservation law that the total variation of the solution is non-increasing. Extension to systems of conservation laws is then achieved in the usual way via approximate Riemann solvers.

The solution of the non-homogeneous equation

$$u_t + f(u)_x = b(x,t),$$

however, does not possess the TVD property. Indeed the presence of the right-hand side will cause the variation of

the solution to increase since it represents a source term. Yet we still wish to solve numerically such equations and desire high resolution oscillation free results. The question then arises as to how to prevent oscillations from forming without inhibiting the natural growth of the solution. Both Roe [6] and Glaister [7] have recently studied the implementation of source terms in schemes for conservation laws and have advocated upwinding of the source, however neither have presented high resolution oscillation free schemes due to the lack of a critereon such as TVD against which to measure the performance. Priestley [8] on the otherhand has obtained empirical results which demonstrates a sucessful implementation of TVD schemes.

We show here how a change of dependent variable transforms the inhomogeneous conservation law into a homogeneous equation of the form

$$v_t + a(u)v_x = 0$$

whose solution does possess the TVD property.

This then gives us a tangible critereon with which to correctly implement high resolution TVD schemes for inhomogeneous conservation laws. Examples are given using the family of Flux Limiter Schemes [2] to illustrate the process both on scalar equations and systems of conservation laws.

References.

1. S. Osher and P.K. Sweby, *Recent developments in the numerical solution of nonlinear conservation laws.* The State of the Art in Numerical Analysis, Eds. A Iserles and M.J.D. Powell, IMA Conference Series 9, OUP (1987).

2. P.K. Sweby, *High resolution schemes using flux limiters for hyperbolic conservation laws.* SIAM J. Numer. Anal. 21 (1984).

3. B. van Leer, *Towards the ultimate finite difference scheme V. A second-order sequel to Godunov's method.* J. Comput. Phys. 32, (1979).

4. A. Harten, *High resolution schemes for hyperbolic conservation laws.* J. Comput. Phys. 49, (1983).

5. A. Harten, S. Osher, B. Engquist, S.R. Chakravarthy, *Some results on uniformly high order accurate essentially non-oscillatory schemes.* J. App. Num. Math. (1986).

6. P.L. Roe, *Upwind differencing schemes for hyperbolic conservation laws with source terms.* Proc. Nonlinear Hyperbolic Problems, Eds. C. Carasso, P.A. Raviart, D. Serre, Lecture Notes in Mathematics 1270 (1986).

7. P. Glaister, *Second order difference schemes for hyperbolic conservation laws with source terms.* University of Reading Numerical Analysis Report 6/87.

8. A. Priestley, *Roe type schemes for the 2-D shallow water equations.* University of Reading Numerical Analysis Report 8/87.

Purely Convective Carrier Transport In Semiconductors

Peter Szmolyan
Department of Mathematics and Statistics
University of Maryland Baltimore County
Balitimore, MD 21228

Carrier transport in semiconductor devices is usually described by the *drift-diffusion model*, a system of two convection- diffusion equations for the concentrations of positive and negative charged particles (holes, resp. electrones), coupled to Poisson's equation, which determines the electric field.

A *singular perturbation analysis*, based on a scaled form of the equations, reveals the complicated structure of solutions, i.e., existence of internal spatial layers of fast variation and temporal evolution on two time scales, a fast and a slow one (see [1], [2]). The fast time scale occurs if the initial data do not have the appropriate spatial layer structure. By rescaling the equations we show that the transport process on the fast time scale is dominated by electric field driven convection, i.e., the impact of *diffusion is small*. The corresponding initial layer problem has the form

$$\begin{aligned} \Phi_{xx} &= n - p - C(x) \\ n_t &= -(n\Phi_x)_x \\ p_t &= (p\Phi_x)_x \end{aligned}$$

subject to appropriate initial values and *'inflow'-boundary conditions* for n and p.

This system describes the flow of electrons and holes in their self-induced electric field. The function C(x) is the doping profile modelling the concentration of fixed charged particles in the device. The equations have been analyzed in [3], where existence and uniqueness of smooth solutions has been proved by the method of characteristics. No shocks occur since the electric field is a smooth, but nonlocal, functional of the carrier concentrations. However, discontinuities can originate at the boundary due to *'switching'*

of the boundary conditions for n and p, which cause the breakdown of the smooth solution.

We interpret the hyperbolic initial layer problem as the limiting system when diffusion approaches zero. This leads, in a natural way, to an existence proof of weak solutions by the method of *vanishing viscosity*. We sketch the proof, which is based on uniformly valid estimates and a compactness argument. These results imply the *convergence* (in suitable topologies) of solutions of the full singularly perturbed problem with small diffusion to the solution of the hyperbolic initial layer problem as diffusion approaches zero.

References

[1] P.A.Markowich, 1987, Spatial temporal structure of solutions of the semiconductor device problem, Studies in Applied Mathematics.

[2] P.Szmolyan, 1987, A singular perturbation analysis of the transient semiconductor device equations, SIAM J.Appl.Math., submitted.

[3] P.Szmolyan, 1987, Ein Hyperbolisches System aus der Halbleiterphysik, Dissertation, Technical University Vienna.

T

CONVERGENCE OF THE SPECTRAL VISCOSITY METHOD FOR NONLINEAR CONSERVATION LAWS.

Eitan Tadmor

School of Mathematical Sciences, Tel-Aviv University, and

Institute for Computer Applications in Science and Engineering

1. INTRODUCTION. In recent years spectral methods have become one of the standard tools for the approximate solution of nonlinear conservation laws, e.g. [3]. It is well known that the spectral methods enjoy high order of accuracy whenever the underlying solution is smooth. On the other hand, one of the main disadvantages in using spectral methods for nonlinear conservation laws, lies in the formation of Gibbs phenomena, once spontaneous shock discontinuities appear in the solution; the global nature of spectral methods then pollutes the unstable Gibbs oscillations overall the computational domain and prevent the convergence of spectral approximation in these cases. One of the standard techniques to mask the oscillatory behavior of spectral approximations is based on spectrally accurate post-processing of these approximations. Indeed, the convergence of such recovery technique can be justified by linear arguments [1], [5]. However, for nonlinear problems we show by a series of prototype counterexamples, that spectral solutions with or without such post-processing techniques, do not converge to the correct 'physically' entropy solutions of the conservation laws. The main reason for this failure of convergence of spectral methods is explained by their lack of entropy dissipation.

A similar situation which involves unstable oscillations, is encountered with finite-difference approximations to nonlinear conservation laws. Here, the problem of oscillations is usually solved by the so called vanishing viscosity method. Namely, one adds artificial viscosity, such that on the one hand it retains the formal accuracy of the basic scheme, while on the other hand, it is sufficient to stabilize the Gibbs oscillations. The Spectral Viscosity Method (SVM) proposed in [6] attempts, in an analogous way, to stabilize the Gibbs oscillations and consequently to guarantee the convergence of spectral approximations, by augmenting them with proper viscous modifications.

2. THE SPECTRAL VISCOSITY METHOD. We consider one-dimensional system of conservation laws

$$\frac{\partial u}{\partial t} + \frac{\partial (f(u))}{\partial x} = 0, \tag{2.1}$$

with prescribed initial data $u_o(x)$. We restrict our attention to the periodic initial-value problem (2.1) which avoids the separate question of boundary treatment. To solve this 2π-periodic problem by spectral methods, we use an N-trigonometric polynomial

$$u_n(x,t) = \sum_{k=-N}^{N} \hat{u}_k(t) e^{ikx},$$

in order to approximate the spectral or pseudospectral Fourier projection $P_N u$ of the exact solution. Starting with $u_n(x,0)=P_N u_o(x)$, the classical Fourier method lets $u_N(x,t)$ evolves at later time according to the approximate model

$$\frac{\partial u_N}{\partial t} + \frac{\partial}{\partial x} [P_N(f(u_N(x,t)))] = 0. \tag{2.2}$$

We have already noted that the convergence to the entropy solution of (2.1), $u_N \xrightarrow[(N\to\infty)]{} u$ may (and in fact, in some cases must) fail. Instead, we propose to replace (2.2) by appending to it a spectrally accurate vanishing viscosity modification which amounts to

$$\frac{\partial u_N}{\partial t} + \frac{\partial}{\partial x} [P_N\, f(u_N(x,t))] = \varepsilon \frac{\partial}{\partial x} \left[Q_m(x,t) * \frac{\partial u_N}{\partial x} \right] \tag{2.3}$$

Here, $Q_m(x,t)$ is a viscosity kernel of the form

$$Q_m(x,t) = \sum_{m \le |k| \le N} \hat{Q}_k(t) e^{ikx} \tag{2.4}$$

This kind of <u>spectral viscosity</u> can be efficiently implemented in the Fourier rather than in the physical space, i.e.,

$$\varepsilon \frac{\partial}{\partial x} \left[Q_m(x,t) * \frac{\partial u_N}{\partial x} \right] = -\varepsilon \sum_{m \le |k| \le N} k^2 \hat{Q}_k(t) \hat{u}_k(t) e^{ikx} \tag{2.5}$$

It depends on two free parameters: the viscosity amplitude, $\varepsilon=\varepsilon(N)$, and the effective size of the <u>inviscid</u> spectrum, $m=m(N)$. In [6] it was shown that these two parameters can be chosen so that we have both, i.e., the spectral viscosity retains the spectral accuracy of the overall approximation and at the same time it is sufficient to enforce the correct amount of entropy dissipation that is missing otherwise (with $\varepsilon=0$).

T

Entropy dissipation is necessary for convergence; the lack of such dissipation in the classical Fourier methods is the main reason for its divergence. On the other hand, under appropriate assumptions, one can use compensated compactness arguments [8] to show that entropy dissipation is sufficient for convergence.

3. CONVERGENCE. We shall discuss two model problems.

Example 3.1 The scalar case. We consider general nonlinear scalar conservation laws (2.1). The pseudospectral viscosity method collocated at the equidistant points $x_\nu=\frac{2\pi\nu}{N}$, takes the form

$$\frac{\partial}{\partial t}\, u_N(x_\nu,t) + \frac{\partial}{\partial x}\,[P_N f(u_N(x_\nu,t))] = +\frac{1}{N} \sum_{|k|=\sqrt{N}}^{N} \frac{k-\sqrt{N}}{N-\sqrt{N}}\, k^2\ \hat{u}_k(t)\, e^{ikx_\nu} \tag{8.1}$$

It can be shown, [7], that the spectral viscosity on the right guarantees entropy dissipation and the L^∞-stability of the overall approximation; consequently convergence follows.

Example 3.2. The isentropic gasdynamics equations

$$\rho_t + (\rho u)_x = 0$$
$$(\rho u)_t + (\rho u^2 + p(\rho))_x = 0 \tag{4.1}$$

for a polytropic gas $p=\text{Const.}\rho^\gamma$, $\gamma>1$ are approximated in a similar fashion. Under appropriate L^∞-stability assumption (in particular, a uniform bound from the vacuum state), it can be shown [3], [7] that the spectral viscosity solution converges.

Finally we will present numerical examples which demonstrate the utility of the method and extensions to nonperiodic problems will be described.

REFERENCES

[1] S. Abarbanel, D. Gottlieb and E. Tadmor, Spectral methods for discontinuous problems, in "Numerical Analysis for Fluid Dynamics II" (K.W. Morton and M.J. Baines, eds.), Oxford University Press, 1986, pp. 129-153.

[2] C. Canuto, M.Y. Hussaini, A. Quartenoni and T. Zang, Spectral Methods with Applications to Fluid Dynamics, Springer-Verlag, 1987.

[3] R. DiPerna, Convergence of approximate solutions to systems of conservation laws, Arch. Rat. Mech. Anal., Vol. 82, pp. 27-70 (1983).

[4] Y. Maday and E. Tadmor, Analysis of the spectral viscosity method for periodic conservation laws, SIAM J. Num. Anal., submitted.

[5] A. Majda, J. McDonough and S. Osher, The Fourier method for nonsmooth initial data, Math. Comp. Vol 30, pp. 1041-1081 (1978).

[6] E. Tadmor, Convergence of spectral methods for nonlinear conservation laws, SIAM J. Num. Anal., to appear.

[7] E. Tadmor, Semi-discrete approximations to nonlinear systems of conservation laws; consistency and stability imply convergence, to appear.

[8] L. Tartar, Compensated compactness and applications to partial differential equations, in Research Notes in Mathematics 39, Nonlinear Analysis and Mechanics, Heriott-Watt Symposium, Vol. 4 (R.J. Knopps, ed.) Pittman Press, pp. 136-211 (1975).

T

THE RIEMANN PROBLEM WITH UMBILIC LINES FOR PLANE WAVES IN ISOTROPIC ELASTIC SOLIDS

by

T. C. T. Ting
Department of Civil Engineering, Mechanics and Metallurgy
University of Illinois at Chicago
Box 4348, Chicago, IL 60680 (U. S. A.)

The governing equations for plane waves in isotropic elastic solids are a system of hyperbolic conservation laws and can be written as

$$\underset{\sim}{U}_x - \underset{\sim}{F}(\underset{\sim}{U})_t = \underset{\sim}{0} , \tag{1}$$

in which $\underset{\sim}{U}$ is a 6-vector, three of which are the velocity components and the other three are the stress components on the surface x = constant. $\underset{\sim}{F}$ is a given function of $\underset{\sim}{U}$ but it depends on the stress components only, not on the velocity components. The characteristic wave speeds c of (1) are $\pm c_i$, i = 1, 2, 3, with

$$c_1 \geq c_2 \geq c_3 . \tag{2}$$

It is shown in [1,2] that c_2 is linearly degenerate. The simple wave associated with c_2 is therefore a shock wave. Thus, it is sufficient for the Riemann problem to consider wave curves associated with c_1 and c_3 only.

For hyperelastic materials for which the stress-strain laws are derivable from a potential (the strain energy) W, one can express W in terms of σ and τ which are, respectively, the normal stress and the resultant

shear stress on the surface x = constant. Since W is invariant with respect to the change of sign in τ, W is a function of σ and τ^2. For the second order materials W has the expression

$$W = \frac{a}{2}\sigma^2 + \frac{d}{2}\tau^2 + \frac{b}{6}\sigma^3 + \frac{e}{2}\sigma\tau^2 , \tag{3}$$

in which a, d, b, e are the material constants. The longitudinal strain ϵ and the shear strain γ are

$$\begin{aligned} \epsilon &= \frac{\partial W}{\partial \sigma} = a\sigma + \frac{1}{2}(b\sigma^2 + e\tau^2) , \\ \gamma &= \frac{\partial W}{\partial \tau} = \tau(d + e\sigma) . \end{aligned} \tag{4}$$

We see that b and e are the second order constants.

With W given by (3), there exists one umbilic point at which

$$c_1 = c_3 .$$

The umbilic point is located at

$$\sigma = \frac{d - a}{b - e} , \quad \tau = 0.$$

The system therefore is not totally hyperbolic (or strictly hyperbolic).

For the modified Riemann problem in which a constant stress state is prescribed for $t = 0$ and $x > 0$ (the initial condition) and a different constant stress state is prescribed for $x = 0$ and $t > 0$ (the boundary condition), the solution consists of wave fans each of which can be a simple wave, a shock wave, or a composite wave in which a shock wave is in contact with a simple wave [3 - 6]. The complete solutions for the strain energy given by (3) for arbitrary initial and boundary conditions have been presented in [2]. Many interesting and unexpected phenomena are

discovered due to the existence of the umbilic point. The same phenomena have also been discovered by Shaeffer and his co-workers [7,8,9] who consider a prototype 2x2 system of non-strictly hyperbolic conservation laws.

If the stresses are not small, the third order terms in the stress-strain laws must be included. The strain energy W then has the expression

$$W = \frac{a}{2}\sigma^2 + \frac{d}{2}\tau^2 + \frac{b}{6}\sigma^3 + \frac{e}{2}\sigma\tau^2 - \rho_o\theta_o\zeta + \frac{1}{12}\varepsilon_1\sigma^4 + \frac{1}{12}\varepsilon_2\tau^4 + \frac{1}{4}\varepsilon_3\sigma^2\tau^2 + \varepsilon\sigma\zeta \quad , \tag{5}$$

in which ε_1, ε_2, ε_3 and ε are the third order material constants and ρ_o, θ_o are the mass density and the initial temperature. ζ is the entropy which can no longer be ignored because entropy jump is of the third order in the discontinuity of the strain [10], and hence of the stress. Depending on the material constants, there may be up to three umbilic points at which $c_1 = c_3$. What is more interesting is that one may have an umbilic line along which $c_1 = c_3$. This is the main subject we will address in this paper.

We will show that there may be one or two umbilic lines. The umbilic line may be a curve. The wave curves, which provide the solution to the modified Riemann problem, will be presented for the system with umbilic lines. As in [2], a shock wave may satisfy the Lax stability conditions for both c_1 wave fan and c_3 wave fan. On the other hand, a shock may not satisfy the Lax stability conditions for either the c_1 wave fan or the c_3 wave fan. Moreover, since the wave speed has more than one extremum along the wave curve, the Lax stability conditions are not sufficient. A more discriminating condition proposed by Liu [11] will be required.

REFERENCES

[1] Li, Yongchi and Ting, T. C. T., "Plane Waves in Simple Elastic Solids and Discontinuous Dependence of Solution on Boundary Conditions," Int. J. Solids Structures, 19, 1983, 989-1008.

[2] Tang, Zhijing and Ting, T. C. T., "Wave Curves for the Riemann Problem of Plane Waves in Isotropic Elastic Solids," Int. J. Engineering Science, in press.

[3] Lax. P. D., "Hyperbolic Systems of Conservation Laws II," Comm. Pure Appl. Math., 10 1957, 537-566.

[4] Smoller, J. A. "On the Solution of the Riemann Problem With General Step Data for an Extended Class of Hyperbolic Systems," Michigan Math. J., 16, 1969, 201-210.

[5] Liu, T.-P., "The Riemann Problem for General Systems of Conservation Laws," J. Diff. Eqs., 18, 1975, 218-234.

[6] Dafermos, C. M., "Hyperbolic Systems of Conservation Laws," Brown Univ. Rept. LCDS #83-5, 1983.

[7] Schaeffer, D. G. and Shearer, M., "The Classification of 2x2 Systems of Non-Strictly Hyperbolic Conservation Laws, With Application to Oil Recovery," Comm. Pure Appl. Math., 40, 1987, 141-178.

[8] Shearer, M., Schaeffer, D. G., Marchesin, D. and Paes-Leme. P. L., "Solution of the Riemann Problem for a Prototype 2x2 System of Non-Strictly Hyperbolic Conservation Laws," Arch. Rat. Mech. Anal., 97, 1987, 299-320.

[9] Schaeffer, D. G. and Shearer, M., "Riemann Problems for Nonstrictly Hyperbolic 2x2 Systems of Conservation Laws," in press.

[10] Bland, D. R., "On the Shock Waves in Hyperelastic Media," IUTAM Symp. on Second-Order Effects in Elasticity, Plasticity and Fluid Dynamics," 1964, 93-108.

[11] Liu, T.-P., "The Riemann Problem for General 2x2 Conservation Laws," Trans. Amer. Math. Soc., 199, 1974, 89-112.

T

Random-Choice Based Hybrid Methods for One and Two Dimensional Gas Dynamics

E F Toro

Department of Aerodynamics, Cranfield Institute of Technology,
Cranfield, MK43 OAL, England

Our theme is numerical solution of the unsteady Euler equations in one and two space dimensions with particular emphasis on the accurate representation of solutions containing strong discontinuities such as shocks and contacts. There are several modern numerical methods that are accurate in the smooth parts of the flow, but discontinuities are smeared. Typically, shocks are spread over two to three zones, but contacts are more difficult to handle and are typically spread over five to six zones. In the gas dynamics associated with combustion phenomena the representation of contacts is very important; they carry discontinuities in temperature on which ignition criteria are based.

The Random Choice Method [1] (RCM), on the other hand, gives zero-width discontinuities but smooth parts of the flow are affected by randomness, which is a feature of the method. In Ref. [2] we presented a hybrid method that combines SORF, a new second order random flux method [3], and RCM. SORF is applied everywhere except at large discontinuities where RCM acts. The performance of this hybrid (SORFRCM) for one-dimensional problems is excellent. Fig. 1 shows results for density and pressure for the Sod's shock tube problem; full lines show the exact solution and symbols show the numerical solution. Here we present some further refinements of SORFRCM concerning three aspects, namely (a) switching mechanisms, (b) monotonicity of the 'smooth component' and (c) extension to multidimensional problems.

Extension of Riemann-problem based methods is normally accomplished by space operator splitting (SOS). Roe [4] has shown that SOS is incorrect under discontinuous data, for certain waves. Here, however we insist in extending the hybrid methods to multi-dimensional problems via SOS. Shock waves must be compromised, that is they must be handled by the smooth component of the hybrid, which must therefore be reasonably accurate for this type of wave. Contact discontinuities however, are cleanly captured. This is

an advantage of the hybrid method over high resolution methods under SOS. Fig. 2 shows results for Sod's shock tube problem with initial data at an angle of 45 degrees to the 2D grid using SORFRCM. Note that there are some small spurious oscillations present; their origin is a start up error. They reveal that we have not yet completely resolved the monotonicity aspect of SORF.

THe second hybrid method (ROERCM) we consider consist of Roe's method [5] and RCM. The advantage of this combination is that the smooth component (Roe) is well understood and developed. Figs. 3 and 4 show the counterparts of Figs. 1 and 2 using the ROERCM Hybrid.

References

1. Chorin A.
   Random Choice Solution of Hyperbolic Systems. J. Comp. Phys., 22, pp 517-536, 1976.

2. Toro E.F. and Roe P.L.
   A Hybridised Higher-Order Random Choice Method for Quasi-Linear Hyperbolic Systems. Proc. 16th International Symposium on Shock Tubes and Waves. July 26-30, 1987, Aachen, W. Germany (to appear).

3. Toro E.F.
   A New Numerical Technique for Quasi-Linear Hyperbolic Systems of Conservation Laws. CoA Report 86/20, Cranfield Institute of Technology, Cranfield, England, December 1986.

4. Roe P.L.
   Discontinuous Solutions to Hyperbolic Systems Under Operator Splitting. ICASE Report 87-64, NASA Langley Research Center, Hampton, VA 23665, 1987.

5. Roe P.L.
   Approximate Riemann Solvers, Parameters, Vectors and Difference Schemes. J. Comp. Phys. 43,pp 357-372, 1981.

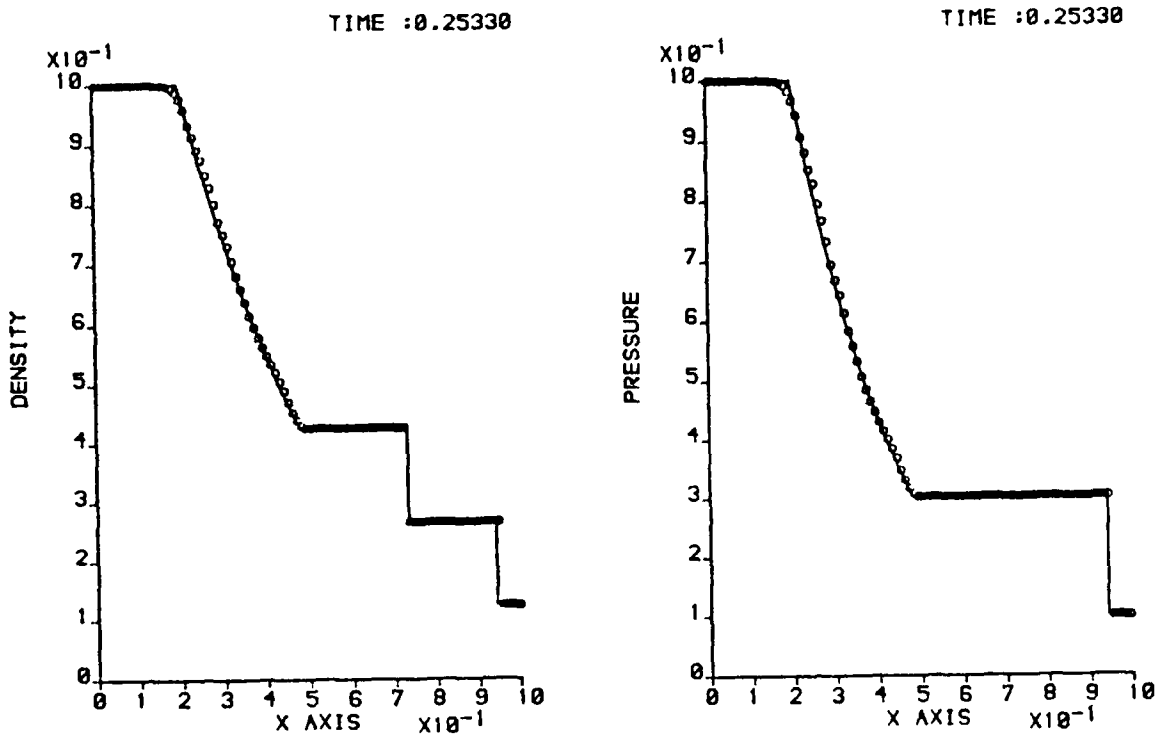

Fig. 1 Shock-tube problem in 1-D solved by the SORFRCM hybrid.

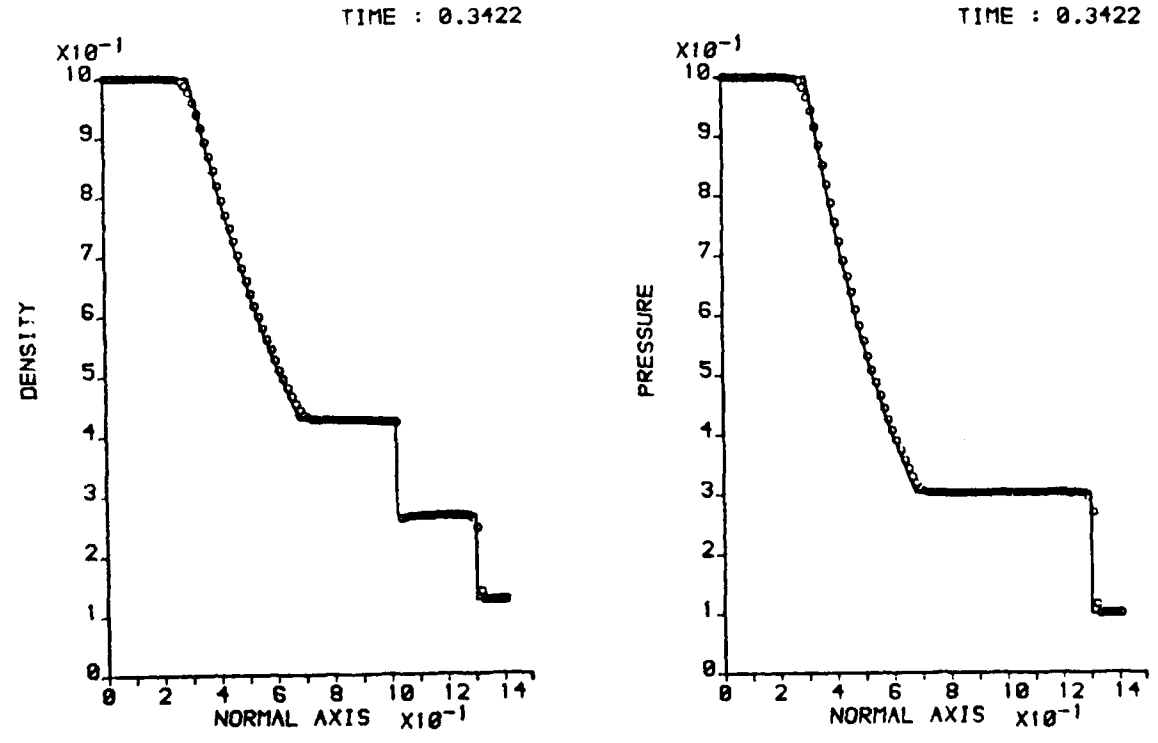

Fig. 2 Shock-tube problem in 2-D solved by the SORFRCM hybrid.

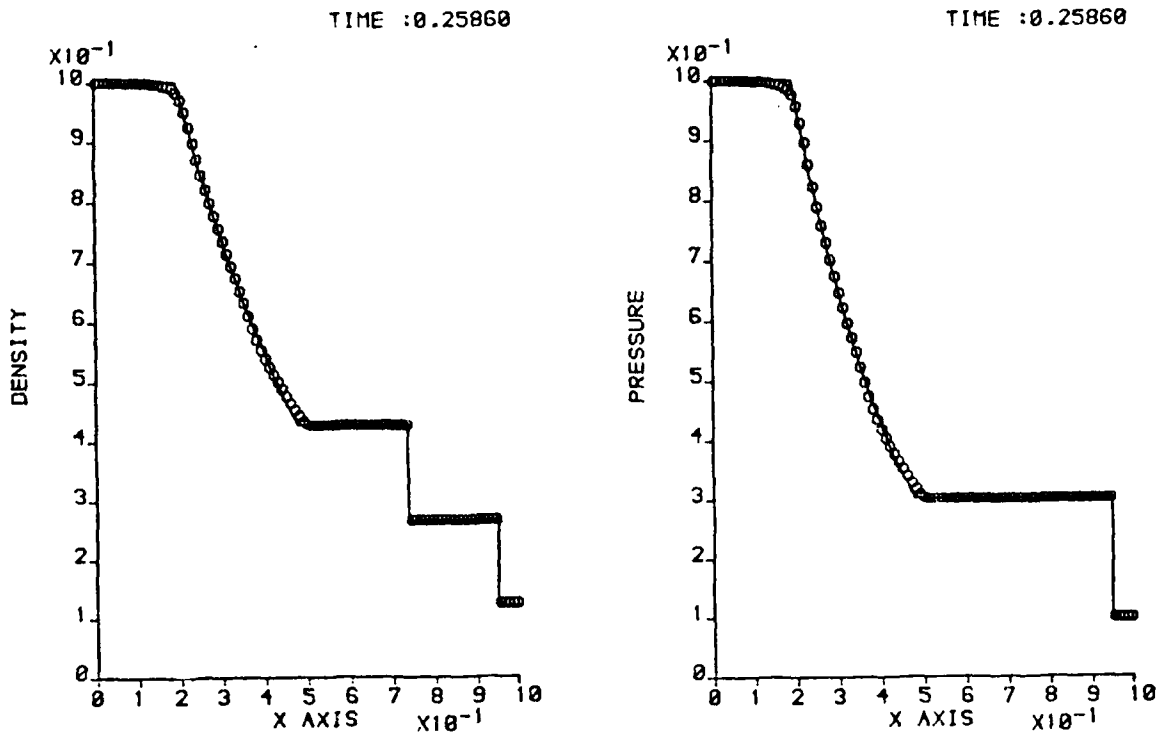

Fig 3. Shock-tube problem in 1-D solved by the ROERCM hybrid.

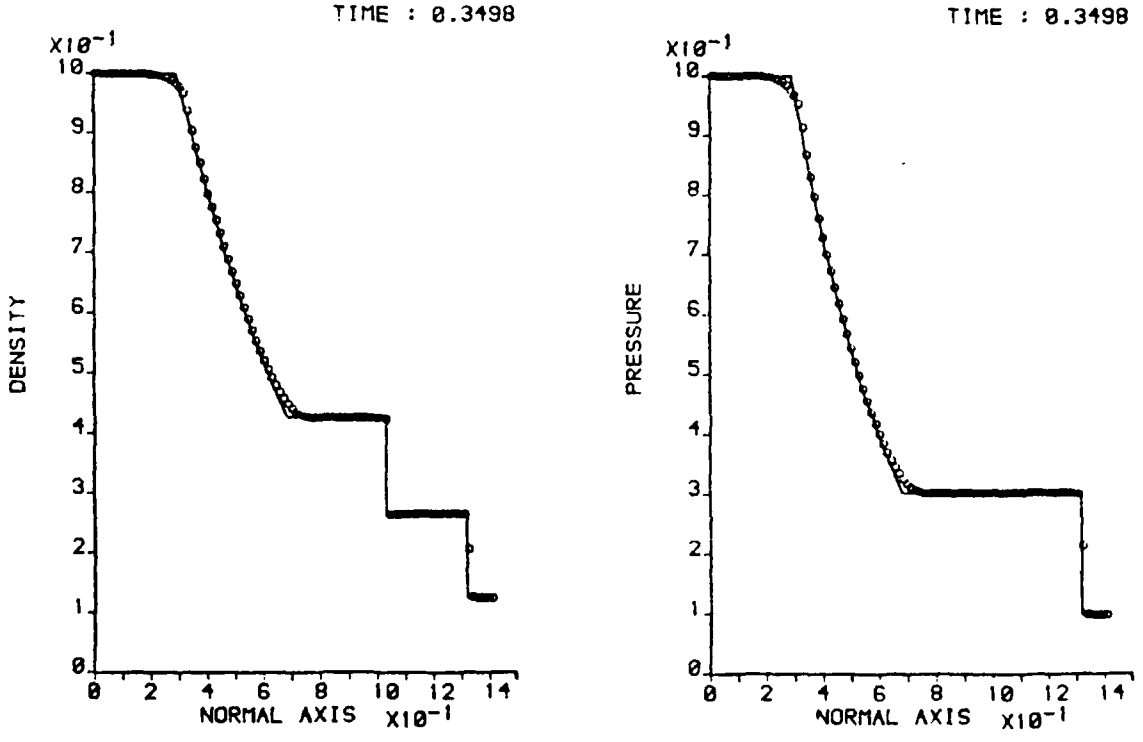

Fig. 4 Shock-tube problem in 2-D solved by the ROERCM hybrid.

Higher-Order Godunov Methods for Compositional Reservoir Simulation

John A. Trangenstein
John B. Bell

Lawrence Livermore National Laboratory
P.O. Box 808
Livermore, California 94550

Simulation of enhanced oil recovery techniques, particularly miscible gas injection, requires numerical models that account for a variety of physical phenomena. Naturally-occuring hydrocarbon fluids are mixtures of a large number of different chemicals, which have widely varying behavior due to changes in pressure, volume and temperature. These hydrocarbons associate to form distinct homogeneous fluids, called phases, in such a way that the Gibbs free energy of the mixture is minimized. As pressure is varied, the concentrations of the hydrocarbon components in the phases varies, even to the point that new phases form or existing phases vanish.

The compositional model of phase behavior is the most successful of all reservoir simulation models in predicting the thermodynamic properties of the reservoir fluids. The basis of this model is a collection of mathematical expressions for the chemical potentials for each component in each phase of the reservoir fluid. Thermodynamic equilibrium is described as a constrained minimization of the Gibbs free energy of the total fluid, subject to constraints representing nonnegativity of the phase compositions and conservation of mass. Because of the representation of the phase behavior in terms of this constrained minimization problem, the resulting system of flow equations is very complicated. The purpose of this talk is to describe the mathematical structure of the flow equations, and to present robust numerical procedures for their solution.

The fluid flow equations consist of component conservation equations, Darcy's law for the volumetric flow rates, balance between the fluid volume and the rock void, and the conditions of thermodynamic equilibrium that determine the distribution of the chemical components into phases. We manipulate the flow equations to form a pressure equation and a modified component conservation equation; these form the basis for our sequential method. We show that the pressure equation is parabolic under reasonable assumptions on the thermodynamic equilibrium model, and that the component conservation equations are hyperbolic in the absence of diffusive forces such as capillary pressure and mixing. (We include other important physical effects, such as interfacial tension.) Our numerical method uses a sequential approach, in which the parabolic pressure equation is solved by taking the chemical compositions to be known functions of space, independent of pressure; afterward, the hyperbolic component conservation equations are solved

by taking the pressure and total fluid velocity to be known functions of space, independent of chemical compositions.

The characteristic structure of the component conservation equations is very interesting. There are always at least as many chemical components as there are phases (at least for these reservoir simulation problems), and there are as many characteristic families as there are chemical components. The characteristic analysis shows that if n phases exist, then there are $n-1$ strongly nonlinear waves with local linear degeneracies (i.e., the the characteristic speeds reach local extrema along the corresponding rarefaction curves). The remaining characteristic speeds are weakly nonlinear, and (relative to the strongly nonlinear waves) behave as if they were linearly degenerate. The hyperbolic system is not strictly hyperbolic, since the various wave speeds can coalesce with a corresponding eigenvector deficiency of the linearized coefficient matrix. Furthermore, in multiple-contact miscible gas injection, the recovery process is designed to drive the fluid composition toward the critical point, where all of the characteristic speeds can become equal and linearly degenerate. These problems are especially difficult to solve numerically, since they are subject to smearing of the linearly degenerate multiple-contact miscible front due to the numerical diffusion in the differencing scheme for the conservation law.

We have used three basic numerical techniques in our numerical method for compositional reservoir simulation. A customized Newton iteration with appropriate adaptive changes of variables is used to solve the thermodynamic equilibrium equations. This view of phase equilibrium is designed to provide the characteristic structure of the component conservation equations as a direct consequence; in fact, the variable changes in the Newton iteration correspond to deflation techniques for the algebraic eigenvalue problem to find the characteristic speeds. The parabolic pressure equation is solved by a particular implementation of the lowest-order mixed finite element method. The component conservation equations are solved by a higher-order Godunov procedure.

Our numerical examples are concerned with the modeling of one-dimensional miscible gas injection in a slim tube. This apparatus effectively eliminates gravitational effects; as a result, all characteristic speeds have the same sign and the Riemann problems required by the Godunov procedure are trivially solved by the upstream state. For the simulation of multi-dimensional petroleum reservoir flow, the Riemann problems could be solved approximately by techniques due to Bell, Colella and Trangenstein.

REFERENCES

"Customized Minimization Techniques for Phase Equilibrium Computations in Reservoir Simulation," to appear in *Chemical Engineering Science*, by John A. Trangenstein

"Mathematical Structure of Compositional Reservoir Simulation," submitted to *SIAM J. Appl. Math.*, by John A. Trangenstein and John B. Bell

"Higher-Order Godunov Methods for General Systems of Hyperbolic Conservation Laws", submitted to *J. Comp. Phys.*, by John B. Bell, Phillip Colella and John A. Trangenstein

GRID CHARACTERISTIC METHODS FOR HYPERBOLIC PROBLEMS

L.I.Turchak, A.S.Kholodov

U.S.S.R. Academy of Sciences Computing Centre
40 Vavilov Str.,117333 Moscow

A method of difference schemes constructing for multidimensional quasilinear equations of hyperbolic type as well as the hyperbolic part of more complicated equations is developed. It is based on a successive transition from the simplest one-dimensional transport equation to a system of linear,and then quasilinear,one-dimensional hyperbolic equations followed by multidimensional ones.

The approach involves an introduction of linear spaces of difference schemes coefficients and characteristic properties of hyperbolic equations systems using. This allows:

(i) to construct the entire set of schemes with positive approximation(monotonic or majorant schemes) for arbitrary grid models;

(ii) to prove in general there are no schmes with the second or higher order of approximation on the solutions of the original equations;

(iii) to find the most accurate scheme among monotonic schemes for each grid model and,conversely,to find among second- and higher-order nonmonotonic schemes the one that is the least oscillating at the discontinuities of the solution;

(iiii)to construct the analogues of all these schemes for a quite general case of linear systems of hyperbolic equations.

GC methods present a wide range of computational algorithms with different properties. These algorithms include explicit and implicit schemes with the first- or higher-order approximations, conservative and hybrid schemes, etc.

Some of the schemes were used for the numerical modeling of many hyperbolic problems: steady and unsteady supersonic flows, plasma physics and mechanics of a deformable body. The results obtained show the effectiveness of the GC methods in solving problems with a complicated structure of the required solution.

Fully Implicit High-Resolution Scheme for Compressible Chemically Reacting Flows

Y. Wada*, H. Kubota**, T. Ishiguro* and S. Ogawa*
* National Aerospace Laboratory
** University of Tokyo

The eigenvalues and eigenvectors are analytically derived for convective terms of general real gas dynamics equations in generalized curvilinear coordinate. This general gas-dynamic equations can include arbitrary non-equilibrium effecs, i.e. chemical reactions or vibrational non-equilibrium etc.

This diagonalization has the following favorable properties :

1. Total mass conservation equation is included.
2. Chemical reaction and vibrational non-equilibrium can be treated in the same manner.
3. Matrix multiplifications are so simple, that the increase in number of additional non-equilibrium equations does not drastically increase the operation counts.
4. This is a natural extention of Warming & Beam's perfect gas-dynamic matrices diagonalization[1], which is included for a special case in our formulation.

Yee and Shinn[2] derived another diagonalizing formulation, but their basic equations do not include the total mass consevation equation, and consequently the total mass is not conserved especially when chemical source terms are treated implicitly. Park[3] suggests that every species equation and the total mass conservation equation should be solved at the same time for the flows in which dominant species do not exist.

The above defects can be overcom in our formulation, which opens the way for general real gas-dynamic equations to the construction of finite difference schemes based on characteristic relations such as TVD schems or the simplification of the solution of block-tridiagonal systems that arise in implicit time-split algorithm such as LU-ADI time integration.

In this paper, we simulate the chemically reacting viscous flows through SCRAM-Jet engine, by the use of TVD scheme[4] in space discretization and Point-Alternative-Direction Implicit(Approximate Factorization) method in time integration, in both of which our diagonalizing formulation is used. The result shows the efficiency , robustness and high resolution of our scheme.

References

1. Warming,R.F., Beam,M. and Hyett,B.J., "Diagonalization and Simultaneous symmetrization of the Gas-Dynamic Matrices," Math. of Comp., Vol 29, Num. 132, October 1975, pp. 1037-1045.

2. Yee,H.C., and Shinn,Judy L., "Semi-Implicit and Fully Implicit Shock-Capturing Methods for Hyperbolic Conservation Laws with Stiff Source Terms," AIAA Paper 87-1116CP, June 1987.

3. Park,Chul, "On Convergence of Computation of Chemically Reacting Flows," AIAA Paper 85-0247, January 1985.

4. Takakura,Y., Ishiguro,T. and Ogawa,S., " On the Recent Difference Schemes for the Three-Dimensional Euler Equations," AIAA Paper 87-1151CP, June 1987.

Two-dimensional calculation:

- inflow condition

p = 1 atm
T = 1000 K
M = 4

mass fraction

$Y_{H_2O} = 0.027$
$Y_{O_2} = 0.022$
$Y_{OH} = 0.001$
$Y_{H_2O} = 0.0$
$Y_{N_2} = 0.75$

} we use Roger's Global Hydrogen - Air Combustion Model

- result

RHO
FMAX= 0.434E+01
FMIN= 0.458E+00
FW= 0.384E-01

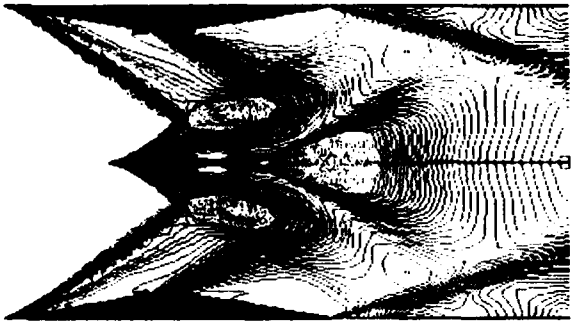

T
FMAX= 0.345E+01
FMIN= 0.818E+00
FW= 0.260E-01

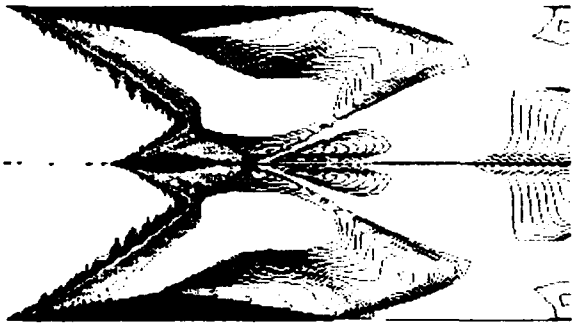

H2O
FMAX= 0.191E+00
FMIN= 0.000E+00
FW= 0.190E-02

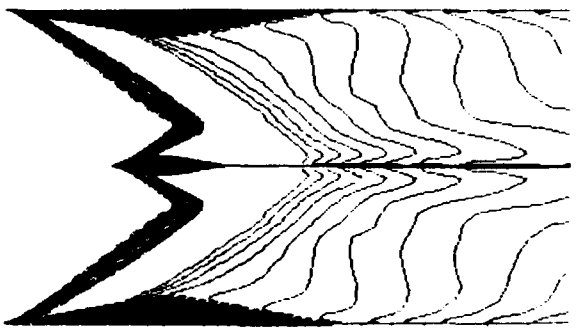

Three-dimensional calculation:

- inflow condition: the same as 2-dimensional calculation
- results (contours of $\zeta\, Y_{H_2O}$)

  above figure: on side wall

  below figure: on symmetric surface

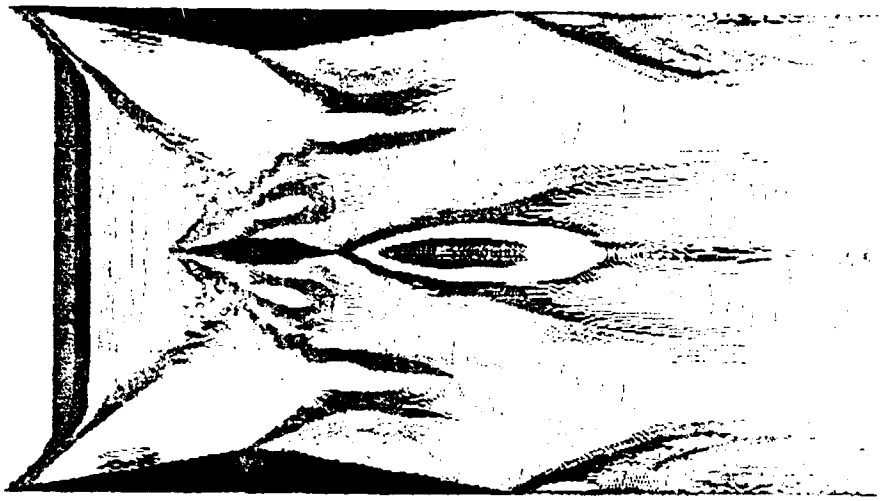

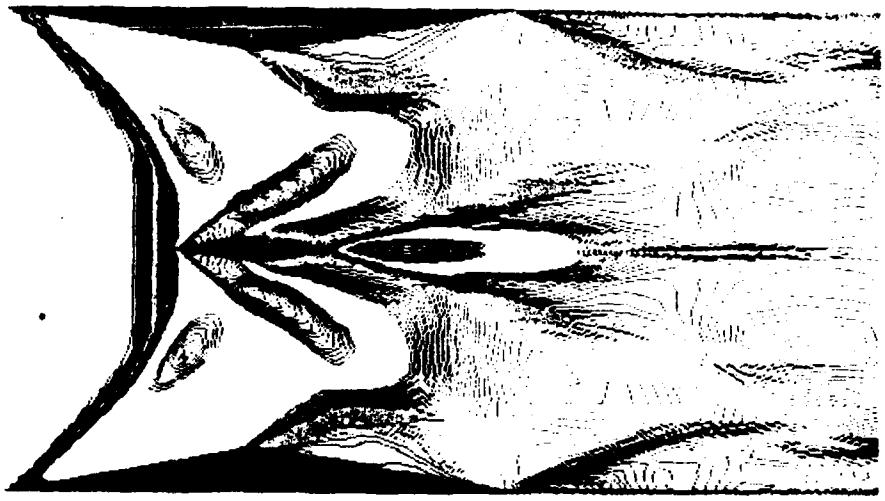

THE EXISTENCE AND BEHAVIOR OF VISCOUS STRUCTURE FOR PLANE DETONATION WAVES

David H. Wagner[1]
Department of Mathematics
University of Houston
Houston, TX 77004

Detonation waves are compressive, exothermically reacting shock waves. One of the curiosities of combustion theory is that there also exist expansive "shock waves" known as *deflagration waves*, which will not be discussed in this paper. We will give a mathematically rigorous, but simple, discussion of the *viscous structure* of plane detonation waves.

In the inviscid theory, known as the Chapman-Jouguet theory, we assume that the thickness of the reaction zone is zero, we neglect all diffusion effects such as viscosity, heat conduction, and diffusion of species, and any external forces such as gravity, and we look for steady plane waves. This yields the following system of differential equations:

(1.1) (a) $(\rho u)_x = 0,$

(b) $[\rho u^2 + p(\rho, T)]_x = 0,$

(c) $\left[\left[\rho[u^2/2 + e(\rho, T, Y)] + p(\rho, T)\right]u\right]_x = 0,$

(d) $(\rho u Y)_x = -\rho u Y \cdot \delta(x - x_0).$

Here x is a space coordinate in the direction normal to the wave, x_0 is the location of the wave, and ρ, T, u, p, e, and Y are the mass density, temperature, x-component of velocity, pressure, specific internal energy, and mass fraction of the reactant, respectively. As is standard practice, we have represented the extremely complicated chemical reaction by a simplified, one-step chemistry: reactant $\rightarrow$ product. From (1.1a) we see that the mass flux, ρu, has a constant value; we denote this value by m. The fluxes of momentum, (1.1b), and energy, (1.1c) are also constant; from this fact we obtain the *Rankine-Hugoniot conditions* for a shock wave. The difference between inert gas dynamics and the exothermic reactive theory discussed here lies in the fact that Y varies from a positive value on the unburned side of the wave, which we take to lie on the right side, to a zero value on the burned, or left side. Because the internal energy e depends on Y, the change in Y causes the classical Hugoniot curve (the solution locus of (1.1c)) of gas dynamics to move. As a

[1]Research supported by NSF Grant #DMS-8601917 and AFOSR Grant # AFOSR 86-0218

consequence, we find that, for a given value of m, a given shock state on the left may now be connected by a shock wave to two possible states on the right, except for certain critical values of m for which there is a unique burned state -- the *Chapman Jouguet point.* In addition, the curve of possible burned states, parameterized by m, has two components. One component, corresponding to compressive waves, is called the detonation branch, and the other component, corresponding to expansive waves, is called the deflagration branch. By way of contrast, in an inert gas, for a given value of m, a state is usually connected to only one state on the right, and the curve of possible terminal shock states is usually connected.

The reacting shock waves of the CJ theory are classified as follows. A wave connecting the unburned state to the closer detonation point is called a weak detonation wave, and a connection to the farther detonation point is called a strong detonation. A detonation wave terminating at the Chapman Jouguet point is called a Chapman Jouguet detonation. Deflagration waves are similarly classified.

The CJ theory for detonation waves is useful for deriving the Rankine Hugoniot conditions, and for classifying the types of wave. However, this theory is physically flawed, because in reality the reaction zone is much thicker than the shock layer. This is due to the fact that the chemical reaction depends on molecular collisions, and requires a distance much longer than the mean free path to achieve significant completion. The shock layer, however, has been experimentally observed to be several mean free paths thick. Consequently the appropriate inviscid model is the one developed independently by Zel'dovich, von Neumann, and Döring, and which is known as the ZND model. In this model equation (1.1d) is replaced by a similar equation, but with a finite reaction rate:

$$(1.1d') \qquad (\rho u Y)_x = -K\rho Y \phi(T)$$

For our purposes it is reasonable to assume that the reaction rate function ϕ is continuous, non-negative, and monotone. Our mathematical treatment will require that we assume that ϕ vanishes whenever the temperature T is less than a given *ignition temperature* T_i. For a known reaction rate ϕ one can solve (1.1a, b, c, d') explicitly; the only detonation wave solutions are strong or CJ detonations. These waves, which are known as ZND waves, begin with a jump discontinuity which is an inert shock wave. This shock wave heats the gas above the ignition temperature; the reaction proceeds, with the velocity and temperature following a curve of equilibrium states for (1.1b, c), parameterized by Y. One of the interesting features of these waves is the peak in the temperature and pressure which is known as the *von Neumann spike.* By way of contrast, in inert shock waves these variables are usually monotone.

One of the purposes of this paper is to examine the *structural stability* of ZND waves. A

shock wave is structurally stable if it is the limit of solutions to models which include more physical effects, such as viscosity and heat conduction, as these models tend to the original inviscid model in which these effects are neglected. For steady plane detonation waves one may consider the effects of viscosity, heat conduction, and species diffusion, to obtain the (steady) *reacting compressible Navier Stokes equations:*

(1.2) (a) $(\rho u)_x = 0,$

(b) $[\rho u^2 + p(\rho, T)]_x = (\mu u_x)_x,$

(c) $\left[\left[\rho[u^2/2 + e(\rho, T, Y)] + p(\rho, T)\right]u\right]_x = (\lambda T_x)_x + (\mu u u_x)_x + (q\rho D Y_x)_x,$

(d) $(\rho u Y)_x = (\rho D Y_x)_x - K\rho Y \phi(T).$

Here μ is the coefficient of bulk viscosity, λ is the heat conductivity, D is the diffusion rate for the reactant, and q is the difference in the heats of formation of the reactant and the product [Wi].

In this paper we prove a necessary condition and a sufficient condition for the existence of heteroclinic solutions of (1.2) which connect an unburned state to the strong detonation point. These conditions also apply to the Chapman Jouguet detonation. See (5.3) and (6.3). For simplicity we restrict our attention to the case where the *Prandtl number* is 3/4 ($\mu = \lambda/c_p$). In the limit as λ, μ, and D tend to zero (with other parameters fixed) these solutions tend to the ZND wave. Thus the ZND wave is structurally stable to this particular perturbation of the model.

For all of these solutions the *stagnation enthalpy* $H = c_p T + u^2/2$ is monotone, as is the *entropy flux:* $mS - \lambda T_x/T$. For most of the strong detonation waves the temperature and the pressure attain their maxima in the interior of the wave; this corresponds to the von Neumann spike which occurs in the ZND wave. However for a certain parameter range, characterized by large values of the diffusion coefficient λ, there exists a continuum of solutions which look like a weak detonation followed by a gas dynamic shock wave. For these waves the pressure and temperature are monotone. This pathological behavior has been noted before in numerical computations of solutions of (1.2), and rigorously for a qualitative model [CMR]. In these numerical computations it was observed that the weak detonation - shock wave solutions are dynamically stable as solutions of the time dependent reacting compressible Navier Stokes equations in one space dimension.

Let $\Lambda_* = \inf(\lambda/\rho D c_p, 1)$, and $\Lambda^* = \sup(\lambda/\rho D c_p, 1)$. For any state variable U let $U_\pm$ be the limit of U at $\pm\infty$. Then a necessary condition for the existence of a strong detonation structure profile is:

$$(5.3) \qquad m^2 V_- \geq \int_0^1 \frac{2\lambda\Lambda_* K}{c_p}(1-\tau)\,\phi(T_- + qY_-\tau/c_p)\,d\tau\,.$$

A sufficient condition is:

$$(6.3) \qquad Y_- > \varepsilon_i + \left(\frac{2\gamma c_p}{(\gamma-1)m^2 q^2 V_*} \int_{T_i}^{T_*} \lambda\Lambda^*(T_* - T)\,\phi(T)\,dT \right)^{\frac{1}{2}}.$$

It is interesting to compare these conditions to the corresponding conditions for existence of a plane premixed laminar flame [BNS, Wg].

References

[BNS] Berestycki, H., Nicolaenko, B., Scheurer, B., Mathematical analysis and singular limits of laminar flame fronts, SIAM J. Math. Anal., *16*, 1985.

[CMR] Colella, P., Majda, A., Roytburd, V., Theoretical and numerical structure for reacting shock waves, SIAM J. Sci. Stat. Comput., *7*, 1986, 1059-1080.

[C] Conley, C.C., *Isolated Invariant Sets and the Morse Index*, CBMS Regional Conference Series in Mathematics, no. 38, American Mathematical Society, 1978.

[HS] Holmes, P., Stewart, D.S., The existence of one dimensional steady detonation waves in a simple model problem, Studies in Applied Math., *66*, 1982, 121-143.

[Wg] Wagner, D. H., "Premixed laminar flames as travelling waves." In: *Reacting Flows: Combustion and Chemical Reactors.* Edited by G. S. S. Ludford. Lecture Notes in Applied Mathematics, no. 24, p. 229-237. American Mathematical Society, Providence, 1986.

[Wz1] Wazewski, T., Sur un principe topologique de l'examen de l'allure asymptotiques des intégrals des équations differentielles, Ann. Soc. Polon. Math., *20*, 1947, 279-313.

[Wz2] Wazewski, T., Sur un méthode topologique de l'examen de l'allure asymptotiques des intégrals des équations differentielles, Proc. Internat. Congr. Math., (Amsterdam, 1954), vol. 3, Noordhoff, Gronigen, 1956, 132-139.

[Wi] Williams, F. A., *Combustion Theory*, Benjamin/Cummings, Menlo Park, 1985.

A New Class of ENO Schemes for Hyperbolic Conservation Laws

Zhong-De Wang
Department of Mathematics and Mechanics
Nanjing Aeronautical Institute
Nanjing, China

In this paper we present a condition that a general 3-point and 5-point finite-difference scheme in conservation form is ENO. By using the UNO2 numerical flux introduced in (1), we obtain the condition that the difference schemes in conservation form is uniformly second-order accurate. We then convert known 3-point schemes into new 5-point schemes by applying Harten's trick in (2). Accordingly, a new class of uniformly second-order accurate ENO schemes has been constructed. Numerical experiment is presented to demonstrate the performance of these new ENO schemes. The result is encouraging.

1. Introduction. In this paper we consider the numerical solutions to the hyperbolic conservation laws

$$u_t + f(u)_x = 0, \qquad u(x,0) = u_0(x), \qquad t > 0, \quad x \in \mathbb{R} \tag{1.1}$$

Let $v_j^n = v_h(x_j, t_n)$, $x_j = jh$, $t_n = n\tau$, denote a numerical approximation in conservation form

$$v_j^{n+1} = v_j^n - \lambda(\hat{f}_{j+1/2} - \hat{f}_{j-1/2}) = (E_h(\tau)\cdot v^n)_j \tag{1.2}$$

Recently, A.Harten & S.Osher have developed Essentially Nonoscillatory (ENO) shock capturing methods for the approximation of (1.1) (see(3), (4)). ENO schemes satisfy

$$TV(E_h(\tau)\cdot v) \le TV(v) + O(h^r) \tag{1.3}$$

for h sufficiently small. Where $u_0(x)$ are piecewise smooth, r is the order of accuracy of (1.2). These schemes overcome the shortcoming — TVD schemes have at most first-order accuracy in the sense of truncation error, at extrema of the solution, and avoid a Gibb-like phenomenon at discontinuities. In this paper we describe a procedure to obtain the uniformly second-order accurate ENO schemes by modifying known TVD schemes. The format of this paper is as follows: In section 2, we present a sufficient condition that scheme (1.2) is ENO; in section 3, we give the condition that scheme (1.2) is uniformly second-order accurate, and propose a new class of uniformly second-order accurate ENO schemes; in section 4, numerical example is included to illustrate the schemes in section 3.

2. The condition for the construction of ENO schemes.
Suppose both the 3-point and 5-point schemes (1.2) can be rewritten in the form

$$v^{n+1} = E_h(\tau)\cdot v^n, \tag{2.1a}$$

$$(E_h(\tau)\cdot v)_j = v_j + C_{+,j+1/2}\Delta_{j+1/2}v - C_{-,j-1/2}\Delta_{j-1/2}v \tag{2.1b}$$

where

(2.1c) $\quad C_{+,j+1/2} = C_+(v_{j-1}, v_j, v_{j+1}, v_{j+2}), \qquad C_{-,j-1/2} = C_-(v_{j-2}, v_{j-1}, v_j, v_{j+1})$

The following theorem states a condition that scheme (1.2) is ENO.

Theorem 2.1. Let the coefficients $C_\pm$ in (2.1c) satisfy the condition

(2.2a) $\quad C_{\pm,j+1/2} = C^+_{\pm,j+1/2} + O(h^r)$

(2.2b) $\quad C^+_{+,j+1/2} = C^+_{-,j+1/2} \le 1$

then $\quad TV(E_h(\tau)\cdot v) \le TV(v) + O(h^r),$ $\quad$ i.e., scheme (2.1) is ENO.

Here $x^+ = (|x| + x)/2$.

Example 2.2. For the UNO2 scheme presented by Harten (see (1)), we can easily show that it satisfies (2.2.)

3. Uniformly second-order accurate ENO schemes

Let us consider a general 3-point scheme (1.2) with a numerical flux of the form

(3.1a) $$\hat{f}_{j+1/2} = \frac{1}{2}(f(v_j) + f(v_{j+1}) - \frac{1}{\lambda}Q(\nu_{j+1/2})\Delta_{j+1/2}v)$$

where

(3.1b) $$\nu_{j+1/2} = \lambda a_{j+1/2}$$

(3.1c) $$a_{j+1/2} = \begin{cases} \frac{f(v_{j+1}) - f(v_j)}{\Delta_{j+1/2}v}, & \Delta_{j+1/2}v \neq 0 \\ a(v_j), & \Delta_{j+1/2}v = 0 \end{cases}$$

Lemma 3.1. If $Q(x)$ in (3.1a) satisfy

(3.2a) $$|Q(x) \mp x| - (Q(x) \mp x) = O(h^r)$$

(3.2b) $$|Q(x) - x| + |Q(x) + x| + 2Q(x) \le 4$$

for $|x| \le \mu + O(h)$, then scheme (1.2) with (3.1) is ENO under the CFL restriction

(3.3) $$\lambda \max_j |a_{j+1/2}| \le \mu + O(h) \qquad (0 < \mu \le 1)$$

A.Harten & S.Osher have proposed the UNO2 scheme (1.2) with a numerical flux of the form

(3.4a)
$$\begin{aligned} \hat{f}^{\mathrm{UNO2}}_{j+1/2} = &\frac{1}{2}(f(v_j) + f(v_{j+1}) - |a_{j+1/2}|(v_{j+1} - v_j) \\ &+ \max(0, a_{j+1/2})(1 - \nu_{j-1/2})\cdot \hat{S}_j \\ &- \min(0, a_{j+1/2})(1 + \nu_{j+3/2})\cdot \hat{S}_{j+1}) \end{aligned}$$

where

(3.4b) $$\hat{S}_j = S_j/(1 + \nu_{j+1/2} - \nu_{j-1/2})$$

By using the UNO2 numerical flux, we obtain the following condition that scheme (1.2) is uniformly second-order accurate.

Lemma 3.2. Let the numerical flux $\hat{f}_{j+1/2}$ in (1.2) satisfy

$$\hat{f}_{j+1/2} - \hat{f}^{\mathrm{UNO2}}_{j+1/2} = O(h^2) \tag{3.5}$$

then scheme (1.2) is uniformly second-order accurate.

We convert 3-point scheme (3.1) into 5-point scheme as follows:

$$\hat{f}^{M}_{j+1/2} = \frac{1}{2}(f(v_j) + f(v_{j+1})) + \frac{1}{2\lambda}(g_j + g_{j+1} - Q(\nu_{j+1/2} + \gamma_{j+1/2})\Delta_{j+1/2}v) \tag{3.6a}$$

$$g_j = g(v_{j-1}, v_j, v_{j+1}), \qquad \gamma_{j+1/2} = (g_{j+1} - g_j)/\Delta_{j+1/2}v \tag{3.6b}$$

Lemma 3.3. Suppose $Q(x)$ is Lipschitz continuous and g_j satisfies

$$\begin{aligned} g_j + g_{j+1} =& \Big(Q(\nu_{j+1/2}) - |\nu_{j+1/2}| + \max(0, \nu_{j+1/2}) \cdot (1 - \nu_{j-1/2})\frac{\hat{S}_j}{\Delta_{j+1/2}v} \\ & - \min(0, \nu_{j+1/2}) \cdot (1 + \nu_{j+3/2})\frac{\hat{S}_{j+1}}{\Delta_{j+1/2}v}\Big) \cdot \Delta_{j+1/2}v + O(h^2) \end{aligned} \tag{3.7a}$$

$$\gamma_{j+1/2} \cdot \Delta_{j+1/2}v = g_{j+1} - g_j = O(h^2) \tag{3.7b}$$

then the numerical flux of (3.6) satisfies (3.5).

We construct $g_j = g(v_{j-1}, v_j, v_{j+1})$ that satisfies (3.7) in the following way:

$$g = m(\tilde{g}_{j+1/2}, \tilde{g}_{j-1/2}) \tag{3.8a}$$

$$\begin{aligned} \tilde{g}_{j+1/2} =& \frac{1}{2}\Big(Q(\nu_{j+1/2}) - |\nu_{j+1/2}| + \max(0, \nu_{j+1/2}) \cdot (1 - \nu_{j-1/2})\frac{\hat{S}_j}{\Delta_{j+1/2}v} \\ & - \min(0, \nu_{j+1/2}) \cdot (1 + \nu_{j+3/2})\frac{\hat{S}_j}{\Delta_{j+1/2}v}\Big) \cdot \Delta_{j+1/2}v \end{aligned} \tag{3.8b}$$

$$m(x, y) = \begin{cases} s \cdot \min(|x|, |y|), & \mathrm{sgn}(x) = \mathrm{sgn}(y) = s \\ 0, & \text{otherwise} \end{cases} \tag{3.8c}$$

Lemma 3.4. Let g_j be defined by (3.8). Suppose

$$S_j = h\frac{du(x_j)}{dx} + O(h^3) \tag{3.9}$$

then relations (3.7) is satisfied, and

$$\begin{aligned} |\gamma_{j+1/2}| =& |g_{j+1} - g_j|/|\Delta_{j+1/2}v| \\ \le& \frac{1}{2}\Big|Q(\nu_{j+1/2}) - |\nu_{j+1/2}| + \max(0, \nu_{j+1/2}) \cdot (1 - \nu_{j-1/2})\frac{\hat{S}_j}{\Delta_{j+1/2}v} \\ & - \min(0, \nu_{j+1/2}) \cdot (1 + \nu_{j+3/2})\frac{\hat{S}_{j+1}}{\Delta_{j+1/2}v}\Big| \end{aligned} \tag{3.10}$$

Lemma 3.5. Suppose $Q(x)$ satisfies (3.2), S_j satisfies (3.9) and g_j is defined by (3.8); then scheme (1.2) with numerical flux (3.6) is ENO under CFL restriction: $\lambda \max_j |a_{j+1/2}| \le \mu$.
As a synthesis of above results, we have
Theorem 3.6. Let us assume that $Q(x)$ satisfies (3.2), S_j satisfies (3.9) and g_j is defined by (3.8), then finite-difference scheme (1.2) with numerical flux (3.6) is uniformly second-order accurate ENO.

4. Numerical Examples. Consider a Riemann problem for the Euler equations of gas dynamics

$$u_t + f(u)_x = 0, \qquad u(x,0) = \begin{cases} u_L, & x < 0 \\ u_R, & x > 0 \end{cases} \tag{4.1a}$$

$$u = (\rho, m, E), \qquad f(u) = (m, m^2/\rho + P, m(E+P)/\rho), \tag{4.1b}$$

$$P = (\gamma - 1)(E - \frac{1}{2}m^2/\rho). \tag{4.1c}$$

Here ρ, m, E and P are the density, momentum, total energy, and pressure, we take $\gamma = 1.4$. We extend the new uniformly second-order accurate ENO scheme (1.2) with numerical flux (3.6) to (4.1) as follows:

$$v_j^{n+1} = v_j^n - \lambda(\hat{f}_{j+1/2} - \hat{f}_{j-1/2}) \tag{4.2a}$$

$$\hat{f}_{j+1/2} = \frac{1}{2}(f(v_j) + f(v_{j+1})) + \frac{1}{2\lambda}\sum_{k=1}^{3} R_{j+1/2}^k((g_j^k + g_{j+1}^k) - Q^k(\nu_{j+1/2}^k + \gamma_{j+1/2}^k)\alpha_{j+1/2}^k) \tag{4.2b}$$

$$g_{j+1/2}^k = \frac{1}{2}((Q^k(\nu_{j+1/2}^k) - |\nu_{j+1/2}^k|^k \cdot \alpha_{j+1/2}^k + \max(0, \nu_{j+1/2}^k) \cdot (1 - \nu_{j-1/2}^k)\hat{S}_j^k - \min(0, \nu_{j+1/2}^k) \cdot (1 + \nu_{j+3/2}^k)\hat{S}_{j+1}^k \tag{4.2c}$$

$$g_j^k = m(\tilde{g}_{j+1/2}^k, \tilde{g}_{j-1/2}^k) \tag{4.2d}$$

$$\gamma_{j+1/2}^k = \begin{cases} (g_{j+1/2}^k - g_j^k)/\alpha_{j+1/2}^k, & \alpha_{j+1/2}^k \neq 0 \\ 0, & \alpha_{j+1/2}^k = 0 \end{cases}, \quad \nu_{j+1/2}^k = \lambda a_{j+1/2}^k \tag{4.2e}$$

We take

$$Q^k(x) = \begin{cases} (x^2 + \varepsilon^2)/2\varepsilon, & |x| < \varepsilon \\ |x|, & |x| \ge \varepsilon \end{cases} \tag{4.3}$$

and $\hat{S}_j^k$ as follows:

$$\hat{S}_j^k = m(S_{-j}^k, S_{+j}^k)/(1 + \nu_{j+1/2}^k - \nu_{j-1/2}^k) \tag{4.4a}$$

$$\hat{S}_{\pm j}^k = \alpha_{j+1/2}^k + \frac{1}{2}m(\alpha_{j+3/2}^k - \alpha_{j+1/2}^k, \alpha_{j+1/2}^k - \alpha_{j-1/2}^k) \tag{4.4b}$$

Here $a_{j+1/2}$ is the k-th eigenvalue of $A(v_{j+1/2})$ corresponding to the right-eigenvector $R_{j+1/2}$, and $\alpha_{j+1/2}^k$ denotes the component of $\Delta_{j+1/2}v = v_{j+1} - v_j$ in the k-th characteristic field.

For (4.1) with $u_L = (0.445, 0.311, 8.928)^T$, $u_R = (0.5, 0.1, 1.4275)^T$, we perform the calculations with 140 cells, $h = 0.1$ and 111 time steps under the CFL numbers $\mu = 0.9$. In calculations we have used Roe's linearization and selected $\epsilon = 0.2$ for genuinely nonlinear fields; $\epsilon = 0$ for linearly degenerate fields. The numerical result is satisfactory.

Acknowledgment. The author would like to thank Dr. Hong-Liang Ren for his valuable suggestions.

Reference

(1) A. Harten & S. Osher "Uniformly High-Order Accurate Non-Oscillatory schemes I". MRC Technical Summary Report 2823.

(2) A. Harten "High Resolution Schemes for Hyperbolic Conservation Laws" J. Comp. Phys. 49, 357–393 (1983)

(3) A. Harten "On High-Order Accurate Interpolation for Non-Oscillatory Shock Capturing Schemes" Technical Summary Report 2829, June 1985.

(4) A. Harten, S. Osher, B. Engquist & S.R. Chkravarthy "An Overview of Uniformly High Order Accurate Essentially Non-Oscillatory Schemes"

STABILITY OF DIFFERENCE APPROXIMATIONS FOR HYPERBOLIC INITIAL-BOUNDARY-VALUE PROBLEMS: STATIONARY MODES

ROBERT F. WARMING AND RICHARD M. BEAM

NASA Ames Research Center
Moffett Field, CA 94035

In this paper we consider the stability of finite-difference approximations to hyperbolic initial-boundary-value problems (IBVPs). For simplicity we restrict our attention to the stability of approximations to the IBVP for the model hyperbolic equation

$$\frac{\partial u}{\partial t} = c\frac{\partial u}{\partial x}, \quad 0 \le x \le L, \quad t \ge 0 \tag{1}$$

where c is a real constant. One must specify initial data at $t = 0$, and the IBVP is well-posed if an *analytical* boundary condition is prescribed at $x = L$

$$u(L,t) = g(t) \quad \text{for} \quad c > 0. \tag{2}$$

A semi-discrete approximation of (1) is obtained by dividing the spatial interval into J subintervals of length Δx where $J\Delta x = L$, $x = x_j = j\Delta x$ and approximating the spatial derivative u_x by a difference quotient. As a prototype approximation we replace u_x by a second-order accurate central difference quotient to obtain a system of ordinary differential equations (ODEs)

$$\frac{du_j}{dt} = \frac{c}{2\Delta x}(u_{j+1} - u_{j-1}), \quad j = 1,2,\cdots,J-1 \tag{3}$$

where $u_j(t) = u_j$ denotes the approximation to $u(x,t)$. The right boundary ($x = L$) is advanced by using the analytical boundary condition (2). We assume that the boundary condition is homogeneous, i.e., $g(t) = 0$, and for the semi-discrete problem we write $u_J = 0$. In this abstact we consider only semi-discrete approximations, but in the final manuscript fully-discrete approximations will be included.

A complication in completing the approximation is the fact that generally more boundary conditions are required for the difference approximation than are specified for the partial differential equation. For example, if we apply (3) at the left boundary ($j = 0$), then the stencil protrudes one point to the left of the boundary. It is clear that an additional *numerical boundary scheme* (NBS) is required. For example, at

the left boundary ($j = 0$) we could change from a centered approximation to a one-sided approximation of u_x and use the following NBS:

$$\frac{du_0}{dt} = \frac{c}{\Delta x}[-\alpha u_2 + (1+2\alpha)u_1 - (1+\alpha)u_0] \tag{4}$$

where α is a parameter. The system of ODEs (3) together with the analytical boundary condition $u_J = 0$ and the NBS (4) can be written in vector-matrix form as

$$\frac{d\mathbf{u}(t)}{dt} = A\mathbf{u}(t) \tag{5}$$

where $\mathbf{u}$ is a J-component vector and A is a $J \times J$ matrix. The essential element in the stability of the semi-discrete approximation (5) is the behavior of the solution as the spatial mesh is refined. Consequently, one must consider an infinite sequence of ODE systems of dimension J where $J \to \infty$ as $\Delta x \to 0$.

Stability of a semi-discrete approximation with homogeneous boundary data means that there exists an estimate of the solution in terms of the initial data. For example, the semi-discrete approximation represented by the sequence of ODE's (5) is Lax-Richtmyer stable if there exists a constant $K > 0$ such that for any initial condition $\mathbf{u}(0)$

$$\|\mathbf{u}(t)\| \leq K\|\mathbf{u}(0)\| \tag{6}$$

for all $J > 0$, $J\Delta x = L$ and for all t, $0 \leq t \leq T$ with T fixed. Here the symbol $\|\cdot\|$ denotes a norm.

Two methods for carrying out a stability analysis are the energy method and the normal mode analysis. The normal mode analysis is an eigenvalue analysis. If we look for a solution of (5) of the form $\mathbf{u}(t) = e^{st}\boldsymbol{\phi}$, then we obtain $A\boldsymbol{\phi} = s\boldsymbol{\phi}$. But this is just the eigenvalue-eigenvector problem for the matrix A where $\boldsymbol{\phi}$ is the eigenvector and s is the eigenvalue. The practical problem of implementing tests on the eigenvalues is that the normal mode analysis for a discrete hyperbolic IBVP on a finite domain is, in general, analytically intractable.

The intractability can easily be demonstrated by the normal mode analysis of the ODE system (5). The components ϕ_j of the eigenvector $\boldsymbol{\phi}$ and the normalized eigenvalue $\hat{s} = (\Delta x/c)s$ are given by

$$\phi_j = [\kappa^j - (-\kappa^2)^J(-1/\kappa)^j], \qquad 2\hat{s} = \kappa - \frac{1}{\kappa} \tag{7a,b}$$

where κ is a root of the algebraic equation

$$q(\kappa) - (-\kappa^2)^{J+1}q(-1/\kappa) = 0. \tag{7c}$$

The polynomial $q(\kappa)$ depends solely on the NBS. In particular, for the NBS (4) the polynomial $q(\kappa)$ is

$$q(\kappa) = (\kappa - 1)^2(2\alpha\kappa - 1). \tag{8}$$

Since $J\Delta x = L$, the degree of (7c) increases as the spatial mesh increment Δx decreases. In general, one cannot solve for the roots of (7c) which accounts for the analytic intractability of the normal mode analysis on a finite-domain.

An alternative but more complicated stability definition is used in the theory developed by Gustafsson, Kreiss, and Sundström (GKS) [1]. The advantage of the GKS theory accrues from the fact that a finite-domain problem with two boundaries is divided into a Cauchy problem and two quarter-plane problems each of which can be analyzed separately by a normal mode analysis. The analogues of (7) for the right-quarter plane problem are

$$\phi_j = \kappa^j, \qquad 2\hat{s} = \kappa - \frac{1}{\kappa} \tag{9a,b}$$

where κ is a root of

$$q(\kappa) = 0. \tag{9c}$$

This is the same polynomial $q(\kappa)$ that appears in (7c) and (8). The roots of (9c) are easily found since $q(\kappa)$ is of low degree. Algebraic tests based on the roots of $q(\kappa)$ and the corresponding eigenvalues $\hat{s}$ provide necessary and sufficient conditions for GKS stability.

Since the Lax-Richtmyer and GKS stability definitions differ, the connection between the normal mode analysis for the finite-domain problem and the normal mode analysis for the quarter-plane problem is rather obscure. In a recent paper [3] we derived asymptotic estimates of the eigenvalues of the finite-domain problem. These estimates were used to relate the normal mode analysis of the finite-domain problem and the GKS quarter-plane analysis.

The notion of stability for the finite-domain problem is intimately associated with the behavior of the eigenvalues $\hat{s}$ as the spatial mesh is refined, i.e., $J \to \infty$. Although we cannot solve for the roots of (7c) analytically, we are primarily interested in asymptotic estimates for large J. In order to derive the asymptotic estimates for the roots of (7c), we assumed in [3] that particular roots can be identified for each J and we write $\kappa = \kappa(J)$. Furthermore, there is no loss of generality in assuming that $|\kappa(J)| \leq 1$. We showed that the roots of the algebraic equation (7c) can be divided into two distinct classes according to the asymptotic behavior of $|\kappa(J)|^J$ in the limit $J \to \infty$. For $|\kappa(J)| < 1$ there are only two possibilites:

$$(I): \quad \lim_{J\to\infty} |\kappa(J)|^J = 0, \qquad (II): \quad \lim_{J\to\infty} |\kappa(J)|^J = \text{constant} > 0. \tag{10}$$

For roots in class (I), it is clear that (7c) reduces to the quarter-plane equation (9c) as $J \to \infty$. Consequently, a root in class (I) becomes a root of the quarter-plane polynomial (9c) in the limit $J \to \infty$.

In addition to (I) and (II), there is a third class of roots

$$(III): \quad |\kappa(J)| = 1. \tag{11}$$

If $|\kappa| = 1$ and is independent of J, then a κ root remains fixed on the unit circle for all J. For this to happen it is obvious from (7c) that the polynomials $q(\kappa)$ and $q(-1/\kappa)$ must have a common factor. This common factor leads to identical roots for both the quarter plane polynomial $q(\kappa)$ and the finite-domain polynomial (7c).

These roots are fixed on the unit circle and from (7b) one obtains $\Re(\hat{s}) = 0$ and $\Im(\hat{s}) =$ fixed. Consequently, there is a *stationary* mode with κ independent of J.

An example with a stationary mode is NBS (4) for $\alpha = -1/2$. The polynomial (8) becomes

$$q(\kappa) = -(\kappa - 1)^2(\kappa + 1), \quad q(-1/\kappa) = -(\kappa + 1)^2(\kappa - 1)/\kappa^3, \quad (\alpha = -1/2) \quad (12)$$

The polynomials $q(\kappa)$ and $q(-1/\kappa)$ have the common factor $(\kappa - 1)(\kappa + 1)$ and consequently, (7c) has the roots $\kappa = \pm 1$ independent of J for $\alpha = -1/2$. From (7b) $\hat{s} = 0$ and this is a stationary mode. According to the GKS stability results, $\alpha = -1/2$ is the *borderline* case between stability ($\alpha > -1/2$) and instability ($\alpha < -1/2$). This borderline case is GKS unstable. If there is a stationary mode for the finite domain problem, the GKS perturbation test will always indicate the presence of a GKS generalized eigenvalue.

The GKS quarter plane analysis cannot detect whether or not a particular mode is stationary for the finite domain problem. The importance of a stationary mode is the following. Gustafsson et al. [2] have proved that if the Cauchy stability requirement of the GKS theory is replaced by a more stringent energy estimate, then GKS stability implies Lax-Richtmyer stability in the L_2 norm. There are known examples showing that Lax-Richtmyer stability does not imply GKS stability. These examples all involve what are called borderline cases. In fact, we show that they are equivalent to the presence of a stationary mode for the finite-domain problem. From our analysis, stationary modes are easy to detect since they occur if and only if $q(\kappa)$ and $q(-1/\kappa)$ have a common factor.

From the point of view of an eigenvalue analysis, a semi-discrete approximation with a stationary mode must be treated separately since any instability derives not from an eigenvalue with a positive real part but from the algebraic growth (as $J \to \infty$) of the norm of the solution. In this paper we examine in detail stationary modes arising from various NBSs for both semi-discrete and fully discrete problems.

References

[1] B. Gustafsson, H.-O. Kreiss, A. Sundström: "Stability theory of difference approximations for mixed initial boundary value problems. II," Mathematics of Computation, 26, 649-686 (1972).

[2] B. Gustafsson, private communication from preliminary manuscript by B. Gustafsson, H.-O. Kreiss, and J. Oliger (1987).

[3] R. F. Warming and R. M. Beam: "Stability of semi-discrete approximations for hyperbolic initial-boundary-value problems: asymptotic estimates," Proceedings of the International Symposium on Computational Fluid Dynamics, Sydney, Australia, North-Holland, Amsterdam (1987).

340 Blank

W

AN ANALYSIS OF THE NUMERICAL SOLUTION OF HYPERBOLIC PDES ON IRREGULAR GRIDS

B. Wendroff and A. B. White, Jr.

Los Alamos National Laboratory
Los Alamos, New Mexico U.S.A.

Extended Abstract

Partial differential equations (PDEs) are often approximated on irregular spatial grids. These irregularities may be required to illuminate particular regions of interest or may be the result of complementary calculations. In any case, many authors have noted that a difference scheme defined on an irregular grid may have significantly larger truncation error than when defined on a regular one. For example, the second divided difference approximates $y''(x_i)$ correct to $O(\Delta x^2)$ on a uniform grid, to $O(\Delta x)$ on an irregular one. Difference approximations of ordinary differential equations on highly irregular grids have been examined in detail in Manteuffel and White [1] and Kreiss et al. [2]. In many cases, this apparent loss of accuracy is an artifact of the classical error analysis, and the discrete solution retains its accuracy even on very irregular grids.

Perhaps the simplest example of this effect for node-centered unknowns is a zeroth order, conservative, upwind scheme, see Pike [3], applied to the scalar wave equation. On a product grid (x_i, t^k), the difference approximation is

$$L_h \bar{u} = \frac{\bar{u}_i^{k+1} - \bar{u}_i^k}{\Delta t} + 2c \, \frac{\bar{u}_i^k - \bar{u}_{i-1}^k}{(\Delta x_{i+1/2} + \Delta x_{i-1/2})} \, . \tag{1.1}$$

The truncation error associated with (1.1) is

$$L_h u \equiv \tau = -c \, \frac{\Delta x_{i+1/2} - \Delta x_{i-1/2}}{\Delta x_{i+1/2} + \Delta x_{i-1/2}} \, u_x + O(\Delta) \, . \tag{1.2}$$

For an irregular grid (e.g., a two-periodic grid: $h, 2h, h, 2h, \ldots$), this difference scheme is inconsistent unless rather stringent restrictions are placed on the mesh spacing. However, a modified exact solution

$$\tilde{u}(x_i, t^k) = u(x_i, t^k) + \frac{1}{2} \, c \, \Delta x_{i+1/2} u_x(x_i, t^k)$$

has $\tilde{\tau} = O(\Delta)$. Thus, the usual error analysis yields

$$\bar{u}_i^k - u(x_i, t^k) = \frac{1}{2} \, c \, \Delta x_{i+1/2} u_x(x_i, t^k) + O(\Delta); \tag{1.3}$$

that is, the discrete solution remains first-order accurate (1.3) despite the zeroth order truncation

error (1.2).

The same basic behavior is observed in the numerical solution of the one-dimensional Lagrangian gas dynamics equations

$$v_t - u_x = 0 \ , \tag{1.4a}$$

$$u_t + p_x = 0 \ , \tag{1.4b}$$

$$e_t + pv_t = 0 \ , \tag{1.4c}$$

via a simple von Neumann-Richtmyer scheme. Here the velocity (u) is node centered (x_i, t^k), both the specific volume (v) and internal energy (e) are cell-centered ($x_{i+1/2}, t^{k+1/2}$), and $p = p(v,e)$. Centered differences are used throughout; for example, Eq. (1.4a) is approximated at ($x_{i+1/2}, t^k$) (see Fig. 1.1),

$$2\,\frac{\bar{v}_{i+1/2}^{\,k+1/2} - \bar{v}_{i+1/2}^{\,k-1/2}}{(\Delta t^{k+1/2} + \Delta t^{k-1/2})} - \frac{\bar{u}_{i+1}^{k} - \bar{u}_{i}^{k}}{\Delta x_{i+1/2}} = 0 \ .$$

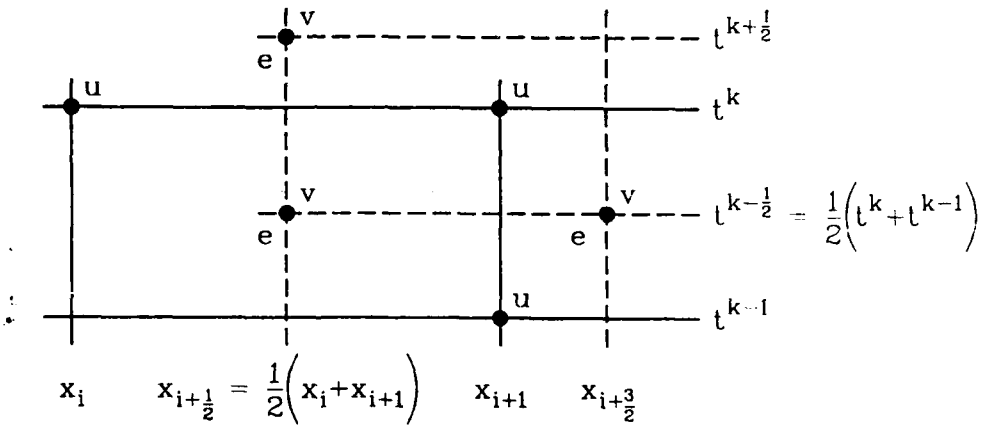

Fig. 1.1. Staggered grid.

Equation (1.4c) is also approximated at $(x_{i+1/2}, t^k)$, Eq. (1.4b) at $(x_{i+1}, t^{k-1/2})$.

Thus, on a regular space-time mesh the truncation error is $O(\Delta^2)$, but only first order on an irregular grid,

$$N_h(v,u,e) \equiv \tau = O(\Delta) \ . \tag{1.5}$$

However, even in this nonlinear problem, a modified solution

$$\tilde{v}_{i-1/2}^{\,k-1/2} = v_{i-1/2}^{\,k-1/2} + O([\Delta t^{k-1/2}]^2 + [\Delta x_{i-1/2}]^2)$$

$$\bar{u}_i^h = u_i^h$$

$$\bar{e}_{i-1/2}^{k-1/2} = e_{i-1/2}^{k-1/2} + O\left((\Delta t^{k-1/2}]^2 + [\Delta x_{i-1/2}]^2\right)$$

can be constructed such that the truncation error is second-order:

$$N_h(\bar{v},\bar{u},\bar{e}) \equiv \bar{\tau} = O(\Delta^2) \ .$$

Thus, it can be shown that the first-order truncation error (1.5) does not imply a merely first-order accurate discrete solution.

A generalized node-centered Lax-Wendroff scheme (Pike [3])

$$\frac{\bar{u}_i^{k+1} - \bar{u}_i^k}{\Delta t} + c\ \frac{\bar{u}_{i+1}^k - \bar{u}_{i-1}^k}{\Delta x_{i+1/2} + \Delta x_{i-1/2}} - c^2 \Delta t\ \frac{1}{\Delta x_{i+1/2} + \Delta x_{i-1/2}} \left[\frac{\bar{u}_{i+1}^k - \bar{u}_i^k}{\Delta x_{i+1/2}} - \frac{\bar{u}_i^k - \bar{u}_{i-1}^k}{\Delta x_{i-1/2}} \right] = 0$$

exhibits supraconvergence on irregular grids under certain restrictions. First, we require that

$$0 < \varepsilon \le c\ \frac{\Delta t}{\Delta x_{i+1/2}} \le p < 1 \ . \tag{1.6}$$

The upper bound is familiar from stability considerations; the lower bound prevents Δt from getting too small (e.g., $\Delta t = O(\Delta x^2)$). Second, we require that the t-grid be uniform (actually quasiuniform is probably sufficient). Numerical experiments will be presented to determine whether these constraints are genuine or, once again, artifacts of the method of analysis.

REFERENCES

[1] Manteuffel, Thomas, A., and Andrew B. White, Jr., *The numerical solution of second-order boundary value problems on nonuniform meshes,* MOC **47** (1986), 511-535.

[2] Kreiss, H.-O., Thomas A. Manteuffel, B. Swartz, B. Wendroff, and Andrew B. White, Jr., *Supraconvergent schemes on irregular grids,* MOC **47** (1986), 537-554.

[3] Pike, J., *Grid adaptive algorithms for the solution of the Euler equations on irregular grids,* JCP **71** (1987), 194-223.

The homogeneous homentropic compression or expansion - a test case for analyzing SOD's operator splitting

WESTENBERGER H.
Lehr- und Forschungsgebiet Mechanik of the RWTH Aachen
D 5100 Aachen, Germany

SOD's operator splitting integrates a hyperbolic conservation law with a source term by splitting the source term from the divergence part and by integrating both parts separately :

$$\underline{y}_t + (\underline{E}(\underline{y}))_r = \underline{Q}(\underline{y}, r)$$

$$\underline{y}_t + (\underline{E}(\underline{y}))_r = \underline{Q} \qquad \underline{y}_t = \underline{Q}(\underline{y}, r)$$

solution operator H solution operator S

This splitting technique can be understood as a special integration of the conservation law with a source term over a region G which leads to

$$\underline{y}_{m,n+1} = \underline{y}_{m,n} - \lambda \left(g_{m+\frac{1}{2},n} - g_{m-\frac{1}{2},n} \right) + \Delta t \underline{Q}_{m,n} .$$

Three variants of the splitting will be considered

$$\{ \underline{y}_{m,n+1} \}_{m \in \mathbb{N}} = \begin{cases} S \circ H \{ \underline{y}_{m,n} \}_{m \in \mathbb{N}} \\ S^{\frac{1}{2}} \circ H \circ S^{\frac{1}{2}} \{ \underline{y}_{m,n} \}_{m \in \mathbb{N}} \\ S + H - I \{ \underline{y}_{m,n} \}_{m \in \mathbb{N}} \end{cases} .$$

There are two special aspects of splitting to be analyzed :

- The choice of dependent variables

The splitting into a homogeneous part and a source term depends on the chosen dependent variables and is therefore not unique. The choice influences the quality of the solution.

- Example : gasdynamic equations

  dependent variables : (*) $\{ \rho, m, e \}$ or (**) $\{ \rho A, m A, e A \}$

  ρ - density, m - momentum, e - total energy, A - cross-section.

Although formulation (*) gives reasonable results with all three variants, formulation (**) can only be combined with variant 3.

- The source term and entropy behaviour

The time integration of the source term does not pay attention to the second law of thermodynamics. Therefore the physical entropy can descend (Figure 1).

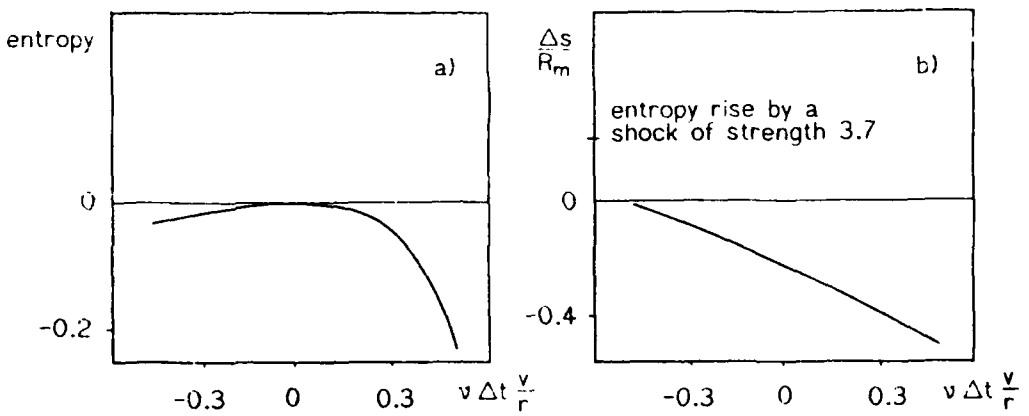

Figure 1 Entropy descent by the time integration of the source term
a) for formulation (*)
b) for formulation (**)

Theorem : A solution of the quasi-one-dimensional gasdynamic equations for variable cross-section $A(r)$ has to be found in $\mathbb{R}_+ \times [0, T)$ with $A(0) < \infty$, $A \in C^2$, entropy $s \equiv$ const., $\rho = \rho(t)$, velocity $v(0, t) = 0$, $v(r_0, 0) = v_0$. Such a solution only exists for

$$A_\delta(r) = \gamma\, r^\delta,\ \gamma > 0,\ \delta \geq 0$$

and for $\frac{v_0}{r_0} t > -1$ it has the form

$$\rho_\delta(t) = \rho_\delta(0) \left(1 + \frac{v_0}{r_0} t \right)^{-(1+\delta)},$$

$$v_\delta(r, t) = \frac{v_c}{1 + \frac{v_0}{r_0} t} \frac{r}{r_0} .$$

To use this analytic solution for a numerical test we choose the initial conditions

$A(r) = r^\nu$, $\nu = 2$ (spherical symmetry)
$\rho(r, 0) = \rho_0$.
$v(r, 0) = \frac{v_0}{r_0} r$, $v_0 = -\frac{1}{2} \frac{a_0}{\varkappa - 1}$. $\varkappa$ - adiabatic exponent, a - sound speed,
$v(0, t) = v(1, t) = 0$.

This leads to a region of undisturbed homogeneous compression which is separated from a rarefaction wave by the characteristic (Figure 2)

$$C(t) = \frac{1}{1+v_0 t} \left(\frac{a_0}{\varepsilon v_0} \left[(1+v_0 t)^{-\varepsilon} - 1 \right] + 1 \right)$$

$$\varepsilon = (\nu+1)\frac{\varkappa-1}{2}$$

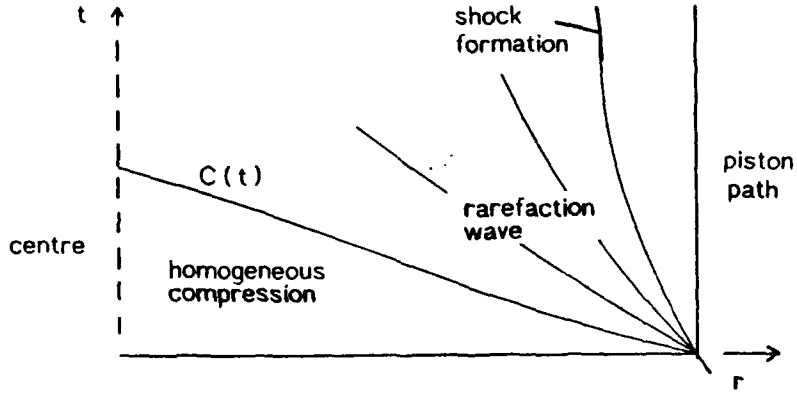

Figure 2 : Wave pattern for the homogeneous compression with a suddenly fixed piston

The *GODUNOV-method* shows very good agreement of the numerical results with the analytic solution. An entropy drop can be found although it is dominated by the entropy rise at the fixed piston (Figure 3).

The *random-choice method* has been treated statistically over several numerical runs. The resulting expectation value and the variance show some oscillations near the centre of symmetry. This agrees with the statement of COLELLA that the combination of the random-choice method with operator splitting diminishes accuracy. In spite of this no entropy rise can be found near the fixed piston (Figure 4).

Literature

COLELLA P. : GLIMM's method for gas dynamics. SIAM J. Sci. Stat. Comput. , 1982, 76-110.

SOD G. : A numerical study of a converging cylindrical shock. J. Fluid Mech. 83, 1977, 785-794.

WESTENBERGER H. : Zur Dynamik des Impulstransportes in blasigen, kompressiblen Flüssigkeiten. Thesis, RWTH Aachen 1987.

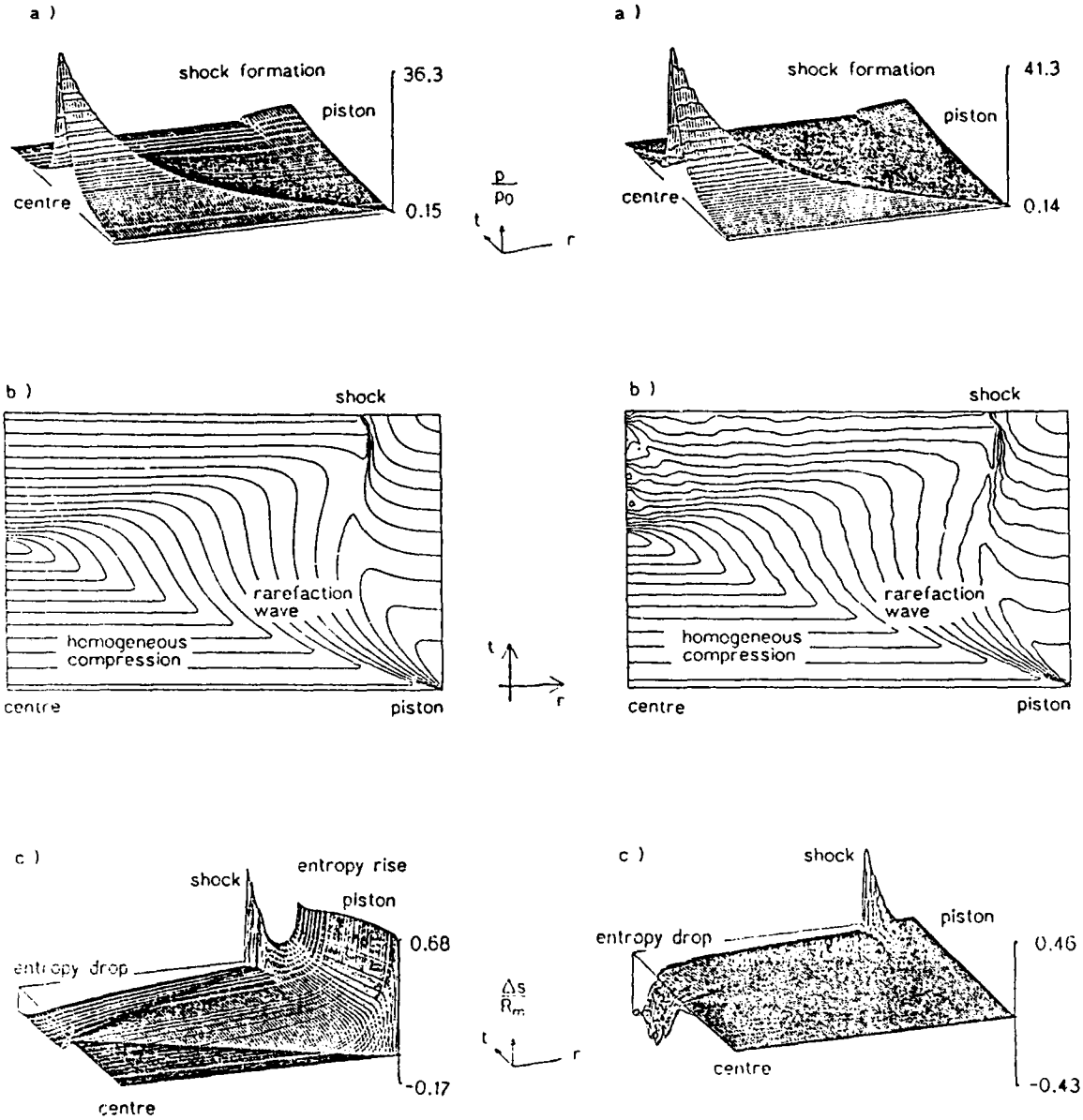

Figure 3 : The homogeneous compression with a suddenly fixed piston with the *GODUNOV-method* (CFL-number: 0.95)
a) space-time pressure profile (variant 2 •)
b) Isobars (variant 2 •)
c) space-time entropy profile (variant 3 •)

Figure 4 : The homogeneous compression with a suddenly fixed piston with the *random-choice method* (CFL-number: 0.95)
a) space-time pressure profile (variant 1 •)
b) Isobars (variant 1 •)
c) space-time entropy profile (variant 1 •)

W

APPLICATIONS OF THE PIECEWISE-PARABOLIC METHOD (PPM) TO THE STUDY OF UNSTABLE FLUID FLOW

Paul R. Woodward

University of Minnesota

The Piecewise-Parabolic Method (PPM) [1-4] is a difference scheme for solving the Euler equations of inviscid fluid flow. PPM is built upon the ideas of Godunov's scheme [5] and its earliest higher-order extension, MUSCL [6,7]. PPM was originally designed to attack transient flow problems involving strong, discontinuous, nonlinear waves. In recent years PPM has been extended to treat milder problems such as compressible convection in stars and terrestrial thunderstorms. In these problems discontinuities also arise, and PPM delivers the same high resolving power which motivated its earlier use in strong shock problems. Applications of both "strong" and "weak" formulations of PPM will be presented, and the merits of the numerical approach as well as the physics of the applications themselves will be discussed. These applications are part of a larger program of investigation of unstable fluid flow. The computed flows are visualized with high-speed interactive color graphics displays, and the results will be shown as video movies.

In the "strong" category of applications, studies of supersonic slip surface instabilities will be presented. These studies were inspired by a larger study of the propagation and stability of gaseous jets, most recently in collaboration with K.-H. Winkler (Los Alamos) and N.J. Zabusky (Pittsburgh). The earliest PPM simulations of slip surface instability showed nonlinear unstable modes not expected from linearized perturbation analysis. This work inspired Artola and Majda at Princeton to extend this analytic theory to the weakly nonlinear regime. They confirmed the existence of the nonlinear modes and gave quantitative formulae for angles and propagation speeds of resonant interactions between a supersonic slip surface and incident sound wave trains. New PPM simulations which correspond more closely to the context of this analytic work have been performed in collaboration with Jeffrey Pedelty at Minnesota. These display interesting nonlinear effects, such as coupling between the various nonlinear modes and broadening of the resonance for strong perturbations. Video movies of these simulations will be presented, and their importance for the understanding of jet stability will be discussed.

In the "weak" category of applications, studies of compressible convection will be presented. This work has been performed in collaboartion with David Porter at Minnesota. These studies are aimed at an understanding of convective heat

transport in the outer layers of stars like the sun. For such stars the regime of interest is one of extremely low thermal conductivity and even more extremely low viscosity (i.e. high Reynolds numbers and low Prandtl numbers). Compressiblity is also very important, because the unstable layers span many density and pressure scale heights. In the PPM simulations we attempt to treat these features of the flows, although the magnetic fields, rotation, and three-dimensional spherical geometry of the stellar flows are not treated. Our simulations of compressible convection between rigid, friction-free plates in 2-D Cartesian geometry are surely quite unlike convection in stars in several respects. Nevertheless, these simulations give important information on the relationship between the predominant sizes of convective eddies and the local pressure and density scale heights in the fluid. We have begun to extend our work to three dimensions, but in this case the demands on the resolution of both the difference scheme and the computational grid add to make the simulations very costly and extremely difficult to carry out and display. The discussion here will focus on the work in 2-D, using video movies to illustrate the approach to a statistically steady spectrum of convective eddy sizes.

REFERENCES

1. Woodward, P. R., and Colella, P., Lecture Notes in Phys. 141, 434 (1981).
2. Woodward, P. R., and Colella, P., J. Comput. Phys. 54, 115 (1984).
3. Colella, P., and Woodward, P. R., J. Comput. Phys. 54, 174 (1984).
4. Woodward, P. R., in "Astrophysical Radiation Hydrodynamics," eds. K.-H. Winkler and M. L. Norman, Reidel, 1986.
5. Godunov, S. K., Nat. Sb. 47, 271 (1959).
6. van Leer, B., J. Comput. Phys. 32, 101 (1979).
7. van Leer, B., and Woodward, P. R., Proc. TICOM Conf., March, 1979.

Global existence of solutions for noncharacteristic mixed problems to nonlinear symmetric hyperbolic systems of the first order with dissipation

W.M. Zajączkowski, Warsaw

Institute of Fundamental Technological Research

We consider the following initial boundary value problem

$$
\begin{aligned}
&E(t,x,u)u_t + \sum_{i=1}^{n} A_i(t,x,u)u_{x_i} + B(t,x,u)u = F(t,x) && \text{in} \quad \Omega\times[0,T],\\
&u_{|t=0} = u_0(x) && \text{in} \quad \Omega,\\
&M(t,x',u)u_{|\partial\Omega} = g(t,x') && \text{on} \quad \partial\Omega\times[0,T],
\end{aligned}
\tag{1}
$$

where Ω is a bounded domain, $x=(x_1,\dots,x_n) \in \Omega \subset \mathbb{R}^n$, $x' \in \partial\Omega$, $u=(u_1,\dots,u_m) \in G \subset \mathbb{R}^m$, G is an open subset of the physical state space $\mathbb{R}^m$, because physical quantities such as the density or temperature should always be positive, $u_0 \in G_0 \subset\subset G$, $E(t,x,u)$, $A_1(t,x,u)$, ..., $A_n(t,x,u)$, $B(t,x,u)$ are real $m\times m$ matrices, $E,A_1,\dots,A_n$ are symmetric, $Eu\cdot u \geq \alpha_0 u^2$, α_0 is a positive constant,

$$
\begin{aligned}
M(t,x',u) = &\sum_{\mu,\nu=1}^{\ell} \alpha_{\mu\nu}(t,x',u)\gamma_\mu^+(t,x',u)\gamma_\nu^+(t,x',u) +\\
&+ \sum_{\mu=1}^{\ell}\sum_{\nu=\ell+1}^{m} \beta_{\mu\nu}(t,x',u)\gamma_\mu^+(t,x',u)\gamma_\nu^-(t,x',u),
\end{aligned}
$$

where γ_μ^+, $\mu=1,\dots,\ell$, γ_ν^-, $\nu=\ell+1,\dots,m$, are eigenvectors to the matrix $-A\cdot\bar{n} = -(A_1n_1+\dots+A_nn_n)$ ($\bar{n}$ is the unit outward vector normal to the boundary), corresponding to the positive (λ_μ^+, $\mu=1,\dots,\ell$) and negative (λ_ν^-, $\nu=\ell+1,\dots,m$) eigenvalues, respectively.

We assume also that the eigenvalues are disjoined from zero, so $\min\limits_{\Omega\times[0,T]\times G}\min\limits_{\mu} |\lambda_\mu| \geq c_0 > 0$, c_0 is a constant, and

$$
\max_{\partial\Omega\times[0,T]\times G} |\alpha_{\mu\nu}^{-1}| \leq \delta_0^{-1}, \qquad \max_{\partial\Omega\times[0,T]\times G} |\beta_{\mu\nu}| \leq \delta_1,
$$

$$
\max_{\nu\in\{1,\dots,\ell\}} \max_{\partial\Omega\times[0,T]\times G} \lambda_\nu^+ \leq c_1',
$$

$$
\max_{\nu\in\{\ell+1,\dots,m\}} \max_{\partial\Omega\times[0,T]\times G} |\lambda_\nu^-| \leq c', \quad (c_0+c')\delta_0^{-2}\delta^2 \leq \frac{1}{4}c_0,
$$

c_1, c_1', δ_0, δ_1 are constants.

Finally we assume the condition of dissipation

(2) $Bu \cdot u \geq \beta_0 u^2, \qquad \beta_0 > 0.$

Under the assumption the following result has been proved

Theorem

Let $F \in H^{\ell}(\Omega \times [0,t])$, $\partial_t^i F \in L_\infty(0,t;H^{\ell-i}(\Omega))$, $i=0,\ldots,\ell$, $g \in H^{\ell}(\partial\Omega \times [0,t])$, $\ell > \frac{n}{2} + 1$, $u_0 \in H^{\ell+1}(\Omega)$, $\partial\Omega \in C^{\ell}$, $E, A_1, \ldots, A_n, B \in C^{\ell}(\Omega \times [0,t] \times G)$, $M \in C^{\ell}(\partial\Omega \times [0,t] \times G)$, $t \leq T \in R_+$ and $F, g, u_0, E, A_1, \ldots, A_n, B, M$ must be sufficiently small in the corresponding norms.

Then there exists a unique global in time solution to the problem (1), (2) such that $u \in H^{\ell}(\Omega \times [0,t]) \cap H^{\ell}(\partial\Omega \times [0,t])$ and $\partial_t^i u \in L_\infty(0,t;H^{\ell-i}(\Omega))$, $i=0,\ldots,\ell$.

RIEMANN PROBLEM FOR GASDYNAMIC COMBUSTION

TONG ZHANG
Institute of Mathematics, Academia Sinica, Beijing
Yuxi Zheng
Department of Mathematics, University of California at Berkeley

The simplest complete system for the flow of combustible gas with an infinite rate of reaction is as follows:

$$u_t + p_x = 0, \qquad \tau_t - u_x = 0, \qquad E_t + (pu)_x = 0,$$

$$E = u^2/2 + e + q, \qquad e = p\tau/(\gamma - 1),$$

chemical binding energy satisfies

$$q(x,t) = \begin{cases} q(x,0) & \sup_{0\le\tau\le t} T(x,\tau) \le T_i \text{ (ignition temperature)} \\ 0 & \text{otherwise,} \end{cases}$$

$$T = p\tau/R, \qquad R > 0,$$

where γ, R and T_i are constants and u, p, τ and q are unknowns. q has only two values: $q = 0$ for the burnt gas and $q = q_0 > 0$ for the unburnt gas.

The Riemann problem is as follows:

$$(u,\tau,p,q)_{t=0} = (u^{\pm},\tau^{\pm},p^{\pm},q^{\pm}), \qquad (x \gtrless 0).$$

We obtained existence and uniqueness constructively for arbitrary Riemann data under the following restrictions: the solutions are selfsimilar and piecewise smooth; the Lax entropy condition is satisfied at the discontinuity points except at the front sides of deflagration waves where the temperatures are assumed to be the ignition point; the number of detonation waves in the solutions is as small as possible; furthermore, the number of times of oscillations of temperature around the ignition point is also as small as possible; and last, the number of deflagration waves is as large as possible. The last three principles are called global entropy condition, without which the number of solutions may be nine at most.

Solutions consist of shocks, centered rarefaction waves, detonations, deflagrations, Chapmann-Jouguet detonations, Chapmann-Jouguet deflagrations and contact discontinuities. There are thirty-six kinds of configurations in all.

Using the Riemann problem, we analyzed the overtaking of shocks and combustion waves: a shock always accelerates detonation, whereas it transforms deflagration into detonation when it is strong enough. Transition from deflagration to detonation in the ignition problem is also investigated.

(to appear in J.D.E.)

References

1. *Courant, R. and Friedrichs, K.O., Supersonic Flow and Shock Waves, Inters. Publ., Inc., New York, 1948*
2. *Chorin, A.J., Random choice methods with application to reacting gas flow, J. Comp. Phys., 25 (1977), 253*
3. *Teng Zhenhuan, Chorin, A.J., Liu, T.-P., Riemann problems for reacting gas with application to transition, SIAM, J. Appl. Math., 42 (1982), 964*
4. *Ying Longan, Teng Zhenhuan, Riemann problem for a reacting and convection hyperbolic system, J. of Approximation Theory and its Applications, 1,1 (1984), 95–122*

SOME RESULTS ON STABILITY AND CONVERGENCE OF DIFFERENCE SCHEMES FOR QUASILINEAR HYPERBOLIC INITIAL-BOUNDARY-VALUE PROBLEMS

You-lan Zhu
The Computing Center, Academia Sinica
Beijing, China

In the seventies[1,2] we obtained some results on stability of difference schemes for initial-boundary-value problems of linear diagonalized hyperbolic systems in two independent variables. Later[3] these results were extended to general linear hyperbolic systems with "moving boundaries" and some convergence theorems were established. In [4], we completed some proofs of 'global' convergence of difference schemes for general quasilinear hyperbolic initial-boundary-value problems with moving boundaries.

In this paper we would like to introduce our main result briefly. The result can be described as follows.

Let us consider the following initial-boundary-value problem for quasilinear hyperbolic systems in two independent variables.

1. A quasilinear hyperbolic system

$$\frac{\partial \bar{U}}{\partial t} + \bar{A}(\bar{U},x,t)\frac{\partial \bar{U}}{\partial x} = \bar{F}(\bar{U},x,t) \qquad (1.1)$$

is given in L regions: $x_{\ell-1}(t) \le x \le x_{\ell}(t)$, $0 \le t \le T$, $\ell = 1,2,\ldots, L$.

2. On external boundaries and internal boundaries $x = x_{\ell}(t)$, $\ell = 0,1,\ldots,L$, a number of nonlinear boundary conditions are prescribed:

$$\begin{cases} B_0(\bar{U}_0^+, x_0, z_0, t) = 0, \\ B_{\ell}(\bar{U}_{\ell}^-, U_{\ell}^+, x_{\ell}, z_{\ell}, t) = 0, \quad \ell = 1,2,\ldots,L-1, \\ B_L(\bar{U}_L^-, x_L, z_L, t) = 0, \end{cases} \qquad (1.2)$$

where

$$z_{\ell} = \frac{dx_{\ell}(t)}{dt}, \qquad \ell = 0,1,\ldots, L. \qquad (1.3)$$

3. At t = 0 initial values are specified:

$$\begin{cases} \bar{U}(x,0) = \bar{D}_{\ell}(x), \text{ for } x_{\ell-1}(0) \leq x \leq x_{\ell}(0), \ \ell=1,2,\ldots,L, \\ x_{\ell}(0) = c_{0,\ell}, \ z_{\ell}(0) = c_{1,\ell}, \quad \ell = 0,1,\ldots,L. \end{cases} \tag{1.4}$$

It is required to determine $\bar{U}$ in the L regions and $x_{\ell}(t)$, $z_{\ell}(t)$ for $0 \leq t \leq T$, $\ell=0,1,\ldots,L$. Here $\bar{U}$, $\bar{F}$, $\bar{D}_{\ell}$ are N_1-dimensional vectors, $\bar{A}$ - an $N_1 \times N_1$ matrix, B_{ℓ} — ν_{ℓ} -dimensional vectors, $c_{0,\ell}$ and $c_{1,\ell}$ are scalars and $\bar{U}_{\ell}^{\pm} \equiv \bar{U}_{\ell}^{\pm}(t) = \lim_{x \to x_{\ell}(t) \pm 0} \bar{U}(x,t)$.

We suppose that in every region: $x_{\ell-1}(t) \leq x \leq x_{\ell}(t)$, $0 \leq t \leq T$, $\bar{U}$ and its first derivatives are Lipschitz continuous with respect to x and t. Obviously, if we take all the discontinuity lines and the first order weak-discontinuity lines (on which the first derivatives are discontinuous) as internal boundaries, this assumption can be satisfied. We further assume that in every region, the second derivatives of $\bar{U}$ are piecewise smooth. Clearly, this assumption usually holds. For this case, the truncation error in L_2 norm will really be $O(\Delta t^3)$ even for the problems with discontinuous solution if the second order schemes in [1] and [2] are adopted. We have proved that when the second order schemes in [1] and [2] are used and when the above two assumptions and a very weak assumption about boundary conditions (1,2) are satisfied, the approximate solution of $\bar{U}$ will converge to the exact solution with a convergence rate of Δt^2 in L_2 norm and the errors of the approximate solutions of $x_{\ell}(t)$ are $O(\Delta t^2)$, no matter whether or not there exist some discontinuities, such as shocks, contact discontinuities.

References

1. You-lan Zhu, Difference schemes for initial-boundary-value problems of the first order hyperbolic system and their stability, Mathematicae Numericae Sinica, 1979, No. 1 (in chinese).
2. You-lan Zhu, Xi-chang Zhong, Bing-mu Chen and Xou-min Zhang, Difference methods for initial-boundary-value problems and flows around bodies, Science Press, Beijing, China, 1980 (in Chinese), The English Edition is in the press.
3. You-lan Zhu, Stability and convergence of difference schemes for linear initial-boundary-value problems, Mathematicae Numericae Sinica, 1982, No. 1 (in English).
4. You-lan Zhu and Wenan Yong, On stability and convergence of difference schemes for quasilinear hyperbolic initial-boundary-value problems (to appear in English).

Stability of Initial-Boundary Value Problems for Hyperbolic Systems

Mariusz Ziółko

Institute of Automatic Control
University of Mining and Metalurgy
Mickiewicza 30, 30–059 Kraków
Poland

Consider the initial-boundary value problem

$$\frac{\partial y}{\partial t} + \Lambda \frac{\partial y}{\partial x} = D\, y \qquad y_{(x,0)} = y_{0(x)} \tag{1}$$

for $y_{(x,t)} \in \mathbb{R}^n$, $0 \le x \le 1$, $0 \le t \le T$. Λ and D are $n \times n$ real matrices. Without loss of generality Λ may be taken to be diagonal

$$\Lambda = \begin{pmatrix} \Lambda^- & 0 \\ 0 & \Lambda^+ \end{pmatrix} \qquad \begin{aligned} \Lambda^- &= \mathrm{diag}(\lambda_1^-, \lambda_2^-, \ldots, \lambda_r^-) < 0 \\ \Lambda &= \mathrm{diag}(\lambda_{r+1}^+, \ldots, \lambda_n^+) > 0 \end{aligned}$$

Well-posed linear homogeneous boundary data can always be written as

$$\begin{aligned} y_{(0,t)}^+ &= S_0\, y_{(0,t)}^- \\ y_{(1,t)}^- &= S_1\, y_{(1,t)}^+ \end{aligned} \tag{2}$$

where vector $y = [y^-, y^+]^T$ is the partition of y corresponding to the partition of Λ, S_0 and S_1 are matrices of dimensions $(n-r) \times r$ and $r \times (n-r)$, respectively. For a positive definite diagonal $n \times n$ matrix G partitioned in the manner of Λ, the Lyapunov functional is defined to be

$$E_{(t)} = \|y\|_G^2 = \int_0^1 y^T\, G\, y\, dx$$

The time rate of change of the Lyapunov functional is given by

$$\frac{dE}{dt} = \frac{dE_b}{dt} + \frac{dE_i}{dt}$$

where

$$\begin{aligned} \frac{dE_b}{dt} &= y_{(0,t)}^{-T}(G^-\Lambda^- + S_0^T G^+ \Lambda^+ S_0) y_{(0,t)}^- - \\ &\quad - y_{(1,t)}^{+T}(G^+\Lambda^+ + S_1^T G^- \Lambda^- S_1) y_{(1,t)}^+ \end{aligned}$$

$$\frac{dE_i}{dt} = 2 \int_0^1 y^T\, GD\, y\, dx$$

Definition 1.

The initial-boundary value problem (1) (2) is interior-stable (resp. boundary-stable) if there is a positive definite diagonal matrix G, independent of initial conditions, such that the inequality $E_{i(t_1)} \geq E_{i(t_2)}$ (resp. $E_{b(t_1)} \geq E_{b(t_2)}$) holds for every $t_1 < t_2$.

Definition 2.

The matrix D is symmetrizable if there exists a diagonal positive definite matrix L that symmetrizes D, i.e. $LD = D^T L$.

Theorem 1.

Assume that the matrix D is symmetrizable. Then problem (1) (2) is interior-stable if and only if all eigenvalues of D are less or equal to zero.

Theorem 2.

If problem (1) (2) is boundary-stable then $\|S_1 S_0\| \leq 1$ and $\|S_0 S_1\| \leq 1$, where $\|\cdot\|$ denotes the matrix Hilbert norm.

Sketch of the proof:
If $\frac{dE_b}{dt} \leq 0$ for every initial condition then

$$y^{-T}(G^-\Lambda^- + S_0^T G^+\Lambda^+ S_0)y^- \leq 0$$
$$y^{+T}(-G^+\Lambda^+ - S_1^T G^-\Lambda^- S_1)y^+ \leq 0$$

Hence we have the following inequalities

$$y^{-T}[(S_1 S_0)^T(-G^-\Lambda^-)\, S_1 S_0 - (-G^-\Lambda^-)]\, y^- \leq 0$$
$$y^{+T}[(S_0 S_1)^T\, G^+\Lambda^+ S_0 S_1 - G^+\Lambda^+]\, y^+ \leq 0$$

If we now take

$$-G^-\Lambda^- = I_{r\times r}$$
$$G^+\Lambda^+ = I_{(n-r)\times(n-r)}$$

we finally obtain

$$\|S_1 S_0\| \leq 1 \qquad \|S_0 S_1\| \leq 1 \quad \blacksquare$$

Theorem 3.

Problem (1) (2) is boundary-stable if there exists $g > 0$ such that $\|S_0\| \leq g$ and $\|S_1\| \leq g^{-1}$.
Sketch of the proof:
If $\|S_0\| \leq g^-/g^+$ and $\|S_1\| \leq g^+/g^-$ then

$$\frac{y^{-T}S_0^T S_0 y^-}{y^{-T}y^-} \leq \frac{g^-}{g^+} \qquad \frac{y^{+T}S_1^T S_1 y^+}{y^{+T}y^+} \leq \frac{g^+}{g^-}$$

for every y^- and y^+. If we now take $G^-\Lambda^- = -g^- I$ and $G^+\Lambda^+ = g^+ I$ we finally obtain $dE_b/dt \leq 0$ ∎

Theorem 4.

Assume that the matrices S_0S_1 and S_1S_0 are symmetrizable. Then problem (1) (2) is boundary-stable if and only if $\|S_0S_1\| \leq 1$ or equivalently, $\|S_1S_0\| \leq 1$.

References

[1] Max. D. Gunzburger, On the stability of Galerkin methods for initial-boundary value problems for hyperbolic systems. Mathematics of Computation. V. 31, 661–675, 1977.

[2] H.-O. Kreiss, Initial boundary value problems for hyperbolic systems. Comm. Pure Appl. Math. V. 23, 277–298, 1970.

[3] W.J. Layton, Stable Galerkin methods for hyperbolic systems. SIAM J. Numer. Anal. V. 20, 221–233, 1983.